

DISTRIBUTION OF *PICEA RUBENS* AND GLOBAL WARMING – A SYSTEMS

APPROACH

by

KYUNG-AH KOO

(Under the Direction of Bernard C. Patten and Marguerite Madden)

ABSTRACT

For half a century the commercially and ecologically important tree species red spruce (*Picea rubens*) has been in decline over its entire range. For understanding the causes of declines at the Great Smoky Mountains National Park (GSMNP), the objectives of this study were: first, to develop a foundation for systematic and comprehensive understanding of the red spruce growth system through interdisciplinary synthesis; second, to investigate the causes of growth decline and the effects of global warming on *Picea rubens* growth from a tree growth model in systems modeling studies; third, to estimate suitable habitat conditions for red spruce from the tree growth model and predict the distribution range of red spruce and the effects of global warming on this range in GIS studies. Based on three study objectives, this study was divided into three main modeling sections: Envirogram of Annual Radial Increment Rate of Red Spruce (ARIRS), a conceptual model; the red spruce Annual Radial Increment Models (ARIMs), which are systems models; and the Red Spruce Habitat Model (RSHM), a spatial landscape GIS model.

The ARIRS envirogram well conceptualized complex interactions affecting red spruce growth and offered a conceptual model for ARIMs. ARIMs significantly showed that air pollution disturbance was the dominant cause of red spruce growth decline at high elevation, and red spruce growth had significant positive relationships with water availability and radiation and

a negative relationship with the air pollution disturbance at low elevation. ARIMs predicted red spruce growth was more affected by air pollution than global warming at high elevation and more by global warming than air pollution at low elevation. The ARIM results were applied to RSHM to find suitable habitat conditions for red spruce. RSHM significantly predicted spatiotemporal distribution of geographical range and habitat suitability of red spruce. RSHM also predicted that global warming would cause red spruce distribution to shrink by degradation of habitat suitability. Overall, this study showed significance and importance of comprehensive modeling for better understanding of tree systems by linking a conceptual modeling effort, the ARIRS envirogram, to a systems modeling effort, ARIMs, and the latter to a spatial landscape modeling effort, RSHM.

INDEX WORDS: Global Warming, *Picea rubens*, Growth decline, Range shift, A systems approach, Conceptual modeling, Envirogram of Annual Radial Increment Rate of Red Spruce (ARIRS), Systems modeling, The red spruce Annual Radial Increment Models (ARIMs), Spatial landscape GIS modeling, Red Spruce Habitat Model (RSHM), Great Smoky Mountain National Park (GSMNP)

DISTRIBUTION OF *PICEA RUBENS* AND GLOBAL WARMING – A SYSTEMS
APPROACH

by

KYUNG-AH KOO

B.S., The Kyunghee University, Seoul, South Korea, 1997

M.Sc., The Kyunghee University, Seoul, South Korea, 2001

A Dissertation Submitted to the Graduate Faculty of The University of Georgia in Partial
Fulfillment of the Requirements for the Degree

DOCTOR OF PHILOSOPHY

ATHENS, GEORGIA

2009

© 2009

Kyung-Ah Koo

All Rights Reserved

DISTRIBUTION OF *PICEA RUBENS* AND GLOBAL WARMING – A SYSTEMS
APPROACH

by

KYUNG-AH KOO

Major Professor: Bernard C. Patten
Co-Major Professor: Marguerite Madden

Committee: David K. Gattie
Robert O. Teskey
Elgene O. Box

Electronic Version Approved:

Maureen Grasso
Dean of the Graduate School
The University of Georgia
May 2009

ACKNOWLEDGEMENTS

Since 2003 spring, I have studied ecology, especially theoretical ecology. At that time, ecology was a kind of subdiscipline of biology and not recognized as an important science field in South Korea. That meant I did not have any background knowledge for the PhD in ecology. However, Dr. Ronald Pulliam gave me a good chance to discover this field by introducing me to ecology and ecological modeling. I am deeply appreciative to Dr. Pulliam for his kind consideration and dedication. Also, I would like to thank my committee members, Dr. R.O. Teskey, Dr. D.K. Gattie, and Dr. E.O. Box. They taught me background knowledge of each field which enabled me to greatly improve my dissertation. I also thank the system group members for encouraging and helping me to build the fundamental knowledge of systems ecology and new perspectives of science. I thank my friends, Jane Shevtsov, Chip Small, Nicole Gottdenker, and Joyce K. Gianato for their warm concerns for me.

Most of all, I would like to specially thank Dr. Bernard C. Patten, who is my main advisor, and Dr. Marguerite Madden, who is a co-advisor. My dissertation could not be completed without their tremendous and comprehensive assistance. Dr. Patten was particularly inspiration in my study of systems ecology and to see the world in a new perspective. For my research, he provided the key, systems ecology, to understand complex *across-scale* and *within-scale* interactions which explain how global climate change influences local tree systems. This key enabled me to make huge progress in my studies and answered questions that I had had since I began my studies of tree systems and global warming. He provided the role model of advisor, scholar, and professor that I want to follow for my entire life. Dr. Madden introduced me to

Geographical Information System and Remote Sensing and provided a chance to learn technical parts of this field with background knowledge. I could not have written Chapter 4, the GIS modeling part, without her assistance.

I would like to thank my family, who have provided invaluable support, my husband (Dong-Geuk Seo), my son (David Hyun-Deog Seo), Mom, Dad, and my brother. They always encouraged me to keep studying whenever I needed their kind words. Finally, I would like to thank God for all the blessings that I have been provided – wisdom, inspiration, the BEST advisors, friends, and family – and His guidance to make the right decisions in my life.

Kyung-Ah Koo, Athens, Georgia, USA, May 2009

TABLE OF CONTENTS

	Page
ACKNOWLEDGEMENTS.....	iv
CHAPTER	
1 INTRODUCTION	1
LITERATURE REVIEW AND PURPOSE OF STUDY	1
2 ANNUAL RADIAL GROWTH OF RED SPRUCE (<i>PICEA RUBENS</i>) IN A PLANT-ENVIRONMENT SYSTEM: LITERATURE REVIEW, DISCIPLINARY PERSPECTIVES, INTERDISCIPLINARY SYNTHESIS, AND ENVIROGRAM	18
3 ARIM: <i>PICEA RUBENS</i> GROWTH DECLINE, GLOBAL WARMING, AND WITHIN- AND ACROSS-SCALE INTERACTIONS: SYSTEMS MODELING AND INTERDISCIPLINARY SYNTHESIS	46
4 RED SPRUCE HABITAT MODEL (RSHM): EFFECTS OF HABITAT SUITABILITY AND GLOBAL WARMING ON THE GEOGRAPHIC DISTRIBUTION OF <i>PICEA RUBENS</i>	94
5 CONCLUSION	169
REFERENCES	175
APPENDICES	191

CHAPTER 1

INTRODUCTION: LITERATURE REVIEW AND PURPOSE OF STUDY

The Greek natural philosophers were interested in the interactions among organisms and surrounding conditions and found inseparable relationships among them. Ecology, which studies organisms and their environment, is descended from this philosophical background. Despite this long historical and philosophical background, modern ecology did not begin until the early eighteenth century. Linnaeus and Buffon made important contributions to lay the foundations of modern ecology (Allee et al. 1949). Linnaeus is the originator of modern phenology, ecology, geographical zoology, and botany and described the effects of external conditions to give an account of the natural phenomena (Allee et al. 1949). Buffon discovered a great principle of ecological study, i.e. environmental induction (Allee et al. 1949).

Since Linnaeus and Buffon, many research results and theories describing the interactions among organisms and environmental conditions have been accumulated in various scientific fields. As a result, ecology became a self-conscious science in the mid-20th century (Kingsland 1991). Ecosystem theory in its current sense, which understands the living world as a complex organized whole in the context of the ensemble of parts and relations existing between them, also began to develop with other ecological theories in that period. Ecologists have increasingly become involved in systems ecology with global issues such as global warming and increasing uncertainties in ecological research results based on reductionism and mechanism (Odum 1962, Patten 1998, Jørgensen and Bendoricchio 2001). Capra (1992) suggested that ecology based on a

systems approach would be a new paradigm in order to solve global issues and complicated problems of the living world.

1. Plant distribution, Uncertainty and System Theory

1.1. Plant distribution, Habitat suitability and Leading factors

Interaction among plant distribution and environmental conditions has been a major subject of ecology and studied for a long time by the successors of Linnaeus. In particular, with rapid and directional environmental changes during the past decade, the range shift of plants associated with environmental gradients and changes have been more focused on ecology (Hamrick 2004). Ecologists such as Clements and Gleason, who studied plant community succession in the early 1900s, and genealogists were interested in this subject. They recognized that all plants have their unique distribution ranges, which have changed in space and time due to interactions with environments. However, researchers have suggested different fundamental ideas about which factors mainly lead to those interactions. Three research trends can be recognized. One is exemplified by Frederick Clements (1916, 1936), who proposed the super-organism and climax concepts based on the postulated equilibrium between climate and plant community composition. Clements (1936) thought that plant communities are determined by climatic conditions and that, ultimately, one species or multiple taxa adapting to climatic conditions come to dominate in some area as a climax. His climax concept has been incorporated into climate–vegetation models of vegetation science and in spatial landscape modeling research of landscape ecology (Holdrige 1947, Seddon 1971, Whittaker 1975, Box 1981, Woodward 1987, Box et al. 1993, Shao and Halpin 1995, Iverson and Prasad 1998, Turner et al. 2001, Matsui et al. 2004). Recently the U.S. Geological Survey (USGS) employed the climax concept to build

climate-vegetation models. These models have been applied to other fields like climatology and paleontology in order to predict climate changes based on tree range shifts. Also, many individual research programs have been implemented in order to elucidate the plant ranges and range changes with climate change, assuming equilibrium between climate and plant range (Huntley et al. 1989, Skov and Borchesenius 1997, Hörsch 2003, Matsui et al. 2004, Chuanyan et al. 2006).

Another trend has followed Gleason's individualism and disequilibrium concepts. Gleason (1926) focused on the different species composition of plant communities, their unclear geographical boundaries, and interannual variations in vegetation structure in every plant association. In order to explain these phenomena, Gleason employed the dispersal mechanism as a causal factor. His concepts have been continued in studies investigating metapopulation dynamics of organisms, estimation of spatiotemporal changes in distribution in relation to environment fluctuations, and community succession (Pulliam 1988, Kiviniemi 1996, Westoby et al. 1996, Eriksson 1996, Fröborg and Eriksson 1997, Pitelka 1997, Clark 1998, Clark et al. 1999, Ehrlén and Eriksson 2000, Nathan and Muller-Landau 2000, Pulliam 2000, Turner et al. 2001, Schwartz et al. 2001, Bullock et al. 2003). For example, Pulliam (1988, 2000) developed "source-sink" theory and a new niche theory. He suggested that environmental tolerance and competition are not enough to account for plant distribution and that the presumed relationship between suitable habitat and plant distribution can become much more complicated with dispersal limitation. Many theoretical and field studies have supported this theory (Skidmore and Heithaus 1988, Primack and Miao 1992, Kiviniemi 1996, Ehrlén and Eriksson 2000, Jones et al. 2005). From a systems ecology perspective, this was nothing more than opening a system that should never have been closed (by population mathematics) in the first place.

The third trend can be seen in the study of geneecology by evolutionary biologists. They have been concerned with how plants adapt to environmental heterogeneity since early biologists found local variations within a species. In evolutionary biology it has been thought that range shift is closely related to adaptation and phenotypic plasticity (acclimation) as well as dispersal mechanisms and environmental tolerance of plants. In addition, range shifts by dispersal could not be simply an alternative to a situation that plants cannot adapt to the novel environments; rather, range shift has to be understood as a complicated interaction among dispersal, environment, and adaptation. David and Shaw (2001) pointed out that “beyond changes in distribution, plants underwent genetic changes, adapting to changes in climate during the Quaternary; therefore, if it is assumed that the tolerance range for a species remains stable and ignoring intraspecific variation, then prediction of plant distribution with climatic change will fail.” Results of many transplant experiments showing genetic differentiation along with environmental gradients have supported the conclusion that modern populations of species that shifted ranges in the past were adapted to the climatic conditions of their present habitats (Campbell 1979, Pitelka 1997, Briggs and Walters 1997, David and Shaw 2001, Hamrick 2004). Hamrick (2004) also suggested that trees may contain adequate genetic diversity through high gene-flow rate among populations to respond to changed climatic conditions.

1.2. Uncertainties in studies of Plant distribution

All three research trends have achieved contributions to understand the relationship between the distribution range of plants and environment in a certain range. However, despite the progress in technique, theories, and quality of data, researchers have faced uncertainties in estimating the current range and predicting future range changes with environmental changes. In

particular, since global-scale environmental changes such as global warming were recognized, uncertainties have kept increasing in this field.

Vegetation scientists and landscape ecologists have pointed out some uncertainties in estimating current distribution ranges and predicting spatiotemporal changes of plant range (David et al. 1998a, David et al. 1998b, Lowton 2000, Pearson and Dawson 2003). These uncertainties originate from the lack of understanding of dispersal mechanisms, biological responses, and the mechanisms describing how environments influence vegetation development, succession and spatiotemporal pattern. As Pulliam (1988, 2000) indicates, dispersal can make plant range dynamics more complicated. Thus spatiotemporal range change of plants could not be correctly predicted by vegetation–climate models. On the other hand, evolutionary biologists have argued that vegetation–climate models cannot predict the real spatiotemporal changes of plant distribution range due to the uncertainty of raw data and the ignoring of adaptation ability (David and Shaw 2001). For example, vegetation scientists and paleontologists have thought that the range of plants has shifted from south to north and from low-elevation to high-elevation along with climate warming. However, several plant physiologists (Battaglia et al. 1996, Gunderson et al. 2000) have reported that high-elevation individual plants are more vulnerable to climate warming than low-elevation ones within a species. Therefore, real changes of plant range can be different from the predictions made by vegetation scientists based on climate–vegetation models. In conclusion, because of interactions among environments, dispersal, adaptation and acclimation (phenotypic plasticity) factors, current vegetation–climate models cannot properly predict distribution ranges and spatiotemporal range changes of plant species.

Theoretical scientists (Higgins et al. 2003, Nathan et al. 2000, Clark et al. 2004) who study dispersal mechanisms have also suggested uncertainties in modeling and predicting plant

range changes and population dynamics. Higgins et al. (2003) identified the three sources of uncertainty of modeling in forecasting range changes: model uncertainty, parameter uncertainty, and inherent uncertainty. Model uncertainty means that in the context of migration, sub-models used to define the life history and dispersal parameters are uncertain; therefore, final models cannot have a high accuracy. Parameter uncertainty originates from sampling size, observation errors, and strategies of sampling and data collection. Also, this uncertainty is linked with model uncertainty. Inherent uncertainty occurs because we cannot perfectly understand all inner-mechanisms of plants; so, this cannot be reduced by improving model and parameter uncertainty. Nathan et al. (2000) suggested we couldn't make accurate predictions without considering subsequent processes, such as herbivory, competition, and mating. Clark et al. (2004) made the point that there are a number of uncertainties in predicting range shift based on dispersal distance, including poor understanding of habitat suitability, interactions among plant species, and their ability of adaptation and acclimation.

Evolutionary biologists have also found uncertainties in estimating adaptation and acclimation (phenotypic plasticity) along with future climate change, in spite of the fact that adaptation of trees to their habitat has been supported by many genetic analyses with field experiments. With physiological experiments in the greenhouse and field, transplant experiments, such as common garden experiments and reciprocal transplant experiments, have been conducted by evolutionary biologists in order to test whether or not trees can adapt to increased temperature conditions (Etterson 2004). The question could not be clearly answered. Such uncertain results originate from the lack of fundamental knowledge about the mechanisms and processes of adaptation associated with habitat conditions. Ability to adapt is determined by all habitat and environmental factors, not just one. Futuyma (1986) pointed out the complexity of the external

ecological world in interpreting adaptation, i.e., there are numerous selective factors and their complexity is difficult to measure.

1.3. Reasons for uncertainties

There could be several reasons why previous studies have not found better solutions, in spite of the advances of theories, methodologies and the availability of high-resolution data. In addition, uncertainty is not decreasing; rather, it seems to keep increasing with advances in these fields. At first, this is because most studies were based on the traditional paradigm of scientific reductionism and statistically-based mechanism. *Reductionism* is originally from the second maxim of Descartes' *Discours de la Methode*, which is "to break down every problem into as many separate, simple elements as might be possible." This was later reformulated by Galileo as the *resolutive method*: to resolve and reduce complex phenomena into elementary parts and processes (Bertalanffy 1975). *Mechanism*, which assumed linear causality among phenomena and a random world, was developed with reductionism. Both mechanism and reductionism have been practiced in physics and chemistry, resulting in outstanding contributions to modern industrial society as leading technical advances. In accordance with advances of physics and chemistry, reductionism and mechanism have moved into biological fields. However, the current paradigm alone is faced with problems in describing a living world (Bertalanffy 1969, 1975). Most researchers thought that the causes of uncertainties found in their researches were the lack of fundamental knowledge and poor understanding of the complexity of the living world. Weinberg (1975) and Bertalanffy (1975), however, suggested that these problems could be because biological fields explored organized complexity as a whole, which cannot be explained by reductionism and mechanism alone.

The second reason for uncertainties is isolation among disciplines, and this is an extension of the first reason. Reductionism has catalyzed the separation of disciplines, emphasizing the specialization of each field in order to find more accurate correlations among elements and solutions to problems. As a result, researchers in each field have concentrated on narrowed research subjects and made special terms (jargon) that can only be understood by colleagues in their field (Bertalanffy 1975, Kuhn 1996, Patten 1998). Researchers studying fluctuation of plant distribution ranges associated with environmental changes also have the same dilemma. Even though the three trends of plant distribution studies identified above have recognized complexity and the demand for knowledge from related disciplines, they have followed their predecessors without considering interdisciplinary aspects. Baker (1989) indicates this issue can also be applied to landscape-ecology fields. Vegetation science and landscape ecology fundamentally attempt to synthesize information. However, spatial landscape models have had problems illustrating the processes and incorporating physiological and genetic information in predicting habitat range.

The third reason could be more specific for ecology and related fields. Ecology is originally an empirical system science (Patten 1980); thus, ecologists have traditionally thought all data should be from the field or laboratory. Field oriented research, together with mechanistic methods, prohibits the consideration of complex indirect interactions among compartments of nature. However, indirect effects induced by hidden relationships among components have been suggested by system scientists as dominant effects. Patten has applied system modeling in his research, concluding that the dominance of indirect (vs. direct) effects is a general feature of connected systems (Higashi and Patten 1989, Patten 1991, 1997, 1998). For example, Patten showed the complexity of relationships and dominance of indirect effects in network environ

analysis of an Okefenokee Swamp water model (Patten 1982) and an ecosystem-based American black bear model (Patten 1997). In addition, Patten (1985a, b, 1990) elucidated the complex pathways in the trophic dynamics and indirect effects dominance among trophic levels through organized complex pathways.

However, most researchers studying plant distribution have tried to find direct relationships with environmental conditions (Skov and Borchesenius 1997, Guisan et al. 2002, Matsui et al. 2004, Engler et al. 2004, Chuanyan et al. 2006). They have not at all recognized indirect effects dominance among environmental factors. Research based on dispersal mechanisms and evolutionary studies has obviously followed mechanism and reductionism. Therefore, they do not fundamentally account for dominant indirect effects in the living world; as a result, phenomena occurring by indirect interactions still remain unanswerable. Vegetation scientists and landscape ecologists have followed the different research trends with two other trends. They have synthesized a set of climate variables and other variables, such as topography, soil, and species composition, in projecting the distribution ranges of organisms, and they made a point that many indirect relationships do exist in nature (Baker 1989, Hörsch 2003). However, they could not develop satisfactory methods and theories to illustrate the hidden relationships among elements (Baker 1989). White et al. (1992) also indicated the lack of any true integration among environmental systems in this field.

1.4. Systems Theory and Modeling

Discerning the limitations of reductionism and mechanism as mentioned above, many system theories involving cybernetics, open system theory, game theory, information theory, and decision theory, were developed in different disciplines. Bertalanffy (1968, 1975) introduced

General Systems Theory (GST) into science in order to organize these system theories and provide a philosophical background and holistic paradigm for interdisciplinary studies. The philosophical foundation for GST originates from the Aristotelian dictum, “The whole is more than the sum of its parts” (Bertalanffy 1975). Based on GST, all phenomena of the living world are understood in the context of the ensemble of the parts and the relations existing between them.

In ecology, the ecosystem concept, first proposed by Tansley (1935), was developed with other system theories; this can be considered as a branch of GST. Evans (1956) extended the ecosystem concept and the term to organizational levels. He regarded the ecosystem as involving “the circulation, transformation, and accumulation of energy and matter through the medium of living things and their activities.” He also stressed that ecosystems are open systems, not closed ones; “energy and matter continuously escape from them in the course of the processes of life, and they must be replaced if the system is to continue to function.” However, systematic treatment and development of the ecosystem concept in its current sense is mostly associated with Eugene Odum beginning with his book, *Fundamentals of Ecology* (Kormondy 1965). Odum (1962) defined ecology as “the study of the structure and function of ecosystems.” Odum (1962) regarded structure as involving the composition of the biological community, the quantity and distribution of the abiotic materials, and the range, or gradient, of conditions of existence. Function is the rate of biological energy flow through the ecosystem, the rate of material or nutrient cycling, and biological or ecological regulation of both organism and environment. Systems ecology and ecosystems ecology have been studied by a combination of modeling and empirical studies because modeling is the only methodology that can deal with complex interactions and integrate empirical knowledge.

2. Global Warming, Habitat Suitability and System Theory

With globalization, our world is more and more interconnected and complicated. We have more chances to contact each other via transportation and various communication systems in spite of long distances. Globalization also has made an impact on our culture and environment. Now we can experience various foreign cultures and goods around our local place through international economic trade and various communication network systems. Patten (2009) wrote that “technology is spearheading the rapid globalization of humanity, and this will ultimately reduce individualistic control because parts will benefit from participating in organized wholes and evolve to belong.” Capra (1992) also said “Ultimately, there are no parts at all; what we call a part is a pattern in an inseparable web of relationships.” Therefore, most or all issues including environmental changes cannot be restricted into the local area at the present time; rather, they are spatiotemporally related with others through organized and complex interaction pathways, as considered by system theories.

The most importantly considered issue of global environmental change is global warming. Many researchers have suggested cyclic climate change in that there are alternating cooling and warming periods. However, after industrialization, directional climate changes, which mean changes of habitat suitability for organisms, have become more and more accelerated with increasing emission of greenhouse gases. Unexpected catastrophes, range shifts of organisms and extinction of alpine species have been reported. Actually, long-term records show earlier onsets of several phenological events (Bradley et al. 1999, Pounds et al. 1999, Walther et al. 2002, Heide 2003, Parmesan and Yohe 2003), and some organisms with southern distribution limits have experienced range shift and shrinking habitats (Pounds et al 1999, McLaughlin et al 2002, Miles et al. 2004). Many scientists have attributed these phenomena to global warming (Corti et

al. 1999, Cox et al. 2000, McLaughlin et al. 2002, Walther et al. 2002, Parmesan and Yohe 2003, Miles et al. 2004). We obviously need a more complete understanding of climate history and plant responses for global warming at local or regional scales in order to argue that global warming is the reason for these phenomena. However, we cannot ignore the possibility that these phenomena are related to global warming. To understand the global warming effects on plants on the local or regional scale, we need to account for interactions among system factors across scales. This can be realized by applying systems theory and modeling which considers interactions across scales, from local to global.

3. Study System, Hypotheses and Objectives

3.1. Study System

The system of study in this dissertation is the red spruce (*Picea rubens* Sarg.) system of the Great Smoky Mountains National Park (GSMNP), located in the southern Appalachian Mountains of Southeastern U.S.A. (Figure 1.1). Red spruce is a long-lived (> 300 years), shade tolerant species, with a low reproduction rate and low genetic diversity (Eagar and Adams 1992). It is a major tree species in high elevation coniferous forests of the Appalachians (Busing 2004) and dominates boreal habitats at the lower elevations (1370-1675m); Fraser fir forests (*Abies fraseri* (Pursh) Poir.) dominate at higher elevations (>1890m). Both species co-dominate at mid elevations (1675-1890m) (Webster et al. 2004).

The growth of red spruce shows a different pattern at lower vs. higher elevations (Deusen 1988, Eagar and Adams 1992) due to differing climatic conditions. The large number of dead and declining red spruce throughout the Adirondacks, in Northeastern U.S.A., and Appalachians raised public and scientific concern about the future of mountain spruce–fir forests (Eagar and

Adams 1992). Dendrochronological studies estimated that red spruce decline in the Southern Appalachians occurred after about 1965 (Deusen 1988, Eagar and Adams 1992). It has been

(a)



(b)

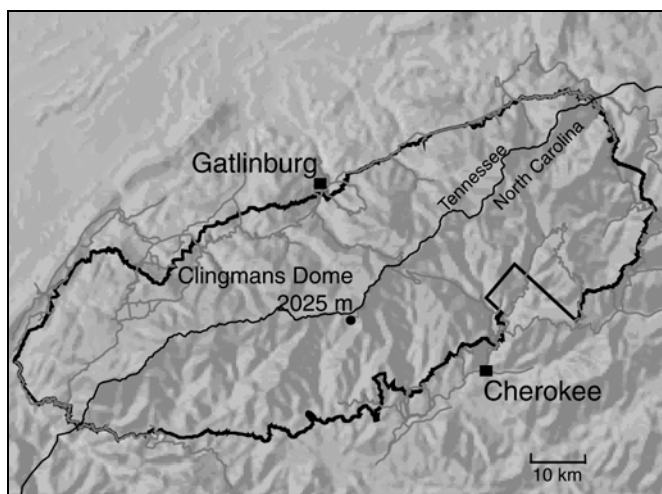


Figure 1.1. (a) shows location of GSMNP in the eastern United States and (b) boundary of GSMNP and elevation of summit area, Clingmans Dome. Source of maps is Madden et al. (2004).

thought that this reduction may be an early indication of more broadly based changes in the structure and functioning of this system (Webster et al. 2004, Eagar and Adams 1992, Johnson et al. 1992). Whether changes in air quality, climate, forest disturbances, and nutrient cycling are major causes of red spruce decline has been a central question within the phytosociological community (Busing 2004).

The red spruce–fir forest has experienced exponential increases of greenhouse gas emissions and acidic pollutants during the past century (EPA 2000). Emissions of greenhouse gases and acidic pollutants with frequent cloud immersion and cloud-water chemistry are implicated in changes of climate and acidification of this montane ecosystem (Webster et al. 2004). Dendroclimatological studies found that warm late-summer temperatures had a negative effect and warm early winter temperatures had a positive effect on radial growth (Cook et al. 1987, Cook 1988, McLaughlin et al. 1987, Eagar and Adams 1992). It has been suggested that acidic pollutants and climate change can influence the red spruce system in multiple ways, such as modification of the atmospheric system, soil system, geochemical system, and physiological system (Eagar and Adams 1992, Barker et al. 2002, Creed et al. 2004, Webster et al. 2004). Another important stress is the infestation of Fraser fir by the balsam woolly adelgid (*Adelges piceae* Ratz.). This has caused extensive Fraser fir mortality in the Great Smoky Mountains (Webster et al. 2004). Such high mortality of a co-dominant species may make an impact on the spruce system's structure and dynamics through modifications of physical environments. Busing and Pauley (1994) reported that loss of Fraser fir from the canopy would leave red spruce vulnerable to wind damage and mortality.

Although many researchers have suggested the possibility of natural and air pollution-related factors in forest decline, considerable uncertainty exists about the roles of those factors

(Eagar and Adams 1992, Busing 2004). Any factors, such as emission of air pollutants, nutrient cycling, climate condition, winter injury, and soil mineral conditions, cannot significantly account for the growth decline alone. Even though laboratory experiments demonstrate the relationship between each factor and growth decline, such results could not be verified in the field. Also, the radial growth decline of red spruce forests shows high regional variation (Eagar and Adams 1992, LeBlanc et al 1992, LeBlanc 1993, Johnson et al. 1995, Reams and Deusen 1995, Webster et al. 2004, Richardson 2004). Busing (2004) reported inconsistent results between mortality and radial growth of red spruce at Mt. Collins, in the Great Smoky Mountains National Park. There, during 1993–2003, red spruce canopy trees continued to grow vigorously, but mortality rate was elevated (Busing 2004).

3.1. Hypotheses and Objectives

In the present study, I employ the system theory approach. The study assumes and implements Patten's theoretical conclusion that indirect effects are dominant over direct effects in ecological networks as a result of organized complex pathways of energy and matter flow interconnecting biota and abiota. In employing system theory, I developed first a set of general hypotheses to guide studies of tree distribution, habitat suitability and environmental change. Then, specific, literature-based hypotheses were developed for the red spruce system of GSMNP. In particular, global warming effects were considered as long-term climatic factors influencing the red spruce system.

General hypotheses for studies of tree distribution, habitat suitability and environmental change are as follows:

- 1) The distribution range of tree species is determined by habitat suitability.
- 2) Habitat suitability is expressed by hierarchically organized direct and indirect interactions among internal system factors of each tree species, external system factors, and relations existing among all of these. Internal system factors are composed of density dependence, physiological responses, acclimation and adaptation. External system factors are environmental factors.
- 3) Indirect interactions among system factors are the dominant determinants of the distribution range of tree species. Indirect effects occur through complex, organized, hidden and hierarchically-ordered, within- and across-scale interactions among system factors.

Corresponding specific hypotheses for the red spruce system at GSMNP are:

- 1) The distribution range and growth of *Picea rubens* in GSMNP is determined by habitat suitability, and habitat suitability is expressed by hierarchically organized direct and indirect interactions among system factors such as physiological responses, temperature, precipitation, herbivory, topographical factors, and air pollution.
- 2) The habitat suitability of *Picea rubens* of GSMNP is influenced by global warming as a cause expressed through direct and indirect interactions among system factors.
- 3) Changes of growth and distribution of *Picea rubens* at GSMNP along with global warming are the result of direct and indirect interactions among system factors.

- 4) Indirect interactions among system factors are the dominant effects in determining the distribution range of *Picea rubens* of GSMNP. Indirect effects occur through complex, organized, hidden and hierarchically ordered, within- and across-scale interactions among system factors.

In the present study, I will examine through modeling the following objectives based on the three specific hypotheses:

- 1) Develop a foundation for systematic and comprehensive understanding of the red spruce growth system through interdisciplinary synthesis;
- 2) Investigate the causes of growth decline and the effects of global warming on *Picea rubens* growth from a tree growth model in systems modeling studies;
- 3) Estimate suitable habitat conditions for red spruce from the tree growth model and predict the distribution range of red spruce and the effects of global warming on this range in GIS studies.

CHAPTER 2

ANNUAL RADIAL GROWTH OF RED SPRUCE (*PICEA RUBENS*) IN A PLANT-ENVIRONMENT SYSTEM: LITERATURE REVIEW, DISCIPLINARY PERSPECTIVES, INTERDISCIPLINARY SYNTHESIS, AND ENVIROGRAM

1. Introduction

The earth system, including all living and nonliving systems, needs energy to maintain itself. It is maintained by energy exchanges across the boundary—incoming solar shortwave radiation and outgoing longwave radiation. Physics recognizes three types of systems: isolated, closed, and open. Isolated systems transfer no matter or energy across their boundaries (White et al. 1992). Closed systems exchange energy but not matter with their surroundings (White et al. 1992). The earth system is to a great extent closed. Most systems on the earth are open; these exchange both energy and matter with systems outside their boundaries (Bertalanffy 1975, White et al. 1992, Lambers et al. 1998).

Systems can also be defined by three different perspectives. One is reductionistic perspective, which focuses on the parts and interactions between them. A second is behavioral, defining a system as a set of behaviors produced as reactions to outside stimuli. The third is holistic, which considers the whole's effects on the parts more than, as in reductionisms, the reverse. Both sets of systems perspectives are related to environmental dualism, which specifies that every non-isolated system has two environments, a stimulus environment incoming and a response environment outgoing (Uexküll 1926, Patten and Finn 1978).

In this study the red spruce (*Picea rubens*) system in the Great Smoky Mountains National Park (GSMNP) is seen as open, behavioral, and holistic. The objective is to provide background information for a simulation model of the annual radial growth increment in red spruce (ARIM) in the Great Smoky Mountains National Park (GSMNP) in chapter 3. This study provides a foundation for a systematic and comprehensive understanding of red spruce growth through interdisciplinary synthesis for ARIM. To initiate this, the envirogram method of S. B. Niven was employed.

2. Methods and Data

2.1. Envirogram

The envirogram method was developed based on the open system and holistic perspectives. Environmental dualism is implemented when outgoing environments are added to the incoming ones of the original method. Envirograms present a compact summary of information about the environmental relations of a subject organism, enabling comprehensive depiction of the whole structure of an organism's complex relationships (Niven and Abel 1991, Niven and Liddell 1994). Susan B. Niven invented the envirogram, and H.G. Andrewartha used it based on her mathematical definition of environment (Niven and Liddell 1994). The total environment (an incoming one) is mathematically defined in two parts, direct and indirect (Niven and Abel 1991, Niven and Liddell 1994).

In envirograms, the direct and indirect environments are called *centrum* and *web*, respectively. The *centrum* is divided (in the dual approach) into input and output environments. The input environment indicates a stimulus environment incoming to a focal system and the output environment a response environment outgoing. Realistic envirograms have multiple webs,

which explains complex and hierarchically organized indirect interactions. In envirograms, more and more indirect interactions lead to increasing web development. Indirect effects produced by indirect interactions are frequently more influential than direct effects; hence, webs frequently outweigh corresponding centrums in importance.

For envirograms of the Annual Radial Increment (growth) Rate of Red Spruce (ARIRS), I regarded the factors that increase radial increment as input environment and the factors that decrease this as the output environment. Both environments are divided into centrum and web according to relationships involved in radial growth. In addition, elements of the system are also categorized into internal and external influences. The internal system elements include intrinsic biological characteristics (age and size effects), phenotypic plasticity, and density-dependent effects. Tree growth is influenced by age and size of tree (Day et al. 2004, Mencuccini et al. 2007), but the study of the annual radial increment rate focuses on the adult stage to understand the long-term relationships between the Annual Radial Increment (growth) Rate of Red Spruce and environment. Therefore, the age and size effects on the red spruce growth are ignored in this study. External system elements are biotic and abiotic factors such as herbivores, co-dominant species, and climate.

2.2. Definition of the Study System

It is assumed that the Annual Radial Increment Rate of Red Spruce (ARIRS) behaves as an open system and expresses phenotypic plasticity in only one type of behavior, annual radial growth increment. The system boundary is defined by the red spruce population instead of an individual tree. The annual variation in ARIRS is therefore the mean variation of the population level. The growth of a tree is a phenomenon of biomass accumulated without loss; however,

ARIRS represents relative variation, obtained by dividing each yearly average value by the corresponding long-term mean. Therefore, ARIRS behaves as an open system, changing with annual variations of photosynthesis and respiration in association with interactions between internal factors and environment. If the annual radial increment in a certain year is higher than the long-term average, then it can be treated as an open system gaining biomass and vice versa.

2.3. Data

A main data source for this study was Eagar and Adams (1992). This book reviewed previous researches on general characteristics of red spruce habitats and the causes of growth decline and high mortality. This reference reports results before 1992; later information was obtained by reviewing research papers and reports. However, the available data do not cover all aspects of the ARIRS envirogram. Such data usually covered disturbance-mediated effects on growth decline and high mortality, but more fundamental information is needed for understanding direct and indirect interactions between the red spruce system and environments, and among environmental factors. Research results from other disciplines are necessary to determine indirect interactions. Basic information was obtained from general physiology, climatology, plant genetics, and ecological studies, among others. Lambers et al. (1998), Geiger et al. (2003), and Aguado and Burt (2004) were principal sources employed for understanding relationships between climate, topography and red spruce growth.

3. Envirogram Construction

Photosynthetic input and respiratory output are key processes in plant growth and thus take a central place in the Annual Radial Increment Rate of Red Spruce. Because energy released

in respiration represents maintenance costs such as repair of damaged parts as well as supplies for photosynthesis, it does not always contribute to growth increment (Lambers et al. 1998). In the ARIRS envirogram, the input environment contains factors increasing photosynthesis, and the output environment contains factors decreasing photosynthesis and increasing respiration for maintenance. Solar radiation, water availability (water), carbon dioxide, and soil nutrients account for the direct environmental factors, consisting of the centrum of input environment. Natural and anthropogenic disturbances account for the output environment, consisting of the centrum of the output environment. For ARIRS, disturbances consist of herbivory and weather disturbances for natural disturbances and air pollution and soil-mediated disturbances including soil acidity and soil aluminum toxicity for anthropogenic disturbances. This study did not consider other disturbances directly due to the deficiency of the information and knowledge cumulated by previous studies.

3.1. Direct Factors (Centrum)

(1) Radiation

In general, tree growth rate increases with increasing light intensity, but each tree species has a critical point such that both low and high light intensity can be limiting (Pandey et al. 2003). Low light reduces net carbon gain due to limited energy for photosynthesis (Lambers et al. 1998). High light can reduce net carbon gain by photoinhibition, which dissipates excess energy through reactions mediated by carotenoids, and direct damage to the photosynthetic apparatus (Lambers et al. 1998, Pandey et al. 2003). Red spruce is a late-successional, shade-tolerant species adapted to regeneration in the understory. Therefore, individuals, mostly seedling and

sapling, have little capacity for photosynthetic acclimation to a rapid increase in light intensity (Dumais and Prévost 2007).

The light condition is regulated by other physical and biological environmental factors. These include temperature, precipitation, cloud immersion, fir (*Abies*, an associated genus) mortality, population density, and topographic factors. Precipitation and (at high elevations) cloud immersion directly block incoming solar radiation. Fir mortality and population density are factors related to competition for radiation. High fir mortality and low population density of red spruce generally increase absorption of radiation.

Temperature is one of most important environmental factors in tree radial growth (Breckle 2002). Temperature controls enzyme activities which catalyze both photosynthesis and respiration. Light absorption increases with increasing temperature until temperature reaches the optimum and then decreases (Lambers et al. 1998, June et al. 2004). Low temperature generally reduces enzyme activities, decreasing light absorption (Lambers et al. 1998). Extremely high temperature can directly damage the photosynthesis apparatus; so, trees shut down photosynthetic mechanisms at very high temperatures (Lambers et al. 1998). Red spruce is highly sensitive to high temperature stress, which inhibits its ability to become established in exposed habitats, showing very low seed germination rate and survival rate of seedlings and saplings, and in extreme cases high air temperature can result in irreversible foliar damage, bleached leaves (Dumais and Prévost 2007).

Topographic factors, including aspect, slope, and elevation, directly influence light conditions by changing local radiation climate. The following observations are from Geiger et al. (2003). The amount of incoming radiation per unit area increases with changing aspect from north-to south-facing slopes, and it increases with slope changes from high to low slope. This is

because southern aspect and low slope have longer daily exposure to radiation during a day. Elevation also affects the light environment of trees. Direct-beam solar radiation increases and diffuse solar radiation decreases with height above sea level because atmospheric mass and turbidity decrease with elevation. Based on field measurements in the Alps, solar radiation increases by 21 percent per 100 m with a clear sky and by 160 percent with cloudy skies. This specific numbers cannot be applied to other places, but are representative of the general relationship between elevation and light intensity.

(2) Water

Water is essential to all known living organisms, as a solvent of many solutes, and as a part of many metabolic processes. In plants, water is the main component of nonwoody tissues such as leaves and roots, the transporter of the raw materials and phytohormones, and the major medium for transporting metabolites through the cell (Lambers et al. 1998). Photosynthetic cells use solar energy to split off hydrogen from the water molecular to form carbohydrate in the carbon reduction cycle. Therefore, water directly affects photosynthetic activity as an electron donor and indirectly as a solvent and transporter of raw materials and phytohormones.

Water availability to trees is fundamentally determined by differing water holding capacities of different soil types (Breckle 2002). But soil type is not a factor in annual variation of growth rates due to adaptation of trees to the soil type and slow changes of nutrient availability compared to water availability. Therefore, in this study, other factors were considered as influential in water relations, such as evapotranspiration. High evapotranspiration causes decrease in water availability, and vice versa. Factors in this are temperature, radiation, precipitation, topographical conditions, fir mortality, population density, and phenotypic plasticity for the ARIRS system.

Precipitation is obviously a direct and fundamental source of water; so, its increase makes water availability increase. Temperature also affects water availability. High temperature condition decreases soil water content due to increasing evaporation and transpiration (Breckle 2002). At high temperatures, more soil water evaporates because of high vapor pressure deficit of the air, and trees need more water for transpiration for cooling down leaf temperatures (Lambers et al. 1998). Low temperature also causes water stress due to decreasing enzyme activity and membrane fluidity (Limbers et al. 1998). Radiation influences water absorption by controlling the demand of water for photosynthesis, showing a positive relationship between them. Influential topographic conditions on water are elevation, aspect, slope, and distance to stream. Some tree can absorb deep soil water using deep roots, so trees rooted are not much influenced by ground water sources such as streams. But for red spruce, stream proximity is important due to generally shallow rooting (Edgar and Adams 1992). Elevation, aspect, and slope determine the local radiation climate. High radiation sites have drier conditions than low radiation sites due to higher evaporation and transpiration rates (Geiger et al. 2003). High fir mortality causes soil to be exposed to more intense radiation due to increased canopy openness, causing water availability to decrease due to increasing the evaporation and transpiration (Edgar and Adams 1992). High fir mortality could be beneficial for red spruce because of reduced competition for water, but in GSMNP this is weakened by high precipitation and cloud immersion. Population density generally accounts for competition for water among red spruce individuals, but this factor is also small due to high precipitation and cloud immersion rates.

(3) Carbon Dioxide (CO₂)

The source for this section is Lambers et al. (1998). Carbon from carbon dioxide is an essential component of carbon assimilation with hydrogen from water. The carbon assimilation

rate is determined by both the supply and demand for CO₂. Diffusion into the leaf supplies CO₂ to the chloroplast, controlled by stomatal conductance and boundary layer conductance, mostly the former under usual conditions.

The stomatal conductance is mainly regulated by temperature, water availability, radiation, and interactions among them. Low temperature decreases stomatal conductance by decreasing enzyme activities. High temperature increases the vapor pressure, increasing evapotranspiration. Thus, the stomatal conductance of leaves is decreased to prevent water loss under high temperature condition. Water availability controls the stomatal conductance to prevent water loss. Water loss is unavoidable if CO₂ is to enter the leaf for photosynthesis. When the water supply from roots does not match the loss from leaves, the stomatal conductance is reduced in order to prevent farther water loss. Roots in dry soil produce chemical materials such as abscisic acid (ABA) and Cytokinin to signal the leaf to restrict stomatal conductance. Radiation is the fundamental energy resource to initiate and maintain photosynthesis, and radiation influences CO₂ absorption by controlling the demand for CO₂.

(4) Nutrients

Nutrients are materials constituting all organs of trees, the photosynthetic apparatus included; therefore, deficiency of nutrients causes metabolic activities to decrease. Many experiments have been accumulated in tree physiology studies to document the role of nutrients in tree growth. Most experiments have concerned nitrogen concentration and cycling because the photosynthetic machinery accounts for more than half of the nitrogen in a leaf (Aber et al. 1998, Lambers et al. 1998, Fernandez et al. 2000, Pregitzer et al. 2008). Experiments have shown that photosynthesis rate declines with decreasing leaf nitrogen concentration associated with declines in ribulose-1, 5-bisphosphate carboxylase/oxygenase (Rubisco), chlorophyll and stomatal

conductance (Lambers et al. 1998). The relationship between nitrogen concentration and photosynthetic rate is not always strong because the entire photosynthetic process, including nitrogen relationships, is complex (Lambers et al. 1998). Other nutrients besides nitrogen, such as phosphorous, calcium, and magnesium, may also be limiting (Lambers et al. 1998, Boyce 2007, Huggett et al. 2007). In particular, calcium and magnesium are limiting factors for red spruce in GSMNP due to acid soil and leaching by acid rain (Eagar and Adams 1992, Sheppard et al. 1993, Borer et al. 2005).

Nutrient absorption is fundamentally controlled by the demand–supply mechanism. Radiation influences nutrient absorption by controlling the demand of nutrients for photosynthesis. Trees, red spruce included, need more nutrients with increasing radiation due to increased photosynthesis, up to the point where radiation induces photoinhibition. Principal factors regulating rates of nutrient supply are temperature, water availability, the air loaded nutrients, and population density. Low temperature decreases nutrient absorption by inhibiting enzymatic activity and membrane fluidity. High temperature coupled with high light intensity decreases it also due to direct damage to the photosynthetic apparatus and photoinhibition (Limbers et al. 1998). Water availability increases nutrient absorption proportionately because water is the solvent and transporter of nutrients (Lambers et al. 1998). The air loaded nutrients are a source of nutrients. For example, field experiments have reported that sulfate and nitrogen are deposited in the soil by throughfall containing SO_4^{2-} or NO_3^- (Eagar and Adams 1992, Aber et al. 1998). Fir mortality and population density are factors related to competition for nutrients. High fir mortality and low population density of red spruce generally increase absorption of nutrients.

(5) Herbivory

Red spruce is consumed by several insects including spruce budworm (*Choristoneura fumiferana*), hemlock looper (*Lambdina fuscicollis*), eastern blackheaded budworm (*Acleris varians*), European spruce sawfly (*Diprion hercyniae*), and the yellowheaded spruce sawfly (*Pikonema alaskensis*); spruce budworm and hemlock looper cause the most injury (Eagar and Adams 1992, Alfaro et al. 1999, MacKinnon and MacLean 2003, Solomon et al. 2003, MacKinnon and MacLean 2004). No research has found a specialized relationship between one of the insects and red spruce in the GSMNP. Therefore, in this study, general herbivores, both insects and diseases included, are assumed for the herbivory environment of ARIRS. Geographic mosaic theory also supports this assumption. This holds that interactions between a pair or group of species, including plants and herbivores, are determined by local habitat conditions (natural selection) instead of any specialized relationship between the interacting species (Thompson 1999, Gomulkiewicz et al. 2000, Thompson & Cunningham 2002).

Plants defend against herbivory by physical parts, such as thorns to restrict approach, and repellent or toxic chemical compounds (Hererra and Pellmyr 2002). Despite many protection mechanisms, plants still suffer damage in proportion to the population size of herbivores. There could other factors, but to a large extent the annual dynamics of herbivore populations can be estimated by temperature and precipitation conditions. Walter reported that egg mortality and development time of an insect predator's embryo are related to air temperature and humidity, as described by a mathematical function (Breckle 2002). The same author in field studies showed reproduction rates for some insect species to differ greatly from year to year, depending on outside air temperature and humidity, without interactions with other species.

(6) Weather Disturbance

Temperature and precipitation account for most weather disturbances. Disturbances associated with temperature were winter cold temperature, late fall and winter warm temperature, and summer hot temperature (Cook et al. 1987, Cook 1988, Deussen 1988, McLaughlin et al. 1987, Eagar and Adams 1992, Schaberg et al. 2000, Dumais and Prévost 2007). Precipitation-related disturbances, associated with episodic disturbances, such as hurricane and drought, are also important factors in red spruce growth but were excluded due to deficiency of literature. Those temperature-related disturbance factors are mostly controlled by topographic variables at the local scale and greenhouse gases at local to global scales. The air pollution factor was added as a controlling factor for cold temperature disturbances because the literature documents compounded effects of air pollution and cold temperature (Eagar and Adams 1992, Schaberg 2000, Schaberg et al. 2000, Dumais and Prévost 2007).

Cold temperature, in general, influences trees in two ways; one is freezing coupled with the behavior inside the tissue and water in the cell; the other one is frost-induced drought (Breckle 2002). Most alpine and subalpine tree species are well adapted to cold temperatures within their natural ranges; however, the maximum frost tolerance levels of red spruce are not enough to resist cold winter condition of the northern Appalachians, suggesting that cold temperature can cause the winter injury (Edgar and Adams 1992, Dumais and Prévost 2007). The maximum cold tolerance levels of red spruce in the southern Appalachians are sufficient to avoid freezing injury, but cold temperature in combination with air pollution produces foliage injury because air pollutants restricted development of maximum frost tolerance levels (Edgar and Adams 1992, Schaberg et al. 2000, Dumais and Prévost 2007). In frost-hardening, the deficiency of membrane-associated Ca negatively affects solution movement across membranes and the

ability of cells to resist dehydration and extracellular ice damage, causing freezing injury on the foliage (Schaberg et al. 2000, Dumais and Prévost 2007). In spite of enough water, low temperature can induce water stress in red spruce. Low soil temperature reduces membrane vibration in roots; membranes turn from fluid to a gel-like state, preventing roots from absorbing water (Limbers et al. 1998).

Winter warm temperatures enhance red spruce growth because they activate photosynthesis in the evergreen leaves. Field surveys showed red spruce photosynthesized during winter thaws (Schaberg et al. 1998, Schaberg 2000). Some studies, however, showed a negative relationship between winter warm temperature and annual growth for alpine and subalpine conifers, including red spruce (Schaberg et al. 1998, Schaberg 2000, Sevanto et al. 2006, Dumais and Prévost 2007). This negative relationship is associated with winter dormancy, associated chilling requirement, and water availability. In general, winter warm temperature reduces the annual growth period by increasing dormancy period, delaying dormancy release in spring, due to a chilling deficit. Winter warm temperature, in combination with frozen soil, is also a major cause of wintertime drought damage in subalpine and alpine evergreen plants (Heide 1993, Myking and Heide 1995, Heide 2003, Sevanto et al. 2006). A robust and clear explanation of dormancy-related mechanisms has not yet been advanced (Rinne et al. 1997, Li et al. 2003b), but some possible mechanisms related to the stress-induced hormone and growth inhibitor ABA, have been suggested (Le Page-Degivry et al. 1997, Schmitz et al. 2002, Jacobsen et al. 2002, Li et al. 2003a). The ABA level showed seasonal changes, being low during the growing season, increasing in autumn, and decreasing in winter (Li et al. 2003a). Dormancy termination is strongly associated with decrease in capacity for ABA synthesis; cold treatment induced a hastening of ABA catabolism and reduced embryo sensitivity to ABA (Le Page-

Degivry et al. 1997, Schmitz et al. 2002). In addition, winter dormancy in red spruce is not deep; so, red spruce decreases in cold hardiness during thaws, frequently causing frost damage (Schaberg et al. 1998, Schaberg 2000, Dumais and Prévost 2007). On the other hand, winter warm temperature can increase the annual growth period through earlier release from dormancy because the chilling requirement is far exceeded (Heide 1993, Myking and Heide 1995). Actually, long-term records show earlier onsets of several phenological events of plants associated with higher temperatures (Bradley et al. 1999, Pounds et al. 1999, Walther et al. 2002, Heide 2003, Parmesan and Yohe 2003). But earlier release from dormancy increases late-season frost damages to tree buds, resulting in lost foliage and consequent decline in annual growth rate (Heide 1993, Myking and Heide 1995).

Summer hot temperature is very understandable as a disturbance factor for red spruce, an alpine and subalpine coniferous species. Usually, most high elevation coniferous species, red spruce included, have lower optimum temperature ranges for photosynthesis (Limbers et al. 1998). Therefore, hot summer temperature likely causes high temperature inhibition of photosynthesis and consequent decline of red spruce radial growth, even though the mechanism of this growth inhibition is not yet documented (Johnson et al. 1988, Dumais and Prévost 2007). Generally, the oxygenation reaction of Rubisco increases more than the carboxylating one so that photorespiration becomes more important at high temperatures (Limbers et al. 1998). In *Quercus pubescens* the thylakoid membranes and photosynthetic electron transport were well protected against high temperature, showing the heat-induced reduction of the Rubisco activation (Haldimann and Feller 2004). In addition, extremely hot summer temperature makes the whole photosynthetic apparatus shut down as a protection from irreversible injury, burning and withering (Lambers et al. 1998, Dumais and Prévost 2007). For red spruce, dendroclimatological

studies generally found that warm late summer temperature had a negative effect on radial growth of red spruce (Cook et al. 1987, Cook 1988, McLaughlin et al. 1987, Eagar and Adams 1992, Dumais and Prévost 2007). The low elevation red spruce also showed a negative relationship with summer temperature at GSMNP (Deusen 1988). Increased water availability, however, can reduce heat-induced foliar damage, cooling down leaf temperature by evapotranspiration (Kolb and Robberecht 1996, Limbers et al. 1998).

(7) Soil Mediated Disturbance

Soil-related hypotheses, including acidification, aluminum toxicity, and base cation deficiency, have played a major role in forest decline research (Eagar and Adams 1992). For red spruce, cation deficiency or aluminum toxicity is a major cause for growth decline (Eagar and Adams 1992, McNulty et al. 2005). In general, soil acidity is directly related to nutrient leaching in both soil and tree. The soils of red spruce forests are typically and naturally acidic due to a combination of high leaching rates and large accumulations of humus (Eagar and Adams 1992). Carbonic acid and organic acid leaching are self-limiting and eventually become inoperable during soil acidification; yet, the introduction of SO_4^{2-} or NO_3^- causes a reduction in the rate of carbonic and organic acid leaching, causing anion shift from carbonic and organic to mineral acid anions (Eagar and Adams 1992). Soil acidification can be relieved by input of atmospheric base cations and soil weathering, but knowledge of the latter has not been successfully applied to soil acidity (Eagar and Adams 1992). Fernandez and Rustad (1990) showed in experiment that SO_4^{2-} concentrations increased with SO_4^{2-} loading, and cation leaching increased with increasing SO_4^{2-} in the order $\text{Mg} > \text{Al} > \text{Ca} > \text{K} > \text{Na}$. In addition, elevated nitrogen concentrations in the soil due to higher loading from the atmosphere can cause red spruce nutrient condition to be unbalanced, resulting in nutrient deficiencies (Aber et al. 1998, McLaughlin and Percy 1999,

McNulty et al. 2005, Kulmatiski et al. 2007). Under high nitrogen concentration and nitrogen saturation, red spruce absorbs more nitrogen than other nutrients and experiences decrease of fine roots, causing reduced uptake of water and mineral nutrients (Aber et al. 1998, McLaughlin and Percy 1999, McNulty et al. 2005, Kulmatiski et al. 2007).

Aluminum toxicity, causing nutrient deficiencies, probably plays a major role in tree growth declines, including red spruce, (Eagar and Adams 1992, Aber et al. 1998, Kinraide 1998, Schaberg et al. 2000, Eldhuset et al. 2006, Bintz and Butcher 2007, Huggett et al. 2007). Shortle and Smith (1988) presented a hypothesis for red spruce decline (Eagar and Adams 1992). It is that Al prevents Ca uptake, Ca deficiency decreases cambial growth, reduced cambial growth causes sapwood function to reduce, and this finally causes a reduction in leaf area. Bondietti et al. (1989) also found a negative correlation between woody Al concentration or Al/Ca ratio and red spruce radial growth from both the Southern and Northern Appalachians (Eagar and Adams 1992). They attributed this to Al mobilization and subsequent inhibition of Ca uptake by Al. Soil and solution culture experiments with spruce-fir also reported a negative correlation between Al and Ca and Mg uptake and decreased root biomass with increased Al concentration at GSMNP (McLaughlin and Percy 1999, Eldhuset et al. 2006, Huggett et al. 2007).

Soil-solution Al is influenced by soil acidification (Eagar and Adams 1992, McLaughlin and Percy 1999, Schaberg et al. 2000). The information of this paragraph was derived from Eagar and Adams (1992). Soil acidification has little effect on the concentration of Al^{3+} in soil solution over base saturation values above 20%. Minor changes of soil acidity in base saturation within the 10 to 20% range, however, can cause large increases in soil-solution Al^{3+} concentration. It leads an abrupt transition from the base cation to the aluminum buffering range. In the aluminum buffering range, Al^{3+} becomes a dominant cation in soil solution. Therefore,

soils within the aluminum buffering range may be vulnerable to huge changes of base saturation with fairly minor changes in soil acidity. Some of the soils from spruce-fir sites, including Clingman's Dome in GSMNP, are in the critical base saturation range (10 to 20%); therefore, even a slight further acidification could lead to an abrupt transition from the base cation to the aluminum buffering.

(8) Air Pollution Disturbance

Air pollution has been considered a main disturbance factor of the red spruce system, causing crown dieback, growth and population declines (Johnson et al. 1992, Eagar and Adams 1992, McLaughlin and Kohut 1992, Sheppard et al. 1993, Webb et al. 1993, McLaughlin and Percy 1999, DeHayes et al. 1999, Sheppard and Pfanzen 2001, Barker et al. 2002, Creed et al. 2004, Webster et al. 2004, Dumais and Prévost 2007). Pollutants initially affect physiological processes and cell ultrastructure, causing cell and tissue injury and leaching of foliar constituents to increase (Eagar and Adams 1992, Schaberg et al. 2000, Dumais and Prévost 2007). Research and monitoring conducted at GSMNP has shown sulfate and nitrate are the main influential air pollutants in this area (Eagar and Adams 1992, McLaughlin and Percy 1999). Sulfate and nitrate strongly influence red spruce through acid precipitation, fog and mist. Laboratory and field studies have shown a positive relationship between leaching rate and the rain solution acidity (Joslin et al. 1988, Eagar and Adams 1992, Jiang and Jagels 1999, McLaughlin and Percy 1999, Schaberg et al. 2000, Borer et al. 2005).

Ozone is another important air pollutant causing foliage injuries of red spruce (Eagar and Adams 1992, McLaughlin and Percy 1999). Ozone enters foliage through the stomata during normal gas exchange (Eagar and Adams 1992, McLaughlin and Percy 1999, Borer et al. 2005). The following information was derived from Eagar and Adams (1992): Ozone reacts with wet

membrane surfaces within the foliage, causing membranes to break down and groups of cells to die. Ozone induces the erosion of epistomatal and epicuticular layers of foliage and accelerates formation of a large number of stomata filled with solid plugs due to increased transition from a crystalline order of fine tube to a shapeless mottled layer. Ozone also reduces photosynthetic pigments, carbohydrate contents, and frost hardiness of red spruce (Dumais and Prévost 2007). Ozone effects are accelerated by other air pollutants. A pH 3.0 acidic mist alone caused only a few needles to turn red; yet, acid mist with $30 \mu\text{g m}^{-3}$ of ozone caused a considerable increase in the number of affected needles, including severe epistomatal injury.

3.2. Indirect Factors (Webs)

(9) Temperature

The information of this paragraph was derived from Geiger et al. (2003). Temperature effects are mainly controlled by topographic conditions and the amount of greenhouse gases. In topographic control, the amount of incoming radiation per unit area increases with changing aspect from north-to south-facing slopes, and it increases with slope changes from high to low slope. This is because southern aspect and low slope have longer daily exposure to radiation during a day. For example, as valleys become steeper and deeper, the sun will rise later and set earlier; so, the shortening of duration of daylight occurs in the valleys. Slope and aspect generally work together in determining ambient temperatures. Radiation is lowest at high slopes and north facing aspects; as a result, such places have lower temperature conditions compared to others at the same elevation. For instance, the probability of frost damage on leaves is generally higher at places with high slopes and north facing aspects at night and during winter. Field experiments showed that the maximum temperature followed from southeastern aspect to

southwestern aspect during summer. This is because in spite of lower incoming solar radiation the southwestern aspect has already been warmed due to diffuse radiation from sky during the morning. Therefore, the southern aspect is generally warmer than the eastern aspect. The contribution of aspect and slope to temperature condition is strongly related to moisture. Precipitation and cloud immersion decrease the temperature difference among different slopes and aspects.

Air temperature is also directly influenced by water vapor and other gases such as CO₂, O₃, O₂, CH₄, and N₂O, called greenhouse gases, because water vapor and these gas particles absorb the warm range of radiation wavelengths in the near infrared wavelengths, longer than 0.76 μ (Geiger et al. 2003). Water vapor could be a key factor in explaining air temperature increase in daily weather changes due to its wide range of radiation absorption spectra, showing a marked absorption band centered at 2.7 μ and a very broad band with its maximum around 6.3 μ (Geiger et al. 2003), but it cannot explain the long term directed air temperature increase due to short residence time in the air. Water vapor has only 10 days' residence time because of the rapidity of global evaporation, condensation, and precipitation (Aguado and Burt 2004). Another important gas is CO₂ because it has a broad range of absorption spectra and higher concentration rate in the air with a residence time of about 150 years as compared to other greenhouse gases; so, CO₂ has been considered the main greenhouse gas (Aguado and Burt 2004). Ozone also needs to be considered as one of factors increasing air temperature because this gas strongly absorbs longwave radiation of around 9.6 μ wavelength in spite of its low concentration in the lower atmosphere (Geiger et al. 2003). Methane (CH₄) is also an extremely effective absorber of thermal radiation emitted by the Earth's surface (Aguado and Burt 2004).

(10) Precipitation

Precipitation is regulated by topographic conditions (Geiger et al. 2003). There is a general tendency for the amount of precipitation to increase with increasing elevation on mountains (Eagar and Adams 1992). Shanks (1954) reported an increase of 73 cm per 1000 m for a 5-year period over an elevation gradient of 445 to 1524 m in the Great Smoky Mountains in Tennessee. Lovet and Kinsman (1990) reported that the altitudinal increase in annual precipitation for the Appalachians ranges between 40 and 90 cm per 1000 m (Eagar and Adams 1992). Other topographical conditions, such as slope and aspect, also influence the amount of precipitation with elevation gradient. The windward side of mountain has abundant rainfall, and the leeward side little due to the lifting of rain clouds by the prevailing winds and föehn-like drying on wind-protected slopes (Geiger et al. 2003). The difference of precipitation also depends on the direction the slope faces, its gradient, and the angle at which the rain is falling (aspect and slope) (Geiger et al. 2003).

(11) Cloud immersion

For high mountain areas like GSMNP, elevation is the main factor in cloud immersion. Low temperatures at high elevations cause condensation and cloud formation; low cloud bases result in emergence. For the southern Appalachian Mountains the cloud base is generally about 1400 m (Eagar and Adams 1992). Cloud base, forming different habitat conditions at different elevations, is an important environmental factor expression of air pollution in GSMNP. Zones of cloud immersion have high humidity and precipitation during summer and high snow during winter. These areas suffer less drought stress but more frost damage during winter and high acidic cloud damage throughout the year (Eagar and Adams 1992). In addition, about 1800m is another elevation of cloud base at GSMNP investigated by Johnson and Lindberg (1992); as a

result, the upper elevations of 1800m have much more effects of acidic rain and cloud than the lower elevation of it at GSMNP.

(12) Topographic factors

Topographic factors are aspect, slope, and elevation. As discussed by Geiger et al. 2003, expression of these factors is controlled by precipitation and cloud immersion frequency. Differences in radiation and temperature at different aspects, slopes and elevations are reduced by precipitation and cloud immersion. Light scattering by cloud droplets introduces complexity into the sky irradiance distribution. Based on field measurements in the Alps, global solar radiation increases by 21 percent with clear sky, and by 160 percent with cloudy skies, respectively, per 100 m. Temperature differences between south- and north-facing slopes are reduced when shading occurs with increased cloudiness.

(13) Fir Mortality

Fir (*Abies fraseri* in GSMNP) mortality is an important factor in understanding the red spruce system because Fraser fir co-exists with red spruce at higher elevations. The fir in GSMNP has experienced huge mortality due to the parasitic balsam woolly adelgid (*Adelges piceae*) (Eagar and Adams 1992, Rabenold et al. 1998, Smith 1998). This is expected to influence the red spruce system by reduced competition and modification of habitat conditions (Eagar and Adams 1992, Busing and Pauley 1994). High fir mortality exposes red spruce to higher light conditions, which causes drier soils and hotter temperatures (Eagar and Adams 1992). These authors note that adelgid populations, as other insect species, are regulated by temperature. They report that in the north adelgids are controlled by severe winter cold; if the approach to temperatures of -25°C to -35°C is gradual, overwintering stages can survive, but a single exposure of -20°C kills other life stages upon prolonged exposure to temperatures below

0°C. Significant reductions of adelgid populations in the south after unusually cold winters have also been observed (Eagar and Adams 1992).

(14) Phenotypic plasticity

Tree species express a broad range of phenotypic plasticity, acclimation included, meaning adjusting to environmental variation without genetic change (Hamrick 2004). In general, trees can maintain photosynthetic rates to match changing environmental conditions (Larigauderie and Körner 1995, Epron 1997, Ladjal et al. 2000, Bolstad et al. 2003, Ghouil et al. 2003). They increase their temperature optima for photosynthesis at higher temperatures and reduce their optima at lower temperatures (Bigras 2000, Atkin and Tjoelker 2003, Bolstad et al. 2003, Ghouil et al. 2003). Trees that experience drought stress during spring are, by producing protective chemical compounds early, better able to tolerate later summer drought and other stresses (Epron 1997, Ladjal et al. 2000). On individual trees, leaves acclimate to different radiation conditions according to their locations. Canopy leaves photosynthesize best at high light intensities, but shade leaves near the bottom have optima at lower light intensities (Lambers et al. 1998). Despite phenotypic plasticity, trees still lose biomass with changing environments. In particular, red spruce is a very shade-tolerant and late-successional species adapted to regeneration in the understory. Photosynthesis of seedlings and saplings is much less efficient in full sunlight, and individuals have little capacity for photosynthetic acclimation to rapid increase in light intensity (Dumais and Prévost 2007).

3.3. The Envirogram

The envirogram constructed for ARIRS is shown below. The envirogram is based on annual variation of relative energy and matter flow among ARIRS and environmental factors in

the context of relations existing among them. The centrum represents direct interactions or factors in the input and output environments. The webs represent progressively more indirect interactions or factors. A factor in a web is also directly controlled by the factors in the next web and indirectly the factors in the webs followed the next web. Numbers in parenthesis correspond to the factors enumerated and discussed in Sections 3.1 and 3.2 above. The notation ® is used for avoiding iterative writing of the same interactions, exhibited in the first part, for the later parts. The factors that do not have the symbol of ® on the right side of them indicate that they do not involve the interactions explained for them before. For example, in the web 2 of (10) Precipitation, the factors of Elevation, Aspect and Slope do not have the symbol of ® on the right side of each factor. This means that those factors are not controlled by any other factors such as precipitation and cloud immersion which usually controlled those factors in other parts, Web 1. The factors without bold letters account for non-webs followed. Its examples are Phenotypic Plasticity, Population Density and Distance to Stream in the envirogram.

An example of how to read the entries is the following from the first row of entries. (1) Radiation refers to Radiation being factor (1) discussed in Section 3.1. (1) Radiation was controlled by all factors, from Temperature to Phenotypic plasticity, in the web 1, those factors are controlled by the factors in the web 2, and so on. The Radiation® signifies that all webs of (1) Radiation are included but not re-presented. For example, (2) Water in the centrum has the Radiation® as a direct controlling factor in the web 1; thus, (2) Water automatically involves all webs of (1) Radiation without re-presenting. The web 1, web 2 and web 3 of (1) Radiation turn into the web 2, web 3 and web 4 for (2) Water, respectively. Therefore, when Temperature®, which has three webs explained in (9) Temperature, in the web 3 of (1) Radiation was considered, (1) Radiation has total six webs and (2) Water seven webs.

Envirogram of the Annual Radial Increment Rate of Red spruce (ARIRS)

A. Input Environments of ARIRS

Input Environments →					Focal System
...	Web 3	Web 2	Web 1	Centrum	Annual Radial Increment Rate of Red Spruce (ARIRS)
		Elevation®	(9) Temperature	(1) Radiation	
		Aspect®			
		Slope®			
		Greenhouse gases			
		Elevation	(10) Precipitation		
		Slope			
		Aspect			
		Elevation	(11) Cloud immersion		
		Precipitation®	(12) Slope		
		Cloud immersion®			
		Precipitation®	(12) Aspect		
		Cloud immersion®			
		Cloud immersion®	(12) Elevation		
		Precipitation®			
	Temperature®	balsam woolly adelgid®	(13) Fir mortality		
	Precipitation®				
			Population Density		
			(14) Phenotypic plasticity		
			Temperature®	(2) Water	
			Precipitation®		
			Radiation®		
			Slope®		
			Aspect®		
			Elevation®		
			Distance to stream		
			Elevation®		

			Slope®		
			Aspect®		
			Fir mortality®		
			Population Density		
			Phenotypic plasticity		
			Temperature®	(3) Carbon dioxide	
			Water ®		
			Radiation®		
			Phenotypic plasticity		
			Temperature®	(4) Nutrients	
			Radiation®		
			Fir mortality®		
			Phenotypic plasticity		
			Water ®		
		Precipitation®	The air loaded nutrients (SO₄²⁻, NO³⁻)		
		Cloud immersion®			
		Phenotypic plasticity			
			Population Density		

B. output Environments of ARIRS

Focal System	→ Output Environments					
Annual Radial Increment Rate of Red Spruce (ARIRS)	Centrum	Web 1	Web 2	Web 3	...	
	(5) Herbivory					
	Herbivory	Temperature®				
		Precipitation®				
	(6) Weather Disturbance					
	Winter Cold Temperature	Elevation®				
		Slope®				
		Aspect®				

	Greenhouse gases			
	Air pollution®			
	Phenotypic plasticity			
Winter Warm Temperature	Elevation®			
	Slope®			
	Aspect®			
	Greenhouse gases			
	Water ®			
	Phenotypic plasticity			
Summer Hot Temperature	Elevation®			
	Slope®			
	Aspect®			
	Greenhouse gases			
	Water ®			
	Phenotypic plasticity			
(7) Soil-mediated Disturbance				
Soil acidity®	Air pollution®			
	Phenotypic plasticity			
Soil-solution Al (soil toxicity)®	Soil acidity®			
	Phenotypic plasticity			
(8) Air pollution Disturbance				
Air pollution® (SO₄²⁻, NO₃⁻)	Precipitation®			
	Cloud immersion®			
	Phenotypic plasticity			
Ozone®	Air pollution®			
	Phenotypic plasticity			

4. Summary and Discussion

This chapter presents background information for a simulation model, the red spruce Annual Radial (growth) Increment Model (ARIM) in Great Smoky Mountains National Park (GSMNP) in the Southeastern USA. The concept of an open system and holistic and behavioral definitions of a system are combined with hierarchical ideas and a dualistic concept of environment to construct a comprehensive species-specific envirogram. This envirogram represents a structured summary of all the environmental factors seen as significant in the generation of annual radial growth increments in this species. These factors are developed in a review of relevant literature from different specific disciplines and organized into the envirogram, which represents an interdisciplinary synthesis. This synthesis distinguishes direct vs. indirect factors in radial growth and takes account of the systems ecology concept that indirect factors may be just as important as or even more important in regulating growth processes than direct ones.

Most factors considered in the envirogram affect the Annual Radial Increment Rate of Red Spruce (ARIRS) both directly and indirectly. The envirogram suggests that indirect interactions are the more significant ones in the context of the multiplicity of interactions. Topography, for example, strongly influences local and regional climatic conditions by indirectly controlling ambient radiation. Temperature influences ARIRS as direct environmental factor, weather disturbance, etc., but also indirectly by controlling the rates of many processes and factors, such as fir mortality, radiation, and herbivory. The chemical constituents of air pollution also directly influence ARIRS, but so does its indirect expressions such as weakening cold tolerance and increasing soil mediated disturbances. On the individual factor level some indirect factors, including topography, temperature, precipitation, air pollution, and cloud immersion, affect each direct factor via multiple interactive pathways. For example, topographic factors

influence radiation conditions directly by blocking solar radiation and indirectly by modifying precipitation, cloud immersion frequency, and fir mortality.

The ARIRS envirogram accounts for hierarchically organized, within- and across-scale, local-to-global interactions. In particular, the processes of envirogram construction make it obvious that ARIRS is strongly influenced by spatiotemporal across-scale interactions. For example, temperature and precipitation are closely associated with global climate change, including global warming, by interacting with the global air circulation system. But they are also obviously modified by local- and regional-scale topography. And also, based on the ARIRS envirogram, air pollution is a global- or continental-scale environmental problem but it also is strongly influenced locally by wind, precipitation, and topography.

The envirogram study for ARIRS contributed to systematic and comprehensive understanding by implementing interdisciplinary synthesis; however, many open questions indicate that mechanistic and empirical studies in various disciplines are still needed to expose other influential factors and hidden interactions among factors. For example, red spruce in GSMNP has more than just Fraser fir as a co-dominant species competing with it for nutrients and radiation, but information is lacking about them, both individually and collectively. In addition, for a more comprehensive understanding of ARIRS in the future, more research on genecology will be needed to clarify the role of phenotypic plasticity and adaptative capacity on nutrient cycling, global-scale environmental change and human disturbance.

CHAPTER 3

ARIM: *PICEA RUBENS* GROWTH DECLINE, GLOBAL WARMING, AND WITHIN- AND ACROSS-SCALE INTERACTIONS: SYSTEMS MODELING AND INTERDISCIPLINARY SYNTHESIS

1. Introduction

Global environmental issues, including global climate change and air pollution, have required ecologists to consider scale as a central issue (Levin 1992, Schneider 2001). Traditional plot-based, fine-scaled studies have faced challenges in trying to understand and explain issues at global scale (Schneider 2001, Kent 2005, Kerr et al. 2007). Patterns and processes measured at fine scales cannot be applied at broad scales; nor do patterns and processes at broad scales account for those at fine scales (Schneider 2001, Carpenter et al. 2006, Peterson in press). Environmental change and its effects on living systems have to be understood at all relevant spatiotemporal scales in order to correctly apply them to conservation policies and sustainable management (Kerr et al. 2007).

With multi-scale studies, understanding across-scale interactions has emerged as a main issue in ecology and related fields (King et al. 2004, Diffenbaugh et al. 2005, Reuter et al. 2005, Cowen et al. 2006, Kerr et al. 2007, Peter et al. 2007). Reuter et al. (2005) indicated, “The important thing in ecosystems is the cross-scale interactions, such as local to global back to local.” Peters et al. (2007) also made point that across-scale interactions result in nonlinear dynamics with thresholds, generating emergent behavior that cannot be predicted by

observations at independent single or multiple scales. It is obvious that living systems are mostly local phenomena, but environmental changes are regional or global phenomena. Therefore, understanding across-scale interactions is essential for studying the effects of environmental changes, including global warming, air pollution increases, and habitat lost, on living systems.

Global warming, for example, has influenced fine-scale processes and patterns through complex, organized, within- and across-scale interactions. Ecologists and conservation biologists are concerned about how and how much global warming has influenced and will influence living systems. In particular, it has been suggested that alpine and sub-alpine species are more vulnerable to global warming due to few refuges and low genetic diversity (Larigauderie and Körner 1995, Hörsch 2003). Red spruce is a representative alpine and sub-alpine species in the eastern United States, showing widespread growth decline and high mortality (Eagar and Adams 1992). Previous studies have suggested various reasons for growth decline and high mortality at the local scales (reviewed in Chapter 1) but have not addressed hierarchically organized across-scale interactions between system factors, including global warming, air pollution, and local system factors. Also, most previous studies have not considered complicated within-scale interactions as well as across-scale interactions. As a result, uncertainty concerning causes of growth decline of red spruce at the Great Smoky Mountains National Park (GSMNP) has increased.

Systems approach, which is appropriate to study hierarchically organized complexity, was employed to reduce this uncertainty in this study. The influences of environmental factors and global warming on the Annual Radial Increment Rate of Red Spruce (ARIRS) were investigated by systems modeling. For this study, it was hypothesized that 1) ARIRS is an open system as documented in Chapter 2; 2) ARIRS is determined by hierarchically organized direct

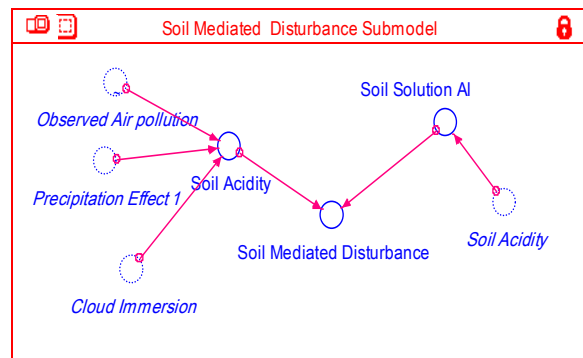
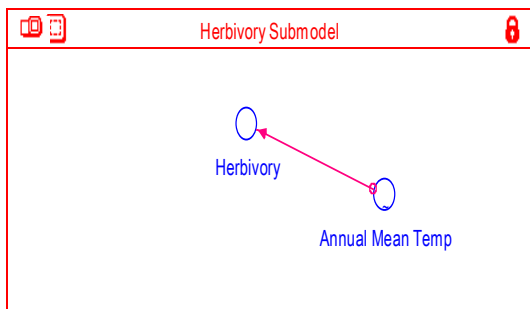
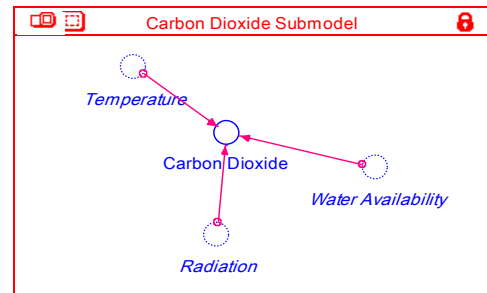
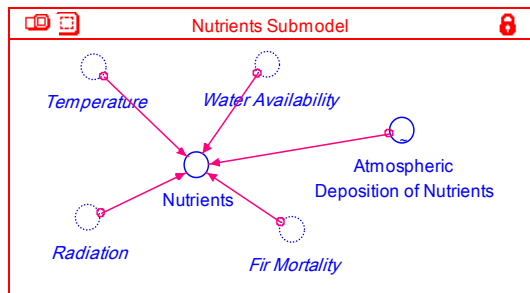
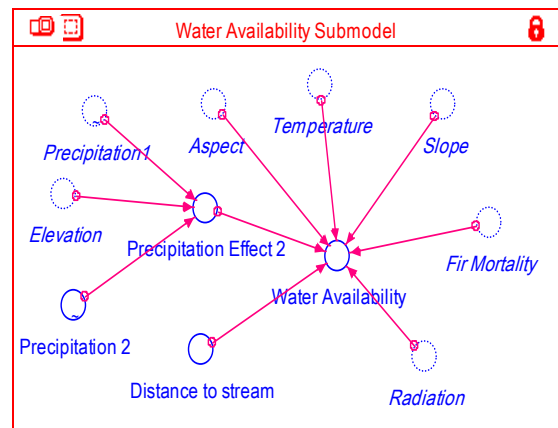
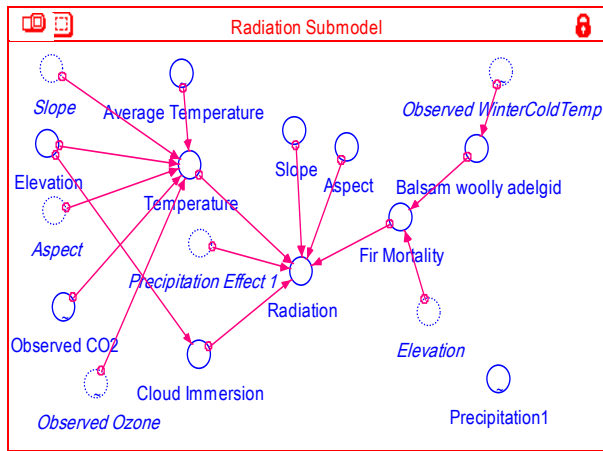
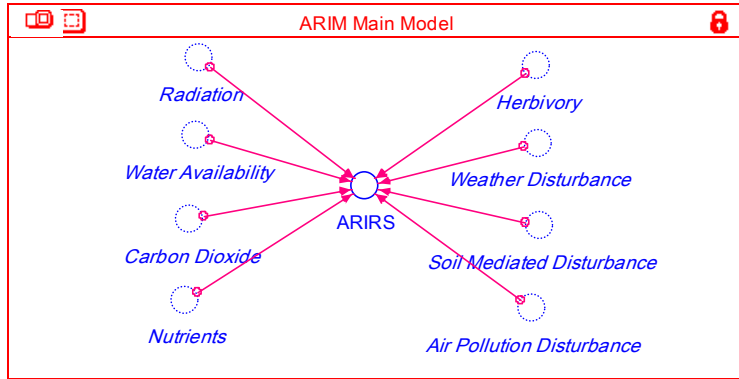
and indirect interactions among system factors; and 3) ARIRS is influenced by global warming through complicated within- and across-scale interactions of system factors.

2. Methods and Materials

2.1. Model Development, ARIMs

Systems modeling was employed to investigate hierarchically organized direct and indirect interactions, including nested within- and across-scale interactions. Systems modeling focuses on parts and relations, which is appropriate to study hierarchically organized complexity. Open system theory understands the focal system in the context of flows of energy and matter. This theory enables hierarchically organized direct and indirect interactions, including within- and across-scale interactions, among system factors to be considered by tracking flows of energy and matter.

The red spruce Annual Radial Increment Model (ARIM) was devised for this study. The steps in development were 1) acquiring literature data, GSMNP monitoring data, and general knowledge of tree physiology and influential environmental factors, 2) assembling the red spruce envirogram described in Chapter 2, 3) constructing conceptual diagrams in Stella (Figure 1) based on the envirogram, and 4) simulation. The simulation process included 1) quantifying parameters, 2) developing mathematical equations, rule based models, and graph functions of processes, 3) verifying the model, 4) calibrating the parameters through sensitivity analysis, and 5) evaluating the models by comparing model outputs with observed data (Jørgensen and Bendoricchio 2001).



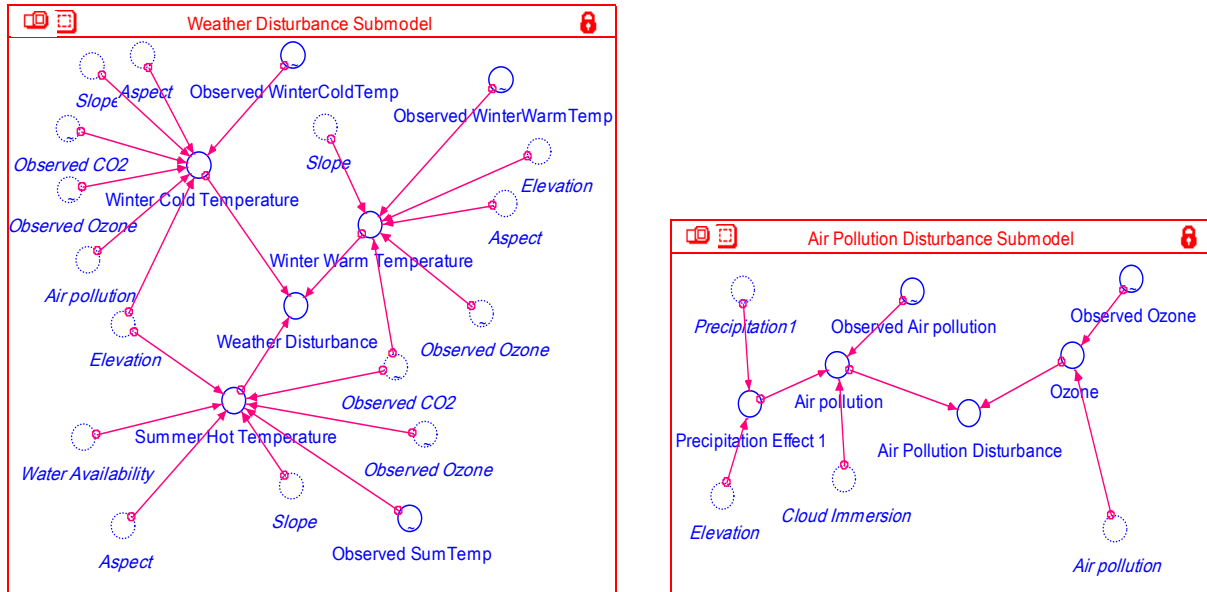


Figure 3.1. The structure of ARIM in Stella.

The model was constructed based on the ARIRS envirogram in Chapter 2. The Main Model consisted of ARIRS and factors contributing to the centrum. Each submodel was constructed based on the interactions between the centrum and webs. Circles represent the parameters and are linked with other factors using arrows based on equations (Appendix 1 and Appendix 2). The factor pointed by an arrow represents a dependent variable or a controlled factor, and the factors located at the other side of an arrow represent independent variables or controlling factors. A circle with solid line represents an original parameter. A circle with dotted line represents a copied parameter of the original parameter by the same name. So, circles with the same name always represent same hierarchically organized interactions and parameter values. For example, Radiation in the main model involves all interactions and parameter values in the Radiation submodel.

In constructing the ARIM conceptual diagram, the parameters, which are acclimation, age effect, and population density, were excluded. Trees generally show different physiological responses to environmental conditions with age and size, resulting in exponential decrease of annual radial increment (Fritts 1976, Day et al. 2004, Mencuccini et al. 2007). However, age and size effects were not included because ARIM focuses on the annual radial increment as a function of environmental factors. Increased population density generally causes self-thinning of

adult trees and high mortality of seedlings. This factor was excluded due to the lack of literature information and complexity of its effects in the field. Acclimation was also excluded due to inadequate literature information, but it was partly covered by the quantification process in the course of ARIM development.

The red spruce Annual Radial Increment Model (ARIM) consists of two models, ARIM_{high} for elevations $\geq 1700\text{m}$, and ARIM_{low} for those $< 1700\text{m}$. Elevation 1700m was arbitrarily taken as the break point to divide habitats into low and high elevation because of the lack of accurate references. Dendrochronological and other research reported that the annual radial increment pattern and its limiting factors were different at high (around 1900m) and low (around 1500m) elevation sites due to significant soil and climatic differences between them at GSMNP (Deusen 1988, Eagar and Adams 1992, Webster et al. 2004). But all studies did not show the exact elevation for defining low and high elevation sites; rather, they were implemented around 1900m for high elevation sites and 1500m for low elevation sites. The two ARIM models have the same conceptual diagram but different combinations of parameter values. Submodels were developed for each main model in order to account for the hierarchically organized indirect interactions (Figure 3.1). For the analyses, interactions among independent parameters and all indirect interactions were considered only in submodels but not in the main models.

In systems modeling, parameter quantification is difficult because different methods, measurements, and units are involved. For ARIM, dimensionless units were obtained for each dimensioned variable by dividing each yearly average value by the corresponding long-term mean, called a Relative Basis Index Value (*RBIV*, Equation (3.1)). *RBIV* partly accounts for acclimation by decreasing annual variations, and data excursions are also compressed by *RBIV*.

In the red spruce Annual Radial Increment Model (ARIM), the focal system is a population of red spruce instead of an individual tree; therefore, results represent the average variation of the annual radial increment rate for a population.

$$RBIV_{ij} = \frac{\chi_{ij}}{\mu_i} \dots\dots\dots \text{Equation (3.1)}$$

where $RBIV_{ij}$ is the Relative Basis Index Value of parameter i in j year, χ_{ij} is the monitored value of parameter i in j year, and μ_i is the mean value of parameter i .

ARIM_{high}, ARIM_{low}, and submodels were simulated using Stella 9.0.0 and 9.0.3. Stella is designed to support research in biological, social, or physical systems and has been widely applied for a variety of systems. In ecology, Stella has been employed for ecosystem models, individual-based models, biochemical models, and hydrological models (Patten 1997, Krivtsov et al. 2000, Jørgensen and Bendoricchio 2001, Voinov 2004). A particular advantage of Stella modeling is that many factors influencing a system can be considered at once. Also, different types of formulations, including linear, non-linear, and rule-based, can be applied to the interactions.

The main models of ARIM_{high} and ARIM_{low} used generalized linear models (GLMs) and classification and regression tree (CART) models to find influential environmental factors and obtain best fits with data. The standardized ring width index values of red spruce, the dependent parameter $ARIRS_{ij}$ in Equation (3.3), were used for GLM and CART modeling. Values of all independent variables in the main models were computed in submodels. CART models were used to determine influential factors, and these were then applied for GLM modeling. GLM and CART modeling were carried out in R.2.6.1, and the procedures of modeling in R.2.6.1 are

displayed in Appendix 3. Before those analyses, randomness of each variable of the main models and row data were tested to understand the characteristics of data and reduce the possible errors in interpretation of results (Appendix 3). For this process, I used Autocorrelation Function (ACF) Shapiro-Wilk normality test using R.2.6.1. The statistical software R.2.6.1 is a free and open source system for statistical analysis and provides an independent implementation of the S language (Venables and Ripley 2002).

A CART model explains variation of a single response variable by one or more explanatory variables and is constructed by repeatedly splitting the data into two mutually exclusive groups, each as homogeneous as possible (De’Ath and Fabricius 2000, Venables and Ripley 2002). CART models are classified into a classification tree and a regression tree based on partitioning criterion, the overall probability of misclassification for the former and the mean square error of the predictions of tree for the later (Venables and Ripley 2002). In ARIM, the regression tree was used for classification. The partitioning process without pruning makes a tree grow fairly big to fit the data set, X , well, but it fits too well to characterize the subsets of X (Venables and Ripley 2002). As a result, the tree is pruned by the criterion for pruning (Equation (3.2)). In Equation (3.2), α size represents the penalty for tree size. The current tree is pruned with increasing α (Venables and Ripley 2002).

$$R_\alpha = R + \alpha \text{ size} \quad \dots\dots\dots \text{Equation (3.2)}$$

where R_α is the mean square error of the predictions of the tree on the current dataset given α , R is the mean square error of the predictions of the tree on the current dataset, and $size$ is the tree size.

In CART modeling, for obtaining realistic estimates of prediction error, cross-validation was employed (Crouse et al. 1987, De'Ath and Fabricius 2000, Venables and Ripley 2002). Cross-validation is implemented by partitioning data into two subsets. One subset, a training set, is used for the analysis, and the other subset is used for validating the initial analysis (Venables and Ripley 2002). Regression trees show the parameters with criterion values used for splitting and a predicted value in each terminal node.

GLMs are the extended forms of classical multiple regressions, where model coefficients are estimated by a Maximum-Likelihood algorithm (Guisan et al. 2002). GLMs are very flexible to apply a variety of probability distributions to accommodate non-linear response distributions (Venables and Ripley 2002). All GLMs for ARIM (Equation (3.3)) were fitted by specifying a Gaussian distribution. This is because all row data and parameters of main models except air pollution data and air pollution related parameters showed significant normality in the Shapiro-Wilk normality test (Appendix 3).

$$ARIRS_j = \sum_{i=k} a_i \times RBIV_{ij} + b \quad \dots\dots\dots \text{Equation (3.3)}$$

where $ARIRS_j$ is the Annual radial increment rate of red spruce in year j , $RBIV_{ij}$ is the index value of parameter i in year j , a_i is the coefficient value of parameter i , b is the intercept value, and $k = \{\text{all independent parameters of the main models of ARIM}\}$.

To decide the best fit model, I used Akaike's Information Criterion (AIC, Equation (3.4), Venables and Ripley 2002) and Dispersion Parameters (DP) obtained from the analysis of deviance. AIC is based on the negative log maximum likelihood algorithm with penalizing with

increasing the number of parameters (Hilborn and Mangel 1997). The model with the lowest AIC represents the best fit model. The analysis of deviance shows the deviance of model as showing the scaled deviance, and the scaled deviance is calculated by dividing the deviance of model by the scale parameter (Venables and Ripley 2002). For Gaussian family, the scale parameter is the variance of model, and the deviance of model is the residual sum of square (Venables and Ripley 2002). DP is an alternative parameter of the scale parameter and is obtained by dividing the sum of squares of the standardized residuals by the degrees of freedom (Venables and Ripley 2002). It is the good and useful reference information to find best fitted model when residuals are widely spread out. In this study, AIC was a dominant criterion to judge which model is the best fitted, but DP was also used as a reference criterion.

$$AIC = 2k - 2\ln(L) \quad \dots\dots\dots \text{Equation (3.4)}$$

where k = the number of parameters, L = the maximized value of the likelihood function for the estimated mode.

For submodels, linear deterministic formulations were mostly used (Appendix 1 and 2). Nonlinear relations were derived for temperature and used to express interactions based on the literature, and 'IF-THEN' statements, rule-based models, were used for spatial parameters such as slope, elevation and aspect (Appendix 1 and 2). The equations and coefficients in the submodels of ARIM_{low} and ARIM_{high} were developed based on documentation of the ARIRS envirogram in Chapter 2.

2.2. *Checking Models and Bootstrapping*

The constant variance, the normality of residuals and the independence of residuals, the fundamental assumptions of linear regression models including GLMs assuming Gaussian probability distribution (Bhattacharyya and Johnson 1977), were tested to check whether or not the assumptions are violated. The violations of three assumptions underestimate *P-value*; as a result, the confidence level of model results, such as confidence intervals and hypotheses test for the parameter estimations, can be suspect (Bhattacharyya and Johnson 1977). The normality test was implemented because the Gaussian distribution was assumed for GLMs. One of the assumptions, constant variance, is that the residuals all come from the same distribution; thus, when the data are subdivided into several groups, variances of those subgroups have to be homogenous. In general, this test was implemented by subdividing the data into appropriate groups, computing the variances of each group and testing the homogeneity among them being sampled from a single distribution (<http://animsci.agrenv.mcgill.ca/servers/anbreed/statisticsII/homogen/index.html>). The Autocorrelation Function (ACF) has been usually used for checking randomness and independence of data. The auto correlation is calculated by dividing the sum of covariance of two data with time lags (one year, two years, ...) by the sum of variance of the model (Equation (3.5), Venables and Ripley 2002). The constant variance was tested by the Fligner-Killeen test, normality by the Shapiro-Wilk normality test, and independence by the Autocorrelation Function. All tests were implemented in R 2.6.1 and the procedures of analyses are displayed in Appendix 3. The Fligner-Killeen test was implemented based on the null hypothesis that the variance is constant. The Shapiro-Wilk normality test was carried out based on the null hypothesis that data have a normal distribution. ACF calculated the autocorrelation with time lags, and the results were presented as a graph (the ACF plot) with lines of significant

levels (mostly 95% significant level). If autocorrelation coefficients are within the boundary of significant levels, then those autocorrelations are rejected.

$$R_h = C_h / C_o \quad \dots\dots\dots \text{Equation (3.5)}$$

$$C_h = \frac{1}{N} \sum_{t=1}^{N-h} (Y_t - \dot{Y})(Y_{t+h} - \dot{Y})$$

$$C_o = \frac{\sum_{t=1}^N (Y_t - \dot{Y})^2}{N}$$

where is R_h = autocorrelation coefficient, C_h = the autocovariance function, C_o = the variance function, N = the number of data points, h = time lag ($h = 1, 2, 3, \dots$), t = time, Y_t = the value at time t , \dot{Y} = the expected value (average value of data).

The three assumptions of regression models are easily violated in ecological studies due to small sample size, autocorrelations frequently found in observations and data from field surveys and experiments, and non-linearity of ecological phenomena (Bhattacharyya and Johnson 1977, Hilborn and Mangel 1997, Johnson 1999). Also, the Autocorrelation Function (ACF) is usually used for checking randomness and independence of data, but when data have a directional trend, such as continuous increase or decrease, the ACF result can be biased. In Equation (3.5), the denominator is a fixed value; therefore, the autocorrelation coefficients are determined by the numerator, and they are high when each data set varies in the same direction (Bhattacharyya and Johnson 1977). In that, even though some data are actually independent, if they vary in the same direction, the ACF analysis results can show significant autocorrelations among data. In fact, the autocorrelation is a natural phenomenon and an important feature of

natural systems. The current year tree growth, for example, is obviously correlated with the previous year tree growth. Tree growth is dominantly influenced by photosynthetic rate determined by the number of leaves (or leaf area) and environmental conditions. The number of buds for new leaves is set in the late summer or early autumn of the previous year; as a result, it depends on the amount of carbon gains of the previous year as well as its environmental conditions. Another example is human-induced disturbances such as air pollution and global warming. The current year air pollutant emissions are influenced by some policies, which are made based on information about the air pollutant emissions of previous years, and sources of air pollutants of previous years such as the number of cars and factories in previous years.

To avoid those limitations coming from complete probability models in estimating parameters and testing hypotheses and confidence intervals, many models and methods have been developed (Gelman et al. 2004). The nonparametric bootstrapping method is one of the models and is used to test generality of model parameter estimations without a specified probability model (Tan et al. 2006). The bootstrapping test is implemented by taking m samples from the observed data set with replacement and calculating t^* for these samples (Venables and Ripley 2002). The asterisk is used to denote bootstrap resamples, and the bootstrap resamples are usually carried out more than 1000 times (Venables and Ripley 2002). For the bootstrapping test, the observed data set is assumed to be a whole of data set we wish to generalize, and a bootstrap resample is a subset of the whole data set (Tan et al. 2006). The plot of bootstrapping test showed the probability distribution that parameter estimations follow, and the statistics of bootstrapping the standardized error and the bias rate of original estimations. For example, if the bootstrapping results show the normal distributions for t^* , then the parameter estimations follow the normal probability distribution, and the estimated parameter values can be generally and

significantly accepted for the observed data set. Also, it can be said that the order of data does not make significant effects on the parameter estimation because data for the bootstrapping test were randomly selected from the observed data set. For this study, the bootstrap resamples were implemented 10000 times.

2.3. Predictions of Global Warming Effects on ARIRS, ARIMs

Global warming effects on the red spruce growth were predicted using ARIM_{high} for high elevation red spruce and ARIM_{low} for low elevation red spruce. For predictions, first, *RBIVs* for annual mean temperature, annual mean winter temperature, annual mean precipitation and air pollution factors were calculated for the 1940 to 2099 period and one year delayed annual mean precipitation for the 1939 to 2098 period. To calculate *RBIVs* (Relative Basis Index Values) for all factors, all factors' data of the 1980 to 1999 period were used for generating the data of the 2000 to 2099 period. This is because IPCC (2007) predictions were calculated based on the data of the 1980 to 1999 period. IPCC (2007) predicted 3.6°C (median value) increase of annual mean temperature, 3.8 °C (median value) increase of annual mean winter temperature and 7% (median value) increase of annual mean precipitation for the 2080 to 2099 period compared to the mean values of the 1980 to 1999 period. Also, data for air pollution factors were calculated for the 1940 to 2099 period based on the assumptions which are 10% increases, 0% increases and 10 % decreases of air pollution emission for the 2000 to 2099 period. Those assumptions were made to test how much air pollution factors influence the global warming effects on red spruce growth. The data of the 2000 to 2099 period were obtained by adding an increment rate to each year data of the 1980 to 1999 period. For example, data of the 2000 to 2019 period were obtained by adding the increment rate to each year data of the 1980 to 1999 period for all factors,

data of the 2020 to 2039 period by adding the increment rate to each year data of the 2000 to 2019 period, ... etc. For air pollution factors, the data of 1998 were used for both 1998 and 1999 due to no data for 1999 in the data set used for ARIM simulations. The increment rate was obtained by dividing 3.6 by 5 (=100 years / 20 years) for annual mean temperature, 3.8 by 5 for annual mean winter temperature, the mean precipitation of the 1980 to 1999 period * 0.07 (7%) by 5 for precipitation and the mean for each air pollution factor of the 1980 to 1999 period * the assumed rates (0.1, 0, -0.1) by 5 for all air pollution factors. Finally, *RBIVs* for all factors were calculated by dividing the yearly value by the long-term mean of the 1940 to 2099 period. All real values used for calculating indices and indices computed in $ARIM_{high}$ and $ARIM_{low}$ of the 1940 to 2099 period are shown in Appendix 4.

All *RBIVs* were applied to $ARIM_{high}$ and $ARIM_{low}$ to calculate red spruce growth during the 1940 to 2099 period. The calculated red spruce growth indices are shown in Appendix 4. The computed annual radial growth of red spruce for the 1940 to 2099 period was plotted in R 2.6.1, and the smoothed local regression lines with simple linear regression lines were obtained using the Loess function and the Spline function in R 2.6.1. The simple linear regression lines were obtained using the `lm` (linear regression model) function, and the local regression lines were obtained using the Loess function. Also, the local regression lines were smoothed by the Spline function. Those regression lines showed the growth trends of red spruce for the 1940 to 2099 period and the changes of red spruce growth in accordance with global warming in interactions with air pollution. All procedures of analyses in R 2.6.1 are displayed in Appendix 4.

2.4. Data

Most information for interactions among factors was explained in the ARIRS (Annual Radial Increment Rate of Red Spruce) envirogram of Chapter 2. Raw data used for ARIM were temperature, precipitation, NO_x and SO_x, ozone, carbon dioxide, and standardized ring width index value of red spruce. Temperature and precipitation data were obtained from the Knoxville, Tennessee airport meteorology station and covered the period 1939 to 1998. The mean annual temperature was obtained by averaging mean daily temperatures. The winter cold temperature and warm temperature for weather disturbances were calculated by averaging the lowest temperatures from November (previous year) to February (current year) and the highest temperatures from November (previous year) to February (current year), respectively. The highest temperature from June to August was averaged for the mean annual summer hot temperature. Mean annual precipitation was employed for the precipitation factor and obtained by averaging daily precipitation records for each year. National mean values of NO_x and SO_x were applied for the air pollution factor and obtained from the year 2000 U.S. Environmental Protection Agency (EPA) report (U.S. EPA 2000). Monitored ozone data of GSMNP were not long enough to cover from 1940 to 1998; thus, ozone emission was estimated by equation (3.6) (<http://www.epa.gov/air/ozonepollution/basic.html>);

$$\text{Ozone} = \text{NO}_x + \text{VOC} + \text{sunlight} \quad \dots\dots\dots \text{Equation (3.6)}$$

where Ozone is ground-level ozone, NO_x is oxides of nitrogen and VOC is volatile organic compounds.

Sunlight was excluded in this estimation because of lack of available long-term monitoring data. National mean values of NO_x and VOC were also obtained from a U.S. EPA report (U.S. EPA 2000). Total national CO₂ emissions from fossil-fuel burning in the U.S.A. were obtained from The Carbon Dioxide Information Analysis Center (CDIAC) and used for the CO₂ parameter in ARIM. Dendrochronology data of red spruce were collected at the National Acid Precipitation Assessment Program (NAPAP) sites at GSMNP by Dr. Creed and her colleagues, and the analysis results were published in 2004 (Webster et al. 2004). Those dendrochronology data were summarized for high (~ 2000m: from 1911 to 2000m) and low (~ 1500m: from 1478 to 1548m) elevation areas.

3. Results

3.1. ARIM, Observed Data and Computed Data

All independent variables of the main models of ARIMs (The red spruce Annual Radial Increment Models) were computed in submodels (Figure 3.1). Randomness and normality were tested for the observed data and all computed data (independent variables) for the main models. These analyses aimed to avoid some possible misinterpretations of results of CART models and GLMs by understanding the characteristics of both the observed and the computed data. In particular, the randomness analysis is also used to explore how much ARIMs, a system model, changes the characteristics of observed data in producing the computed data. These and all test results are shown in Appendix 3 with R programming procedures.

Various probability distribution functions including Poisson, Gaussian (= Normal), Inverse Gaussian, Gama and Binomial can be applied for GLMs (Venables and Ripley 2002). From these, the Gaussian probability distribution was assumed for GLMs of ARIMs. This is

because dendrochronological studies have used a linear regression model, which achieves the same purpose as a GLM assumed Gaussian probability distribution (Venables and Ripley 2002), to explain the effects of environmental conditions on red spruce growth (Edgar and Adams 1992, Webster et al. 2004). As it is assumed that the distribution of the whole population is Gaussian, the normality tests showed how the observed and computed data significantly explain the whole population. The test showed significant normality for the high and low elevation red spruce standardized ring indices, temperature and precipitation. For ARIM_{high}, Radiation (RA), Water Availability (WA), Nutrients (NU), Herbivory (HB) and Weather Disturbance (WD) showed significant normality (Table 3.1). For ARIM_{low}, Radiation, Nutrients, Herbivory and WD showed significant normality. On the other hand, the observed air pollution data showed insignificant normality. Also, the computed data for CO₂, Air Pollution Disturbance (APD) and Soil Mediated Disturbance (SMD) of ARIM_{high}, and CO₂, APD, Water Availability and SMD of ARIM_{low} did not show significant normality. Based on the test results, natural climate factors showed significant normality but the data, including both observed and computed, gave insignificant normality for human induced disturbances (Figure 3.1). The observed air pollution data for CO₂, ozone and air pollutants (combined NO_x and SO_x) are given in Appendix 3.

Table 3.1. Factors in ARIMs and Abbreviations for all factors

Factors in ARIMs	Abbreviation
Radiation	RA
Water Availability	WA
Nutrients	NU
Carbon dioxide (CO ₂)	CO ₂
Herbivory	HB
Weather Disturbance	WD
Soil Mediated Disturbance	SMD
Air Pollution Disturbance	APD

The Autocorrelation Function (ACF) analysis was used for testing randomness, as is usually done for statistical analyses, especially time series analyses (Venables and Ripley 2002). ACF analysis showed insignificant autocorrelation, indicating randomness of yearly data for temperature and precipitation. The computed data, Radiation, CO₂, Herbivory and WD of ARIM_{high} and Radiation, Herbivory and WD of ARIM_{low} also showed insignificant autocorrelation (Appendix 3). On the other hand, the observed air pollution data and the standardized ring indices for ARIM_{high} and ARIM_{low} showed significant autocorrelations and violated the randomness assumption (Appendix 3). Also, the computed data, APD, SMD, Water Availability, and Nutrients of ARIM_{high} and APD, SMD, Water Availability, Nutrients, and CO₂ of ARIM_{low}, which are controlled by air pollution data in submodels, showed significant autocorrelations (Appendix 3). In the case of Water Availability, the significant autocorrelation was not caused by the precipitation effect 2 (Figure 3.1, Appendix 1 and 2) which was a main controlling factor in the Water Availability submodel. The precipitation effect 2 was calculated by dividing the current year precipitation + the previous year precipitation by 2; as a result, the autocorrelation with one year time lag was created by the overlapping effect on two continuous years. In Nutrients, Nutrients of ARIM_{low} showed stronger autocorrelation than the one of ARIM_{high}. This is because Nutrients of ARIM_{low} is more strongly influenced by the observed CO₂ through Radiation and Temperature, but Nutrients of ARIM_{high} was more dominantly affected by precipitation effect 2 via Water Availability. When the autocorrelation patterns of Nutrients of ARIM_{high} and ARIM_{low} are compared, the pattern of Nutrients of ARIM_{high} follows the one of Water Availability and the pattern of Nutrients of ARIM_{low} the one of observed CO₂ (Appendix 3). In CO₂, CO₂ of ARIM_{high} does not show significant autocorrelation, but CO₂ of

ARIM_{low} shows significant autocorrelation with one year time lag. This is probably because of stronger effects of the observed CO₂ through Radiation and Temperature on CO₂ of ARIM_{low}.

In the ACF analyses, all observed air pollution data and the standardized ring indices for ARIMs showed strong autocorrelation. This is because the air pollution factors have been strongly influenced by human decisions, such as economical and political policies, and global economic growth trends. The global economic growth is an accumulated phenomenon instead of being independent from year to year. Also, human decisions have been made based on the data from the past. Therefore, the autocorrelations of APD, SMD, and Nutrients of ARIM_{high} and APD, SMD, Nutrients, and CO₂ of ARIM_{low} originating from the observed data are not avoidable. The current year tree growth is obviously correlated with the previous year tree growth. Tree growth is dominantly influenced by photosynthetic rate determined by the number of leaves (or leaf area) and environmental conditions. The number of buds for new leaves is set in the late summer or early autumn of the previous year; as a result, it depends on the amount of carbon gain the previous year. Also the autocorrelation of Water Availability created based on the ARIM purpose is necessary for this study because previous studies addressed the effects of previous precipitation condition on the current year tree growth (Webster et al. 2004). Thus, these limitations of data have to be accepted for this study, even though they can make some violations against the randomness assumption of statistical modeling. In addition, it cannot be ignored that all violations can be partly caused by the autocorrelation analysis itself, as explained in the methods section (Section 2.2).

The randomness analysis also aimed to understand the effects of observed data on the computed data. This is essential to show how well the ARIM modeling methodology can be applied for other studies. The ARIM modeling tried to combine systems modeling with statistical

modeling to find the influential submodels and coefficients. The statistical models were applied to the main model of ARIM. Statistical modeling always has the fundamental assumption of randomness (independence) of data; as a result, data collections are planned and implemented in the field or laboratory based on the ways not to violate this assumption. Therefore, if ARIM unintentionally generates autocorrelations in computed data which do not exist in observed data, this methodology cannot be generally and reliably used for other studies based on observed data sets or can be restricted to use for some specific studies.

The ACF analyses well addressed that ARIM, the system model, could keep the features of observed data in spite of the complicated model structure. The variables dominantly related with temperature and precipitation did not show any violation of randomness in the autocorrelation analyses. The variables related with the air pollution factors, however, showed violation of randomness. On the other hand, the autocorrelation of Water Availability is definitely caused by the system modeling process; however, this is justified by the purpose of ARIM in that it was created on purpose. Previous research has documented the significant effects of previous precipitation on the current year tree growth as controlling the number of leaves and leaf area (Webster et al. 2004, Meier and Leuschner 2008). Therefore, it is concluded that the features of computed data originate from the observed data and are created based on the special purpose of study not from the unknown operations of the systems model or model structure. Thus, the ARIM modeling methodology can be generally applied for other modeling studies considering hierarchically organized complexity, in that, if the observed data do not have significant autocorrelations, the computed data will not have significant unintended autocorrelations either.

3.2. *CART Models, GLMs and ARIM*

The CART model results for ARIM_{high} and ARIM_{low} are shown in Table 3.2 and Figure 3.2. Table 3.2 shows the pruning processes, and Figure 3.2 shows the final result of the CART model. CP is a complexity parameter, α/R : R is the mean square error of the predictions and α is a given value. The complexity parameter is used for deciding tree size to have minimum error rate of X (Xerror and Xstd in Table 3.2). The error rates of X (Xerror and Xstd) verse CP for the pruned tree were computed on the validation data set (Venables and Ripley 2002), and 10-fold cross-validation was employed for this study. Ten-fold cross-validation was implemented by splitting the training data set into ten equally sized groups and using nine groups to grow the tree and the tenth for testing (Venables and Ripley 2002). Table 3.2 shows that CP (complexity parameter) = 0.01 represents the best tree size, six branches, three split for ARIM_{high}, and eight branches, four split for ARIM_{low}, showing the minimum Xerror and Xstd. In Figure 3.2, the length of edge branches shows the strength of the parameter used for classification. The parameters used for splitting (edges) are presented at the nodes and the predicted values at the terminal nodes. APD is only selected for ARIM_{high} as the significant explanatory variable (Figure 3.2 (a)). Radiation, APD, and Water Availability are selected for ARIM_{low} as the significant explanatory variables (Figure 3.2 (b)). Those variables were applied for GLMs of ARIMs; therefore, ARIM_{high} had just one variable for GLM modeling, and ARIM_{low} had three variables (Radiation, Air Pollution Disturbance, and Water Availability).

Table 3.2. The results of CART model of ARIM_{high} (a) and ARIM_{low} (b). Symbols: WA = Water Availability, Radiation = Radiation, APD = Air pollution disturbance, X = independent variables, CP = complexity parameter ($= \alpha / R$ (Equation (2))), rel error = X-value relative error, Xerror = error rate of X in partitioning, Xstd = standard deviation of X in partitioning, N split = Number of splits, representing tree size. All the errors are proportions of the error for the root tree (Root node error).

(a) CART result for ARIM_{high}

Variables	# of Node	Root node error			
APD	59	0.05179			
	CP	nsplit	rel error	xerror	xstd
1	0.450634	0	1	1.02346	0.14224
2	0.062608	1	0.54937	0.79882	0.19267
3	0.04317	2	0.48676	0.72451	0.16225
4	0.01	3	0.44359	0.71192	0.1547

(b) CART result for ARIM_{low}

Variables	# of Node	Root node error			
APD Radiation WA	59	0.043735			
	CP	nsplit	rel error	xerror	xstd
1	0.085985	0	1	1.0345	0.14777
2	0.038081	2	0.82803	1.3207	0.21803
3	0.02671	3	0.78995	1.3519	0.21698
4	0.01	4	0.76324	1.3519	0.21698

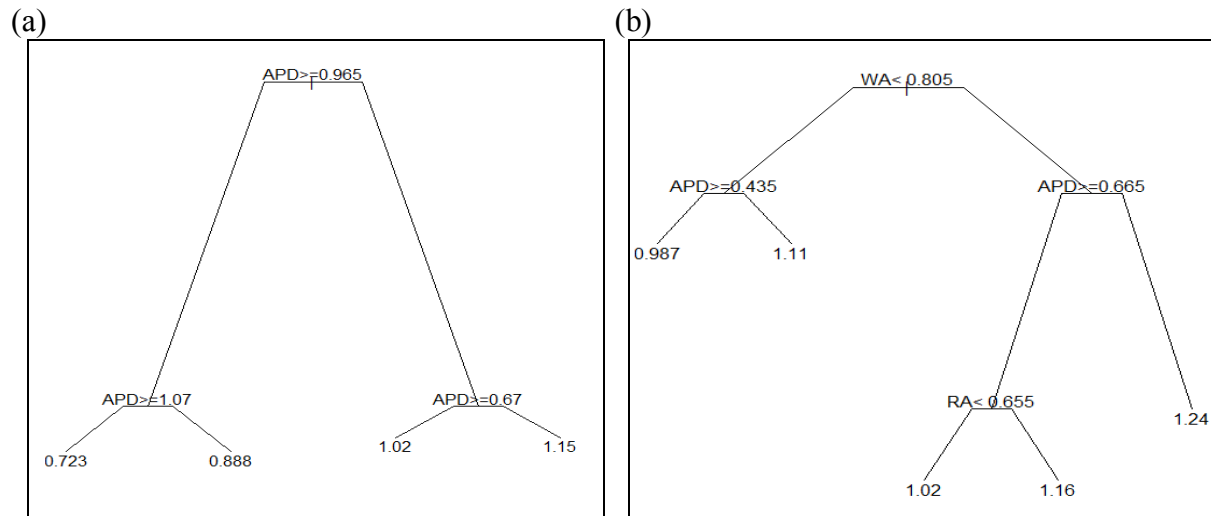


Figure 3.2. Trees of CART models. (a) Graph trees (nodes and edges) for ARIM_{high}; (b) for ARIM_{low}. Both trees show the parameters with criterion values (at the nodes) used for splitting (edges) and a predicted red spruce growth rate value in each terminal node. The length of the edge branches shows the strength of the parameter used for splitting in classification.

The first table (Table 3.3 (a)) shows the GLM result of ARIM_{high}. AIC and DP are the criteria to judge the best fitted model (Equation (4) in Section 2.1). AIC and DP, however, were not necessary for ARIM_{high} because there was no competing model; thus, *P-values* are more important to look for GLM of ARIM_{high}. Table 3.3 (a) shows the model to explain annual variation of red spruce growth at high elevation. *P-values* support that both factors are significant and explain that Air Pollution Disturbance is the dominant parameter to explain the high elevation red spruce growth.

The second table (Table 3.3 (b)) shows the GLMs' result of ARIM_{low}. As compared to ARIM_{high}, ARIM_{low} showed relatively lower AIC and non significant *P* value for Air Pollution Disturbance (*P* value = 0.134244) (Table 3.3 (b)). Based on AIC (Akaike's information criterion) and DP (dispersion parameter), Model 1 is the best model for ARIM_{low}, but the *P*-value for the Air Pollution Disturbance parameter is not significant. AIC value is penalized by the number of parameters (Equation 3.4 in Section 2.2); therefore, the model which has more variables always shows higher AIC values. It is concluded that Model 1 is the best fitted GLM for ARIM_{low} with the lowest AIC (= -23.219) and DP (= 0.035768).

Table 3.3. The GLMs results of ARIM_{high} (a) and ARIM_{low} (b). Symbols: RA=Radiation, WA=Water Availability, APD = Air pollution disturbance, * means significant level based on *P* value ($Pr>|t|$): ***=0.001, **=0.01, *=0.1, AIC = Akaike's information criterion, and DP = dispersion parameter. The minimum value of AIC and DP shows the best fit model to observed data.

(a) GLMs for ARIMhigh								
Variable	APD						DP	AIC
	Estimate	Std. Error	t value	Pr(> t)				
(Intercept)	1.55774	0.08863	17.575	< 2e-16	***	0.0278332	-39.91	
APD	-0.67955	0.09354	-7.265	1.15E-09	***			

(b) GLMs for ARIM_{low}								
Model 1	Variables	WA, RA, APD						
		Estimate	Std. Error	t value	Pr(> t)		DP	AIC
	(Intercept)	-11.4031	3.2042	-3.559	0.000776	***	0.035768	-23.219
	WA	11.3237	2.747	4.122	0.000128	***		
	APD	-0.2697	0.1774	-1.52	0.134244			
RA	5.3397	1.8696	2.856	0.006042	**			
Model 2	Variables	WA, APD						
		Estimate	Std. Error	t value	Pr(> t)		DP	AIC
	(Intercept)	-3.3103	1.5885	-2.084	0.04175	*	0.040339	-17.06
	WA	5.6473	2.0138	2.804	0.00692	**		
	APD	-0.2648	0.1884	-1.406	0.1654			
Model 3	Variables	WA, RA						
		Estimate	Std. Error	t value	Pr(> t)		DP	AIC
	(Intercept)	-10.604	3.198	-3.316	0.001606	**	0.036605	-22.792
	WA	10.154	2.668	3.806	0.000352	***		
	RA	5.312	1.891	2.809	0.006833	**		
Model 4	Variables	RA, APD						
		Estimate	Std. Error	t value	Pr(> t)		DP	AIC
	(Intercept)	1.29449	1.00043	1.294	0.201		0.045982	-9.3348
	APD	-0.06487	0.19313	-0.336	0.738			
	RA	-0.23655	1.46332	-0.162	0.872			
Model 5	Variable	WA						
		Estimate	Std. Error	t value	Pr(> t)		DP	AIC
	(Intercept)	-2.566	1.51	-1.699	0.0948	.	0.041029	-17.015
WA	4.527	1.865	2.427	0.0184	*			
Model 6	Variable	APD						
		Estimate	Std. Error	t value	Pr(> t)		DP	AIC
	(Intercept)	1.13387	0.11571	9.799	7.87E-14	***	0.045197	-11.307
APD	-0.05577	0.18317	-0.304	0.762				
Model 7	Variable	RA						
		Estimate	Std. Error	t value	Pr(> t)		DP	AIC
	(Intercept)	1.1609	0.9108	1.275	0.208		0.045266	-11.216
RA	-0.0934	1.3889	-0.067	0.947				

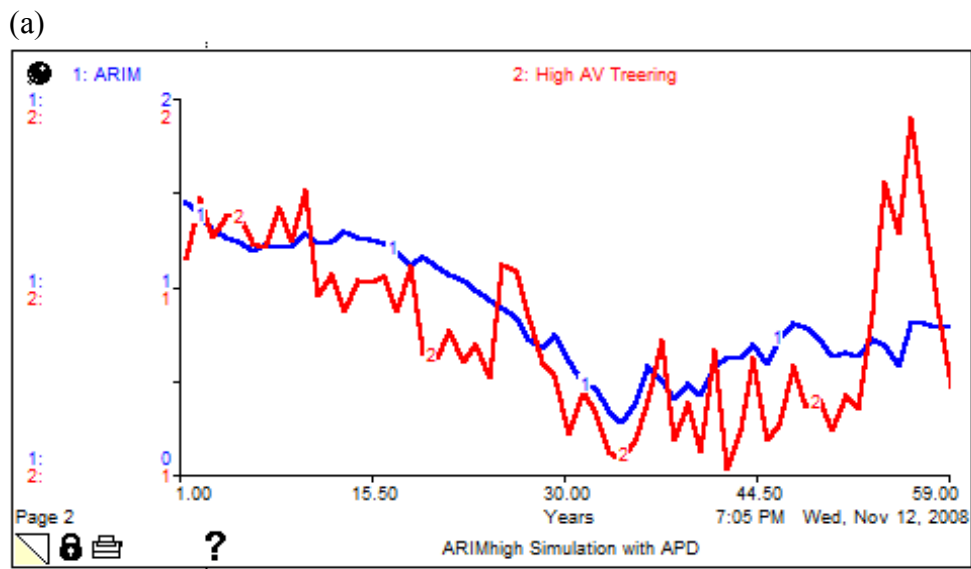
Equation (3.7) was developed for ARIM_{high} based on the GLM in Table 3.3 (a). Equation (8) was developed for ARIM_{low} based on Model 1 of GLMs in Table 3.3 (b). Then, Equations

(3.7) and (8) were employed for simulations of $ARIM_{high}$ and $ARIM_{low}$ respectively. The $ARIM_{high}$ simulation accounted for the high elevation red spruce growth fairly well but could not very well explain recent one or two years growths (Figure 3.3 (a)). The $ARIM_{low}$ simulation also accounts for red spruce growth at low elevation but has some unmatched years between the predicted and the original (Figure 3.3 (b)). Based on the results of simulations, CART models and GLMs, it is concluded that GLMs of $ARIM_{high}$ and $ARIM_{low}$ explain red spruce growth trends at low and high elevation significantly, even though some unmatched years exist.

$$ARIM_{highi} = -0.67955APD_i + 1.55774 \quad \dots\dots\dots \text{Equation (3.7)}$$

$$ARIM_{lowi} = 5.3397RA_i + 11.3237WA_i - 0.26971APD_i - 11.4031 \quad \dots\dots \text{Equation (3.8)}$$

Where $ARIM_{highi}$ is red spruce growth at high elevation in year i , $ARIM_{lowi}$ is red spruce growth at low elevation in year i , RA_i is Radiation in year i , WA_i is Water Availability in year i , and APD_i is Air Pollution Disturbance in year i .



(b)

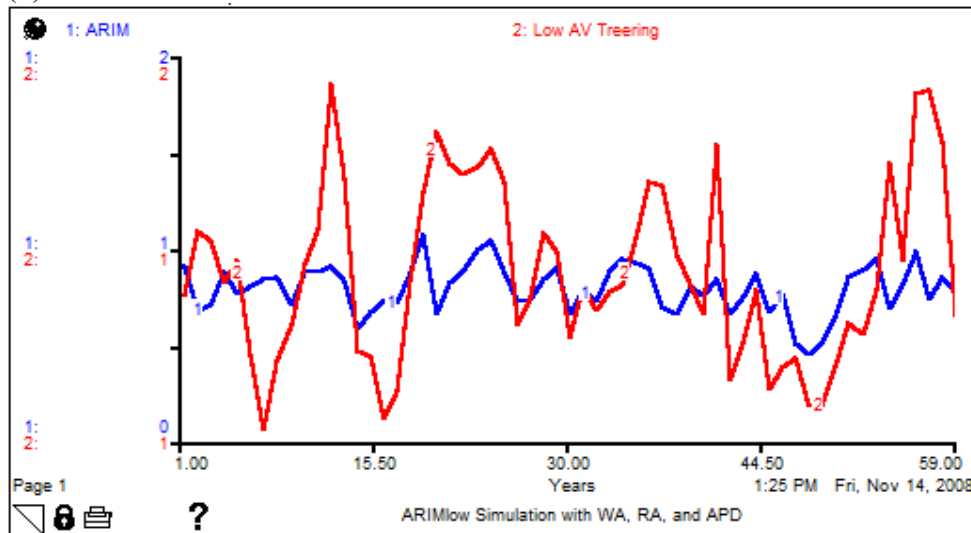


Figure 3.3. Simulations of (a) $ARIM_{high}$ and (b) $ARIM_{low}$. The x axis represents the number of years simulated and y axis indices are ($0 < ARIM < 2$, $0 < High\ AV\ Treering < 2$, $0 < Low\ AV\ Treering < 2$). High AV Treering means the standardized ring width index values at high elevation and Low AV Treering at low elevation.

3.3. Checking GLMs and Bootstrapping Test

The three fundamental assumptions of linear regression models were checked for the GLMs of $ARIM_{high}$ (Equation (3.7)) and $ARIM_{low}$ (Equation (3.8)) in order to check whether their confidence levels were suspect (Appendix 3). The test results were summarized in Table 3.4 and Figure 3.4. In Table 3.4, the GLM of $ARIM_{high}$ showed significance in the constant variance test, showing the P -value higher than 0.05, but insignificance in the normality test, showing the P -value lower than 0.05. The GLM of $ARIM_{low}$, however, showed significance in both the constant variance test and the normality test, showing the P -value higher than 0.05.

Table 3.4. The results of model checks: Normality and Constant variance tests of residuals. W = Wilks Shapiro test statistic, $m\chi^2$ = Fligner-Killeen (median) chi-squared test statistic and df = degree of freedom. Constant variance test was performed by Fligner-Killeen (median) test, and the null this test is that the variances in each of the groups (samples) are the same. Normality test was performed by the Shapiro-Wilk normality test, and it was carried out based on the null hypothesis that data have a normal distribution

	ARIM _{high}			ARIM _{low}		
	Statistics	df	<i>P-value</i>	Statistics	df	<i>P-value</i>
Normality test	$W = 0.8862$		4.911e-05	$W = 0.9652$		0.08995
Constant Variance test	$m\chi^2 = 38.2489$	36	0.3677	$m\chi^2 = 32.6082$	26	0.1738

The two assumptions, constant variance and normality of residuals, were easily violated by small sample size. Independence of residuals is generally the most important assumption in checking the confidence and generality of models (Bhattacharyya and Johnson 1977). The autocorrelation analyses showed the existence of significant autocorrelations in the residuals of both GLMs of ARIM_{high} and ARIM_{low} (Figure 3.4). The GLM of ARIM_{high} showed significant autocorrelation at one- and two-year time lags and the GLM of ARIM_{low} at one-year time lag. Based on the autocorrelation analyses, the assumption of independence of residuals is violated for both models, and the GLM of ARIM_{high} is more seriously violated than the one of ARIM_{low}. Therefore, the confidence levels and generality of GLMs shown by *P*-values are suspect. The violations of independence of residuals could be induced by the autocorrelations that already exist in the raw data, standardized ring indices, and response variables for GLMs (shown in Appendix 3). Most autocorrelations of standardized red spruce ring indices were removed by the ones for air pollution disturbances in GLM of ARIM_{high} and water availability and air pollution disturbances in GLM of ARIM_{low} in the modeling processes, but some of them still exist due to unknown factors and lack of information. Also, it is possible that all positive autocorrelations detected in the analyses for standardized ring indices and residuals just present the continuous

increases and decreases of yearly data instead of real autocorrelations based on the feature of autocorrelation analysis explained in Section 2.2.

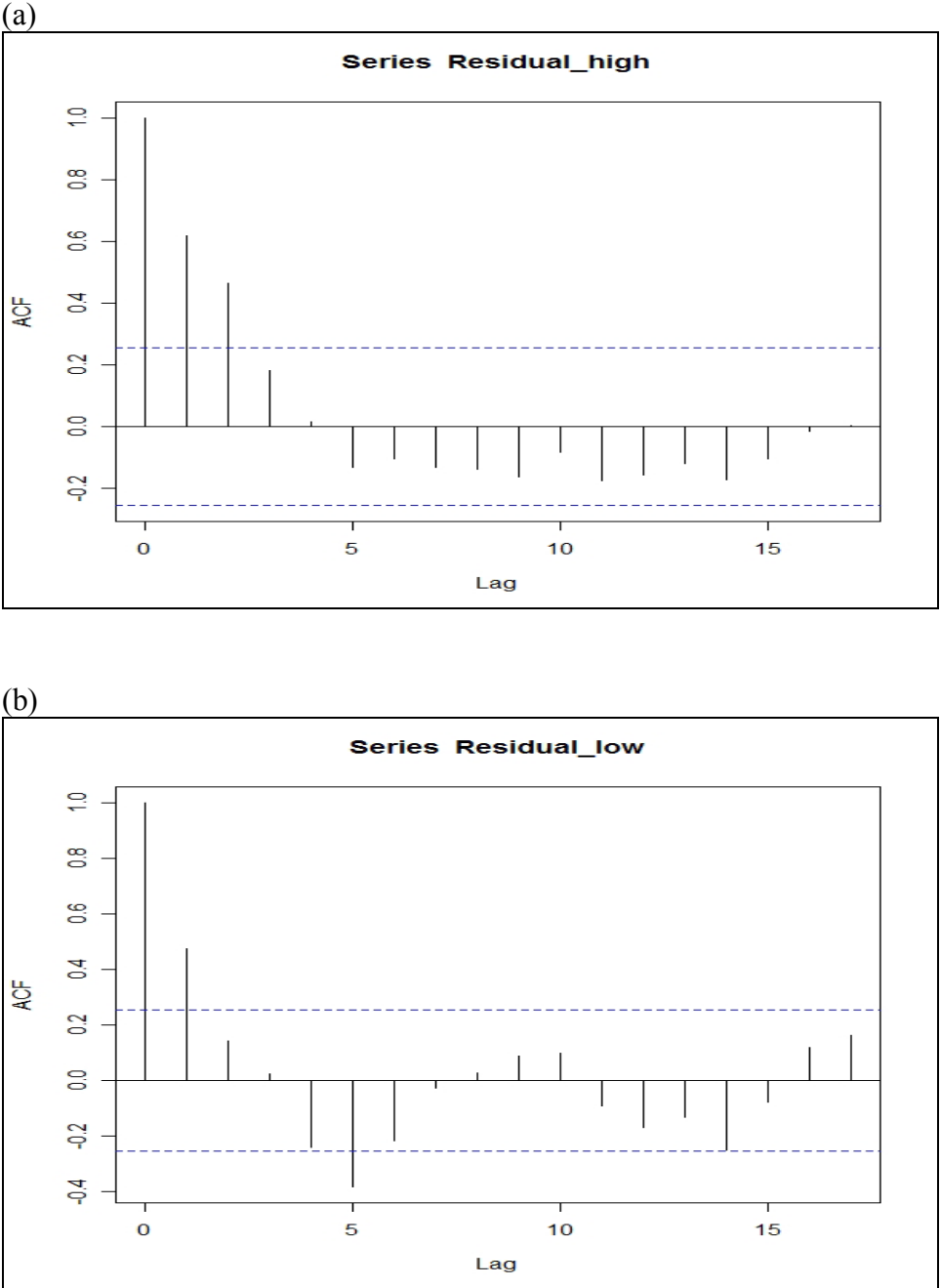


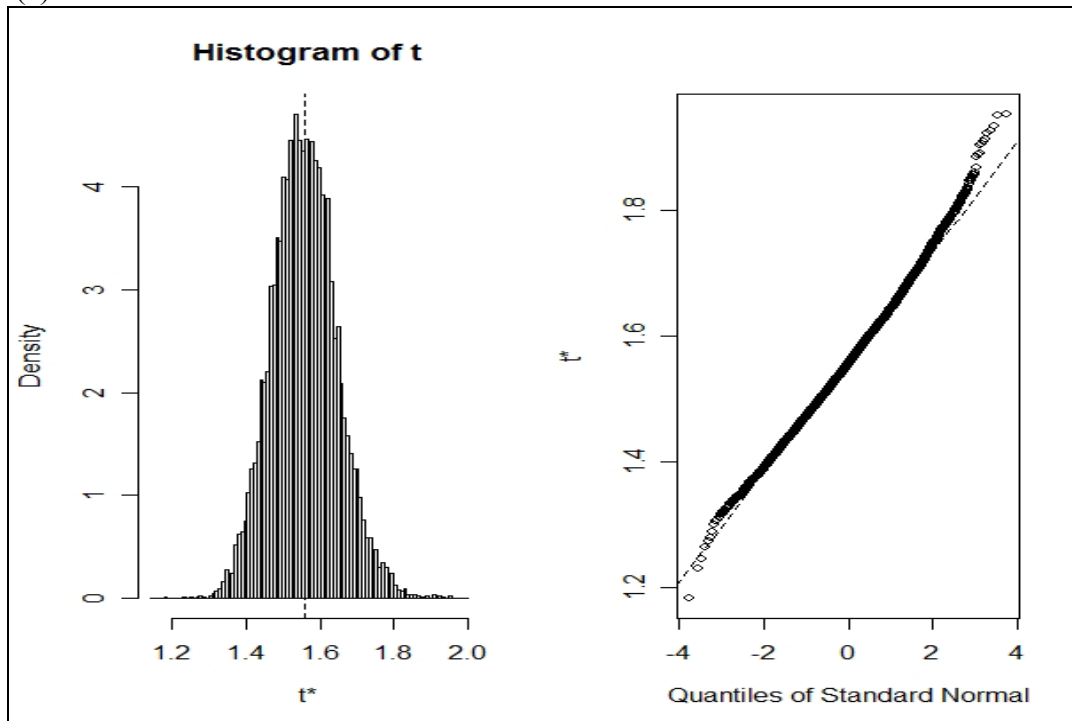
Figure 3.4. The ACF plots of residuals. (a) ACF plot of GLM of $ARIM_{high}$ and (b) ACF plot of GLM of $ARIM_{low}$. In the plots, ACF = autocorrelation coefficients and Lag = time lags (year). The dotted lines in the plot show the 95% confidence interval. The autocorrelations within the lines are not significant, so they are rejected.

Complete probability models assume the observed data as a subset of the universal population, and how well the observed data explain the universal population, confidence interval and hypothesis test, is tested based on an assumed probability distribution (Bhattacharyya and Johnson 1977). However, complete probability models in testing hypotheses and estimating confidence intervals showed many limitations in ecological and biological studies due to the features of living systems, such as nonlinearity, small sample size and complexity (Gelman et al. 2004). Thus, many nonparametric models and methods have been developed to avoid those limitations (Gelman et al. 2004). In this study, nonparametric bootstrapping methods, assuming the observed data set as the universal population, were employed, and the results of bootstrapping tests are shown in Table 3.5 and Figure 3.5. Table 3.5 explains the standardized errors of original parameter estimations and biased range for each parameter. Figure 3.5 shows parameter estimations for bootstrap resamples (t^*) of GLMs of $ARIM_{high}$ and $ARIM_{low}$ are normally distributed. Therefore, when the observed data are regarded as the universal data, the bootstrapping results for both GLMs well support the Gaussian probability distribution assumed for GLMs, with some error and bias ranges presented in Table 3.5. In addition, the bootstrapping results showed the autocorrelations detected in the autocorrelation analyses did not significantly influence the generality and confidence level of models as considered from the random resampling process of the bootstrapping test.

Table 3.5. The bootstrap statistics for (a) ARIM_{high} and (b) ARIM_{low} GLMs. In the tables, * means the bootstrap resamples for each parameter and the original estimated parameter values in GLMs modeling. The names of original parameters are presented in the second column.

(a) ARIM_{high} Bootstrap Statistics				
Bootstrap resamples	Parameter in GLMs	Original	Bias	Standardized error
t1*	Intercept	1.5577449	6.634789e-05	0.08784153
t2*	APD	-0.6795544	1.250802e-05	0.09246660
(b) ARIM_{low} Bootstrap Statistics				
t1*	Intercept	-11.4030854	0.0073056171	3.0727770
t2*	Water Availability	11.3237405	-0.0019962561	2.6305096
t3*	Air Pollution	-0.2696905	0.0006411868	0.1716500
t4*	Radiation	5.3397221	-0.0084959440	1.8014611

(a)



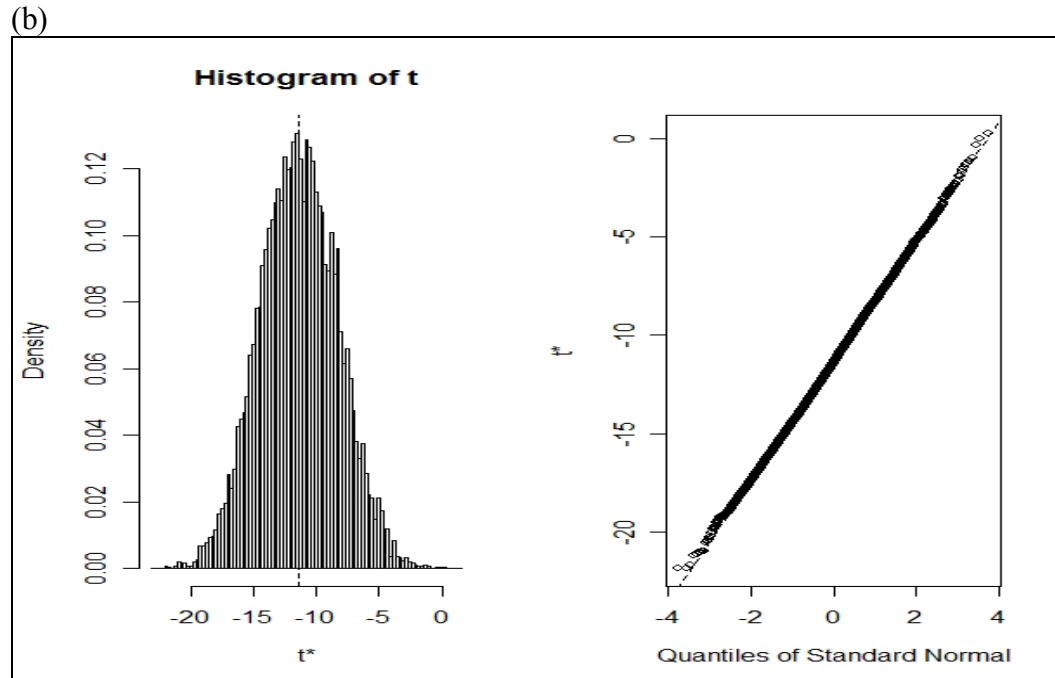


Figure 3.5. The bootstrapping test results of GLMs of (a) $ARIM_{high}$ and (b) $ARIM_{low}$. In the graphs, t^* means the bootstrap resamples, and the dotted line on the histogram shows the original estimated parameter value from GLMs. t^* is the estimated parameter values of intercepts in GLMs of $ARIM_{high}$ and $ARIM_{low}$ (Table 3.5).

3.4. Causes of Red Spruce Growth Decline at GSMNP

GLM and CART modeling and ARIM simulations showed a negative relationship between Air Pollution Disturbance and red spruce growth at high elevation (Table 3.3 (a), Figure 3.2 (a), and Figure 3.3 (a)). This corresponds to literature results (Johnson 1992, Eagar and Adams 1992, McLaughlin and Kohut 1992, Sheppard et al. 1993, Webb et al. 1993, McLaughlin and Percy 1999, DeHayes et al. 1999, Sheppard and Pfanz 2001, Barker et al. 2002, Webster et al. 2004, Dumais and Prévost 2007). High precipitation and cloud immersion frequencies at high elevations account for dominance of the air pollution effect on red spruce growth decline. Acidic rain and clouds cause more serious injuries on foliage and foliage nutrient leaching than dry air

pollutants (Eagar and Adams 1992). In addition, it is reported that the effect of ozone on the red spruce foliage is increased twofold by acidic rain and clouds (Eagar and Adams 1992).

The GLM and CART results showed, as expected, that red spruce growth was positively related to Water Availability and Radiation and negatively related to Air Pollution Disturbance (Table 3.3 (b), Figure 3.2 (b), Figure 3.3 (b)) at low elevation. Warmer temperatures and less precipitation at low elevations account for the positive relationships between red spruce growth and Water Availability and Radiation. Warmer temperature causes radiation absorption and water availability of red spruce to decrease due to high evapotranspiration and reduced photosynthetic activity. Less precipitation directly explains the lack of water resources for photosynthesis. Comparing the results of ARIM_{high} and ARIM_{low}, air pollution disturbances were shown to be less important in explaining the red spruce growth at low elevations due to lower rates of exposure to acid rain and cloud immersion. However, dry air pollutants, especially ozone, still caused negative effects on the low elevation system by direct foliar damage.

3.5. Global Warming Effects on Red Spruce Growth

Accelerated global warming, directional climate change, has driven forest scientists and ecologists to focus on global warming effects on forest systems. Field experimental research has reported positive effects of elevated CO₂ concentration and temperature on most plant species, except some herbaceous ones (Norby and Luo 2004, Ainsworth and Long 2005). Predictions of global warming effects on tree growth are, however, always difficult due to the complexity of nature, lack of knowledge and short periods for most experimental research.

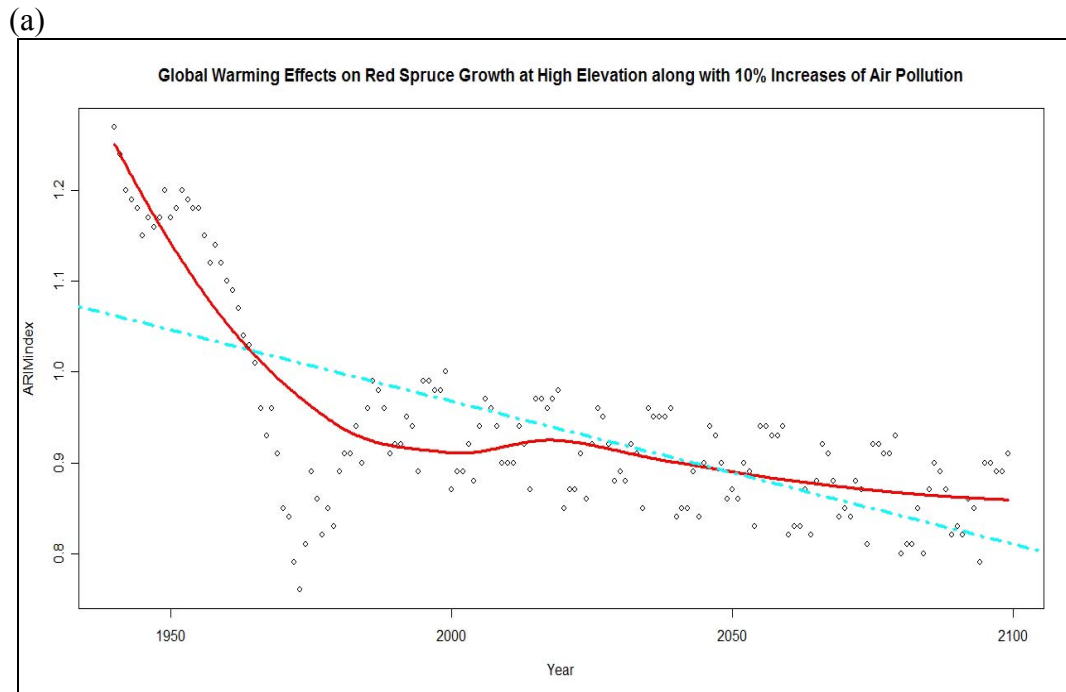
Despite such difficulties, global warming effects on red spruce were predicted by ARIM simulations for the period of 2000 to 2099. The predictions were based on reports of *The Intergovernmental Panel on Climate Change* (IPCC) for eastern North America that annual mean temperature will increase 3.6°C (median), annual mean winter temperature 3.8°C (median) and annual mean precipitation 7% (median) (IPCC 2007). The IPCC predictions were made by comparing the average temperature and precipitation of the period of 1980 to 1999 with simulated ones for the period of 2080 to 2099. Based on the IPCC predictions, *RBIVs* of annual mean temperature, annual mean winter temperature and annual mean precipitation were computed based on equation (3.1) (Appendix 4). Also, *RBIVs* of air pollution factors were calculated to apply the changed air pollution conditions – 10% increase, no increase and 10% decrease. All detail explanations are in Section 2.3, and all data and procedures in Appendix 4. The aim is to understand global warming effects on red spruce growth in interactions with air pollution disturbances in predictions of red spruce growth during 2000 to 2099. For ARIM simulations, Equations (3.7) and (3.8) were applied for ARIM_{high} and ARIM_{low}, respectively. Red spruce growth indices were computed based on those equations, and the results are displayed in Appendix 4.

Growth indices were computed in ARIMs during the whole period 1940 to 2099 (Appendix 4) to show long-term trends. For this, *RBIVs* of all data were calculated for the period 1940 to 2099 by dividing yearly data by the average during this period (Appendix 4). The longer-term average was used for calculating *RBIVs* to predict global warming effects because this can better represent red spruce growth of the whole population. The computed red spruce indices were applied in the simple linear regression and local regression models smoothed by the Spline function, and the results are shown in Figure 3.6.

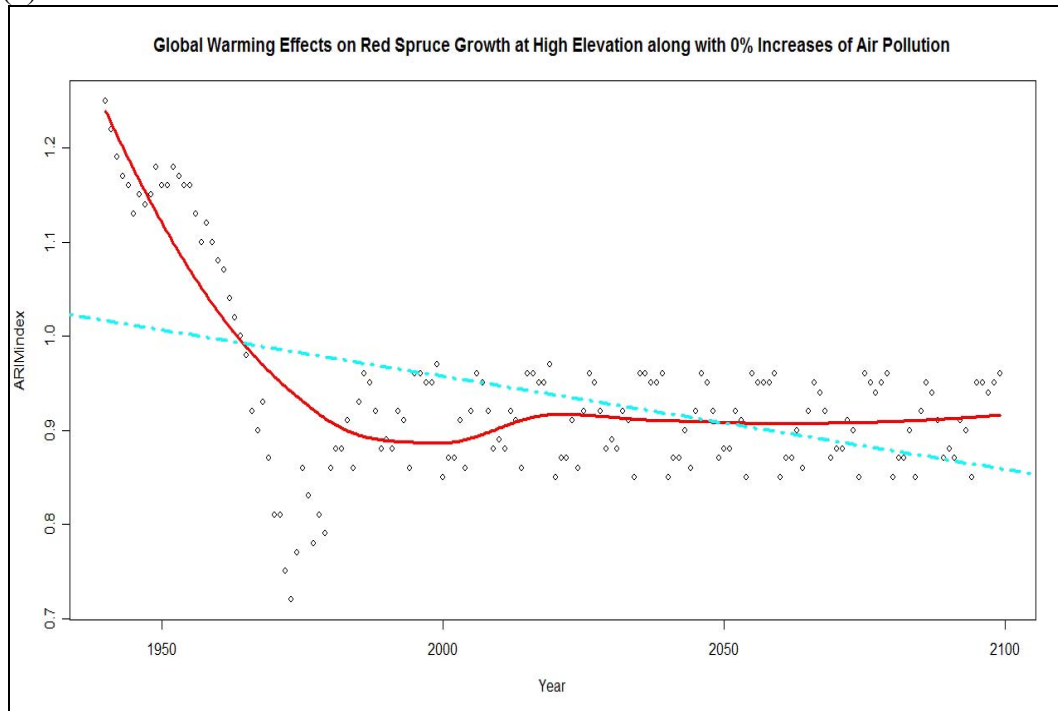
Red spruce growth during 2000 to 2099 was compared with that for 1980 to 1999. This is because global warming and air pollution predictions of the period 2000 to 2099 were made based on the data from 1980 to 1999. Figure 3.6 shows that red spruce growth is more affected by air pollution than global warming at high elevation (Figure 3.6 (a), (b), and (c)) and global warming than air pollution at low elevation (Figure 3.6 (d), (e), and (f)). Red spruce growth at high elevation decreases with increased temperature and precipitation when air pollution increases (Figure 3.6 (a)). But it increases with either no change (Figure 3.6 (b)) or decrease (Figure 3.6 (c)) of air pollution, showing increased slopes of both regressions. In particular, red spruce growth is well recovered with 10% air pollution decrease, showing an almost horizontal simple regression line and remarkably increased slope of the local regression line after 2000 (Figure 3.6 (c)). Equation (3.7) and ARIM (Figure 3.1) explain these results as showing the deterministic effects of Air Pollution Disturbance variable. In Air Pollution Disturbance submodel (Figure 3.1, Appendix 1), the Air Pollution Disturbance effect on red spruce growth increases with increasing precipitation at high elevation due to increased acidic rains. Therefore, increases in air pollution and precipitation together both have negative effects on red spruce growth, but precipitation by itself only indirectly influences red spruce growth in interactions with air pollution factors.

On the other hand, red spruce growth at low elevations always decreases in all three figures, 3.6 (d), (e), and (f). Red spruce growth is barely affected by air pollution factors at low elevations, showing almost no difference of slopes of regression lines among figures (Figure 3.6 (d), (e), and (f)). This is because red spruce growth at low elevations is more dominantly influenced by temperature and precipitation conditions than air pollution via Radiation and Water Availability submodels (Equation (3.8) and ARIM (The red spruce Annual Radial

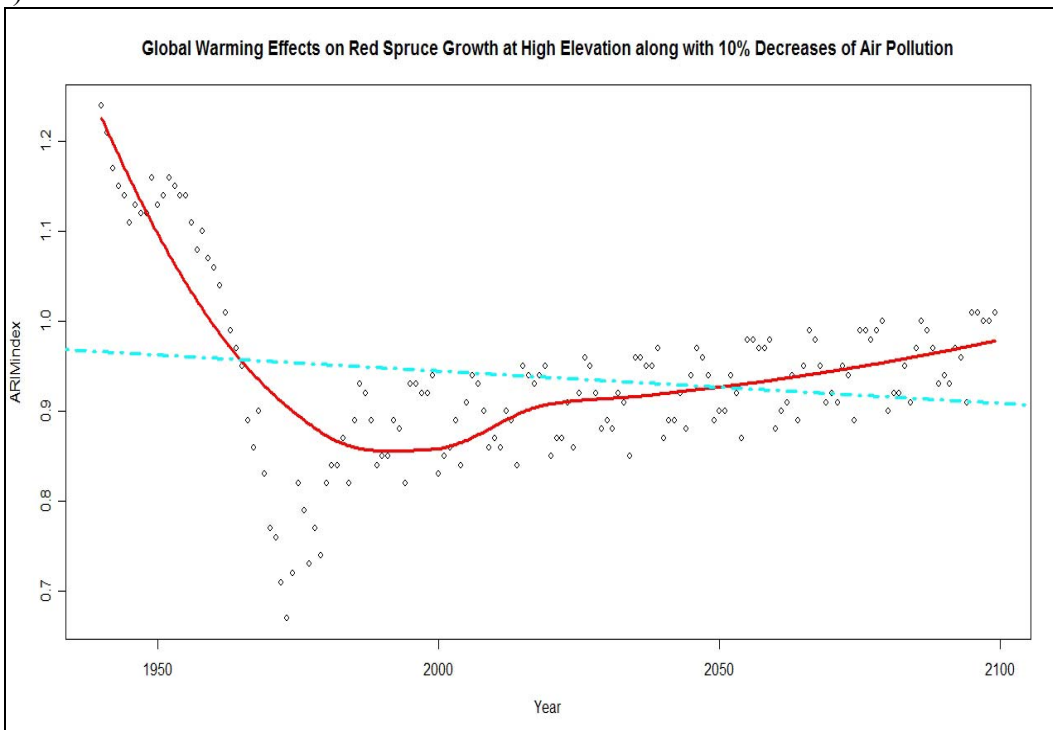
Increment Model) (Figure 3.1)). Based on equation (3.8), increased precipitation has positive effects on red spruce growth at low elevation via Water Availability. But, temperature increase is much greater than that of precipitation; therefore the positive effects of increased precipitation cannot compensate the negative effects of increased temperature. Also, increased precipitation causes negative effects on red spruce growth through a negative relationship with Radiation and positive Air Pollution Disturbance (Figure 3.1, Appendix 2).



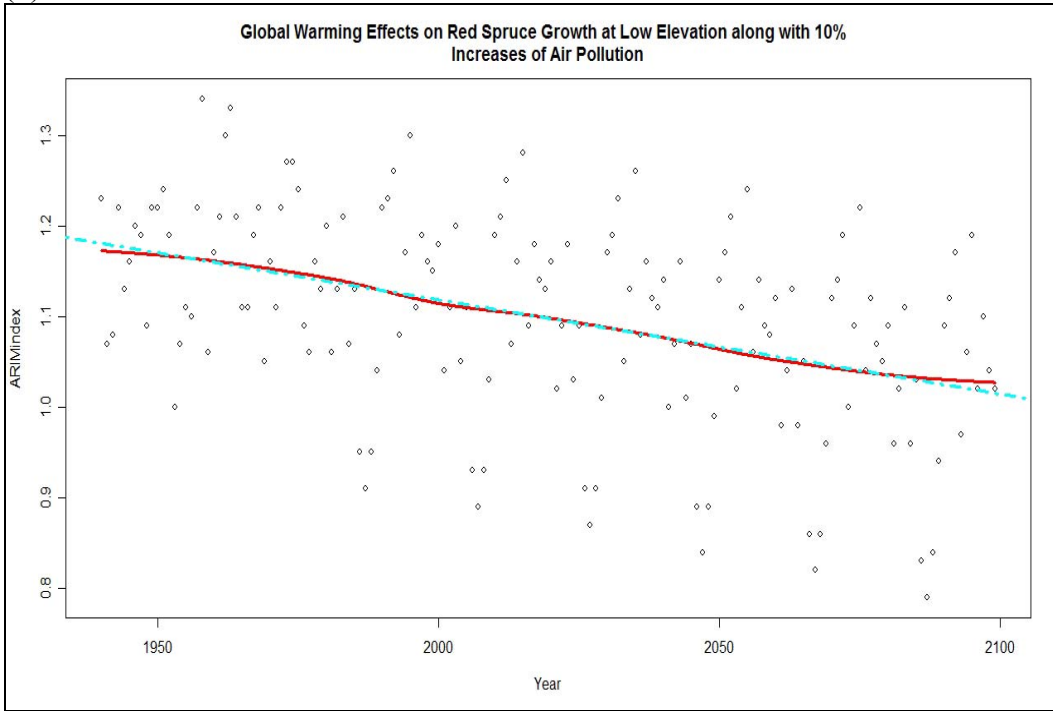
(b)



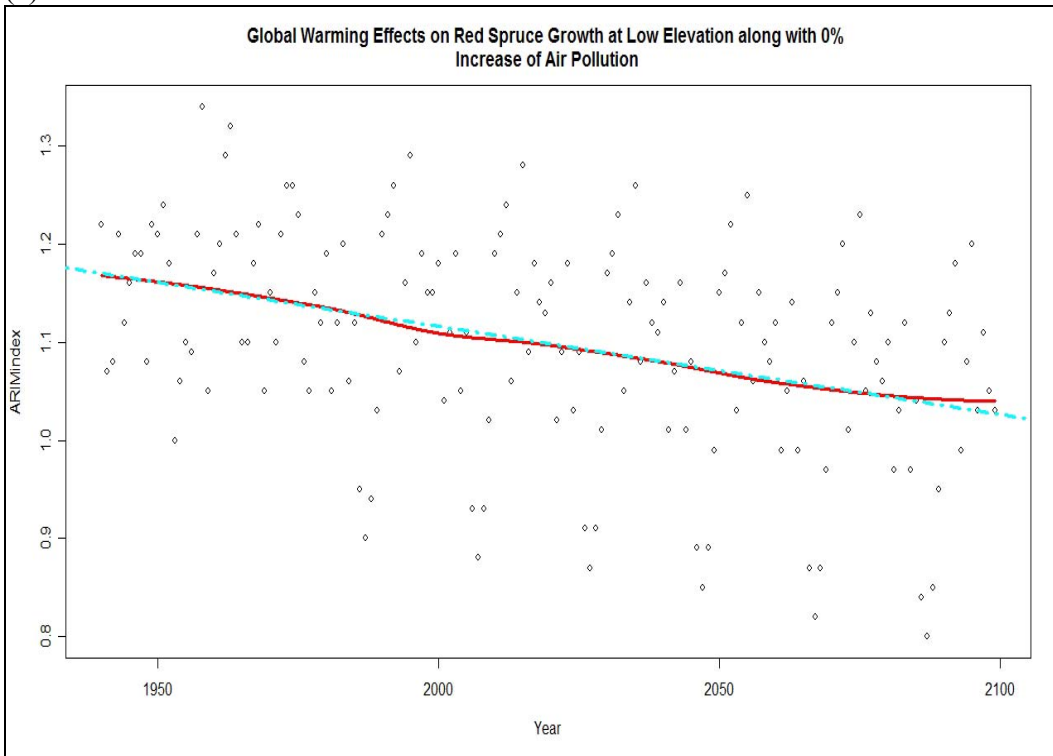
(c)



(d)



(e)



(f)

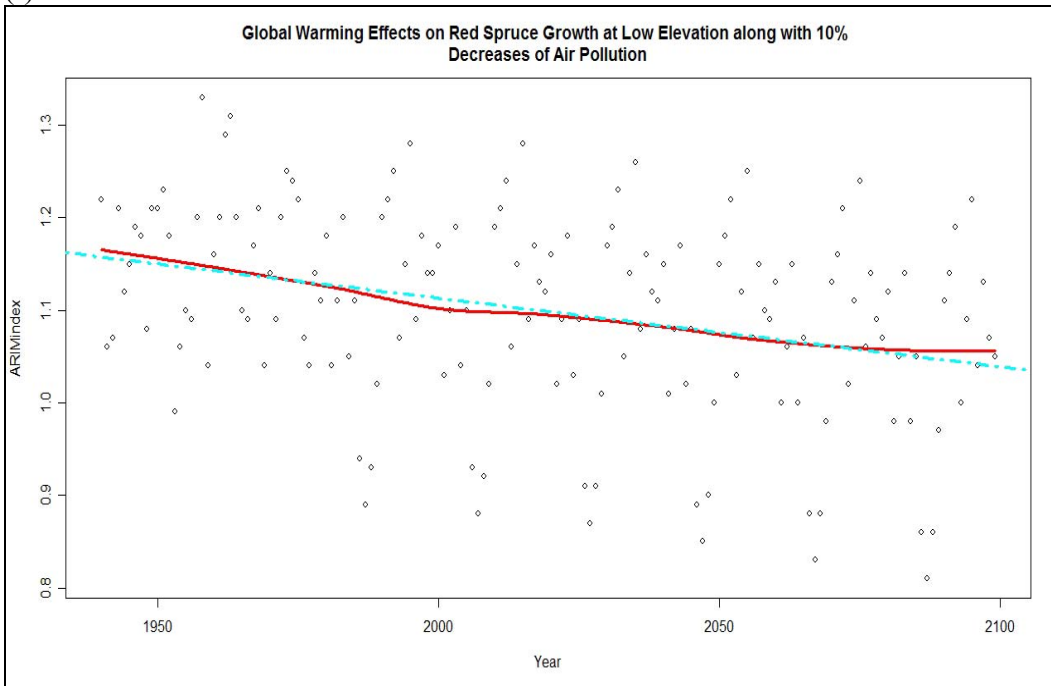


Figure 3.6. Panels (a), (b), and (c) show the red spruce growth predicted by $ARIM_{high}$ simulation with global warming and air pollution changes, 10% increase, no increase, and 10% decrease respectively, at high elevation. Panels (d), (e), and (f) show the red spruce growth predicted by $ARIM_{low}$ simulation according to global warming and air pollution changes, 10% increase, no increase, and 10% decrease respectively, at low elevation. The x axis represents years simulated and y axis the range of the ARIM index ($0 < ARIM \text{ index} < 2$, no units). The small circles are computed red spruce growth generated in ARIMs for each year. Two lines on each graph are regression lines to show long-term trends of growth. The dotted line (light blue) is the simple regression line, and the solid line (red) the local regression line smoothed by the Spline function.

On the other hand, it should be remembered in these predictions that acclimation is a very important factor in tree growth responses (Hamrick 2004). For example, the optimal temperature for photosynthesis and respiration will shift according to temperature increase; thus, tree growth will not show a linear correlation with temperature change (Bigras 2000, Atkin and Tjoelker 2003, Bolstad et al. 2003, Ghouil et al. 2003). Absence of information about the acclimation range of red spruce prevents exact quantitative prediction of global warming on this system. However, the direction of effects predicted by ARIMs will not change because trees lose biomass during acclimation, and also, ARIMs already consider the range of acclimation in tuning

the annual variation by the long-term average (*RBIV*). Therefore, ARIM can offer reliable predictions and comprehensive information about global warming effects on red spruce growth in support of long-term conservation policies and management of red spruce at GSMNP.

4. Discussion

4.1. ARIMs vs. Previous Research: Direct vs. Indirect Factors

The results of ARIM_{high} and ARIM_{low} strongly supported previous research results. These include negative correlations between red spruce growth and air pollution and high temperature, and positive correlation with precipitation (Deusen 1988, Edgar and Adams 1992, Webster et al. 2004, Dumais and Prevost 2007). In particular, the red spruce Annual Radial Increment Models (ARIMs) showed more significant and obvious correlations between red spruce growth and air pollution disturbances than previous research. This suggested the potential effects of air pollution on red spruce growth based on laboratory experiments and field observations, but could not significantly document the negative effects of air pollution in the field studies (Edgar and Adams 1992, Webster et al. 2004, Dumais and Prevost 2007). ARIMs, however, demonstrated that air pollution was the dominant cause of red spruce growth decline at high elevation, and not dominant but still an influential cause at low elevation (Table 3.3 (a), (b)). Also, while dendrochronological studies could not always find significant direct correlations between temperature and precipitation and red spruce growth (Deusen 1988, Edgar and Adams 1992), ARIM showed the importance of those factors as indirect controlling factors, regulating all direct factors (Figure 3.1).

On the other hand, some results of both ARIM_{high} and ARIM_{low} were inconsistent with previous research which showed negative effects of intensive radiation. The predictions of global

warming effects on the red spruce were also inconsistent with the general experimental research results showing positive effects of increased temperature and CO₂ on tree growth (Norby and Luo 2004, Ainsworth and Long 2005). Age and size effects partly explain the inconsistent results in relation to the radiation factor. Age and size effects explain the different physiological responses between young trees, including seedlings and saplings, and adult trees (Day et al. 2004, Mencuccini et al. 2007). Shade tolerant tree species such as red spruce are generally very sensitive to intensive radiation when they are young, but adult trees develop the ability to adapt to and tolerate these conditions. For example, seedling and sapling survival rates are much lower than for Fraser fir in mixed spruce-fir forest, yet red spruce surviving through the seedling and sapling stages lives longer than Fraser fir (Eagar and Adams 1992).

The unique feature of ARIM is its attention to indirect as well as direct causes. Most previous research has not considered the former, and as a result has failed to obtain significant correlations between red spruce growth and environmental conditions in the field. In the ARIM model, indirect interactions are dominant, and this feature mostly explains the reasons for inconsistent results and higher significances shown in the consistent results. As shown in Figure 3.1, many indirect interactions exist in the submodels compared to only eight direct interactions in the main model. These indirect interactions allowed realistically complicated habitat conditions to be considered in understanding red spruce growth at GSMNP. For example, radiation in ARIM represents the amount absorbed by red spruce as mediated by many indirect factors influencing real radiation conditions for red spruce growth (Figure 3.1). As a result, radiation as modeled in ARIM cannot be compared with that used in other studies using raw data collected directly in the field. In ARIM, global warming effects were also predicted by considering complicated indirect interactions in Section 3.5, showing opposite results with the

experimental research such as FACE (Free Air CO₂ Enrichment) research (Ainsworth and Long 2005) (Figure 3.6). The predictions showed the negative effects of global warming on red spruce growth in interactions with air pollution disturbance at high and low elevations (Figure 3.6). The negative effects have been supported by many field observations, such as range shifts of organisms, even though experimental research has been unable to show significant negative effects of global warming due to limitations of the number of parameters considered and the short-term experimental periods (Bradley et al. 1999, Corti et al. 1999, Pounds et al. 1999, Cox et al. 2000, McLaughlin et al. 2002, Walther et al. 2002, Parmesan and Yohe 2003, Miles et al. 2004).

4.2. ARIM: Modeling, System Modeling, and Interdisciplinary Synthesis

In modeling, in general, generality and reality have been considered as a mutually exclusive concept (Guisan and Zimmermann 2000). It has been thought that generality can be achieved by analytical and mathematical models, including the classical logistic growth and Lotka-Volterra population equations, developed for predicting responses within simplified reality (Guisan and Zimmermann 2000). Those models can be applied for other idealized phenomena also, but they cannot explain the real causes of realistic phenomena (Guisan and Zimmermann 2000). Reality can only be approached by considering complicated cause-and-effect relationships among multiple factors. Thus, models to encompass reality must have more variables. Process-based models and ecosystem models do consider reality more specifically, and to that extent lose generality. These model types involve many factors and comprehensive synthesis of data to express these, and they give better explanations and fits with observed data in model evaluation. But, being too case- and species-specific hampers broad application of

those models to other studies. Generality is sacrificed. Also, many variables make parameter estimation and checking the confidence level of estimates technically difficult or impossible. As a result, such models cannot quantitatively show the confidence levels and generality of model results like those described in Sections 3.1, 3.2, and 3.3.

For understanding complicated ecological phenomena and improving model applicability, ecologists need to chase two hares at once, generality and reality. These need be not always mutually exclusive but can be achieved with new kinds of models (Guisan and Zimmermann 2000). In the ARIM study, systems modeling was applied as such a new modeling methodology in order to achieve both generality and reality. ARIM, as a modeling process, can be classified into two parts, structural and functional part. The structure of ARIM explains its generality. Its structure is based on general metabolic processes, photosynthesis and respiration, of all tree species. Its disturbance factors reflect general disturbances known from long-term tree growth studies. Therefore, the ARIM model structure can be applied for studies of other tree species with a few modifications for special cases. For example, the weather disturbance submodel may need to involve fire disturbance for a fire sensitive species. The functional part of ARIM, accounting for reality of this model, was explained by mathematical, statistical and rule-based models employed for each interaction. Although some models applied for each interaction were based on general functional relationships, most models were based on the red spruce-specific research results (see Chapter 2). Therefore, in spite of some limitations, ARIM exhibited generality and reality that could both be achieved at once.

Model reality can be improved by understanding the complexity of nature through interdisciplinary synthesis. In ecology, interdisciplinary synthesis has been suggested as one of the most important issues due to the known complexity and connectivity of ecosystems.

Separation among disciplines, different measurement units in collecting data, and narrowed perspectives of researchers due to reductive thinking system have prevented interdisciplinary studies (Bertalanffy 1969, 1975). System theory and systems modeling ultimately pursue interdisciplinary synthesis in understanding hierarchically organized complexity in the living world (Bertalanffy 1969, 1975). ARIM, as a systems model, has provided a general framework for the interdisciplinary synthesis, including integration of knowledge, data and submodels, in studying tree growth. The model structure of ARIM includes all possible direct and indirect interactions among factors which studied in various disciplines – climatology, soil ecology, disturbance ecology, tree physiology, etc. (Figure 3.1). Also, a variety of models, including linear deterministic models, non-linear deterministic models, and rule-based models, were employed in accounting for each functional relationship between submodel factors (Appendices 1 and 2). In particular, statistical models – GLMs and CART models – were used for the main models of ARIM to estimate coefficients of direct factors and determine the influential factors in the ARIM submodels. In employing statistical models to the main models, ARIM shows the flexibility of a systems model in incorporating a variety of model approaches and shows that a systems model can quantitatively explain the confidence level and generality of modeling results. The fact that the ARIM structure does not change the features of observed data without a reason, when the computed data for the main models are calculated in submodels, makes incorporation of statistical models into a systems model possible, as explained in Section 3.1. In addition, a dimensionless index value, Relative Basis Index Value (*RBI*), developed for ARIM modeling fundamentally enabled data from different disciplines and monitoring systems to quantitatively integrate (Equation (3.1)). This index value can be applied for other interdisciplinary studies due to its dimensionless feature.

4.3. ARIM: Scale , Across-scale Interaction, and Global Warming

Since the late 1970s and 1980s, consideration of scale has increased exponentially in ecology (Schneider 2001). Earlier studies showed discontinuous hierarchical structures and processes of natural phenomena over time and space, and scale dependency of study results (Holling 1992, Allen and Holling 2002, Willis and Whittaker 2002). With the orientation to scale issues, increased global environmental problems, global warming and air pollution, have raised concerns about across-scale interactions in order to understand how global scale phenomena influence local phenomena and vice versa. Importance of understanding across-scale interactions has been supported by much research population dynamics, genetics, biogeography, and environmental change (King et al. 2004, Diffenbaugh et al. 2005, Cowen et al. 2006, Kerr et al. 2007).

Hierarchy theory partly accounts for across-scale interactions. Higher-scale factors constrain focal-scale interactions, and lower-scale factors explain the processes of focal-level interactions (Turner et al. 2001). However, hierarchy theory has been applied to ecological studies by separating broad and fine scales (Peterson, in press). Separation among scales calls for explanations about some mediator factors, which show connectivity across scales. Peters et al. (2007) suggested a framework, consisting of fine-scale, intermediate-scale and broad-scale pattern–process relationships. In this framework, intermediate-scale pattern–process relationships are influenced by transfer vectors, such as wind, water, and dispersal animals, linking fine-scale and broad-scale pattern and process relationships.

Hierarchy theory and the framework of Peters et al. (2007) have contributed to explain across-scale interactions, but ecologists still need a more advanced conceptual framework and quantitative methodologies. In addition, three subjective classes of scale cannot involve complex

across-scale interactions that can often be found in nature. Some modeling approaches, including process-based models and ecosystem models, have been applied to explain across-scale interactions as well as within-scale interactions. Process-based models have contributed to mechanistic understanding of broad-scale phenomena using fine-scale data as considering cause-effect relationships among elements (Kerr et al. 2007). Ecosystem models have provided the comprehensive understanding via descriptive integration of data and information. However, process-based models and ecosystem models still have problems in quantitatively dealing with the hierarchically organized complexity of nature.

The red spruce Annual Radial Increment Model (ARIM), as a systems model, provided the conceptual framework, the ARIM model structure, and quantitative methodology, *RBIV*, for studying complicated and nested within- and across-scale interactions. *RBIV* and a variety of models for each interaction enable the within- and across-scale interactions to be quantitatively integrated in ARIM (Section 2.1). ARIM involved a variety of within- and across-scale interactions through the hierarchical model structure (Figure 1). For example, in ARIM, radiation, temperature, precipitation, and air pollution represent large spatial scale parameters, and those factors were modified by regional scale parameters such as elevation. These factors were also modified by aspect, slope, and others at local scale and affected by co-existent species such as Fraser fir at finer scale. The within and across-scale interactions frequently cause self-organized emergent phenomena that cannot be predicted based on observations at single or multiple, independent scales (Peters et al. 2007). ARIM explained and involved some self-organized emergent phenomena. For example, in ARIM, acidic rain and cloud environment account for an emergent phenomenon. The interactions involved in the acidic rain and cloud environment are: within-scale interaction between air pollution and precipitation at continental spatial scale;

within-scale interaction between cloud immersion and elevation at regional spatial scale; and, across-scale interactions between large scale and regional scale, including interactions among all four factors.

In predicting the global warming effects on the red spruce growth system in Section 3.5, many within- and across-scale interactions were also involved. For example, in ARIM, increased temperature and precipitation conditions interact; with elevation at regional scale; with aspect and slope at local scale; and, with air pollution at continental scale (CO_2 and O_3 for global warming) and at regional scale (NO_x and SO_x for acidic rain) (Figure 3.1). The air pollution factor also involved interactions between acidic rain and clouds and ozone at regional scale (Figure 3.1). Those within- and across-scale interactions involved in ARIM enabled the global warming effects on the red spruce growth to be more comprehensively explained and predicted at GSMNP in Section 3.5.

5. Conclusion

The causes of red spruce growth decline and the effects of global warming on the growth of red spruce were explored through systems modeling at GSMNP. The red spruce Annual Radial Increment Model (ARIM) was devised for this study. The modeling results showed that air pollution disturbance was the dominant cause of red spruce growth decline at high elevation, and red spruce growth had significant positive relationships with water availability and radiation and a negative relationship with the air pollution disturbance at low elevation. Based on the results of ARIMs in predicting global warming effects on red spruce growth, growth was more affected by air pollution than global warming at high elevation (Figure 3.6 (a), (b), and (c)), and more by global warming than air pollution at low elevation (Figure 3.6 (d), (e), and (f)). In

particular, red spruce growth is well recovered with 10% air pollution decrease, showing an almost horizontal simple regression line and remarkably increased slope of local regression line after 2000 (Figure 3.6 (c)). Red spruce growth is barely affected by air pollution factors at low elevation, showing almost no difference in slopes of regression lines among Figures 3.6 (d), (e), and (f). However, deficient information about acclimation range of red spruce prevents the exact quantitative prediction of global warming effects on this system. We need further genecological and physiological research about acclimation ability of red spruce to improve understanding of causes of growth decline and prediction of global warming effects on growth. In particular, more ecological research, such as interactions with co-existent species and insects, and general physiological research, are needed at low elevations.

ARIM exhibited the concept and methodology to implement quantitative multifactorial, interdisciplinary research and contributed to solving ecological issues of within- and across-scales interactions and complexity, in three ways. First, ARIM, in modeling perspectives, provided a general model structure including complex direct and indirect interactions for studying tree systems. Second, ARIM was demonstrated to be a practical methodology to quantitatively integrate knowledge and data from different disciplines, as developing *RBIV* and flexibility in incorporation of models within the ARIM structure without modifications of observed data features. Third, ARIM provided the conceptual framework and methodology to study hierarchically organized within- and across-scale interactions.

CHAPTER 4

RED SPRUCE HABITAT MODEL (RSHM): EFFECTS OF HABITAT SUITABILITY AND GLOBAL WARMING ON THE GEOGRAPHIC DISTRIBUTION OF *PICEA* *RUBENS*

1. Introduction

There is increasing need to predict the spatiotemporal variations of plant distributions for exploring land cover changes, planning restorations and implementing sustainable management (Dymond and Johnson 2002). Predictions of spatial distribution of plant species have utilized a variety of spatial landscape models (Münier et al. 2001, Dymond and Johnson 2002, Chuanyan et al. 2006). Predictive Species Distribution Models (PSDMs) are a special type of spatial landscape models and result in spatial predictions indicating locations of the most suitable habitats for a target species and community (Engler et al. 2004). These spatial predictions have been used for plant distribution maps and applied to predict range shifts with environmental change (Engler et al. 2004).

Most predictions of PSDMs have relied on the direct relationship between a taxon and its direct environment (Skov and Borchsenius 1997, Guisan et al. 2002, Matsui et al. 2004, Engler et al. 2004, Chuanyan et al. 2006). Also, those studies have been focused on understanding the relationships at one fixed spatial and temporal scale. The characteristics of PSDMs, focusing on only direct interactions, have restricted PSDMs to explain detailed cause-effect relationships explained by complicated indirect interactions. Also, PSDMs developed at one fixed scale cannot well predict the spatiotemporal changes of plant distribution according to global-scale

environmental changes. This is because the global-scale environmental changes influence local plants via complicated across-scale interactions. Thus, with increases of environmental catastrophes and lost of species diversity, global-scale environmental changes have impelled ecologists to understand knowledge of within- and across-scale system interdependencies. This need has required developing submodels, which explore complicated within- and across-scale interactions and diverse direct and indirect interactions, for PSDMs. In addition, spatiotemporal dynamics of plant distributions rely on mutual interactions between plants and environment. Plants can tolerate certain level of environmental changes using their defense mechanisms, such as photoinhibition. Also they can acclimate themselves to environmental changes as changing optimal conditions for growth and survival, such as shifting optimal temperature of photosynthesis and respiration with increased temperature condition. Therefore, the submodels of PSDMs have to explain ecological and physiological processes of plants as well as environmental conditions.

Scientists who have studied environment and plants have focused on global warming as one of the most serious global environmental changes in understanding habitat loss, population decline and species extinction (Corti et al. 1999, Cox et al. 2000, McLaughlin et al. 2002, Walther et al. 2002, Parmesan and Yohe 2003, Miles et al. 2004). In particular, understanding global warming effects on the species distributed in areas such as high mountains and southern distribution limits is very important because they are more sensitive and vulnerable to warming than other species (Hörsch 2003, Guisan and Thuiller 2005). Field observations have reported range shifts of organisms, such as *Bufo periglenes*, *Euphydryas editha bayensis*, and *Fagus crenata*, toward northern areas with global warming even though details of processes have not yet been explained (Pounds et al 1999, McLaughlin et al 2002, Matsui et al. 2004, Miles et al.

2004). Therefore, it is reasonably expected that red spruce, a typical alpine and subalpine species of the eastern United States, is very sensitive and vulnerable to global warming. The red spruce populations of Great Smoky Mountains National Park (GSMNP), the southern distribution limit, can lose their suitable habitats due to degradation of habitat suitability via interactions between global warming and local environmental factors.

This study aimed at predicting the current distribution range of red spruce and accounting for the possible global warming effects on the changes of red spruce distribution. To do this, I made the following three hypotheses. First, the distribution range of red spruce can be projected by the suitable habitat conditions, which is determined by hierarchically organized complex interactions among factors. Second, the spatiotemporal changes of the red spruce distribution can be predicted by predicting suitable habitat changes induced by global warming in interactions with other environmental factors. Third, the spatiotemporal changes of the red spruce distribution are not directly limited by distance of seed dispersal. The dispersal mechanisms of red spruce include long distance dispersal, like other coniferous species; thus, the dispersal distance of red spruce can catch up to the rate of habitat change within the study area, GSMNP. In this study, ARIMs (The red spruce Annual Radial Increment Models) developed in Chapter 3 were used as the submodels of PSDM of red spruce, and PSDM modeling was implemented by geoprocessing and spatial data analyses of a Geographic Information System (GIS) using raster and vector data and statistics, Pearson's χ^2 statistics for a goodness of fit test.

2. Methods and Data

2.1. Study Species, Red Spruce (*Picea rubens*)

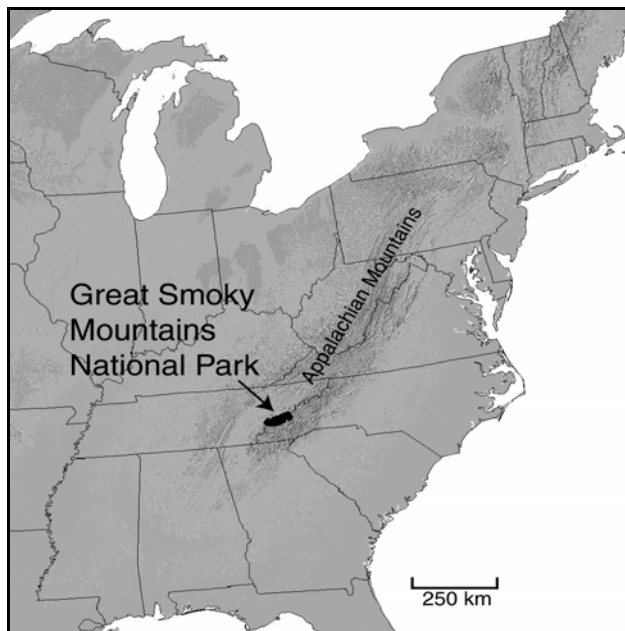
The study species of this study is red spruce (*Picea rubens* Sarg.). Red spruce is a long-lived (> 300 years), shade-tolerant species, with a low reproduction rate and low genetic diversity (Eagar and Adams 1992). It is a major tree species in high elevation coniferous forests of the Appalachians (Busing 2004, Webster et al. 2004). Red spruce dominates boreal habitats at the lower elevations (1370-1675m), Fraser fir forests (*Abies fraseri* (Pursh) Poir.) mostly at higher elevations (>1890m), and both species co-dominate at mid elevations (1675-1890m) (Webster et al. 2004).

Dendrochronological studies estimated that red spruce decline in the Southern Appalachians occurred after about 1965 (Deusen 1988, Eagar and Adams 1992). It has been thought that this reduction may be an early indication of more broadly based changes in the structure and functioning of this system (Webster et al. 2004, Eagar and Adams 1992, Johnson et al. 1992). It has been suggested that acidic pollutants and climate change have caused red spruce growth decline and high mortality rate via modification of the atmospheric system, soil system, geochemical system, and physiological system (Eagar and Adams 1992, Barker et al. 2002, Creed et al. 2004, Webster et al. 2004). Another important stress suggested is the infestation of Fraser fir by the balsam woolly adelgid (*Adelges piceae* Ratz.), causing extensive Fraser fir mortality in the Great Smoky Mountains (Webster et al. 2004). Such high mortality of a co-dominant species may make an impact on the spruce system's structure and dynamics through modifications of physical environments. Busing and Pauley (1994) reported that loss of Fraser fir from the canopy would leave red spruce vulnerable to wind damage and mortality.

2.2. Study Area, GSMNP

The Study area is the Great Smoky Mountains National Park (GSMNP), located in the southern Appalachian Mountains of Southeastern U.S.A. (Figure 4.1). Elevations in GSMNP range from approximately 250 m to 2,025 m at Clingman's Dome (Welch et al. 2002, Madden et al. 2004). Soils in GSMNP are Inceptisols to have large contents of organic matter at the surface, and textures of soils are silt to sandy loam (Creed et al. 2004, Madden et al. 2004). GSMNP has a cool, temperate rainforest climate with the mean annual air temperature of 8.5°C, ranging from an average of -2 °C in January to 18 °C in July, and annual mean precipitation of 230 cm, ranging from 150 to 300 cm (Creed et al. 2004, Webster et al. 2004). These climatic conditions result in short growing seasons (about 100–150 days), frequent cloud immersion and strong winds (Johnson et al. 1992).

(a)



(b)

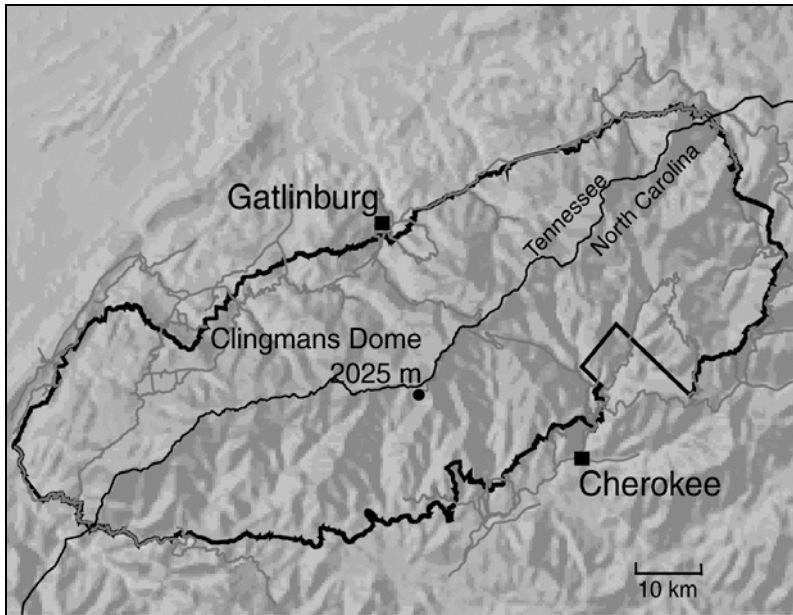


Figure 4.1. (a) shows location of GSMNP in the eastern United States and (b) boundary of GSMNP and elevation of summit area, Clingmans Dome. Source of maps is Madden et al. (2004).

2.3. Model Development, RSHM

A Species-Habitat Model (SHM) is a special type of PSDM which explains a spatial species distribution as a function of mapped environmental variables (Guisan and Thuiller 2005). In general, SHMs have been developed to cover various research fields including species management with environmental changes (Guisan and Zimmermann 2000). SHM as a spatial landscape model is very flexible to incorporate literature information, field measurements and observations that can be converted into geospatial data.

SHM modeling is implemented under the functions and construction of GIS; therefore, understanding of GIS is necessary for this modeling. GIS has become an important field of academic studies and an essential part of the information technology infrastructure of our society since the early 1960s (Aronoff 1989). There have been three kinds of GIS definitions: Toolbox-

based definition, database definition, and organization-based definition (Burrough and McDonnell 1998). Ozemoy, Smith, and Sicherman (1981) defined GIS as “an automated set of functions that provides professionals with advanced capabilities for the storage, retrieval, manipulation and display of geographically located data”. It is an early example of organization-based definition. Burrough (1986) and Burrough and McDonnell (1998) defined GIS as “a powerful set of tools for collecting, storing, retrieving at will, transforming and displaying spatial data from the real world”. It is an example of toolbox-based definition. Aronoff (1989) defined GIS as “computer-based systems used to store and manipulate geographic information”. It is an example of database definition of GIS. Recently, Lo and Yeung (2007) comprehensively defined GIS as “computer-based systems specially designed and implemented for two subtle but interrelated purposes: managing geospatial data and using these data to solve spatial problems”.

GIS consists of five components, data input, geoprocessing, spatial analysis, output, and people (Burrough and McDonnell 1998, Lo and Yeung 2007). GIS data must be georeferenced to a particular map coordinate system. Georeferencing means for data to have their own coordinate system (x, y) related to the real world and attributes of the geodata expressed in a particular map coordinate system (Aronoff 1989, Burrough and McDonnell 1998, Lo and Yeung 2007). Geoprocessing is defined as processes of creating and modifying geospatial data using geoprocessing tools (DeMers 2002, Lo and Yeung 2007). A GIS contains many geoprocessing tools for implementing data creation and modification, producing cartographic products and conducting spatial analysis (Lo and Yeung 2007). Spatial analysis cannot be simply defined because it has been evolved with advances in techniques, concepts and capability of application, and each discipline has developed a terminology such as spatial data analysis, statistical spatial analysis, spatial statistics, and spatial data mining and methodology for spatial analysis (Bailey

1994, Lo and Yeung 2007). In the face of such a diversity of analytical perspectives, Bailey (1994) defined spatial analysis, including spatial data analysis, statistical spatial analysis, spatial statistics, and spatial data mining, as “a general ability to manipulate spatial data into different forms and extract additional meaning as a result”. Spatial analysis is also defined as a collection of techniques for analyzing spatial arrangement of point, line or area objects, located in geographical space, with a set of attribute values (Goodchild 1987, Haining 1994). Modern spatial analysis, more focusing on the spatial aspects of geospatial data, consists of three components: database models, such as raster-based models and object-based models, to explore and manipulate geospatial data: statistical and graphical analysis including geostatistical analysis, image analysis and spatial visualization (Lo and Yeung 2007). Also, spatial analysis includes spatial modeling and spatial data mining in accordance with the research purposes (Lo and Yeung 2007). Spatial analysis is used for spatial modeling, which includes many kinds of spatial landscape modeling, to model spatial relationships and heterogeneity for improving spatial understanding and predicting spatial patterns and processes (Bailey 1994). When spatial data analysis is applied to geospatial data to assist data exploration processes, it is spatial data mining and could be used as a preprocess for spatial modeling.

Species-Habitat Model (SHM) modeling is spatial (landscape) modeling implemented by raster geoprocessing, which is defined as creating and modifying the raster geospatial data using geoprocessing tools (DeMers 2002, Lo and Yeung 2007). The spatial modeling conducted by raster geoprocessing is usually called raster GIS modeling. Raster GIS modeling is the heart of the GIS modeling framework, called cartographic modeling, and has become the standard methodology, providing an increase in flexibility of modeling of surfaces beyond the vector models in environmental modeling and describing diffusion events such as air pollution and seed

dispersal (Burrough and McDonnell 1998, DeMers 2002, Lo and Yeung 2007). A surface means a statistical space in GIS. For understanding raster GIS modeling, we need fundamental understanding of raster models (raster geospatial data). The following explanation of raster models in this paragraph are summarized from Lo and Yeung (2007). Geographical space is represented by two different types of models, a vector model (object-based model) and a raster model. The vector model treats geographical spaces as discrete and distinguishable objects and the raster model treats one or more spatial phenomena, varying continuously over space with no obvious boundary. In the raster data model, the geographical space is divided into cells (pixels), and the attribute or value of each cell is coded by a digital alphanumeric code. Also, the raster data are organized into layers (raster layers) according to themes, for example, forest layer, road layer, elevation layer, etc. This feature makes area calculation and overlay possible for spatial modeling.

Raster GIS modeling has used a variety of data sources, such as observed field data and Remote Sensing (RS) data. In particular, raster GIS modeling has been increased with increased availability of raster data sets, especially, the advanced RS data with decreased cost and increased resolution (DeMers 2002). Currently, RS, defined as the collecting and processing of natural and cultural information of Earth by the use of photographs and data related with aircraft and satellite, has been preferred for spatial modeling studies due to various spatial resolutions and temporally recorded data sets (DeMers 2002, Lo and Yeung 2007). Also, the RS data have been indirectly used for raster GIS modeling by being used for developing many kinds of raster geospatial data such as DEMs (digital elevation models). This study used a DEM as an essential data source for developing a red spruce habitat model with the digital stream map (Figure 4.2).

In this study a red spruce habitat model (RSHM) as SHM of red spruce was developed in the functions and constructions of GIS. Its aim is to project the red spruce distribution range and habitat suitability distribution within the distribution range at GSMNP. ArcGIS 9.2 and 9.3 produced by Environmental System Research Institute (ESRI), Inc., in Redlands, CA, was used for RSHM modeling. The result of RSHM was used for predicting the global warming effects on the red spruce distribution at GSMNP. The RSHM development procedure was mainly made up of four steps: 1) finding the suitable habitat conditions of red spruce using submodels, ARIMs in Chapter 3; 2) developing geospatial variables representing habitat suitability conditions, called geospatial habitat suitability variables, using raster geoprocessing tools; 3) developing RSHM by overlaying geospatial habitat suitability variables using overlay analysis, a raster geoprocessing tool; and finally, 4) evaluating RSHM by comparing its results with the real distribution range of red spruce at GSMNP by Pearson's χ^2 statistics for goodness of fit test. The development procedures of RSHM are shown in figure 4.2. The real distribution range of red spruce was extracted from the digital vegetation map of GSMNP developed by National Park Service (Figure 4.3).

RSHM used the results of the red spruce Annual Radial Increment Model (ARIM) modeling in Chapter 3 (Equations (7) and (8) for high- and low-elevation habitats, respectively) to find suitable habitat conditions. ARIM, a systems model, explained the red spruce growth via energy and matter flows between red spruce and environmental factors and among environmental factors. In ARIM, hierarchically organized direct and indirect interactions including within- and across-interactions were explored by tracking energy and matter flows. ARIMs included natural and anthropogenic disturbances and physiological responses of the red spruce to disturbances at a variety of scales. For applications of ARIMs' results to determine

suitable habitat conditions, it was assumed that the conditions for better growth indicated more suitable habitat for red spruce. In ARIMs (ARIM_{high} and ARIM_{low}), the suitable habitat information of red spruce growth was converted into geospatial information using sensitivity analysis. The sensitivity analysis results of ARIMs showed the relationship between red spruce growth and the four geospatial variables, Elevation (E), Aspect (A), Slope (S), and Distance to Stream (DS). The sensitivity analysis was carried in Stella 9.0.3 by changing values of the geospatial variables. The sensitivity of red spruce growth to Elevation was calculated at five elevation ranges and averaged (Appendix 5, Table 4.1). For the sensitivity analysis, Aspect was divided into four ranges, Slope was divided into five ranges, and Distance to Stream was divided into three ranges (Table 4.1). The four ranges of Aspect, which are four different directions of aspect: North, East, South, and West, were determined based on literature information documenting different radiation climate conditions according to aspect directions (Geiger et al. 2003). The amount of incoming radiation per unit area increases with changing aspect from north-to south-facing slopes (Geiger et al. 2003). The five ranges of Slope and three ranges of Distance to Stream were arbitrarily divided for sensitivity analyses in ARIMs, and then real numbers for these ranges were obtained by the natural breaks (Jenks) system of the Reclassify function in Spatial Analyst, ArcGIS 9.2 (Table 4.1). The natural breaks (Jenks) system classifies the data into groups based on similar values, maximizing the differences between classes through being divided by relatively big differences in the data values (ArcGIS 9.2 Desktop Help: Natural breaks (Jenks)).

Table 4.1. The ranges of four habitat suitability variables for sensitivity analysis ranges. The ranges of Elevation and Aspect were divided by the ARIM results and literature information. The ranges of Slope and Distance to Stream were divided by the natural breaks (Jenks) system of the Reclassify function in Spatial Analyst, ArcGIS 9.2. For Aspect, Slope and Distance to Stream,

the range values for sensitivity analyses in ARIMs are shown as integer numbers such as 1, 2, and 3, and the real break values obtained from the natural breaks (Jenks) system in parenthesis.

Geospatial Habitat Suitability Variables	Elevations (m)	Aspect (°)	Slope (°)	Distance to Stream (m)
Ranges	1400-1450	North (0 – 45, 315 – 360)	1 (0 – 11.7)	1 (0 – 149.3)
	1450-1550	East (45 – 135)	2 (11.8 – 19.5)	2 (149.4 – 482.3)
	1550-1650	South (135 – 225)	3 (19.6 – 26.5)	3 (482.3 – 979.9)
	1650-1850	West (225 – 315)	4 (26.6 – 33.1)	
	>1850		5 (33.2 – 62.3)	

Elevation was classified into three ranges – high (>1850m), buffer (1650 to 1850m) and low (1400 to 1650m) – in estimating the sensitivity of red spruce growth according to variations of Aspect, Slope and Distance to Stream. The sensitivity of red spruce growth for Aspect, Slope and Distance to Stream were computed and averaged at three elevation ranges separately (Appendix 5). The classification of three elevation ranges was based on the results of ARIMs studies. The red spruce Annual Radial Increment Models (ARIMs) showed different growth pattern and suitable habitat conditions of red spruce at high elevation and low elevation. The result of ARIMs were explained in Chapter 3 and summarized in the result section of the present chapter. Therefore, the high- and low-elevation ranges were explained by ARIM_{high} and ARIM_{low}, respectively. The buffer range, however, was created by averaging values from values at 1700m estimated by ARIM_{low} and values at 1700 and 1800m estimated by ARIM_{high} (Appendix 5). This is because ARIM_{high} represents high-elevation area around 1950m (from 1911 to 2000m), and ARIM_{low} represents low-elevation area around 1500m (from 1478 to 1548m); thus, these models cannot represent the habitat condition of the buffer area (1650– 1850m). All sensitivity analysis

results of four geospatial variables were expressed by index values of ARIM in the range 0 to 2. For example, elevation 170m is expressed by ARIM index of 0.9337. For convenience in ArcGIS spatial modeling, these index values were modified by multiplying each value of the four geospatial variables by 10000. For example, an index value 0.9871 is modified into 9871. The ARIM indices computed for all four geospatial variables in the sensitivity analyses, and the modified index values are displayed in Appendix 5.

All geospatial variables were modified by raster geoprocessing to develop geospatial habitat suitability variables (Figure 4.2). At first, Aspect and Slope were calculated from a DEM, and called the Digital Aspect Model and Digital Slope Model respectively (Figure 4.2, Figure 4.6 (a)). Distance to Stream was calculated from the digital stream map and called the Digital Distance to Stream Model (Figure 4.2, Figure 4.6 (b)). The Digital Aspect Model was developed using the Aspect function of Spatial Analyst, ArcGIS 9.2, and the Digital Slope Model used the Slope function of Spatial Analyst, ArcGIS 9.2. The Digital Distance to Stream Model was obtained using the Straight line function of Spatial Analyst, ArcGIS 9.2. Next, all geospatial variables were reclassified, and the modified index values were assigned for them based on the relationships found in sensitivity analyses (Figure 4.2). This process is called reclassification, a type of raster geoprocessing, and produced the geospatial habitat suitability variables which are raster layers for raster GIS modeling (Figure 4.2). Reclassification has been used for creating a new raster layer by changing the attribute values of the cells of the input layer (Lo and Yeung 2007). The Reclassify function in Spatial Analyst, ArcGIS 9.2, implemented all reclassification geoprocessing.

Calculator function of Spatial Analyst, ArcGIS 9.2. Finally, the overlaid layer was reclassified, and simplified habitat indices were assigned to all ranges of numbers, first produced by the raster calculation, to make the final product look better and the predictions of global warming effects on red spruce distribution convenient (Figure 4.2). RSHM showed the habitat suitability distribution map with distribution limit of red spruce at GSMNP. The habitat suitability map of RSHM informs relative habitat suitability; thus, the higher value means the higher probability of presence, higher density, better growth, and less probability of damages.

2.4. Model Evaluation

The Red Spruce Habitat Model (RSHM) result was compared with the vegetation map of red spruce obtained from the digital vegetation map for GSMNP developed by the Center for Remote Sensing and Mapping Science (CRMS), Department of Geography at the University of Georgia, funded by the U.S. National Park Service (NPS) for model evaluation (Figure 4.3). The evaluation processes included several steps, including reclassifications, generating random points, and Pearson's χ^2 statistics for a goodness of fit test. First, the indices of RSHM were reclassified, and new indices, ranging from 10 to 40, were assigned to make comparison convenient. An index value of 10 indicates absence of red spruce; 20, low habitat suitability; 30, medium habitat suitability; and 40, the highest habitat suitability. Then, 1000 random points were generated on RSHM and saved as a shapefile using Generate Random Point Tool of Hawth's Analysis Tools in ArcGIS 9.2 extension. The predicted suitability indices of RSHM and the original habitat information of the digital vegetation maps for GSMNP, including presence/absence and dominance of red spruce in vegetation communities, were collected at random points using Intersect Point Tool of Hawth's Analysis Tools in ArcGIS extension. Hawth's Analysis Tools is

mostly developed for ecological spatial modeling and applications and is designed to perform spatial analysis and functions that cannot be conveniently carried out by ArcGIS (<http://www.spataleecology.com/htools/tooldesc.php>). The original habitat information of red spruce on the random points was reclassified, and new indices ranging 10 to 40 were assigned based on presence/absence and dominance of red spruce. An index value of 10 indicates absence of red spruce; 20 denotes understory only; 30, third and second vegetation levels of overstory; and 40, dominant overstory vegetation based on information in the vegetation codes of Table 4.2. In reclassification, if two different vegetation categories overlapped at the same location, then the upper class was reflected in the index system. For example, when dominant vegetation overlapped with second or third-level vegetation, an index value of 40 was assigned for this habitat.

The collected information and index values assigned on the random points are shown in Appendix 6. Finally, the correspondence between predicted suitability and the original suitability were tested on the random points by Pearson's χ^2 statistics for goodness of fit (Equation (4.1)). This test was carried out in R 2.6.1., and R-programming and data for these tests are shown in Appendix 6. This goodness of fit test attempts to determine whether or not a significant discrepancy exists between the observed frequencies or values and the expected or predicted frequencies or values (Bhattacharyya and Johnson 1977). The null hypothesis of this test is that the observed frequencies or values correspond with the expected (or predicted) frequencies or values estimated by assumption, knowledge or a model. Therefore, if the *P-value* from this test is larger than 0.05 at the 5% significance level, then the observed frequencies or values correspond with the expected ones. For this study, the big-enough *P-value* (>0.05) says there is no

significant discrepancy between the predicted habitat suitability values of RSHM and the observed ones on the digital vegetation map for GSMNP. The Chi-square statistic (χ^2) is

$$\chi^2 = \sum_{i=1}^n \frac{(O_i - E_i)^2}{E_i} \quad \text{..... Equation (4.1)}$$

where O_i = observed values or frequencies, E_i = expected or predicted values or frequencies, and $i = 1, \dots, n$ indexes the total number of values of each of n variables.

2.5. Global Warming Effect on the Red Spruce Range at GSMNP

Global warming effects on the red spruce range at GSMNP were predicted based on the results of ARIMs in Chapter 3. In Chapter 3, the differences of red spruce growth between the period of 1980 to 1999 and 2080 to 2099 were predicted based on IPCC (2007) predictions, which showed the differences of temperature and precipitation between two periods – 3.6°C (median) increase of annual mean temperature, 3.8°C (median) increase of annual mean winter temperature, and 7% (median) increase of annual mean precipitation, with different change rates (10% increase, 0% increase, and 10% decrease) for air pollution (Chapter 3, Figure 3.6). In figure 3.6, red spruce growth at high elevation decreases with increased temperature and precipitation when air pollution increases but increases with either no change or decrease of air pollution. On the other hand, Figure 3.6 shows that red spruce growth at low elevations always decreases. Red spruce growth is barely affected by air pollution factors at low elevations, showing almost no difference in slopes of regression lines among figures (Figure 3.6).

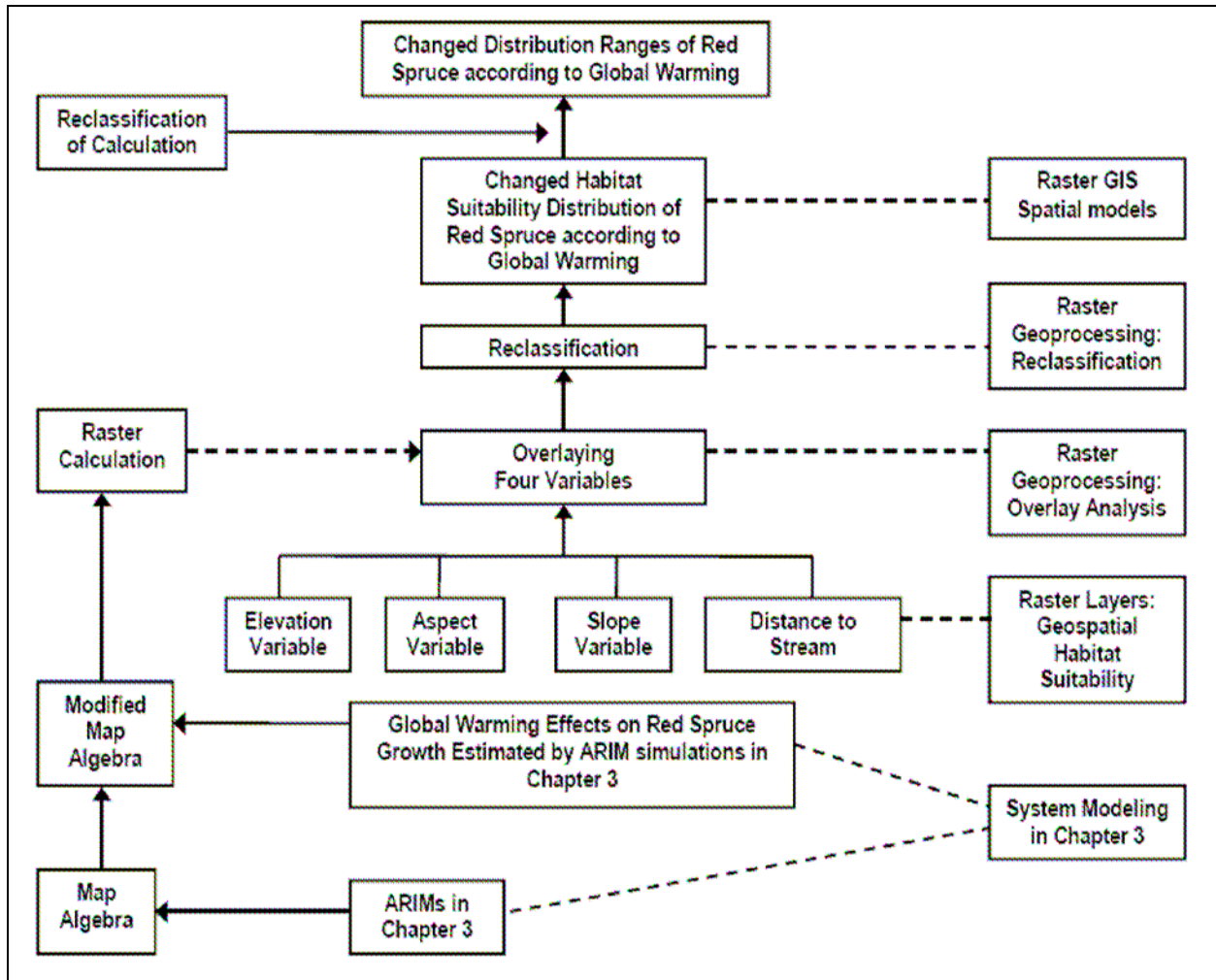


Figure 4.3. The procedure for estimating global warming effects on red spruce range at GSMNP. The solid line shows the prediction processes (from bottom to top), the dotted line toward the right side shows raster geoprocessing of raster GIS modeling and linkage between system modeling and GIS spatial modeling, and the dotted line toward the left side shows information sources and a tool for raster geoprocessing.

The predictions of global warming effects on the red spruce distribution range were implemented by four steps shown in Figure 4.3. For the predictions of range change, red spruce growth was computed using ARIMs for the period of 1940 to 2099 (Appendix 7). The computed growth amounts were averaged for the period of 1980 to 1999 and the period of 2080 to 2099

separately, and growth differences between these periods were calculated (Appendix 7). Then, these calculated differences were used to modify the map algebra used for the RSHM projection. Next, the modified map algebras were applied for raster calculations to overlay four geospatial habitat suitability variables, Elevation, Aspect, Slope, and Distance to Stream variables. The raster calculation results were reclassified and assigned by the same values used for the RSHM projection. This process visually showed variations of suitable habitat of red spruce according to global warming in interaction with air pollution. In addition, the total area of each habitat index value was calculated by multiplying the number of pixels by 900 m², which is the area of a pixel with 30 m spatial resolution, quantitatively showing suitable habitat changes along with global warming. Finally, the changes of red spruce distribution ranges were predicted by the changes of habitat suitability.

2.6. Data

The Red Spruce Habitat Model (RSHM) used the digital vegetation map for the Great Smokey Mountains National Park for the model evaluation process (Figure 4.5). Also, the current distribution range of red spruce, including the information of vegetation classes, was extracted from both overstory and understory vegetation maps (Figure 4.5, Table 4.1). The overstory vegetation consisted of dominant vegetation, second vegetation, and third vegetation. Those classes were classified by the relative abundance of red spruce in relation to other species. The Center for Remote Sensing and Mapping Science, Department of Geography at the University of Georgia, funded by the U. S. National Park Service (NPS), produced this digital vegetation map in 2004 (Madden et al. 2004). The U. S. NPS implemented accuracy assessment for the vegetation map and showed 80% accuracy overall, but nearly 100% accuracy for red

spruce (Jenkins 2007). What follows is summarized from Welch et al. (2002) and Madden et al. (2004). The digital vegetation map developed in vector format contains polygons for over 100 overstory and 70 understory plant communities, which are plotted to within approximately ± 5 to ± 10 m of their true ground locations. The overstory vegetation map in Figure 4.4 (a) was produced using 1:12,000-scale color infrared aerial photographs and the understory vegetation map in Figure 4.4 (b) 1:40,000-scale color infrared photographs. The digital vegetation map was created by a combination of photogrammetry, manual photointerpretation and GIS procedures. The photogrammetric process provides the passpoints with their *X*-, *Y*- and *Z*-coordinates, showing planimetric errors of approximately 2-3 m for *X*- and *Y*- coordinates and much less than 10 m for the *Z*-coordinate, driven from aerotriangulation to compute orientation parameters for the photos. Aerotriangulation is “the process of assigning ground control values to points on a block of photographs by determining the relationship between the photographs and known ground control points” (<http://www.rain.org/gis/data-classroom/data-formats-aerotriangulation.html>). The manual photointerpretation was ground-truthed by field work in cooperation with Nature Serve.

The digital stream map and the level II DEM (Digital elevation model) data, 30m spatial resolution, of GSMNP were used for developing geospatial habitat suitability variables in the process of RSHM development (Figure 4.6). The digital stream map was obtained from the U. S. Geological Survey (USGS) Digital Line Graph (DLG) and NPS, and the level II DEM from USGS (Figure 4.6). This error range of the USGS Level II DEMs is less than 10m for the *X* and *Y* coordinates and a few meters for the *Z* coordinate (Welch et al. 2002). The USGS digital stream map used to calculate Distance to Stream is one of large-scale USGS Digital Line Graph

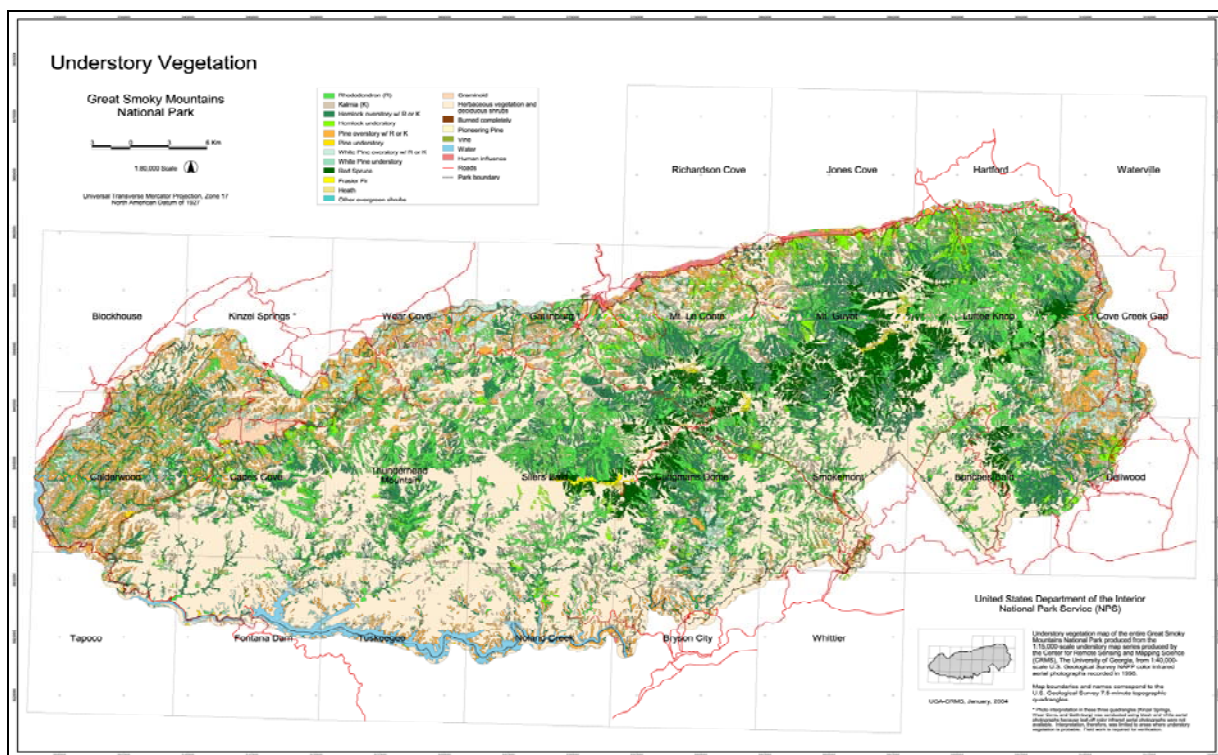
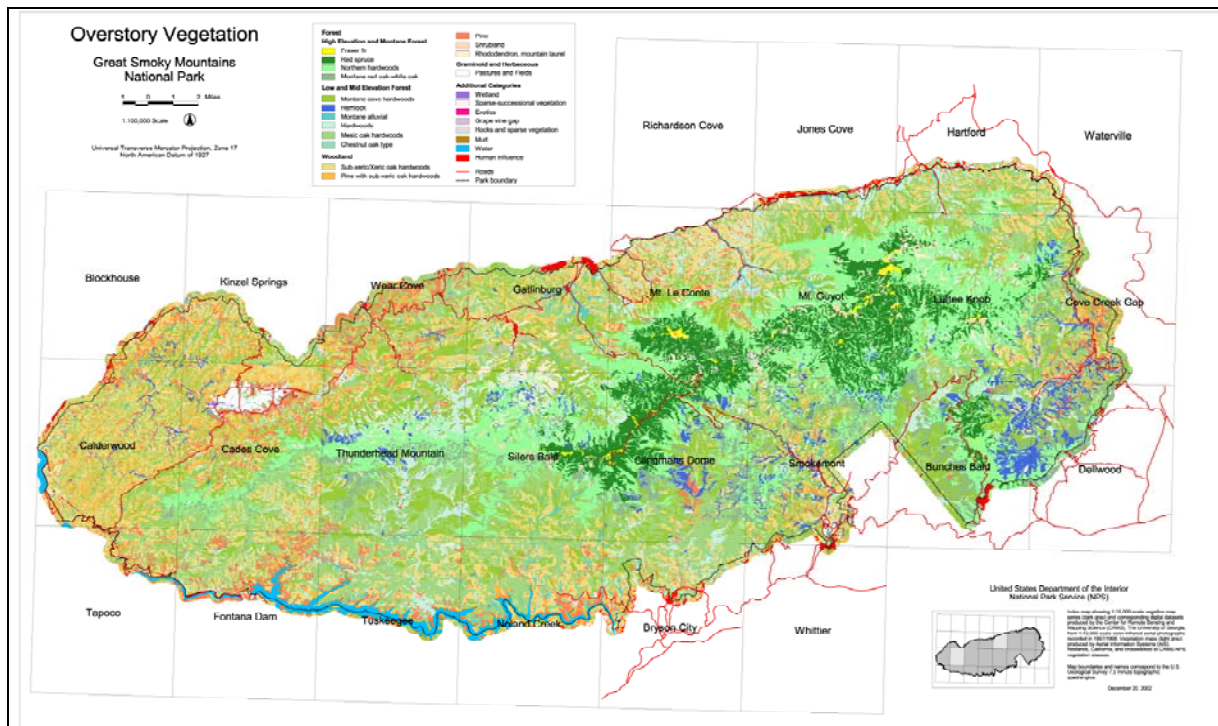
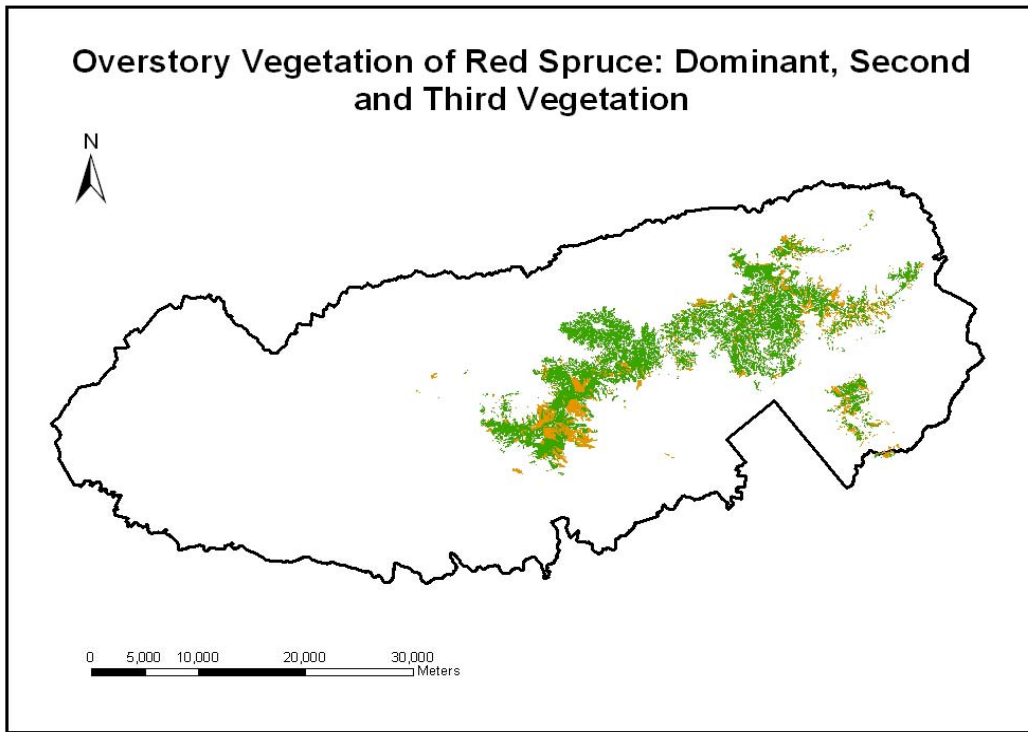


Figure 4.4. Digital vegetation map for the Great Smoky Mountains National Park: Overstory and Understory vegetation maps. The Center for Remote Sensing and Mapping Science, Department of Geography at the University of Georgia, funded by the U. S. National Park Service (NPS), produced this digital vegetation map in 2004 (Jordan 2002, Welch et al. 2002, Madden et al. 2004).

(a)



(b)

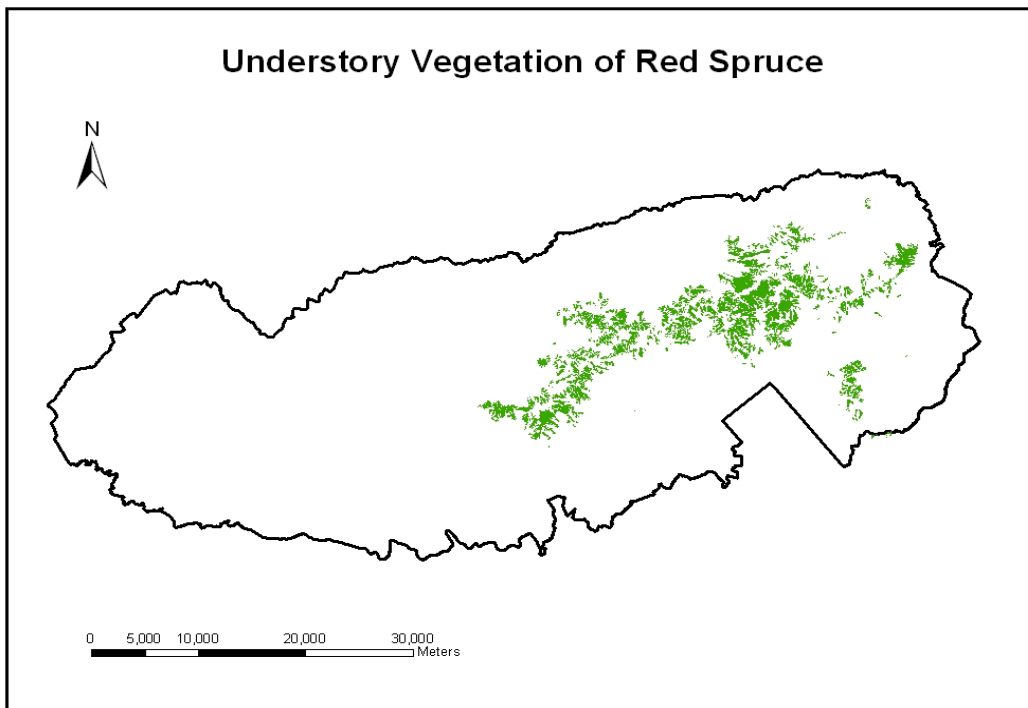


Figure 4.5. The red spruce vegetation maps extracted from both overstory and understory vegetation maps for GSMNP. The overstory map (a) included dominant vegetation (green color in the map), second-level vegetation (orange color), and third-level vegetation (red color). In the map the red color does not show well because third-level vegetation was mostly distributed under dominant or second vegetations. If different vegetation types were overlapped, the upper class is displayed in the map, obscuring lower classes. For example, if dominant vegetation overlapped with second-level vegetation, the map shows only the dominant vegetation, green color. The understory red spruce vegetation map (b) does not have second- and third-level vegetation but has only dominant vegetation including mixed classes. The codes for vegetation classes for understory and overstory are explained in Table 4.2 below. This information was used in the model evaluation process.

files (1:24,000-scale). The large-scale DLG files are digital vector representations of cartographic information and involve a certain error range (<http://eros.usgs.gov/guides/dlg.html#dlg1>). The large-scale DLG files (1:24,000-scale) were derived from the 1: 24,000-scale topographic quadrangle maps, and the data are manually digitized using equipment with a resolution of 0.001 inch (<http://eros.usgs.gov/guides/dlg.html>). An absolute accuracy of the DLG files is from 0.003 to 0.005 inch at scale (<http://eros.usgs.gov/guides/dlg.html>).

Table 4.2. The Vegetation Classification System of Red Spruce at GSMNP (Madden et al. 2004): Overstory (a) and Understory (b). Symbols: (-) designates an equal mix; (/) designates the first class listed as dominant (>50 percent) over the second class listed; x with class name means mixed; and “i” (implied) signifies that conditions are suitable for the presence of red spruce and it is reasonably believed to be found there. The symbol “p” indicating possible presence was included in the understory system, but not in the present study.

(a) Vegetation Classification System of Red spruce, Overstory

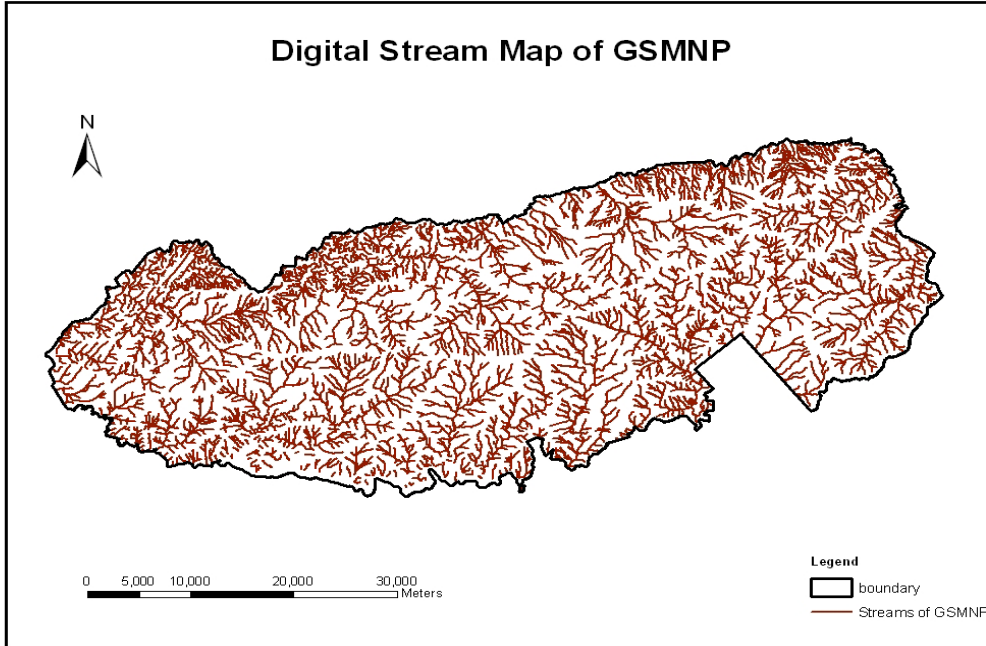
Vegetation type	Code
Red Spruce with Formerly Fraser Fir, Fraser Fir/ Red Spruce	(F)S, F/S
Red Spruce - Fraser Fir	S(F), S/F, S-F
Red Spruce - (Fraser Fir)/ Highbush Cranberry-Deciduous	S-F/Sb
Red Spruce-(Fraser Fir)/ Rhododendron	S-F/R

Red Spruce	S
Red Spruce/Southern Mountain Cranberry Low	S/Sb
Red Spruce/Rhododendron	S/R
Red Spruce - Birch – Southern Appalachian Northern Hardwood	S/NHxB, S-NHxB, NHxB/S, NHxB-S, S/NHx, S-NHx, NHx/S
Red Spruce/Southern Appalachian Mixed Hardwood, Acidic	S/NHxA
Red Spruce-Hemlock/Rhododendron	S/T, S-T, T/S, S-T/R

(b) Vegetation Classification System of Red spruce, Understory

Vegetation type	Code	Vegetation type	Code
Fir implied with spruce implied and shadow	Fi/Si/Sd	Spruce with hemlock and Rhododendron possible	S/T/Rp
Fir understory with spruce understory	Fu/Su	Spruce implied with fir medium density	Si/Fum
Fir understory light density with spruce implied	Ful/Si	Spruce implied with Rhododendron heavy density	Si/Rh
Fir understory light density with spruce understory light density	Ful/Sul	Spruce implied with Rhododendron medium density	Si/Rm
Fir understory medium density with spruce implied	Fum/Si	Spruce implied with hemlock and Rhododendron possible	Si/T/Rp
Rhododendron medium density with spruce implied	Rm/Si	Spruce understory	Su
Spruce with Fir understory	S/Fu	Spruce understory with fir understory	Su/Fu
Spruce with heath bald species	S/Hth	Spruce understory with Rhododendron heavy density	Su/Rh
Spruce with heath bald species medium density	S/Hum	Spruce understory with Rhododendron implied	Su/Ri
Spruce with Rhododendron heavy density	S/Rh	Spruce understory with Rhododendron light density	Su/RI
Spruce with Rhododendron implied	S/Ri	Spruce understory with Rhododendron heavy density	Su/Rm
Spruce with Rhododendron light density	S/RI	Spruce understory with Rhododendron possible	Su/Rp
Spruce with Rhododendron medium density	S/Rm	Spruce understory with hemlock understory	Su/Tu
Spruce with Rhododendron possible	S/Rp	Spruce understory light density with fir understory light density	Sul/Ful
Spruce with shrubs	S/Sb	Spruce understory implied	Sui
Spruce with hemlock and Rhododendron heavy density	S/T/Rh	Spruce understory implied with fir understory implied	Sui/Fui
Spruce with hemlock and Rhododendron implied	S/T/Ri	Hemlock understory with spruce understory implied	Sui/Tui
Spruce with hemlock and Rhododendron light density	S/T/RI	Hemlock with spruce and Rhododendron medium density	T-S/Rm
Spruce with hemlock and Rhododendron medium density	S/T/Rm	Hemlock understory implied with spruce understory implied	Tui/Sui

(a)



(b)

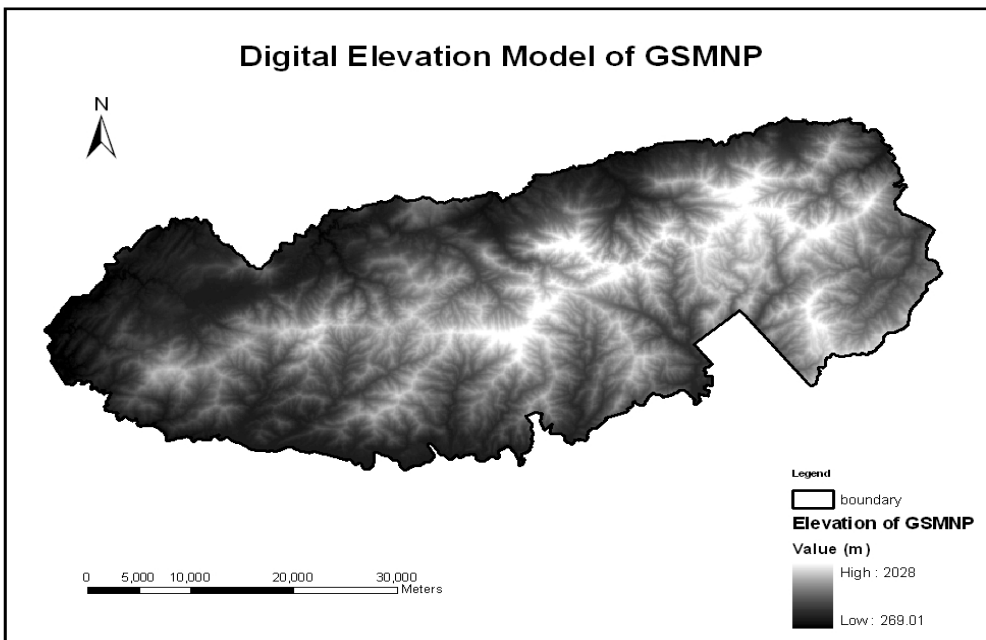


Figure 4.6. The digital stream map (a) and the level II DEM (Digital elevation model) data (b) of GSMNP. The digital stream map was obtained from the U. S. Geological Survey (USGS) Digital Line Graph (DLG) and NPS. The level II DEM was also developed by USGS. Both models were used for developing geospatial habitat suitability variables in the process of RSHM development.

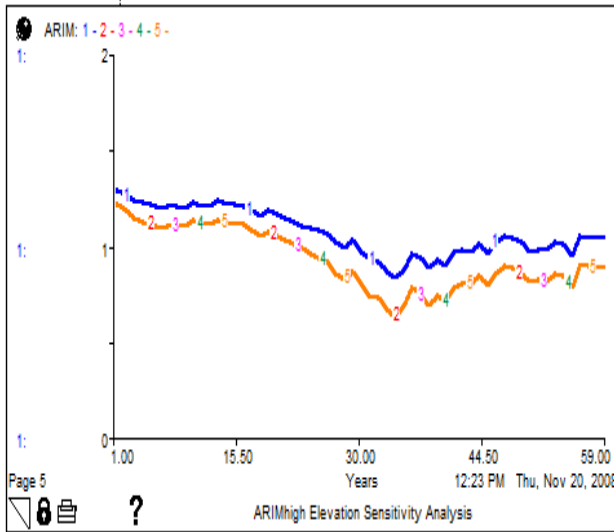
3. Results

3.1. RSHM: Suitable Habitat Conditions and Sensitivity Analyses

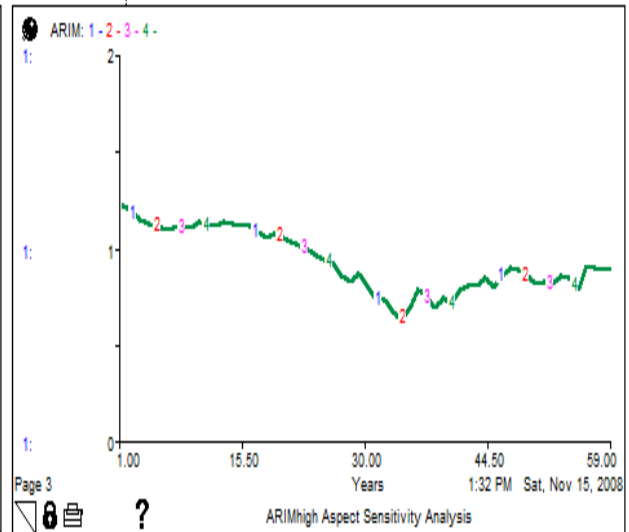
The Red Spruce Habitat Model (RSHM) was developed based on the suitable habitat conditions found in the red spruce Annual Radial Increment Model (ARIM) modeling (Chapter 3). ARIM_{high} showed a negative relationship with air pollution at high elevations, and ARIM_{low} showed a positive relationship with radiation and water availability and a negative relationship with air pollution at low elevations (Table 3.1, Table 3.2, Equation 3.7, and Equation 3.8 in Chapter 3). These relationships were applied as suitable habitat conditions for RSHM, assuming better growth of red spruce represents higher habitat suitability. Sensitivity analyses using ARIM_{high} and ARIM_{low} were employed to evaluate the relationship between topographical factors and red spruce growth. These analyses were performed by varying the values of topographical factors in order to convert suitable habitat conditions to geospatial information in Stella 9.0.3. The results of sensitivity analyses were shown in Figures 4.7.1–4.7.3, and the ARIM indices computed from these were displayed in Appendix 5. The ARIM indices computed for the period 1940 to 1998 were averaged, and the average value of each class was regarded as the representative value of red spruce growth for the class (Appendix 5, Table 4.3). These values were modified by multiplying by 10,000 for RSHM modeling in GIS (Table 4.3).

The sensitivity analyses well documented the effects of topographical factors on red spruce growth. The sensitivity analyses in ARIM_{high} showed that Aspect, Slope and Distance to Stream have no effects (Figure 4.7.1). This is because the equation developed in Chapter 3 for ARIM_{high} involves air pollution factor as an independent variable in explaining high-elevation growth. ARIM index values of the elevation factor in the sensitivity analyses are shifted down at 1800m (the number “2” in Figure 4.7.1 (a)). This is because 1800m is the cloud base at GSMNP

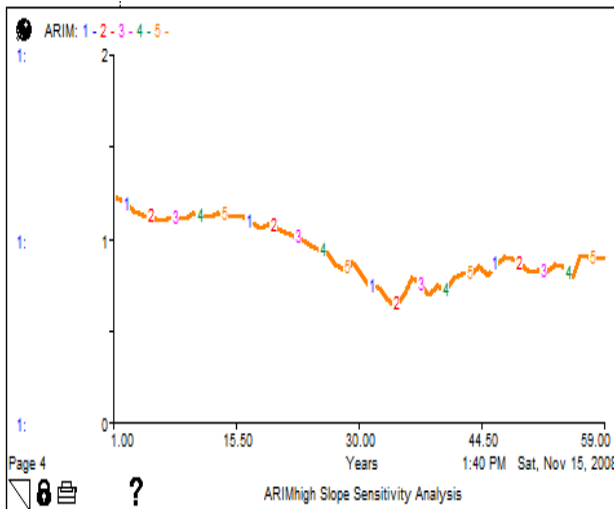
(a) ARIM_{high} sensitivity to Elevation



(b) ARIM_{high} sensitivity to Aspect



(c) ARIM_{high} sensitivity to Slope Stream



(d) ARIM_{high} sensitivity to Distance to

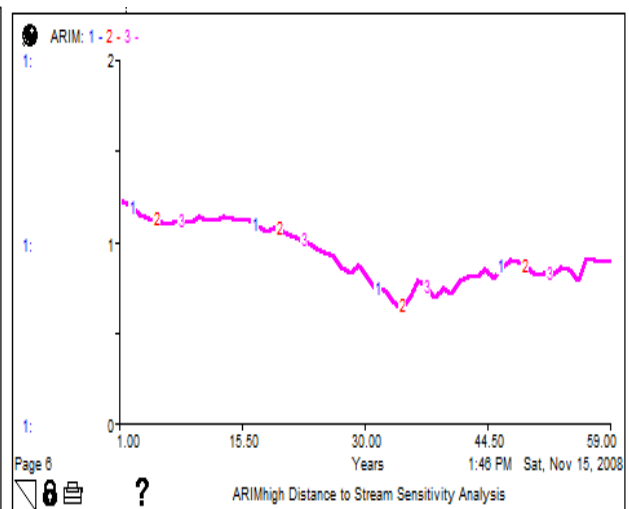
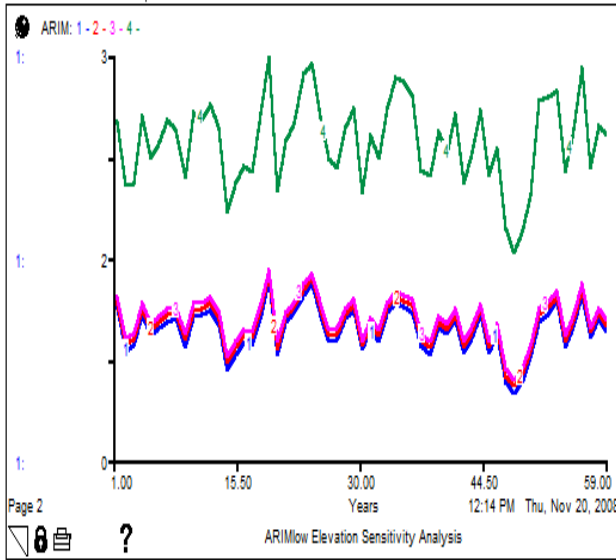
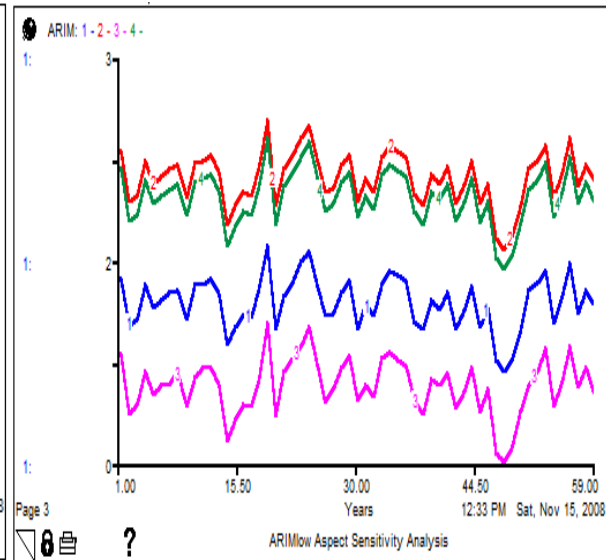


Figure 4.7.1. Sensitivity analysis results at high elevation using ARIM_{high} (>1850m). Figures (a) to (d) show the sensitivity results for Elevation (a), Aspect (b), Slope (c), and Distance to Stream (d) for ARIM_{high}. The ARIM_{high} index value ranged 0 – 2 (y axis). Red spruce growth for 59 years (x axis) was tested in this study. The number 1, 2, 3, 4, and 5 for lines in Figure (a) indicate elevation 1700, 1800, 1900, 2000, and 2100m, respectively. The numbers 1, 2, 3, and 4 for lines in Figure (b), showing ARIM sensitivity to Aspect, represent north, east, south, and west, respectively. The numbers for lines increase with increasing Elevation for Figure (a), Slope for Figure (c), and Distance to Stream for Figure (d). All figures except figure (a) showed that Aspect, Slope, and Distance to Stream do not have any significant effects on red spruce growth at high elevation. In Figure (a), the ARIM index was shifted down at elevation 1800m (the number “2”). This is because this elevation is the cloud-base in GSMNP; so, the upper elevations of 1800m were influenced by air pollution more than the lower elevations (Webster et al. 2004).

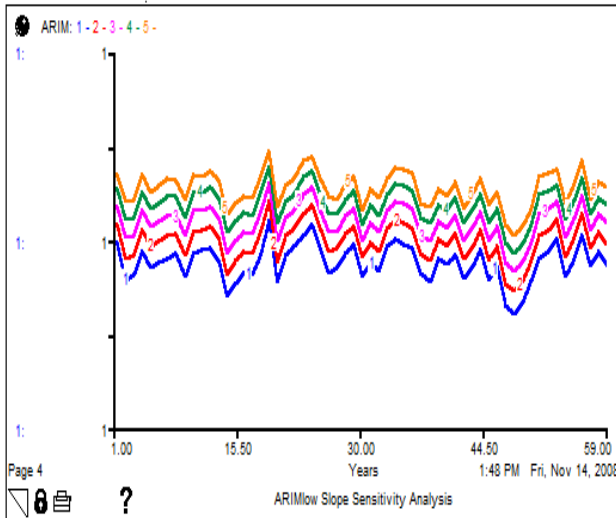
(a) ARIM_{low} sensitivity to Elevation



(b) ARIM_{low} sensitivity to Aspect



(c) ARIM_{low} sensitivity to Slope



(d) ARIM_{low} sensitivity to Distance to Stream

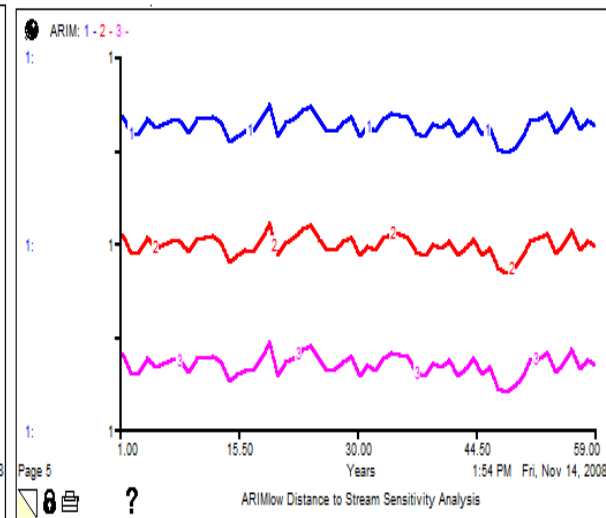
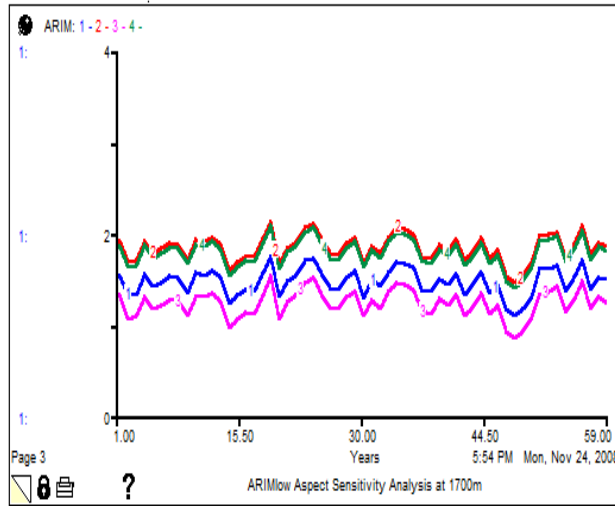
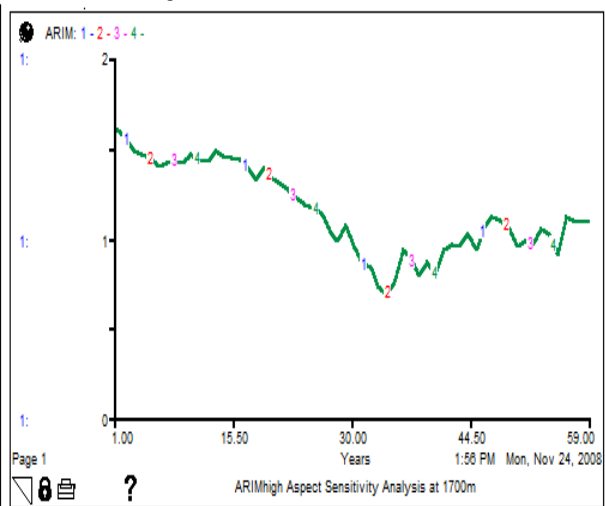


Figure 4.7.2. Sensitivity analysis results at low elevation using ARIM_{low} (1400 to 1650m). Figures (a) to (d) exhibit the sensitivity analysis results of Elevation (a), Aspect (b), Slope (c), and Distance to Stream (d) for ARIM_{low}. ARIM_{low} has an index value range 0 to 2 (y axis). Red spruce growth for 59 years (x axis) was tested in this study. The numbers 1, 2, 3, 4, and 5 for lines in Figure (a) indicate 1400, 1500, 1600, and 1700m respectively. All number in figure (a), (b), (c), and (d) indicate the same ranges of each variable explained in figure 4.7.1. All figures showed strong effects of topographical factors in red spruce growth at low elevations. In particular, the ARIM index in Figure (a) was shifted up at elevation 1700m (the number “4”). This is because this elevation is the elevation to divide the habitat of red spruce into two distinct habitats: those of low and high elevation.

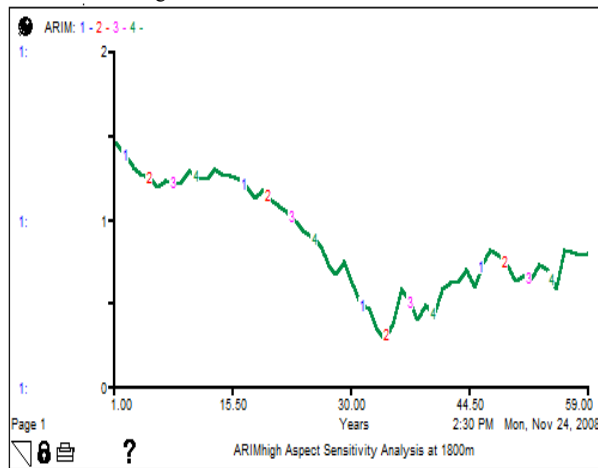
(a) ARIM_{low} sensitivity to Aspect at 1700m



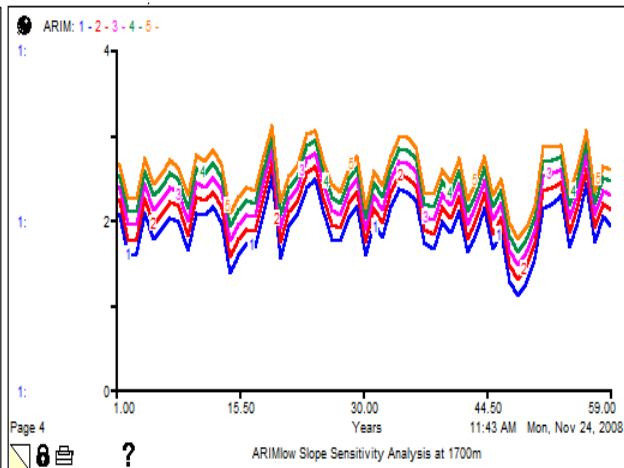
(b) ARIM_{high} sensitivity to Aspect at 1700m



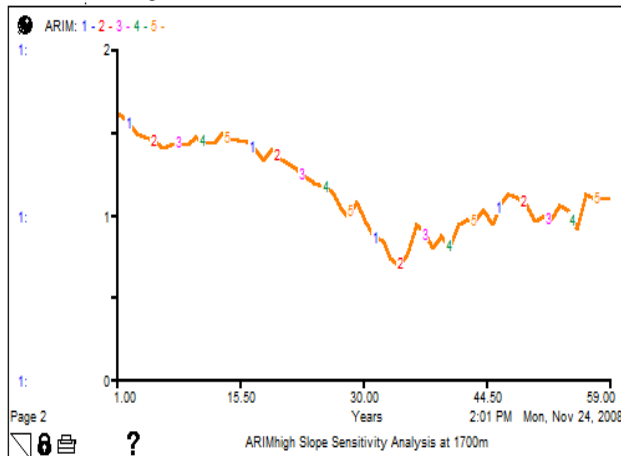
(c) ARIM_{high} sensitivity to Aspect at 1800m



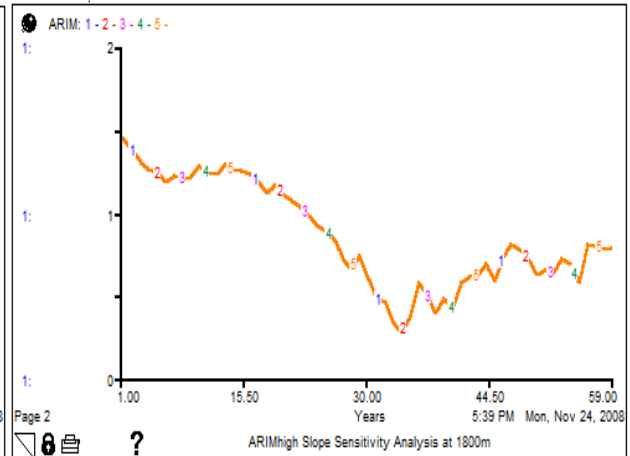
(d) ARIM_{low} sensitivity to Slope at 1700m



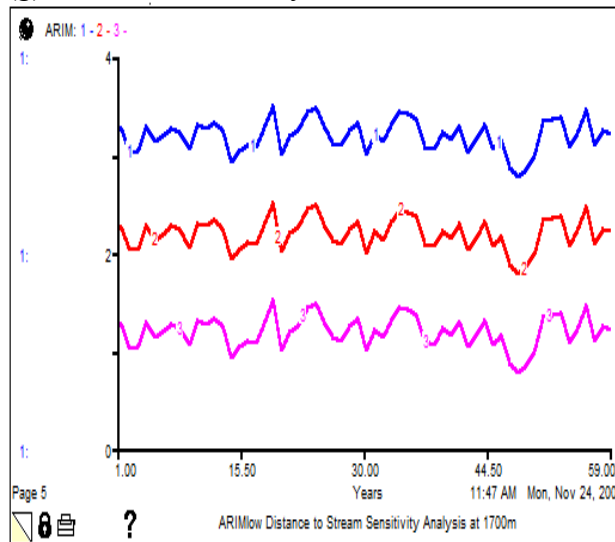
(e) ARIM_{high} sensitivity to Slope at 1700m



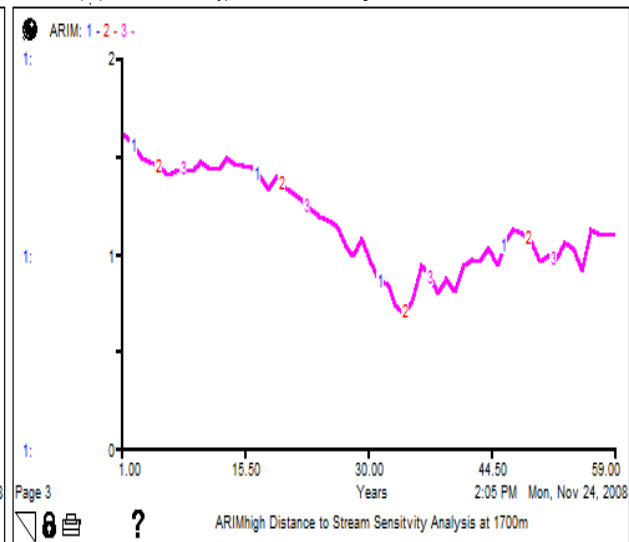
(f) ARIM_{high} sensitivity to Slope at 1800m



(g) ARIM_{low} sensitivity to DS at 1700m



(h) ARIM_{high} sensitivity to DS at 1700m



(i) ARIM_{high} sensitivity to DS at 1800m

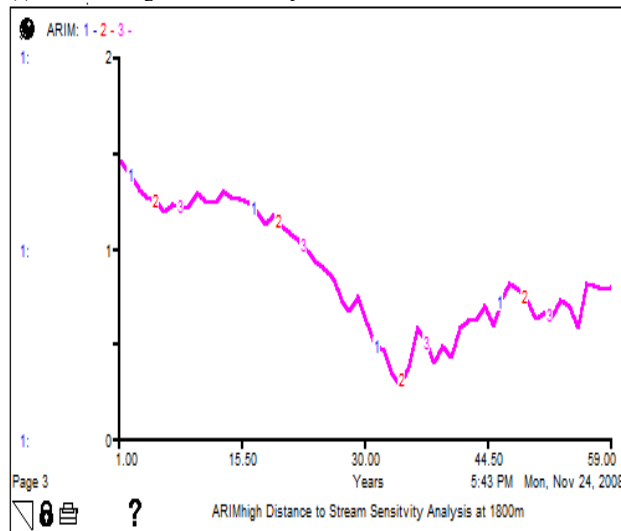


Figure 4.7.3. Sensitivity analysis results for the buffer zone (1650 to 1850m). Figures (a) through (i) exhibit results for Aspect (a), (b), and (c); Slope (d), (e), and (f); and Distance to Stream (g), (h), and (i). Figure (a), (d), and (g) were computed using ARIM_{low}, and the other figures were computed using ARIM_{high} to estimate the sensitivity of red spruce to all four factors in the buffer zone. The computed values at three elevations were averaged and applied for the buffer zone (shown in Appendix 5). The x-axis ARIM index values ranged 0 to 2. The x axis is time, 1–59 years. DS indicates Distance to Stream.

(Johnson and Lindberg, 1992). As a result, elevations above 1800m have much more effects of acidic rain and clouds than elevations below this altitude. However, ARIM_{high} represents elevations above 1850m, and Elevation sensitivity results for the range of 1900 to 2100m were used to defining red spruce habitat condition at high elevations (Table 4.3 (a)). Also, the sensitivity results of Aspect, Slope and Distance to Stream at 1900m were used for defining red spruce habitat conditions at high elevation. This is because the raw tree-ring data used for ARIM modeling represent elevation greater than 1900m. The tree-ring data were collected between 1911 and 2000m (Chapter 3, Webster et al. 2004). All computed index values are displayed in Appendix 5.

On the other hand, sensitivity analyses for ARIM_{low} showed strong topographic effects (Figure 4.7.2). The analyses showed: first, that habitat suitability is highest at east-facing and lowest at south-facing sites (Figure 4.7.2 (b)), second, that it increases with increasing Slope (Figure 4.7.2 (c)); third, that suitability increases with decreasing Distance to Stream at low elevations (Figure 4.7.2 (d)); and fourth, gradually increases with increasing Elevation, showing one shifting point at 1700m (the number “4”). In Figure 4.7.2(a), the shifting point originates from the definition of low-elevation and high-elevation habitat in ARIM modeling in Chapter 3. In ARIM modeling, 1700m, which is almost the middle of the elevation range 1400 – 2028m, was decided as the elevation to divide the habitats of red spruce into two distinct ones, low and high. The greatest difference between high- and low-elevation habitats revealed in ARIM modeling is precipitation. High-elevation habitat had much higher precipitation than low, and as a result, ARIM_{low} is very sensitive to water availability. Those features of ARIM_{low} caused the shifting point to be at 1700m in the Elevation sensitivity analysis. However, ARIM_{low} applied only below 1650m, and therefore Elevation sensitivity results in the range 1400 – 1650m were

used to define red spruce habitat condition at low elevation (Table 4.3 (a)). Also, the sensitivity results of Aspect, Slope and Distance to Stream at 1600m were used for defining red spruce low-elevation habitat conditions (Table 4.3 (b) and (c)). This is because the raw tree-ring data used for ARIM modeling were collected at elevations lower than 1600m, 1478 to 1548m (Chapter 3, Webster et al. 2004). All computed index values are shown in Appendix 5.

The buffer zone (1650 to 1850m) was created by averaging the indices estimated at 1700m from both ARIM_{low} and ARIM_{high} and at 1800m from ARIM_{high} in order to compensate for limitations of the raw tree-ring data (Figure 4.7.3, Appendix 5). The tree-ring data used for ARIM modeling explained the elevation ranges of lower than 1600m and higher than 1900m (Chapter 3, Webster et al. 2004). The ARIM indices of the period of 1940 to 1998 were averaged to decide the representative value for each class at all three elevation ranges: 1700m for ARIM_{low}, and 1700 and 1800m for ARIM_{high} (Appendix 5). In the buffer zone the indices at all three elevations were averaged for each variable (Table 4.3, Appendix 5). In addition, representative index values were multiplied by 10,000 for RSHM spatial modeling in GIS, as shown in Table 4.3.

Table 4.3. Summary of sensitivity analyses of red spruce growth for four geospatial variables. Elevation was classified into five ranges (a), Aspect four ranges (b), Slope five (c) and Distance to Stream three (d). The five ranges of Slope and three ranges of Distance to Stream were divided by natural breaks (Jenks system) of the Reclassify function in Spatial Analyst, ArcGIS 9.2, and the break ranges are displayed in parentheses in Tables (c) and (d). All index values of red spruce growth are averages for the period 1940 to 1998. For Distance to Stream (DS), the original index values were divided by two because the relatively big ARIM indices make RSHM unrealistically sensitive to the DS variable. Also, all ARIM indices were multiplied by 10000 for GIS modeling, as shown in the columns of ‘Modified ARIM Index’ in Table (a), (b), and (c).

(a)

	ARIM index	Elevations ×10,000 (Modified ARIM index)
Elevations (m)		
1400-1450	1.05	10500
1450-1550	1.07508	10750.8
1550-1650	1.09915	10991.5
1650-1850	1.28661	12866.1
>1850	0.93373	9337.3

(b)

Elevation	ARIM index			Aspect×10,000 (Modified ARIM index)		
	High Elevation (1900m)	Low Elevation (1600m)	Buffering Zone (1650 to 1850m)	High Elevation (1900m)	Low Elevation (1600m)	Buffering Zone (1650 to 1850m)
Aspect (°)						
North (0 – 45, 315 – 360)	0.93373	1.09915	1.28661	9337.3	10991.5	12866.1
East (45 – 135)	0.93373	1.56288	1.44226	9337.3	15628.8	14422.6
South (135 – 225)	0.93373	0.78847	1.18740	9337.3	7884.7	11874.0
West (225 – 315)	0.93373	1.49440	1.42028	9337.3	14944.0	14202.8

(c)

Slope (°)	ARIM index			Slope×10,000 (Modified ARIM index)		
	High Elevation (1900m)	Low Elevation (1600m)	Buffering Zone (1650 to 1850m)	High Elevation (1900m)	Low Elevation (1600m)	Buffering Zone (1650 to 1850m)
1 (0–11.6)	0.93373	0.88559	1.21808	9337.3	8855.9	12180.8
2 (11.7–19.5)	0.93373	0.99593	1.25345	9337.3	9959.3	12534.5
3 (19.6–26.5)	0.93373	1.09915	1.28661	9337.3	10991.5	12866.1
4 (26.6–33.1)	0.93373	1.19458	1.31729	9337.3	11945.8	13172.9
5 (33.2–62.3)	0.93373	1.28322	1.34559	9337.3	12832.2	13455.9

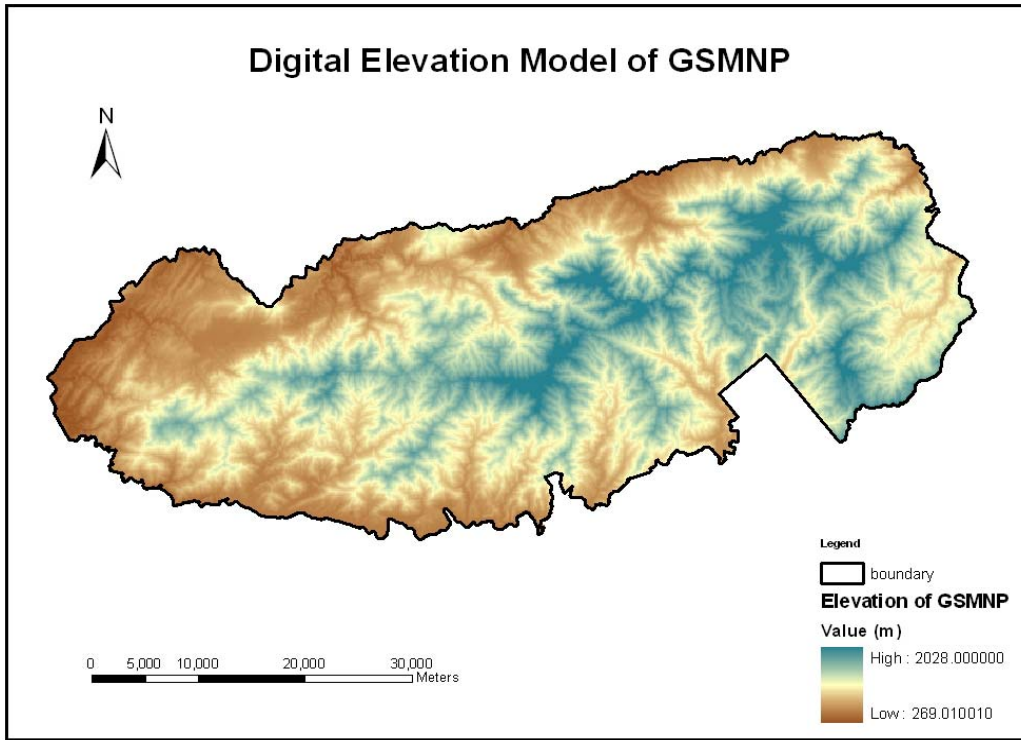
(d)

Distance to Stream (m)	ARIM index			Distance to Stream×10,000 (Modified ARIM index)		
	High Elevation (1900m)	Low Elevation (1600m)	Buffering Zone (1650 to 1850m)	High Elevation (1900m)	Low Elevation (1600m)	Buffering Zone (1650 to 1850m)
1 (0–149.3)	0.93373	1.68161	1.35585	9337.3	16816.1	13558.5
2 (149.4–482.3)	0.93373	1.11585	1.16701	9337.3	11158.5	11670.1
3 (482.4–979.9)	0.93373	0.54958	0.97839	9337.3	5495.8	9783.9

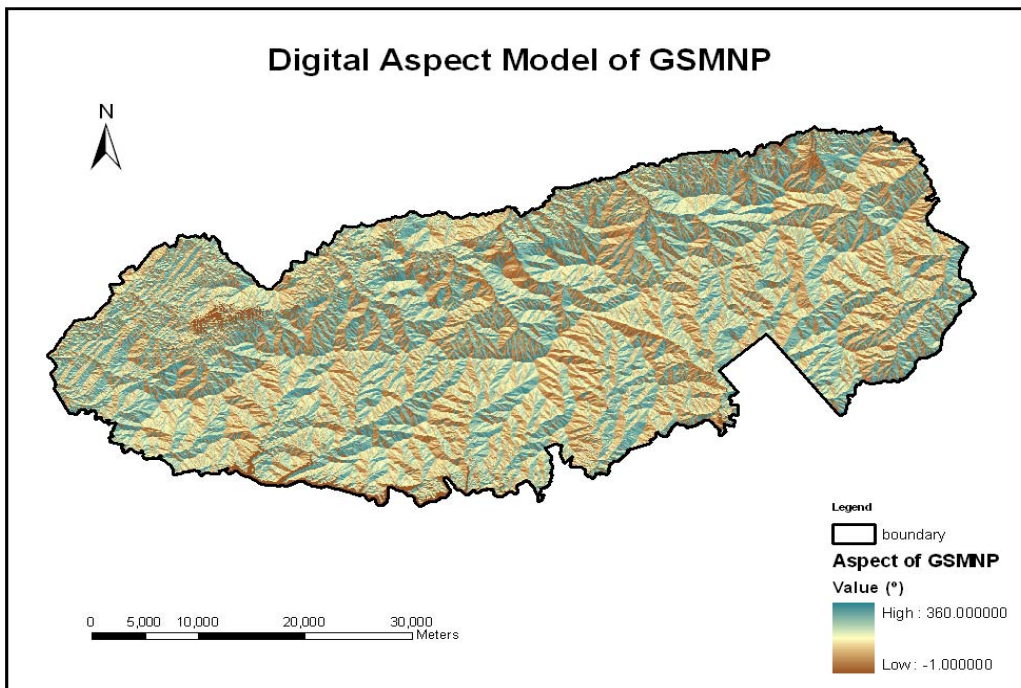
3.1. Digital Models for Four Variables

Digital Aspect Model and Digital Slope Model were calculated using USGS Level 2 DEMs in ArcGIS (Figure 4.8 (b) and (c)) and Digital Distance to Stream Model using USGS Digital Stream Map (Figure 4.8 (d)). The calculations show that the Elevation range of GSMNP is 269 to 2028m (Figure 4.8 (a)), the range of Aspect -1 to 360° (Figure 4.8 (b)), the range of Slope 0 to 62.31° (Figure 4.8 (c)), and the range of Distance to Stream 0 to 979.87m (Figure 4.8 (d)). All digital models consist of raster data to develop geospatial habitat suitability variables.

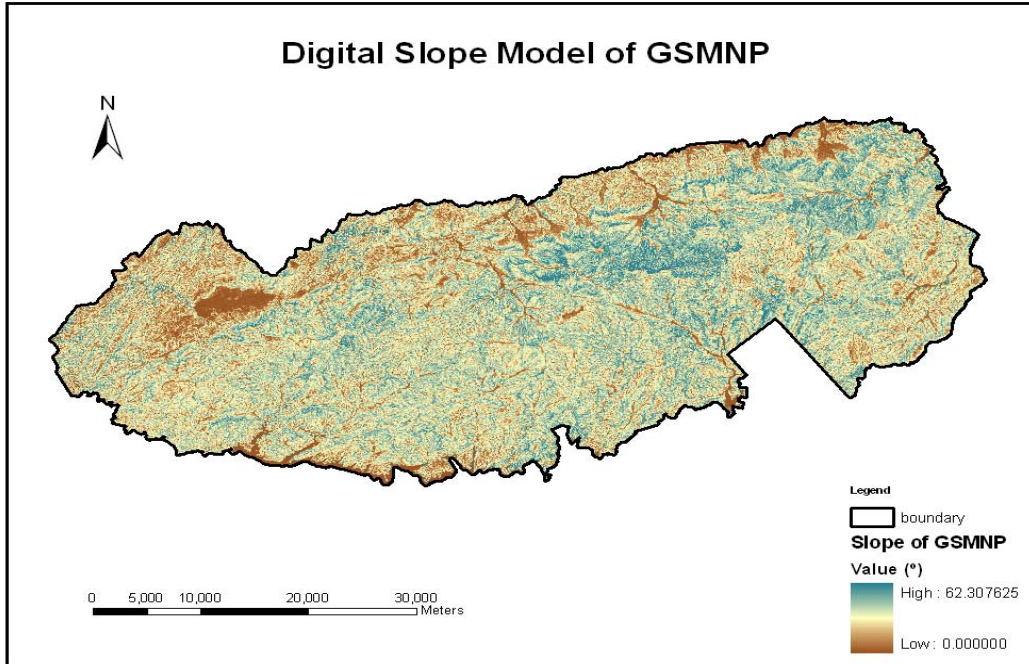
(a)



(b)



(c)



(d)

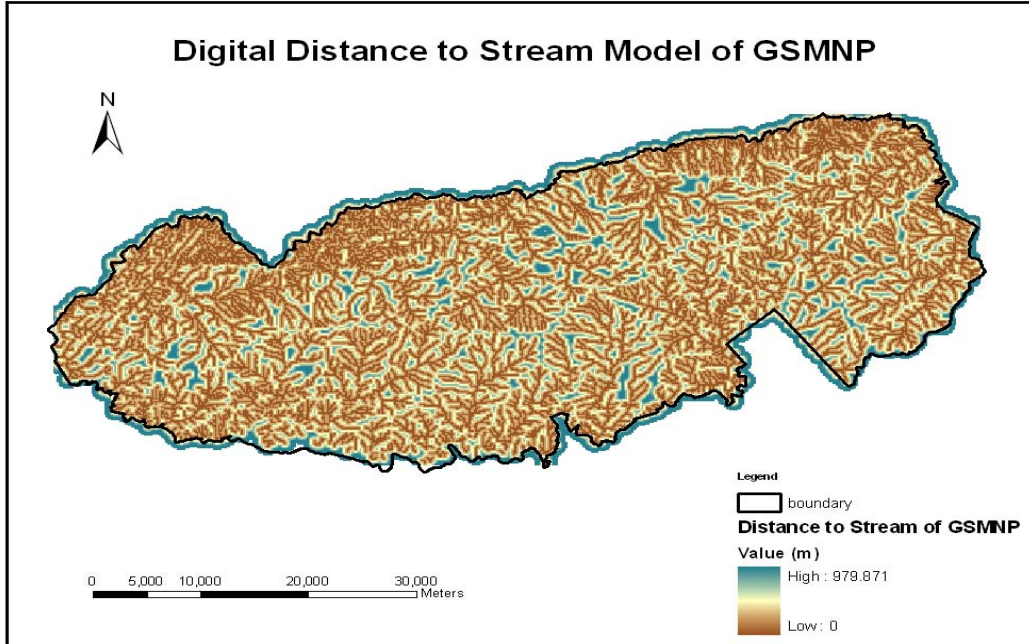
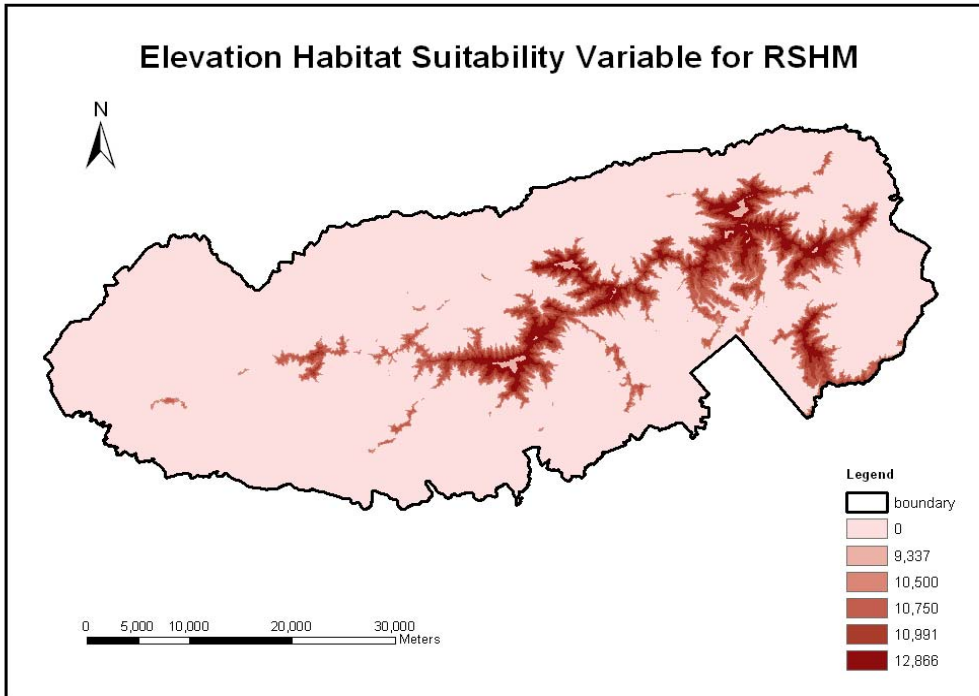


Figure 4.8. Digital Models of Four Variables: Digital Elevation Model (a), Digital Aspect Model (b), Digital Slope Model (c), and Digital Distance to Stream Model (d). Digital Aspect Model and Digital Slope Model were calculated using USGS Level 2 DEMs in ArcGIS (Figure 4.8 (b) and (c)) and Digital Distance to Stream Model using USGS Digital Stream Map (Figure 4.8 (d)).

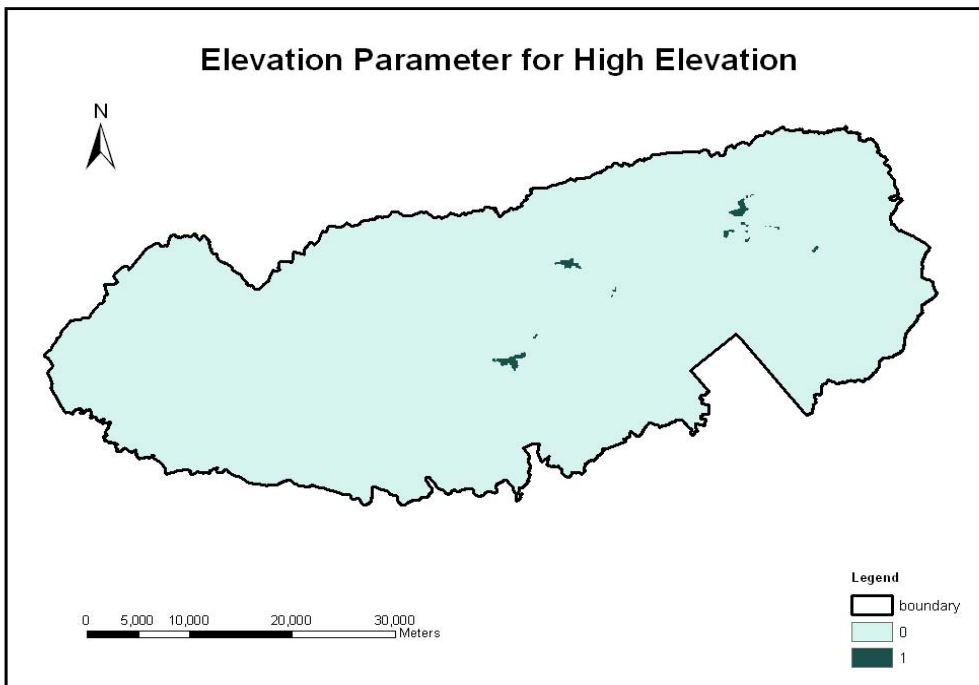
3.2. Geospatial Habitat Suitability Variables

Digital Aspect Model (*A*), Digital Slope Model (*S*), Digital Elevation Model (*E*), and Digital Distance to Stream Model (*DS*) were reclassified, and the modified suitability indices found in the sensitivity analyses (Table 4.3) were assigned in order to produce geospatial habitat suitability variables (from Figure 4.9.1 to Figure 4.9.4). Figure 4.9.1(a) shows the spatial distribution of indices in the right columns of Table 4.3 (a), representing the Elevation geospatial habitat suitability variable reclassified based on Table 4.3 (a). Figures (b), (c), and (d) show the elevation parameters for the other three geospatial suitability variables. These three elevation parameters were developed for three elevation ranges, low elevation (Ep_l), high elevation (Ep_h), and buffer zone (Ep_b). Those three elevation parameters were obtained by reclassifying DEM. For example, Ep_h (elevation parameter for high elevation) was obtained by reclassifying DEM into two groups, 1850 to 2028m and others, and a value of one was assigned for the range of 1850 to 2028 and zero for the others.

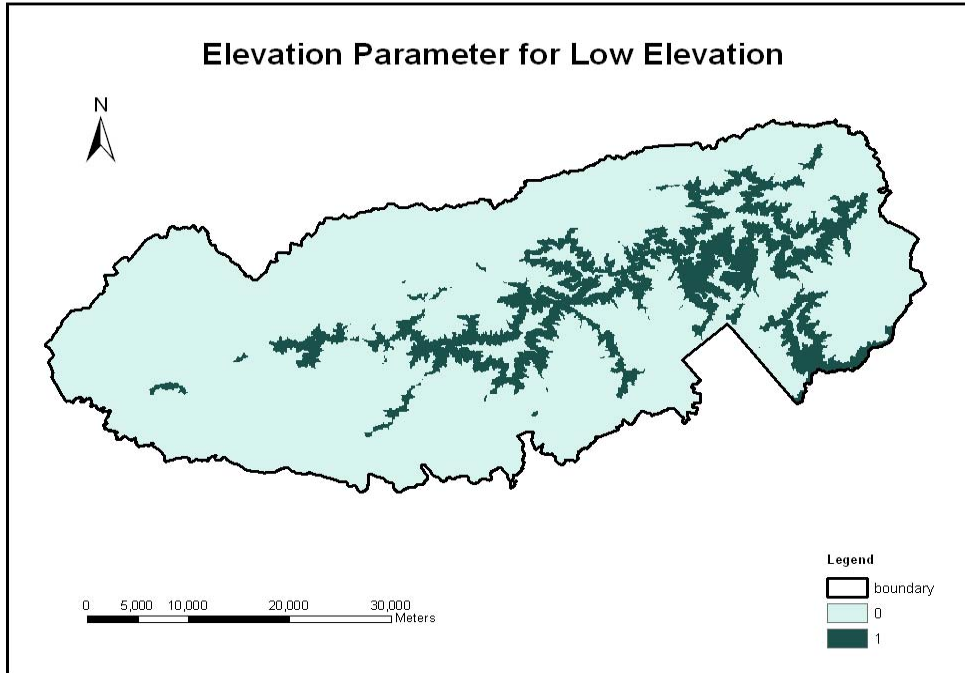
(a)



(b)



(c)



(d)

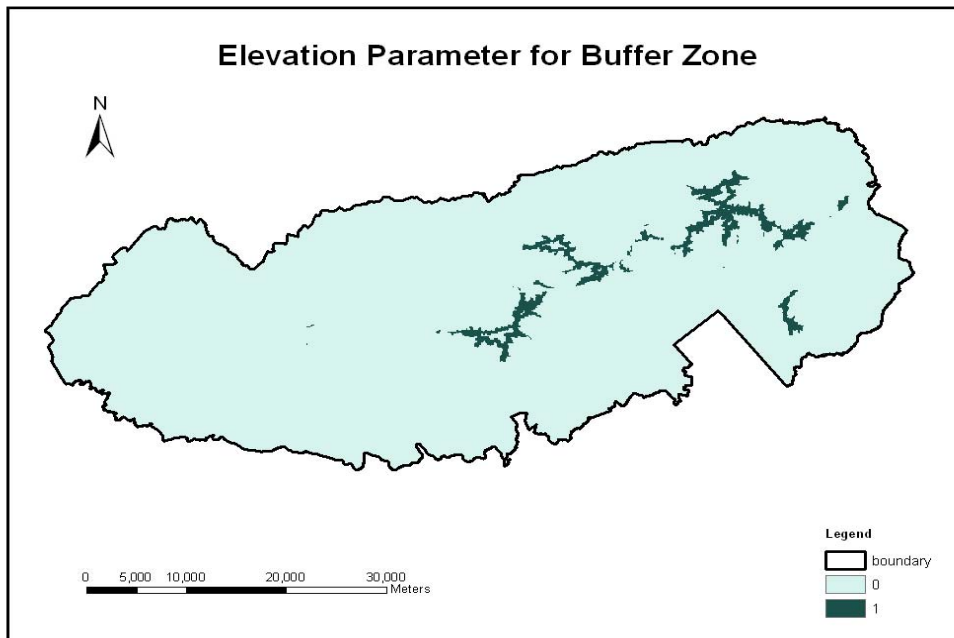
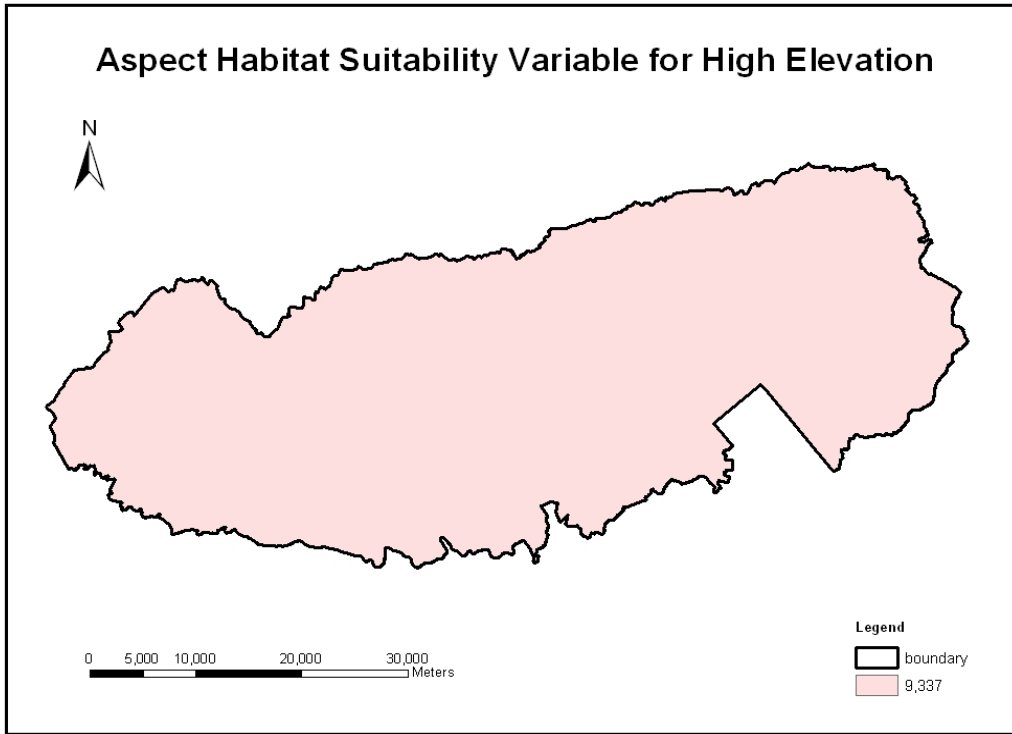


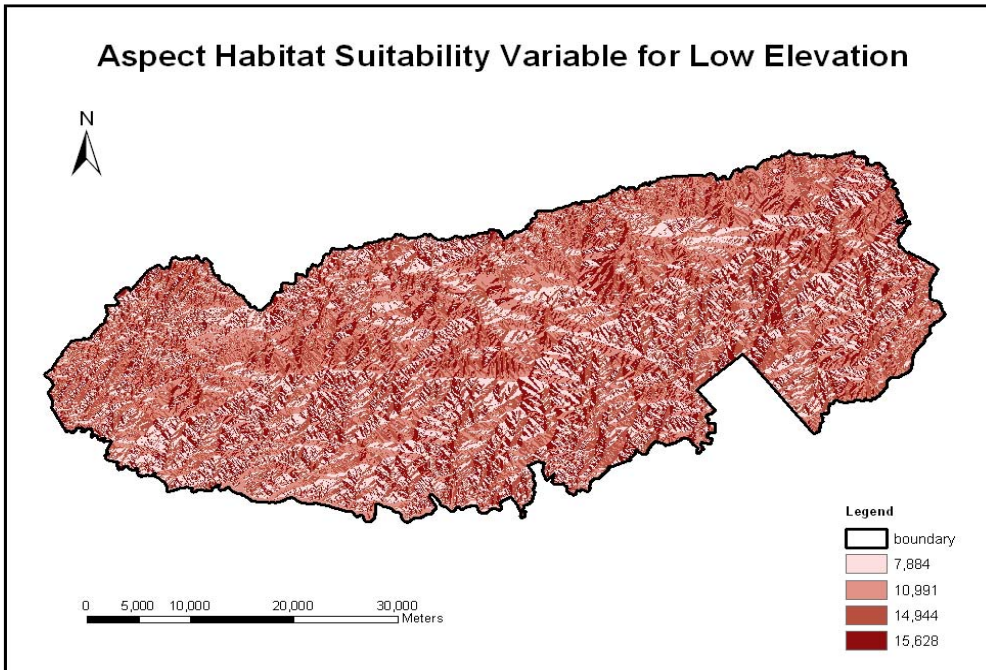
Figure 4.9.1. Elevation geospatial habitat suitability variable for RSHM and elevation parameters for Aspect, Slope, and Distance to Stream variables: Elevation (a), Ep_h (b), Ep_l (c), and Ep_b (d). Ep_h indicates the elevation parameter for high elevation, Ep_l that for low elevation, and Ep_b that for the buffer zone. All values in the figures do not have units because they are indices.

Figure 4.9.2, 4.9.3, and 4.9.4 showed geospatial habitat suitability variables: Aspect, Slope, and Distance to Stream, respectively. All variables were reclassified based on the ranges shown in the first columns of Table 4.3 (b), (c), and (d), and modified index values shown in the fifth to seventh columns of Table 4.3 (b), (c), and (d) were assigned as new attributes. Figure 4.9.2 shows the spatial distribution of habitat suitability indices in the first column of Table 4.3 (b), of Aspect geospatial variable at three elevation ranges: high elevation (>1850m, Figure 4.9.2 (a)), low elevation (1400 to 1650m, Figure 4.9.2 (b)), and buffer zone (1650 to 1850m, Figure 4.9.2 (c)). Figure 4.9.3 show the spatial distribution of indices from the first column of Table 4.3 (c), of the Slope geospatial habitat suitability variable at high elevation (Figure 4.9.3 (a)), low elevation (Figure 4.9.3 (b)) and buffer zone (Figure 4.9.3(c)). Figure 4.9.4 shows the spatial distribution of indices, in the first column of Table 4.3 (d), of Distance to Stream geospatial habitat suitability variable at high elevation (Figure 4.9.4 (a)), low elevation (Figure 4.9.4 (b)), and buffer zone (Figure 4.9.4 (c)). All four geospatial habitat suitability variables consist of raster layers for overlay analysis in GIS.

(a)



(b)



(c)

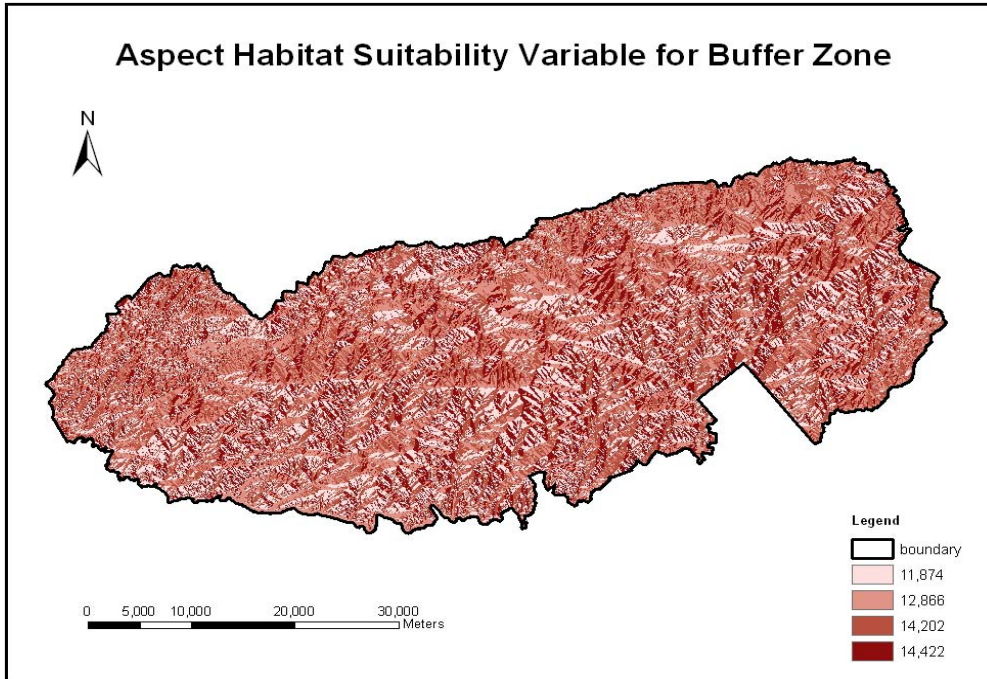
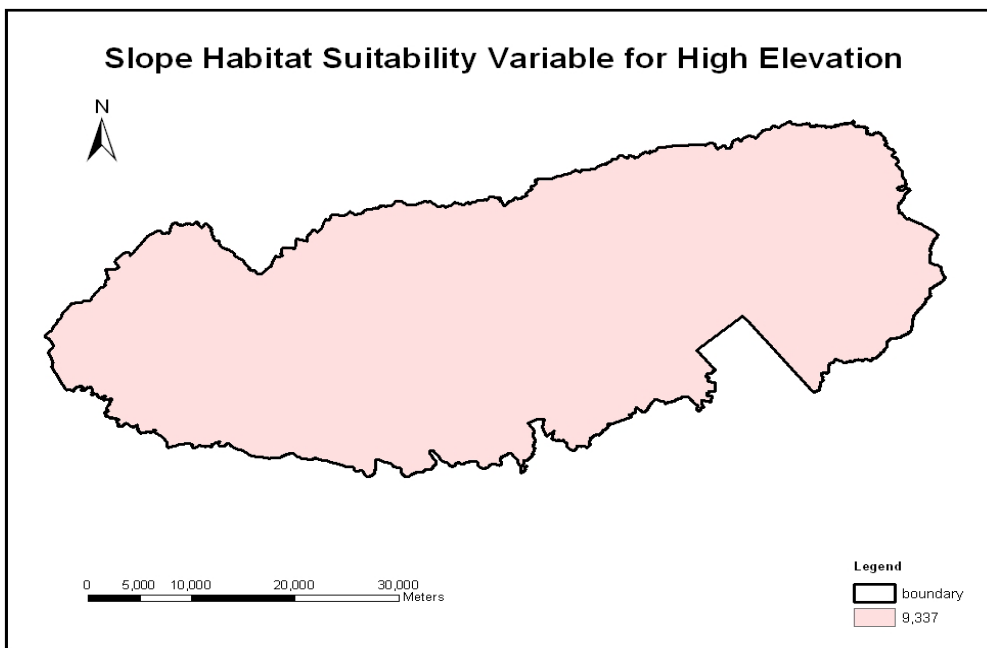
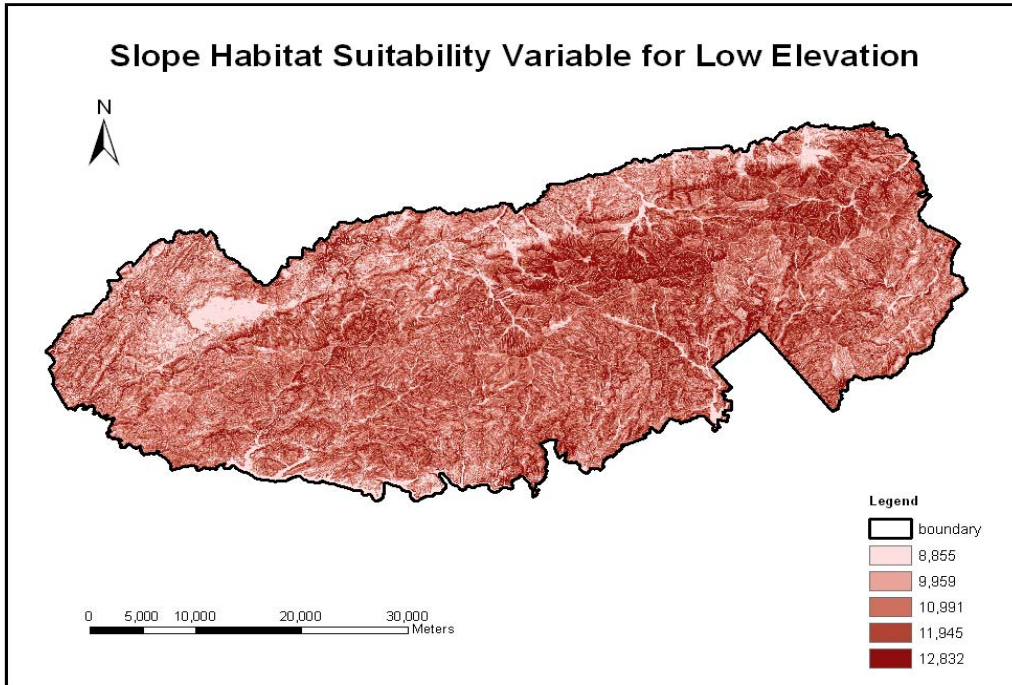


Figure 4.9.2. The spatial distribution of indices of Aspect geospatial habitat suitability variables at high elevation (a), low elevation (b), and buffer zone (c). All values in figures do not have units because they are indices.

(a)



(b)



(c)

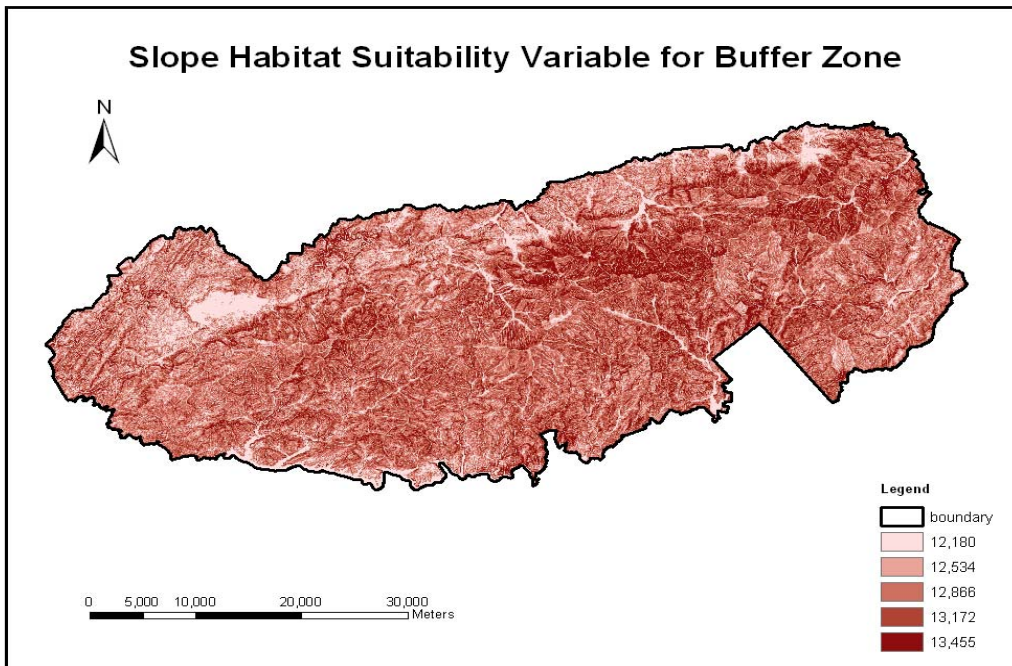
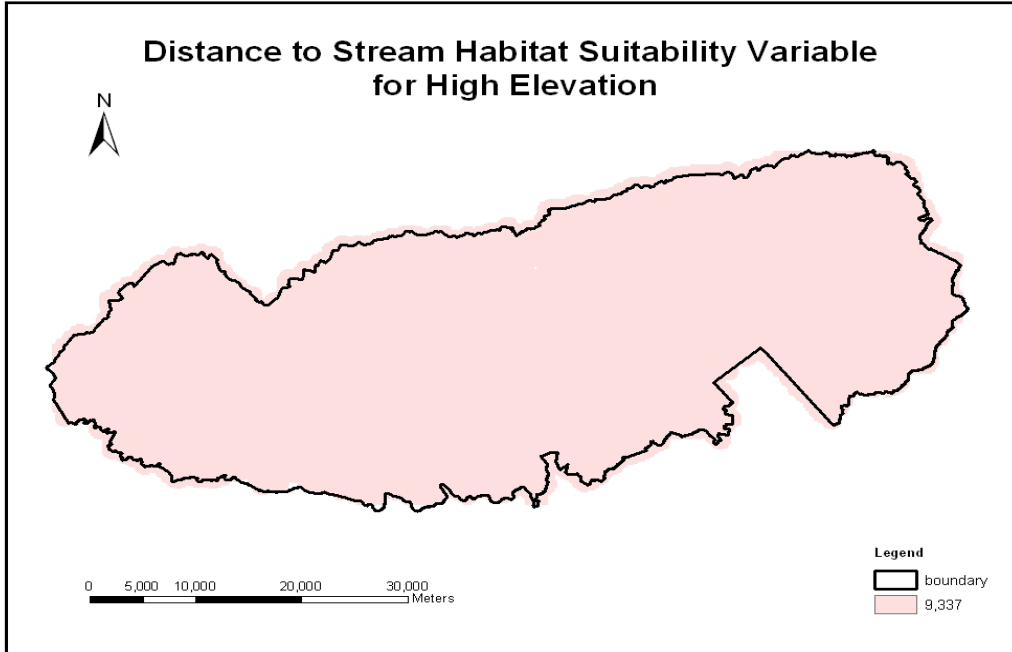
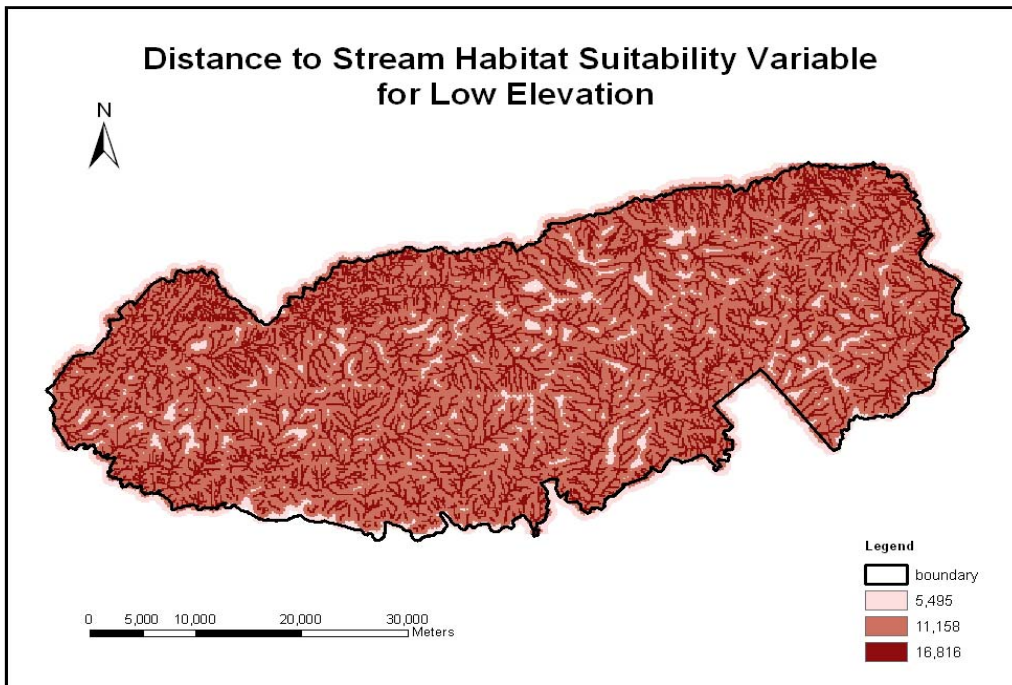


Figure 4.9.3. The spatial distribution of indices of Slope geospatial habitat suitability variables at high elevation (a), low elevation (b), and buffer zone (c). All values in the figures do not have units because they are indices.

(a)



(b)



(c)

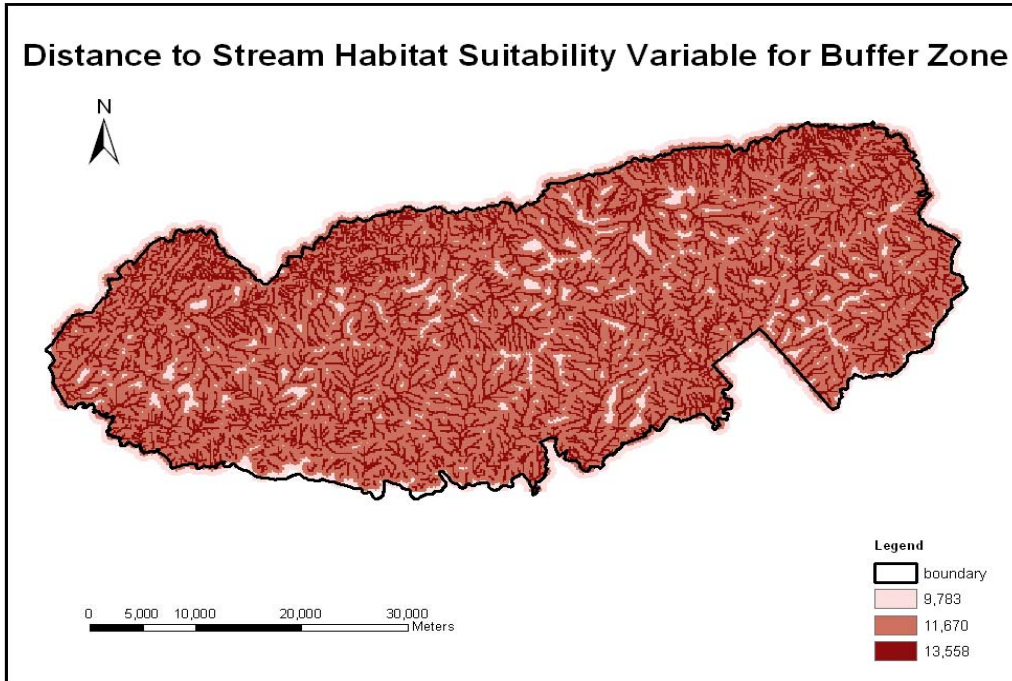


Figure 4.9.4. The spatial distribution of indices of Distance to Stream geospatial habitat suitability variables at high elevation (a), low elevation (b), and buffer zone (c). All values in the figures do not have units because they are indices.

3.3. RSHM and Model Evaluation

The geospatial habitat suitability variables were integrated using overlay analysis to produce RSHM (Red Spruce Habitat Model) (Figure 4.10). Overlay analysis was implemented by the Raster Calculation Function of Spatial Analyst in ArcGIS 9.2. This raster calculation overlaid raster layers consisting of four geospatial habitat suitability variables: Elevation, Aspect, Slope, and Distance to Stream based on equation (4.2), map algebra. In equation 4.2, Elevation was added once, but Aspect, Slope, and Distance to Stream were added for each elevation zone by multiplying elevation parameters, Ep_h , Ep_l , and Ep_b . Then, all added values were divided by

the number of variables, four, in order to keep the value range of the final product similar to the original indices shown in Table 4.3.

Habitat Suitability index of RSHM

$$= (E + ((A_h + S_h + DS_h) * Ep_h) + ((A_l + S_l + DS_l) * Ep_l) + ((A_b + S_b + DS_b) * Ep_b))/4$$

..... Equation 4.2)

Here, *A* is Aspect, *S* is Slope, *DS* is Distance to Stream, *E* is Elevation, *Ep* Elevation parameter: *Ep_h* high elevation, *Ep_l* low elevation, and *Ep_b* buffer zone. The capitalized italic letters indicate variables and the subscribed italic letters locations. For example, *A_h* is Aspect at high elevation.

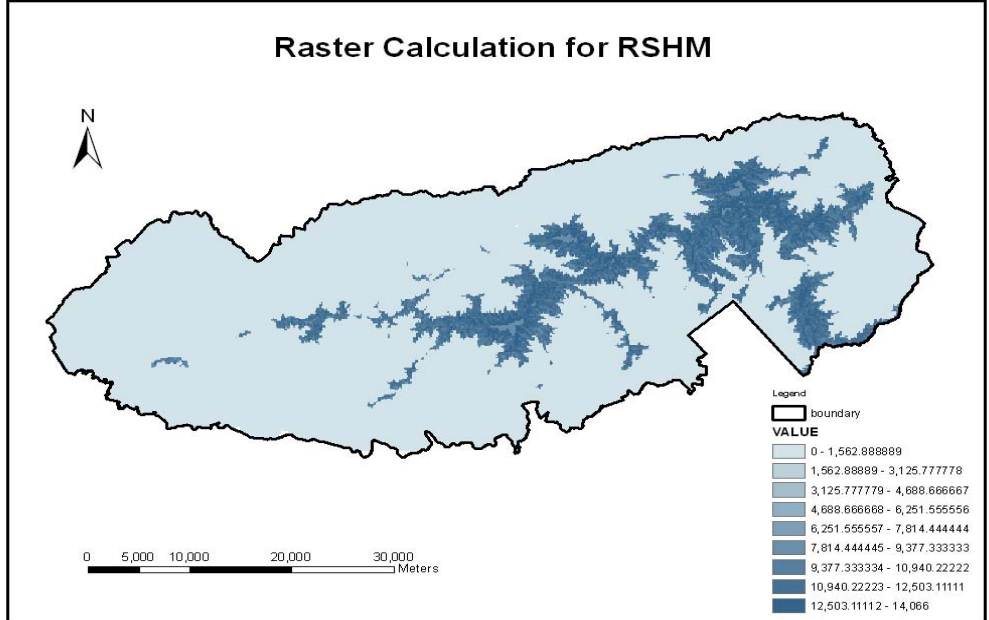
The final product of raster calculation is shown in the first column of Table 4.4 and Figure 4.10 (a). It was reclassified by the Natural Break (Jenks) system in the Reclassification function of Spatial Analyst, ArcGIS 9.2 (the second column of Table 4.4). Then, new index values were attributed to the ranges divided by the Natural Break (Jenks) system (the third column of Table 4.4, Figure 4.10 (b)). The highest value of each range was chosen for the new attribute value, but the ranges 11289 – 12652, and 12652 – 14066 were given the average value (13359) of 12652 and 14066 in order to simplify the habitat suitability ranges: low suitability (9617), medium suitability (11289), and high suitability (13359). The index value of zero indicates the absolute absence of red spruce at elevations below 1400m, and the value of 9617 indicates the lower probability of presence and lower density and the higher probability of mortality. 9617 includes all habitat suitability index values lower than 9617, including the index of zero, at elevations higher than 1400m; therefore, some areas with the indices of zero or near-

zero do not have red spruce (Table 4.4). This is because the equation for raster calculation treated the elevations below 1400m as zero by multiplying the elevation parameters, Ep_h , Ep_l , and Ep_b . For example, Ep_l assigned zero values to all areas below 1400m. The value of 11289 indicates a lower probability of presence, lower density, and higher mortality rate than the value of 13359 and higher probability of presence, higher density and lower mortality rate than the value of 9617. The value of 13359 represents the most suitable habitat condition for red spruce in RSHM.

Table 4.4. The results of raster calculation and reclassification. The final product of raster calculation is shown in the first column. It was reclassified by the Natural Break (Jenks) system in the Reclassification function of Spatial Analyst, ArcGIS 9.2 (second column). The third column shows the new attribute values for the ranges divided by the Natural Break (Jenks) system.

Raster Calculation	Reclassification	
Raster Calculation Result	Reclassified by the Natural Break (Jenks)	New Attribute Values for RSHM
0 - 1,562.8	0	0
1,562.9 - 3,125.8	0 - 9617	9617
3,125.9 - 4,688.7	9617 - 11289	11289
4,688.8 - 6,251.6	11289 - 12652	13359
6,251.7 - 7,814.4	12652 - 14066	13359
7,814.5 - 9,377.3		
9,377.4 - 10,940.2		
10,940.3 - 12,503.1		
12,503.2 - 14,066		

(a)



(b)

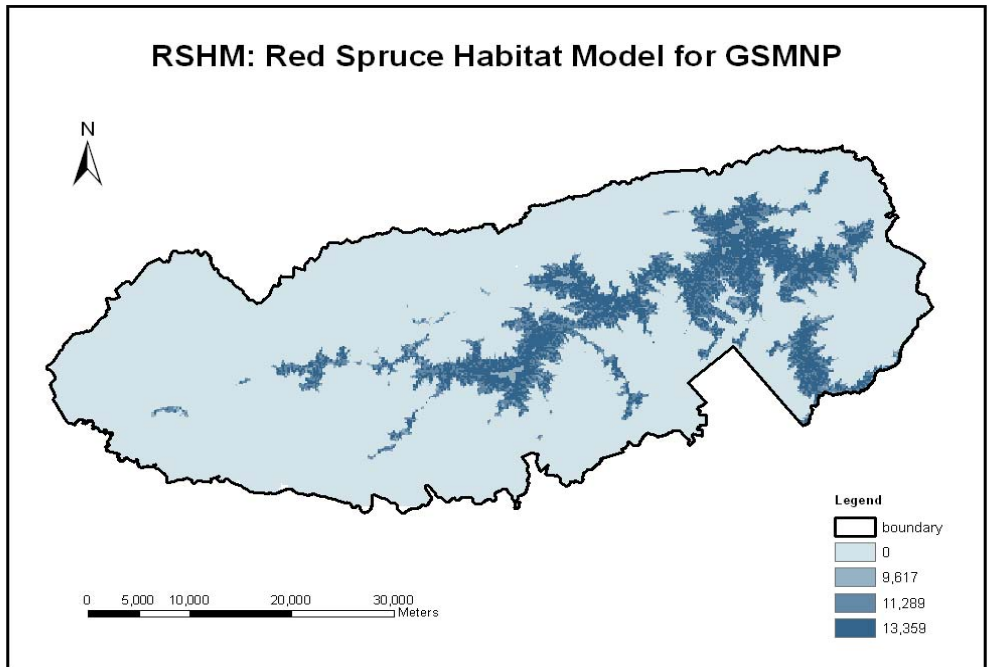


Figure 4.10. The result of raster calculation (a) and the final product of RSHM (b). The highest value of each range was chosen for the new attribute values (new indices) for each range or class, but the ranges of 11289 – 12652 and 12652 – 14066 were expressed by the average value (13359) of 12652 and 14066 in order to simplify the habitat suitability ranges: low suitability (9617), medium suitability (11289) and high suitability (13359).

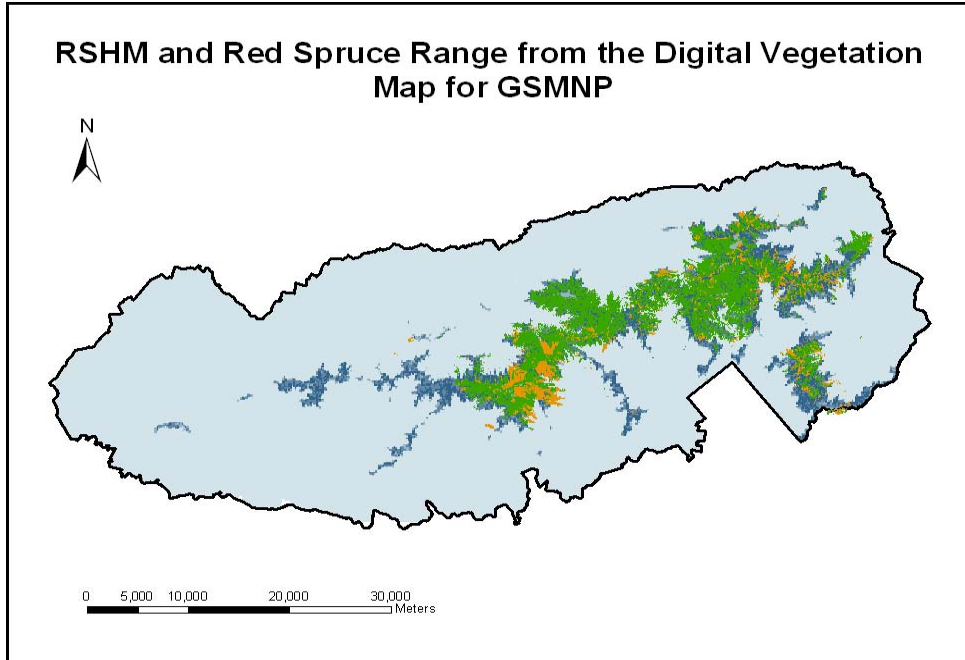
The Red Spruce Habitat Model result (RSHM) was compared with the red spruce vegetation maps of NPS (Figure 4.11), overstory and understory, for evaluating RSHM. For comparison, 1,000 random points were generated on RSHM (Figure 4.11 (b)). The RSHM index values and vegetation information were collected at these random points, and the new index values were assigned to both for a quantitative comparison (Appendix 6). For this process, red spruce vegetation was reclassified into three classes based on forest types. This reclassification was based on the assumption that red spruce dominated forests represented the most suitable habitat conditions for red spruce. Index values of 10 were assigned for no red spruce, 20 for the red spruce understory forests, 30 for second and third vegetations of overstory forests, and 40 for the red spruce-dominated overstory forests (Appendix 6). In reclassification, if two different vegetation types overlapped at the same location, then the upper class was reflected in the index system. For example, when dominant vegetation overlapped with second or third vegetation, an index value of 40 was assigned for this habitat. The result of RSHM was also reclassified to assign new index values in the range 10 to 40 (Appendix 6). Range10 represented absence of red spruce, 20 the index 9617, 30 the index 11289, and 40 the index 13359 (Appendix 6).

The correspondence between index values of RSHM and the Digital Vegetation Map for GSMNP was tested by Pearson's χ^2 goodness of fit test. The result showed $\chi^2 = 865.8151$, df (degree of freedom) = 999 and p -value = 0.999, indicating that hypothesis H_0 , observed values or frequencies correspondent to expected or predicted values or frequencies, was not significantly rejected by the random points data. Therefore, the habitat suitability distribution predicted by RSHM significantly corresponds to that on the Digital Vegetation Map for GSMNP. This result is also supported by the visual contrast shown in Figure 4.11 (a). However, in Figure 4.11, the some of western areas of GSMNP showing suitable habitats in RSHM do not have any red

spruce vegetation. This is due to factors such as dispersal, competition between co-existing species, and physical environmental conditions not considered in ARIM and RSHM, such as soil types. In general, the concept of a "suitable habitat" in this work does not necessarily mean a realized habitat. There is not yet sufficient literature information to explain the reasons for red spruce absence from areas of suitable habitat.

In conclusion, the Red Spruce Habitat Model (RSHM) showed lowest habitat suitability (9617) at high elevation habitats (1850 to 2028m); medium suitability (11289) at habitats located on south-facing, gentle slopes far from streams at low elevation (1400 to 1650m); and highest suitability (13359) for habitats located at higher, east-facing slopes closer to streams at low elevation (1400 to 1650m) and for all habitats of the buffer zone (1650 to 1850m) (Figure 4.10). RSHM therefore well explained the red spruce distribution range, including both presence and absence of red spruce at GSMNP (Figure 4.11 (a)). As relationships between habitat suitability levels and vegetation associations were considered, the index of 13359 mostly represented red spruce dominated vegetation and 11289 more second and third vegetations of red spruce than 13359 (orange and yellow colors in the map) (Figure 4.11 (a)). In addition, absence of red spruce increased with decreasing habitat suitability. The index of zero represented red spruce absence at elevations below 1400m and was involved in the index of 9617 at elevations above 1400m. The index value of 9617 covered habitat suitability ranges of zero to 9617; therefore, it relatively involved more absent areas than 11289 and 13359. The areas of 9617 are shown in the top areas of Figure 4.11 (a) as the light blue colored areas surrounded by green colors.

(a)



(b)

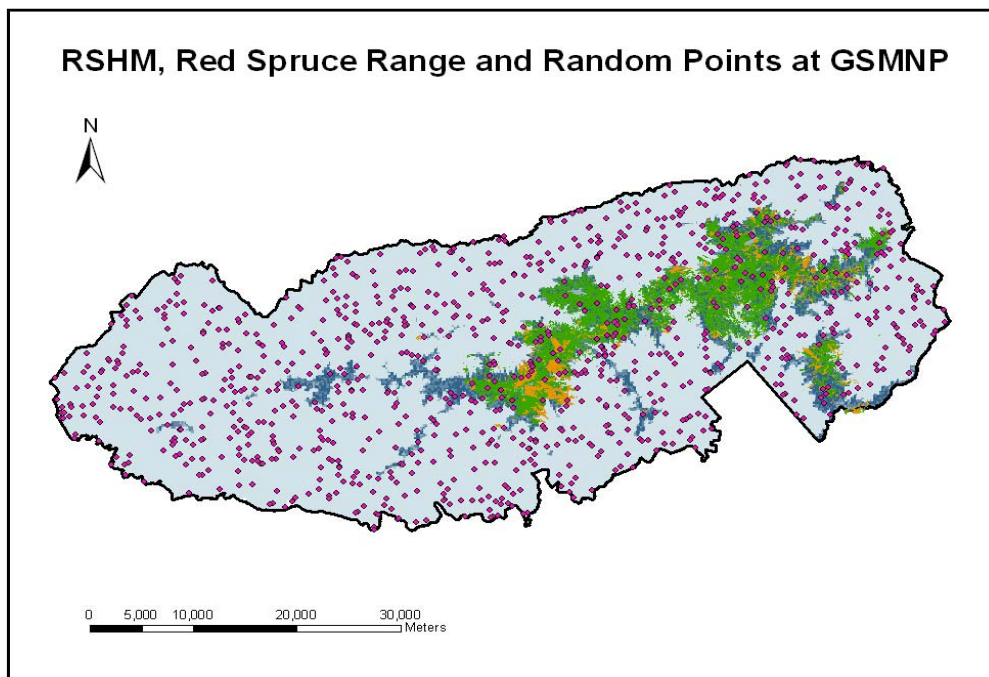


Figure 4.11. Visual comparison between predicted and original red spruce range (a) and 1,000 randompoints, dots of pink color, on RSHM (b) for model evaluation. The colors shown in both figures are explained in Figure 4.2.

RSHM showed the habitat suitability distribution of red spruce to be mostly determined by the Elevation geospatial variable at GSMNP. The amount of precipitation and the frequency of cloud immersion in interactions with air pollution disturbances, which increase with increasing elevation, and temperature, which decreases with increasing elevation, account for the elevation-dominated habitat suitability distribution pattern. In particular, high elevation areas are influenced by air pollution more than lower elevation areas because of higher acid rain and cloud exposure according to higher precipitation and cloud immersion frequencies at higher elevations. This is the reason for the lowest habitat suitability, index value of 9617, at high elevation areas (Figure 4.10). In addition, high precipitation and cloud immersion rate combined with low temperature at high elevation explain no effects of Aspect, Slope, and Distance to Stream on red spruce growth and distribution (Geiger et al. 2003). On the other hand, red spruce at low elevation sites is very sensitive to water availability and temperature conditions, showing strong sensitivity to topographical factors, Elevation, Slope, Aspect, and Distance to Stream in the sensitivity analyses (Figure 4.7.2). The ARIM (The red spruce Annual Radial Increment Model) sensitivity results in Figure 4.7.2 showed red spruce growth to increase with increasing slope and decreasing distance to stream and better growth on east- and north-facing slopes. As a result, in RSHM, the habitats located at south-facing and gentle slopes far from streams showed lower habitat suitability, which is mostly the index value of 11289 (Figure 4.10).

3.4. Global warming effects on the Red Spruce Distribution at GSMNP

IPCC reported that all of North America is very likely to warm during this century, exceeding the global mean warming in most areas, and annual mean precipitation is likely to increase in the eastern USA (IPCC 2007). To evaluate this, RSHM was modified to predict

changes in red spruce range and habitat suitability distribution. The modifications were implemented by modifying map algebras (Equations 4.3, 4.4, and 4.5) based on predicted growth declines of red spruce according to global warming in interactions with air pollution (AP). The growth declines of red spruce were estimated from ARIM simulations (Appendix 7). Red spruce growth for the period of 1940 to 2099 was computed using ARIM and displayed in Appendix 7. The average red spruce growth for the periods of 1980 – 1999 and 2080 – 2099 were obtained from the calculated growth values (Appendix 7, Table 4.5 (a)). These two periods were selected to assess the global warming effects and air pollution effects on red spruce because IPCC predicted the temperature and precipitation changes as comparing those two periods' data. The differences in red spruce growth between two periods were separately calculated for all air pollution change rates: 10% increase, 0% increase, and 10% decrease (Table 4.5 (b)). Those growth differences were multiplied by 10,000 in order to apply them to modify each geospatial habitat suitability variable (Table 4.5 (c)).

Table 4.5. The averaged ARIM indices for two periods: 1980 to 1999 and 2080 to 2099 at high and low elevations (Table (a)). Table (b) showed differences of red spruce growth between the two periods. Buffer Zone was calculated by averaging ARIM indices of $ARIM_{high}$ (High Elevation) and $ARIM_{low}$ (Low Elevation). These values were then multiplied by 10,000 to apply them to map algebra modifications (Table (c)). All values in Table (a), (b), and (c) are index values without unit.

(a)

Elevation Range	Period	Air Pollution (AP) Change Rates		
		10% increase	0% increase	10% decrease
High Elevation	1980-1999	0.9455	0.914	0.8795
	2080-2099	0.853	0.9045	0.96
Low Elevation	1980-1999	1.121	1.1125	1.1025
	2080-2099	1.008	1.023	1.0365

(b)

Elevation Range	Air Pollution (AP) Change Rates		
	10% increase	0% increase	10% decrease
High Elevation	-0.0925	-0.0095	0.0805
Low Elevation	-0.113	-0.0895	-0.066
Buffer Zone (1650-1850)	-0.10275	-0.0495	0.00725

(c)

Elevation Range	Air Pollution (AP) Change Rates (Modified values)		
	10% increase	0% increase	10% decrease
High Elevation	-925	-95	805
Low Elevation	-1130	-895	-660
Buffer Zone (1650-1850)	-1027.5	-495	72.5

The Elevation geospatial habitat suitability variable was modified directly by adding the differences in Table 4.5 (c) to the current values of all elevation ranges (Table 4.6). These new index values were applied in the reclassification process to produce new Elevation geospatial habitat suitability variables (Figure 4.12 (a), (b), and (c)). The new Elevation geospatial habitat suitability variables, *TenInE* (10% increase of AP), *TenNoE* (0% increase of AP), and *TenDeE* (10% decrease of AP), consisted of one of the raster layers for overlay analyses in predicting the global warming effects on red spruce distribution at GSMNP in interactions with air pollution (Equations 4.3, 4.4, and 4.5). The map algebra for RSHM (Equation 4.2) was also modified by red spruce growth differences between two periods (Table 4.5 (c)). The modified map algebras are shown in equations 4.3 – 4.5, and these were used for projecting new RSHMs changed by global warming with different air pollution change rates: 10% increase, 0% increase, and 10% decrease respectively. When the algebra was modified, all differences were multiplied by three to apply the differences to all three geospatial habitat suitability variables, Aspect, Slope, and Distance to Stream. For example, in equation 4.3, the value of 925 was multiplied by the 3 in parentheses to apply this difference to A_h , S_h , and DS_h .

Table 4.6. Modified Elevation variable for assessing global warming effects on red spruce distribution changes in interactions with air pollution. Indices in the Current column indices of red spruce growth multiplied by 10,000. These indices were modified by adding the growth differences shown in Table 4.5 (c) to indices in the Current column.

Elevations	Elevations geospatial habitat suitability variables with Air Pollution (AP) changes			
	Current	10% increase of AP	0% increase of AP	10% decrease of AP
1400-1450	10500	9370.0	9605.0	9840.0
1450-1550	10750.8	9620.8	9855.8	10090.8
1550-1650	10991.5	9861.5	10096.5	10331.5
1650-1850	12866.1	11838.6	12371.1	12938.6
>1850	9337.3	8412.3	9242.3	10142.3

RSHM with global warming with 10% increased AP

$$= (([TenInE]) + ([Ep_h] \times ([A_h] + [S_h] + [DS_h] - (925 \times 3))) + ([Ep_l] \times ([A_l] + [S_l] + [DS_l] - (1130 \times 3))) + ([Ep_b] \times ([A_b] + [S_b] + [DS_b] - (1028 \times 3)))) / 4 \dots \text{Equation 4.3}$$

RSHM with global warming with 0% increased AP

$$= (([TenNoE]) + ([Ep_h] \times ([A_h] + [S_h] + [DS_h] - (95 \times 3))) + ([Ep_l] \times ([A_l] + [S_l] + [DS_l] - (895 \times 3))) + ([Ep_b] \times ([A_b] + [S_b] + [DS_b] - (495 \times 3)))) / 4 \dots \text{Equation 4.4}$$

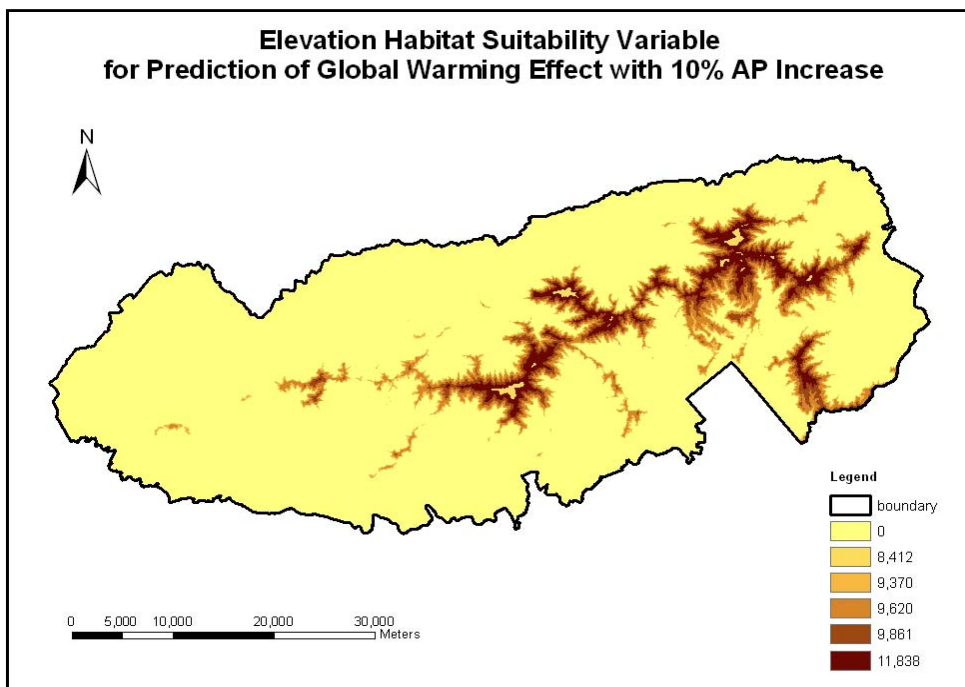
RSHM with global warming with 10% decreased AP

$$= (([TenDeE]) + ([Ep_h] \times ([A_h] + [S_h] + [DS_h] + (805 \times 3))) + ([Ep_l] \times ([A_l] + [S_l] + [DS_l] - (660 \times 3))) + ([Ep_b] \times ([A_b] + [S_b] + [DS_b] + (73 \times 3)))) / 4 \dots \text{Equation 4.5}$$

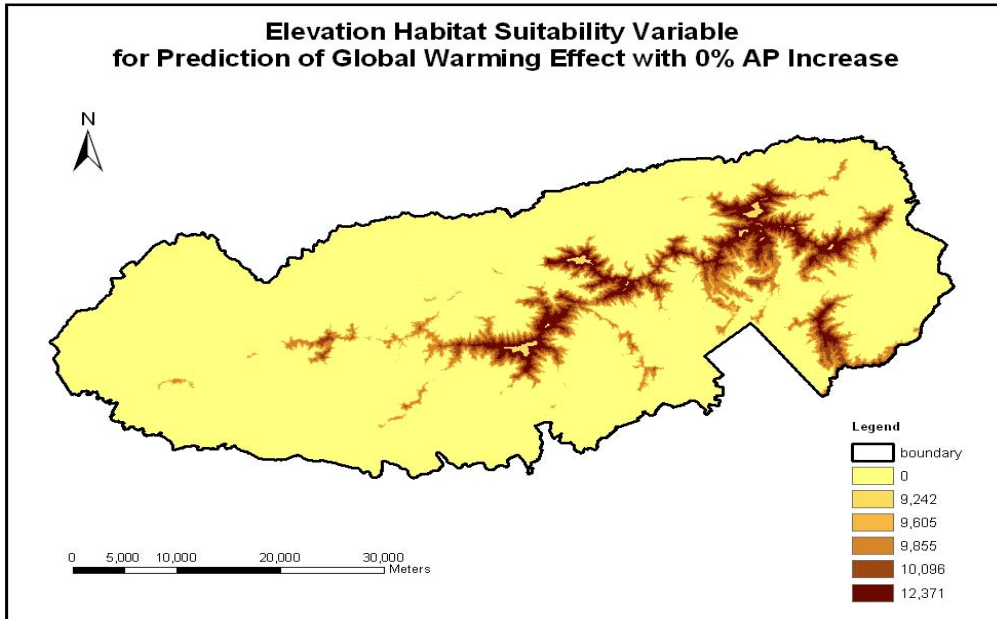
Here, *A* is Aspect, *S* is Slope, *DS* is Distance to Stream, *E* is Elevation, *Ep* Elevation parameter: *Ep_h* high elevation, *Ep_l* low elevation, and *Ep_b* buffer zone. The capitalized italic letters indicate variables and the subscribed italic letters locations. *TenInE* in equation 4.3, *TenNoE* in equation 4.4, and *TenDeE* in equation 4.5 indicate Elevation geospatial habitat

suitability variables changed by global warming with air pollution change rates: 10% increase, 0% increase, and 10% decrease respectively. For example, A_h is Aspect at high elevation. The values added in equations were obtained from Table 4.5 (c).

(a)



(b)



(c)

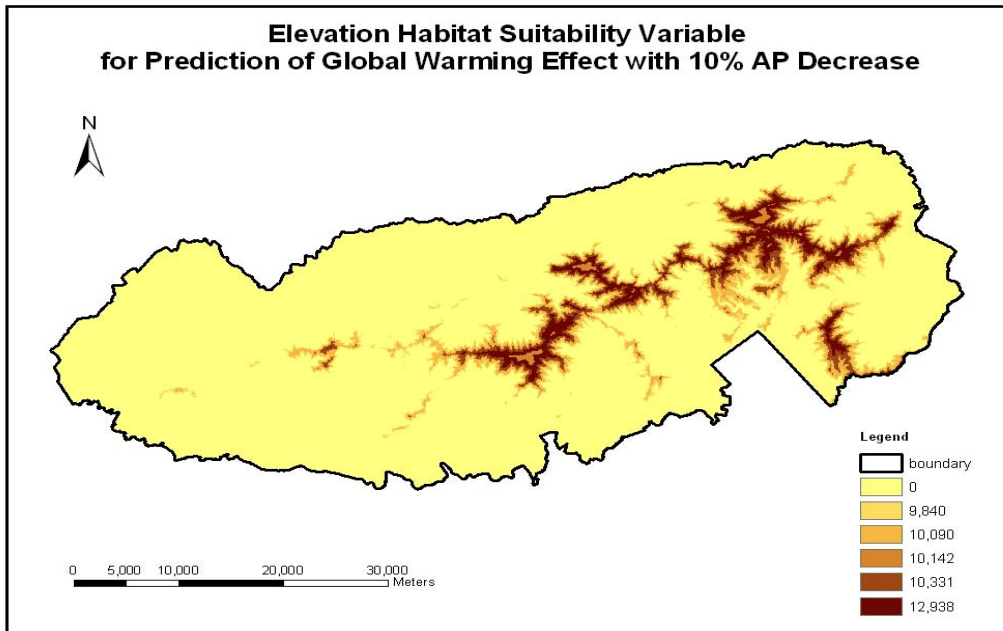
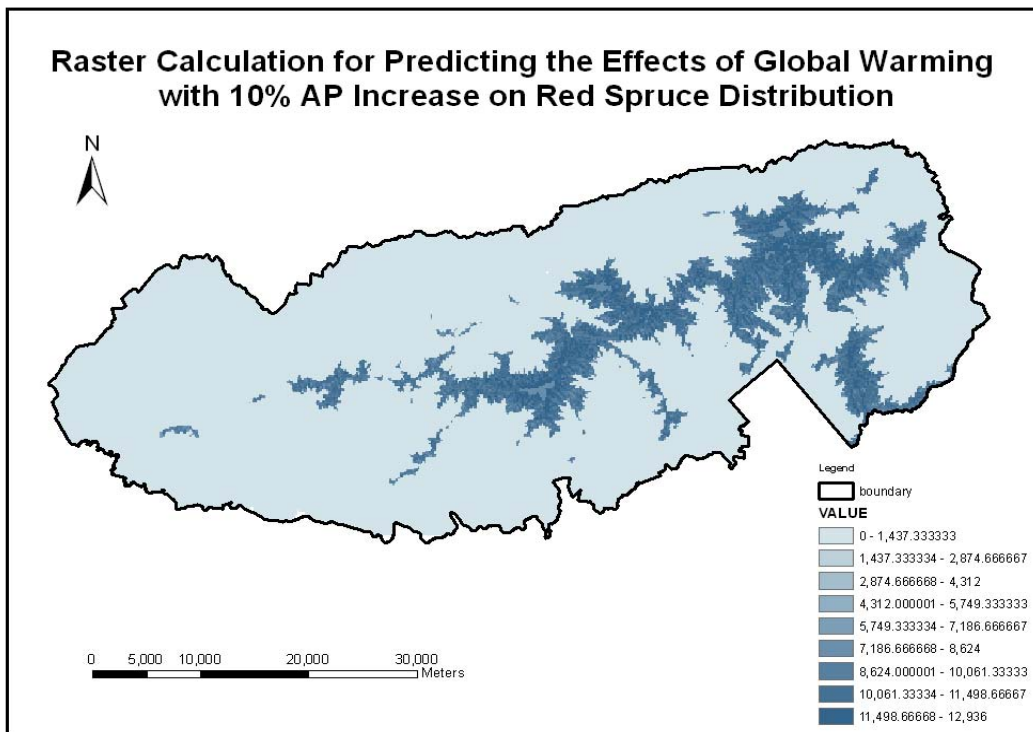


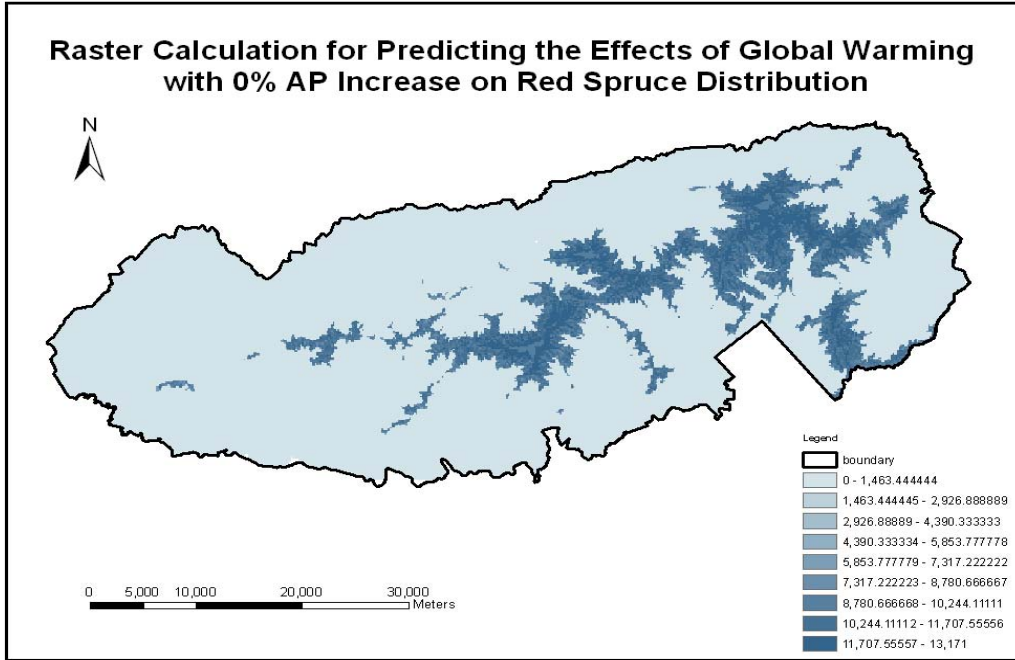
Figure 4.12. Elevation geospatial habitat suitability variables changed by global warming and air pollution changes for predicting global warming effects on red spruce ranges in interaction with air pollution. These raster layers were used for raster calculations; *TenInE* (10% increase of AP), *TenNoE* (0% increase of AP), and *TenDeE* (10% decrease of AP) indicate the changed Elevation geospatial habitat suitability variables in equations 4.3, 4.4, and 4.5, respectively. AP denotes air pollution.

The equations were employed for raster calculations, and the raster calculations produced the results shown in Figure 4.13 and Table 4.7 (a). These results were reclassified using the ranges used for the Red Spruce Habitat Model (RSHM), and the same indices used for RSHM were also applied as attributing processes (Table 4.7 (b)) in order to compare the current habitat condition with those changed by global warming in interaction with air pollution. All reclassification results are shown in Figures 4.14.2 (a), 4.14.3 (a), and 4.14.4 (a). Also, areas of all indices, 9617, 11289, and 13359, were calculated as the number of pixels (30m spatial resolution) and multiplied by 900 (the area of a pixel) (Table 4.7 (c)). Then, the area of each index value of new RSHMs was compared with the current area of corresponding index values in order to show quantitative changes (Figures 4.14.2 (b), 4.14.3 (b), and 4.14.4 (b)).

(a)



(b)



(c)

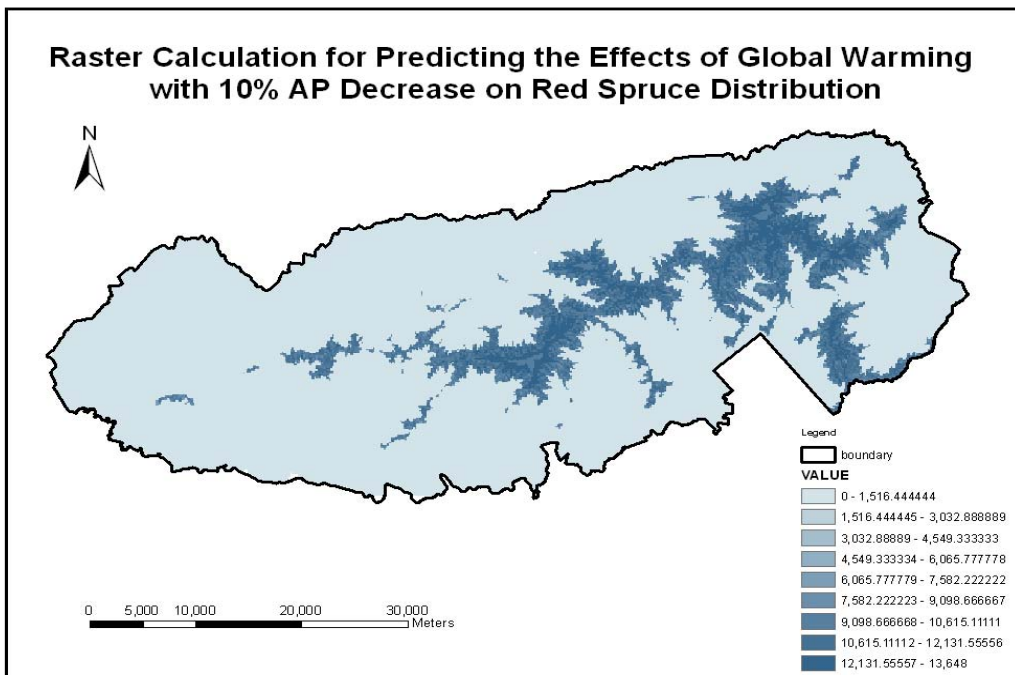


Figure 4.13. Raster calculations for predicting global warming effects on red spruce ranges with different air pollution (AP) change rates: (a) 10% increase, (b) 0% increase, and (c) 10% decrease.

Table 4.7. Reclassification results (b) of raster calculations (a) and calculated area changes (c). Panel (a) shows raster calculation results for RSHM and new RSHMs according to global warming and air pollution. Panel (b) shows the reclassification processes for each raster calculation result. In reclassification, the habitat suitability indices were all identical to compare the habitat suitability changes according to global warming and air pollution changes. Panel (c) is the areas (m²) calculated by multiplying the number of pixels (spatial resolution of each pixel is 30m) by the area of a pixel (900m²). In panel (c), the habitat index of zero was not changed by global warming and air pollution changes. This is index value corresponds to areas below 1400m, and the equations for raster calculations always treated elevations below 1400m as zero by being multiplied by the elevation parameters, Ep_h , Ep_l , and Ep_b . For example, Ep_l assigned zero values to all areas below 1400m. Therefore, the habitats with index value zero were involved in the areas of the index of 9617 at elevations higher than 1400m.

(a)

RSHM	10% AP Increase & GW	0% AP Increase & GW	10% AP Decrease & GW
0 – 1,562.8	0 – 1,437.3	0 – 1,463.4	0 – 1,516.4
1,562.9 – 3,125.8	1,437.4 – 2,874.7	1,463.5 – 2,926.9	1,516.5 – 3,032.9
3,125.9 – 4,688.7	2,874.8 – 4,312	2,927.0 – 4,390.3	3,033.0 – 4,549.3
4,688.8 – 6,251.6	4312.1 – 5,749.3	4,390.4 – 5,853.8	4,549.4 – 6,065.8
6,251.7 – 7,814.4	5,749.4 – 7,186.7	5,853.9 – 7,317.2	6,065.9 – 6,582.2
7,814.5 – 9,377.3	7,186.8 – 8,624	7,317.3 – 8,780.7	7,582.3 – 9,098.7
9,377.4 – 10,940.2	8,624.1 – 10,061.3	8,780.8 – 10,244.1	9,098.8 – 10,615.1
10,940.3 – 12,503.1	10,061.4 – 11,498.7	10,244.2 – 11,707.6	10,615.2 – 12,131.6
12,503.2 – 14,066	11,498.8 – 12,936	11,707.7 – 13,171	12,131.7 – 13,648

(b)

Current Suitability Habitat Area		10% increase of AP & GW		0% increase of AP & GW		10% decrease of AP & GW	
Ranges	Habitat Suitability Index	Ranges	Habitat Suitability Index	Ranges	Habitat Suitability Index	Ranges	Habitat Suitability Index
0	0	0	0	0	0	0	0
0 – 9617	9617	0 – 9617	9617	0 – 9617	9617	0 – 9617	9617
9617 – 11289	11289	9617 – 11289	11289	9617 – 11289	11289	9617 – 11289	11289
11289 – 14066	13359	11289 – 13359	13359	11289 – 13359	13359	11289 – 13648	13359

(c)

Habitat Index Value	Current Suitability Habitat Area		10% Increase of AP with Global Warming		0% Increase of AP with Global Warming		10% Decrease of AP with Global Warming	
	Pixels	Area (m ²)	Pixels	Area (m ²)	Pixels	Area (m ²)	Pixels	Area (m ²)
0	73140	65826000	73140	65826000	73140	65826000	73140	65826000

9617	1553	1397700	4495	4045500	3942	3547800	2978	2680200
11289	4550	4095000	6291	5661900	5244	4719600	4961	4464900
13359	8642	7777800	3959	3563100	5559	5003100	6806	6125400

The change analyses of habitat suitability for red spruce at GSMNP according to global warming in interactions with air pollution show that global warming will cause red spruce distribution to shrink due to degradation of habitat suitability at GSMNP (Figures 4.14.1 – 4.14.4). Global warming effects will be generally augmented by interactions with air pollution, causing increases of low (9617) and medium (11289) habitat suitability areas and decreases of high (13359) habitat suitability areas with increasing air pollution (Figure 4.15, Table 4.7 (c)). Figures of 4.14.1 – 4.14.4 show visually the changes of areas of all three indices with the different air pollution change rates: 10% increase, 0% increase, and 10% decrease. Figures 4.14.2 (b), 4.14.3 (b), and 4.14.4 (b) quantitatively show changes in the areas of all three indices compared with current areas as estimated in RSHM. These figures show that the slopes of lines for all three habitat suitability indices were decreased with decreasing air pollution, showing less decrease for 13359 and less increases for 11289 and 9617. In particular, increase for the habitat suitability index of 9617 indicates increasing habitat loss and growth decline at elevations higher than 1400m. This is because the habitat index of zero indicates absence of red spruce in areas below 1400m with index 9617, which represents the suitability indices of zero to 9617 (Table 4.7 (b)) in areas above 1400m. Therefore, areal changes of the index of 9617 shown in Figures 4.14.1 – 4.14.4 and 4.15 strongly support the range contraction of the red spruce at GSMNP in response to global warming in interaction with air pollution.

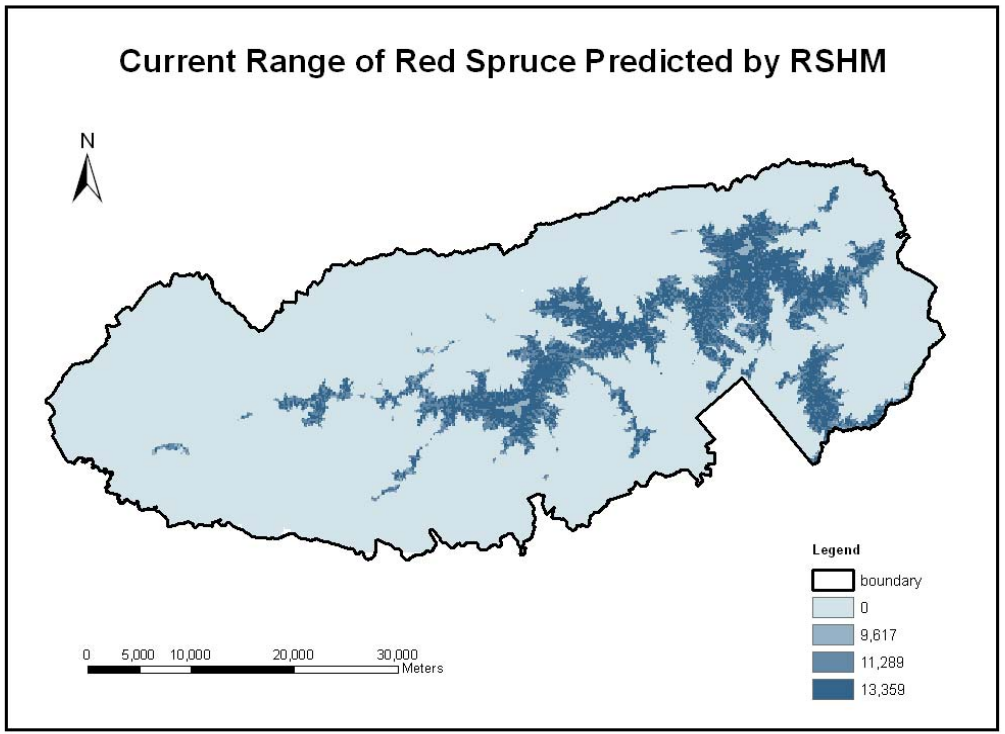
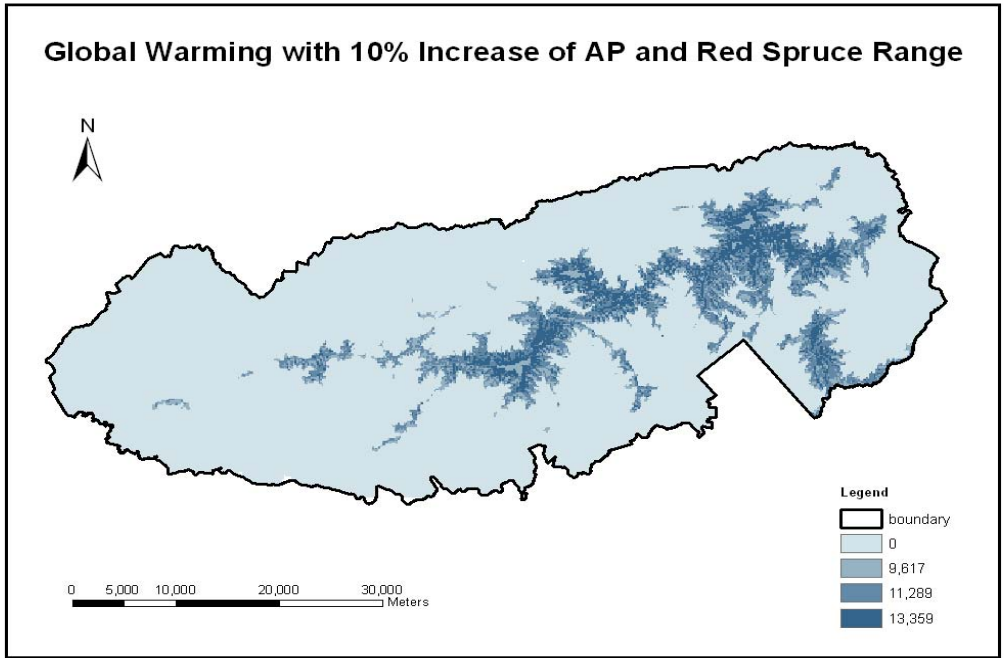


Figure 4.14.1. The current red spruce range at GSMNP estimated by RSHM. This range and spatial habitat suitability distribution were estimated by RSHM.

(a)



(b)

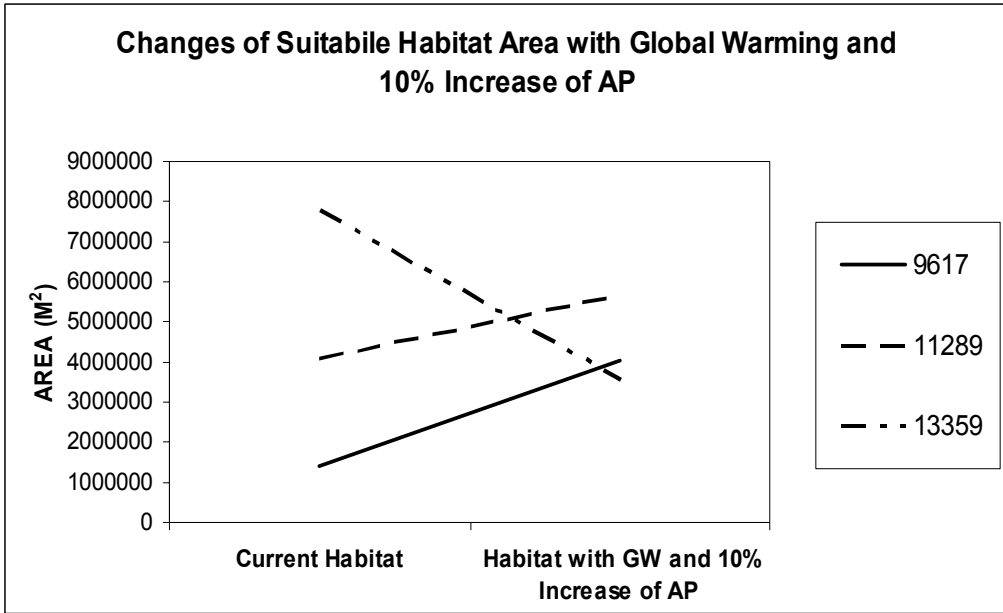
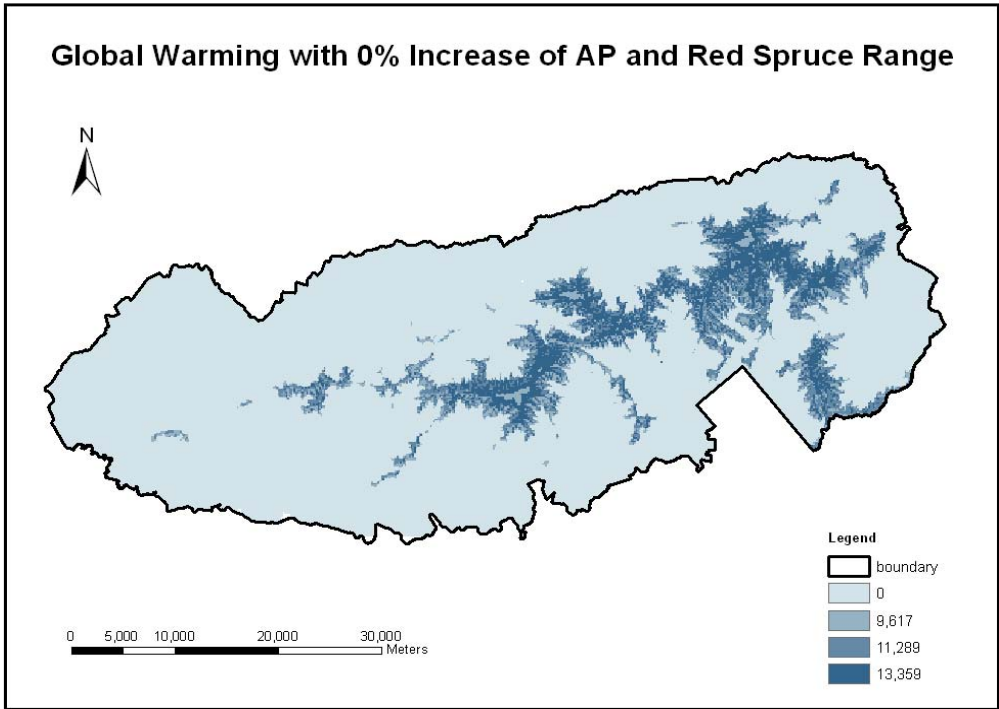


Figure 4.14.2. Global warming effects on red spruce ranges with 10% increase in air pollution: raster GIS spatial model (a) and quantitative comparison of areal changes (b). Figure (a) visually shows spatial changes of the areas of habitat suitability indices due to global warming and 10% increase in air pollution, and Figure (b) quantitatively. AP indicates air pollution.

(a)



(b)

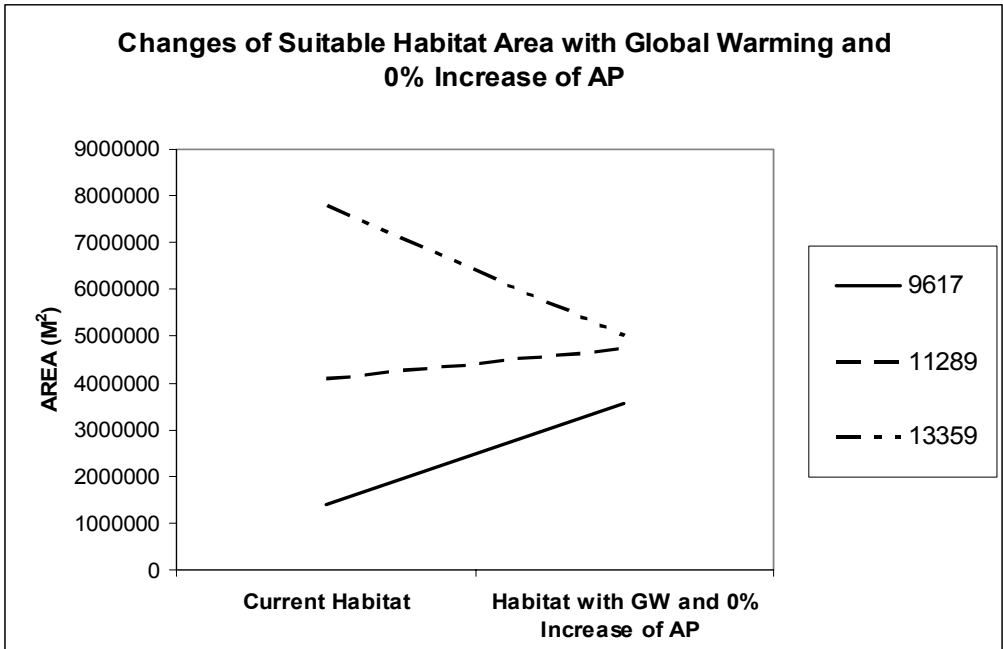
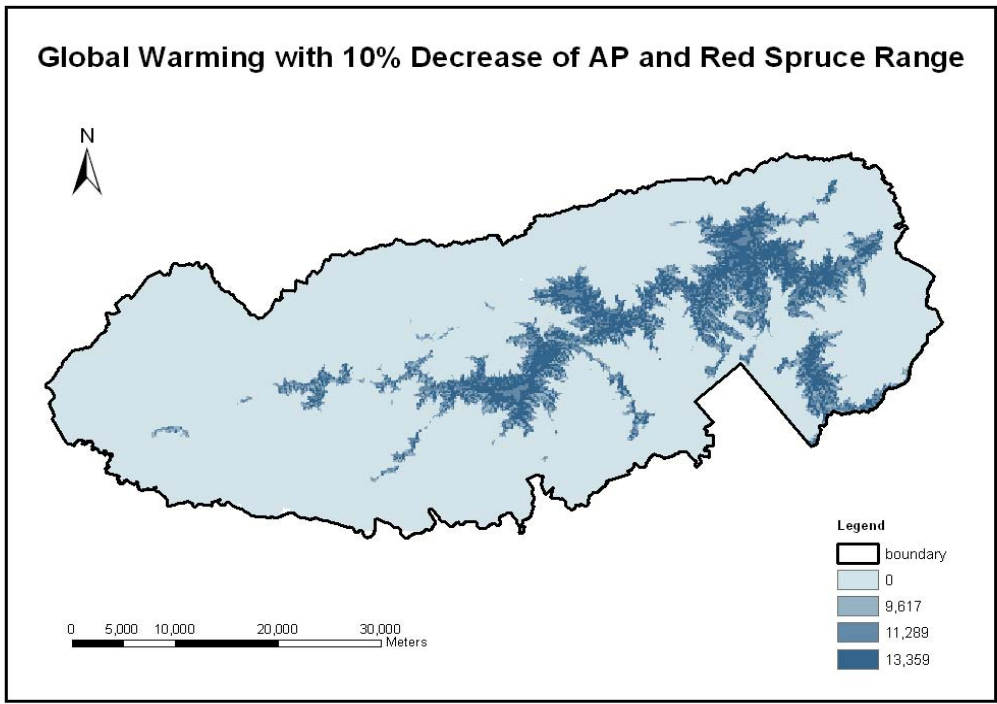


Figure 4.14.3. Global warming effects on red spruce ranges with 0% increase in air pollution: raster GIS spatial model product (a), and quantitative comparison of areal changes (b). Figure (a) shows the spatial changes in the areas of habitat suitability indices according to global warming and 0% increased air pollution visually, and Figure (b) quantitatively

(a)



(b)

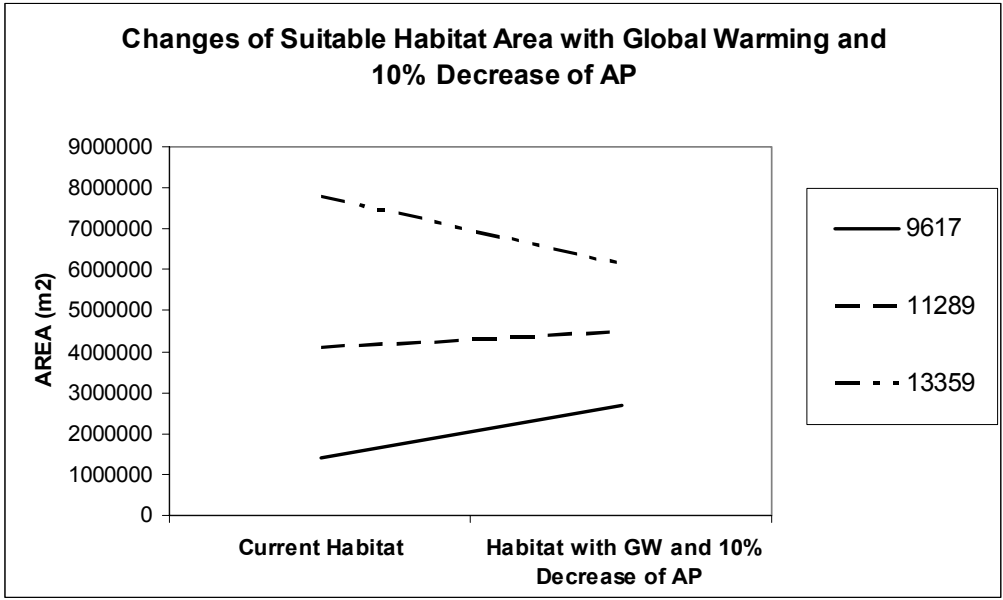


Figure 4.14.4. Global warming effects on red spruce ranges with 10% decrease in air pollution: raster GIS spatial model product (a) and quantitative comparison of areal changes (b). Figure (a) shows the spatial changes of the areas of habitat suitability indices due to global warming and 10% decreased air pollution visually, and Figure (b) quantitatively.

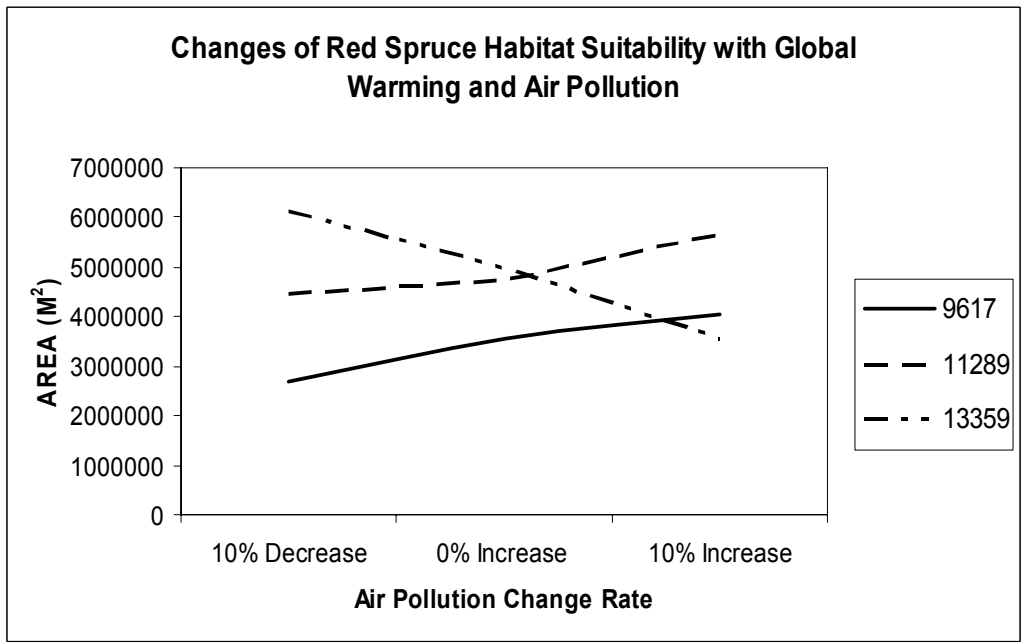


Figure 4.15. Changes in areas of each habitat suitability index associated with air pollution change. The area of 13359 (high habitat suitability) decreased with increasing air pollution, 11289 (medium habitat suitability) increased, and 9617 (low habitat suitability) also increased.

The red spruce Annual Radial Increment Models (ARIMs) used as submodels of RSHM (Red Spruce Habitat Model) explained detailed causes of predicted range decreases of red spruce at GSMNP. ARIMs showed that red spruce growth was decreased with global warming and increasing air pollution at both high and low elevation (Table 4.5 (b) and (c)). In particular, red spruce growth was much more sensitive to air pollution than increased temperature and precipitation at high elevation and the buffer zone. Table 4.5 (b) and (c) showed increased red spruce growth with 10% air pollution decrease, almost no changes of red spruce growth with 0% air pollution increase and decreased red spruce growth with 10% air pollution increase. High elevation sites already have sufficient precipitation and low enough temperature conditions; thus, the temperature increase does not exceed the optimum temperature range of photosynthesis for red spruce. Also, precipitation influences red spruce growth via acidic rain and clouds at high elevations and most of the buffer zone. Therefore, increased precipitation by itself does not have any effects on red spruce growth. That means that global warming alone does not influence red spruce growth, but it does so via interactions with air pollution at high elevations and the buffer zone. Red spruce growth in the buffer zone mostly follows the trend of high elevation due to greater sensitivity in ARIM_{high} than ARIM_{low} (Section 3.1).

On the other hand, increased temperature influences red spruce growth more than air pollution and precipitation at low elevation (Table 4.5 (b) and (c)). In Tables 4.5 (b) and (c), red spruce growth decline is slightly decreased with decreasing air pollution but still a dominant trend at low elevation. This is because of much less acidic rain and cloud effects than effects of water availability, radiation, climate and the factors related with these, such as temperature at low elevations. Increased temperatures at low elevations will cause red spruce growth to decline by causing radiation absorption and water availability for photosynthesis to decrease. Even

though the effects of increased temperature will be compensated by increased precipitation, increased temperature will be much higher than corresponding precipitation; as a result, compensation from increased precipitation will not prevent red spruce growth decline at low elevation.

Based on the assumption that better red spruce growth indicates more suitable habitat condition, it is predicted that increased temperature and precipitation with increased air pollution will cause degradation of habitat suitability at both high and low elevations. Global warming with no change or decrease of air pollution does not seriously influence changes of red spruce range at high elevation and the buffer zone, but is still the strong and dominant cause of range reduction at low elevation. Therefore, global warming will generally result in range contraction at GSMNP, though its effects will be modified by air pollution. With high air pollution, global warming will make red spruce lose more area at high than low elevation, and with low air pollution most areas of range loss will be at low elevations. Also, red spruce range can be expanded with decreased air pollution at high elevation but still shrink at low elevation (Table 4.5 (b) and (c)).

On the other hand, complexity of interactions among system factors, and lack of knowledge prevent exact quantitative predictions of the extent of range shift and degradation of habitat suitability. In particular, lack of genecological information, adaptation and phenotypic plasticity account for the difficulties in making exact quantitative predictions. Many transplant experiments have documented that plant populations are adapted to current local environmental conditions (Davis and Shaw 2001); therefore, the extent of range shift depends on the adaptation speed and range of phenotypic plasticity. Hamrick (2004) suggested that trees may contain adequate genetic diversity to acclimate and adapt to new environmental conditions through high

gene-flow among populations. If red spruce can fully adapt to the changing environment, its range will not change. However, high mortality and growth decline of red spruce strongly support the conclusion that the red spruce system cannot fully adapt and tolerate environmental stresses related to air pollution and climatic change. Therefore, in spite of the limitations, the predictions based on RSHM can provide valuable information to understand the potential global warming effects on the spatiotemporal changes of red spruce distribution at GSMNP.

4. Discussion

4.1. Ecological and physiological processes behind environmental predictors

The Predicted Species Distribution Models (PSDMs), including the Species Habitat Models (SHMs), are generally classified as empirical and phenomenological. This is because PSDMs depend on the field-basis of direct observations without explanations of cause-and-effect relationships. PSDMs have used topographic variables, sampled from digital maps, for relatively small spatial scales such as mountains (Guisan and Zimmermann 2000). Large-scale PSDMs have used biophysical variables developed by elevation-sensitive interpolations (Guisan and Zimmermann 2000). Recently, PSDMs have advanced with new powerful statistical techniques, such as Generalized Linear Models (GLM), neural networks, environmental envelopes, etc., augmented by Geographic Information System (GIS) tools (Guisan and Zimmermann 2000, Guisan and Thuiller 2005). However, these advances cannot explain the ecological and physiological causes of species distribution patterns and processes. Moreover, this limitation produced uncertainty in predicting the effects of environmental change on species distribution (Guisan and Zimmermann 2000, Guisan and Thuiller 2005).

PSDMs have incorporated ecological theories in order to explain ecological and physiological causes of species distribution pattern and process. PSDMs fundamentally assumed the equilibrium between environment and species distribution based on niche theory (Guisan and Thuiller 2005). PSDMs have applied the dispersal factor as well as niche theory, and its application improved understanding of the spatiotemporal species distribution changes (Turner et al. 2001, Guisan and Thuiller 2005). Applications of metapopulation theory also helped in predicting territory ranges and population dynamics of animals, which migrate seasonally or move among fragmented habitats (Turner et al. 2001). However, despite of those efforts, most PSDMs could not successfully explain ecological and physiological processes and causes; as a result, the difficulties in predicting species distribution changes with environmental changes still remain unsolved.

The Red Spruce Habitat Model (RSHM) involved ecological and physiological processes and causes in developing two submodels, ARIM_{high} and ARIM_{low} (Chapter 3). ARIMs, a systems model, explained red spruce growth via energy and matter flows between red spruce and environmental factors and among environmental factors. The red spruce Annual Radial Increment Models (ARIMs) included natural and anthropogenic disturbances and physiological responses of red spruce to disturbances at a variety of scales. In ARIMs, hierarchically organized direct and indirect interactions including within and across interactions were also explored by tracking energy and matter flows. Those ARIMs features were involved in RSHM via the following procedures. First, the ARIMs results were used as suitable habitat conditions of red spruce in Section 3.1. Second, the sensitivity analysis results of ARIMs were employed to convert suitable habitat information to geospatial information in Sections 3.1 and 3.3. Third, indices computed in sensitivity analyses were used for habitat suitability indices with

modifications in Section 3.3 and 3.4. Finally, red spruce growth changes according to global warming in interactions with air pollution were directly applied for modifying map algebras in Section 3.5. Therefore, geospatial habitat suitability variables, Elevation, Aspect, Slope and Distance to Stream, of RSHM involved information about physiological responses of red spruce to various disturbances as well as climatic conditions via ARIMs submodel systems. For example, the Elevation geospatial habitat suitability variable in RSHM included information about air pollution disturbances in relation to precipitation and cloud immersion frequencies and the effects of fir mortality rate, precipitation and temperature in relation to physiological responses to those factors.

Ecological and physiological information in RSHM enabled more realistic and detailed predictions of spatial habitat suitability distribution, red spruce range and global warming effects on the potential distribution changes of red spruce at GSMNP (Sections 3.4 and 3.5). It has been generally expected that habitat suitability increases with increasing elevation for alpine and subalpine species, including red spruce. RSHM showed the diverse habitat suitability distribution pattern at GRMNP, indicating low habitat suitability at high elevation (1850 to 2028m), medium habitat suitability at low elevation (1400 to 1650m) and highest habitat suitability in the buffer zone (1650 to 1850m) (Figure 4.10). This prediction was well supported by previous ecological, dendrochronological and physiological research. Ecological studies have reported that anthropogenic disturbances such as air pollution are dominant causes of high mortality rate and growth decline of red spruce (Eagar and Adams 1992, Busing 2004, Webster et al. 2004). Dendrochronological studies have showed that the high elevation red spruce has experienced severer growth declines than low elevation red spruce (Eagar and Adams 1992, Webster et al. 2004).

The predictions of global warming effects on red spruce range in Section 3.5 showed spatial differences of the global warming effects on red spruce in relation to elevation, aspect, slope and distance to stream. Especially, the high elevation red spruce system is more vulnerable to air pollution in interaction with global warming than the low elevation system. Increased temperature influences the red spruce system more than air pollution and precipitation at low elevation. Therefore, global warming will generally result in range reduction of red spruce at GSMNP, but its effects will be modified by air pollution. With high air pollution global warming will make red spruce lose more area at high elevation than low elevation and with low air pollution most areas at low elevation. Also, red spruce range can be expanded with decreased air pollution at high elevation but still shrink at low elevation.

RSHM significantly predicted the red spruce distribution and spatial distribution of suitable habitats of red spruce at GSMNP in Section 3.4. There, the predicted habitat suitability of RSHM and the original habitat suitability obtained from the Digital Vegetation Map for GSMNP were compared at 1,000 random points, and significance of correspondence between them was tested by Pearson's χ^2 goodness of fit test. This test showed significant correspondence, with *p-value* of 0.999. However, the result of model evaluation revealed a need for further studies, because the western side of GSMNP showed a discrepancy between RSHM and the digital vegetation map for GSMNP (Figure 4.11). This could be caused by competition among species, or environmental factors not considered in RSHM. The exact reasons cannot be known due to the lack of sufficient information and literature.

Despite of the significant evaluation result shown in Section 3.4, some possible uncertainty originating from raw data, the vegetation maps, the USGS digital stream map, and DEMs, should be considered. When the Digital Vegetation Map for GSMNP was projected, the

plant communities were plotted to within approximately ± 5 to ± 10 m of their true ground locations (Madden et al. 2004, Welch et al. 2002). This error range originated from the error range of the USGS Level II DEMs, less than 10m for the X and Y coordinates and a few meters for the Z coordinate (Welch et al. 2002). This error range of the USGS Level II DEMs also influenced RSHM because the variables, Elevation, Aspect and Slope, were calculated from the USGS Level II DEMs. The USGS digital stream map used to calculate Distance to Stream is one of large-scale USGS Digital Line Graph (DLG) files (1:24,000-scale). The large-scale DLG files are digital vector representations of cartographic information and also involve a certain error range (http://eros.usgs.gov/guides/dlg.html#_dlg1). The large-scale DLG files (1:24,000-scale) were derived from the 1: 24,000-scale topographic quadrangle maps, and the data are manually digitized using equipment with a resolution of 0.001 inch (<http://eros.usgs.gov/guides/dlg.html>). An absolute accuracy of the DLG files is from 0.003 to 0.005 inch at scale (<http://eros.usgs.gov/guides/dlg.html>). Therefore, there could be some errors originating in the raw data in RSHM.

4.2. Global issues, Nested across-scale interactions, and Interdisciplinary synthesis

Traditional ecology has been based on plot-based, fine-scale studies (Schneider 2001, Kent 2005, Kerr et al. 2007). Recognition of global issues, including global warming and air pollution, have motivated need for new approaches, such as macroecology and landscape ecology integrated with traditional studies. New ecological fields have played an important role in understanding global issues, such as declining species diversity and range shift toward the poles related to global warming and air pollution (Kerr et al. 2007). However, we need new frameworks to analyze ecological processes at multiple scales (Carpenter et al. 2006). This is

because ecosystems are hierarchically organized, and their processes operate at a variety of scales (Peterson in press).

With needs of multi-scale studies, ecologists have automatically faced problems in: selecting an appropriate scale for each study; upscaling and downscaling data from different study scales; and understanding across-scale interactions (Peter et al. 2007, Peterson in press). With theoretical and technical advances, landscape ecologists have achieved great advances in developing statistical methods to lump and extrapolate data. However, simple up- and down-scaling based on traditional hierarchy theory fails to explain the connectivity among scales due to features of ecological patterns and processes, including non-linearity, heterogeneity, scale dependency of processes, and emergent properties (Peterson in press). Those ecological features can be explained by understanding complicated within- and across-scale interactions, recently emerging as a main issue in this field (King et al. 2004, Diffenbaugh et al. 2005, Reuter et al. 2005, Cowen et al. 2006, Kerr et al. 2007, Peter et al. 2007). Reuter et al. (2005) indicated, “The important thing in ecosystems is the cross-scale interactions, such as local to global back to local.” Peters et al. (2007) also made pointed, “Cross-scale interactions refer to processes at one spatial or temporal scale interacting with processes at another scale to result in nonlinear dynamics with thresholds, generating emergent behavior that cannot be predicted based on observations at single or multiple, independent scales.”

The Predicted Species Distribution Models (PSDMs) also has faced the same issues as other spatial landscape models. The Red Spruce Habitat Model (RSHM) suggests the alternatives to solve the problems of traditional PSDMs. In general, the spatial landscape models are very flexible to incorporate submodels, and a variety of submodels have been applied for these models (Baker 1989). So, RSHM involved within- and across-scale interactions through

developing hierarchically organized submodels, ARIMs (ARIM_{high} and ARIM_{low}). ARIMs explained within-scale interactions at fine scale to continental scale and across-scale interactions among them (Chapter 3). For instance, ARIMs involved interactions between: Fraser fir and red spruce at fine scale; elevation and cloud immersion at regional scale; and, precipitation and air pollution at continental scale. Acidic rain and clouds accounted for across-scale interactions between regional scale (elevation) and continental or global scale (precipitation and air pollution). Within-and across-interactions considered in RSHM enabled RSHM to predict more detailed and reasonable spatial habitat conditions of red spruce in Section 3.4 and the global warming effects on red spruce distribution in interactions with air pollution and local environmental factors represented by topographical factors, Elevation, Aspect, Slope and Distance to Stream, in Section 3.5. Even though complexity of interactions among system factors and the lack of knowledge, such as genetic information, prevent exact quantitative predictions of the extent of range shift and degradation of habitat suitability, high mortality and growth decline of red spruce have strongly supported the predictions based on RSHM.

5. Conclusion

The objective of this study was to project the current distribution range of red spruce and account for possible global warming effects on the changes in this distribution range. The Red Spruce Habitat Model (RSHM) was devised for this study. RSHM exhibited low habitat suitability (9617) at high elevation habitats (1850 to 2028m), medium habitat suitability (11289) at habitats located at south-facing and gentle slopes and far from streams at low elevation (1400 to 1650m) and high habitat suitability (13359) at habitats located on east-facing and higher slopes closer to streams at low elevation (1400 to 1650m) and for all habitats in the buffer zone

(1650 to 1850m) (Figure 4.10). RSHM was well matched with the red spruce distribution range including both presence and absence of red spruce at GSMNP (Figure 4.11 (a)). Habitat suitability predicted by RSHM explained well red spruce associations, showing significant correspondence between predicted habitat suitability and observed habitat suitability in Section 3.4.

RSHM predicted that global warming would cause red spruce distribution to shrink by degradation of habitat suitability at GSMNP. The global warming effects will be generally augmented by interactions with air pollution, showing increases of low and medium habitat suitability and decreases of high habitat suitability with increasing air pollution (Figure 4.15). In particular, increased areas of habitat suitability index of 9617 indicate increasing red spruce habitat loss and growth decline at elevations higher than 1400m at GSMNP. Therefore, the increases of the index of 9617 shown in figures of 4.14.1 – 4.14.4 and 4.15 strongly support the range contraction of red spruce at GSMNP associated with global warming in interaction with air pollution. However, complexity of interactions among system factors and lack of knowledge prevent exact quantitative predictions of range shifts and degradation of habitat suitability.

RSHM involved ecological and physiological processes and causes in explaining the distribution patterns of red spruce based on habitat suitability. For this, two systems models, ARIM_{high} and ARIM_{low}, were developed in Chapter 3 and applied for developing RSHM as submodels. The predictors of RSHM—Elevation, Aspect, Slope, and Distance to Stream—involved hierarchically organized within- and across-scale interactions as well as ecological and physiological processes and causes via ARIMs. This feature of RSHM allowed predicting more detailed spatial habitat conditions for red spruce and global warming effects on temporal changes in red spruce habitat suitability and range at GSMNP.

CHAPTER 5

CONCLUSION

For half a century the commercially and ecologically important tree species red spruce (*Picea rubens*) has been in decline over its entire range. Air quality, climate change, forest disturbance, and nutrient cycling have been most frequently cited as possible causes. Direct and indirect effects of air pollution, alone or in combination with other factors, have been most studied, but with inconclusive results.

The lack of knowledge and methodology may account for the inconclusive results. However, reductionistic and mechanistic perspectives could also be fundamental reasons. Those perspectives have shown problems in treating the concept of organized complexity, a unique feature of the living world, in spite of outstanding contributions to the advances of science and industrial society. System theory, focusing on parts and relations, is appropriate to study organized complexity, and E. P. Odum championed in the ecosystem concept its use in ecology. Open system theory enabled all possible direct and indirect interactions among factors to be considered by tracking flows of energy and matter. Also, a theoretical basis was achieved for interdisciplinary synthesis implemented by systems modeling. Thus, this study employed system theory and systems modeling to understand red spruce growth decline and global warming effects on red spruce growth and geographic ranges changes.

This study was implemented based on four hypotheses. First, the distribution range and growth of *Picea rubens* in GSMNP is determined by habitat suitability, and habitat suitability is expressed by hierarchically organized direct and indirect interactions among system factors.

Second, the habitat suitability of *Picea rubens* in GSMNP is influenced by global warming as a cause expressed through direct and indirect interactions among system factors. Third, changes of growth and distribution of *Picea rubens* at GSMNP along with global warming are the result of direct and indirect interactions among many system factors. Fourth, indirect interactions among system factors are the dominant effects in determining the distribution range of *Picea rubens* of GSMNP. Indirect effects occur through complex, organized, hidden and hierarchically ordered, within- and across-scale interactions among system factors. Based on the four hypotheses, the objectives of this study were; first, to develop a foundation for systematic and comprehensive understanding of the red spruce growth system through interdisciplinary synthesis; second, to investigate the causes of growth decline and the effects of global warming on *Picea rubens* growth from a tree growth model in systems modeling studies; third, to estimate suitable habitat conditions for red spruce from the tree growth model and predict the distribution range of red spruce and the effects of global warming on this range in GIS studies.

Based on three study objectives, this study was divided into three main modeling sections: Envirogram of Annual Radial Increment Rate of Red Spruce (ARIRS), a conceptual model (Chapter 2); The red spruce Annual Radial Increment Models (ARIMs), which are systems models (Chapter 3); and the Red Spruce Habitat Model (RSHM), a spatial landscape model (Chapter 4). Chapter 2 presented background information for a simulation model of the annual radial (growth) increment in red spruce (ARIM) in the Great Smoky Mountains National Park (GSMNP) in the Southeastern USA. The concept of an open system and holistic and behavioral definitions of a system are combined with hierarchical ideas and a dualistic concept of environment to construct a comprehensive species-specific envirogram. This envirogram represents a structured summary of all the environmental factors seen as significant in the

generation of annual radial growth increments in this species. These factors are developed in a review of relevant literature from different specific disciplines and organized into the envirogram, which represents an interdisciplinary synthesis. This synthesis distinguishes direct vs. indirect factors in radial growth and took account of the systems ecology concept that indirect factors might be just as important as or even more important in regulating growth processes than direct ones.

In Chapter 3, the causes of red spruce growth decline and the effects of global warming on the growth of red spruce were explored through ARIMs systems modeling. ARIMs were developed based on the ARIRS envirogram. For quantitative synthesis, Relative Basis Index Value (*RBI*) was developed by dividing annual values by long-term averages. Also, various linear and nonlinear models, rule-based models and modeling techniques were applied to ARIMs to find significant factors and interactions to explain red spruce growth at GSMNP. The modeling results showed that air pollution disturbance was the dominant cause of red spruce growth decline at high elevation, and red spruce growth had significant positive relationships with water availability and radiation and a negative relationship with air pollution disturbance at low elevation. Based on the results of ARIMs in predicting global warming effects on red spruce growth, growth was more affected by air pollution than global warming at high elevation and more by global warming than air pollution at low elevation. In particular, red spruce growth is well recovered with 10% air pollution decrease at high elevation. However, deficient information about acclimation range of red spruce prevents the exact quantitative prediction of global warming effects on this system. We need further genecological and physiological research about acclimation ability of red spruce to improve understanding of causes of growth decline and prediction of global warming effects on growth. In particular, more ecological research, such as

interactions with co-existent species and insects, and general physiological research, are needed at low elevations.

In Chapter 4, the objective of this study was to project the current distribution range of red spruce and account for possible global warming effects on the changes in this distribution range. The Red Spruce Habitat Model (RSHM), a spatial landscape model, was devised for this study in GIS concept and function. In RSHM, suitable habitat conditions of red spruce were explained by the sensitivity results of ARIMs. Those conditions were used to develop geospatial habitat suitability variables to produce RSHM. The modeling was carried out by raster GIS modeling processes explained in Section 2.3, Chapter 4. RSHM exhibited the low habitat suitability (9617) at high elevation habitats (1850 to 2028m), medium habitat suitability (11289) at the habitats located at south-facing and gentle slopes and distant from streams at low elevation (1400 to 1650m) and high habitat suitability (13359) at the habitats located at east-facing and higher slopes and closer distances to streams at low elevation (1400 to 1650m) and for all habitats in the intermediate buffer zone (1650 to 1850m). RSHM well predicted red spruce distribution range, including both presence and absence, and habitat suitability at GSMNP, showing *P-value* of 0.999 in Pearson's χ^2 statistics for goodness of fit test, in Section 3.4, Chapter 4. RSHM also predicted that global warming would cause the red spruce distribution to shrink by degradation of habitat suitability at GSMNP. The global warming effects will be generally augmented by interactions with air pollution, showing the increases of low and medium habitat suitability and decreases of high habitat suitability with increasing air pollution. In particular, increases of the index of 9617 strongly support the range reduction of red spruce at GSMNP due to global warming in interactions with air pollution. However, complexity of

interactions among system factors and lack of knowledge prevent the exact quantitative predictions of range shift and degradation of habitat suitability.

In conclusion, the Annual Radial Increment Rate of Red Spruce (ARIRS) envirogram well conceptualized complex interactions affecting red spruce growth and offered a conceptual model for ARIMs. ARIMs significantly explained the habitat-specific causes of red spruce growth declines and global warming effects. RSHM significantly predicted spatiotemporal distribution of geographic range and habitat suitability of red spruce at GSMNP. In modeling perspectives, ARIMs practically exhibited the concept and methodology to implement quantitative multifactorial, interdisciplinary research and contributed to solving ecological issues of within- and across-scale interactions and complexity, in three ways. First, ARIM, in modeling perspectives, provided a general model structure including complex direct and indirect interactions for studying tree systems. Second, ARIM was demonstrated to be a practical methodology to quantitatively integrate knowledge and data from different disciplines, as developing RBIV. ARIM also showed flexibility in incorporation of models within the ARIM structure without modifications of observed data features. Third, ARIM provided the conceptual framework and methodology to study hierarchically organized within- and across-scale interactions. RSHM successfully explained ecological and physiological processes and causes in explaining the distribution patterns of red spruce based on habitat suitability by applying ARIMs as submodels, $ARIM_{high}$ and $ARIM_{low}$. The predictors of RSHM, Elevation, Aspect, Slope and Distance to Stream, also involved hierarchically organized within- and cross-scale interactions as well as ecological and physiological processes and causes via ARIMs. This feature of RSHM allowed predicting more detailed spatial habitat conditions for red spruce and global warming effects on the temporal changes of red spruce habitat suitability and range at GSMNP. Overall,

this study showed the significance and importance of comprehensive multifactorial modeling for better understanding of tree systems by linking a conceptual model, the ARIRS envirogram, to a systems model, ARIMs, and to a spatial landscape model, RSHM.

REFERENCES

- Aber, J., W. McDowell, K. Nadelhoffer, A. Magill, G. Bernston, M. Kamakea, S. McNulty, W. Currie, L. Rustad, and I. Fernandez. 1998. Nitrogen saturation in temperate forest ecosystems. *BioScience* 48:921-934.
- Aguad, E. and J. Burt. 2004. *Understanding weather and climate* (3rd ed.). Prentice Hall, Upper Saddle River, NJ, 560pp.
- Ainsworth, E.A. and S.P. Long. 2005. What have we learned from 15 years of free-air CO₂ enrichment (FACE)? A meta-analytic review of the responses of photosynthesis, canopy properties and plant production to rising CO₂. *New Phytologist* 165(2): 351-372.
- Alfaro, R.I., S. Taylor, G. Brown, and E. Wegwitz. 1999. Tree mortality caused by the western hemlock looper in landscape of central British Columbia. *Forest Ecology and Management* 124(2-3): 285-291.
- Allee, W.C., W.C. Emerson, O. Park, T. Park, and K.P. Schmidt. 1949. *Principles of animal ecology*. Saunders, Philadelphia & London. 837p.
- Allen, C.R. and C.S. Holling. 2002. Cross-scale Structure and Scale Breaks in Ecosystems and Other Complex System. *Ecosystems* 5(4): 315-318.
- Atkin, O.W. and M.G. Tjoelker. 2003. Thermal acclimation and the dynamic response of plant respiration to temperature. *Trends in Plant Science* 8(7): 343-351.
- Aronoff, S. 1989. *Geographic information systems: a management perspective*. WDL Publications, Ontario, Canada. 294pp.
- Bailey, T.C. 1994. 1994. A review of statistical spatial analysis in geographical information systems. In *Spatial Analysis and GIS* (S. Fotheringham and P. Rogerson eds.). Taylor & Francis Ltd, London. 281pp.
- Baker, W.L. 1989. A review of models of landscape change. *Landscape Ecology* 2(2): 111-133.
- Barker M., H.V. Miegroet, N.S. Micholas, and I.F. Creed. 2002. Variation in overstory nitrogen uptake in a small, high-elevation southern Appalachian spruce-fir watershed. *Canadian Journal of Forest Research* 32: 1741-1752.
- Battaglia, M., C. Beadle, and S. Loughhead. 1996. Photosynthetic temperature responses of *Eucalyptus globulus* and *Eucalyptus nitens*. *Tree Physiology* 16: 81-89.

- Bertalanffy, L.V. 1969. General system theory: foundations, development, applications. George Braziller, Inc., New York. 295p.
- Bertalanffy, M. 1975. Perspectives on general system theory: Scientific-philosophical studies (The international library of systems theory and philosophy). George Braziller, Inc., New York. 183p.
- Bhattacharyya, G.K. and R.A. Johnson. 1977. Statistical Concepts and Methods. John Wiley & Sons, New York. 639pp.
- Bigras, F.J.. 2000. Selection of white spruce families in the context of climate change: heat tolerance. *Tree Physiology* 20: 1227-1234.
- Bintz, W.W. and D.J. Butcher. 2007. Characterization of the health of southern Appalachian red spruce (*Picea rubens*) through determination of calcium, magnesium, and aluminum concentrations in foliage and soil. *Microchemical Journal* 87: 170-174.
- Bolstad, P.V., P. Reich, and T. Lee. 2003. Rapid temperature acclimation of leaf respiration rates in *Quercus alba* and *Quercus rubra*. *Tree Physiology* 23: 969-976.
- Borer, C.H., P.G. Schaberg, and D.H. Dehayes. 2005. Acidic mist reduces foliar membrane-associated calcium and impairs stomatal responsiveness in red spruce. *Tree Physiology* 25: 673-680.
- Box, E.O. 1981. Macroclimate and plant forms: an introduction to predictive modeling in phytogeography, Dr. W. Junk, The Hague, Boston. 258pp.
- Box, E.O., D.W. Crumpacker, and E.D. Hardin. 1993. A climatic model for location of plant species in Florida, U.S.A. *Journal of Biogeography* 20(16): 629-644.
- Boyce, R.L. 2007. Chlorophyll fluorescence response of red spruce and balsam fir to a watershed calcium fertilization experiment in New Hampshire. *Canadian Journal of Forest Research* 37(8): 1518-1522.
- Bradley, N.L., A.C. Leopold, J. Ross, and W. Huffaker. 1999. Phenological changes reflect climate change in Wisconsin. *Proceedings of the National Academy of Sciences of the United States of America*. 96 (17), 9701-9704.
- Breckle, S.-W. 2002. Walter's Vegetation of the Earth: The Ecological Systems of the Geobiosphere (4th edition). Springer, New York, USA. 527pp.
- Briggs, D. and S.M. Walters. 1997. Plant variation and evolution (3rd edition). Cambridge University Press, New York, USA. 512pp.

- Bullock, J.M., I.L. Moy, S.J. Coulson, and R.T. Clarke. 2003. Habitat-specific dispersal: environmental effects on the mechanisms and patterns of seed movement in a grassland herb *Rhinanthus minor*. *Ecography* 26: 692-704
- Busing, R.T. 2004. Red spruce dynamics in an old southern Appalachian forest. *Journal of the Torrey Botanical Society*. 131 (4), 337-342.
- Busing, R.T. and E.F. Pauley. 1994. Mortality trends in a southern Appalachian red spruce population. *Forest Ecology and Management* 64(1): 41-45.
- Burrough, P.A. 1986. Principles of geographical information systems for land resources assessment. Oxford University Press, Oxford. 194pp.
- Burrough, P.A. and R.A. McDonnell. 1998. Principles of geographical information systems. Oxford University Press, New York. 333pp.
- Campbell, R.K. 1979. Genecology of Douglas-Fir in a watershed in the Oregon cascades. *Ecology* 60(5): 1036-1050.
- Capra, F., D. Steindl-Rast, and T. Matus. 1992. *Belonging to the universe: explorations on the frontiers of science & spirituality* (1st ed.). HarperCollins, New York, USA. 217p.
- Carpenter, S.R., R. DeFries, T. Dietz, H.A. Mooney and S. Polasky. 2006. Millennium Ecosystem Assessment: Research Needs. *Science* 314: 257-258.
- Chuanyan, Z., N. Zhongren, C. Guodong, Z. Junhua, and F. Zhaodong. 2006. GIS-assisted modeling of the spatial distribution of Qinghai spruce (*Picea crassifolia*) in the Qilian Mountains, northwestern China based on biophysical parameters. *Ecological Modelling* 191: 487-500.
- Clark, J.S. 1998. Why tree migrate so fast: confronting theory with dispersal biology and the paleorecord. *American Naturalist* 152(2): 204-224.
- Clark, J.S., B. Beckage, P. Camill, B. Cleveland, J. HilleRisLambers, J. Lichter, J. McLachlan, J. Mohan, and P. Wyckoff. 1999. Interpreting recruitment limitation in forests. *American Journal of Botany* 86 (1), 1-16.
- Clark, J.S., S. LaDeau, and I. Ibanez. 2004. Fecundity of trees and the colonization-competition hypothesis. *Ecological Monographs* 74(3): 415-442.
- Clements, F.E. 1916. *Plant succession: an analysis of the development of vegetation*. Carnegie Institution of Washington, Washington. 512pp.
- Clements, F.E. 1936. Nature and structure of the climax. *The Journal of Ecology* 24: 252-284.

- Cook, E.R. 1988. A tree ring analysis of red spruce in the southern Appalachian Mountains. In Van Deusen, P. ed., *Analyses of Great Smoky Mountain red spruce tree ring data*. USDA Forest Service General Technical Report SO-69: 6-19.
- Cook, E.R., A.H. Johnson, and T.J. Blasing. 1987. Forest decline: modeling the effect of climate in tree rings. *Tree Physiology* 3: 27-40.
- Corti, S., F. Molteni, and T.N. Palmer. 1999. Signature of recent climate change in frequencies of natural atmospheric circulation regimes. *Nature*. 398 (6730), 799-802.
- Cowen, R.K., C.B. Paris, and A. Srinivasan. 2006. Scaling of connectivity in marine populations. *Science* 311(5760): 522-527.
- Cox, P.M., R.A. Betts, C.D. Jones, S.A. Spall, and I.J. Totterdell. 2000. Acceleration of global warming due to carbon-cycle feedbacks in a coupled climate model. *Nature* 408: 184-187.
- Creed, I.F., D.L. Morrison, and N.S. Nicholas. 2004. Is coarse woody debris a net sink or source of nitrogen in the red spruce – Fraser fir forest of the southern Appalachians, U.S.A.? *Canadian Journal of Forest Research* 34(3): 716-727.
- Crouse, D.T., L.B. Crowder, and H. Caswell. 1987. A stage-based population model for longhead sea turtle and implications for conservation. *Ecology* 68:1412-1423.
- David, M.B. and R.G. Shaw. 2001. Range shifts and adaptive response to Quaternary climate change. *Science* 292: 673-182.
- Davis, A.J., L.S. Jenkinson, J.L. Lawton, B. Shorrocks, and S. Wood. 1998a. Making mistakes when predicting shifts in species range in response to global warming. *Nature* 391: 783-789.
- Davis, A.J., J.L. Lawton, B. Shorrocks, and L.S. Jenkinson. 1998b. Individualistic species responses invalidate simple physiological models of community dynamics under global environmental change. *Journal of Animal Ecology* 67: 600-612.
- Day, M.E., M.S. Greenwood, and A.S. White. 2004. Age-related changes in foliar morphology and physiology in red spruce and their influence on declining photosynthetic rates and productivity with tree age. *Tree Physiology* 21: 1195-1204.
- De'Ath, G. and K.E. Fabricius. 2000. Classification and Regression Trees: A Powerful yet Simple Technique for Ecological Data Analysis. *Ecology* 81(11): 3178-3192
- DeHayes, D.H., P.G. Schaberg, G. J. Hawley, and G.R. Strimbeck. 1999. Acid rain impacts on calcium nutrition and forest health alteration of membrane-associated calcium leads to membrane destabilization and foliar injury in red spruce. *BioScience* 49(10) 789-800.
- DeMers, M.N.. 2002. GIS modeling in raster. John Wiley & Sons, Inc. New York, USA. 203p.

- Deusen, P.C., 1988. Analyses of Great Smoky Mountain Red Spruce Tree Ring Data. Gen. Tech. Rep. SO-69. New Orleans, LA: U.S. Dept of Agriculture, Forest Service, Southern Forest Experiment Station. 67p.
- Diffenbaugh, N.S., J.S. Pal, R.J. Trapp, and F. Giorgi. 2005. Fine-scale processes regulate the response of extreme events to global climate change. PANS 102(44): 15774-15778.
- Dumais, D. and M. Prévost. 2007. Management for red spruce conservation in Quebec: The importance of some physiological and ecological characteristics – A review. Forestry Chronicle 83(3): 378-392.
- Dymond, C.C. and E.A. Johnson. 2002. Mapping vegetation spatial patterns from modeled water, temperature and solar radiation gradients. ISPRS Journal of Photogrammetry and Remote Sensing 57(1-2): 69-85.
- Eagar, C. and M.B. Adams, editors. 1992. Ecology and decline of red spruce in the eastern United States. Springer-Verlag, New York, USA. 417pp.
- Ehrlén, J. and O. Eriksson. 2000. Dispersal limitation and patch occupancy in forest herbs. Ecology 81(6): 1667-1674.
- Eldhuset, T.D., H. Lange, and H.A. de Wit. 2006. Fine root biomass, necromass and chemistry during seven years of elevated aluminum concentrations in the soil solution of a middle-aged *Picea abies* stand. Science of the Total Environment 369: 344-356.
- Engler, R., A. Guisan, and L. Rechsteiner. 2004. An improved approach for predicting the distribution of rare and endangered species from occurrence and pseudo-absence data. Journal of Applied Ecology 41(2): 263-274.
- Epron, D. 1997. Effects of drought on photosynthesis and on the thermotolerance of photosystem II in seedlings of cedar (*Cedrus atlantica* and *C. libani*). Journal of Experimental Botany 48(315): 1835-1841.
- EPA. 2000. National air pollution emission trends 1900-1998. EPA 454/R-00-002.
- Eriksson, O. 1996. Regional dynamics of plants: a review of evidence for remnant, source-sink and metapopulations. Oikos 77: 248-258.
- Etterson, J.R. 2004. Evolutionary potential of *Chamaecrista fasciculata* in relation to climate change. I. Clinal patterns of selection along an environmental gradient in the great plains. Evolution 58(7): 1446-1458.
- Evans, F.C. 1956. Ecosystem as the basic unit in ecology. Science 123: 1127-1128.
- Fernandez, I.J. and L.R. Rustad. 1990. Soil response to S and N treatments in a northern New England low elevation coniferous forest. Water Air Soil Pollution 52: 23-39.

- Fernandez, I.J., J.A. Simmons, and R.D. Briggs. 2000. Indices of forest floor nitrogen status along a climate gradient in Maine, USA. *Forest Ecology and Management* 134: 177-187.
- Fritts . H.C. 1976. *Tree rings and climate*. Academic Press, New York. 567pp.
- Fröberg, H. and O. Eriksson. 1997. Local colonization and extinction of field layer plants in a deciduous forest and their dependence upon life history features. *Journal of Vegetation Science* 8: 395-400.
- Futuyma. D.J. 1986. *Evolutionary biology* (2nd ed.). Sinauer Associates Inc., Massachusetts. 600pp.
- Geiger , R., R.H. Aron, and P. Todhunter. 2003. *The climate near the ground* (6th ed.). Rowman & Littlefield Publishers, Inc., Maryland. 584pp.
- Gelman. A., J.B. Carlin, H.S. Stern, and D.B. Rubin. 2004. *Bayesian data analysis* (2nd ed.). Chapman & Hall/CRC, New York. 668pp.
- Ghouil, H., P. Montpied, D. Epron, M. Ksontini, B. Hanchi, and E. Dreyer. 2003. Thermal optima of photosynthetic functions and thermostability of photochemistry in cork oak seedlings. *Tree Physiology* 23: 1031-1039.
- Gleason, H.A. 1926. The individualistic concept of the plant association. *Bulletin of the Torrey Botanical Club* 53: 7-26.
- Gomulkiewicz, R., J.N. Thompson, R.D. Holt, S.L. Nuismer, and M.E. Hochberg. 2000. Hot spots, cold spots, and the geographic mosaic theory of coevolution. *The American Naturalist* 156(2): 156-174.
- Goodchild, M.F. 1987. A spatial analytical perspective on geographical information systems, *International Journal of Geographical Information Systems* 1(4): 327-334.
- Guisan, A. and W. Thuiller. 2005. Predicting species distribution: offering more than simple habitat models. *Ecology Letters* 8(9): 993-1009.
- Guisan, A. and N.E. Zimmermann. 2000. Predictive habitat distribution models in ecology. *Ecological Modelling* 135: 147-186.
- Guisan, A., T.C. Edwards, and T. Hastie. 2002. Generalized linear and generalized additive models in studies of species distributions: setting the scene. *Ecological Modelling* 157(2-3): 89-100.
- Gunderson, C.A., R.J. Norby, and S. Wullschleger. 2000. Acclimation of photosynthesis and respiration to simulated climatic warming in northern and southern populations of *Acer saccharum*: laboratory and field evidence. *Tree Physiology* 20: 87-96.

- Haining, R. 1994. Designing spatial data analysis modules for geographical information systems. In *Spatial Analysis and GIS* (S. Fotheringham and P. Rogerson eds.). Taylor & Francis Ltd, London. 281pp.
- Haldimann, P. and U. Feller. 2004. Inhibition of photosynthesis by high temperature in oak (*Quercus pubescens* L.) leaves grown under natural conditions closely correlates with a reversible heat-dependent reduction of the activation state of ribulose-1, 5-bisphosphate carboxylase/oxygenase. *Plant, Cell and Environment* 27: 1169-1183.
- Hamrick, J.L. 2004. Response of forest trees to global environmental changes. *Forest Ecology and Management* 197: 323-335.
- Heide, O.M. 1993. Dormancy release in beech buds (*Fagus sylvatica*) requires both chilling and long days. *Physiologia Plantarum* 89: 187-191.
- Heide, O.M.. 2003. High autumn temperature delays spring bud burst in boreal trees, counterbalancing the effect of climatic warming. *Tree Physiology* 23: 931-936.
- Hererra, C.M and O. Pellmyr. 2002. *Plant Animal Interactions: An Evolutionary Approach*. Blackwell Science Ltd., Malden, USA. 328pp.
- Higashi, M. and Patten, B. C. 1989. Dominance of indirect causality in ecosystems. *Amer. Nat.* 133: 288-302.
- Higgins, S.I., J.S. Clark, R. Nathan, T. Hovestadt, F. Schurr, J.M.V. Fragoso, M.R. Aguiar, E. Ribbens, and S. Lavorel. 2003. Forecasting plant migration rates: managing uncertainty for risk assessment. *Journal of Ecology* 91: 341-347.
- Hilborn, R. and M. Mangel. 1997. *The ecological detective: confronting models with data*. Princeton University Press, New Jersey, USA. 315pp.
- Holdrige, L.R. 1947. Determination of world plant formations from simple climatic data. *Science* 105(2727): 367 – 368.
- Holling, C.S. 1992. Cross-scale morphology, geometry, and dynamics of ecosystem. *Ecological Monographs* 62(4): 447-502.
- Hörsch, B. 2003. Modelling the spatial distribution of montane and subalpine forests in the central Alps using digital elevation models. *Ecological Modelling* 168(3): 267-282.
- Huggett, B.A., P.G. Schaberg, G.J. Hawley, and C. Eagar. 2007. Long-term calcium addition increases growth release, wound closure, and health of sugar maple (*Acer saccharum*) trees at the Hubbard Brook experimental forest. *Canadian Journal of Forest Research* 37: 1692-1700.

- Huntley, B., P.J. Bartlein, and I.C. Prentice. 1989. Climate control of the distribution and abundance of beech (*Fagus L.*) in Europe and North America. *Journal of Biogeography* 16: 551-560
- IPCC 2007, IPCC fourth assessment report: The physical science basis, contribution of working group 1 report, Chapter 11.
- Iverson, L.R. and A.M. Prasad. 1998. Predicting abundance of 80 tree species following climate change in the eastern United States. *Ecological Monographs* 68(4): 465-485.
- Jacobsen, J.V., D.W. Pearce, A. T. Poole, R.P. Pharis, and L.N. Mander. 2002. Abscisic acid, phaseic acid and gibberellin contents associated with dormancy and germination in barley. *Physiologia Plantarum* 115: 428-441.
- Jenkins, M. 2007. Thematic accuracy assessment: Great Smoky Mountains National Park vegetation map. 26pp.
- Jiang, M. and R. Jagels. 1999. Detection and quantification of changes in membrane-associated calcium in red spruce saplings exposed to acid fog. *Tree Physiology* 19(14): 909-916.
- Johnson, A.H., E.R. Cook, and T.G. Siccama. 1988. Climate and red spruce growth and decline in the northern Appalachians. *Proceedings Natural Academic of Sciences of the United State of America* 85: 5369-5373.
- Johnson, A.H., S.B. McLaughlin, M.B. Adams, E.R. Cook, D.H. DeHayes, C. Eagar, I.J. Fernandez, D.W. Johnson, R.J. Kohut, and V.A. Mohnen. 1992. Synthesis and conclusions from epidemiological and mechanistic studies of red spruce decline. In: *Ecology and decline of red spruce in the Eastern United States*, Springer-Verlag, New York, pages 385-411.
- Johnson, A.H., E.R. Cook, T.G. Siccama, J.J. Battles, S.B. McLaughlin, D.C. LeBlanc, and P.M. Wargo. 1995. Comment: synchronic large-scale disturbances and red spruce decline. *Canadian Journal of Forest Research* 25: 851-858.
- Johnson, D.W. and S.E. Lindberg, editors. 1992. *Atmospheric Deposition and nutrient cycling in forest ecosystem*. Springer-Verlag, New York. 707pp.
- Johnson, D.H. 1999. The insignificance of statistical significance testing. *Journal of Wildlife Management* 63(3): 763-772.
- Jones, F.A., J. Chen, G. -J. Weng, and S.P. Hubbell. 2005. A genetic evaluation of seed dispersal in the neotropical tree *Jacaranda copaia* (Bignoniaceae). *The American Naturalist* 166: 543-555.
- Jørgensen, S.E. and G. Bendoricchio. 2001. *Fundamentals of Ecological Modelling (3rd Edition)*, *Developments in Environmental Modelling* 21. Elsevier, Amsterdam, 530pp.

- Joslin, J.D., C. McDuffie, and P.F. Brewer. 1988. Acidic cloud water and cation loss from red spruce foliage, *Water Air Soil Pollution* 39: 355-363.
- June, T., J.R. Evans and G.D. Farquhar. 2004. A simple new equation for the reversible temperature dependence of photosynthetic electron transport: a study on soybean leaf. *Functional Plant Biology* 31: 275-283.
- Kent, M., R.A. Moyeed, C.L. Reid, R. Pakeman, and R. Weaver. 2005. Geostatistics, spatial rate of change analysis and boundary detection in plant ecology and biogeography. *Progress in Physical Geography* 30(2): 201-231.
- Kerr, J.T., H.M. Kharouba and D.J. Currie. 2007. The macroecological contribution to global change solutions. *Science* 316: 1581-1584.
- King, R.S., C.J. Richardson, D.L. Urban, and E.A. Romanowicz. 2004. Spatial dependency of vegetation-environment linkages in an anthropogenically influenced wetland ecosystem. *Ecosystems* 7: 75-97.
- Kingsland, S.E. 1991. Definition as a science. In: *Foundations of ecology: classic papers with commentaries* (Reak, L., and J.H. Brown, eds.), University of Chicago Press, Chicago, pages 1-13.
- Kinraide, T.B. 1998. Three mechanisms for the calcium alleviation of mineral toxicities. *Plant Physiology* 118:513-520.
- Kiviniemi, K. 1996. A study of adhesive seed dispersal of three species under natural conditions. *Acta Biotheoretica*. 45(1): 73-83
- Kolb, P.F. and R. Robberecht. 1996. High temperature and drought stress effects on survival of *Pinus ponderosa* seedlings. *Tree Physiology* 16: 665-672.
- Kormondy, E.J. 1965. *Readings in ecology*. Prentice Hall, Englewood Cliffs, New Jersey. 219pp.
- Krivtsov, V., J. Corliss, E. Bellinger, and D. Sigeo. 2000. Indirect regulation rule for consecutive stages of ecological succession. *Ecological Modelling* 133: 73-82.
- Kuhn, T.S. 1996. *The structure of scientific revolutions* (3rd ed.). University of Chicago Press, Chicago. 212pp.
- Kulmatiski, A., K.A. Vogt, D.J. Vogt, P.M. Wargo, J.P. Tilley, T.G. Siccama, R. Sigurdardottir and D. Ludwig. 2007. Nitrogen and calcium additions increase forest growth in northeastern USA spruce-fir forests. *Canadian Journal of Forest Research* 37: 1574-1585.
- Ladjal, M., D. Epron, and M. Ducrey. 2000. Effects of drought preconditioning on thermotolerance of photosystem II and susceptibility of photosynthesis to heat stress in cedar seedlings. *Tree physiology* 20: 1325-1241.

- Lambers, H., F.S. Chapin III, and T.L. Pons. 1998. Plant physiological ecology. Springer, New York. 540p.
- Larigauderie, A. and C. Körner. 1995. Acclimation of leaf dark respiration to temperature in alpine and lowland plant species. *Annals of Botany* 76: 245-252.
- Lawton, J.L. 2000. Concluding remarks: a review of some open questions. In *Ecological consequences of heterogeneity* (ed. By M.J. Hutchings, E. John, and A.J.A. Stewart). Cambridge University Press, Cambridge. pp. 401-424.
- Le Page-Degivry, M.T., G. Garello, and P. Barthe. 1997. Changes in abscisic acid biosynthesis and catabolism during dormancy breaking in *Fagus sylvatica* embryo. *Journal of Plant Growth Regulation* 16: 57-61.
- LeBlanc, D.C., N.S. Nicholas, and S.M. Zedaker. 1992. Prevalence of individual-tree growth decline in red spruce populations of the southern Appalachian Mountains. *Canadian Journal of Forest Research* 22: 905-914.
- LeBlanc, D.C. 1993. Spatial and temporal variations in the prevalence of growth decline in red spruce populations of the northeastern United States: reply. *Canadian Journal of Forest Research* 23(7): 1494-1496.
- Levin S.A. 1992. The problem of pattern and scale in ecology. *Ecology* 73(6): 1943-1967.
- Li, C., A. Viherä-Aarnio, T. Puhakainen, O. Junttila, P. Heino, and E.T. Palva. 2003a. Ecotype-dependent control of growth, dormancy and freezing tolerance under seasonal changes in *Betula pendula* Roth. *Trees* 17:127-132.
- Li, C., O. Junttila, P. Heino, and E.T. Palva. 2003b. Different responses of northern and southern ecotypes of *Betula pendula* to exogenous ABA application. *Tree Physiology* 23: 481-487.
- Lo, C.P. and A.K.W. Yeung. 2007. *Concepts and techniques in Geographic Information Systems*. Pearson Education Inc., New Jersey. 532pp.
- MacKinnon, W.E. and D.A. MacLean. 2003. The influence of forest and stand conditions on spruce budworm defoliation in New Brunswick, Canada. *Forest Science* 49(5): 657-667.
- MacKinnon, W.E. and D.A. MacLean. 2004. Effects of surrounding forest and site conditions on growth reduction of balsam fir and spruce caused by spruce budworm defoliation. *Canadian Journal of Forest Research* 34: 2351-2362.
- Madden, M., R. Welch, T. Jordan, P. Jackson, R. Seavey, and J. Seavey. 2004. Digital vegetation maps of the Great Smoky Mountains National Park, final report, Center for Remote Sensing and Mapping Science, Department of Geography, The University of Georgia, Athens, Georgia. 121pp.

- Matsui, T., T. Yagihashi, T. Nakaya, N. Tanaka, and H. Taoda. 2004. Climatic controls on distribution of *Fagus crenata* forest in Japan. *Journal of Vegetation Science* 15: 57-66.
- McLaughlin, S. and K. Percy. 1999. Forest health in North America: some perspectives on actual and potential roles of climate and air pollution. *Water, Air, and Soil Pollution* 116: 151-197.
- McLaughlin, J.F., J.J. Hellmann, C.L. Boggs, and P.R. Ehrlich. 2002. Climate change hastens population extinctions. *PNAS* 99(9): 6070-6074.
- McLaughlin, S.B., D.J. Downing, T.J. Blasing, E.R. Cook, and H.S. Adams. 1987. An analysis of climate and competition as contributors to decline of red spruce in high elevation Appalachian forests of the Eastern United States. *Oecologia* 72: 487-501.
- McLaughlin, S.B. and R.J. Kohut. 1992. The effects of atmospheric deposition and ozone on carbon allocation and associated physiological processes in red spruce. In: *Ecology and decline of red spruce in the Eastern United States*, Springer-Verlag, New York, pages 338-382.
- McNulty, S.G., J. Boggs, J.D. Aber, L. Rustad, and A. Magill. 2005. Red spruce ecosystem level changes following 14 years of chronic N fertilization. *Forest Ecology and Management* 219: 279-291.
- Meier, I.C. and C. Leuschner. 2008. Leaf size and leaf area index in *Fagus sylvatica* forests: competing effects of precipitation, temperature, and nitrogen availability. *Ecosystems* 11(5): 655-669.
- Mencuccini, M., J. Martínez-Vilalta, H.A. Hamid, E. Korakaki, and D. Vanderklein. 2007. Evidence for age- and size-mediated controls of tree growth from grafting studies. *Tree Physiology* 27: 463-473.
- Miles, L., A. Grainger, and O. Phillips. 2004. The impact of global climate change on tropical forest biodiversity in Amazonia. *Global Ecology and Biogeography*. 13 (6), 553-565.
- Münier, B., B. Nygaard, R. Ejrnæs, and H.G. Bruun. 2001. A biotope landscape model for prediction of semi-natural vegetation in Denmark. *Ecological Modelling* 139: 221-233.
- Myking, T. and O.M. Heide. 1995. Dormancy release and chilling requirement of buds of latitudinal ecotypes of *Betula pendula* and *B. pubescens*. *Tree Physiology* 15: 697-704.
- Nathan, R. and H.C. Muller-Landau. 2000. Spatial patterns of seed dispersal, their determinants and consequences for recruitment. *Tree* 15(7): 278-285.
- Nathan, R., G.G. Katul, H.S. Horn, S.M. Thomas, R. Oren, R. Avissar, S.W. Pacala, and S.A. Levin. 2000. Mechanisms of long-distance dispersal of seeds by wind. *Nature* 418: 409-413.

- Niven, B.S. and D.E. Abel. 1991. Logical synthesis of environment of King Penguin, *Aptenodytes-Patagonicus*. *Ecological Modelling*. 56 (1-4), 291-311.
- Niven, B.S. and M.J. Liddle. 1994. Towards a classification of the environment and the community of *Quercus-Robur*. *Journal of Vegetation Science*. 5 (3), 317-326.
- Norby, R. and Y. Luo. 2004. Evaluating ecosystem responses to rising atmospheric CO₂ and global warming in a multi-factor world. *New Phytologist* 162: 282-293.
- Odum, E.P. 1962. Relationships between structure and function in ecosystems. *The Japanese Journal of Ecology* 12: 108-118.
- Ozemoy, V.M., D.R. Smith, and A. Sicherman. 1981. Evaluating computerized geographic information systems using decision analysis. *Interfaces* 11:92-8.
- Pandey, S., S. Kumar, and P.K. Nagar. 2003. Photosynthetic performance of *Ginkgo biloba* L. grown under high and low irradiance. *Photosynthetica* 41(4): 505-511.
- Parmesan, C. and G.A. Yohe. 2003. Globally coherent fingerprint of climate change impacts across natural systems. *Nature*. 421 (6918), 37-42.
- Patten, B.C. and J.T. Finn. 1978. Systems approach to continental shelf ecosystem. In: *Theoretical systems ecology* (E. Halfon ed.). Academic Press, New York, pages 183-212.
- Patten, B.C. and G.T. Auble. 1980. Systems-Approach to the concept of niche. *Syntheses* 43 (1), 155-181
- Patten, B.C. 1982. Indirect causality in ecosystems: its significance for environmental protection. In: Mason, W.T., Iker, S. (Eds.), *Research on Fish and Wildlife Habitat. Commemorative Monograph in Honor of the First Decade of the US Environmental Protection Agency. Office of Research and Development, US Environmental Protection Agency, EPA-600/8-82-022, Washington, DC, pp. 92-107.*
- Patten, B. C. 1985a. Energy cycling in the ecosystem. *Ecological Modelling* 28: 1-71.
- Patten, B. C. 1985b. Energy cycling, length of food chains, and direct vs. indirect effects in ecosystems. *Can. Bull. Fish. Aqu. Sci.* 213: 119-138.
- Patten, B.C., 1990. Environ theory and indirect effects – reply. *Ecology*. 71(6), 2386-2393.
- Patten, B.C. 1991. Network ecology: indirect determination of the life-environment relationship in ecosystems. In: Higashi, M., Burns, T.P. (Eds.), *Theoretical Ecosystem Ecology: The Network Perspective*. Cambridge University Press, London, pp. 288-351.
- Patten, B.C., 1997. Synthesis of chaos and sustainability in a nonstationary linear dynamic model of the American black bear (*Ursus americanus pallas*) in the Adirondack Mountains of New York. *Ecological Modelling*. 100 (1-3), 11-42.

- Patten, B.C., 1998. Ecology's AWFUL theorem: sustaining sustainability. *Ecological Modelling*. 108 (1-3), 97-105.
- Patten, B.C. 2009. *Holoecology, The Unification of Nature by Network Indirect Effects*. Complexity in Ecological Systems series, Columbia University Press, New York. In preparation.
- Pearson, R.G. and T.P. Dawson. 2003. Predicting the impacts of climate change on the distribution of species: are bioclimate envelope models useful? *Global Ecology & Biogeography* 12: 361-371.
- Peter, D.P.C., B.T. Bestelmeyer, and M.G. Turner. 2007. Cross-scale interactions and changing pattern-process relationships: Consequences for system dynamics. *Ecosystems* 10(5): 790-796.
- Peterson, G.D. 2008. Scaling ecological dynamics: self-organization, hierarchical structure, and ecological resilience. *Climate Change*. In press.
- Pitelka, L.F. 1997. Plant migration and climate change. *American Scientist* 85(5): 464-473.
- Pounds, J.A., M.P.L. Fogden, and J.H. Campbell. 1999. Biological response to climate change on a tropical mountain. *Nature* 398 (6728): 611-615.
- Pregitzer, K.S., A.J. Burton, D.R. Zak, and A.F. Talhelm. 2008. Simulated chronic nitrogen deposition increases carbon storage in northern temperate forests. *Global Change Biology* 14: 142-153.
- Primack. R.B. and S.L. Miao. 1992. Dispersal can limit local plant distribution. *Conservation Biology* 6(4): 513-519.
- Pulliam, H.R. 1988. Sources, Sinks, and Population Regulation. *The American Naturalist* 132: 652-661.
- Pulliam, H.R. 2000. On the relationship between niche and distribution. *Ecology Letters* 3(4): 349-361.
- Rabenold, K.N., P.T. Fauth, B.W. Goodner, J.A. Sadowski, and P.G. Parker. 1998. Response of avian communities to disturbance by an exotic insect in spruce-fir forests of the Southern Appalachians. *Conservation Biology* 12: 177-189.
- Reams, G.A. and P.C.V. Deusen. 1995. Synchronic large-scale disturbances and red spruce growth decline. *Canadian Journal of Forest Research* 25(5): 859-869.
- Reuter, H., F. Hölker, U. Middelhoff, F. Jopp, C. Eschenbach, and B. Breckling. 2005. Emergent properties in individual-based models case studies from the Bornhöved project (Northern Germany). *Ecological Modelling* 186(4): 489-501.

- Richardson, A.D., G.P. Berlyn, and T.G. Gregoire. 2004. Spectral reflectance of *Picea rubens* (Pinaceae) and *Abies balsamea* (Pinaceae) needles along an elevational gradient, Mt. Moosilauke, New Hampshire, USA. *American Journal of Botany* 88(4): 667-676.
- Rinne, P., H. Hänninen, P. Kaikuranta, J.E. Jalonen, and T. Repo. 1997. Freezing exposure releases bud dormancy in *Betula pubescens* and *B. pendula*. *Plant, Cell and Environment* 20: 1199-1204.
- Schaberg, P.G. 2000. Winter photosynthesis in red spruce (*Picea rubens* Sarg.): limitations, potential benefits, and risks. *Arctic, Antarctic, and Alpine Research* 32(4): 375-380.
- Schaberg, P.G., J.B. Shane, P.F. Cali, J.R. Donnelly, and G.R. Strimbeck. 1998. Photosynthetic capacity of red spruce during winter. *Tree Physiology* 18: 271-276.
- Schaberg, P.G., D.H. Dehayes, G.J. Hawley, G.R. Strimbeck, J.R. Cumming, P.F. Murakami, and C.H. Borer. 2000. Acid mist and soil Ca and Al alter the mineral nutrition and physiology of red spruce. *Tree Physiology* 20: 73-85.
- Schmitz, N., S.R. Abrams, and A.R. Kermode. 2002. Changes in ABA turnover and sensitivity that accompany dormancy termination of yellow-cedar (*Chamaecyparis nootkatensis*) seeds. *Journal of Experimental Botany* 53(366): 89-101.
- Schneider, D.C. 2001. The rise of the concept of scale in ecology. *BioScience* 51(7): 545-553.
- Schwartz, M.W., L.R. Iverson, and A.M. Parsad. 2001. Predicting the potential future distribution of four tree species in Ohio using current habitat availability and climatic forcing. *Ecosystem* 4: 568-581.
- Seddon, B. 1971. *Introduction to biogeography*. Gerald Duckworth and C. Ltd. London, UK. 220p.
- Sevanto, S., T. Suni, J. Pumpanen, T. Grönholm, P. Kolari, E. Nikinmaa, P. Hari, and T. Vesala. 2006. Wintertime photosynthesis and water uptake in a boreal forest. *Tree Physiology* 26: 749-757.
- Shanks, R.E. 1954. Climates of the Great Smoky Mountains. *Ecology* 35(3): 354-361.
- Shao, G. and P.N. Halpin. 1995. Climate controls of eastern North American coastal tree and shrubs distribution. *Journal of Biogeography* 22(6): 1083-1089.
- Sheppard, L.J., J.N. Cape, and I.D. Leith. 1993. Influence of acidic mist on frost hardiness and nutrient concentrations in red spruce seedlings: effects of misting frequency and rainfall exclusion. *New Phytologist* 124: 607-615.
- Sheppard, L. and H. Pfanz. 2001. Impacts of air pollutants on cold hardiness in Conifer cold hardiness (Bigras, F.J., and J.C. Stephen, editors). Springer, New York. 569pp.

- Shortle, W.C. and K.T. Smith. 1988. Aluminum-induced calcium deficiency syndrome in declining red spruce. *Science* 240(4855): 1071-1018.
- Skidmore, B.A. and E.R. Heithaus. 1988. Lipid cues for seed-carrying by ants in *Hepatica*. *Journal of Chemical Ecology*. 14(12) 2185-2196.
- Skov, F. and F. Borchsenius. 1997. Predicting plant species distribution patterns using simple climatic parameters: a case study of Ecuadorian palms. *Ecography* 20: 347-355.
- Smith, G.F. 1998. Patterns of overstory composition in the Fir and Fir-spruce forests of the Great Smoky Mountain after Balsam Woolly Adelgid infestation. *Am. Midl. Nat.* 139: 340-352.
- Solomon, D.S., L. Zhang, T.B. Brann, and D.S. Larrick. 2003. Mortality patterns following spruce budworm infestation in unprotected spruce-fir forests in Maine. *Northern Journal of Applied Forestry* 20(4): 148-153.
- Tan, C.O., U. Özesmi, M. Beklioglu, E. Per, and B. Kurt. 2006. Predictive models in ecology: Comparison of performances and assessment of applicability. *Ecological Informatics* 1: 195-211.
- Tansley, A.G. 1935. The use and abuse of vegetational concepts and terms. *Ecology* 16: 284-307.
- Thompson, J.N. and B.M. Cunningham. 2002. Geographic structure and dynamics of coevolutionary selection. *Nature* 417: 735-738.
- Thompson, J.N. 1999. Specific Hypotheses on the geographic mosaic of coevolution. *The American Naturalist* 153: S1-S14.
- Turner, M.G., R.H. Gardner, and R.V. O'Neill. 2001. *Landscape Ecology in Theory and Practice: Pattern and Process*. Springer-Verlag New York, Inc., New York, USA. 401p.
- Uexküll, J. von. 1926. *Theoretical Biology* (Transl. by D. L. MacKinnon. International Library of Psychology, Philosophy and Scientific Method.). Kegan Paul, Trench, Trubner & Co, Ltd., London, UK. 362pp.
- Venables, W.N. and B.D. Ripley. 2002. *Modern Applied Statistics with S* (4th ed.). Springer-Verlag New York, Inc., New York. 495pp.
- Voinov, A., C. Fitz, R. Bounmans, and R. Costanza. 2004. Modular ecosystem modeling. *Environmental Modelling & Software*. 19(3): 285-304.
- Walther, G.R., E. Post, P. Convey, A. Menzel, C. Parmesan, T.J.C. Beebee, J.M. Fromentin, O. Hoegh-Guldberg, and F. Bairlein. 2002. Ecological responses to recent climate change. *Nature* 416: 389-395.

- Webb, S.L., M.G. Glenn, E.R. Cook, W.S. Wagner, and R.D. Thetford. 1993. Range edge red spruce in New Jersey, U.S.A.: Bog versus upland population structure and climate responses. *Journal of Biogeography* 20(1): 63-78.
- Webster, K.L., I.F. Creed, N.S. Nicholas, and H. Van Miegroet. 2004. Exploring interactions between pollutant emissions and climatic variability in growth of red spruce in the Great Smoky Mountains National Park. *Water Air and Soil Pollution*. 159 (1-4), 225-248.
- Weinberg, G.M. 1975. *An introduction to general systems thinking*. John Wiley & Sons Inc., New York. 302pp.
- Welch, R., M. Madden, and T. Jordan. 2002. Photogrammetric and GIS techniques for the development of vegetation databases of mountainous areas: Great Smoky Mountains National Park. *ISPRS Journal of Photogrammetry & Remote Sensing* 57: 53-68.
- Westoby, M., M. Leishman, J. Lord, H. Pooter, and D.J. Schoen. 1996. Comparative ecology of seed size and dispersal [and discussion]. *Philosophical Transactions of the Royal Society* 351: 1309-1318.
- White, I.D., D.N. Mottershead, and S.J. Harrison. 1992. *Environmental systems: An introductory text* (2nd edition). Chapman & Hall, London, 616pp.
- Whittaker, R.H. 1975. *Communities and ecosystem* (2nd ed.). Macmillan, New York. 385pp.
- Willis, K.J. and R.J. Whittaker. 2002. Species diversity-Scale matters. *Science* 295: 1245-1248.
- Woodward, F.I. 1987. *Climate and plant distribution*. Cambridge University Press, Cambridge. 188pp.

APPENDICES

Appendix 1

Equations, Data and documents for ARIM_{high}

The followings show and explain equations and data used for ARIM_{high} simulation in Stella.

Main model

ARIM = 0*Radiation + 0*Nutrients + 0*Carbon Dioxide + 0* Water Availability -0.67955*Air Pollution Disturbance - 0*Herbivory + 0* Soil Mediated Disturbance -0*Weather Disturbance + 1.55774

DOCUMENT: Apply the GLM model in Table 2 (a) in section 3.2 of Results. In GLM and CART models, Radiation = RA, Nutrient = NU, Carbon Dioxide = CO2, Water Availability = WA, Weather Disturbance = WD, Air Pollution Disturbance = APD, Herbivory = HB, and Soil Mediated Disturbance = SMD.

High AV Treering = GRAPH(TIME)

(1.00, 1.12), (2.00, 1.29), (3.00, 1.18), (4.00, 1.24), (5.00, 1.25), (6.00, 1.17), (7.00, 1.16), (8.00, 1.26), (9.00, 1.17), (10.0, 1.31), (11.0, 1.03), (12.0, 1.09), (13.0, 0.989), (14.0, 1.07), (15.0, 1.07), (16.0, 1.08), (17.0, 0.985), (18.0, 1.11), (19.0, 0.876), (20.0, 0.863), (21.0, 0.934), (22.0, 0.85), (23.0, 0.895), (24.0, 0.81), (25.0, 1.11), (26.0, 1.09), (27.0, 0.977), (28.0, 0.852), (29.0, 0.813), (30.0, 0.655), (31.0, 0.772), (32.0, 0.72), (33.0, 0.612), (34.0, 0.591), (35.0, 0.639), (36.0, 0.748), (37.0, 0.906), (38.0, 0.639), (39.0, 0.742), (40.0, 0.608), (41.0, 0.879), (42.0, 0.564), (43.0, 0.665), (44.0, 0.858), (45.0, 0.641), (46.0, 0.682), (47.0, 0.839), (48.0, 0.728), (49.0, 0.751), (50.0, 0.666), (51.0, 0.763), (52.0, 0.725), (53.0, 0.983), (54.0, 1.33), (55.0, 1.19), (56.0, 1.50), (57.0, 1.23), (58.0, 1.01), (59.0, 0.785)

DOCUMENT: High AV Treering means the average standardized ring width index value of red spruce at high elevation. In the parentheses, the first entry shows the simple order and the second one the index value.

Radiation Submodel

Radiation = (if Aspect=2 then 2 else (if Aspect =3 then 3 else (if Aspect=4 then 2.5 else 1))) + Fir Mortality + (if Slope=5 then 1 else (if Slope=4 then 2 else (if Slope=3 then 3 else (if Slope=2 then 4 else 5)))) - Cloud Immersion - Precipitation Effect 1 + ((1.276949 - Temperature)*Temperature)/6

DOCUMENT: For the Temperature parameter, the logistic map was applied:

$$X_{n+1} = r * X_n (1 - X_n)$$

where X_n is a population in year n , and r is bifurcation parameter (>0)

Aspect = 1

DOCUMENT: N(316-45); E(46-135); S(136-225); W(226-315)--> N=1; E=2; S=3; W=4

Balsam woolly adelgid = Observed Winter Cold Temp

Cloud Immersion = (If (Elevation <1400) Then (0) Else (If (Elevation >=1400 and Elevation<1800) Then (1) Else (2)))/2

Elevation = 1900

Fir Mortality = Balsam woolly adelgid*((if (Elevation>=1700) then (2) else (1))/3)

Slope = 2

DOCUMENT: 5 classes (1:0-20; 2:21-40...): 1=0-20; 2=21-40; 3=41-60; 4=61-80; 5=81-100.
Slope is %value

Temperature = Average Temperature*((2 + 0*Observed CO2 + 0*Observed Ozone + 1*(if Aspect=2 then 0.65 else (if Aspect=3 then 1 else (if Aspect=4 then 0.65 else 0.3))) + 1*(if Elevation =1000 then 1 else (if Elevation = 1100 then 0.9 else (if Elevation =1200 then 0.8 else (if Elevation = 1300 then 0.7 else (if Elevation = 1400 then 0.6 else (if Elevation = 1500 then 0.5 else (if Elevation = 1600 then 0.4 else (if Elevation = 1700 then 0.3 else (if Elevation = 1800 then 0.2 else 0.1)))))))))) + 1*(if Slope=5 then 0.2 else (if Slope=4 then 0.4 else (if Slope=3 then 0.6 else (if Slope=2 then 0.8 else 1)))))/5)

Average Temperature = GRAPH(TIME)

(1.00, 0.957), (2.00, 1.03), (3.00, 1.00), (4.00, 1.02), (5.00, 1.02), (6.00, 1.01), (7.00, 1.05), (8.00, 0.992), (9.00, 1.02), (10.0, 1.04), (11.0, 0.997), (12.0, 1.03), (13.0, 1.04), (14.0, 1.07), (15.0, 1.05), (16.0, 1.03), (17.0, 1.03), (18.0, 1.04), (19.0, 0.961), (20.0, 1.02), (21.0, 0.959), (22.0, 0.95), (23.0, 1.00), (24.0, 0.948), (25.0, 0.968), (26.0, 1.02), (27.0, 0.951), (28.0, 0.958), (29.0, 0.955), (30.0, 0.93), (31.0, 0.988), (32.0, 0.986), (33.0, 0.944), (34.0, 0.983), (35.0, 1.01), (36.0, 1.01), (37.0, 0.966), (38.0, 1.01), (39.0, 0.974), (40.0, 0.957), (41.0, 0.991), (42.0, 0.978), (43.0, 0.993), (44.0, 0.984), (45.0, 1.01), (46.0, 0.986), (47.0, 1.05), (48.0, 1.04), (49.0, 1.02), (50.0, 0.98), (51.0, 1.07), (52.0, 1.03), (53.0, 0.961), (54.0, 0.999), (55.0, 1.00), (56.0, 1.00), (57.0, 0.945), (58.0, 0.961), (59.0, 1.04)

DOCUMENT: Average Temperature is an index value, which is calculated by dividing each yearly average value of maximum temperature by the corresponding long-term mean. In parentheses, the first entry shows the simple order and the second one the index value.

Precipitation Effect 1 = Precipitation1*((If Elevation < 1700 then 1 else 2)/3)

Precipitation 1 = GRAPH(TIME)

(1.00, 0.882), (2.00, 0.744), (3.00, 1.08), (4.00, 0.921), (5.00, 0.935), (6.00, 1.04), (7.00, 1.06), (8.00, 0.791), (9.00, 1.09), (10.0, 1.02), (11.0, 1.07), (12.0, 1.11), (13.0, 0.787), (14.0, 0.853), (15.0, 0.916), (16.0, 0.877), (17.0, 1.00), (18.0, 1.30), (19.0, 0.811), (20.0, 0.959), (21.0, 0.953), (22.0, 1.17), (23.0, 1.20), (24.0, 1.07), (25.0, 0.982), (26.0, 0.89), (27.0, 0.997), (28.0, 1.18), (29.0, 0.77), (30.0, 1.07), (31.0, 0.956), (32.0, 1.09), (33.0, 1.22), (34.0, 1.23), (35.0, 1.24), (36.0, 0.952), (37.0, 0.889), (38.0, 1.08), (39.0, 0.922), (40.0, 1.17), (41.0, 0.87), (42.0, 0.932), (43.0, 1.15), (44.0, 0.901), (45.0, 1.02), (46.0, 0.811), (47.0, 0.699), (48.0, 0.765), (49.0, 0.745), (50.0, 1.19), (51.0, 1.15), (52.0, 1.22), (53.0, 0.918), (54.0, 0.968), (55.0, 1.33), (56.0, 0.854), (57.0, 1.04), (58.0, 1.03), (59.0, 1.12)

DOCUMENT: Precipitation 1 is an index value, which is calculated by dividing each yearly average value by the corresponding long-term mean. In the parentheses, the first element shows the simple order and the second one the index value.

Water Availability Submodel

Water Availability = ((3* Precipitation Effect 2 + (if Distance to Stream =1 then 3 else (if Distance to Stream = 2 then 2 else 1)) - Fir Mortality – Temperature + (if Aspect=2 then 2.5 else (if Aspect =3 then 1 else (if Aspect=4 then 2 else 3))) + (if Slope=1 then 1 else (if Slope=2 then 2 else (if Slope=3 then 3 else (if Slope=4 then 4 else 5)))) + ((1.276949 - Temperature)*Temperature) + Radiation)/10)

Distance to Stream = 2

DOCUMENT: 1=near the stream, 2=slope, 3=ridge

Precipitation Effect 2 = ((Precipitation 1+ Precipitation 2)/2)*((If Elevation < 1700 then 1 else 2)/3)

Precipitation 2 = GRAPH(TIME)

(1.00, 1.00), (2.00, 0.882), (3.00, 0.744), (4.00, 1.08), (5.00, 0.921), (6.00, 0.935), (7.00, 1.04), (8.00, 1.06), (9.00, 0.791), (10.0, 1.09), (11.0, 1.02), (12.0, 1.07), (13.0, 1.11), (14.0, 0.787), (15.0, 0.853), (16.0, 0.916), (17.0, 0.877), (18.0, 1.00), (19.0, 1.30), (20.0, 0.811), (21.0, 0.959), (22.0, 0.953), (23.0, 1.17), (24.0, 1.20), (25.0, 1.07), (26.0, 0.982), (27.0, 0.89), (28.0, 0.997), (29.0, 1.18), (30.0, 0.77), (31.0, 1.07), (32.0, 0.956), (33.0, 1.09), (34.0, 1.22), (35.0, 1.23), (36.0, 1.24), (37.0, 0.952), (38.0, 0.889), (39.0, 1.08), (40.0, 0.922), (41.0, 1.17), (42.0, 0.87), (43.0, 0.932), (44.0, 1.15), (45.0, 0.901), (46.0, 1.02), (47.0, 0.811), (48.0, 0.699), (49.0, 0.765), (50.0, 0.745), (51.0, 1.19), (52.0, 1.15), (53.0, 1.22), (54.0, 0.918), (55.0, 0.968), (56.0, 1.33), (57.0, 0.854), (58.0, 1.04), (59.0, 1.03)

DOCUMENT: Precipitation 2 is the previous year precipitation and an index value, which is calculated by dividing each yearly average value by the corresponding long-term mean. In the parentheses, the first column shows the simple order and the second one the index value.

Carbon Dioxide Submodel

Carbon Dioxide = (((1.276949-Temperature)*Temperature) + Radiation + Water Availability)/3

Observed CO2 = GRAPH(TIME)

(1.00, 0.493), (2.00, 0.538), (3.00, 0.576), (4.00, 0.596), (5.00, 0.635), (6.00, 0.614), (7.00, 0.592), (8.00, 0.653), (9.00, 0.68), (10.0, 0.573), (11.0, 0.674), (12.0, 0.695), (13.0, 0.678), (14.0, 0.694), (15.0, 0.66), (16.0, 0.723), (17.0, 0.759), (18.0, 0.753), (19.0, 0.729), (20.0, 0.759), (21.0, 0.777), (22.0, 0.779), (23.0, 0.807), (24.0, 0.843), (25.0, 0.877), (26.0, 0.915), (27.0, 0.962), (28.0, 1.00), (29.0, 1.04), (30.0, 1.09), (31.0, 1.12), (32.0, 1.13), (33.0, 1.18), (34.0, 1.23), (35.0, 1.18), (36.0, 1.14), (37.0, 1.20), (38.0, 1.22), (39.0, 1.26), (40.0, 1.28), (41.0, 1.23), (42.0, 1.18), (43.0, 1.12), (44.0, 1.13), (45.0, 1.17), (46.0, 1.17), (47.0, 1.18), (48.0, 1.22), (49.0, 1.28), (50.0, 1.30), (51.0, 1.28), (52.0, 1.28), (53.0, 1.28), (54.0, 1.36), (55.0, 1.38), (56.0, 1.38), (57.0, 1.41), (58.0, 1.52), (59.0, 1.50)

DOCUMENT: Observed CO2 is index value, which is calculated by dividing each yearly average value by the corresponding long-term mean. In the parentheses, the first element shows the simple order and the second one the index value.

Nutrients Submodel

Nutrients = (Fir Mortality + Radiation + Water Availability + Atmospheric Deposition of Nutrients + ((1.276949-Temperature)*Temperature))/5

Atmospheric Deposition of Nutrients = GRAPH(TIME)

(1.00, 0.644), (2.00, 0.733), (3.00, 0.776), (4.00, 0.844), (5.00, 0.861), (6.00, 0.885), (7.00, 0.784), (8.00, 0.866), (9.00, 0.808), (10.0, 0.732), (11.0, 0.765), (12.0, 0.754), (13.0, 0.751), (14.0, 0.755), (15.0, 0.75), (16.0, 0.765), (17.0, 0.775), (18.0, 0.79), (19.0, 0.84), (20.0, 0.852), (21.0, 0.857), (22.0, 0.847), (23.0, 0.88), (24.0, 0.925), (25.0, 0.97), (26.0, 1.02), (27.0, 1.09), (28.0, 1.09), (29.0, 1.15), (30.0, 1.17), (31.0, 1.23), (32.0, 1.21), (33.0, 1.25), (34.0, 1.30), (35.0, 1.25), (36.0, 1.19), (37.0, 1.24), (38.0, 1.26), (39.0, 1.22), (40.0, 1.22), (41.0, 1.19), (42.0, 1.15), (43.0, 1.11), (44.0, 1.10), (45.0, 1.13), (46.0, 1.10), (47.0, 1.08), (48.0, 1.08), (49.0, 1.11), (50.0, 1.11), (51.0, 1.12), (52.0, 1.11), (53.0, 1.12), (54.0, 1.12), (55.0, 1.11), (56.0, 1.04), (57.0, 1.03), (58.0, 1.05), (59.0, 1.04)

DOCUMENT: Atmospheric Deposition of Nutrients is index value, which is calculated by dividing each yearly average value by the corresponding long-term mean. In the parenthesis, the first entry shows the simple order and the second one the index value. These values were obtained from $(\text{NO}_x \text{ emission} + \text{SO}_x \text{ emission})/2$.

Herbivory Submodel

Herbivory = Annual Mean Temp

Annual Mean Temp = GRAPH(TIME)

(1.00, 1.09), (2.00, 0.956), (3.00, 1.07), (4.00, 0.979), (5.00, 0.98), (6.00, 1.03), (7.00, 1.02), (8.00, 1.06), (9.00, 0.977), (10.0, 1.04), (11.0, 1.08), (12.0, 1.01), (13.0, 1.01), (14.0, 1.05), (15.0, 1.05), (16.0, 1.04), (17.0, 1.03), (18.0, 1.06), (19.0, 1.09), (20.0, 0.952), (21.0, 1.04), (22.0, 0.957), (23.0, 0.937), (24.0, 0.999), (25.0, 0.898), (26.0, 0.949), (27.0, 1.04), (28.0, 0.97), (29.0, 0.947), (30.0, 0.925), (31.0, 0.928), (32.0, 1.01), (33.0, 1.03), (34.0, 0.987), (35.0, 1.03), (36.0, 1.06), (37.0, 1.03), (38.0, 0.91), (39.0, 1.03), (40.0, 0.99), (41.0, 0.987), (42.0, 1.02), (43.0, 0.994), (44.0, 1.01), (45.0, 0.935), (46.0, 0.944), (47.0, 0.917), (48.0, 1.00), (49.0, 0.964), (50.0, 0.911), (51.0, 0.955), (52.0, 1.08), (53.0, 1.07), (54.0, 0.98), (55.0, 0.997), (56.0, 0.997), (57.0, 0.996), (58.0, 0.934), (59.0, 0.976)

DOCUMENT: Average Mean Temp is index value, which is calculated by dividing each yearly average value by the corresponding long-term mean. In the parenthesis, the first entry shows the simple order and the second one the index value. For the Herbivory submodel, the previous temperature value was applied for the current year because in general insect reproduction is controlled by previous temperature (Breckle 2002).

Weather Disturbance Submodel

Weather Disturbance = (0* Summer Hot Temperature + 2* Winter Cold Temperature + 1* Winter Warm Temperature)/3)

Summer Hot Temperature = Observed Sum Temp *((2+1*(if Aspect=2 then 0.5 else (if Aspect =3 then 1 else (if Aspect=4 then 0.65 else 0.3)))) - 1* Water Availability + 0*Observed CO2+ 0* Observed Ozone + 1*(if Elevation =1000 then 1 else (if Elevation = 1100 then 0.9 else (if Elevation =1200 then 0.8 else (if Elevation = 1300 then 0.7 else (if Elevation = 1400 then 0.6 else (if Elevation = 1500 then 0.5 else (if Elevation = 1600 then 0.4 else (if Elevation = 1700 then 0.3 else (if Elevation = 1800 then 0.2 else 0.1)))))))))) + 1*(if Slope=5then 0.2 else (if Slope=4 then 0.4 else (if Slope=3 then 0.6 else (if Slope=2 then 0.8 else 1)))))/6)

Winter Cold Temperature = Observed Winter Cold Temp *((2 + 4* Air Pollution - 0* Observed CO2 - 0* Observed Ozone + 1*(if Elevation =1000 then 0.1 else (if Elevation = 1100 then 0.2 else (if Elevation =1200 then 0.3 else (if Elevation = 1300 then 0.4 else (if Elevation = 1400 then 0.5 else (if Elevation = 1500 then 0.6 else (if Elevation = 1600 then 0.7 else (if Elevation = 1700 then 0.8 else (if Elevation = 1800 then 0.9 else 1)))))))))))+1*(if Slope=5then 0.2 else (if Slope=4 then 0.4 else (if Slope=3 then 0.6 else (if Slope=2 then 0.8 else 1)))) + 1*(if Aspect=2 then 0.5 else (if Aspect =3 then 1 else (if Aspect=4 then 0.65 else 0.3))))/9)

Winter Warm Temperature = Observed Winter Warm Temp * ((2 + 0*Observed CO2+0* Observed Ozone + 1*(if Aspect=2 then 0.5 else (if Aspect =3 then 1 else (if Aspect=4 then 0.65 else 0.3))) + 1*(if Elevation =1000 then 0.1 else (if Elevation = 1100 then 0.2 else (if Elevation =1200 then 0.3 else (if Elevation = 1300 then 0.4 else (if Elevation = 1400 then 0.5 else (if Elevation = 1500 then 0.6 else (if Elevation = 1600 then 0.7 else (if Elevation = 1700 then 0.8 else (if Elevation = 1800 then 0.9 else 1)))))))))) + 1*(if Slope=5then 0.2 else (if Slope=4 then 0.4 else (if Slope=3 then 0.6 else (if Slope=2 then 0.8 else 1))))/5)

Observed Sum Temp = GRAPH(TIME)

(1.00, 0.989), (2.00, 1.02), (3.00, 1.01), (4.00, 1.06), (5.00, 1.04), (6.00, 1.00), (7.00, 0.989), (8.00, 0.997), (9.00, 1.02), (10.0, 1.02), (11.0, 0.956), (12.0, 1.04), (13.0, 1.07), (14.0, 1.05), (15.0, 1.07), (16.0, 1.01), (17.0, 1.01), (18.0, 1.04), (19.0, 1.00), (20.0, 1.02), (21.0, 1.00), (22.0, 0.924), (23.0, 1.01), (24.0, 0.939), (25.0, 0.964), (26.0, 0.979), (27.0, 0.991), (28.0, 0.904), (29.0, 1.00), (30.0, 0.976), (31.0, 0.977), (32.0, 0.961), (33.0, 0.936), (34.0, 0.954), (35.0, 0.948), (36.0, 1.00), (37.0, 0.973), (38.0, 1.02), (39.0, 0.989), (40.0, 0.937), (41.0, 1.06), (42.0, 1.02), (43.0, 0.959), (44.0, 1.02), (45.0, 0.965), (46.0, 0.977), (47.0, 1.06), (48.0, 1.05), (49.0, 1.06), (50.0, 0.974), (51.0, 1.02), (52.0, 0.992), (53.0, 0.942), (54.0, 1.07), (55.0, 0.981), (56.0, 1.05), (57.0, 0.972), (58.0, 0.973), (59.0, 1.01)

DOCUMENT: Observed Sum Temp (= Observed Summer Hot Temperature) is index value, which is calculated by dividing each yearly average value by the corresponding long-term mean. In the parentheses, the first element shows the simple order and the second one the index value.

Observed Winter Cold Temp = GRAPH(TIME)

(1.00, 0.779), (2.00, 1.18), (3.00, 0.687), (4.00, 1.03), (5.00, 1.19), (6.00, 0.886), (7.00, 1.18), (8.00, 0.752), (9.00, 1.02), (10.0, 1.72), (11.0, 1.52), (12.0, 1.20), (13.0, 1.54), (14.0, 1.25), (15.0, 1.09), (16.0, 0.984), (17.0, 1.64), (18.0, 1.62), (19.0, 0.31), (20.0, 1.06), (21.0, 0.774), (22.0, 1.01), (23.0, 0.955), (24.0, 0.0133), (25.0, 0.787), (26.0, 0.968), (27.0, 0.968), (28.0, 1.17), (29.0, 0.391), (30.0, 0.89), (31.0, 0.666), (32.0, 1.29), (33.0, 1.31), (34.0, 0.928), (35.0, 1.64), (36.0, 1.31), (37.0, 0.736), (38.0, 0.373), (39.0, 0.453), (40.0, 0.669), (41.0, 0.936), (42.0, 0.665), (43.0, 1.05), (44.0, 0.749), (45.0, 0.976), (46.0, 0.086), (47.0, 0.634), (48.0, 1.05), (49.0, 0.44), (50.0, 0.758), (51.0, 1.63), (52.0, 1.33), (53.0, 1.29), (54.0, 1.18), (55.0, 0.944), (56.0, 0.935), (57.0, 0.865), (58.0, 1.25), (59.0, 1.66)

DOCUMENT: Observed Winter Cold Temp is index value, which is calculated by dividing each yearly average value by the corresponding long-term mean. In the parentheses, the first element shows the simple order and the second one the index value.

Observed Winter Warm Temp = GRAPH(TIME)

(1.00, 0.791), (2.00, 0.963), (3.00, 0.822), (4.00, 1.10), (5.00, 1.04), (6.00, 0.872), (7.00, 1.17), (8.00, 0.991), (9.00, 0.911), (10.0, 1.35), (11.0, 1.21), (12.0, 1.21), (13.0, 1.18), (14.0, 1.16), (15.0, 1.11), (16.0, 0.992), (17.0, 1.21), (18.0, 1.23), (19.0, 0.7), (20.0, 1.06), (21.0, 0.849), (22.0, 0.978), (23.0, 1.01), (24.0, 0.591), (25.0, 0.895), (26.0, 1.07), (27.0, 0.798), (28.0, 1.04), (29.0, 0.754), (30.0, 0.757), (31.0, 0.875), (32.0, 1.13), (33.0, 1.06), (34.0, 0.945), (35.0, 1.19), (36.0, 1.18), (37.0, 1.07), (38.0, 0.813), (39.0, 0.701), (40.0, 0.797), (41.0, 0.916), (42.0, 0.873), (43.0, 1.05), (44.0, 0.895), (45.0, 1.19), (46.0, 0.665), (47.0, 1.04), (48.0, 1.02), (49.0, 0.969), (50.0, 0.92), (51.0, 1.36), (52.0, 1.12), (53.0, 1.05), (54.0, 0.986), (55.0, 0.982), (56.0, 0.865), (57.0, 0.977), (58.0, 1.02), (59.0, 1.14)

DOCUMENT: Observed Winter Warm Temp is index value, which is calculated by dividing each yearly average value by the corresponding long-term mean. In the parentheses, the first entry shows the simple order and the second one the index value.

Soil-mediated Submodel

$$\text{Soil Mediated Disturbance} = (\text{Soil Acidity} + \text{Soil Solution Al})/2$$

$$\text{Soil Acidity} = \text{Observed Air Pollution} * ((1+2* \text{Precipitation Effect} 1 + 3*\text{Cloud Immersion})/6)$$

$$\text{Soil Solution Al} = (1+ 2* \text{Soil Acidity})/3$$

Air Pollution Submodel

$$\text{Air Pollution Disturbance} = (\text{Air Pollution} + \text{Ozone})/2$$

$$\text{Air Pollution} = \text{Observed Air Pollution} * ((1 + 3*\text{Cloud Immersion} + 2* \text{Precipitation Effect} 1)/6)$$

DOCUMENT: Observed Air Pollution is the monitoring data of NO_x and SO_x of U.S.A.

$$\text{Ozone} = \text{Observed Ozone} * ((1 + 2* \text{Air Pollution})/3)$$

$$\text{Precipitation Effect} = \text{Precipitation} * ((\text{If Elevation} < 1700 \text{ then } 1 \text{ else } 2)/3)$$

$$\text{Observed Air Pollution} = \text{GRAPH}(\text{TIME})$$

(1.00, 0.644), (2.00, 0.733), (3.00, 0.776), (4.00, 0.844), (5.00, 0.861), (6.00, 0.885), (7.00, 0.784), (8.00, 0.866), (9.00, 0.808), (10.0, 0.732), (11.0, 0.765), (12.0, 0.754), (13.0, 0.751), (14.0, 0.755), (15.0, 0.75), (16.0, 0.765), (17.0, 0.775), (18.0, 0.79), (19.0, 0.84), (20.0, 0.852), (21.0, 0.857), (22.0, 0.847), (23.0, 0.88), (24.0, 0.925), (25.0, 0.97), (26.0, 1.02), (27.0, 1.09), (28.0, 1.09), (29.0, 1.15), (30.0, 1.17), (31.0, 1.23), (32.0, 1.21), (33.0, 1.25), (34.0, 1.30), (35.0, 1.25), (36.0, 1.19), (37.0, 1.24), (38.0, 1.26), (39.0, 1.22), (40.0, 1.22), (41.0, 1.19), (42.0, 1.15), (43.0, 1.11), (44.0, 1.09), (45.0, 1.13), (46.0, 1.10), (47.0, 1.08), (48.0, 1.08), (49.0, 1.11), (50.0, 1.11), (51.0, 1.12), (52.0, 1.11), (53.0, 1.12), (54.0, 1.12), (55.0, 1.11), (56.0, 1.04), (57.0, 1.03), (58.0, 1.05), (59.0, 1.04)

DOCUMENT: Observed Air Pollution is index value, which is calculated by dividing each yearly average value by the corresponding long-term mean. In the parentheses, the first entry shows the simple order and the second one the index value.

$$\text{Observed Ozone} = \text{GRAPH}(\text{TIME})$$

(1.00, 0.594), (2.00, 0.618), (3.00, 0.599), (4.00, 0.613), (5.00, 0.63), (6.00, 0.65), (7.00, 0.74), (8.00, 0.726), (9.00, 0.71), (10.0, 0.726), (11.0, 0.752), (12.0, 0.749), (13.0, 0.757), (14.0, 0.784), (15.0, 0.797), (16.0, 0.812), (17.0, 0.842), (18.0, 0.849), (19.0, 0.844), (20.0, 0.877), (21.0, 0.935), (22.0, 0.93), (23.0, 0.955), (24.0, 1.02), (25.0, 1.04), (26.0, 1.07), (27.0, 1.10), (28.0,

1.11), (29.0, 1.09), (30.0, 1.10), (31.0, 1.26), (32.0, 1.25), (33.0, 1.28), (34.0, 1.29), (35.0, 1.23), (36.0, 1.18), (37.0, 1.24), (38.0, 1.27), (39.0, 1.28), (40.0, 1.26), (41.0, 1.23), (42.0, 1.19), (43.0, 1.15), (44.0, 1.18), (45.0, 1.22), (46.0, 1.15), (47.0, 1.12), (48.0, 1.13), (49.0, 1.17), (50.0, 1.12), (51.0, 1.09), (52.0, 1.10), (53.0, 1.10), (54.0, 1.11), (55.0, 1.14), (56.0, 1.11), (57.0, 1.05), (58.0, 1.06), (59.0, 1.03)

DOCUMENT: Observed Ozone is index value, which is calculated by dividing each yearly average value by the corresponding long-term mean. In the parenthesis, the first element shows the simple order and the second one the index value.

Appendix 2

Equations, Data and Documents for ARIM_{low}

The followings show and explain equations and data used for ARIM_{low} simulation in Stella.

Main Model

ARIM = 5.3397*Radiation + 0*Nutrients + 0*Carbon Dioxide + 11.3237*Water Availability - 0.2697*Air Pollution Disturbance - 0*Herbivory + 0*Soil Mediated Disturbance - 0*Weather Disturbance - 11.4031

DOCUMENT: Apply GLM model 1 in Table 2 (b). In GLM and CART models, Radiation = RA, Nutrient = NU, Carbon Dioxide = CO2, Water Availability = WA, Weather Disturbance = WD, Air Pollution Disturbance = APD, Herbivory = HB, and Soil Mediated Disturbance = SMD.

Low AV Treering = GRAPH(TIME)

(1.00, 1.04), (2.00, 1.19), (3.00, 1.17), (4.00, 1.07), (5.00, 1.13), (6.00, 0.906), (7.00, 0.728), (8.00, 0.887), (9.00, 0.976), (10.0, 1.12), (11.0, 1.20), (12.0, 1.54), (13.0, 1.32), (14.0, 0.912), (15.0, 0.902), (16.0, 0.752), (17.0, 0.817), (18.0, 1.08), (19.0, 1.29), (20.0, 1.43), (21.0, 1.36), (22.0, 1.33), (23.0, 1.34), (24.0, 1.39), (25.0, 1.31), (26.0, 0.975), (27.0, 1.04), (28.0, 1.19), (29.0, 1.15), (30.0, 0.944), (31.0, 1.07), (32.0, 1.01), (33.0, 1.05), (34.0, 1.07), (35.0, 1.18), (36.0, 1.31), (37.0, 1.30), (38.0, 1.14), (39.0, 1.07), (40.0, 0.998), (41.0, 1.40), (42.0, 0.844), (43.0, 0.933), (44.0, 1.06), (45.0, 0.824), (46.0, 0.876), (47.0, 0.896), (48.0, 0.784), (49.0, 0.784), (50.0, 0.876), (51.0, 0.978), (52.0, 0.952), (53.0, 1.05), (54.0, 1.35), (55.0, 1.12), (56.0, 1.52), (57.0, 1.53), (58.0, 1.41), (59.0, 0.996)

DOCUMENT: Low AV Treering means the average standardized ring width index value of red spruce at low elevation. In the parentheses, the first element shows the simple order and the second one the index value.

Radiation Submodel

Radiation = ((if Aspect=2 then 2 else (if Aspect =3 then 3 else (if Aspect=4 then 2.5 else 1))) + Fir Mortality + (if Slope=5 then 1 else (if Slope=4 then 2 else (if Slope=3 then 3 else (if Slope=2 then 4 else 5)))) - Cloud Immersion - Precipitation Effect + ((1.317288136 - Temperature)*Temperature)/6

DOCUMENT: For the Temperature parameter, the logistic map was applied:

$$X_{n+1} = r * X_n (1 - X_n)$$

Where: X_n is a population in year n , and r is bifurcation parameter (>0)

Aspect = 1

DOCUMENT: N(316-45); E(46-135); S(136-225); W(226-315)--> N=1; E=2; S=3; W=4

Balsam woolly adelgid = Observed Winter Cold Temp

Cloud Immersion = (If(Elevation <1400) Then (0) Else (If (Elevation <1800 and Elevation >=1400) Then (1) Else (2)))/2

Elevation = 1600

Fir Mortality = Balsam woolly adelgid * ((if (Elevation>=1700) then (2) else (1))/3)

Slope = 3

DOCUMENT: 5 classes (1:0-20; 2:21-40...): 1=0-20; 2=21-40; 3=41-60; 4=61-80; 5=81-100.
Slope is %value

Temperature = Average Temperature * ((2 + 0*Observed CO2 + 0* Observed Ozone + 1*(if Aspect=2 then 0.5 else (if Aspect =3 then 1 else (if Aspect=4 then 0.65 else 0.3))) + 1* (if Elevation =1000 then 1 else (if Elevation = 1100 then 0.9 else (if Elevation =1200 then 0.8 else (if Elevation = 1300 then 0.7 else (if Elevation = 1400 then 0.6 else (if Elevation = 1500 then 0.5 else (if Elevation = 1600 then 0.4 else (if Elevation = 1700 then 0.3 else (if Elevation = 1800 then 0.2 else 0.1)))))))))) + 1*(if Slope=5 then 0.2 else (if Slope=4 then 0.4 else (if Slope=3 then 0.6 else (if Slope=2 then 0.8 else 1)))))/5)

Average Temperature = GRAPH(TIME)

(1.00, 0.957), (2.00, 1.03), (3.00, 1.00), (4.00, 1.02), (5.00, 1.02), (6.00, 1.01), (7.00, 1.05), (8.00, 0.992), (9.00, 1.02), (10.0, 1.04), (11.0, 0.997), (12.0, 1.03), (13.0, 1.04), (14.0, 1.07), (15.0, 1.05), (16.0, 1.03), (17.0, 1.03), (18.0, 1.04), (19.0, 0.961), (20.0, 1.02), (21.0, 0.959), (22.0, 0.95), (23.0, 1.00), (24.0, 0.948), (25.0, 0.968), (26.0, 1.02), (27.0, 0.951), (28.0, 0.958), (29.0, 0.955), (30.0, 0.93), (31.0, 0.988), (32.0, 0.986), (33.0, 0.944), (34.0, 0.983), (35.0, 1.01), (36.0, 1.01), (37.0, 0.966), (38.0, 1.01), (39.0, 0.974), (40.0, 0.957), (41.0, 0.991), (42.0, 0.978), (43.0, 0.993), (44.0, 0.984), (45.0, 1.01), (46.0, 0.986), (47.0, 1.05), (48.0, 1.04), (49.0, 1.02), (50.0, 0.98), (51.0, 1.07), (52.0, 1.03), (53.0, 0.961), (54.0, 0.999), (55.0, 1.00), (56.0, 1.00), (57.0, 0.945), (58.0, 0.961), (59.0, 1.04)

DOCUMENT: Average Temperature is index value, which is calculated by dividing each yearly average value of maximum temperature by the corresponding long-term mean. In the parentheses, the first element shows the simple order and the second one the index value.

Precipitation Effect 1 = Precipitation1*((If Elevation < 1700 then 1 else 2)/3)

Precipitation 1 = GRAPH(TIME)

(1.00, 0.882), (2.00, 0.744), (3.00, 1.08), (4.00, 0.921), (5.00, 0.935), (6.00, 1.04), (7.00, 1.06), (8.00, 0.791), (9.00, 1.09), (10.0, 1.02), (11.0, 1.07), (12.0, 1.11), (13.0, 0.787), (14.0, 0.853), (15.0, 0.916), (16.0, 0.877), (17.0, 1.00), (18.0, 1.30), (19.0, 0.811), (20.0, 0.959), (21.0, 0.953),

(22.0, 1.17), (23.0, 1.20), (24.0, 1.07), (25.0, 0.982), (26.0, 0.89), (27.0, 0.997), (28.0, 1.18), (29.0, 0.77), (30.0, 1.07), (31.0, 0.956), (32.0, 1.09), (33.0, 1.22), (34.0, 1.23), (35.0, 1.24), (36.0, 0.952), (37.0, 0.889), (38.0, 1.08), (39.0, 0.922), (40.0, 1.17), (41.0, 0.87), (42.0, 0.932), (43.0, 1.15), (44.0, 0.901), (45.0, 1.02), (46.0, 0.811), (47.0, 0.699), (48.0, 0.765), (49.0, 0.745), (50.0, 1.19), (51.0, 1.15), (52.0, 1.22), (53.0, 0.918), (54.0, 0.968), (55.0, 1.33), (56.0, 0.854), (57.0, 1.04), (58.0, 1.03), (59.0, 1.12)

DOCUMENT: Precipitation 1 is index value, which is calculated by dividing each yearly average value by the corresponding long-term mean. In the parentheses, the first element shows the simple order and the second one the index value.

Water Availability Submodel

Water Availability = (3*Precipitation Effect 2 +(if Distance to Stream =1 then 3 else (if Distance to Stream=2 then 2 else 1)) - Fir Mortality – Temperature + (if Aspect=2 then 2.5 else (if Aspect =3 then 1 else (if Aspect=4 then 2 else 3))) + (if Slope=1 then 1 else (if Slope=2 then 2 else (if Slope=3 then 3 else (if Slope=4 then 4 else 5)))) + ((1.317288136-Temperature)*Temperature) + Radiation)/10

Distance to Stream = 3

DOCUMENT: 1=near the stream; 2=slope; 3=ridge

Precipitation Effect 2 = ((Precipitation_1 + precipitation_2)/2)*((If Elevation < 1700 then 1 else 2)/3)

Precipitation_2 = GRAPH(TIME)

(1.00, 1.00), (2.00, 0.882), (3.00, 0.744), (4.00, 1.08), (5.00, 0.921), (6.00, 0.935), (7.00, 1.04), (8.00, 1.06), (9.00, 0.791), (10.0, 1.09), (11.0, 1.02), (12.0, 1.07), (13.0, 1.11), (14.0, 0.787), (15.0, 0.853), (16.0, 0.916), (17.0, 0.877), (18.0, 1.00), (19.0, 1.30), (20.0, 0.811), (21.0, 0.959), (22.0, 0.953), (23.0, 1.17), (24.0, 1.20), (25.0, 1.07), (26.0, 0.982), (27.0, 0.89), (28.0, 0.997), (29.0, 1.18), (30.0, 0.77), (31.0, 1.07), (32.0, 0.956), (33.0, 1.09), (34.0, 1.22), (35.0, 1.23), (36.0, 1.24), (37.0, 0.952), (38.0, 0.889), (39.0, 1.08), (40.0, 0.922), (41.0, 1.17), (42.0, 0.87), (43.0, 0.932), (44.0, 1.15), (45.0, 0.901), (46.0, 1.02), (47.0, 0.811), (48.0, 0.699), (49.0, 0.765), (50.0, 0.745), (51.0, 1.19), (52.0, 1.15), (53.0, 1.22), (54.0, 0.918), (55.0, 0.968), (56.0, 1.33), (57.0, 0.854), (58.0, 1.04), (59.0, 1.03)

DOCUMENT: Precipitation 2 is the previous year precipitation and an index value, which is calculated by dividing each yearly average value by the corresponding long-term mean. In the parentheses, the first element shows the simple order and the second one the index value.

Carbon Dioxide Submodel

Carbon Dioxide = (((((1.317288136 -Temperature)*Temperature) + Radiation + Water Availability)/3

Observed CO2 = GRAPH(TIME)

(1.00, 0.493), (2.00, 0.538), (3.00, 0.576), (4.00, 0.596), (5.00, 0.635), (6.00, 0.614), (7.00, 0.592), (8.00, 0.653), (9.00, 0.68), (10.0, 0.573), (11.0, 0.674), (12.0, 0.695), (13.0, 0.678), (14.0, 0.694), (15.0, 0.66), (16.0, 0.723), (17.0, 0.759), (18.0, 0.753), (19.0, 0.729), (20.0, 0.759), (21.0, 0.777), (22.0, 0.779), (23.0, 0.807), (24.0, 0.843), (25.0, 0.877), (26.0, 0.915), (27.0, 0.962), (28.0, 1.00), (29.0, 1.04), (30.0, 1.09), (31.0, 1.12), (32.0, 1.13), (33.0, 1.18), (34.0, 1.23), (35.0, 1.18), (36.0, 1.14), (37.0, 1.20), (38.0, 1.22), (39.0, 1.26), (40.0, 1.28), (41.0, 1.23), (42.0, 1.18), (43.0, 1.12), (44.0, 1.13), (45.0, 1.17), (46.0, 1.17), (47.0, 1.18), (48.0, 1.22), (49.0, 1.28), (50.0, 1.30), (51.0, 1.28), (52.0, 1.28), (53.0, 1.28), (54.0, 1.36), (55.0, 1.38), (56.0, 1.38), (57.0, 1.41), (58.0, 1.52), (59.0, 1.50)

DOCUMENT: Observed CO2 is index value, which is calculated by dividing each yearly average value by the corresponding long-term mean. In the parentheses, the first element shows the simple order and the second one the index value.

Nutrients Submodel

Nutrients = (Fir Mortality + Radiation + Water Availability + Atmospheric Deposition of Nutrients + (((1.317288136-Temperature)*Temperature))/5

Atmospheric Deposition of Nutrients = GRAPH(TIME)

(1.00, 0.644), (2.00, 0.733), (3.00, 0.776), (4.00, 0.844), (5.00, 0.861), (6.00, 0.885), (7.00, 0.784), (8.00, 0.866), (9.00, 0.808), (10.0, 0.732), (11.0, 0.765), (12.0, 0.754), (13.0, 0.751), (14.0, 0.755), (15.0, 0.75), (16.0, 0.765), (17.0, 0.775), (18.0, 0.79), (19.0, 0.84), (20.0, 0.852), (21.0, 0.857), (22.0, 0.847), (23.0, 0.88), (24.0, 0.925), (25.0, 0.97), (26.0, 1.02), (27.0, 1.09), (28.0, 1.09), (29.0, 1.15), (30.0, 1.17), (31.0, 1.23), (32.0, 1.21), (33.0, 1.25), (34.0, 1.30), (35.0, 1.25), (36.0, 1.19), (37.0, 1.24), (38.0, 1.26), (39.0, 1.22), (40.0, 1.22), (41.0, 1.19), (42.0, 1.15), (43.0, 1.11), (44.0, 1.10), (45.0, 1.13), (46.0, 1.10), (47.0, 1.08), (48.0, 1.08), (49.0, 1.11), (50.0, 1.11), (51.0, 1.12), (52.0, 1.11), (53.0, 1.12), (54.0, 1.12), (55.0, 1.11), (56.0, 1.04), (57.0, 1.03), (58.0, 1.05), (59.0, 1.04)

DOCUMENT: Atmospheric Deposition of Nutrients is index value, which is calculated by dividing each yearly average value by the corresponding long-term mean. In the parentheses, the first element shows the simple order and the second one the index value. These values were obtained from (NO_x emission + SO_x emission)/2.

Herbivory Submodel

Herbivory = Annual Mean Temp

Annual Mean Temp = GRAPH(TIME)

(1.00, 1.09), (2.00, 0.956), (3.00, 1.07), (4.00, 0.979), (5.00, 0.98), (6.00, 1.03), (7.00, 1.02), (8.00, 1.06), (9.00, 0.977), (10.0, 1.04), (11.0, 1.08), (12.0, 1.01), (13.0, 1.01), (14.0, 1.05), (15.0, 1.05), (16.0, 1.04), (17.0, 1.03), (18.0, 1.06), (19.0, 1.09), (20.0, 0.952), (21.0, 1.04), (22.0, 0.957), (23.0, 0.937), (24.0, 0.999), (25.0, 0.898), (26.0, 0.949), (27.0, 1.04), (28.0, 0.97), (29.0,

0.947), (30.0, 0.925), (31.0, 0.928), (32.0, 1.01), (33.0, 1.03), (34.0, 0.987), (35.0, 1.03), (36.0, 1.06), (37.0, 1.03), (38.0, 0.91), (39.0, 1.03), (40.0, 0.99), (41.0, 0.987), (42.0, 1.02), (43.0, 0.994), (44.0, 1.01), (45.0, 0.935), (46.0, 0.944), (47.0, 0.917), (48.0, 1.00), (49.0, 0.964), (50.0, 0.911), (51.0, 0.955), (52.0, 1.08), (53.0, 1.07), (54.0, 0.98), (55.0, 0.997), (56.0, 0.997), (57.0, 0.996), (58.0, 0.934), (59.0, 0.976)

DOCUMENT: Average Mean Temp is index value, which is calculated by dividing each yearly average value by the corresponding long-term mean. In the parentheses, the first entry shows the simple order and the second one the index value.

Weather Disturbance Submodel

Weather Disturbance = (2*Summer Hot Temperature + 0*Winter Cold Temperature + 2*Winter Warm Temperature)/4

Summer Hot Temperature = Observed Sum Hot Temp*((2 + 1*(if Aspect=2 then 0.5 else (if Aspect =3 then 1 else (if Aspect=4 then 0.65 else 0.3))) - 1*Water Availability + 0*Observed CO2 + 0*Observed Ozone + 1*(if Elevation =1000 then 1 else (if Elevation = 1100 then 0.9 else (if Elevation =1200 then 0.8 else (if Elevation = 1300 then 0.7 else (if Elevation = 1400 then 0.6 else (if Elevation = 1500 then 0.5 else (if Elevation = 1600 then 0.4 else (if Elevation = 1700 then 0.3 else (if Elevation = 1800 then 0.2 else 0.1)))))))))) + 1*(if Slope=5 then 0.2 else (if Slope=4 then 0.4 else (if Slope=3 then 0.6 else (if Slope=2 then 0.8 else 1)))))/6

Winter Cold Temperature = Observed Winter Cold Temp*((2 + 4*Air Pollution - 0*Observed CO2 - 0* Observed Ozone + 1*(if Elevation =1000 then 0.1 else (if Elevation = 1100 then 0.2 else (if Elevation =1200 then 0.3 else (if Elevation = 1300 then 0.4 else (if Elevation = 1400 then 0.5 else (if Elevation = 1500 then 0.6 else (if Elevation = 1600 then 0.7 else (if Elevation = 1700 then 0.8 else (if Elevation = 1800 then 0.9 else 1)))))))))) + 1*(if Slope=5 then 0.2 else (if Slope=4 then 0.4 else (if Slope=3 then 0.6 else (if Slope=2 then 0.8 else 1)))) + 1*(if Aspect=2 then 0.5 else (if Aspect =3 then 1 else (if Aspect=4 then 0.65 else 0.3))))/9

Winter Warm Temperature = Observed Winter Warm Temp * ((2 + 0*Observed CO2 + 0* Observed Ozone + 1*(if Aspect=2 then 0.5 else (if Aspect =3 then 1 else (if Aspect=4 then 0.65 else 0.3))) + 1*(if Elevation =1000 then 0.1 else (if Elevation = 1100 then 0.2 else (if Elevation =1200 then 0.3 else (if Elevation = 1300 then 0.4 else (if Elevation = 1400 then 0.5 else (if Elevation = 1500 then 0.6 else (if Elevation = 1600 then 0.7 else (if Elevation = 1700 then 0.8 else (if Elevation = 1800 then 0.9 else 1)))))))))) + 1*(if Slope=5 then 0.2 else (if Slope=4 then 0.4 else (if Slope=3 then 0.6 else (if Slope=2 then 0.8 else 1))))/5

Observed Sum Temp = GRAPH(TIME)

(1.00, 0.989), (2.00, 1.02), (3.00, 1.01), (4.00, 1.06), (5.00, 1.04), (6.00, 1.00), (7.00, 0.989), (8.00, 0.997), (9.00, 1.02), (10.0, 1.02), (11.0, 0.956), (12.0, 1.04), (13.0, 1.07), (14.0, 1.05), (15.0, 1.07), (16.0, 1.01), (17.0, 1.01), (18.0, 1.04), (19.0, 1.00), (20.0, 1.02), (21.0, 1.00), (22.0, 0.924), (23.0, 1.01), (24.0, 0.939), (25.0, 0.964), (26.0, 0.979), (27.0, 0.991), (28.0, 0.904), (29.0, 1.00), (30.0, 0.976), (31.0, 0.977), (32.0, 0.961), (33.0, 0.936), (34.0, 0.954), (35.0, 0.948), (36.0, 1.00), (37.0, 0.973), (38.0, 1.02), (39.0, 0.989), (40.0, 0.937), (41.0, 1.06), (42.0, 1.02), (43.0,

0.959), (44.0, 1.02), (45.0, 0.965), (46.0, 0.977), (47.0, 1.06), (48.0, 1.05), (49.0, 1.06), (50.0, 0.974), (51.0, 1.02), (52.0, 0.992), (53.0, 0.942), (54.0, 1.07), (55.0, 0.981), (56.0, 1.05), (57.0, 0.972), (58.0, 0.973), (59.0, 1.01)

DOCUMENT: Observed Sum Temp (= Observed Summer Hot Temperature) is index value, which is calculated by dividing each yearly average value by the corresponding long-term mean. In the parentheses, the first entry shows the simple order and the second one the index value.

Observed Winter Cold Temp = GRAPH(TIME)

(1.00, 0.779), (2.00, 1.18), (3.00, 0.687), (4.00, 1.03), (5.00, 1.19), (6.00, 0.886), (7.00, 1.18), (8.00, 0.752), (9.00, 1.02), (10.0, 1.72), (11.0, 1.52), (12.0, 1.20), (13.0, 1.54), (14.0, 1.25), (15.0, 1.09), (16.0, 0.984), (17.0, 1.64), (18.0, 1.62), (19.0, 0.31), (20.0, 1.06), (21.0, 0.774), (22.0, 1.01), (23.0, 0.955), (24.0, 0.0133), (25.0, 0.787), (26.0, 0.968), (27.0, 0.968), (28.0, 1.17), (29.0, 0.391), (30.0, 0.89), (31.0, 0.666), (32.0, 1.29), (33.0, 1.31), (34.0, 0.928), (35.0, 1.64), (36.0, 1.31), (37.0, 0.736), (38.0, 0.373), (39.0, 0.453), (40.0, 0.669), (41.0, 0.936), (42.0, 0.665), (43.0, 1.05), (44.0, 0.749), (45.0, 0.976), (46.0, 0.086), (47.0, 0.634), (48.0, 1.05), (49.0, 0.44), (50.0, 0.758), (51.0, 1.63), (52.0, 1.33), (53.0, 1.29), (54.0, 1.18), (55.0, 0.944), (56.0, 0.935), (57.0, 0.865), (58.0, 1.25), (59.0, 1.66)

DOCUMENT: Observed Winter Cold Temp is index value, which is calculated by dividing each yearly average value by the corresponding long-term mean. In the parentheses, the first entry shows the simple order and the second one the index value.

Observed Winter Warm Temp = GRAPH(TIME)

(1.00, 0.791), (2.00, 0.963), (3.00, 0.822), (4.00, 1.10), (5.00, 1.04), (6.00, 0.872), (7.00, 1.17), (8.00, 0.991), (9.00, 0.911), (10.0, 1.35), (11.0, 1.21), (12.0, 1.21), (13.0, 1.18), (14.0, 1.16), (15.0, 1.11), (16.0, 0.992), (17.0, 1.21), (18.0, 1.23), (19.0, 0.7), (20.0, 1.06), (21.0, 0.849), (22.0, 0.978), (23.0, 1.01), (24.0, 0.591), (25.0, 0.895), (26.0, 1.07), (27.0, 0.798), (28.0, 1.04), (29.0, 0.754), (30.0, 0.757), (31.0, 0.875), (32.0, 1.13), (33.0, 1.06), (34.0, 0.945), (35.0, 1.19), (36.0, 1.18), (37.0, 1.07), (38.0, 0.813), (39.0, 0.701), (40.0, 0.797), (41.0, 0.916), (42.0, 0.873), (43.0, 1.05), (44.0, 0.895), (45.0, 1.19), (46.0, 0.665), (47.0, 1.04), (48.0, 1.02), (49.0, 0.969), (50.0, 0.92), (51.0, 1.36), (52.0, 1.12), (53.0, 1.05), (54.0, 0.986), (55.0, 0.982), (56.0, 0.865), (57.0, 0.977), (58.0, 1.02), (59.0, 1.14)

DOCUMENT: Observed Winter Warm Temp is index value, which is calculated by dividing each yearly average value by the corresponding long-term mean. In the parentheses, the first entry shows the simple order and the second one the index value.

Soil Mediated Submodel

Soil Mediated Disturbance = (Soil Acidity + Soil Solution Al)/2

Soil Acidity = Observed Air Pollution * ((1+2*Precipitation Effect 1 + 3*Cloud Immersion)/6)

Soil Solution Al = (1+2*Soil Acidity)/3

Air Pollution Submodel

Air Pollution Disturbance = (Air Pollution + Ozone)/2

Air Pollution = Observed Air Pollution *((1 + 3*Cloud Immersion + 2*Precipitation Effect 1)/6)

DOCUMENT: Observed Air Pollution is the monitoring data of NO_x and SO_x of U.S.A.

Ozone = Observed Ozone *((1+2*Air Pollution)/3)

Precipitation Effect 1 = Precipitation 1 *((If Elevation < 1700 then 1 else 2)/3)

Observed Air Pollution = GRAPH(TIME)

(1.00, 0.644), (2.00, 0.733), (3.00, 0.776), (4.00, 0.844), (5.00, 0.861), (6.00, 0.885), (7.00, 0.784), (8.00, 0.866), (9.00, 0.808), (10.0, 0.732), (11.0, 0.765), (12.0, 0.754), (13.0, 0.751), (14.0, 0.755), (15.0, 0.75), (16.0, 0.765), (17.0, 0.775), (18.0, 0.79), (19.0, 0.84), (20.0, 0.852), (21.0, 0.857), (22.0, 0.847), (23.0, 0.88), (24.0, 0.925), (25.0, 0.97), (26.0, 1.02), (27.0, 1.09), (28.0, 1.09), (29.0, 1.15), (30.0, 1.17), (31.0, 1.23), (32.0, 1.21), (33.0, 1.25), (34.0, 1.30), (35.0, 1.25), (36.0, 1.19), (37.0, 1.24), (38.0, 1.26), (39.0, 1.22), (40.0, 1.22), (41.0, 1.19), (42.0, 1.15), (43.0, 1.11), (44.0, 1.09), (45.0, 1.13), (46.0, 1.10), (47.0, 1.08), (48.0, 1.08), (49.0, 1.11), (50.0, 1.11), (51.0, 1.12), (52.0, 1.11), (53.0, 1.12), (54.0, 1.12), (55.0, 1.11), (56.0, 1.04), (57.0, 1.03), (58.0, 1.05), (59.0, 1.04)

DOCUMENT: Observed Air Pollution is index value, which is calculated by dividing each yearly average value by the corresponding long-term mean. In the parentheses, the first entry shows the simple order and the second one the index value.

Observed Ozone = GRAPH(TIME)

(1.00, 0.594), (2.00, 0.618), (3.00, 0.599), (4.00, 0.613), (5.00, 0.63), (6.00, 0.65), (7.00, 0.74), (8.00, 0.726), (9.00, 0.71), (10.0, 0.726), (11.0, 0.752), (12.0, 0.749), (13.0, 0.757), (14.0, 0.784), (15.0, 0.797), (16.0, 0.812), (17.0, 0.842), (18.0, 0.849), (19.0, 0.844), (20.0, 0.877), (21.0, 0.935), (22.0, 0.93), (23.0, 0.955), (24.0, 1.02), (25.0, 1.04), (26.0, 1.07), (27.0, 1.10), (28.0, 1.11), (29.0, 1.09), (30.0, 1.10), (31.0, 1.26), (32.0, 1.25), (33.0, 1.28), (34.0, 1.29), (35.0, 1.23), (36.0, 1.18), (37.0, 1.24), (38.0, 1.27), (39.0, 1.28), (40.0, 1.26), (41.0, 1.23), (42.0, 1.19), (43.0, 1.15), (44.0, 1.18), (45.0, 1.22), (46.0, 1.15), (47.0, 1.12), (48.0, 1.13), (49.0, 1.17), (50.0, 1.12), (51.0, 1.09), (52.0, 1.10), (53.0, 1.10), (54.0, 1.11), (55.0, 1.14), (56.0, 1.11), (57.0, 1.05), (58.0, 1.06), (59.0, 1.03)

DOCUMENT: Observed Ozone is index value, which is calculated by dividing each yearly average value by the corresponding long-term mean. In the parentheses, the first entry shows the simple order and the second one the index value.

Appendix 3

R programming for GLMs, CART and Data and Model Checking

3.1. R programming for Checking Randomness for all Raw Data and Results

High Elevation Red Spruce Standardized Tree-ring Index Value (HighRSTI)

```
require(graphics)
```

```
HighRSTI <- c(1.1249, 1.2915, 1.1823, 1.2409, 1.2462, 1.1691, 1.1591, 1.2623, 1.1748, 1.312,  
1.0275, 1.0878, 0.9885, 1.0689, 1.0654, 1.078, 0.9852, 1.1063, 0.8762, 0.863, 0.9336, 0.8504,  
0.895, 0.8099, 1.1139, 1.0933, 0.977, 0.8521, 0.8134, 0.655, 0.7724, 0.7195, 0.6118, 0.5907,  
0.6395, 0.7478, 0.9056, 0.6389, 0.7421, 0.6077, 0.879, 0.5641, 0.6654, 0.8583, 0.6411, 0.6818,  
0.8394, 0.7276, 0.7511, 0.666, 0.7634, 0.7254, 0.9833, 1.3323, 1.1925, 1.5019, 1.2294, 1.0087,  
0.7849) # Index values and no measurement unit
```

```
shapiro.test(HighRSTI) # Normality test: check normality
```

```
acf(HighRSTI) # autocorrelation function: check randomness
```

Low Elevation Red Spruce Standardized Tree-ring Index Value (LowRSTI)

```
LowRSTI <- c(1.04, 1.19, 1.17, 1.08, 1.13, 0.91, 0.73, 0.89, 0.98, 1.12, 1.2, 1.54, 1.32, 0.91, 0.9,  
0.75, 0.82, 1.08, 1.29, 1.43, 1.36, 1.33, 1.34, 1.39, 1.31, 0.97, 1.04, 1.19, 1.15, 0.94, 1.07, 1.01,  
1.05, 1.07, 1.18, 1.31, 1.3, 1.14, 1.07, 1, 1.4, 0.84, 0.93, 1.06, 0.82, 0.88, 0.9, 0.78, 0.78, 0.88,  
0.98, 0.95, 1.05, 1.35, 1.12, 1.52, 1.53, 1.41, 1) # Index values and no measurement unit
```

```
shapiro.test(LowRSTI)
```

```
acf(LowRSTI)
```

Observed Air Pollution (OAP)

```
OAP <- c(27326, 31119, 32930, 35818, 36547, 37555, 33290, 36768, 34269, 31048, 32450,  
32012, 31882, 32024, 31844, 32446, 32906, 33520, 35646, 36140, 36367, 35951, 37363,  
39233, 41172, 43329, 46239, 46128, 48635, 49808, 52089, 51245, 53130, 55283, 52947,  
50643, 52486, 53431, 51947, 51657, 50289, 48823, 47104, 46446, 48138, 46856, 45700,  
45743, 47259, 47186, 47709, 47290, 47402, 47427, 47242, 44102, 43797, 44446, 44101)  
# Observed air pollutant data: NOx+SOx, Unit=ppm
```

```
shapiro.test(OAP)
```

```
acf(OAP)
```

Observed Ozone (OOZONE)

```
OOZONE <- c(24535, 25497, 24747, 25295, 25994, 26856, 30542, 29977, 29334, 29967,
31029, 30933, 31264, 32362, 32895, 33536, 34769, 35032, 34858, 36189, 38599, 38393,
39444, 42162, 42819, 44209, 45217, 45844, 44940, 45611, 51910, 51598, 53037, 53402,
50957, 48711, 51042, 52234, 52725, 51877, 50720, 49167, 47651, 48717, 50337, 47626, 46425,
46538, 48430, 46406, 44985, 45351, 45255, 45829, 46907, 45738, 43412, 43700, 42371)
# Observed ozone data (ppm)
```

```
shapiro.test(OOZONE)
acf(OOZONE)
```

Observed CO₂ (OCO₂)

```
OCO2 <- c(506732, 553466, 592489, 612491, 652733, 631014, 608629, 671101, 699510,
589091, 692968, 715047, 697302, 713521, 679214, 743859, 780754, 774883, 749322,
780345, 798700, 801386, 830035, 866683, 902394, 940910, 988857, 1028564, 1068013,
1119151, 1156871, 1162393, 1211928, 1263643, 1213915, 1167855, 1238157, 1255274,
1299052, 1313359, 1262744, 1216628, 1155139, 1161816, 1201975, 1208067, 1209394,
1252563, 1321103, 1336439, 1315008, 1317751, 1311226, 1393487, 1420718, 1420827,
1450290, 1560577, 1545558)
# observed CO2 data (ppm)
```

```
shapiro.test(OCO2)
acf(OCO2)
```

Observed Temperature (TEM)

```
TEM <- c(16.1, 14.3, 15.8, 14.8, 14.9, 15.4, 15.2, 15.8, 14.7, 15.4, 15.9, 15.0, 15.2,
15.6, 15.8, 15.7, 15.4, 15.6, 16.0, 14.3, 15.4, 14.3, 14.1, 15.0, 13.7, 14.3, 15.5, 14.4,
14.2, 14.0, 13.9, 15.0, 15.1, 14.5, 15.1, 15.6, 15.3, 13.9, 15.3, 14.7, 14.6, 15.0,
14.8, 15.0, 14.3, 14.5, 14.1, 15.3, 14.8, 14.3, 14.4, 16.1, 15.8, 14.5, 14.9, 15.0,
14.9, 14.0, 14.5, 16.1)
# Observed Temperature (°C)
```

```
shapiro.test(TEM)
acf(TEM)
```

Observed Precipitation (PRE)

```
PRE <- c(3.372706023, 2.961724447, 2.499916641, 3.628629579, 3.095166551, 3.140851582,
3.506407898, 3.551465911, 2.657839186, 3.670383584, 3.411630165, 3.599181138,
3.734580338, 2.643781022, 2.865840675, 3.075975115, 2.945142518, 3.374507802,
4.353497248, 2.723383481, 3.221474002, 3.201727135, 3.920155268, 4.016539196,
3.585309005, 3.299289615, 2.990237111, 3.349453488, 3.950281189, 2.586422259,
3.601177503, 3.210533013, 3.662698208, 4.112057437, 4.128677823, 4.173986194,
```

3.197942748, 2.9875871, 3.627426933, 3.097507565, 3.938692358, 2.922336161, 3.131725384,
 3.875979199, 3.027292595, 3.415787118, 2.725201831, 2.347783257, 2.570772139,
 2.502208828, 3.994929525, 3.849898029, 4.10477916, 3.082042859, 3.250800077,
 4.464623874, 2.869834217, 3.494622874, 3.468153456, 3.770344201)

Observed precipitation (m)

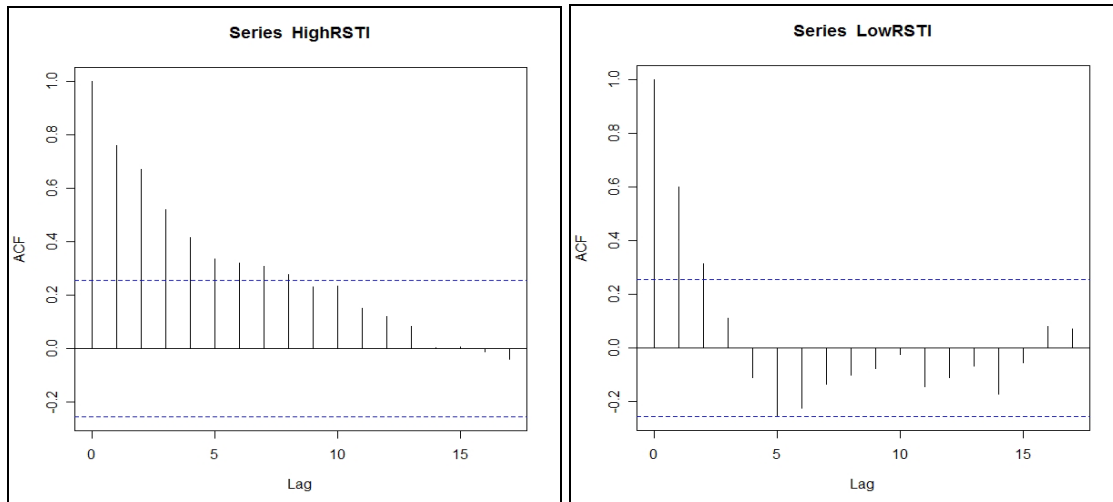
shapiro.test(PRE)
 acf(PRE)

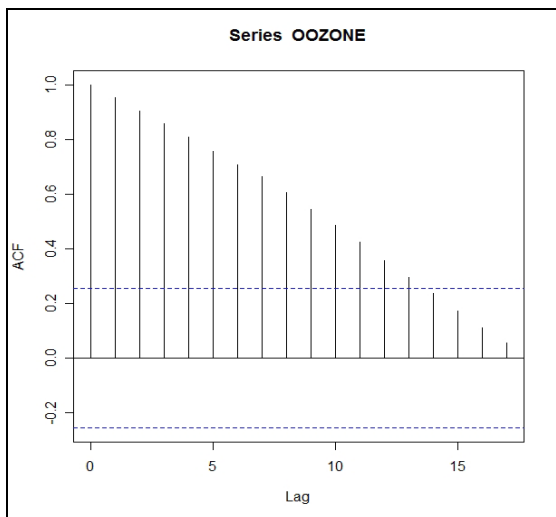
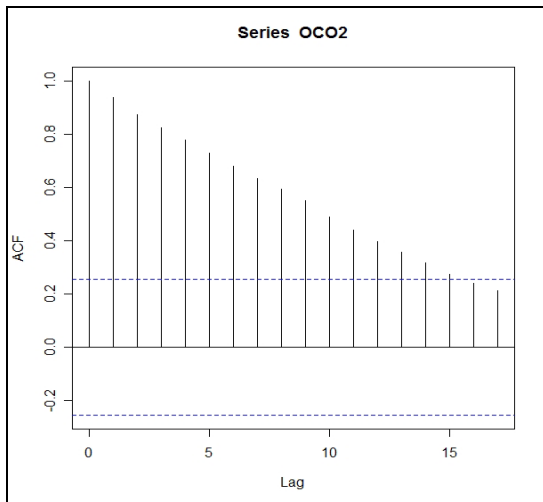
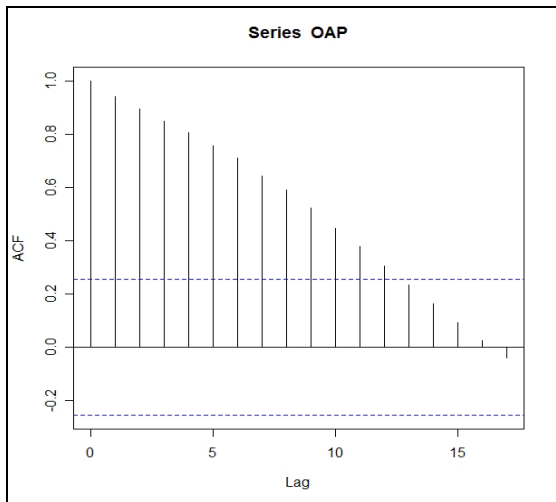
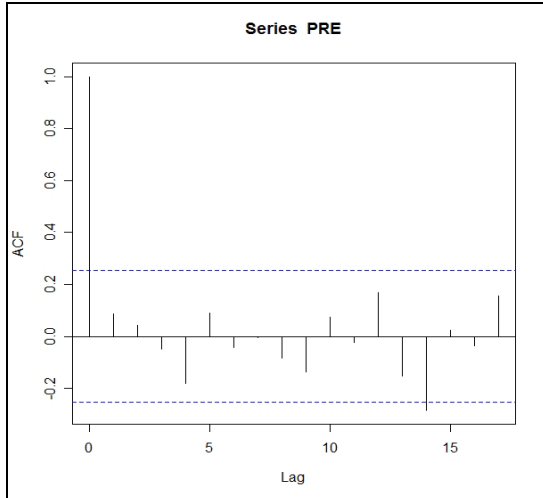
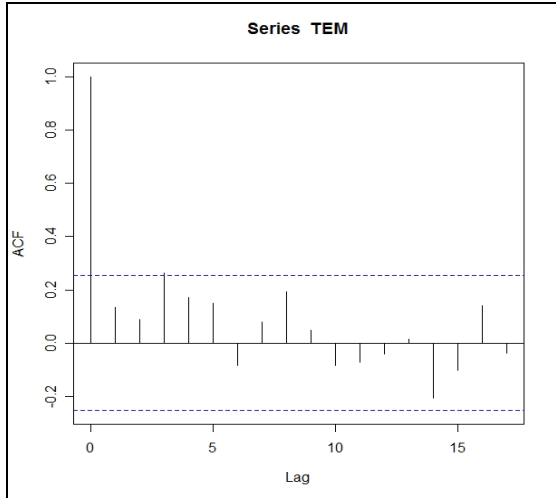
Results of normality tests for the observed data

	<i>HighRSTI</i>	<i>LowRSTI</i>	<i>TEM</i>	<i>PRE</i>	<i>OAP</i>	<i>OOZONE</i>	<i>OCO₂</i>
<i>W-value</i>	0.9632	0.9683	0.9702	0.9853	0.9218	0.9119	0.9257
<i>P-value</i>	0.07154	0.1267	0.1489	0.6876	0.00102	0.00041	0.00146

W-value: It is Wilks Shapiro test statistic.

Results of autocorrelation tests for raw data





3.2. R programming for CART and GLMs

Checking Randomness for Variables for CART and GLMs and Results for ARIMhigh

```
require(graphics)
```

```
HighRSTI <- c( 1.1249, 1.2915, 1.1823, 1.2409, 1.2462, 1.1691, 1.1591, 1.2623, 1.1748, 1.312,  
1.0275, 1.0878, 0.9885, 1.0689, 1.0654, 1.078, 0.9852, 1.1063, 0.8762, 0.863, 0.9336, 0.8504,  
0.895, 0.8099, 1.1139, 1.0933, 0.977, 0.8521, 0.8134, 0.655, 0.7724, 0.7195, 0.6118, 0.5907,  
0.6395, 0.7478, 0.9056, 0.6389, 0.7421, 0.6077, 0.879, 0.5641, 0.6654, 0.8583, 0.6411, 0.6818,  
0.8394, 0.7276, 0.7511, 0.666, 0.7634, 0.7254, 0.9833, 1.3323, 1.1925, 1.5019, 1.2294, 1.0087,  
0.7849) # High elevation observed standardized ring width of red spruce  
# Index values and no measurement unit
```

```
shapiro.test(HighRSTI) # Shapiro-Wilk normality test  
acf(HighRSTI) # autocorrelation: check randomness of variables
```

```
Radiation_high <- c(0.72, 0.78, 0.69, 0.75, 0.76, 0.72, 0.75, 0.73, 0.73, 0.81, 0.78, 0.74, 0.82,  
0.78, 0.75, 0.75, 0.81, 0.77, 0.68, 0.75, 0.71, 0.72, 0.71, 0.62, 0.71, 0.74, 0.73, 0.73, 0.69, 0.71,  
0.7, 0.76, 0.74, 0.7, 0.78, 0.77, 0.72, 0.66, 0.68, 0.68, 0.74, 0.7, 0.72, 0.72, 0.73, 0.65, 0.73, 0.77,  
0.7, 0.69, 0.79, 0.75, 0.78, 0.76, 0.69, 0.74, 0.71, 0.76, 0.79) # radiation simulated in ARIMhigh  
# Index values and no measurement unit
```

```
shapiro.test(Radiation_high)  
acf(Radiation_high)
```

```
Water_high <- c(0.89, 0.84, 0.88, 0.88, 0.86, 0.89, 0.88, 0.88, 0.87, 0.85, 0.86, 0.89, 0.84, 0.83,  
0.85, 0.86, 0.83, 0.87, 0.94, 0.86, 0.89, 0.9, 0.92, 0.97, 0.9, 0.87, 0.88, 0.89, 0.92, 0.88, 0.91, 0.87,  
0.9, 0.93, 0.89, 0.89, 0.89, 0.91, 0.92, 0.91, 0.89, 0.88, 0.89, 0.91, 0.88, 0.92, 0.85, 0.83, 0.87,  
0.89, 0.88, 0.9, 0.88, 0.86, 0.91, 0.91, 0.88, 0.88, 0.86)  
# water availability simulated in ARIMhigh  
# Index values and no measurement unit
```

```
shapiro.test(Water_high)  
acf(Water_high)
```

```
Nutrients_high <- c(0.64, 0.71, 0.64, 0.71, 0.74, 0.7, 0.72, 0.68, 0.7, 0.79, 0.77, 0.72, 0.77, 0.72,  
0.7, 0.69, 0.78, 0.78, 0.61, 0.71, 0.68, 0.71, 0.71, 0.58, 0.7, 0.74, 0.75, 0.78, 0.68, 0.75, 0.74, 0.82,  
0.84, 0.79, 0.88, 0.83, 0.75, 0.7, 0.71, 0.73, 0.77, 0.72, 0.77, 0.72, 0.76, 0.63, 0.7, 0.76, 0.68, 0.72,  
0.86, 0.81, 0.81, 0.79, 0.75, 0.74, 0.72, 0.79, 0.84) # Nutrient simulated in ARIMhigh  
# Index values and no measurement unit
```

```
shapiro.test(Nutrients_high)  
acf(Nutrients_high)
```

```
CO2_high <- c(0.67, 0.68, 0.66, 0.68, 0.68, 0.67, 0.68, 0.67, 0.67, 0.69, 0.68, 0.68, 0.69, 0.67,
0.67, 0.67, 0.68, 0.68, 0.67, 0.67, 0.67, 0.67, 0.67, 0.68, 0.66, 0.67, 0.67, 0.67, 0.68, 0.67, 0.67, 0.67,
0.68, 0.68, 0.68, 0.69, 0.69, 0.67, 0.66, 0.67, 0.67, 0.68, 0.67, 0.67, 0.68, 0.67, 0.66, 0.66, 0.67,
0.66, 0.66, 0.69, 0.68, 0.69, 0.68, 0.67, 0.69, 0.67, 0.68, 0.69)
#CO2 simulated in ARIMhigh
# Index values and no measurement unit
```

```
shapiro.test(CO2_high)
acf(CO2_high)
```

```
Herbivory_high <- c(1.09, 0.96, 1.07, 0.98, 0.98, 1.03, 1.02, 1.06, 0.98, 1.04, 1.08, 1.01, 1.01,
1.05, 1.05, 1.04, 1.03, 1.06, 1.09, 0.95, 1.04, 0.96, 0.94, 1, 0.9, 0.95, 1.04, 0.97, 0.95, 0.92, 0.93,
1.01, 1.03, 0.99, 1.03, 1.06, 1.03, 0.91, 1.03, 0.99, 0.99, 1.02, 0.99, 1.01, 0.93, 0.94, 0.92, 1, 0.96,
0.91, 0.96, 1.08, 1.07, 0.98, 1, 1, 1, 0.93, 0.98) #Herbivory simulated in ARIMhigh
# Index values and no measurement unit
```

```
shapiro.test(Herbivory_high)
acf(Herbivory_high)
```

```
WD_high <- c(0.58, 0.83, 0.58, 0.84, 0.91, 0.72, 0.92, 0.66, 0.78, 1.22, 1.1, 0.94, 1.08, 0.94, 0.85,
0.76, 1.17, 1.19, 0.35, 0.84, 0.64, 0.81, 0.8, 0.17, 0.68, 0.84, 0.79, 0.99, 0.44, 0.76, 0.65, 1.12,
1.14, 0.88, 1.4, 1.13, 0.75, 0.46, 0.47, 0.64, 0.82, 0.64, 0.93, 0.68, 0.92, 0.23, 0.64, 0.88, 0.52,
0.71, 1.37, 1.12, 1.05, 0.97, 0.85, 0.77, 0.77, 1.01, 1.29)
# Weather Disturbance simulated in ARIMhigh
# Index values and no measurement unit
```

```
shapiro.test(WD_high)
acf(WD_high)
```

```
SMD_high <- c(0.63, 0.68, 0.75, 0.78, 0.79, 0.83, 0.76, 0.77, 0.78, 0.71, 0.74, 0.74, 0.69, 0.71,
0.71, 0.72, 0.74, 0.8, 0.76, 0.79, 0.79, 0.82, 0.85, 0.86, 0.88, 0.9, 0.97, 1.01, 0.97, 1.05, 1.07, 1.08,
1.15, 1.19, 1.15, 1.04, 1.06, 1.12, 1.06, 1.11, 1.02, 1, 1.02, 0.96, 1.01, 0.95, 0.9, 0.92, 0.94, 1.03,
1.03, 1.04, 0.98, 0.99, 1.06, 0.91, 0.94, 0.95, 0.96)
# Soil Mediated Disturbance simulated in ARIMhigh
# Index values and no measurement unit
```

```
shapiro.test(SMD_high)
acf(SMD_high)
```

```
APD_high <- c(0.49, 0.53, 0.59, 0.62, 0.64, 0.68, 0.65, 0.66, 0.66, 0.61, 0.64, 0.64, 0.6, 0.62,
0.63, 0.64, 0.68, 0.73, 0.7, 0.74, 0.77, 0.79, 0.83, 0.87, 0.9, 0.93, 1.02, 1.06, 1.01, 1.11, 1.2, 1.21,
1.3, 1.36, 1.28, 1.13, 1.18, 1.26, 1.2, 1.25, 1.13, 1.1, 1.1, 1.04, 1.12, 1.02, 0.96, 0.98, 1.02, 1.09,
1.08, 1.09, 1.02, 1.04, 1.13, 0.96, 0.96, 0.98, 0.97)
# Air Pollution Disturbance simulated in ARIMhigh
# Index values and no measurement unit
```

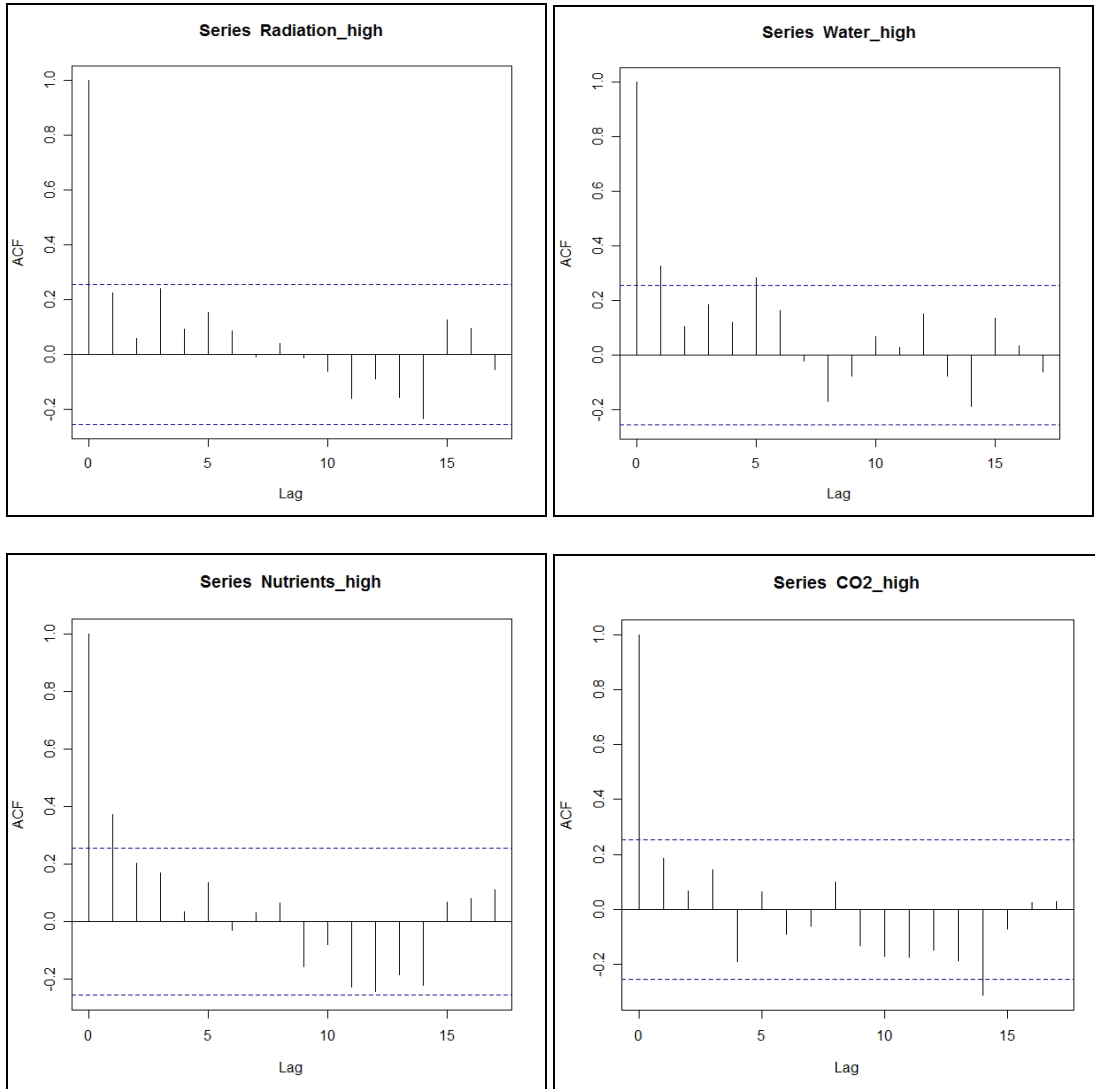
```
shapiro.test(APD_high)
acf(APD_high)
```

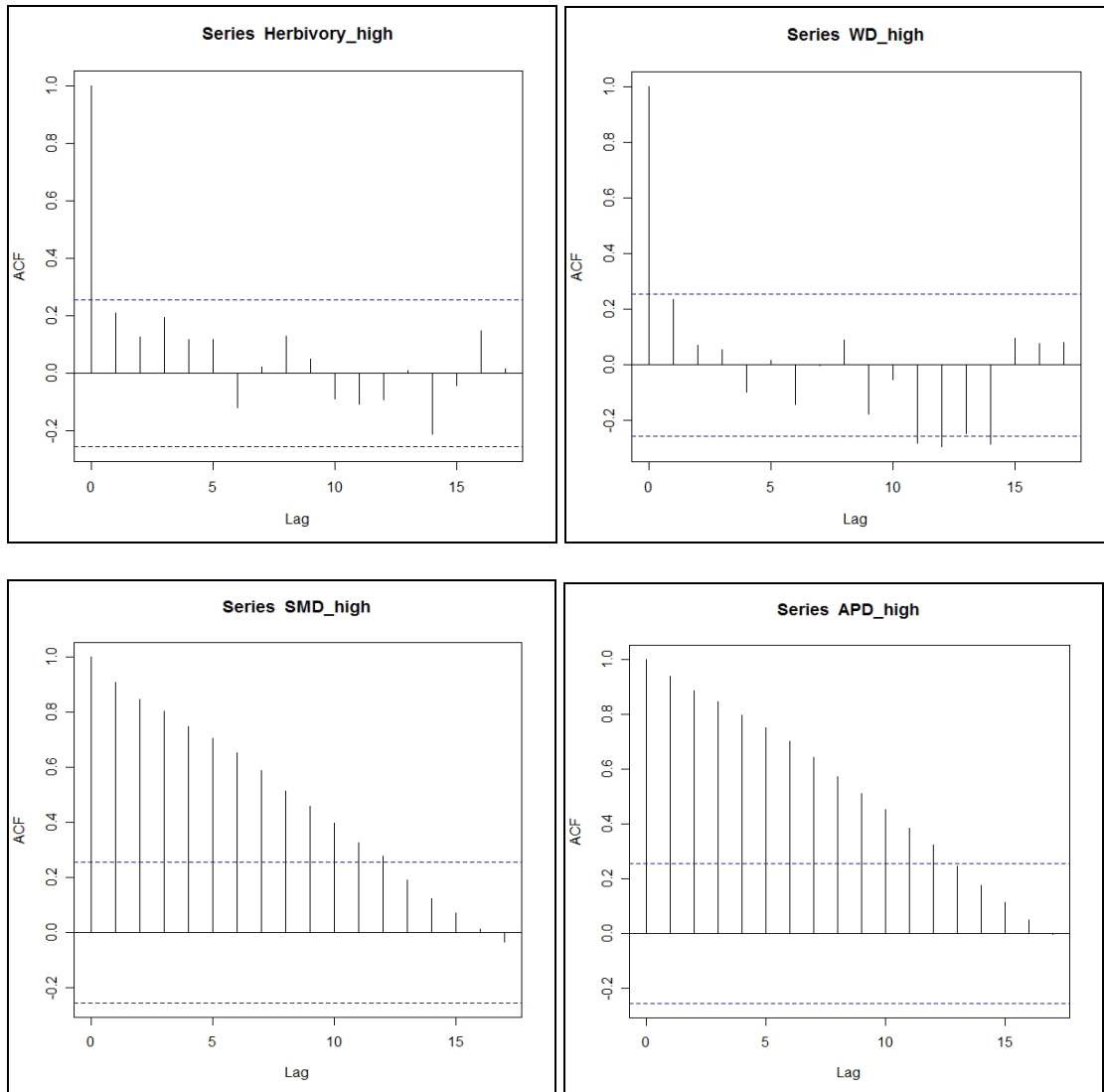
Results of normality tests for variables of ARIM_{high} main model

	<i>Radiation</i>	<i>Water</i>	<i>Nutrients</i>	<i>CO2</i>	<i>Herbivory</i>	<i>WD</i>	<i>SMD</i>	<i>APD</i>
W-value	0.9886	0.9707	0.9834	0.8695	0.9753	0.9882	0.9595	0.9384
P-value	0.8567	0.1656	0.5992	1.394e-05	0.2724	0.8389	0.04719	0.00501

W-value: It is Wilks Shapiro test statistic.

Results of autocorrelation tests for variables of ARIM_{high} main model





Checking Randomness for Variables for CART and GLMs and Results for ARIM_{low}

require(graphics)

```
LowRSTI <- c( 1.04, 1.19, 1.17, 1.08, 1.13, 0.91, 0.73, 0.89, 0.98, 1.12, 1.2, 1.54, 1.32, 0.91, 0.9,
0.75, 0.82, 1.08, 1.29, 1.43, 1.36, 1.33, 1.34, 1.39, 1.31, 0.97, 1.04, 1.19, 1.15, 0.94, 1.07, 1.01,
1.05, 1.07, 1.18, 1.31, 1.3, 1.14, 1.07, 1, 1.4, 0.84, 0.93, 1.06, 0.82, 0.88, 0.9, 0.78, 0.78, 0.88,
0.98, 0.95, 1.05, 1.35, 1.12, 1.52, 1.53, 1.41, 1)
```

```
# Low elevation observed standardized ring index of red spruce
```

```
# Index values and no measurement unit
```

```
shapiro.test(LowRSTI) # Shapiro-Wilk normality test
```

```
acf(LowRSTI) # autocorrelation: check randomness of independent and dependent variables
```

```
Radiation_low <- c(0.65, 0.68, 0.63, 0.66, 0.67, 0.65, 0.66, 0.65, 0.65, 0.69, 0.68, 0.66, 0.7, 0.68,
0.67, 0.66, 0.69, 0.67, 0.63, 0.66, 0.65, 0.65, 0.64, 0.6, 0.64, 0.66, 0.65, 0.66, 0.63, 0.65, 0.64,
0.67, 0.66, 0.64, 0.68, 0.68, 0.65, 0.62, 0.63, 0.63, 0.66, 0.64, 0.65, 0.65, 0.65, 0.62, 0.65, 0.67,
0.64, 0.63, 0.68, 0.66, 0.68, 0.67, 0.63, 0.66, 0.65, 0.67, 0.69) # Radiation simulated in ARIMlow
# Index values and no measurement unit
```

```
shapiro.test(Radiation_low)
acf(Radiation_low)
```

```
Water_low <- c(0.81, 0.79, 0.81, 0.81, 0.8, 0.81, 0.81, 0.81, 0.8, 0.79, 0.8, 0.81, 0.79, 0.78, 0.79,
0.8, 0.78, 0.8, 0.84, 0.8, 0.81, 0.82, 0.83, 0.85, 0.82, 0.8, 0.81, 0.82, 0.83, 0.81, 0.82, 0.8, 0.82,
0.83, 0.81, 0.81, 0.81, 0.82, 0.83, 0.83, 0.81, 0.81, 0.81, 0.82, 0.81, 0.83, 0.79, 0.78, 0.8, 0.81, 0.8,
0.82, 0.81, 0.8, 0.82, 0.82, 0.81, 0.81, 0.8) # Water availability simulated in ARIMlow
# Index values and no measurement unit
```

```
shapiro.test(Water_low)
acf(Water_low)
```

```
Nutrients_low <- c(0.56, 0.6, 0.58, 0.62, 0.63, 0.61, 0.62, 0.6, 0.61, 0.64, 0.64, 0.61, 0.64, 0.61,
0.6, 0.6, 0.65, 0.65, 0.57, 0.62, 0.6, 0.62, 0.62, 0.56, 0.63, 0.65, 0.66, 0.68, 0.63, 0.67, 0.67, 0.71,
0.72, 0.7, 0.74, 0.71, 0.67, 0.65, 0.65, 0.67, 0.68, 0.65, 0.67, 0.65, 0.67, 0.6, 0.63, 0.66, 0.63, 0.65,
0.72, 0.69, 0.69, 0.68, 0.66, 0.65, 0.64, 0.67, 0.7) # Nutrient simulated in ARIMlow
# Index values and no measurement unit
```

```
shapiro.test(Nutrients_low)
acf(Nutrients_low)
```

```
CO2_low <- c(0.63, 0.63, 0.63, 0.63, 0.63, 0.63, 0.63, 0.63, 0.63, 0.64, 0.64, 0.63, 0.64, 0.63,
0.63, 0.63, 0.64, 0.64, 0.63, 0.63, 0.63, 0.63, 0.63, 0.63, 0.63, 0.63, 0.63, 0.63, 0.63, 0.63, 0.63,
0.63, 0.64, 0.64, 0.64, 0.64, 0.63, 0.62, 0.63, 0.63, 0.64, 0.63, 0.63, 0.63, 0.63, 0.63, 0.63, 0.63,
0.62, 0.63, 0.64, 0.64, 0.64, 0.63, 0.63, 0.64, 0.63, 0.64, 0.64) #CO2 simulated in ARIMlow
# Index values and no measurement unit
```

```
shapiro.test(CO2_low)
acf(CO2_low)
```

```
Herbivory_low <- c(1.09, 0.96, 1.07, 0.98, 0.98, 1.03, 1.02, 1.06, 0.98, 1.04, 1.08, 1.01, 1.01,
1.05, 1.05, 1.04, 1.03, 1.06, 1.09, 0.95, 1.04, 0.96, 0.94, 1, 0.9, 0.95, 1.04, 0.97, 0.95, 0.92, 0.93,
1.01, 1.03, 0.99, 1.03, 1.06, 1.03, 0.91, 1.03, 0.99, 0.99, 1.02, 0.99, 1.01, 0.93, 0.94, 0.92, 1, 0.96,
0.91, 0.96, 1.08, 1.07, 0.98, 1, 1, 1, 0.93, 0.98) #Herbivory simulated in ARIMlow
# Index values and no measurement unit
```

```
shapiro.test(Herbivory_low)
acf(Herbivory_low)
```

```
WD_low <- c(0.49, 0.56, 0.51, 0.62, 0.59, 0.52, 0.63, 0.56, 0.54, 0.7, 0.64, 0.65, 0.65, 0.64, 0.62,
0.57, 0.65, 0.66, 0.46, 0.59, 0.51, 0.54, 0.57, 0.4, 0.52, 0.59, 0.49, 0.56, 0.48, 0.48, 0.52, 0.61,
0.57, 0.54, 0.63, 0.63, 0.59, 0.5, 0.46, 0.48, 0.55, 0.52, 0.58, 0.53, 0.63, 0.44, 0.6, 0.59, 0.57,
0.53, 0.7, 0.61, 0.57, 0.58, 0.56, 0.53, 0.55, 0.57, 0.62)
```

```
# Weather Disturbance simulated in ARIMlow
# Index values and no measurement unit
```

```
shapiro.test(WD_low)
acf(WD_low)
```

```
SMD_low <- c(0.44, 0.47, 0.51, 0.53, 0.54, 0.56, 0.52, 0.53, 0.53, 0.49, 0.51, 0.51, 0.48, 0.49,
0.49, 0.49, 0.51, 0.54, 0.52, 0.54, 0.54, 0.55, 0.57, 0.58, 0.59, 0.61, 0.65, 0.66, 0.65, 0.69, 0.7,
0.71, 0.74, 0.77, 0.74, 0.69, 0.7, 0.73, 0.7, 0.72, 0.67, 0.67, 0.67, 0.64, 0.67, 0.63, 0.61, 0.62,
0.63, 0.68, 0.68, 0.68, 0.65, 0.65, 0.69, 0.61, 0.62, 0.63, 0.64)
```

```
# Soil Mediated Disturbance simulated in ARIMlow
# Index values and no measurement unit
```

```
shapiro.test(SMD_low)
acf(SMD_low)
```

```
APD_low <- c(0.33, 0.36, 0.39, 0.41, 0.42, 0.45, 0.44, 0.45, 0.44, 0.41, 0.43, 0.43, 0.41, 0.42,
0.43, 0.44, 0.46, 0.49, 0.47, 0.5, 0.52, 0.53, 0.56, 0.59, 0.6, 0.63, 0.68, 0.7, 0.68, 0.73, 0.8, 0.8,
0.86, 0.89, 0.84, 0.75, 0.79, 0.83, 0.8, 0.82, 0.76, 0.74, 0.73, 0.7, 0.75, 0.69, 0.65, 0.66, 0.69, 0.72,
0.71, 0.72, 0.68, 0.69, 0.74, 0.65, 0.64, 0.65, 0.64)
```

```
# Air Pollution Disturbance simulated in ARIMlow
# Index values and no measurement unit
```

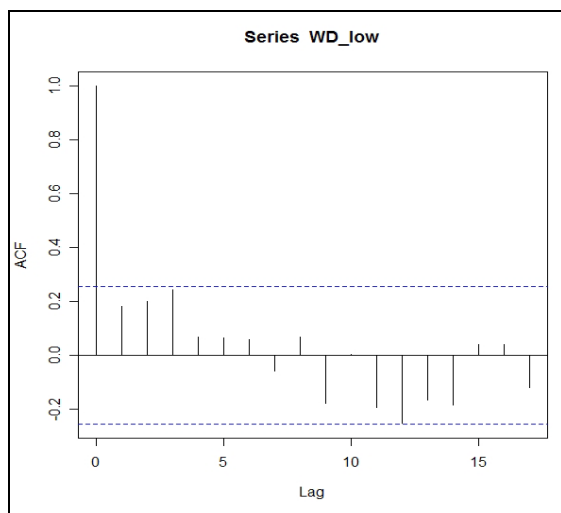
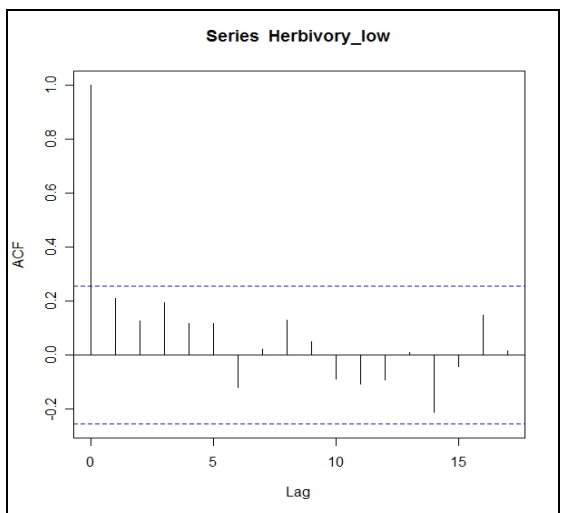
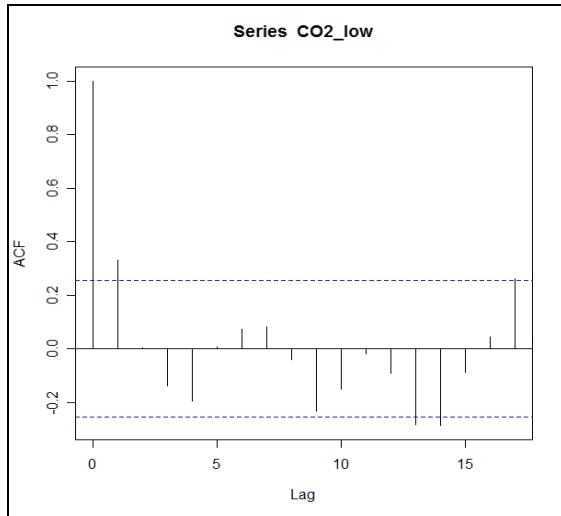
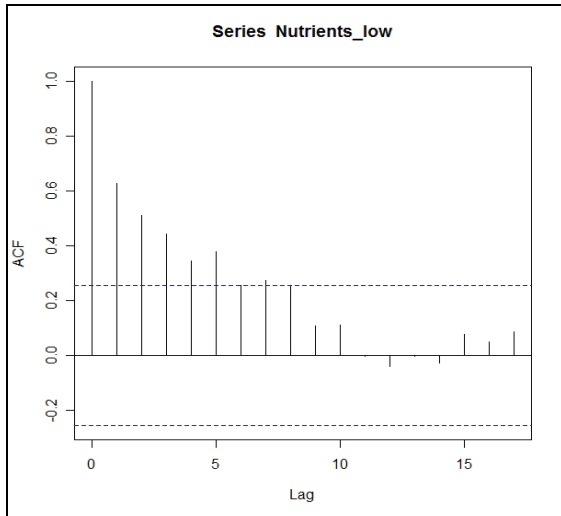
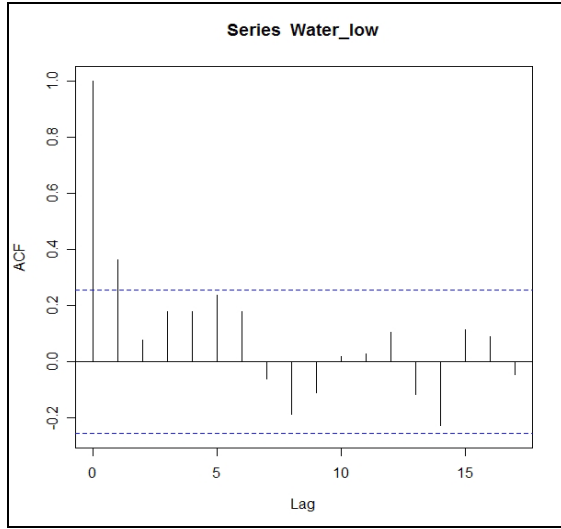
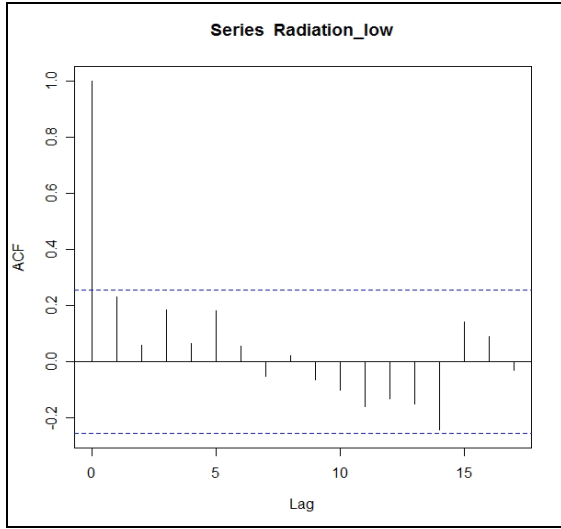
```
shapiro.test(APD_low)
acf(APD_low)
```

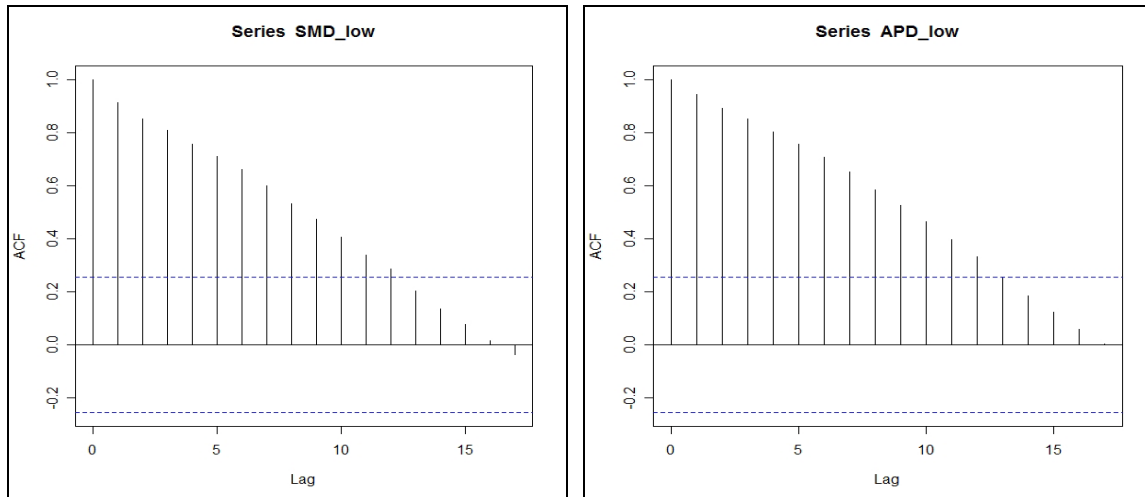
Results of normality tests for variables of ARIM_{low} main model

	<i>Radiation</i>	<i>Water</i>	<i>Nutrient s</i>	<i>CO2</i>	<i>Herbivo ry</i>	<i>WD</i>	<i>SMD</i>	<i>APD</i>
<i>W- value</i>	0.9732	0.9481	0.9859	0.6678	0.9753	0.99	0.9552	0.9351
<i>P-value</i>	0.2181	0.0137 7	0.7246	2.784e- 10	0.2724	0.9104	0.0294	0.0036

```
# W-value: It is Wilks Shapiro test statistic.
```

Results of autocorrelation tests for variables of ARIM_{low} main model





CART and GLM for ARIMhigh

```
library(rpart)
```

```
highAV<-read.table("highAV_193.csv", header=T, sep=",")
```

```
AVhightree<-rpart(formula = highAV ~ RA+WA+NU+CO2+WD+SMD+APD+HB,  
data=highAV, method="anova") # Regression Tree modeling
```

```
printcp(AVhightree)
```

```
AVhightree1<-prune(AVhightree, cp=0.01)
```

```
plot(AVhightree1, branch=0.3) # Plot of CART results as a tree
```

```
text(AVhightree1, digits=3) # Summary of CART results
```

```
highAVglm1<-glm(formula=highAV~APD, family=gaussian, data=highAV) # GLM modeling  
summary(highAVglm1) # Result Summary
```

CART and GLM for ARIMlow

```
library(rpart)
```

```
lowAV_N2<-read.table("lowAV_N2.csv", header=T, sep=",")
```

```
AVNlowtree<-rpart(formula = lowAV_N2 ~ RA+WA+NU+CO2+WD+SMD+APD+HB,  
data=lowAV_N2, method="anova")
```

```
printcp(AVNlowtree)
```

```
AVNlowtree1<-prune(AVNlowtree, cp=0.01)  
plot(AVNlowtree1, branch=0.3)  
text(AVNlowtree1, digits=3)
```

```
lowAVNglm1<-glm(formula=lowAV_N2~WA+APD+RA, family=gaussian, data=lowAV_N2)  
summary(lowAVNglm1)
```

```
lowAVNglm2<-glm(formula=lowAV_N2~WA+APD, family=gaussian, data=lowAV_N2)  
summary(lowAVNglm2)
```

```
lowAVNglm3<-glm(formula=lowAV_N2~WA+RA, family=gaussian, data=lowAV_N2)  
summary(lowAVNglm3)
```

```
lowAVNglm4<-glm(formula=lowAV_N2~APD+RA, family=gaussian, data=lowAV_N2)  
summary(lowAVNglm4)
```

```
lowAVNglm5<-glm(formula=lowAV_N2~WA, family=gaussian, data=lowAV_N2)  
summary(lowAVNglm5)
```

```
lowAVNglm6<-glm(formula=lowAV_N2~APD, family=gaussian, data=lowAV_N2)  
summary(lowAVNglm6)
```

```
lowAVNglm7<-glm(formula=lowAV_N2~RA, family=gaussian, data=lowAV_N2)  
summary(lowAVNglm7)
```

3.3. R programming for Model Check and Bootstrapping

Model Checks and Bootstrapping for ARIM_{high}

```
require(graphics)
```

```
pr <- c(1.23, 1.2, 1.16, 1.14, 1.12, 1.1, 1.12, 1.11, 1.11, 1.15, 1.12, 1.12, 1.15, 1.13, 1.13, 1.12,  
1.1, 1.06, 1.08, 1.06, 1.04, 1.02, 0.99, 0.96, 0.95, 0.92, 0.86, 0.84, 0.87, 0.81, 0.74, 0.73, 0.67,  
0.64, 0.69, 0.79, 0.76, 0.7, 0.74, 0.71, 0.79, 0.81, 0.81, 0.85, 0.8, 0.87, 0.9, 0.89, 0.86, 0.82, 0.83,  
0.82, 0.86, 0.85, 0.79, 0.91, 0.9, 0.89, 0.9) # Predicted values from ARIMhigh simulation  
# Index values and no measurement unit
```

```
or <- c(1.1249, 1.2915, 1.1823, 1.2409, 1.2462, 1.1691, 1.1591, 1.2623, 1.1748, 1.312, 1.0275,  
1.0878, 0.9885, 1.0689, 1.0654, 1.078, 0.9852, 1.1063, 0.8762, 0.863, 0.9336, 0.8504, 0.895,  
0.8099, 1.1139, 1.0933, 0.977, 0.8521, 0.8134, 0.655, 0.7724, 0.7195, 0.6118, 0.5907, 0.6395,
```

```
0.7478 ,0.9056, 0.6389, 0.7421, 0.6077, 0.879, 0.5641, 0.6654, 0.8583, 0.6411, 0.6818, 0.8394,
0.7276, 0.7511, 0.666, 0.7634, 0.7254, 0.9833, 1.3323, 1.1925, 1.5019, 1.2294, 1.0087, 0.7849)
# Original red spruce ring index values for high elevation red spruce
# Index values and no measurement unit
```

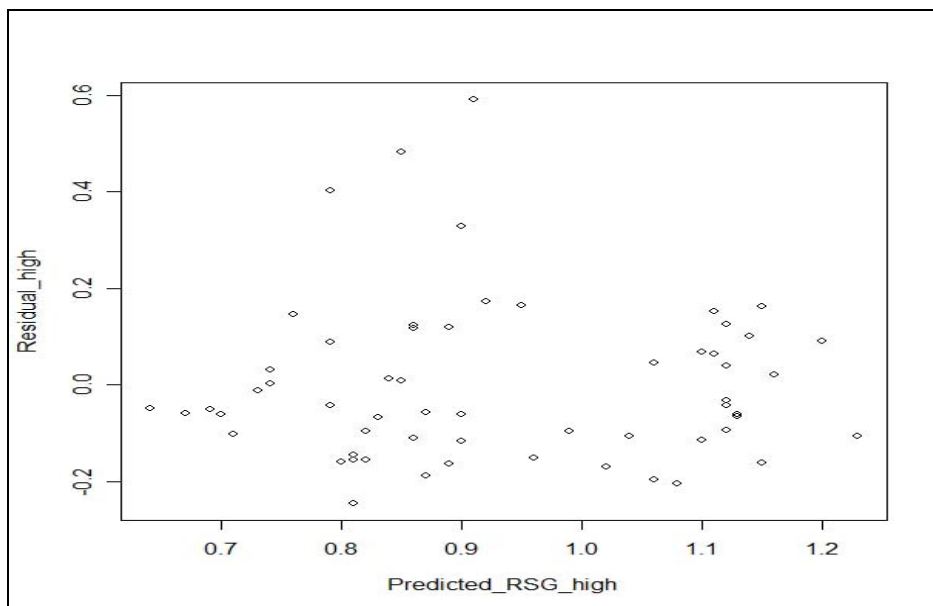
```
Predicted_RSG_high <- pr
Observed_RSG_high <- or
```

```
CV <- (list(Predicted_RSG_high, Observed_RSG_high))
```

Constance Variance Test

```
fligner.test(Observed_RSG_high ~ Predicted_RSG_high, data=CV)
# Contant variance test: Performs a Fligner-Killeen (median) test of the null that
# the variances in each of the groups (samples) are the same
```

```
Residual_high <- Observed_RSG_high - Predicted_RSG_high
plot(Predicted_RSG_high, Residual_high) # plot of residuals vs. predicted values
# It shows the randomness of residuals vs.
predicted values
```



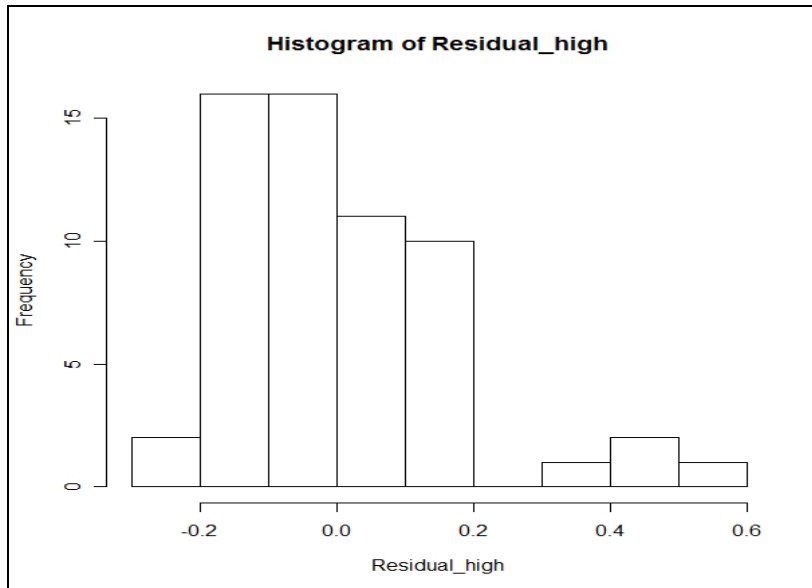
Independence of Residual Test

```
acf(Residual_high) # Autocorrelation function: independence test: The most important
#assumption for hypothesis test and confidence interval
```

Normality of Residual Test

```
shapiro.test(Residual_high) # Normality test
```

```
hist(Residual_high) #histogram: it shows the normality of residuals
```



Bootstrapping Test

```
library(boot)
```

```
highTR<-read.table("highAV_195.csv", header=T, sep=",")
```

```
fit<-glm(formula=highAV~APD, family=gaussian, data=highTR)
```

```
RShigh<-data.frame(highTR, res=resid(fit), fitted=fitted(fit))
```

```
RShigh.fun<- function(data, i) {  
  d <- data  
  d$highAV <- d$fitted + d$res[i]  
  coef(update(fit, data=d))  
}
```

```
RShigh_glm_boot1 <- boot(RShigh, RShigh.fun, R=10000, sim="ordinary", stype="i")  
# non parametric bootstrapping simulation with 10000 run times
```

```
plot(RShigh_glm_boot1) # It shows the bootstrapping results
```

Model Checks and Bootstrapping for ARIM_{low}

```
require(graphics)
```

```
pr <- c(1.19, 1.02, 1.03, 1.17, 1.08, 1.11, 1.14, 1.14, 1.03, 1.16, 1.17, 1.19, 1.13, 0.94, 1, 1.05,  
1.04, 1.16, 1.31, 1, 1.13, 1.17, 1.25, 1.29, 1.16, 1.05, 1.05, 1.14, 1.18, 1, 1.1, 1.05, 1.17, 1.21, 1.2,  
1.18, 1.03, 1, 1.11, 1.07, 1.14, 1, 1.07, 1.16, 1.01, 1.08, 0.89, 0.84, 0.89, 0.98, 1.14, 1.17, 1.21,  
1.02, 1.11, 1.25, 1.06, 1.14, 1.09) # ARIMlow predicted index value with no measurement unit
```

```
or <- c(1.04, 1.19, 1.17, 1.08, 1.13, 0.91, 0.73, 0.89, 0.98, 1.12, 1.2, 1.54, 1.32, 0.91, 0.9, 0.75,  
0.82, 1.08, 1.29, 1.43, 1.36, 1.33, 1.34, 1.39, 1.31, 0.97, 1.04, 1.19, 1.15, 0.94, 1.07, 1.01,  
1.05, 1.07, 1.18, 1.31, 1.3, 1.14, 1.07, 1, 1.4, 0.84, 0.93, 1.06, 0.82, 0.88, 0.9,  
0.78, 0.78, 0.88, 0.98, 0.95, 1.05, 1.35, 1.12, 1.52, 1.53, 1.41, 1) # Red Spruce Standardized  
#Tree-ring Index value for low elevation sites with no measurement unit
```

```
Predicted_RSG_low <- pr  
Observed_RSG_low <- or
```

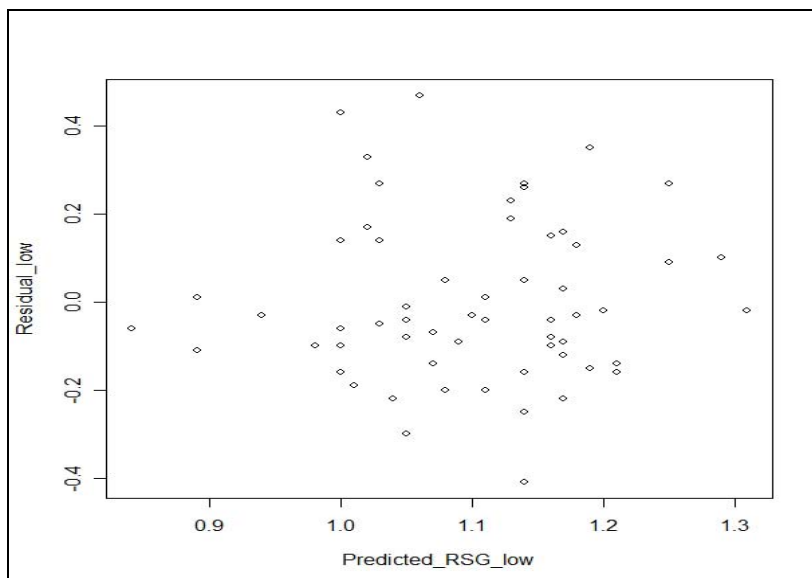
```
CV <- (list(Predicted_RSG_low, Observed_RSG_low))
```

Constant Variance Test

```
fligner.test(Observed_RSG_low ~ Predicted_RSG_low, data=CV) # Contant variance test:  
# Performs a Fligner-Killeen (median) test of the null that the  
variances in each of # the groups(samples) are the same
```

```
Residual_low <- Observed_RSG_low - Predicted_RSG_low
```

```
plot(Predicted_RSG_low, Residual_low)
```



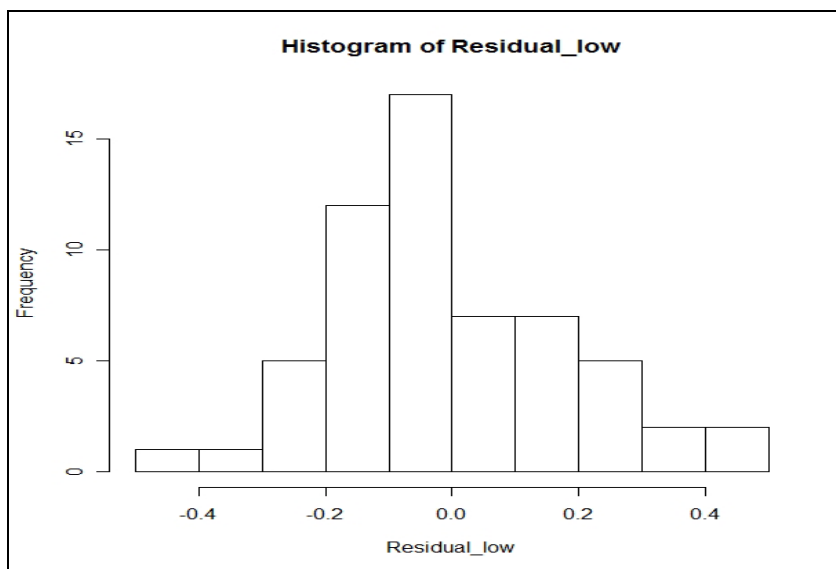
Independence of Residual Test

```
acf(Residual_low) # Independence test: The most important assumption for hypothesis test and  
#confidence interval (the dotted line: 95% confidence interval)
```

Normality of Residual Test

```
shapiro.test(Residual_low) # Normality test: violation of normality is not serious if  
#independence is not violated.
```

```
hist(Residual_low) #histogram of residuals
```



Bootstrapping Test

```
library(boot)
```

```
lowTR<-read.table("lowAV_N4.csv", header=T, sep=",")
```

```
fit<-glm(formula=lowAV_N2~WA+APD+RA, family=gaussian, data=lowTR)
```

```
RSlow<-data.frame(lowTR, res=resid(fit), fitted=fitted(fit))
```

```
RSlow.fun<- function(data, i) {  
  d <- data  
  d$lowAV_N2 <- d$fitted + d$res[i]
```

```
coef(update(fit, data=d))  
}
```

```
RSlow_glm_boot1 <- boot(RSlow, RSlow.fun, R=10000, sim="ordinary", stype="i")  
plot(RSlow_glm_boot1)
```

Appendix 4

Data for ARIM Simulation and R programming for Predicting Global Warming Effects on Red Spruce Growth

4.1. Data for ARIM Simulations for Predicting Global Warming Effects on Red Spruce Growth

Data for ARIMhigh

(NOSO = (NO_x+SO_x)/2, OZONE = Ozone, PRE = Precipitation, RBIVs = Relative Basis Index Values). Unit for NOSO is ppm, OZONE ppm and PRE m. *RBIVs* (Relative Basis Index Values) are unitless index values

Real Values with 10% increase of AP				RBIVs		
Year	NOSO	OZONE	PRE	NOSO	OZONE	PRE
1940	27326	24535	2.9617	0.5843	0.5307	0.8670
1941	31119	25497	2.4999	0.6654	0.5516	0.7318
1942	32930	24747	3.6286	0.7041	0.5353	1.0622
1943	35818	25295	3.0952	0.7659	0.5472	0.9061
1944	36547	25994	3.1409	0.7814	0.5623	0.9194
1945	37555	26856	3.5064	0.8030	0.5810	1.0264
1946	33290	30542	3.5515	0.7118	0.6607	1.0396
1947	36768	29977	2.6578	0.7862	0.6485	0.7780
1948	34269	29334	3.6704	0.7327	0.6346	1.0744
1949	31048	29967	3.4116	0.6639	0.6483	0.9987
1950	32450	31029	3.5992	0.6938	0.6712	1.0536
1951	32012	30933	3.7346	0.6845	0.6692	1.0932
1952	31882	31264	2.6438	0.6817	0.6763	0.7739
1953	32024	32362	2.8658	0.6847	0.7001	0.8389
1954	31844	32895	3.0760	0.6809	0.7116	0.9004
1955	32446	33536	2.9451	0.6938	0.7255	0.8621
1956	32906	34769	3.3745	0.7036	0.7521	0.9878
1957	33520	35032	4.3535	0.7167	0.7578	1.2744
1958	35646	34858	2.7234	0.7622	0.7541	0.7972
1959	36140	36189	3.2215	0.7727	0.7829	0.9430
1960	36367	38599	3.2017	0.7776	0.8350	0.9372
1961	35951	38393	3.9202	0.7687	0.8305	1.1476
1962	37363	39444	4.0165	0.7989	0.8533	1.1758
1963	39233	42162	3.5853	0.8389	0.9121	1.0495
1964	41172	42819	3.2993	0.8803	0.9263	0.9658
1965	43329	44209	2.9902	0.9265	0.9563	0.8753
1966	46239	45217	3.3495	0.9887	0.9781	0.9805
1967	46128	45844	3.9503	0.9863	0.9917	1.1564
1968	48635	44940	2.5864	1.0399	0.9722	0.7571
1969	49808	45611	3.6012	1.0650	0.9867	1.0542
1970	52089	51910	3.2105	1.1138	1.1229	0.9398
1971	51245	51598	3.6627	1.0957	1.1162	1.0722

1972	53130	53037	4.1121	1.1360	1.1473	1.2037
1973	55283	53402	4.1287	1.1821	1.1552	1.2086
1974	52947	50957	4.1740	1.1321	1.1023	1.2219
1975	50643	48711	3.1979	1.0828	1.0537	0.9361
1976	52486	51042	2.9876	1.1223	1.1042	0.8746
1977	53431	52234	3.6274	1.1425	1.1299	1.0619
1978	51947	52725	3.0975	1.1107	1.1406	0.9067
1979	51657	51877	3.9387	1.1045	1.1222	1.1530
1980	50289	50720	2.9223	1.0753	1.0972	0.8555
1981	48823	49167	3.1317	1.0439	1.0636	0.9168
1982	47104	47651	3.8760	1.0072	1.0308	1.1346
1983	46446	48717	3.0273	0.9931	1.0539	0.8862
1984	48138	50337	3.4158	1.0293	1.0889	0.9999
1985	46856	47626	2.7252	1.0019	1.0303	0.7978
1986	45700	46425	2.3478	0.9772	1.0043	0.6873
1987	45743	46538	2.5708	0.9781	1.0067	0.7525
1988	47259	48430	2.5022	1.0105	1.0477	0.7325
1989	47186	46406	3.9949	1.0089	1.0039	1.1694
1990	47709	44985	3.8499	1.0201	0.9731	1.1270
1991	47290	45351	4.1048	1.0112	0.9810	1.2016
1992	47402	45255	3.0820	1.0135	0.9790	0.9022
1993	47427	45829	3.2508	1.0141	0.9914	0.9516
1994	47242	46907	4.4646	1.0101	1.0147	1.3069
1995	44102	45738	2.8698	0.9430	0.9894	0.8401
1996	43797	43412	3.4946	0.9365	0.9391	1.0230
1997	44446	43700	3.4682	0.9503	0.9453	1.0152
1998	44101	42371	3.7703	0.9430	0.9166	1.1037
1999	44101	42371	3.3590	0.9430	0.9166	0.9833
2000	51220.161	51647.936	2.9687	1.0952	1.1173	0.8690
2001	49754.161	50094.936	3.1781	1.0638	1.0837	0.9303
2002	48035.161	48578.936	3.9223	1.0271	1.0509	1.1482
2003	47377.161	49644.936	3.0737	1.0130	1.0739	0.8998
2004	49069.161	51264.936	3.4621	1.0492	1.1090	1.0135
2005	47787.161	48553.936	2.7716	1.0218	1.0503	0.8113
2006	46631.161	47352.936	2.3941	0.9971	1.0244	0.7008
2007	46674.161	47465.936	2.6171	0.9980	1.0268	0.7661
2008	48190.161	49357.936	2.5486	1.0304	1.0677	0.7460
2009	48117.161	47333.936	4.0413	1.0288	1.0239	1.1830
2010	48640.161	45912.936	3.8963	1.0400	0.9932	1.1406
2011	48221.161	46278.936	4.1511	1.0311	1.0011	1.2152
2012	48333.161	46182.936	3.1284	1.0335	0.9990	0.9158
2013	48358.161	46756.936	3.2972	1.0340	1.0115	0.9652
2014	48173.161	47834.936	4.5110	1.0300	1.0348	1.3205
2015	45033.161	46665.936	2.9162	0.9629	1.0095	0.8537
2016	44728.161	44339.936	3.5410	0.9564	0.9592	1.0366
2017	45377.161	44627.936	3.5145	0.9703	0.9654	1.0288
2018	45032.161	43298.936	3.8167	0.9629	0.9367	1.1173
2019	45032.161	43298.936	3.4054	0.9629	0.9367	0.9969

2020	52151.322	52575.872	3.0151	1.1151	1.1373	0.8826
2021	50685.322	51022.872	3.2244	1.0838	1.1037	0.9439
2022	48966.322	49506.872	3.9687	1.0470	1.0709	1.1618
2023	48308.322	50572.872	3.1200	1.0329	1.0940	0.9133
2024	50000.322	52192.872	3.5085	1.0691	1.1291	1.0271
2025	48718.322	49481.872	2.8179	1.0417	1.0704	0.8249
2026	47562.322	48280.872	2.4405	1.0170	1.0444	0.7144
2027	47605.322	48393.872	2.6635	1.0179	1.0469	0.7797
2028	49121.322	50285.872	2.5949	1.0503	1.0878	0.7596
2029	49048.322	48261.872	4.0876	1.0488	1.0440	1.1966
2030	49571.322	46840.872	3.9426	1.0599	1.0133	1.1541
2031	49152.322	47206.872	4.1975	1.0510	1.0212	1.2287
2032	49264.322	47110.872	3.1748	1.0534	1.0191	0.9294
2033	49289.322	47684.872	3.3435	1.0539	1.0315	0.9788
2034	49104.322	48762.872	4.5573	1.0499	1.0549	1.3341
2035	45964.322	47593.872	2.9626	0.9828	1.0296	0.8672
2036	45659.322	45267.872	3.5873	0.9763	0.9792	1.0501
2037	46308.322	45555.872	3.5609	0.9902	0.9855	1.0424
2038	45963.322	44226.872	3.8631	0.9828	0.9567	1.1308
2039	45963.322	44226.872	3.4517	0.9828	0.9567	1.0104
2040	53082.483	53503.808	3.0614	1.1350	1.1574	0.8962
2041	51616.483	51950.808	3.2708	1.1037	1.1238	0.9575
2042	49897.483	50434.808	4.0151	1.0669	1.0910	1.1753
2043	49239.483	51500.808	3.1664	1.0528	1.1141	0.9269
2044	50931.483	53120.808	3.5549	1.0890	1.1491	1.0406
2045	49649.483	50409.808	2.8643	1.0616	1.0905	0.8385
2046	48493.483	49208.808	2.4869	1.0369	1.0645	0.7280
2047	48536.483	49321.808	2.7099	1.0378	1.0669	0.7933
2048	50052.483	51213.808	2.6413	1.0702	1.1079	0.7732
2049	49979.483	49189.808	4.1340	1.0687	1.0641	1.2102
2050	50502.483	47768.808	3.9890	1.0798	1.0334	1.1677
2051	50083.483	48134.808	4.2439	1.0709	1.0413	1.2423
2052	50195.483	48038.808	3.2211	1.0733	1.0392	0.9429
2053	50220.483	48612.808	3.3899	1.0738	1.0516	0.9923
2054	50035.483	49690.808	4.6037	1.0699	1.0749	1.3476
2055	46895.483	48521.808	3.0089	1.0027	1.0496	0.8808
2056	46590.483	46195.808	3.6337	0.9962	0.9993	1.0637
2057	47239.483	46483.808	3.6072	1.0101	1.0056	1.0560
2058	46894.483	45154.808	3.9094	1.0027	0.9768	1.1444
2059	46894.483	45154.808	3.4981	1.0027	0.9768	1.0240
2060	54013.644	54431.744	3.1078	1.1549	1.1775	0.9097
2061	52547.644	52878.744	3.3172	1.1236	1.1439	0.9710
2062	50828.644	51362.744	4.0614	1.0868	1.1111	1.1889
2063	50170.644	52428.744	3.2127	1.0727	1.1342	0.9405
2064	51862.644	54048.744	3.6012	1.1089	1.1692	1.0542
2065	50580.644	51337.744	2.9106	1.0815	1.1106	0.8520
2066	49424.644	50136.744	2.5332	1.0568	1.0846	0.7416
2067	49467.644	50249.744	2.7562	1.0577	1.0870	0.8068

2068	50983.644	52141.744	2.6876	1.0901	1.1279	0.7868
2069	50910.644	50117.744	4.1804	1.0886	1.0842	1.2237
2070	51433.644	48696.744	4.0353	1.0998	1.0534	1.1813
2071	51014.644	49062.744	4.2902	1.0908	1.0613	1.2559
2072	51126.644	48966.744	3.2675	1.0932	1.0593	0.9565
2073	51151.644	49540.744	3.4362	1.0937	1.0717	1.0059
2074	50966.644	50618.744	4.6501	1.0898	1.0950	1.3612
2075	47826.644	49449.744	3.0553	1.0226	1.0697	0.8944
2076	47521.644	47123.744	3.6801	1.0161	1.0194	1.0773
2077	48170.644	47411.744	3.6536	1.0300	1.0256	1.0695
2078	47825.644	46082.744	3.9558	1.0226	0.9969	1.1580
2079	47825.644	46082.744	3.5445	1.0226	0.9969	1.0376
2080	54944.805	55359.68	3.1541	1.1748	1.1976	0.9233
2081	53478.805	53806.68	3.3635	1.1435	1.1640	0.9846
2082	51759.805	52290.68	4.1078	1.1067	1.1312	1.2025
2083	51101.805	53356.68	3.2591	1.0927	1.1542	0.9540
2084	52793.805	54976.68	3.6476	1.1288	1.1893	1.0678
2085	51511.805	52265.68	2.9570	1.1014	1.1306	0.8656
2086	50355.805	51064.68	2.5796	1.0767	1.1046	0.7551
2087	50398.805	51177.68	2.8026	1.0776	1.1071	0.8204
2088	51914.805	53069.68	2.7340	1.1100	1.1480	0.8003
2089	51841.805	51045.68	4.2267	1.1085	1.1042	1.2373
2090	52364.805	49624.68	4.0817	1.1197	1.0735	1.1948
2091	51945.805	49990.68	4.3366	1.1107	1.0814	1.2695
2092	52057.805	49894.68	3.3138	1.1131	1.0793	0.9701
2093	52082.805	50468.68	3.4826	1.1136	1.0918	1.0195
2094	51897.805	51546.68	4.6964	1.1097	1.1151	1.3748
2095	48757.805	50377.68	3.1016	1.0425	1.0898	0.9079
2096	48452.805	48051.68	3.7264	1.0360	1.0395	1.0908
2097	49101.805	48339.68	3.7000	1.0499	1.0457	1.0831
2098	48756.805	47010.68	4.0021	1.0425	1.0170	1.1716
2099	48756.805	47010.68	3.5908	1.0425	1.0170	1.0511

Real Values with 0% increase of AP				<i>RBIVs</i>		
Year	NOSO	OZONE	PRE	NOSO	OZONE	PRE
1940	27326	24535	2.9617	0.6069	0.5515	0.8670
1941	31119	25497	2.4999	0.6912	0.5731	0.7318
1942	32930	24747	3.6286	0.7314	0.5563	1.0622
1943	35818	25295	3.0952	0.7956	0.5686	0.9061
1944	36547	25994	3.1409	0.8118	0.5843	0.9194
1945	37555	26856	3.5064	0.8341	0.6037	1.0264
1946	33290	30542	3.5515	0.7394	0.6865	1.0396
1947	36768	29977	2.6578	0.8167	0.6738	0.7780
1948	34269	29334	3.6704	0.7612	0.6594	1.0744
1949	31048	29967	3.4116	0.6896	0.6736	0.9987
1950	32450	31029	3.5992	0.7208	0.6975	1.0536
1951	32012	30933	3.7346	0.7110	0.6953	1.0932

1952	31882	31264	2.6438	0.7081	0.7028	0.7739
1953	32024	32362	2.8658	0.7113	0.7274	0.8389
1954	31844	32895	3.0760	0.7073	0.7394	0.9004
1955	32446	33536	2.9451	0.7207	0.7538	0.8621
1956	32906	34769	3.3745	0.7309	0.7815	0.9878
1957	33520	35032	4.3535	0.7445	0.7875	1.2744
1958	35646	34858	2.7234	0.7917	0.7836	0.7972
1959	36140	36189	3.2215	0.8027	0.8135	0.9430
1960	36367	38599	3.2017	0.8078	0.8676	0.9372
1961	35951	38393	3.9202	0.7985	0.8630	1.1476
1962	37363	39444	4.0165	0.8299	0.8866	1.1758
1963	39233	42162	3.5853	0.8714	0.9477	1.0495
1964	41172	42819	3.2993	0.9145	0.9625	0.9658
1965	43329	44209	2.9902	0.9624	0.9937	0.8753
1966	46239	45217	3.3495	1.0270	1.0164	0.9805
1967	46128	45844	3.9503	1.0246	1.0305	1.1564
1968	48635	44940	2.5864	1.0802	1.0102	0.7571
1969	49808	45611	3.6012	1.1063	1.0253	1.0542
1970	52089	51910	3.2105	1.1570	1.1669	0.9398
1971	51245	51598	3.6627	1.1382	1.1598	1.0722
1972	53130	53037	4.1121	1.1801	1.1922	1.2037
1973	55283	53402	4.1287	1.2279	1.2004	1.2086
1974	52947	50957	4.1740	1.1760	1.1454	1.2219
1975	50643	48711	3.1979	1.1248	1.0949	0.9361
1976	52486	51042	2.9876	1.1658	1.1473	0.8746
1977	53431	52234	3.6274	1.1868	1.1741	1.0619
1978	51947	52725	3.0975	1.1538	1.1852	0.9067
1979	51657	51877	3.9387	1.1474	1.1661	1.1530
1980	50289	50720	2.9223	1.1170	1.1401	0.8555
1981	48823	49167	3.1317	1.0844	1.1052	0.9168
1982	47104	47651	3.8760	1.0462	1.0711	1.1346
1983	46446	48717	3.0273	1.0316	1.0951	0.8862
1984	48138	50337	3.4158	1.0692	1.1315	0.9999
1985	46856	47626	2.7252	1.0407	1.0706	0.7978
1986	45700	46425	2.3478	1.0150	1.0436	0.6873
1987	45743	46538	2.5708	1.0160	1.0461	0.7525
1988	47259	48430	2.5022	1.0497	1.0886	0.7325
1989	47186	46406	3.9949	1.0481	1.0431	1.1694
1990	47709	44985	3.8499	1.0597	1.0112	1.1270
1991	47290	45351	4.1048	1.0504	1.0194	1.2016
1992	47402	45255	3.0820	1.0529	1.0173	0.9022
1993	47427	45829	3.2508	1.0534	1.0302	0.9516
1994	47242	46907	4.4646	1.0493	1.0544	1.3069
1995	44102	45738	2.8698	0.9796	1.0281	0.8401
1996	43797	43412	3.4946	0.9728	0.9758	1.0230
1997	44446	43700	3.4682	0.9872	0.9823	1.0152
1998	44101	42371	3.7703	0.9795	0.9524	1.1037
1999	44101	42371	3.3590	0.9795	0.9524	0.9833

2000	50289	50720	2.9687	1.1170	1.1401	0.8690
2001	48823	49167	3.1781	1.0844	1.1052	0.9303
2002	47104	47651	3.9223	1.0462	1.0711	1.1482
2003	46446	48717	3.0737	1.0316	1.0951	0.8998
2004	48138	50337	3.4621	1.0692	1.1315	1.0135
2005	46856	47626	2.7716	1.0407	1.0706	0.8113
2006	45700	46425	2.3941	1.0150	1.0436	0.7008
2007	45743	46538	2.6171	1.0160	1.0461	0.7661
2008	47259	48430	2.5486	1.0497	1.0886	0.7460
2009	47186	46406	4.0413	1.0481	1.0431	1.1830
2010	47709	44985	3.8963	1.0597	1.0112	1.1406
2011	47290	45351	4.1511	1.0504	1.0194	1.2152
2012	47402	45255	3.1284	1.0529	1.0173	0.9158
2013	47427	45829	3.2972	1.0534	1.0302	0.9652
2014	47242	46907	4.5110	1.0493	1.0544	1.3205
2015	44102	45738	2.9162	0.9796	1.0281	0.8537
2016	43797	43412	3.5410	0.9728	0.9758	1.0366
2017	44446	43700	3.5145	0.9872	0.9823	1.0288
2018	44101	42371	3.8167	0.9795	0.9524	1.1173
2019	44101	42371	3.4054	0.9795	0.9524	0.9969
2020	50289	50720	3.0151	1.1170	1.1401	0.8826
2021	48823	49167	3.2244	1.0844	1.1052	0.9439
2022	47104	47651	3.9687	1.0462	1.0711	1.1618
2023	46446	48717	3.1200	1.0316	1.0951	0.9133
2024	48138	50337	3.5085	1.0692	1.1315	1.0271
2025	46856	47626	2.8179	1.0407	1.0706	0.8249
2026	45700	46425	2.4405	1.0150	1.0436	0.7144
2027	45743	46538	2.6635	1.0160	1.0461	0.7797
2028	47259	48430	2.5949	1.0497	1.0886	0.7596
2029	47186	46406	4.0876	1.0481	1.0431	1.1966
2030	47709	44985	3.9426	1.0597	1.0112	1.1541
2031	47290	45351	4.1975	1.0504	1.0194	1.2287
2032	47402	45255	3.1748	1.0529	1.0173	0.9294
2033	47427	45829	3.3435	1.0534	1.0302	0.9788
2034	47242	46907	4.5573	1.0493	1.0544	1.3341
2035	44102	45738	2.9626	0.9796	1.0281	0.8672
2036	43797	43412	3.5873	0.9728	0.9758	1.0501
2037	44446	43700	3.5609	0.9872	0.9823	1.0424
2038	44101	42371	3.8631	0.9795	0.9524	1.1308
2039	44101	42371	3.4517	0.9795	0.9524	1.0104
2040	50289	50720	3.0614	1.1170	1.1401	0.8962
2041	48823	49167	3.2708	1.0844	1.1052	0.9575
2042	47104	47651	4.0151	1.0462	1.0711	1.1753
2043	46446	48717	3.1664	1.0316	1.0951	0.9269
2044	48138	50337	3.5549	1.0692	1.1315	1.0406
2045	46856	47626	2.8643	1.0407	1.0706	0.8385
2046	45700	46425	2.4869	1.0150	1.0436	0.7280
2047	45743	46538	2.7099	1.0160	1.0461	0.7933

2048	47259	48430	2.6413	1.0497	1.0886	0.7732
2049	47186	46406	4.1340	1.0481	1.0431	1.2102
2050	47709	44985	3.9890	1.0597	1.0112	1.1677
2051	47290	45351	4.2439	1.0504	1.0194	1.2423
2052	47402	45255	3.2211	1.0529	1.0173	0.9429
2053	47427	45829	3.3899	1.0534	1.0302	0.9923
2054	47242	46907	4.6037	1.0493	1.0544	1.3476
2055	44102	45738	3.0089	0.9796	1.0281	0.8808
2056	43797	43412	3.6337	0.9728	0.9758	1.0637
2057	44446	43700	3.6072	0.9872	0.9823	1.0560
2058	44101	42371	3.9094	0.9795	0.9524	1.1444
2059	44101	42371	3.4981	0.9795	0.9524	1.0240
2060	50289	50720	3.1078	1.1170	1.1401	0.9097
2061	48823	49167	3.3172	1.0844	1.1052	0.9710
2062	47104	47651	4.0614	1.0462	1.0711	1.1889
2063	46446	48717	3.2127	1.0316	1.0951	0.9405
2064	48138	50337	3.6012	1.0692	1.1315	1.0542
2065	46856	47626	2.9106	1.0407	1.0706	0.8520
2066	45700	46425	2.5332	1.0150	1.0436	0.7416
2067	45743	46538	2.7562	1.0160	1.0461	0.8068
2068	47259	48430	2.6876	1.0497	1.0886	0.7868
2069	47186	46406	4.1804	1.0481	1.0431	1.2237
2070	47709	44985	4.0353	1.0597	1.0112	1.1813
2071	47290	45351	4.2902	1.0504	1.0194	1.2559
2072	47402	45255	3.2675	1.0529	1.0173	0.9565
2073	47427	45829	3.4362	1.0534	1.0302	1.0059
2074	47242	46907	4.6501	1.0493	1.0544	1.3612
2075	44102	45738	3.0553	0.9796	1.0281	0.8944
2076	43797	43412	3.6801	0.9728	0.9758	1.0773
2077	44446	43700	3.6536	0.9872	0.9823	1.0695
2078	44101	42371	3.9558	0.9795	0.9524	1.1580
2079	44101	42371	3.5445	0.9795	0.9524	1.0376
2080	50289	50720	3.1541	1.1170	1.1401	0.9233
2081	48823	49167	3.3635	1.0844	1.1052	0.9846
2082	47104	47651	4.1078	1.0462	1.0711	1.2025
2083	46446	48717	3.2591	1.0316	1.0951	0.9540
2084	48138	50337	3.6476	1.0692	1.1315	1.0678
2085	46856	47626	2.9570	1.0407	1.0706	0.8656
2086	45700	46425	2.5796	1.0150	1.0436	0.7551
2087	45743	46538	2.8026	1.0160	1.0461	0.8204
2088	47259	48430	2.7340	1.0497	1.0886	0.8003
2089	47186	46406	4.2267	1.0481	1.0431	1.2373
2090	47709	44985	4.0817	1.0597	1.0112	1.1948
2091	47290	45351	4.3366	1.0504	1.0194	1.2695
2092	47402	45255	3.3138	1.0529	1.0173	0.9701
2093	47427	45829	3.4826	1.0534	1.0302	1.0195
2094	47242	46907	4.6964	1.0493	1.0544	1.3748
2095	44102	45738	3.1016	0.9796	1.0281	0.9079

2096	43797	43412	3.7264	0.9728	0.9758	1.0908
2097	44446	43700	3.7000	0.9872	0.9823	1.0831
2098	44101	42371	4.0021	0.9795	0.9524	1.1716
2099	44101	42371	3.5908	0.9795	0.9524	1.0511

Real Values with 10% decrease of AP			RBIVs			
Year	NOSO	OZONE	PRE	NOSO	OZONE	PRE
1940	27326	24535	2.9617	0.6314	0.5740	0.8670
1941	31119	25497	2.4999	0.7191	0.5965	0.7318
1942	32930	24747	3.6286	0.7609	0.5789	1.0622
1943	35818	25295	3.0952	0.8277	0.5917	0.9061
1944	36547	25994	3.1409	0.8445	0.6081	0.9194
1945	37555	26856	3.5064	0.8678	0.6282	1.0264
1946	33290	30542	3.5515	0.7692	0.7145	1.0396
1947	36768	29977	2.6578	0.8496	0.7013	0.7780
1948	34269	29334	3.6704	0.7919	0.6862	1.0744
1949	31048	29967	3.4116	0.7174	0.7010	0.9987
1950	32450	31029	3.5992	0.7498	0.7259	1.0536
1951	32012	30933	3.7346	0.7397	0.7236	1.0932
1952	31882	31264	2.6438	0.7367	0.7314	0.7739
1953	32024	32362	2.8658	0.7400	0.7571	0.8389
1954	31844	32895	3.0760	0.7358	0.7695	0.9004
1955	32446	33536	2.9451	0.7497	0.7845	0.8621
1956	32906	34769	3.3745	0.7604	0.8134	0.9878
1957	33520	35032	4.3535	0.7746	0.8195	1.2744
1958	35646	34858	2.7234	0.8237	0.8154	0.7972
1959	36140	36189	3.2215	0.8351	0.8466	0.9430
1960	36367	38599	3.2017	0.8403	0.9030	0.9372
1961	35951	38393	3.9202	0.8307	0.8981	1.1476
1962	37363	39444	4.0165	0.8634	0.9227	1.1758
1963	39233	42162	3.5853	0.9066	0.9863	1.0495
1964	41172	42819	3.2993	0.9514	1.0017	0.9658
1965	43329	44209	2.9902	1.0012	1.0342	0.8753
1966	46239	45217	3.3495	1.0685	1.0578	0.9805
1967	46128	45844	3.9503	1.0659	1.0724	1.1564
1968	48635	44940	2.5864	1.1238	1.0513	0.7571
1969	49808	45611	3.6012	1.1509	1.0670	1.0542
1970	52089	51910	3.2105	1.2036	1.2143	0.9398
1971	51245	51598	3.6627	1.1841	1.2070	1.0722
1972	53130	53037	4.1121	1.2277	1.2407	1.2037
1973	55283	53402	4.1287	1.2774	1.2492	1.2086
1974	52947	50957	4.1740	1.2235	1.1921	1.2219
1975	50643	48711	3.1979	1.1702	1.1395	0.9361
1976	52486	51042	2.9876	1.2128	1.1940	0.8746
1977	53431	52234	3.6274	1.2346	1.2219	1.0619
1978	51947	52725	3.0975	1.2004	1.2334	0.9067
1979	51657	51877	3.9387	1.1937	1.2136	1.1530

1980	50289	50720	2.9223	1.1620	1.1865	0.8555
1981	48823	49167	3.1317	1.1282	1.1502	0.9168
1982	47104	47651	3.8760	1.0884	1.1147	1.1346
1983	46446	48717	3.0273	1.0732	1.1396	0.8862
1984	48138	50337	3.4158	1.1123	1.1775	0.9999
1985	46856	47626	2.7252	1.0827	1.1141	0.7978
1986	45700	46425	2.3478	1.0560	1.0860	0.6873
1987	45743	46538	2.5708	1.0570	1.0887	0.7525
1988	47259	48430	2.5022	1.0920	1.1329	0.7325
1989	47186	46406	3.9949	1.0903	1.0856	1.1694
1990	47709	44985	3.8499	1.1024	1.0523	1.1270
1991	47290	45351	4.1048	1.0927	1.0609	1.2016
1992	47402	45255	3.0820	1.0953	1.0587	0.9022
1993	47427	45829	3.2508	1.0959	1.0721	0.9516
1994	47242	46907	4.4646	1.0916	1.0973	1.3069
1995	44102	45738	2.8698	1.0191	1.0700	0.8401
1996	43797	43412	3.4946	1.0120	1.0155	1.0230
1997	44446	43700	3.4682	1.0270	1.0223	1.0152
1998	44101	42371	3.7703	1.0191	0.9912	1.1037
1999	44101	42371	3.3590	1.0191	0.9912	0.9833
2000	49357.839	49792.064	2.9687	1.1405	1.1648	0.8690
2001	47891.839	48239.064	3.1781	1.1066	1.1285	0.9303
2002	46172.839	46723.064	3.9223	1.0669	1.0930	1.1482
2003	45514.839	47789.064	3.0737	1.0517	1.1179	0.8998
2004	47206.839	49409.064	3.4621	1.0908	1.1558	1.0135
2005	45924.839	46698.064	2.7716	1.0612	1.0924	0.8113
2006	44768.839	45497.064	2.3941	1.0345	1.0643	0.7008
2007	44811.839	45610.064	2.6171	1.0355	1.0670	0.7661
2008	46327.839	47502.064	2.5486	1.0705	1.1112	0.7460
2009	46254.839	45478.064	4.0413	1.0688	1.0639	1.1830
2010	46777.839	44057.064	3.8963	1.0809	1.0306	1.1406
2011	46358.839	44423.064	4.1511	1.0712	1.0392	1.2152
2012	46470.839	44327.064	3.1284	1.0738	1.0370	0.9158
2013	46495.839	44901.064	3.2972	1.0744	1.0504	0.9652
2014	46310.839	45979.064	4.5110	1.0701	1.0756	1.3205
2015	43170.839	44810.064	2.9162	0.9976	1.0483	0.8537
2016	42865.839	42484.064	3.5410	0.9905	0.9938	1.0366
2017	43514.839	42772.064	3.5145	1.0055	1.0006	1.0288
2018	43169.839	41443.064	3.8167	0.9975	0.9695	1.1173
2019	43169.839	41443.064	3.4054	0.9975	0.9695	0.9969
2020	48426.678	48864.128	3.0151	1.1190	1.1431	0.8826
2021	46960.678	47311.128	3.2244	1.0851	1.1068	0.9439
2022	45241.678	45795.128	3.9687	1.0454	1.0713	1.1618
2023	44583.678	46861.128	3.1200	1.0302	1.0962	0.9133
2024	46275.678	48481.128	3.5085	1.0693	1.1341	1.0271
2025	44993.678	45770.128	2.8179	1.0397	1.0707	0.8249
2026	43837.678	44569.128	2.4405	1.0130	1.0426	0.7144
2027	43880.678	44682.128	2.6635	1.0140	1.0453	0.7797

2028	45396.678	46574.128	2.5949	1.0490	1.0895	0.7596
2029	45323.678	44550.128	4.0876	1.0473	1.0422	1.1966
2030	45846.678	43129.128	3.9426	1.0594	1.0089	1.1541
2031	45427.678	43495.128	4.1975	1.0497	1.0175	1.2287
2032	45539.678	43399.128	3.1748	1.0523	1.0152	0.9294
2033	45564.678	43973.128	3.3435	1.0529	1.0287	0.9788
2034	45379.678	45051.128	4.5573	1.0486	1.0539	1.3341
2035	42239.678	43882.128	2.9626	0.9760	1.0265	0.8672
2036	41934.678	41556.128	3.5873	0.9690	0.9721	1.0501
2037	42583.678	41844.128	3.5609	0.9840	0.9789	1.0424
2038	42238.678	40515.128	3.8631	0.9760	0.9478	1.1308
2039	42238.678	40515.128	3.4517	0.9760	0.9478	1.0104
2040	47495.517	47936.192	3.0614	1.0975	1.1214	0.8962
2041	46029.517	46383.192	3.2708	1.0636	1.0851	0.9575
2042	44310.517	44867.192	4.0151	1.0239	1.0496	1.1753
2043	43652.517	45933.192	3.1664	1.0087	1.0745	0.9269
2044	45344.517	47553.192	3.5549	1.0478	1.1124	1.0406
2045	44062.517	44842.192	2.8643	1.0182	1.0490	0.8385
2046	42906.517	43641.192	2.4869	0.9915	1.0209	0.7280
2047	42949.517	43754.192	2.7099	0.9924	1.0236	0.7933
2048	44465.517	45646.192	2.6413	1.0275	1.0678	0.7732
2049	44392.517	43622.192	4.1340	1.0258	1.0205	1.2102
2050	44915.517	42201.192	3.9890	1.0379	0.9872	1.1677
2051	44496.517	42567.192	4.2439	1.0282	0.9958	1.2423
2052	44608.517	42471.192	3.2211	1.0308	0.9935	0.9429
2053	44633.517	43045.192	3.3899	1.0314	1.0070	0.9923
2054	44448.517	44123.192	4.6037	1.0271	1.0322	1.3476
2055	41308.517	42954.192	3.0089	0.9545	1.0048	0.8808
2056	41003.517	40628.192	3.6337	0.9475	0.9504	1.0637
2057	41652.517	40916.192	3.6072	0.9625	0.9572	1.0560
2058	41307.517	39587.192	3.9094	0.9545	0.9261	1.1444
2059	41307.517	39587.192	3.4981	0.9545	0.9261	1.0240
2060	46564.356	47008.256	3.1078	1.0760	1.0997	0.9097
2061	45098.356	45455.256	3.3172	1.0421	1.0633	0.9710
2062	43379.356	43939.256	4.0614	1.0024	1.0279	1.1889
2063	42721.356	45005.256	3.2127	0.9872	1.0528	0.9405
2064	44413.356	46625.256	3.6012	1.0263	1.0907	1.0542
2065	43131.356	43914.256	2.9106	0.9966	1.0273	0.8520
2066	41975.356	42713.256	2.5332	0.9699	0.9992	0.7416
2067	42018.356	42826.256	2.7562	0.9709	1.0018	0.8068
2068	43534.356	44718.256	2.6876	1.0060	1.0461	0.7868
2069	43461.356	42694.256	4.1804	1.0043	0.9988	1.2237
2070	43984.356	41273.256	4.0353	1.0164	0.9655	1.1813
2071	43565.356	41639.256	4.2902	1.0067	0.9741	1.2559
2072	43677.356	41543.256	3.2675	1.0093	0.9718	0.9565
2073	43702.356	42117.256	3.4362	1.0098	0.9853	1.0059
2074	43517.356	43195.256	4.6501	1.0056	1.0105	1.3612
2075	40377.356	42026.256	3.0553	0.9330	0.9831	0.8944

2076	40072.356	39700.256	3.6801	0.9260	0.9287	1.0773
2077	40721.356	39988.256	3.6536	0.9410	0.9355	1.0695
2078	40376.356	38659.256	3.9558	0.9330	0.9044	1.1580
2079	40376.356	38659.256	3.5445	0.9330	0.9044	1.0376
2080	45633.195	46080.32	3.1541	1.0545	1.0780	0.9233
2081	44167.195	44527.32	3.3635	1.0206	1.0416	0.9846
2082	42448.195	43011.32	4.1078	0.9809	1.0062	1.2025
2083	41790.195	44077.32	3.2591	0.9657	1.0311	0.9540
2084	43482.195	45697.32	3.6476	1.0048	1.0690	1.0678
2085	42200.195	42986.32	2.9570	0.9751	1.0056	0.8656
2086	41044.195	41785.32	2.5796	0.9484	0.9775	0.7551
2087	41087.195	41898.32	2.8026	0.9494	0.9801	0.8204
2088	42603.195	43790.32	2.7340	0.9844	1.0244	0.8003
2089	42530.195	41766.32	4.2267	0.9828	0.9771	1.2373
2090	43053.195	40345.32	4.0817	0.9948	0.9438	1.1948
2091	42634.195	40711.32	4.3366	0.9852	0.9524	1.2695
2092	42746.195	40615.32	3.3138	0.9877	0.9501	0.9701
2093	42771.195	41189.32	3.4826	0.9883	0.9636	1.0195
2094	42586.195	42267.32	4.6964	0.9840	0.9888	1.3748
2095	39446.195	41098.32	3.1016	0.9115	0.9614	0.9079
2096	39141.195	38772.32	3.7264	0.9044	0.9070	1.0908
2097	39790.195	39060.32	3.7000	0.9194	0.9137	1.0831
2098	39445.195	37731.32	4.0021	0.9115	0.8827	1.1716
2099	39445.195	37731.32	3.5908	0.9115	0.8827	1.0511

Data for ARIMlow

(NOSO = (NO_x+SO_x)/2 (ppm), OZONE = Ozone (ppm), PRE = Precipitation (m), DPRE = Previous year precipitation (m), TEM = Annual mean temperature (°C), WTem = Annual mean winter temperature (°C), RBIVs = Relative Basis Index Values)

Year	Real Values with 10% increase of AP						RBIVs					
	NOSO	OZONE	PRE	DPRE	TEM	WTem	NOSO	OZONE	PRE	DPRE	TEM	WTem
1940	27326	24535	2.9617	3.3727	19.8542	3.4878	0.5843	0.5307	0.8670	0.9818	0.8950	0.5951
1941	31119	25497	2.4999	2.9617	21.4650	5.2656	0.6654	0.5516	0.7318	0.8622	0.9677	0.8984
1942	32930	24747	3.6286	2.4999	20.8422	3.0737	0.7041	0.5353	1.0622	0.7278	0.9396	0.5244
1943	35818	25295	3.0952	3.6286	21.1893	4.6015	0.7659	0.5472	0.9061	1.0564	0.9552	0.7851
1944	36547	25994	3.1409	3.0952	21.1210	5.3354	0.7814	0.5623	0.9194	0.9011	0.9522	0.9103
1945	37555	26856	3.5064	3.1409	21.0443	3.9651	0.8030	0.5810	1.0264	0.9144	0.9487	0.6765
1946	33290	30542	3.5515	3.5064	21.8147	5.2660	0.7118	0.6607	1.0396	1.0208	0.9834	0.8985
1947	36768	29977	2.6578	3.5515	20.5791	3.3675	0.7862	0.6485	0.7780	1.0339	0.9277	0.5745
1948	34269	29334	3.6704	2.6578	21.1521	4.5439	0.7327	0.6346	1.0744	0.7737	0.9536	0.7753
1949	31048	29967	3.4116	3.6704	21.6614	7.6796	0.6639	0.6483	0.9987	1.0685	0.9765	1.3103
1950	32450	31029	3.5992	3.4116	20.6807	6.7819	0.6938	0.6712	1.0536	0.9932	0.9323	1.1571
1951	32012	30933	3.7346	3.5992	21.3327	5.3838	0.6845	0.6692	1.0932	1.0478	0.9617	0.9186
1952	31882	31264	2.6438	3.7346	21.6523	6.8792	0.6817	0.6763	0.7739	1.0872	0.9761	1.1737

1953	32024	32362	2.8658	2.6438	22.1755	5.6166	0.6847	0.7001	0.8389	0.7696	0.9997	0.9583
1954	31844	32895	3.0760	2.8658	21.8359	4.8910	0.6809	0.7116	0.9004	0.8343	0.9844	0.8345
1955	32446	33536	2.9451	3.0760	21.3591	4.4016	0.6938	0.7255	0.8621	0.8955	0.9629	0.7510
1956	32906	34769	3.3745	2.9451	21.2987	7.3557	0.7036	0.7521	0.9878	0.8574	0.9602	1.2550
1957	33520	35032	4.3535	3.3745	21.5424	7.2378	0.7167	0.7578	1.2744	0.9824	0.9711	1.2349
1958	35646	34858	2.7234	4.3535	19.9284	1.3868	0.7622	0.7541	0.7972	1.2674	0.8984	0.2366
1959	36140	36189	3.2215	2.7234	21.1770	4.7258	0.7727	0.7829	0.9430	0.7928	0.9547	0.8063
1960	36367	38599	3.2017	3.2215	19.8901	3.4660	0.7776	0.8350	0.9372	0.9378	0.8967	0.5914
1961	35951	38393	3.9202	3.2017	19.7103	4.4991	0.7687	0.8305	1.1476	0.9321	0.8886	0.7676
1962	37363	39444	4.0165	3.9202	20.8218	4.2759	0.7989	0.8533	1.1758	1.1412	0.9387	0.7295
1963	39233	42162	3.5853	4.0165	19.6687	0.0597	0.8389	0.9121	1.0495	1.1693	0.8867	0.0102
1964	41172	42819	3.2993	3.5853	20.0858	3.5200	0.8803	0.9263	0.9658	1.0437	0.9055	0.6006
1965	43329	44209	2.9902	3.2993	21.0779	4.3316	0.9265	0.9563	0.8753	0.9605	0.9502	0.7390
1966	46239	45217	3.3495	2.9902	19.7221	4.3309	0.9887	0.9781	0.9805	0.8705	0.8891	0.7389
1967	46128	45844	3.9503	3.3495	19.8619	5.2293	0.9863	0.9917	1.1564	0.9751	0.8954	0.8922
1968	48635	44940	2.5864	3.9503	19.8080	1.7495	1.0399	0.9722	0.7571	1.1500	0.8930	0.2985
1969	49808	45611	3.6012	2.5864	19.2879	3.9819	1.0650	0.9867	1.0542	0.7529	0.8695	0.6794
1970	52089	51910	3.2105	3.6012	20.4887	2.9800	1.1138	1.1229	0.9398	1.0484	0.9236	0.5084
1971	51245	51598	3.6627	3.2105	20.4555	5.7644	1.0957	1.1162	1.0722	0.9346	0.9221	0.9835
1972	53130	53037	4.1121	3.6627	19.5705	5.8750	1.1360	1.1473	1.2037	1.0663	0.8823	1.0024
1973	55283	53402	4.1287	4.1121	20.3967	4.1545	1.1821	1.1552	1.2086	1.1971	0.9195	0.7088
1974	52947	50957	4.1740	4.1287	20.9481	7.3541	1.1321	1.1023	1.2219	1.2019	0.9444	1.2547
1975	50643	48711	3.1979	4.1740	20.9337	5.8722	1.0828	1.0537	0.9361	1.2151	0.9437	1.0019
1976	52486	51042	2.9876	3.1979	20.0371	3.2952	1.1223	1.1042	0.8746	0.9310	0.9033	0.5622
1977	53431	52234	3.6274	2.9876	20.9561	1.6692	1.1425	1.1299	1.0619	0.8697	0.9447	0.2848
1978	51947	52725	3.0975	3.6274	20.2074	2.0283	1.1107	1.1406	0.9067	1.0560	0.9110	0.3461
1979	51657	51877	3.9387	3.0975	19.8455	2.9920	1.1045	1.1222	1.1530	0.9017	0.8947	0.5105
1980	50289	50720	2.9223	3.9387	20.5613	4.1884	1.0753	1.0972	0.8555	1.1466	0.9269	0.7146
1981	48823	49167	3.1317	2.9223	20.2879	2.9783	1.0439	1.0636	0.9168	0.8507	0.9146	0.5082
1982	47104	47651	3.8760	3.1317	20.5942	4.7120	1.0072	1.0308	1.1346	0.9117	0.9284	0.8039
1983	46446	48717	3.0273	3.8760	20.4067	3.3534	0.9931	1.0539	0.8862	1.1284	0.9199	0.5721
1984	48138	50337	3.4158	3.0273	20.9172	4.3666	1.0293	1.0889	0.9999	0.8813	0.9430	0.7450
1985	46856	47626	2.7252	3.4158	20.4608	0.3851	1.0019	1.0303	0.7978	0.9944	0.9224	0.0657
1986	45700	46425	2.3478	2.7252	21.8201	2.8392	0.9772	1.0043	0.6873	0.7933	0.9837	0.4844
1987	45743	46538	2.5708	2.3478	21.5013	4.7120	0.9781	1.0067	0.7525	0.6835	0.9693	0.8039
1988	47259	48430	2.5022	2.5708	21.1997	1.9689	1.0105	1.0477	0.7325	0.7484	0.9557	0.3359
1989	47186	46406	3.9949	2.5022	20.3321	3.3941	1.0089	1.0039	1.1694	0.7284	0.9166	0.5791
1990	47709	44985	3.8499	3.9949	22.1700	7.2828	1.0201	0.9731	1.1270	1.1630	0.9994	1.2426
1991	47290	45351	4.1048	3.8499	21.3918	5.9404	1.0112	0.9810	1.2016	1.1208	0.9644	1.0135
1992	47402	45255	3.0820	4.1048	19.9281	5.7764	1.0135	0.9790	0.9022	1.1950	0.8984	0.9855
1993	47427	45829	3.2508	3.0820	20.7166	5.2951	1.0141	0.9914	0.9516	0.8972	0.9339	0.9034
1994	47242	46907	4.4646	3.2508	20.8423	4.2228	1.0101	1.0147	1.3069	0.9464	0.9396	0.7205
1995	44102	45738	2.8698	4.4646	20.7945	4.1822	0.9430	0.9894	0.8401	1.2997	0.9374	0.7136
1996	43797	43412	3.4946	2.8698	19.6012	3.8701	0.9365	0.9391	1.0230	0.8355	0.8836	0.6603
1997	44446	43700	3.4682	3.4946	19.9288	5.5949	0.9503	0.9453	1.0152	1.0173	0.8984	0.9546
1998	44101	42371	3.7703	3.4682	21.5090	7.4405	0.9430	0.9166	1.1037	1.0096	0.9696	1.2695
1999	44101	42371	3.3590	3.7703	22.6538	6.0139	0.9430	0.9166	0.9833	1.0976	1.0213	1.0261
2000	51220	51648	2.9687	3.9855	21.2813	4.9484	1.0952	1.1173	0.8690	1.1602	0.9594	0.8443
2001	49754	50095	3.1781	2.9691	21.0079	3.7383	1.0638	1.0837	0.9303	0.8644	0.9471	0.6378

2002	48035	48579	3.9223	3.1785	21.3142	5.4720	1.0271	1.0509	1.1482	0.9253	0.9609	0.9336
2003	47377	49645	3.0737	3.9227	21.1267	4.1134	1.0130	1.0739	0.8998	1.1420	0.9524	0.7018
2004	49069	51265	3.4621	3.0741	21.6372	5.1266	1.0492	1.1090	1.0135	0.8949	0.9754	0.8747
2005	47787	48554	2.7716	3.4626	21.1808	1.1451	1.0218	1.0503	0.8113	1.0080	0.9548	0.1954
2006	46631	47353	2.3941	2.7720	22.5401	3.5992	0.9971	1.0244	0.7008	0.8070	1.0161	0.6141
2007	46674	47466	2.6171	2.3945	22.2213	5.4720	0.9980	1.0268	0.7661	0.6971	1.0018	0.9336
2008	48190	49358	2.5486	2.6175	21.9197	2.7289	1.0304	1.0677	0.7460	0.7620	0.9882	0.4656
2009	48117	47334	4.0413	2.5490	21.0521	4.1541	1.0288	1.0239	1.1830	0.7420	0.9490	0.7088
2010	48640	45913	3.8963	4.0417	22.8900	8.0428	1.0400	0.9932	1.1406	1.1766	1.0319	1.3722
2011	48221	46279	4.1511	3.8967	22.1118	6.7004	1.0311	1.0011	1.2152	1.1344	0.9968	1.1432
2012	48333	46183	3.1284	4.1515	20.6481	6.5364	1.0335	0.9990	0.9158	1.2086	0.9308	1.1152
2013	48358	46757	3.2972	3.1288	21.4366	6.0551	1.0340	1.0115	0.9652	0.9108	0.9664	1.0331
2014	48173	47835	4.5110	3.2976	21.5623	4.9828	1.0300	1.0348	1.3205	0.9600	0.9720	0.8501
2015	45033	46666	2.9162	4.5114	21.5145	4.9422	0.9629	1.0095	0.8537	1.3133	0.9699	0.8432
2016	44728	44340	3.5410	2.9166	20.3212	4.6301	0.9564	0.9592	1.0366	0.8491	0.9161	0.7900
2017	45377	44628	3.5145	3.5414	20.6488	6.3549	0.9703	0.9654	1.0288	1.0310	0.9309	1.0843
2018	45032	43299	3.8167	3.5149	22.2290	8.2005	0.9629	0.9367	1.1173	1.0232	1.0021	1.3991
2019	45032	43299	3.4054	3.8171	23.3738	6.7739	0.9629	0.9367	0.9969	1.1112	1.0537	1.1557
2020	52151	52576	3.0151	4.0322	22.0013	5.7084	1.1151	1.1373	0.8826	1.1738	0.9918	0.9739
2021	50685	51023	3.2244	3.0159	21.7279	4.4983	1.0838	1.1037	0.9439	0.8780	0.9795	0.7675
2022	48966	49507	3.9687	3.2253	22.0342	6.2320	1.0470	1.0709	1.1618	0.9389	0.9933	1.0633
2023	48308	50573	3.1200	3.9695	21.8467	4.8734	1.0329	1.0940	0.9133	1.1556	0.9849	0.8315
2024	50000	52193	3.5085	3.1208	22.3572	5.8866	1.0691	1.1291	1.0271	0.9085	1.0079	1.0043
2025	48718	49482	2.8179	3.5093	21.9008	1.9051	1.0417	1.0704	0.8249	1.0216	0.9873	0.3250
2026	47562	48281	2.4405	2.8187	23.2601	4.3592	1.0170	1.0444	0.7144	0.8206	1.0486	0.7438
2027	47605	48394	2.6635	2.4413	22.9413	6.2320	1.0179	1.0469	0.7797	0.7107	1.0342	1.0633
2028	49121	50286	2.5949	2.6643	22.6397	3.4889	1.0503	1.0878	0.7596	0.7756	1.0206	0.5953
2029	49048	48262	4.0876	2.5957	21.7721	4.9141	1.0488	1.0440	1.1966	0.7557	0.9815	0.8384
2030	49571	46841	3.9426	4.0885	23.6100	8.8028	1.0599	1.0133	1.1541	1.1902	1.0644	1.5019
2031	49152	47207	4.1975	3.9434	22.8318	7.4604	1.0510	1.0212	1.2287	1.1480	1.0293	1.2729
2032	49264	47111	3.1748	4.1983	21.3681	7.2964	1.0534	1.0191	0.9294	1.2222	0.9633	1.2449
2033	49289	47685	3.3435	3.1756	22.1566	6.8151	1.0539	1.0315	0.9788	0.9245	0.9988	1.1628
2034	49104	48763	4.5573	3.3443	22.2823	5.7428	1.0499	1.0549	1.3341	0.9736	1.0045	0.9798
2035	45964	47594	2.9626	4.5582	22.2345	5.7022	0.9828	1.0296	0.8672	1.3270	1.0023	0.9729
2036	45659	45268	3.5873	2.9634	21.0412	5.3901	0.9763	0.9792	1.0501	0.8627	0.9486	0.9196
2037	46308	45556	3.5609	3.5882	21.3688	7.1149	0.9902	0.9855	1.0424	1.0446	0.9633	1.2139
2038	45963	44227	3.8631	3.5617	22.9490	8.9605	0.9828	0.9567	1.1308	1.0369	1.0346	1.5288
2039	45963	44227	3.4517	3.8639	24.0938	7.5339	0.9828	0.9567	1.0104	1.1248	1.0862	1.2854
2040	53082	53504	3.0614	4.0790	22.7213	6.4684	1.1350	1.1574	0.8962	1.1875	1.0243	1.1036
2041	51616	51951	3.2708	3.0626	22.4479	5.2583	1.1037	1.1238	0.9575	0.8916	1.0120	0.8972
2042	49897	50435	4.0151	3.2720	22.7542	6.9920	1.0669	1.0910	1.1753	0.9525	1.0258	1.1929
2043	49239	51501	3.1664	4.0163	22.5667	5.6334	1.0528	1.1141	0.9269	1.1692	1.0173	0.9611
2044	50931	53121	3.5549	3.1676	23.0772	6.6466	1.0890	1.1491	1.0406	0.9221	1.0403	1.1340
2045	49649	50410	2.8643	3.5561	22.6208	2.6651	1.0616	1.0905	0.8385	1.0352	1.0198	0.4547
2046	48493	49209	2.4869	2.8655	23.9801	5.1192	1.0369	1.0645	0.7280	0.8342	1.0810	0.8734
2047	48536	49322	2.7099	2.4881	23.6613	6.9920	1.0378	1.0669	0.7933	0.7243	1.0667	1.1929
2048	50052	51214	2.6413	2.7111	23.3597	4.2489	1.0702	1.1079	0.7732	0.7892	1.0531	0.7249
2049	49979	49190	4.1340	2.6425	22.4921	5.6741	1.0687	1.0641	1.2102	0.7693	1.0140	0.9681
2050	50502	47769	3.9890	4.1352	24.3300	9.5628	1.0798	1.0334	1.1677	1.2038	1.0968	1.6316

2051	50083	48135	4.2439	3.9902	23.5518	8.2204	1.0709	1.0413	1.2423	1.1616	1.0617	1.4025
2052	50195	48039	3.2211	4.2451	22.0881	8.0564	1.0733	1.0392	0.9429	1.2358	0.9957	1.3745
2053	50220	48613	3.3899	3.2223	22.8766	7.5751	1.0738	1.0516	0.9923	0.9381	1.0313	1.2924
2054	50035	49691	4.6037	3.3911	23.0023	6.5028	1.0699	1.0749	1.3476	0.9872	1.0370	1.1095
2055	46895	48522	3.0089	4.6049	22.9545	6.4622	1.0027	1.0496	0.8808	1.3406	1.0348	1.1026
2056	46590	46196	3.6337	3.0101	21.7612	6.1501	0.9962	0.9993	1.0637	0.8763	0.9810	1.0493
2057	47239	46484	3.6072	3.6349	22.0888	7.8749	1.0101	1.0056	1.0560	1.0582	0.9958	1.3436
2058	46894	45155	3.9094	3.6084	23.6690	9.7205	1.0027	0.9768	1.1444	1.0505	1.0670	1.6585
2059	46894	45155	3.4981	3.9106	24.8138	8.2939	1.0027	0.9768	1.0240	1.1384	1.1186	1.4151
2060	54014	54432	3.1078	4.1258	23.4413	7.2284	1.1549	1.1775	0.9097	1.2011	1.0568	1.2333
2061	52548	52879	3.3172	3.1094	23.1679	6.0183	1.1236	1.1439	0.9710	0.9052	1.0444	1.0268
2062	50829	51363	4.0614	3.3188	23.4742	7.7520	1.0868	1.1111	1.1889	0.9662	1.0582	1.3226
2063	50171	52429	3.2127	4.0630	23.2867	6.3934	1.0727	1.1342	0.9405	1.1828	1.0498	1.0908
2064	51863	54049	3.6012	3.2144	23.7972	7.4066	1.1089	1.1692	1.0542	0.9357	1.0728	1.2637
2065	50581	51338	2.9106	3.6028	23.3408	3.4251	1.0815	1.1106	0.8520	1.0488	1.0522	0.5844
2066	49425	50137	2.5332	2.9123	24.7001	5.8792	1.0568	1.0846	0.7416	0.8478	1.1135	1.0031
2067	49468	50250	2.7562	2.5348	24.3813	7.7520	1.0577	1.0870	0.8068	0.7379	1.0991	1.3226
2068	50984	52142	2.6876	2.7578	24.0797	5.0089	1.0901	1.1279	0.7868	0.8028	1.0855	0.8546
2069	50911	50118	4.1804	2.6893	23.2121	6.4341	1.0886	1.0842	1.2237	0.7829	1.0464	1.0978
2070	51434	48697	4.0353	4.1820	25.0500	10.3228	1.0998	1.0534	1.1813	1.2174	1.1293	1.7612
2071	51015	49063	4.2902	4.0370	24.2718	8.9804	1.0908	1.0613	1.2559	1.1752	1.0942	1.5322
2072	51127	48967	3.2675	4.2918	22.8081	8.8164	1.0932	1.0593	0.9565	1.2494	1.0282	1.5042
2073	51152	49541	3.4362	3.2691	23.5966	8.3351	1.0937	1.0717	1.0059	0.9517	1.0638	1.4221
2074	50967	50619	4.6501	3.4379	23.7223	7.2628	1.0898	1.0950	1.3612	1.0008	1.0694	1.2391
2075	47827	49450	3.0553	4.6517	23.6745	7.2222	1.0226	1.0697	0.8944	1.3542	1.0673	1.2322
2076	47522	47124	3.6801	3.0569	22.4812	6.9101	1.0161	1.0194	1.0773	0.8899	1.0135	1.1790
2077	48171	47412	3.6536	3.6817	22.8088	8.6349	1.0300	1.0256	1.0695	1.0718	1.0282	1.4733
2078	47826	46083	3.9558	3.6552	24.3890	10.4805	1.0226	0.9969	1.1580	1.0641	1.0995	1.7881
2079	47826	46083	3.5445	3.9574	25.5338	9.0539	1.0226	0.9969	1.0376	1.1521	1.1511	1.5447
2080	54945	55360	3.1541	4.1725	24.1613	7.9884	1.1748	1.1976	0.9233	1.2147	1.0892	1.3630
2081	53479	53807	3.3635	3.1562	23.8879	6.7783	1.1435	1.1640	0.9846	0.9188	1.0769	1.1565
2082	51760	52291	4.1078	3.3656	24.1942	8.5120	1.1067	1.1312	1.2025	0.9798	1.0907	1.4523
2083	51102	53357	3.2591	4.1098	24.0067	7.1534	1.0927	1.1542	0.9540	1.1964	1.0822	1.2205
2084	52794	54977	3.6476	3.2611	24.5172	8.1666	1.1288	1.1893	1.0678	0.9494	1.1053	1.3934
2085	51512	52266	2.9570	3.6496	24.0608	4.1851	1.1014	1.1306	0.8656	1.0625	1.0847	0.7140
2086	50356	51065	2.5796	2.9590	25.4201	6.6392	1.0767	1.1046	0.7551	0.8614	1.1460	1.1328
2087	50399	51178	2.8026	2.5816	25.1013	8.5120	1.0776	1.1071	0.8204	0.7515	1.1316	1.4523
2088	51915	53070	2.7340	2.8046	24.7997	5.7689	1.1100	1.1480	0.8003	0.8165	1.1180	0.9843
2089	51842	51046	4.2267	2.7360	23.9321	7.1941	1.1085	1.1042	1.2373	0.7965	1.0789	1.2274
2090	52365	49625	4.0817	4.2288	25.7700	11.0828	1.1197	1.0735	1.1948	1.2311	1.1617	1.8909
2091	51946	49991	4.3366	4.0837	24.9918	9.7404	1.1107	1.0814	1.2695	1.1888	1.1267	1.6619
2092	52058	49895	3.3138	4.3386	23.5281	9.5764	1.1131	1.0793	0.9701	1.2630	1.0607	1.6339
2093	52083	50469	3.4826	3.3159	24.3166	9.0951	1.1136	1.0918	1.0195	0.9653	1.0962	1.5518
2094	51898	51547	4.6964	3.4846	24.4423	8.0228	1.1097	1.1151	1.3748	1.0144	1.1019	1.3688
2095	48758	50378	3.1016	4.6985	24.3945	7.9822	1.0425	1.0898	0.9079	1.3678	1.0997	1.3619
2096	48453	48052	3.7264	3.1037	23.2012	7.6701	1.0360	1.0395	1.0908	0.9035	1.0459	1.3086
2097	49102	48340	3.7000	3.7285	23.5288	9.3949	1.0499	1.0457	1.0831	1.0854	1.0607	1.6029
2098	48757	47011	4.0021	3.7020	25.1090	11.2405	1.0425	1.0170	1.1716	1.0777	1.1319	1.9178
2099	48757	47011	3.5908	4.0042	26.2538	9.8139	1.0425	1.0170	1.0511	1.1657	1.1835	1.6744

Real Values with 0% increase of AP							RBIVs					
Year	NOSO	OZON E	PRE	DPRE	TEM	WTem	NOSO	OZON E	PRE	DPRE	TEM	WTem
1940	27326	24535	2.9617	3.3727	19.8542	3.4878	0.6069	0.5515	0.8670	0.9818	0.8950	0.5951
1941	31119	25497	2.4999	2.9617	21.4650	5.2656	0.6912	0.5731	0.7318	0.8622	0.9677	0.8984
1942	32930	24747	3.6286	2.4999	20.8422	3.0737	0.7314	0.5563	1.0622	0.7278	0.9396	0.5244
1943	35818	25295	3.0952	3.6286	21.1893	4.6015	0.7956	0.5686	0.9061	1.0564	0.9552	0.7851
1944	36547	25994	3.1409	3.0952	21.1210	5.3354	0.8118	0.5843	0.9194	0.9011	0.9522	0.9103
1945	37555	26856	3.5064	3.1409	21.0443	3.9651	0.8341	0.6037	1.0264	0.9144	0.9487	0.6765
1946	33290	30542	3.5515	3.5064	21.8147	5.2660	0.7394	0.6865	1.0396	1.0208	0.9834	0.8985
1947	36768	29977	2.6578	3.5515	20.5791	3.3675	0.8167	0.6738	0.7780	1.0339	0.9277	0.5745
1948	34269	29334	3.6704	2.6578	21.1521	4.5439	0.7612	0.6594	1.0744	0.7737	0.9536	0.7753
1949	31048	29967	3.4116	3.6704	21.6614	7.6796	0.6896	0.6736	0.9987	1.0685	0.9765	1.3103
1950	32450	31029	3.5992	3.4116	20.6807	6.7819	0.7208	0.6975	1.0536	0.9932	0.9323	1.1571
1951	32012	30933	3.7346	3.5992	21.3327	5.3838	0.7110	0.6953	1.0932	1.0478	0.9617	0.9186
1952	31882	31264	2.6438	3.7346	21.6523	6.8792	0.7081	0.7028	0.7739	1.0872	0.9761	1.1737
1953	32024	32362	2.8658	2.6438	22.1755	5.6166	0.7113	0.7274	0.8389	0.7696	0.9997	0.9583
1954	31844	32895	3.0760	2.8658	21.8359	4.8910	0.7073	0.7394	0.9004	0.8343	0.9844	0.8345
1955	32446	33536	2.9451	3.0760	21.3591	4.4016	0.7207	0.7538	0.8621	0.8955	0.9629	0.7510
1956	32906	34769	3.3745	2.9451	21.2987	7.3557	0.7309	0.7815	0.9878	0.8574	0.9602	1.2550
1957	33520	35032	4.3535	3.3745	21.5424	7.2378	0.7445	0.7875	1.2744	0.9824	0.9711	1.2349
1958	35646	34858	2.7234	4.3535	19.9284	1.3868	0.7917	0.7836	0.7972	1.2674	0.8984	0.2366
1959	36140	36189	3.2215	2.7234	21.1770	4.7258	0.8027	0.8135	0.9430	0.7928	0.9547	0.8063
1960	36367	38599	3.2017	3.2215	19.8901	3.4660	0.8078	0.8676	0.9372	0.9378	0.8967	0.5914
1961	35951	38393	3.9202	3.2017	19.7103	4.4991	0.7985	0.8630	1.1476	0.9321	0.8886	0.7676
1962	37363	39444	4.0165	3.9202	20.8218	4.2759	0.8299	0.8866	1.1758	1.1412	0.9387	0.7295
1963	39233	42162	3.5853	4.0165	19.6687	0.0597	0.8714	0.9477	1.0495	1.1693	0.8867	0.0102
1964	41172	42819	3.2993	3.5853	20.0858	3.5200	0.9145	0.9625	0.9658	1.0437	0.9055	0.6006
1965	43329	44209	2.9902	3.2993	21.0779	4.3316	0.9624	0.9937	0.8753	0.9605	0.9502	0.7390
1966	46239	45217	3.3495	2.9902	19.7221	4.3309	1.0270	1.0164	0.9805	0.8705	0.8891	0.7389
1967	46128	45844	3.9503	3.3495	19.8619	5.2293	1.0246	1.0305	1.1564	0.9751	0.8954	0.8922
1968	48635	44940	2.5864	3.9503	19.8080	1.7495	1.0802	1.0102	0.7571	1.1500	0.8930	0.2985
1969	49808	45611	3.6012	2.5864	19.2879	3.9819	1.1063	1.0253	1.0542	0.7529	0.8695	0.6794
1970	52089	51910	3.2105	3.6012	20.4887	2.9800	1.1570	1.1669	0.9398	1.0484	0.9236	0.5084
1971	51245	51598	3.6627	3.2105	20.4555	5.7644	1.1382	1.1598	1.0722	0.9346	0.9221	0.9835
1972	53130	53037	4.1121	3.6627	19.5705	5.8750	1.1801	1.1922	1.2037	1.0663	0.8823	1.0024
1973	55283	53402	4.1287	4.1121	20.3967	4.1545	1.2279	1.2004	1.2086	1.1971	0.9195	0.7088
1974	52947	50957	4.1740	4.1287	20.9481	7.3541	1.1760	1.1454	1.2219	1.2019	0.9444	1.2547
1975	50643	48711	3.1979	4.1740	20.9337	5.8722	1.1248	1.0949	0.9361	1.2151	0.9437	1.0019
1976	52486	51042	2.9876	3.1979	20.0371	3.2952	1.1658	1.1473	0.8746	0.9310	0.9033	0.5622
1977	53431	52234	3.6274	2.9876	20.9561	1.6692	1.1868	1.1741	1.0619	0.8697	0.9447	0.2848
1978	51947	52725	3.0975	3.6274	20.2074	2.0283	1.1538	1.1852	0.9067	1.0560	0.9110	0.3461
1979	51657	51877	3.9387	3.0975	19.8455	2.9920	1.1474	1.1661	1.1530	0.9017	0.8947	0.5105
1980	50289	50720	2.9223	3.9387	20.5613	4.1884	1.1170	1.1401	0.8555	1.1466	0.9269	0.7146
1981	48823	49167	3.1317	2.9223	20.2879	2.9783	1.0844	1.1052	0.9168	0.8507	0.9146	0.5082
1982	47104	47651	3.8760	3.1317	20.5942	4.7120	1.0462	1.0711	1.1346	0.9117	0.9284	0.8039
1983	46446	48717	3.0273	3.8760	20.4067	3.3534	1.0316	1.0951	0.8862	1.1284	0.9199	0.5721
1984	48138	50337	3.4158	3.0273	20.9172	4.3666	1.0692	1.1315	0.9999	0.8813	0.9430	0.7450
1985	46856	47626	2.7252	3.4158	20.4608	0.3851	1.0407	1.0706	0.7978	0.9944	0.9224	0.0657

1986	45700	46425	2.3478	2.7252	21.8201	2.8392	1.0150	1.0436	0.6873	0.7933	0.9837	0.4844
1987	45743	46538	2.5708	2.3478	21.5013	4.7120	1.0160	1.0461	0.7525	0.6835	0.9693	0.8039
1988	47259	48430	2.5022	2.5708	21.1997	1.9689	1.0497	1.0886	0.7325	0.7484	0.9557	0.3359
1989	47186	46406	3.9949	2.5022	20.3321	3.3941	1.0481	1.0431	1.1694	0.7284	0.9166	0.5791
1990	47709	44985	3.8499	3.9949	22.1700	7.2828	1.0597	1.0112	1.1270	1.1630	0.9994	1.2426
1991	47290	45351	4.1048	3.8499	21.3918	5.9404	1.0504	1.0194	1.2016	1.1208	0.9644	1.0135
1992	47402	45255	3.0820	4.1048	19.9281	5.7764	1.0529	1.0173	0.9022	1.1950	0.8984	0.9855
1993	47427	45829	3.2508	3.0820	20.7166	5.2951	1.0534	1.0302	0.9516	0.8972	0.9339	0.9034
1994	47242	46907	4.4646	3.2508	20.8423	4.2228	1.0493	1.0544	1.3069	0.9464	0.9396	0.7205
1995	44102	45738	2.8698	4.4646	20.7945	4.1822	0.9796	1.0281	0.8401	1.2997	0.9374	0.7136
1996	43797	43412	3.4946	2.8698	19.6012	3.8701	0.9728	0.9758	1.0230	0.8355	0.8836	0.6603
1997	44446	43700	3.4682	3.4946	19.9288	5.5949	0.9872	0.9823	1.0152	1.0173	0.8984	0.9546
1998	44101	42371	3.7703	3.4682	21.5090	7.4405	0.9795	0.9524	1.1037	1.0096	0.9696	1.2695
1999	44101	42371	3.3590	3.7703	22.6538	6.0139	0.9795	0.9524	0.9833	1.0976	1.0213	1.0261
2000	50289	50720	2.9687	3.9855	21.2813	4.9484	1.1170	1.1401	0.8690	1.1602	0.9594	0.8443
2001	48823	49167	3.1781	2.9691	21.0079	3.7383	1.0844	1.1052	0.9303	0.8644	0.9471	0.6378
2002	47104	47651	3.9223	3.1785	21.3142	5.4720	1.0462	1.0711	1.1482	0.9253	0.9609	0.9336
2003	46446	48717	3.0737	3.9227	21.1267	4.1134	1.0316	1.0951	0.8998	1.1420	0.9524	0.7018
2004	48138	50337	3.4621	3.0741	21.6372	5.1266	1.0692	1.1315	1.0135	0.8949	0.9754	0.8747
2005	46856	47626	2.7716	3.4626	21.1808	1.1451	1.0407	1.0706	0.8113	1.0080	0.9548	0.1954
2006	45700	46425	2.3941	2.7720	22.5401	3.5992	1.0150	1.0436	0.7008	0.8070	1.0161	0.6141
2007	45743	46538	2.6171	2.3945	22.2213	5.4720	1.0160	1.0461	0.7661	0.6971	1.0018	0.9336
2008	47259	48430	2.5486	2.6175	21.9197	2.7289	1.0497	1.0886	0.7460	0.7620	0.9882	0.4656
2009	47186	46406	4.0413	2.5490	21.0521	4.1541	1.0481	1.0431	1.1830	0.7420	0.9490	0.7088
2010	47709	44985	3.8963	4.0417	22.8900	8.0428	1.0597	1.0112	1.1406	1.1766	1.0319	1.3722
2011	47290	45351	4.1511	3.8967	22.1118	6.7004	1.0504	1.0194	1.2152	1.1344	0.9968	1.1432
2012	47402	45255	3.1284	4.1515	20.6481	6.5364	1.0529	1.0173	0.9158	1.2086	0.9308	1.1152
2013	47427	45829	3.2972	3.1288	21.4366	6.0551	1.0534	1.0302	0.9652	0.9108	0.9664	1.0331
2014	47242	46907	4.5110	3.2976	21.5623	4.9828	1.0493	1.0544	1.3205	0.9600	0.9720	0.8501
2015	44102	45738	2.9162	4.5114	21.5145	4.9422	0.9796	1.0281	0.8537	1.3133	0.9699	0.8432
2016	43797	43412	3.5410	2.9166	20.3212	4.6301	0.9728	0.9758	1.0366	0.8491	0.9161	0.7900
2017	44446	43700	3.5145	3.5414	20.6488	6.3549	0.9872	0.9823	1.0288	1.0310	0.9309	1.0843
2018	44101	42371	3.8167	3.5149	22.2290	8.2005	0.9795	0.9524	1.1173	1.0232	1.0021	1.3991
2019	44101	42371	3.4054	3.8171	23.3738	6.7739	0.9795	0.9524	0.9969	1.1112	1.0537	1.1557
2020	50289	50720	3.0151	4.0322	22.0013	5.7084	1.1170	1.1401	0.8826	1.1738	0.9918	0.9739
2021	48823	49167	3.2244	3.0159	21.7279	4.4983	1.0844	1.1052	0.9439	0.8780	0.9795	0.7675
2022	47104	47651	3.9687	3.2253	22.0342	6.2320	1.0462	1.0711	1.1618	0.9389	0.9933	1.0633
2023	46446	48717	3.1200	3.9695	21.8467	4.8734	1.0316	1.0951	0.9133	1.1556	0.9849	0.8315
2024	48138	50337	3.5085	3.1208	22.3572	5.8866	1.0692	1.1315	1.0271	0.9085	1.0079	1.0043
2025	46856	47626	2.8179	3.5093	21.9008	1.9051	1.0407	1.0706	0.8249	1.0216	0.9873	0.3250
2026	45700	46425	2.4405	2.8187	23.2601	4.3592	1.0150	1.0436	0.7144	0.8206	1.0486	0.7438
2027	45743	46538	2.6635	2.4413	22.9413	6.2320	1.0160	1.0461	0.7797	0.7107	1.0342	1.0633
2028	47259	48430	2.5949	2.6643	22.6397	3.4889	1.0497	1.0886	0.7596	0.7756	1.0206	0.5953
2029	47186	46406	4.0876	2.5957	21.7721	4.9141	1.0481	1.0431	1.1966	0.7557	0.9815	0.8384
2030	47709	44985	3.9426	4.0885	23.6100	8.8028	1.0597	1.0112	1.1541	1.1902	1.0644	1.5019
2031	47290	45351	4.1975	3.9434	22.8318	7.4604	1.0504	1.0194	1.2287	1.1480	1.0293	1.2729
2032	47402	45255	3.1748	4.1983	21.3681	7.2964	1.0529	1.0173	0.9294	1.2222	0.9633	1.2449
2033	47427	45829	3.3435	3.1756	22.1566	6.8151	1.0534	1.0302	0.9788	0.9245	0.9988	1.1628
2034	47242	46907	4.5573	3.3443	22.2823	5.7428	1.0493	1.0544	1.3341	0.9736	1.0045	0.9798

2035	44102	45738	2.9626	4.5582	22.2345	5.7022	0.9796	1.0281	0.8672	1.3270	1.0023	0.9729
2036	43797	43412	3.5873	2.9634	21.0412	5.3901	0.9728	0.9758	1.0501	0.8627	0.9486	0.9196
2037	44446	43700	3.5609	3.5882	21.3688	7.1149	0.9872	0.9823	1.0424	1.0446	0.9633	1.2139
2038	44101	42371	3.8631	3.5617	22.9490	8.9605	0.9795	0.9524	1.1308	1.0369	1.0346	1.5288
2039	44101	42371	3.4517	3.8639	24.0938	7.5339	0.9795	0.9524	1.0104	1.1248	1.0862	1.2854
2040	50289	50720	3.0614	4.0790	22.7213	6.4684	1.1170	1.1401	0.8962	1.1875	1.0243	1.1036
2041	48823	49167	3.2708	3.0626	22.4479	5.2583	1.0844	1.1052	0.9575	0.8916	1.0120	0.8972
2042	47104	47651	4.0151	3.2720	22.7542	6.9920	1.0462	1.0711	1.1753	0.9525	1.0258	1.1929
2043	46446	48717	3.1664	4.0163	22.5667	5.6334	1.0316	1.0951	0.9269	1.1692	1.0173	0.9611
2044	48138	50337	3.5549	3.1676	23.0772	6.6466	1.0692	1.1315	1.0406	0.9221	1.0403	1.1340
2045	46856	47626	2.8643	3.5561	22.6208	2.6651	1.0407	1.0706	0.8385	1.0352	1.0198	0.4547
2046	45700	46425	2.4869	2.8655	23.9801	5.1192	1.0150	1.0436	0.7280	0.8342	1.0810	0.8734
2047	45743	46538	2.7099	2.4881	23.6613	6.9920	1.0160	1.0461	0.7933	0.7243	1.0667	1.1929
2048	47259	48430	2.6413	2.7111	23.3597	4.2489	1.0497	1.0886	0.7732	0.7892	1.0531	0.7249
2049	47186	46406	4.1340	2.6425	22.4921	5.6741	1.0481	1.0431	1.2102	0.7693	1.0140	0.9681
2050	47709	44985	3.9890	4.1352	24.3300	9.5628	1.0597	1.0112	1.1677	1.2038	1.0968	1.6316
2051	47290	45351	4.2439	3.9902	23.5518	8.2204	1.0504	1.0194	1.2423	1.1616	1.0617	1.4025
2052	47402	45255	3.2211	4.2451	22.0881	8.0564	1.0529	1.0173	0.9429	1.2358	0.9957	1.3745
2053	47427	45829	3.3899	3.2223	22.8766	7.5751	1.0534	1.0302	0.9923	0.9381	1.0313	1.2924
2054	47242	46907	4.6037	3.3911	23.0023	6.5028	1.0493	1.0544	1.3476	0.9872	1.0370	1.1095
2055	44102	45738	3.0089	4.6049	22.9545	6.4622	0.9796	1.0281	0.8808	1.3406	1.0348	1.1026
2056	43797	43412	3.6337	3.0101	21.7612	6.1501	0.9728	0.9758	1.0637	0.8763	0.9810	1.0493
2057	44446	43700	3.6072	3.6349	22.0888	7.8749	0.9872	0.9823	1.0560	1.0582	0.9958	1.3436
2058	44101	42371	3.9094	3.6084	23.6690	9.7205	0.9795	0.9524	1.1444	1.0505	1.0670	1.6585
2059	44101	42371	3.4981	3.9106	24.8138	8.2939	0.9795	0.9524	1.0240	1.1384	1.1186	1.4151
2060	50289	50720	3.1078	4.1258	23.4413	7.2284	1.1170	1.1401	0.9097	1.2011	1.0568	1.2333
2061	48823	49167	3.3172	3.1094	23.1679	6.0183	1.0844	1.1052	0.9710	0.9052	1.0444	1.0268
2062	47104	47651	4.0614	3.3188	23.4742	7.7520	1.0462	1.0711	1.1889	0.9662	1.0582	1.3226
2063	46446	48717	3.2127	4.0630	23.2867	6.3934	1.0316	1.0951	0.9405	1.1828	1.0498	1.0908
2064	48138	50337	3.6012	3.2144	23.7972	7.4066	1.0692	1.1315	1.0542	0.9357	1.0728	1.2637
2065	46856	47626	2.9106	3.6028	23.3408	3.4251	1.0407	1.0706	0.8520	1.0488	1.0522	0.5844
2066	45700	46425	2.5332	2.9123	24.7001	5.8792	1.0150	1.0436	0.7416	0.8478	1.1135	1.0031
2067	45743	46538	2.7562	2.5348	24.3813	7.7520	1.0160	1.0461	0.8068	0.7379	1.0991	1.3226
2068	47259	48430	2.6876	2.7578	24.0797	5.0089	1.0497	1.0886	0.7868	0.8028	1.0855	0.8546
2069	47186	46406	4.1804	2.6893	23.2121	6.4341	1.0481	1.0431	1.2237	0.7829	1.0464	1.0978
2070	47709	44985	4.0353	4.1820	25.0500	10.3228	1.0597	1.0112	1.1813	1.2174	1.1293	1.7612
2071	47290	45351	4.2902	4.0370	24.2718	8.9804	1.0504	1.0194	1.2559	1.1752	1.0942	1.5322
2072	47402	45255	3.2675	4.2918	22.8081	8.8164	1.0529	1.0173	0.9565	1.2494	1.0282	1.5042
2073	47427	45829	3.4362	3.2691	23.5966	8.3351	1.0534	1.0302	1.0059	0.9517	1.0638	1.4221
2074	47242	46907	4.6501	3.4379	23.7223	7.2628	1.0493	1.0544	1.3612	1.0008	1.0694	1.2391
2075	44102	45738	3.0553	4.6517	23.6745	7.2222	0.9796	1.0281	0.8944	1.3542	1.0673	1.2322
2076	43797	43412	3.6801	3.0569	22.4812	6.9101	0.9728	0.9758	1.0773	0.8899	1.0135	1.1790
2077	44446	43700	3.6536	3.6817	22.8088	8.6349	0.9872	0.9823	1.0695	1.0718	1.0282	1.4733
2078	44101	42371	3.9558	3.6552	24.3890	10.4805	0.9795	0.9524	1.1580	1.0641	1.0995	1.7881
2079	44101	42371	3.5445	3.9574	25.5338	9.0539	0.9795	0.9524	1.0376	1.1521	1.1511	1.5447
2080	50289	50720	3.1541	4.1725	24.1613	7.9884	1.1170	1.1401	0.9233	1.2147	1.0892	1.3630
2081	48823	49167	3.3635	3.1562	23.8879	6.7783	1.0844	1.1052	0.9846	0.9188	1.0769	1.1565
2082	47104	47651	4.1078	3.3656	24.1942	8.5120	1.0462	1.0711	1.2025	0.9798	1.0907	1.4523
2083	46446	48717	3.2591	4.1098	24.0067	7.1534	1.0316	1.0951	0.9540	1.1964	1.0822	1.2205

2084	48138	50337	3.6476	3.2611	24.5172	8.1666	1.0692	1.1315	1.0678	0.9494	1.1053	1.3934
2085	46856	47626	2.9570	3.6496	24.0608	4.1851	1.0407	1.0706	0.8656	1.0625	1.0847	0.7140
2086	45700	46425	2.5796	2.9590	25.4201	6.6392	1.0150	1.0436	0.7551	0.8614	1.1460	1.1328
2087	45743	46538	2.8026	2.5816	25.1013	8.5120	1.0160	1.0461	0.8204	0.7515	1.1316	1.4523
2088	47259	48430	2.7340	2.8046	24.7997	5.7689	1.0497	1.0886	0.8003	0.8165	1.1180	0.9843
2089	47186	46406	4.2267	2.7360	23.9321	7.1941	1.0481	1.0431	1.2373	0.7965	1.0789	1.2274
2090	47709	44985	4.0817	4.2288	25.7700	11.0828	1.0597	1.0112	1.1948	1.2311	1.1617	1.8909
2091	47290	45351	4.3366	4.0837	24.9918	9.7404	1.0504	1.0194	1.2695	1.1888	1.1267	1.6619
2092	47402	45255	3.3138	4.3386	23.5281	9.5764	1.0529	1.0173	0.9701	1.2630	1.0607	1.6339
2093	47427	45829	3.4826	3.3159	24.3166	9.0951	1.0534	1.0302	1.0195	0.9653	1.0962	1.5518
2094	47242	46907	4.6964	3.4846	24.4423	8.0228	1.0493	1.0544	1.3748	1.0144	1.1019	1.3688
2095	44102	45738	3.1016	4.6985	24.3945	7.9822	0.9796	1.0281	0.9079	1.3678	1.0997	1.3619
2096	43797	43412	3.7264	3.1037	23.2012	7.6701	0.9728	0.9758	1.0908	0.9035	1.0459	1.3086
2097	44446	43700	3.7000	3.7285	23.5288	9.3949	0.9872	0.9823	1.0831	1.0854	1.0607	1.6029
2098	44101	42371	4.0021	3.7020	25.1090	11.2405	0.9795	0.9524	1.1716	1.0777	1.1319	1.9178
2099	44101	42371	3.5908	4.0042	26.2538	9.8139	0.9795	0.9524	1.0511	1.1657	1.1835	1.6744

Real Values with 10% decrease of AP							RBIVs					
Year	NOSO	OZON E	PRE	DPRE	TEM	Wtem	NOSO	OZON E	PRE	DPRE	TEM	Wtem
1940	27326	24535	2.9617	3.3727	19.8542	3.4878	0.6314	0.5740	0.8670	0.9818	0.8950	0.5951
1941	31119	25497	2.4999	2.9617	21.4650	5.2656	0.7191	0.5965	0.7318	0.8622	0.9677	0.8984
1942	32930	24747	3.6286	2.4999	20.8422	3.0737	0.7609	0.5789	1.0622	0.7278	0.9396	0.5244
1943	35818	25295	3.0952	3.6286	21.1893	4.6015	0.8277	0.5917	0.9061	1.0564	0.9552	0.7851
1944	36547	25994	3.1409	3.0952	21.1210	5.3354	0.8445	0.6081	0.9194	0.9011	0.9522	0.9103
1945	37555	26856	3.5064	3.1409	21.0443	3.9651	0.8678	0.6282	1.0264	0.9144	0.9487	0.6765
1946	33290	30542	3.5515	3.5064	21.8147	5.2660	0.7692	0.7145	1.0396	1.0208	0.9834	0.8985
1947	36768	29977	2.6578	3.5515	20.5791	3.3675	0.8496	0.7013	0.7780	1.0339	0.9277	0.5745
1948	34269	29334	3.6704	2.6578	21.1521	4.5439	0.7919	0.6862	1.0744	0.7737	0.9536	0.7753
1949	31048	29967	3.4116	3.6704	21.6614	7.6796	0.7174	0.7010	0.9987	1.0685	0.9765	1.3103
1950	32450	31029	3.5992	3.4116	20.6807	6.7819	0.7498	0.7259	1.0536	0.9932	0.9323	1.1571
1951	32012	30933	3.7346	3.5992	21.3327	5.3838	0.7397	0.7236	1.0932	1.0478	0.9617	0.9186
1952	31882	31264	2.6438	3.7346	21.6523	6.8792	0.7367	0.7314	0.7739	1.0872	0.9761	1.1737
1953	32024	32362	2.8658	2.6438	22.1755	5.6166	0.7400	0.7571	0.8389	0.7696	0.9997	0.9583
1954	31844	32895	3.0760	2.8658	21.8359	4.8910	0.7358	0.7695	0.9004	0.8343	0.9844	0.8345
1955	32446	33536	2.9451	3.0760	21.3591	4.4016	0.7497	0.7845	0.8621	0.8955	0.9629	0.7510
1956	32906	34769	3.3745	2.9451	21.2987	7.3557	0.7604	0.8134	0.9878	0.8574	0.9602	1.2550
1957	33520	35032	4.3535	3.3745	21.5424	7.2378	0.7746	0.8195	1.2744	0.9824	0.9711	1.2349
1958	35646	34858	2.7234	4.3535	19.9284	1.3868	0.8237	0.8154	0.7972	1.2674	0.8984	0.2366
1959	36140	36189	3.2215	2.7234	21.1770	4.7258	0.8351	0.8466	0.9430	0.7928	0.9547	0.8063
1960	36367	38599	3.2017	3.2215	19.8901	3.4660	0.8403	0.9030	0.9372	0.9378	0.8967	0.5914
1961	35951	38393	3.9202	3.2017	19.7103	4.4991	0.8307	0.8981	1.1476	0.9321	0.8886	0.7676
1962	37363	39444	4.0165	3.9202	20.8218	4.2759	0.8634	0.9227	1.1758	1.1412	0.9387	0.7295
1963	39233	42162	3.5853	4.0165	19.6687	0.0597	0.9066	0.9863	1.0495	1.1693	0.8867	0.0102
1964	41172	42819	3.2993	3.5853	20.0858	3.5200	0.9514	1.0017	0.9658	1.0437	0.9055	0.6006
1965	43329	44209	2.9902	3.2993	21.0779	4.3316	1.0012	1.0342	0.8753	0.9605	0.9502	0.7390
1966	46239	45217	3.3495	2.9902	19.7221	4.3309	1.0685	1.0578	0.9805	0.8705	0.8891	0.7389
1967	46128	45844	3.9503	3.3495	19.8619	5.2293	1.0659	1.0724	1.1564	0.9751	0.8954	0.8922

1968	48635	44940	2.5864	3.9503	19.8080	1.7495	1.1238	1.0513	0.7571	1.1500	0.8930	0.2985
1969	49808	45611	3.6012	2.5864	19.2879	3.9819	1.1509	1.0670	1.0542	0.7529	0.8695	0.6794
1970	52089	51910	3.2105	3.6012	20.4887	2.9800	1.2036	1.2143	0.9398	1.0484	0.9236	0.5084
1971	51245	51598	3.6627	3.2105	20.4555	5.7644	1.1841	1.2070	1.0722	0.9346	0.9221	0.9835
1972	53130	53037	4.1121	3.6627	19.5705	5.8750	1.2277	1.2407	1.2037	1.0663	0.8823	1.0024
1973	55283	53402	4.1287	4.1121	20.3967	4.1545	1.2774	1.2492	1.2086	1.1971	0.9195	0.7088
1974	52947	50957	4.1740	4.1287	20.9481	7.3541	1.2235	1.1921	1.2219	1.2019	0.9444	1.2547
1975	50643	48711	3.1979	4.1740	20.9337	5.8722	1.1702	1.1395	0.9361	1.2151	0.9437	1.0019
1976	52486	51042	2.9876	3.1979	20.0371	3.2952	1.2128	1.1940	0.8746	0.9310	0.9033	0.5622
1977	53431	52234	3.6274	2.9876	20.9561	1.6692	1.2346	1.2219	1.0619	0.8697	0.9447	0.2848
1978	51947	52725	3.0975	3.6274	20.2074	2.0283	1.2004	1.2334	0.9067	1.0560	0.9110	0.3461
1979	51657	51877	3.9387	3.0975	19.8455	2.9920	1.1937	1.2136	1.1530	0.9017	0.8947	0.5105
1980	50289	50720	2.9223	3.9387	20.5613	4.1884	1.1620	1.1865	0.8555	1.1466	0.9269	0.7146
1981	48823	49167	3.1317	2.9223	20.2879	2.9783	1.1282	1.1502	0.9168	0.8507	0.9146	0.5082
1982	47104	47651	3.8760	3.1317	20.5942	4.7120	1.0884	1.1147	1.1346	0.9117	0.9284	0.8039
1983	46446	48717	3.0273	3.8760	20.4067	3.3534	1.0732	1.1396	0.8862	1.1284	0.9199	0.5721
1984	48138	50337	3.4158	3.0273	20.9172	4.3666	1.1123	1.1775	0.9999	0.8813	0.9430	0.7450
1985	46856	47626	2.7252	3.4158	20.4608	0.3851	1.0827	1.1141	0.7978	0.9944	0.9224	0.0657
1986	45700	46425	2.3478	2.7252	21.8201	2.8392	1.0560	1.0860	0.6873	0.7933	0.9837	0.4844
1987	45743	46538	2.5708	2.3478	21.5013	4.7120	1.0570	1.0887	0.7525	0.6835	0.9693	0.8039
1988	47259	48430	2.5022	2.5708	21.1997	1.9689	1.0920	1.1329	0.7325	0.7484	0.9557	0.3359
1989	47186	46406	3.9949	2.5022	20.3321	3.3941	1.0903	1.0856	1.1694	0.7284	0.9166	0.5791
1990	47709	44985	3.8499	3.9949	22.1700	7.2828	1.1024	1.0523	1.1270	1.1630	0.9994	1.2426
1991	47290	45351	4.1048	3.8499	21.3918	5.9404	1.0927	1.0609	1.2016	1.1208	0.9644	1.0135
1992	47402	45255	3.0820	4.1048	19.9281	5.7764	1.0953	1.0587	0.9022	1.1950	0.8984	0.9855
1993	47427	45829	3.2508	3.0820	20.7166	5.2951	1.0959	1.0721	0.9516	0.8972	0.9339	0.9034
1994	47242	46907	4.4646	3.2508	20.8423	4.2228	1.0916	1.0973	1.3069	0.9464	0.9396	0.7205
1995	44102	45738	2.8698	4.4646	20.7945	4.1822	1.0191	1.0700	0.8401	1.2997	0.9374	0.7136
1996	43797	43412	3.4946	2.8698	19.6012	3.8701	1.0120	1.0155	1.0230	0.8355	0.8836	0.6603
1997	44446	43700	3.4682	3.4946	19.9288	5.5949	1.0270	1.0223	1.0152	1.0173	0.8984	0.9546
1998	44101	42371	3.7703	3.4682	21.5090	7.4405	1.0191	0.9912	1.1037	1.0096	0.9696	1.2695
1999	44101	42371	3.3590	3.7703	22.6538	6.0139	1.0191	0.9912	0.9833	1.0976	1.0213	1.0261
2000	49358	49792	2.9687	3.3590	21.2813	4.9484	1.1405	1.1648	0.8690	1.1602	0.9594	0.8443
2001	47892	48239	3.1781	2.9687	21.0079	3.7383	1.1066	1.1285	0.9303	0.8644	0.9471	0.6378
2002	46173	46723	3.9223	3.1781	21.3142	5.4720	1.0669	1.0930	1.1482	0.9253	0.9609	0.9336
2003	45515	47789	3.0737	3.9223	21.1267	4.1134	1.0517	1.1179	0.8998	1.1420	0.9524	0.7018
2004	47207	49409	3.4621	3.0737	21.6372	5.1266	1.0908	1.1558	1.0135	0.8949	0.9754	0.8747
2005	45925	46698	2.7716	3.4621	21.1808	1.1451	1.0612	1.0924	0.8113	1.0080	0.9548	0.1954
2006	44769	45497	2.3941	2.7716	22.5401	3.5992	1.0345	1.0643	0.7008	0.8070	1.0161	0.6141
2007	44812	45610	2.6171	2.3941	22.2213	5.4720	1.0355	1.0670	0.7661	0.6971	1.0018	0.9336
2008	46328	47502	2.5486	2.6171	21.9197	2.7289	1.0705	1.1112	0.7460	0.7620	0.9882	0.4656
2009	46255	45478	4.0413	2.5486	21.0521	4.1541	1.0688	1.0639	1.1830	0.7420	0.9490	0.7088
2010	46778	44057	3.8963	4.0413	22.8900	8.0428	1.0809	1.0306	1.1406	1.1766	1.0319	1.3722
2011	46359	44423	4.1511	3.8963	22.1118	6.7004	1.0712	1.0392	1.2152	1.1344	0.9968	1.1432
2012	46471	44327	3.1284	4.1511	20.6481	6.5364	1.0738	1.0370	0.9158	1.2086	0.9308	1.1152
2013	46496	44901	3.2972	3.1284	21.4366	6.0551	1.0744	1.0504	0.9652	0.9108	0.9664	1.0331
2014	46311	45979	4.5110	3.2972	21.5623	4.9828	1.0701	1.0756	1.3205	0.9600	0.9720	0.8501
2015	43171	44810	2.9162	4.5110	21.5145	4.9422	0.9976	1.0483	0.8537	1.3133	0.9699	0.8432
2016	42866	42484	3.5410	2.9162	20.3212	4.6301	0.9905	0.9938	1.0366	0.8491	0.9161	0.7900

2017	43515	42772	3.5145	3.5414	20.6488	6.3549	1.0055	1.0006	1.0288	1.0310	0.9309	1.0843
2018	43170	41443	3.8167	3.5149	22.2290	8.2005	0.9975	0.9695	1.1173	1.0232	1.0021	1.3991
2019	43170	41443	3.4054	3.8171	23.3738	6.7739	0.9975	0.9695	0.9969	1.1112	1.0537	1.1557
2020	48427	48864	3.0151	4.0322	22.0013	5.7084	1.1190	1.1431	0.8826	1.1738	0.9918	0.9739
2021	46961	47311	3.2244	3.0159	21.7279	4.4983	1.0851	1.1068	0.9439	0.8780	0.9795	0.7675
2022	45242	45795	3.9687	3.2253	22.0342	6.2320	1.0454	1.0713	1.1618	0.9389	0.9933	1.0633
2023	44584	46861	3.1200	3.9695	21.8467	4.8734	1.0302	1.0962	0.9133	1.1556	0.9849	0.8315
2024	46276	48481	3.5085	3.1208	22.3572	5.8866	1.0693	1.1341	1.0271	0.9085	1.0079	1.0043
2025	44994	45770	2.8179	3.5093	21.9008	1.9051	1.0397	1.0707	0.8249	1.0216	0.9873	0.3250
2026	43838	44569	2.4405	2.8187	23.2601	4.3592	1.0130	1.0426	0.7144	0.8206	1.0486	0.7438
2027	43881	44682	2.6635	2.4413	22.9413	6.2320	1.0140	1.0453	0.7797	0.7107	1.0342	1.0633
2028	45397	46574	2.5949	2.6643	22.6397	3.4889	1.0490	1.0895	0.7596	0.7756	1.0206	0.5953
2029	45324	44550	4.0876	2.5957	21.7721	4.9141	1.0473	1.0422	1.1966	0.7557	0.9815	0.8384
2030	45847	43129	3.9426	4.0885	23.6100	8.8028	1.0594	1.0089	1.1541	1.1902	1.0644	1.5019
2031	45428	43495	4.1975	3.9434	22.8318	7.4604	1.0497	1.0175	1.2287	1.1480	1.0293	1.2729
2032	45540	43399	3.1748	4.1983	21.3681	7.2964	1.0523	1.0152	0.9294	1.2222	0.9633	1.2449
2033	45565	43973	3.3435	3.1756	22.1566	6.8151	1.0529	1.0287	0.9788	0.9245	0.9988	1.1628
2034	45380	45051	4.5573	3.3443	22.2823	5.7428	1.0486	1.0539	1.3341	0.9736	1.0045	0.9798
2035	42240	43882	2.9626	4.5582	22.2345	5.7022	0.9760	1.0265	0.8672	1.3270	1.0023	0.9729
2036	41935	41556	3.5873	2.9634	21.0412	5.3901	0.9690	0.9721	1.0501	0.8627	0.9486	0.9196
2037	42584	41844	3.5609	3.5882	21.3688	7.1149	0.9840	0.9789	1.0424	1.0446	0.9633	1.2139
2038	42239	40515	3.8631	3.5617	22.9490	8.9605	0.9760	0.9478	1.1308	1.0369	1.0346	1.5288
2039	42239	40515	3.4517	3.8639	24.0938	7.5339	0.9760	0.9478	1.0104	1.1248	1.0862	1.2854
2040	47496	47936	3.0614	4.0790	22.7213	6.4684	1.0975	1.1214	0.8962	1.1875	1.0243	1.1036
2041	46030	46383	3.2708	3.0626	22.4479	5.2583	1.0636	1.0851	0.9575	0.8916	1.0120	0.8972
2042	44311	44867	4.0151	3.2720	22.7542	6.9920	1.0239	1.0496	1.1753	0.9525	1.0258	1.1929
2043	43653	45933	3.1664	4.0163	22.5667	5.6334	1.0087	1.0745	0.9269	1.1692	1.0173	0.9611
2044	45345	47553	3.5549	3.1676	23.0772	6.6466	1.0478	1.1124	1.0406	0.9221	1.0403	1.1340
2045	44063	44842	2.8643	3.5561	22.6208	2.6651	1.0182	1.0490	0.8385	1.0352	1.0198	0.4547
2046	42907	43641	2.4869	2.8655	23.9801	5.1192	0.9915	1.0209	0.7280	0.8342	1.0810	0.8734
2047	42950	43754	2.7099	2.4881	23.6613	6.9920	0.9924	1.0236	0.7933	0.7243	1.0667	1.1929
2048	44466	45646	2.6413	2.7111	23.3597	4.2489	1.0275	1.0678	0.7732	0.7892	1.0531	0.7249
2049	44393	43622	4.1340	2.6425	22.4921	5.6741	1.0258	1.0205	1.2102	0.7693	1.0140	0.9681
2050	44916	42201	3.9890	4.1352	24.3300	9.5628	1.0379	0.9872	1.1677	1.2038	1.0968	1.6316
2051	44497	42567	4.2439	3.9902	23.5518	8.2204	1.0282	0.9958	1.2423	1.1616	1.0617	1.4025
2052	44609	42471	3.2211	4.2451	22.0881	8.0564	1.0308	0.9935	0.9429	1.2358	0.9957	1.3745
2053	44634	43045	3.3899	3.2223	22.8766	7.5751	1.0314	1.0070	0.9923	0.9381	1.0313	1.2924
2054	44449	44123	4.6037	3.3911	23.0023	6.5028	1.0271	1.0322	1.3476	0.9872	1.0370	1.1095
2055	41309	42954	3.0089	4.6049	22.9545	6.4622	0.9545	1.0048	0.8808	1.3406	1.0348	1.1026
2056	41004	40628	3.6337	3.0101	21.7612	6.1501	0.9475	0.9504	1.0637	0.8763	0.9810	1.0493
2057	41653	40916	3.6072	3.6349	22.0888	7.8749	0.9625	0.9572	1.0560	1.0582	0.9958	1.3436
2058	41308	39587	3.9094	3.6084	23.6690	9.7205	0.9545	0.9261	1.1444	1.0505	1.0670	1.6585
2059	41308	39587	3.4981	3.9106	24.8138	8.2939	0.9545	0.9261	1.0240	1.1384	1.1186	1.4151
2060	46564	47008	3.1078	4.1258	23.4413	7.2284	1.0760	1.0997	0.9097	1.2011	1.0568	1.2333
2061	45098	45455	3.3172	3.1094	23.1679	6.0183	1.0421	1.0633	0.9710	0.9052	1.0444	1.0268
2062	43379	43939	4.0614	3.3188	23.4742	7.7520	1.0024	1.0279	1.1889	0.9662	1.0582	1.3226
2063	42721	45005	3.2127	4.0630	23.2867	6.3934	0.9872	1.0528	0.9405	1.1828	1.0498	1.0908
2064	44413	46625	3.6012	3.2144	23.7972	7.4066	1.0263	1.0907	1.0542	0.9357	1.0728	1.2637
2065	43131	43914	2.9106	3.6028	23.3408	3.4251	0.9966	1.0273	0.8520	1.0488	1.0522	0.5844

2066	41975	42713	2.5332	2.9123	24.7001	5.8792	0.9699	0.9992	0.7416	0.8478	1.1135	1.0031
2067	42018	42826	2.7562	2.5348	24.3813	7.7520	0.9709	1.0018	0.8068	0.7379	1.0991	1.3226
2068	43534	44718	2.6876	2.7578	24.0797	5.0089	1.0060	1.0461	0.7868	0.8028	1.0855	0.8546
2069	43461	42694	4.1804	2.6893	23.2121	6.4341	1.0043	0.9988	1.2237	0.7829	1.0464	1.0978
2070	43984	41273	4.0353	4.1820	25.0500	10.3228	1.0164	0.9655	1.1813	1.2174	1.1293	1.7612
2071	43565	41639	4.2902	4.0370	24.2718	8.9804	1.0067	0.9741	1.2559	1.1752	1.0942	1.5322
2072	43677	41543	3.2675	4.2918	22.8081	8.8164	1.0093	0.9718	0.9565	1.2494	1.0282	1.5042
2073	43702	42117	3.4362	3.2691	23.5966	8.3351	1.0098	0.9853	1.0059	0.9517	1.0638	1.4221
2074	43517	43195	4.6501	3.4379	23.7223	7.2628	1.0056	1.0105	1.3612	1.0008	1.0694	1.2391
2075	40377	42026	3.0553	4.6517	23.6745	7.2222	0.9330	0.9831	0.8944	1.3542	1.0673	1.2322
2076	40072	39700	3.6801	3.0569	22.4812	6.9101	0.9260	0.9287	1.0773	0.8899	1.0135	1.1790
2077	40721	39988	3.6536	3.6817	22.8088	8.6349	0.9410	0.9355	1.0695	1.0718	1.0282	1.4733
2078	40376	38659	3.9558	3.6552	24.3890	10.4805	0.9330	0.9044	1.1580	1.0641	1.0995	1.7881
2079	40376	38659	3.5445	3.9574	25.5338	9.0539	0.9330	0.9044	1.0376	1.1521	1.1511	1.5447
2080	45633	46080	3.1541	4.1725	24.1613	7.9884	1.0545	1.0780	0.9233	1.2147	1.0892	1.3630
2081	44167	44527	3.3635	3.1562	23.8879	6.7783	1.0206	1.0416	0.9846	0.9188	1.0769	1.1565
2082	42448	43011	4.1078	3.3656	24.1942	8.5120	0.9809	1.0062	1.2025	0.9798	1.0907	1.4523
2083	41790	44077	3.2591	4.1098	24.0067	7.1534	0.9657	1.0311	0.9540	1.1964	1.0822	1.2205
2084	43482	45697	3.6476	3.2611	24.5172	8.1666	1.0048	1.0690	1.0678	0.9494	1.1053	1.3934
2085	42200	42986	2.9570	3.6496	24.0608	4.1851	0.9751	1.0056	0.8656	1.0625	1.0847	0.7140
2086	41044	41785	2.5796	2.9590	25.4201	6.6392	0.9484	0.9775	0.7551	0.8614	1.1460	1.1328
2087	41087	41898	2.8026	2.5816	25.1013	8.5120	0.9494	0.9801	0.8204	0.7515	1.1316	1.4523
2088	42603	43790	2.7340	2.8046	24.7997	5.7689	0.9844	1.0244	0.8003	0.8165	1.1180	0.9843
2089	42530	41766	4.2267	2.7360	23.9321	7.1941	0.9828	0.9771	1.2373	0.7965	1.0789	1.2274
2090	43053	40345	4.0817	4.2288	25.7700	11.0828	0.9948	0.9438	1.1948	1.2311	1.1617	1.8909
2091	42634	40711	4.3366	4.0837	24.9918	9.7404	0.9852	0.9524	1.2695	1.1888	1.1267	1.6619
2092	42746	40615	3.3138	4.3386	23.5281	9.5764	0.9877	0.9501	0.9701	1.2630	1.0607	1.6339
2093	42771	41189	3.4826	3.3159	24.3166	9.0951	0.9883	0.9636	1.0195	0.9653	1.0962	1.5518
2094	42586	42267	4.6964	3.4846	24.4423	8.0228	0.9840	0.9888	1.3748	1.0144	1.1019	1.3688
2095	39446	41098	3.1016	4.6985	24.3945	7.9822	0.9115	0.9614	0.9079	1.3678	1.0997	1.3619
2096	39141	38772	3.7264	3.1037	23.2012	7.6701	0.9044	0.9070	1.0908	0.9035	1.0459	1.3086
2097	39790	39060	3.7000	3.7285	23.5288	9.3949	0.9194	0.9137	1.0831	1.0854	1.0607	1.6029
2098	39445	37731	4.0021	3.7020	25.1090	11.2405	0.9115	0.8827	1.1716	1.0777	1.1319	1.9178
2099	39445	37731	3.5908	4.0042	26.2538	9.8139	0.9115	0.8827	1.0511	1.1657	1.1835	1.6744

4.2. R programming for Prediction of Global Warming Effects on Red Spruce Growth

Global Warming Effects on ARIMhigh

x<-c(1940, 1941,1942, 1943, 1944, 1945, 1946, 1947, 1948, 1949, 1950, 1951, 1952, 1953, 1954, 1955, 1956, 1957, 1958, 1959, 1960, 1961, 1962, 1963, 1964, 1965, 1966, 1967, 1968, 1969, 1970, 1971, 1972, 1973, 1974, 1975, 1976, 1977, 1978, 1979, 1980, 1981, 1982, 1983, 1984, 1985, 1986, 1987, 1988, 1989, 1990, 1991, 1992, 1993, 1994, 1995, 1996, 1997, 1998, 1999, 2000, 2001, 2002, 2003, 2004, 2005, 2006, 2007, 2008, 2009, 2010, 2011, 2012, 2013, 2014, 2015, 2016, 2017, 2018, 2019, 2020, 2021, 2022, 2023, 2024, 2025, 2026, 2027, 2028, 2029, 2030, 2031, 2032, 2033, 2034, 2035, 2036, 2037, 2038, 2039, 2040, 2041, 2042, 2043, 2044,

2045, 2046, 2047, 2048, 2049, 2050, 2051, 2052, 2053, 2054, 2055, 2056, 2057, 2058, 2059, 2060, 2061, 2062, 2063, 2064, 2065, 2066, 2067, 2068, 2069, 2070, 2071, 2072, 2073, 2074, 2075, 2076, 2077, 2078, 2079, 2080, 2081, 2082, 2083, 2084, 2085, 2086, 2087, 2088, 2089, 2090, 2091, 2092, 2093, 2094, 2095, 2096, 2097, 2098, 2099) # years

10% increase of AP(Air Pollution) and global warming at high elevation: x=years, yI10=global warming with 10%increase AP

yI10<-c(1.27, 1.24, 1.2, 1.19, 1.18, 1.15, 1.17, 1.16, 1.17, 1.2, 1.17, 1.18, 1.2, 1.19, 1.18, 1.18, 1.15, 1.12, 1.14, 1.12, 1.1, 1.09, 1.07, 1.04, 1.03, 1.01, 0.96, 0.93, 0.96, 0.91, 0.85, 0.84, 0.79, 0.76, 0.81, 0.89, 0.86, 0.82, 0.85, 0.83, 0.89, 0.91, 0.91, 0.94, 0.9, 0.96, 0.99, 0.98, 0.96, 0.91, 0.92, 0.92, 0.95, 0.94, 0.89, 0.99, 0.99, 0.98, 0.98, 1, 0.87, 0.89, 0.89, 0.92, 0.88, 0.94, 0.97, 0.96, 0.94, 0.9, 0.9, 0.9, 0.94, 0.92, 0.87, 0.97, 0.97, 0.96, 0.97, 0.98, 0.85, 0.87, 0.87, 0.91, 0.86, 0.92, 0.96, 0.95, 0.92, 0.88, 0.89, 0.88, 0.92, 0.91, 0.85, 0.96, 0.95, 0.95, 0.95, 0.96, 0.84, 0.85, 0.85, 0.89, 0.84, 0.9, 0.94, 0.93, 0.9, 0.86, 0.87, 0.86, 0.9, 0.89, 0.83, 0.94, 0.94, 0.93, 0.93, 0.94, 0.82, 0.83, 0.83, 0.87, 0.82, 0.88, 0.92, 0.91, 0.88, 0.84, 0.85, 0.84, 0.88, 0.87, 0.81, 0.92, 0.92, 0.91, 0.91, 0.93, 0.8, 0.81, 0.81, 0.85, 0.8, 0.87, 0.9, 0.89, 0.87, 0.82, 0.83, 0.82, 0.86, 0.85, 0.79, 0.9, 0.9, 0.89, 0.89, 0.91) # Indices with no unit computed in ARIM_{high} with 10% increased AP and Global #warming

```
dumI10 <- data.frame (x, yI10)
```

```
ARIMhigh_GWI10 <- lm(yI10 ~ x, data=dumI10) # linear regression model
```

```
summary(ARIMhigh_GWI10)
```

```
lrfI10 <- loess(yI10~x, dumI10) # Fit a smooth regression curve using a modern regression #function.
```

```
attach(dumI10)
```

```
plot(x, yI10, xlab = "Year",ylab = "ARIMindex")
```

```
lines(spline(x, fitted(lrfI10)), lwd=3, col=2) # First add smooth lines in the local regression curve #using a Spline interpolation between the calculated points
```

```
abline(ARIMhigh_GWI10, lwd=3, lty=4, col=5) # Add the regression line estimated from the #simple linear regression model
```

```
title("Global Warming Effects on Red Spruce Growth at High Elevation along with 10% Increases of Air Pollution") # Add title
```

No change AP and global warming at high elevation: x=years, yno=no change of AP

```
yno<-c(1.25, 1.22, 1.19, 1.17, 1.16, 1.13, 1.15, 1.14, 1.15, 1.18, 1.16, 1.16, 1.18, 1.17, 1.16, 1.16,  
1.13, 1.1, 1.12, 1.1, 1.08, 1.07, 1.04, 1.02, 1, 0.98, 0.92, 0.9, 0.93, 0.87, 0.81, 0.81, 0.75, 0.72,  
0.77, 0.86, 0.83, 0.78, 0.81, 0.79, 0.86, 0.88, 0.88, 0.91, 0.86, 0.93, 0.96, 0.95, 0.92, 0.88, 0.89,  
0.88, 0.92, 0.91, 0.86, 0.96, 0.96, 0.95, 0.95, 0.97, 0.85, 0.87, 0.87, 0.91, 0.86, 0.92, 0.96, 0.95,  
0.92, 0.88, 0.89, 0.88, 0.92, 0.91, 0.86, 0.96, 0.96, 0.95, 0.95, 0.97, 0.85, 0.87, 0.87, 0.91, 0.86,  
0.92, 0.96, 0.95, 0.92, 0.88, 0.89, 0.88, 0.92, 0.91, 0.85, 0.96, 0.96, 0.95, 0.95, 0.96, 0.85, 0.87,  
0.87, 0.9, 0.86, 0.92, 0.96, 0.95, 0.92, 0.87, 0.88, 0.88, 0.92, 0.91, 0.85, 0.96, 0.95, 0.95, 0.95,  
0.96, 0.85, 0.87, 0.87, 0.9, 0.86, 0.92, 0.95, 0.94, 0.92, 0.87, 0.88, 0.88, 0.91, 0.9, 0.85, 0.96, 0.95,  
0.94, 0.95, 0.96, 0.85, 0.87, 0.87, 0.9, 0.85, 0.92, 0.95, 0.94, 0.91, 0.87, 0.88, 0.87, 0.91, 0.9, 0.85,  
0.95, 0.95, 0.94, 0.95, 0.96) # Indices with no unit computed in ARIMhigh with 0% increased AP  
# and Global warming
```

```
dumno <- data.frame(x, yno)
```

```
ARIMhigh_GWno <- lm(yno ~ x, data=dumno)
```

```
summary(ARIMhigh_GW0)
```

```
lrfno <- loess(yno ~ x, dumno)
```

```
attach(dumno)
```

```
plot(x, yno, xlab = "Year", ylab = "ARIMindex")
```

```
lines(spline(x, fitted(lrfno)), lwd=3, col=2)
```

```
abline(ARIMhigh_GWno, lwd=3, lty=4, col=5)
```

```
title("Global Warming Effects on Red Spruce Growth at High Elevation along with 0% Increases  
of Air Pollution")
```

10% decrease of AP and Global warming at high elevation: x=years, yd10=10%decrease of AP.

```
yd10<-c(1.24, 1.21, 1.17, 1.15, 1.14, 1.11, 1.13, 1.12, 1.12, 1.16, 1.13, 1.14, 1.16, 1.15, 1.14,  
1.14, 1.11, 1.08, 1.1, 1.07, 1.06, 1.04, 1.01, 0.99, 0.97, 0.95, 0.89, 0.86, 0.9, 0.83, 0.77, 0.76, 0.71,  
0.67, 0.72, 0.82, 0.79, 0.73, 0.77, 0.74, 0.82, 0.84, 0.84, 0.87, 0.82, 0.89, 0.93, 0.92, 0.89, 0.84,  
0.85, 0.85, 0.89, 0.88, 0.82, 0.93, 0.93, 0.92, 0.92, 0.94, 0.83, 0.85, 0.86, 0.89, 0.84, 0.91, 0.94,  
0.93, 0.9, 0.86, 0.87, 0.86, 0.9, 0.89, 0.84, 0.95, 0.94, 0.93, 0.94, 0.95, 0.85, 0.87, 0.87, 0.91, 0.86,  
0.92, 0.96, 0.95, 0.92, 0.88, 0.89, 0.88, 0.92, 0.91, 0.85, 0.96, 0.96, 0.95, 0.95, 0.97, 0.87, 0.89,  
0.89, 0.92, 0.88, 0.94, 0.97, 0.96, 0.94, 0.89, 0.9, 0.9, 0.94, 0.92, 0.87, 0.98, 0.98, 0.97, 0.97, 0.98,
```

```
0.88, 0.9, 0.91, 0.94, 0.89, 0.95, 0.99, 0.98, 0.95, 0.91, 0.92, 0.91, 0.95, 0.94, 0.89, 0.99, 0.99,
0.98, 0.99, 1, 0.9, 0.92, 0.92, 0.95, 0.91, 0.97, 1, 0.99, 0.97, 0.93, 0.94, 0.93, 0.97, 0.96, 0.91,
1.01, 1.01, 1, 1, 1.01) # Indices with no unit computed in ARIMhigh with 10% decreased AP and
# Global warming
```

```
dumd10 <- data.frame (x, yd10)
```

```
ARIMhigh_GWd10 <- lm(yd10 ~ x, data=dumd10)
```

```
summary(ARIMhigh_GWd10)
```

```
lrfd10 <- loess(yd10~x, dumd10)
```

```
attach(dumd10)
```

```
plot(x, yd10, xlab = "Year", ylab = "ARIMindex")
```

```
lines(spline(x, fitted(lrfd10)), lwd=3, col=2)
```

```
abline(ARIMhigh_GWd10, lwd=3, lty=4, col=5)
```

```
title("Global Warming Effects on Red Spruce Growth at High Elevation along with 10%
Decreases of Air Pollution")
```

Global Warming Effects on ARIM_{low}

```
x<-c(1940, 1941,1942, 1943, 1944, 1945, 1946, 1947, 1948, 1949, 1950, 1951, 1952,
1953, 1954, 1955, 1956, 1957, 1958, 1959, 1960, 1961, 1962, 1963, 1964, 1965, 1966,
1967, 1968, 1969, 1970, 1971, 1972, 1973, 1974, 1975, 1976, 1977, 1978, 1979, 1980,
1981, 1982, 1983, 1984, 1985, 1986, 1987, 1988, 1989, 1990, 1991, 1992, 1993, 1994,
1995, 1996, 1997, 1998, 1999, 2000, 2001, 2002, 2003, 2004, 2005, 2006, 2007, 2008,
2009, 2010, 2011, 2012, 2013, 2014, 2015, 2016, 2017, 2018, 2019, 2020, 2021, 2022,
2023, 2024, 2025, 2026, 2027, 2028, 2029, 2030, 2031, 2032, 2033, 2034, 2035, 2036,
2037, 2038, 2039, 2040, 2041, 2042, 2043, 2044, 2045, 2046, 2047, 2048, 2049, 2050,
2051, 2052, 2053, 2054, 2055, 2056, 2057, 2058, 2059, 2060, 2061, 2062, 2063, 2064,
2065, 2066, 2067, 2068, 2069, 2070, 2071, 2072, 2073, 2074, 2075, 2076, 2077, 2078,
2079, 2080, 2081, 2082, 2083, 2084, 2085, 2086, 2087, 2088, 2089, 2090, 2091, 2092,
2093, 2094, 2095, 2096, 2097, 2098, 2099) # years
```

10% increase of AP and global warming at low elevation: x=years, yI10=global warming with 10%increase AP

```

yI10<-c(1.23, 1.07, 1.08, 1.22, 1.13, 1.16, 1.2, 1.19, 1.09, 1.22, 1.22, 1.24, 1.19,
1, 1.07, 1.11, 1.1, 1.22, 1.34, 1.06, 1.17, 1.21, 1.3, 1.33, 1.21, 1.11, 1.11, 1.19,
1.22, 1.05, 1.16, 1.11, 1.22, 1.27, 1.27, 1.24, 1.09, 1.06, 1.16, 1.13, 1.2, 1.06,
1.13, 1.21, 1.07, 1.13, 0.95, 0.91, 0.95, 1.04, 1.22, 1.23, 1.26, 1.08, 1.17, 1.3,
1.11, 1.19, 1.16, 1.15, 1.18, 1.04, 1.11, 1.2, 1.05, 1.11, 0.93, 0.89, 0.93, 1.03,
1.19, 1.21, 1.25, 1.07, 1.16, 1.28, 1.09, 1.18, 1.14, 1.13, 1.16, 1.02, 1.09, 1.18,
1.03, 1.09, 0.91, 0.87, 0.91, 1.01, 1.17, 1.19, 1.23, 1.05, 1.13, 1.26, 1.08, 1.16,
1.12, 1.11, 1.14, 1, 1.07, 1.16, 1.01, 1.07, 0.89, 0.84, 0.89, 0.99, 1.14, 1.17, 1.21,
1.02, 1.11, 1.24, 1.06, 1.14, 1.09, 1.08, 1.12, 0.98, 1.04, 1.13, 0.98, 1.05, 0.86,
0.82, 0.86, 0.96, 1.12, 1.14, 1.19, 1, 1.09, 1.22, 1.04, 1.12, 1.07, 1.05, 1.09, 0.96,
1.02, 1.11, 0.96, 1.03, 0.83, 0.79, 0.84, 0.94, 1.09, 1.12, 1.17, 0.97, 1.06, 1.19,
1.02, 1.1, 1.04, 1.02) # Indices with no unit computed in ARIMIlow with 10% increased AP and
# Global warming.

```

```
dumI10 <- data.frame (x, yI10)
```

```
ARIMlow_GWI10 <- lm(yI10 ~ x, data=dumI10)
```

```
summary(ARIMlow_GWI10)
```

```
lrfI10 <- loess(yI10~x, dumI10)
```

```
attach(dumI10)
```

```
plot(x, yI10, xlab = "Year", ylab = "ARIMindex")
```

```
lines(spline(x, fitted(lrfI10)), lwd=3, col=2)
```

```
abline(ARIMlow_GWI10, lwd=3, lty=4, col=5)
```

```
title("Global Warming Effects on Red Spruce Growth at Low Elevation along with 10%
Increases of Air Pollution")
```

```
# No change AP and global warming at low elevation: x=years, yno=no change of AP
```

```

yno<-c(1.22, 1.07, 1.08, 1.21, 1.12, 1.16, 1.19, 1.19, 1.08, 1.22, 1.21, 1.24, 1.18,
1, 1.06, 1.1, 1.09, 1.21, 1.34, 1.05, 1.17, 1.2, 1.29, 1.32, 1.21, 1.1, 1.1, 1.18,
1.22, 1.05, 1.15, 1.1, 1.21, 1.26, 1.26, 1.23, 1.08, 1.05, 1.15, 1.12, 1.19, 1.05,
1.12, 1.2, 1.06, 1.12, 0.95, 0.9, 0.94, 1.03, 1.21, 1.23, 1.26, 1.07, 1.16, 1.29, 1.1,

```

1.19, 1.15, 1.15, 1.18, 1.04, 1.11, 1.19, 1.05, 1.11, 0.93, 0.88, 0.93, 1.02, 1.19,
 1.21, 1.24, 1.06, 1.15, 1.28, 1.09, 1.18, 1.14, 1.13, 1.16, 1.02, 1.09, 1.18, 1.03,
 1.09, 0.91, 0.87, 0.91, 1.01, 1.17, 1.19, 1.23, 1.05, 1.14, 1.26, 1.08, 1.16, 1.12,
 1.11, 1.14, 1.01, 1.07, 1.16, 1.01, 1.08, 0.89, 0.85, 0.89, 0.99, 1.15, 1.17, 1.22,
 1.03, 1.12, 1.25, 1.06, 1.15, 1.1, 1.08, 1.12, 0.99, 1.05, 1.14, 0.99, 1.06, 0.87,
 0.82, 0.87, 0.97, 1.12, 1.15, 1.2, 1.01, 1.1, 1.23, 1.05, 1.13, 1.08, 1.06, 1.1, 0.97,
 1.03, 1.12, 0.97, 1.04, 0.84, 0.8, 0.85, 0.95, 1.1, 1.13, 1.18, 0.99, 1.08, 1.2, 1.03,
 1.11, 1.05, 1.03) #Indices with no unit computed in ARIM_{low} with 0% increased AP and Global
 #warming

```
dumno <- data.frame(x, yno)
```

```
ARIMlow_GWno <- lm(yno ~ x, data=dumno)
```

```
summary(ARIMlow_GWno)
```

```
lrfno <- loess(yno ~ x, dumno)
```

```
attach(dumno)
```

```
plot(x, yno, xlab = "Year", ylab = "ARIMindex")
```

```
lines(spline(x, fitted(lrfno)), lwd=3, col=2)
```

```
abline(ARIMlow_GWno, lwd=3, lty=4, col=5)
```

```
title("Global Warming Effects on Red Spruce Growth at Low Elevation along with 0%  

  Increase of Air Pollution")
```

10% decrease of AP and Global warming at low elevation: x=years, yd10=10%decrease of AP.

```
yd10<-c(1.22, 1.06, 1.07, 1.21, 1.12, 1.15, 1.19, 1.18, 1.08, 1.21, 1.21, 1.23, 1.18,  

  0.99, 1.06, 1.1, 1.09, 1.2, 1.33, 1.04, 1.16, 1.2, 1.29, 1.31, 1.2, 1.1, 1.09, 1.17,  

  1.21, 1.04, 1.14, 1.09, 1.2, 1.25, 1.24, 1.22, 1.07, 1.04, 1.14, 1.11, 1.18, 1.04,  

  1.11, 1.2, 1.05, 1.11, 0.94, 0.89, 0.93, 1.02, 1.2, 1.22, 1.25, 1.07, 1.15, 1.28,  

  1.09, 1.18, 1.14, 1.14, 1.17, 1.03, 1.1, 1.19, 1.04, 1.1, 0.93, 0.88, 0.92, 1.02,  

  1.19, 1.21, 1.24, 1.06, 1.15, 1.28, 1.09, 1.17, 1.13, 1.12, 1.16, 1.02, 1.09, 1.18,  

  1.03, 1.09, 0.91, 0.87, 0.91, 1.01, 1.17, 1.19, 1.23, 1.05, 1.14, 1.26, 1.08, 1.16,  

  1.12, 1.11, 1.15, 1.01, 1.08, 1.17, 1.02, 1.08, 0.89, 0.85, 0.9, 1, 1.15, 1.18, 1.22,  

  1.03, 1.12, 1.25, 1.07, 1.15, 1.1, 1.09, 1.13, 1, 1.06, 1.15, 1, 1.07, 0.88, 0.83,
```

```
0.88, 0.98, 1.13, 1.16, 1.21, 1.02, 1.11, 1.24, 1.06, 1.14, 1.09, 1.07, 1.12, 0.98,  
1.05, 1.14, 0.98, 1.05, 0.86, 0.81, 0.86, 0.97, 1.11, 1.14, 1.19, 1, 1.09, 1.22, 1.04,  
1.13, 1.07, 1.05) # Indices with no unit computed in ARIMlow with 10% decreased AP and  
#Global warming.
```

```
dumd10 <- data.frame (x, yd10)
```

```
ARIMlow_GWd10 <- lm(yd10 ~ x, data=dumd10)
```

```
summary(ARIMlow_GWd10)
```

```
lrfd10 <- loess(yd10~x, dumd10)
```

```
attach(dumd10)
```

```
plot(x, yd10, xlab = "Year",ylab = "ARIMindex")
```

```
lines(spline(x, fitted(lrfd10)), lwd=3, col=2)
```

```
abline(ARIMlow_GWd10, lwd=3, lty=4, col=5)
```

```
title("Global Warming Effects on Red Spruce Growth at Low Elevation along with 10%  
Decreases of Air Pollution")
```

Appendix 5

Data of Sensitivity Analyses of Red Spruce Growth in ARMs

5.1. Sensitivity Analyses with Elevation Gradients

The high elevation ranges, 1700 to 2100 m, were calculated by ARIM_{high} and the low elevation ranges, 1400 to 1700 m, by ARIM_{low}. Actually, 2100 m in ARIM_{high} represents the highest elevation. The index values of the buffer range were obtained by averaging ARIM indices at 1700m estimated by ARIM_{low} and 1700 and 1800 m estimated by ARIM_{high} (elevations written in italics and underlined in the table). All values in the table are unitless indices of the ARIMs.

Year	Elevation (ARIM _{low})				Elevation (ARIM _{high})					Elevation (buffering zone)
	1400	1500	1600	<u>1700</u>	<u>1700</u>	<u>1800</u>	1900	2000	2100	<u>1650 - 1850</u>
1940	1.15	1.17	1.19	1.93	1.3	1.23	1.23	1.23	1.23	1.4867
1941	0.96	0.99	1.02	1.66	1.28	1.2	1.2	1.2	1.2	1.3800
1942	0.98	1.01	1.03	1.67	1.25	1.16	1.16	1.16	1.16	1.3600
1943	1.11	1.14	1.17	1.96	1.24	1.14	1.14	1.14	1.14	1.4467
1944	1.02	1.05	1.08	1.78	1.23	1.12	1.12	1.12	1.12	1.3767
1945	1.06	1.08	1.11	1.84	1.2	1.1	1.1	1.1	1.1	1.3800
1946	1.08	1.11	1.14	1.94	1.21	1.12	1.12	1.12	1.12	1.4233
1947	1.1	1.12	1.14	1.9	1.22	1.11	1.11	1.11	1.11	1.4100
1948	0.98	1.01	1.03	1.69	1.21	1.11	1.11	1.11	1.11	1.3367
1949	1.11	1.14	1.16	1.97	1.24	1.15	1.15	1.15	1.15	1.4533
1950	1.12	1.14	1.17	1.94	1.22	1.12	1.12	1.12	1.12	1.4267
1951	1.13	1.16	1.19	2.01	1.22	1.12	1.12	1.12	1.12	1.4500
1952	1.07	1.1	1.13	1.91	1.24	1.15	1.15	1.15	1.15	1.4333
1953	0.88	0.91	0.94	1.55	1.23	1.13	1.13	1.13	1.13	1.3033
1954	0.95	0.98	1	1.67	1.23	1.13	1.13	1.13	1.13	1.3433
1955	1	1.03	1.05	1.74	1.22	1.12	1.12	1.12	1.12	1.3600
1956	0.99	1.01	1.04	1.72	1.2	1.1	1.1	1.1	1.1	1.3400
1957	1.1	1.13	1.16	1.97	1.17	1.06	1.06	1.06	1.06	1.4000
1958	1.26	1.29	1.31	2.21	1.2	1.08	1.08	1.08	1.08	1.4967
1959	0.95	0.97	1	1.64	1.17	1.06	1.06	1.06	1.06	1.2900
1960	1.08	1.11	1.13	1.85	1.15	1.04	1.04	1.04	1.04	1.3467
1961	1.12	1.15	1.17	1.92	1.14	1.02	1.02	1.02	1.02	1.3600
1962	1.2	1.22	1.25	2.14	1.12	0.99	0.99	0.99	0.99	1.4167

1963	1.25	1.27	1.29	2.18	1.1	0.96	0.96	0.96	0.96	1.4133
1964	1.12	1.14	1.16	1.95	1.09	0.95	0.95	0.95	0.95	1.3300
1965	1	1.03	1.05	1.77	1.07	0.92	0.92	0.92	0.92	1.2533
1966	1.01	1.03	1.05	1.74	1.02	0.86	0.86	0.86	0.86	1.2067
1967	1.1	1.12	1.14	1.91	1	0.84	0.84	0.84	0.84	1.2500
1968	1.14	1.16	1.18	1.99	1.04	0.87	0.87	0.87	0.87	1.3000
1969	0.97	0.99	1	1.63	0.98	0.81	0.81	0.81	0.81	1.1400
1970	1.05	1.07	1.1	1.88	0.93	0.74	0.74	0.74	0.74	1.1833
1971	1	1.03	1.05	1.78	0.92	0.73	0.73	0.73	0.73	1.1433
1972	1.13	1.15	1.17	1.99	0.87	0.67	0.67	0.67	0.67	1.1767
1973	1.17	1.19	1.21	2.12	0.84	0.64	0.64	0.64	0.64	1.2000
1974	1.15	1.18	1.2	2.1	0.88	0.69	0.69	0.69	0.69	1.2233
1975	1.13	1.15	1.18	2.05	0.97	0.79	0.79	0.79	0.79	1.2700
1976	0.99	1.01	1.03	1.73	0.95	0.76	0.76	0.76	0.76	1.1467
1977	0.95	0.97	1	1.7	0.9	0.7	0.7	0.7	0.7	1.1000
1978	1.06	1.09	1.11	1.89	0.93	0.74	0.74	0.74	0.74	1.1867
1979	1.03	1.05	1.07	1.8	0.9	0.71	0.71	0.71	0.71	1.1367
1980	1.09	1.12	1.14	1.96	0.97	0.79	0.79	0.79	0.79	1.2400
1981	0.96	0.98	1	1.67	0.99	0.81	0.81	0.81	0.81	1.1567
1982	1.02	1.04	1.07	1.8	0.98	0.81	0.81	0.81	0.81	1.1967
1983	1.11	1.14	1.16	1.98	1.01	0.85	0.85	0.85	0.85	1.2800
1984	0.95	0.98	1.01	1.7	0.97	0.8	0.8	0.8	0.8	1.1567
1985	1.03	1.05	1.08	1.82	1.03	0.87	0.87	0.87	0.87	1.2400
1986	0.83	0.86	0.89	1.48	1.06	0.9	0.9	0.9	0.9	1.1467
1987	0.78	0.81	0.84	1.38	1.05	0.89	0.89	0.89	0.89	1.1067
1988	0.83	0.86	0.89	1.47	1.03	0.86	0.86	0.86	0.86	1.1200
1989	0.94	0.96	0.98	1.62	0.98	0.82	0.82	0.82	0.82	1.1400
1990	1.08	1.11	1.14	2.02	0.99	0.83	0.83	0.83	0.83	1.2800
1991	1.12	1.14	1.17	2.04	0.98	0.82	0.82	0.82	0.82	1.2800
1992	1.17	1.19	1.21	2.06	1.03	0.86	0.86	0.86	0.86	1.3167
1993	0.97	1	1.02	1.71	1.01	0.85	0.85	0.85	0.85	1.1900
1994	1.06	1.09	1.11	1.9	0.96	0.79	0.79	0.79	0.79	1.2167
1995	1.2	1.22	1.25	2.16	1.06	0.91	0.91	0.91	0.91	1.3767
1996	1.02	1.04	1.06	1.73	1.05	0.9	0.9	0.9	0.9	1.2267
1997	1.1	1.12	1.14	1.91	1.05	0.89	0.89	0.89	0.89	1.2833
1998	1.04	1.07	1.09	1.88	1.05	0.9	0.9	0.9	0.9	1.2767
Average	1.05	1.075	1.099	1.849	1.077	0.934	0.934	0.93	0.934	1.2866

5.2. Sensitivity Analyses with Aspect Gradients

In estimating the sensitivity of red spruce growth according to variations of Aspect, the elevation was classified into three ranges – high (>1850 m), buffer (1650 to 1850m) and low (1400 to 1650 m). Therefore, the sensitivity of red spruce growth for Aspect was computed and

averaged for four classes (**North, East, South and West**) at three elevation ranges separately. The indices of high elevation were computed by $ARIM_{high}$ at 1900m and low elevation by $ARIM_{low}$ at 1600m. The index values of the buffer zone were obtained by averaging values at 1700 m estimated by $ARIM_{low}$ and 1700 and 1800 m estimated by $ARIM_{high}$. (Aspect headings are written in italics and underlined in the following table). All values in the table are unitless indices of ARIMs.

Year	Aspect (ARIM Index of $ARIM_{low}$)				Aspect (ARIM Index of $ARIM_{high}$)			
	North	East	South	West	North	East	South	West
1940	1.19	1.66	0.91	1.6	1.23	1.23	1.23	1.23
1941	1.02	1.48	0.68	1.4	1.2	1.2	1.2	1.2
1942	1.03	1.5	0.72	1.43	1.16	1.16	1.16	1.16
1943	1.17	1.63	0.84	1.56	1.14	1.14	1.14	1.14
1944	1.08	1.54	0.75	1.47	1.12	1.12	1.12	1.12
1945	1.11	1.57	0.79	1.5	1.1	1.1	1.1	1.1
1946	1.14	1.59	0.79	1.52	1.12	1.12	1.12	1.12
1947	1.14	1.61	0.84	1.54	1.11	1.11	1.11	1.11
1948	1.03	1.49	0.71	1.42	1.11	1.11	1.11	1.11
1949	1.16	1.62	0.82	1.54	1.15	1.15	1.15	1.15
1950	1.17	1.63	0.86	1.56	1.12	1.12	1.12	1.12
1951	1.19	1.65	0.86	1.57	1.12	1.12	1.12	1.12
1952	1.13	1.59	0.79	1.51	1.15	1.15	1.15	1.15
1953	0.94	1.39	0.58	1.31	1.13	1.13	1.13	1.13
1954	1	1.46	0.66	1.38	1.13	1.13	1.13	1.13
1955	1.05	1.51	0.72	1.44	1.12	1.12	1.12	1.12
1956	1.04	1.5	0.71	1.43	1.1	1.1	1.1	1.1
1957	1.16	1.61	0.82	1.54	1.06	1.06	1.06	1.06
1958	1.31	1.78	1.02	1.71	1.08	1.08	1.08	1.08
1959	1	1.46	0.67	1.39	1.06	1.06	1.06	1.06
1960	1.13	1.6	0.84	1.53	1.04	1.04	1.04	1.04
1961	1.17	1.64	0.89	1.58	1.02	1.02	1.02	1.02
1962	1.25	1.71	0.94	1.64	0.99	0.99	0.99	0.99
1963	1.29	1.76	1.01	1.7	0.96	0.96	0.96	0.96
1964	1.16	1.63	0.87	1.57	0.95	0.95	0.95	0.95
1965	1.05	1.51	0.73	1.44	0.92	0.92	0.92	0.92
1966	1.05	1.53	0.78	1.46	0.86	0.86	0.86	0.86
1967	1.14	1.61	0.85	1.55	0.84	0.84	0.84	0.84
1968	1.18	1.65	0.9	1.59	0.87	0.87	0.87	0.87

1969	1	1.48	0.74	1.42	0.81	0.81	0.81	0.81
1970	1.1	1.56	0.79	1.5	0.74	0.74	0.74	0.74
1971	1.05	1.51	0.75	1.45	0.73	0.73	0.73	0.73
1972	1.17	1.64	0.89	1.58	0.67	0.67	0.67	0.67
1973	1.21	1.68	0.91	1.61	0.64	0.64	0.64	0.64
1974	1.2	1.66	0.88	1.59	0.69	0.69	0.69	0.69
1975	1.18	1.64	0.86	1.57	0.79	0.79	0.79	0.79
1976	1.03	1.5	0.74	1.44	0.76	0.76	0.76	0.76
1977	1	1.46	0.68	1.39	0.7	0.7	0.7	0.7
1978	1.11	1.57	0.81	1.51	0.74	0.74	0.74	0.74
1979	1.07	1.54	0.79	1.48	0.71	0.71	0.71	0.71
1980	1.14	1.6	0.84	1.54	0.79	0.79	0.79	0.79
1981	1	1.47	0.71	1.4	0.81	0.81	0.81	0.81
1982	1.07	1.53	0.76	1.46	0.81	0.81	0.81	0.81
1983	1.16	1.63	0.86	1.56	0.85	0.85	0.85	0.85
1984	1.01	1.47	0.69	1.4	0.8	0.8	0.8	0.8
1985	1.08	1.54	0.78	1.48	0.87	0.87	0.87	0.87
1986	0.89	1.34	0.54	1.26	0.9	0.9	0.9	0.9
1987	0.84	1.3	0.5	1.22	0.89	0.89	0.89	0.89
1988	0.89	1.35	0.56	1.27	0.86	0.86	0.86	0.86
1989	0.98	1.45	0.69	1.39	0.82	0.82	0.82	0.82
1990	1.14	1.6	0.79	1.52	0.83	0.83	0.83	0.83
1991	1.17	1.63	0.84	1.56	0.82	0.82	0.82	0.82
1992	1.21	1.68	0.93	1.62	0.86	0.86	0.86	0.86
1993	1.02	1.49	0.71	1.42	0.85	0.85	0.85	0.85
1994	1.11	1.58	0.8	1.51	0.79	0.79	0.79	0.79
1995	1.25	1.71	0.93	1.64	0.91	0.91	0.91	0.91
1996	1.06	1.53	0.78	1.47	0.9	0.9	0.9	0.9
1997	1.14	1.61	0.86	1.55	0.89	0.89	0.89	0.89
1998	1.09	1.55	0.76	1.48	0.9	0.9	0.9	0.9
Average	1.0992	1.5629	0.7885	1.4944	0.9337	0.9337	0.9337	0.9337

Year	<i>Aspect (ARIM Index of ARIM_{low} at 1700m)</i>				<i>Aspect (ARIM Index of ARIM_{high} at 1700m)</i>			
	North	East	South	West	North	East	South	West
1940	1.93	2.41	1.66	2.35	1.3	1.3	1.3	1.3
1941	1.66	2.12	1.34	2.05	1.28	1.28	1.28	1.28
1942	1.67	2.14	1.37	2.07	1.25	1.25	1.25	1.25
1943	1.96	2.42	1.65	2.35	1.24	1.24	1.24	1.24
1944	1.78	2.24	1.47	2.17	1.23	1.23	1.23	1.23
1945	1.84	2.31	1.53	2.24	1.2	1.2	1.2	1.2
1946	1.94	2.39	1.6	2.32	1.21	1.21	1.21	1.21
1947	1.9	2.37	1.61	2.3	1.22	1.22	1.22	1.22
1948	1.69	2.16	1.38	2.09	1.21	1.21	1.21	1.21
1949	1.97	2.43	1.64	2.36	1.24	1.24	1.24	1.24
1950	1.94	2.41	1.64	2.34	1.22	1.22	1.22	1.22
1951	2.01	2.47	1.69	2.4	1.22	1.22	1.22	1.22
1952	1.91	2.37	1.58	2.29	1.24	1.24	1.24	1.24

1953	1.55	2.01	1.21	1.93	1.23	1.23	1.23	1.23
1954	1.67	2.13	1.34	2.05	1.23	1.23	1.23	1.23
1955	1.74	2.2	1.43	2.13	1.22	1.22	1.22	1.22
1956	1.72	2.18	1.41	2.11	1.2	1.2	1.2	1.2
1957	1.97	2.43	1.64	2.35	1.17	1.17	1.17	1.17
1958	2.21	2.68	1.93	2.62	1.2	1.2	1.2	1.2
1959	1.64	2.1	1.33	2.04	1.17	1.17	1.17	1.17
1960	1.85	2.32	1.58	2.26	1.15	1.15	1.15	1.15
1961	1.92	2.4	1.65	2.34	1.14	1.14	1.14	1.14
1962	2.14	2.6	1.84	2.54	1.12	1.12	1.12	1.12
1963	2.18	2.65	1.91	2.59	1.1	1.1	1.1	1.1
1964	1.95	2.42	1.67	2.36	1.09	1.09	1.09	1.09
1965	1.77	2.24	1.47	2.17	1.07	1.07	1.07	1.07
1966	1.74	2.21	1.47	2.15	1.02	1.02	1.02	1.02
1967	1.91	2.38	1.64	2.32	1	1	1	1
1968	1.99	2.47	1.72	2.41	1.04	1.04	1.04	1.04
1969	1.63	2.11	1.37	2.05	0.98	0.98	0.98	0.98
1970	1.88	2.35	1.59	2.28	0.93	0.93	0.93	0.93
1971	1.78	2.24	1.49	2.18	0.92	0.92	0.92	0.92
1972	1.99	2.46	1.72	2.4	0.87	0.87	0.87	0.87
1973	2.12	2.59	1.83	2.53	0.84	0.84	0.84	0.84
1974	2.1	2.57	1.8	2.5	0.88	0.88	0.88	0.88
1975	2.05	2.51	1.74	2.45	0.97	0.97	0.97	0.97
1976	1.73	2.2	1.45	2.14	0.95	0.95	0.95	0.95
1977	1.7	2.17	1.4	2.1	0.9	0.9	0.9	0.9
1978	1.89	2.36	1.61	2.3	0.93	0.93	0.93	0.93
1979	1.8	2.28	1.53	2.22	0.9	0.9	0.9	0.9
1980	1.96	2.43	1.67	2.36	0.97	0.97	0.97	0.97
1981	1.67	2.14	1.38	2.07	0.99	0.99	0.99	0.99
1982	1.8	2.27	1.51	2.21	0.98	0.98	0.98	0.98
1983	1.98	2.45	1.69	2.39	1.01	1.01	1.01	1.01
1984	1.7	2.16	1.4	2.1	0.97	0.97	0.97	0.97
1985	1.82	2.29	1.53	2.22	1.03	1.03	1.03	1.03
1986	1.48	1.94	1.15	1.87	1.06	1.06	1.06	1.06
1987	1.38	1.84	1.06	1.77	1.05	1.05	1.05	1.05
1988	1.47	1.93	1.16	1.86	1.03	1.03	1.03	1.03
1989	1.62	2.09	1.34	2.03	0.98	0.98	0.98	0.98
1990	2.02	2.47	1.68	2.4	0.99	0.99	0.99	0.99
1991	2.04	2.5	1.72	2.43	0.98	0.98	0.98	0.98
1992	2.06	2.54	1.79	2.48	1.03	1.03	1.03	1.03
1993	1.71	2.18	1.42	2.12	1.01	1.01	1.01	1.01
1994	1.9	2.37	1.6	2.3	0.96	0.96	0.96	0.96
1995	2.16	2.62	1.86	2.56	1.06	1.06	1.06	1.06
1996	1.73	2.21	1.47	2.15	1.05	1.05	1.05	1.05
1997	1.91	2.39	1.64	2.33	1.05	1.05	1.05	1.05
1998	1.88	2.34	1.55	2.27	1.05	1.05	1.05	1.05

Year	<i>Aspect (ARIM Index of ARIM_{high} at 1800m)</i>				<i>Aspect (ARIM Index of Buffering Zone)</i>			
	North	East	South	West	North	East	South	West
1940	1.23	1.23	1.23	1.23	1.4867	1.6467	1.3967	1.6267
1941	1.2	1.2	1.2	1.2	1.38	1.5333	1.2733	1.51
1942	1.16	1.16	1.16	1.16	1.36	1.5167	1.26	1.4933
1943	1.14	1.14	1.14	1.14	1.4467	1.6	1.3433	1.5767
1944	1.12	1.12	1.12	1.12	1.3767	1.53	1.2733	1.5067
1945	1.1	1.1	1.1	1.1	1.38	1.5367	1.2767	1.5133
1946	1.12	1.12	1.12	1.12	1.4233	1.5733	1.31	1.55
1947	1.11	1.11	1.11	1.11	1.41	1.5667	1.3133	1.5433
1948	1.11	1.11	1.11	1.11	1.3367	1.4933	1.2333	1.47
1949	1.15	1.15	1.15	1.15	1.4533	1.6067	1.3433	1.5833
1950	1.12	1.12	1.12	1.12	1.4267	1.5833	1.3267	1.56
1951	1.12	1.12	1.12	1.12	1.45	1.6033	1.3433	1.58
1952	1.15	1.15	1.15	1.15	1.4333	1.5867	1.3233	1.56
1953	1.13	1.13	1.13	1.13	1.3033	1.4567	1.19	1.43
1954	1.13	1.13	1.13	1.13	1.3433	1.4967	1.2333	1.47
1955	1.12	1.12	1.12	1.12	1.36	1.5133	1.2567	1.49
1956	1.1	1.1	1.1	1.1	1.34	1.4933	1.2367	1.47
1957	1.06	1.06	1.06	1.06	1.4	1.5533	1.29	1.5267
1958	1.08	1.08	1.08	1.08	1.4967	1.6533	1.4033	1.6333
1959	1.06	1.06	1.06	1.06	1.29	1.4433	1.1867	1.4233
1960	1.04	1.04	1.04	1.04	1.3467	1.5033	1.2567	1.4833
1961	1.02	1.02	1.02	1.02	1.36	1.52	1.27	1.5
1962	0.99	0.99	0.99	0.99	1.4167	1.57	1.3167	1.55
1963	0.96	0.96	0.96	0.96	1.4133	1.57	1.3233	1.55
1964	0.95	0.95	0.95	0.95	1.33	1.4867	1.2367	1.4667
1965	0.92	0.92	0.92	0.92	1.2533	1.41	1.1533	1.3867
1966	0.86	0.86	0.86	0.86	1.2067	1.3633	1.1167	1.3433
1967	0.84	0.84	0.84	0.84	1.25	1.4067	1.16	1.3867
1968	0.87	0.87	0.87	0.87	1.3	1.46	1.21	1.44
1969	0.81	0.81	0.81	0.81	1.14	1.3	1.0533	1.28
1970	0.74	0.74	0.74	0.74	1.1833	1.34	1.0867	1.3167
1971	0.73	0.73	0.73	0.73	1.1433	1.2967	1.0467	1.2767
1972	0.67	0.67	0.67	0.67	1.1767	1.3333	1.0867	1.3133
1973	0.64	0.64	0.64	0.64	1.2	1.3567	1.1033	1.3367
1974	0.69	0.69	0.69	0.69	1.2233	1.38	1.1233	1.3567
1975	0.79	0.79	0.79	0.79	1.27	1.4233	1.1667	1.4033
1976	0.76	0.76	0.76	0.76	1.1467	1.3033	1.0533	1.2833
1977	0.7	0.7	0.7	0.7	1.1	1.2567	1	1.2333
1978	0.74	0.74	0.74	0.74	1.1867	1.3433	1.0933	1.3233
1979	0.71	0.71	0.71	0.71	1.1367	1.2967	1.0467	1.2767
1980	0.79	0.79	0.79	0.79	1.24	1.3967	1.1433	1.3733
1981	0.81	0.81	0.81	0.81	1.1567	1.3133	1.06	1.29
1982	0.81	0.81	0.81	0.81	1.1967	1.3533	1.1	1.3333
1983	0.85	0.85	0.85	0.85	1.28	1.4367	1.1833	1.4167
1984	0.8	0.8	0.8	0.8	1.1567	1.31	1.0567	1.29
1985	0.87	0.87	0.87	0.87	1.24	1.3967	1.1433	1.3733

1986	0.9	0.9	0.9	0.9	1.1467	1.3	1.0367	1.2767
1987	0.89	0.89	0.89	0.89	1.1067	1.26	1	1.2367
1988	0.86	0.86	0.86	0.86	1.12	1.2733	1.0167	1.25
1989	0.82	0.82	0.82	0.82	1.14	1.2967	1.0467	1.2767
1990	0.83	0.83	0.83	0.83	1.28	1.43	1.1667	1.4067
1991	0.82	0.82	0.82	0.82	1.28	1.4333	1.1733	1.41
1992	0.86	0.86	0.86	0.86	1.3167	1.4767	1.2267	1.4567
1993	0.85	0.85	0.85	0.85	1.19	1.3467	1.0933	1.3267
1994	0.79	0.79	0.79	0.79	1.2167	1.3733	1.1167	1.35
1995	0.91	0.91	0.91	0.91	1.3767	1.53	1.2767	1.51
1996	0.9	0.9	0.9	0.9	1.2267	1.3867	1.14	1.3667
1997	0.89	0.89	0.89	0.89	1.2833	1.4433	1.1933	1.4233
1998	0.9	0.9	0.9	0.9	1.2767	1.43	1.1667	1.4067
Average					1.2866	1.4423	1.1874	1.4203

5.3. Sensitivity Analyses with Slope Gradients

In estimating the sensitivity of red spruce growth according to variations of Slope, the elevation was classified into three ranges – high (>1850 m), buffer (1650 to 1850 m) and low (1400 to 1650 m). Therefore, the sensitivity of red spruce growth for Slope was computed and averaged for five classes (**1, 2, 3, 4 and 5**) at three elevation ranges separately. The indices of high elevation were computed by $ARIM_{high}$ at 1900m and low elevation $ARIM_{low}$ at 1600m. The index values of the buffer zone were obtained by averaging values at 1700 m estimated by $ARIM_{low}$ and 1700 and 1800 m estimated by $ARIM_{high}$ (Slope headings are written in italics and underlined in the following table). All values in the table are unitless indices of ARIMs.

Year	Slope (ARIM Index of $ARIM_{low}$)					Slope (ARIM Index of $ARIM_{high}$)				
	1	2	3	4	5	1	2	3	4	5
1940	0.99	1.09	1.19	1.28	1.36	1.23	1.23	1.23	1.23	1.23
1941	0.79	0.91	1.02	1.12	1.21	1.2	1.2	1.2	1.2	1.2
1942	0.82	0.93	1.03	1.13	1.22	1.16	1.16	1.16	1.16	1.16
1943	0.95	1.06	1.17	1.27	1.36	1.14	1.14	1.14	1.14	1.14
1944	0.86	0.97	1.08	1.17	1.27	1.12	1.12	1.12	1.12	1.12

1945	0.89	1	1.11	1.21	1.3	1.1	1.1	1.1	1.1	1.1
1946	0.91	1.03	1.14	1.24	1.34	1.12	1.12	1.12	1.12	1.12
1947	0.93	1.04	1.14	1.24	1.33	1.11	1.11	1.11	1.11	1.11
1948	0.81	0.93	1.03	1.13	1.22	1.11	1.11	1.11	1.11	1.11
1949	0.93	1.05	1.16	1.27	1.36	1.15	1.15	1.15	1.15	1.15
1950	0.95	1.06	1.17	1.26	1.35	1.12	1.12	1.12	1.12	1.12
1951	0.96	1.08	1.19	1.29	1.38	1.12	1.12	1.12	1.12	1.12
1952	0.9	1.02	1.13	1.23	1.33	1.15	1.15	1.15	1.15	1.15
1953	0.7	0.82	0.94	1.05	1.14	1.13	1.13	1.13	1.13	1.13
1954	0.77	0.89	1	1.11	1.21	1.13	1.13	1.13	1.13	1.13
1955	0.83	0.94	1.05	1.15	1.24	1.12	1.12	1.12	1.12	1.12
1956	0.82	0.93	1.04	1.14	1.23	1.1	1.1	1.1	1.1	1.1
1957	0.93	1.05	1.16	1.26	1.35	1.06	1.06	1.06	1.06	1.06
1958	1.11	1.21	1.31	1.4	1.48	1.08	1.08	1.08	1.08	1.08
1959	0.78	0.89	1	1.1	1.19	1.06	1.06	1.06	1.06	1.06
1960	0.93	1.03	1.13	1.22	1.3	1.04	1.04	1.04	1.04	1.04
1961	0.97	1.07	1.17	1.25	1.34	1.02	1.02	1.02	1.02	1.02
1962	1.03	1.15	1.25	1.35	1.43	0.99	0.99	0.99	0.99	0.99
1963	1.09	1.19	1.29	1.37	1.46	0.96	0.96	0.96	0.96	0.96
1964	0.96	1.07	1.16	1.25	1.34	0.95	0.95	0.95	0.95	0.95
1965	0.83	0.95	1.05	1.15	1.24	0.92	0.92	0.92	0.92	0.92
1966	0.86	0.96	1.05	1.14	1.22	0.86	0.86	0.86	0.86	0.86
1967	0.94	1.04	1.14	1.23	1.31	0.84	0.84	0.84	0.84	0.84
1968	0.98	1.08	1.18	1.27	1.35	0.87	0.87	0.87	0.87	0.87
1969	0.81	0.91	1	1.09	1.17	0.81	0.81	0.81	0.81	0.81
1970	0.89	1	1.1	1.19	1.28	0.74	0.74	0.74	0.74	0.74
1971	0.84	0.95	1.05	1.14	1.23	0.73	0.73	0.73	0.73	0.73
1972	0.97	1.07	1.17	1.25	1.33	0.67	0.67	0.67	0.67	0.67
1973	1.01	1.11	1.21	1.31	1.39	0.64	0.64	0.64	0.64	0.64
1974	0.98	1.1	1.2	1.3	1.39	0.69	0.69	0.69	0.69	0.69
1975	0.96	1.07	1.18	1.27	1.36	0.79	0.79	0.79	0.79	0.79
1976	0.83	0.94	1.03	1.12	1.21	0.76	0.76	0.76	0.76	0.76
1977	0.78	0.89	1	1.1	1.19	0.7	0.7	0.7	0.7	0.7
1978	0.9	1.01	1.11	1.2	1.28	0.74	0.74	0.74	0.74	0.74
1979	0.87	0.98	1.07	1.16	1.24	0.71	0.71	0.71	0.71	0.71
1980	0.93	1.04	1.14	1.23	1.32	0.79	0.79	0.79	0.79	0.79
1981	0.8	0.9	1	1.09	1.18	0.81	0.81	0.81	0.81	0.81
1982	0.86	0.97	1.07	1.16	1.25	0.81	0.81	0.81	0.81	0.81
1983	0.95	1.06	1.16	1.25	1.34	0.85	0.85	0.85	0.85	0.85
1984	0.79	0.9	1.01	1.1	1.19	0.8	0.8	0.8	0.8	0.8
1985	0.87	0.98	1.08	1.17	1.26	0.87	0.87	0.87	0.87	0.87
1986	0.65	0.77	0.89	0.99	1.09	0.9	0.9	0.9	0.9	0.9
1987	0.61	0.73	0.84	0.94	1.03	0.89	0.89	0.89	0.89	0.89
1988	0.67	0.78	0.89	0.99	1.08	0.86	0.86	0.86	0.86	0.86
1989	0.78	0.89	0.98	1.08	1.16	0.82	0.82	0.82	0.82	0.82
1990	0.91	1.03	1.14	1.25	1.35	0.83	0.83	0.83	0.83	0.83
1991	0.95	1.06	1.17	1.27	1.36	0.82	0.82	0.82	0.82	0.82
1992	1.01	1.12	1.21	1.3	1.39	0.86	0.86	0.86	0.86	0.86

1993	0.81	0.92	1.02	1.12	1.21	0.85	0.85	0.85	0.85	0.85
1994	0.9	1.01	1.11	1.21	1.3	0.79	0.79	0.79	0.79	0.79
1995	1.03	1.14	1.25	1.34	1.43	0.91	0.91	0.91	0.91	0.91
1996	0.86	0.96	1.06	1.15	1.23	0.9	0.9	0.9	0.9	0.9
1997	0.94	1.05	1.14	1.23	1.32	0.89	0.89	0.89	0.89	0.89
1998	0.87	0.98	1.09	1.2	1.29	0.9	0.9	0.9	0.9	0.9
Average	0.8856	0.9959	1.0992	1.1946	1.2832	0.9337	0.9337	0.9337	0.9337	0.9337

Year	<i>Slope (ARIM Index of ARIM_{low} at 1700m)</i>					<i>Slope (ARIM Index of ARIM_{high} at 1700m)</i>				
	1	2	3	4	5	1	2	3	4	5
1940	1.74	1.84	1.93	2.02	2.1	1.3	1.3	1.3	1.3	1.3
1941	1.45	1.56	1.66	1.76	1.85	1.28	1.28	1.28	1.28	1.28
1942	1.46	1.57	1.67	1.76	1.85	1.25	1.25	1.25	1.25	1.25
1943	1.74	1.85	1.96	2.05	2.14	1.24	1.24	1.24	1.24	1.24
1944	1.56	1.67	1.78	1.87	1.96	1.23	1.23	1.23	1.23	1.23
1945	1.63	1.74	1.84	1.94	2.02	1.2	1.2	1.2	1.2	1.2
1946	1.71	1.83	1.94	2.04	2.13	1.21	1.21	1.21	1.21	1.21
1947	1.7	1.8	1.9	1.99	2.07	1.22	1.22	1.22	1.22	1.22
1948	1.48	1.59	1.69	1.79	1.88	1.21	1.21	1.21	1.21	1.21
1949	1.75	1.86	1.97	2.07	2.16	1.24	1.24	1.24	1.24	1.24
1950	1.73	1.84	1.94	2.03	2.11	1.22	1.22	1.22	1.22	1.22
1951	1.79	1.9	2.01	2.1	2.19	1.22	1.22	1.22	1.22	1.22
1952	1.69	1.8	1.91	2.01	2.1	1.24	1.24	1.24	1.24	1.24
1953	1.32	1.44	1.55	1.65	1.75	1.23	1.23	1.23	1.23	1.23
1954	1.44	1.56	1.67	1.77	1.86	1.23	1.23	1.23	1.23	1.23
1955	1.53	1.64	1.74	1.84	1.93	1.22	1.22	1.22	1.22	1.22
1956	1.51	1.62	1.72	1.82	1.91	1.2	1.2	1.2	1.2	1.2
1957	1.75	1.86	1.97	2.06	2.15	1.17	1.17	1.17	1.17	1.17
1958	2.01	2.11	2.21	2.29	2.37	1.2	1.2	1.2	1.2	1.2
1959	1.43	1.54	1.64	1.74	1.82	1.17	1.17	1.17	1.17	1.17
1960	1.66	1.76	1.85	1.94	2.02	1.15	1.15	1.15	1.15	1.15
1961	1.73	1.83	1.92	2.01	2.09	1.14	1.14	1.14	1.14	1.14
1962	1.93	2.04	2.14	2.23	2.31	1.12	1.12	1.12	1.12	1.12
1963	1.99	2.09	2.18	2.26	2.34	1.1	1.1	1.1	1.1	1.1
1964	1.76	1.86	1.95	2.04	2.12	1.09	1.09	1.09	1.09	1.09
1965	1.56	1.67	1.77	1.87	1.96	1.07	1.07	1.07	1.07	1.07
1966	1.55	1.65	1.74	1.82	1.9	1.02	1.02	1.02	1.02	1.02
1967	1.72	1.82	1.91	2	2.08	1	1	1	1	1
1968	1.8	1.9	1.99	2.08	2.16	1.04	1.04	1.04	1.04	1.04
1969	1.45	1.54	1.63	1.71	1.79	0.98	0.98	0.98	0.98	0.98
1970	1.68	1.78	1.88	1.97	2.05	0.93	0.93	0.93	0.93	0.93
1971	1.57	1.68	1.78	1.87	1.95	0.92	0.92	0.92	0.92	0.92
1972	1.8	1.9	1.99	2.07	2.15	0.87	0.87	0.87	0.87	0.87
1973	1.92	2.02	2.12	2.21	2.29	0.84	0.84	0.84	0.84	0.84
1974	1.9	2	2.1	2.2	2.28	0.88	0.88	0.88	0.88	0.88

1975	1.84	1.95	2.05	2.14	2.23	0.97	0.97	0.97	0.97	0.97
1976	1.54	1.64	1.73	1.82	1.9	0.95	0.95	0.95	0.95	0.95
1977	1.49	1.6	1.7	1.8	1.88	0.9	0.9	0.9	0.9	0.9
1978	1.69	1.79	1.89	1.98	2.06	0.93	0.93	0.93	0.93	0.93
1979	1.61	1.71	1.8	1.89	1.97	0.9	0.9	0.9	0.9	0.9
1980	1.76	1.86	1.96	2.05	2.13	0.97	0.97	0.97	0.97	0.97
1981	1.47	1.57	1.67	1.76	1.84	0.99	0.99	0.99	0.99	0.99
1982	1.6	1.7	1.8	1.89	1.98	0.98	0.98	0.98	0.98	0.98
1983	1.78	1.88	1.98	2.07	2.15	1.01	1.01	1.01	1.01	1.01
1984	1.49	1.6	1.7	1.79	1.88	0.97	0.97	0.97	0.97	0.97
1985	1.62	1.72	1.82	1.91	1.99	1.03	1.03	1.03	1.03	1.03
1986	1.26	1.38	1.48	1.58	1.68	1.06	1.06	1.06	1.06	1.06
1987	1.16	1.27	1.38	1.47	1.56	1.05	1.05	1.05	1.05	1.05
1988	1.25	1.36	1.47	1.56	1.65	1.03	1.03	1.03	1.03	1.03
1989	1.43	1.53	1.62	1.71	1.8	0.98	0.98	0.98	0.98	0.98
1990	1.79	1.91	2.02	2.12	2.22	0.99	0.99	0.99	0.99	0.99
1991	1.82	1.93	2.04	2.13	2.22	0.98	0.98	0.98	0.98	0.98
1992	1.87	1.97	2.06	2.15	2.23	1.03	1.03	1.03	1.03	1.03
1993	1.51	1.62	1.71	1.81	1.89	1.01	1.01	1.01	1.01	1.01
1994	1.69	1.8	1.9	1.99	2.08	0.96	0.96	0.96	0.96	0.96
1995	1.95	2.06	2.16	2.25	2.34	1.06	1.06	1.06	1.06	1.06
1996	1.54	1.64	1.73	1.82	1.89	1.05	1.05	1.05	1.05	1.05
1997	1.72	1.82	1.91	2	2.08	1.05	1.05	1.05	1.05	1.05
1998	1.66	1.77	1.88	1.97	2.06	1.05	1.05	1.05	1.05	1.05

Year	<i>Slope (ARIM Index of ARIM_{high} at 1800m)</i>					<i>Slope (ARIM Index of Buffering Zone (1650 - 1850m))</i>				
	1	2	3	4	5	1	2	3	4	5
1940	1.23	1.23	1.23	1.23	1.23	1.4233	1.4567	1.4867	1.5167	1.5433
1941	1.2	1.2	1.2	1.2	1.2	1.31	1.3467	1.38	1.4133	1.4433
1942	1.16	1.16	1.16	1.16	1.16	1.29	1.3267	1.36	1.39	1.42
1943	1.14	1.14	1.14	1.14	1.14	1.3733	1.41	1.4467	1.4767	1.5067
1944	1.12	1.12	1.12	1.12	1.12	1.3033	1.34	1.3767	1.4067	1.4367
1945	1.1	1.1	1.1	1.1	1.1	1.31	1.3467	1.38	1.4133	1.44
1946	1.12	1.12	1.12	1.12	1.12	1.3467	1.3867	1.4233	1.4567	1.4867
1947	1.11	1.11	1.11	1.11	1.11	1.3433	1.3767	1.41	1.44	1.4667
1948	1.11	1.11	1.11	1.11	1.11	1.2667	1.3033	1.3367	1.37	1.4
1949	1.15	1.15	1.15	1.15	1.15	1.38	1.4167	1.4533	1.4867	1.5167
1950	1.12	1.12	1.12	1.12	1.12	1.3567	1.3933	1.4267	1.4567	1.4833
1951	1.12	1.12	1.12	1.12	1.12	1.3767	1.4133	1.45	1.48	1.51
1952	1.15	1.15	1.15	1.15	1.15	1.36	1.3967	1.4333	1.4667	1.4967
1953	1.13	1.13	1.13	1.13	1.13	1.2267	1.2667	1.3033	1.3367	1.37
1954	1.13	1.13	1.13	1.13	1.13	1.2667	1.3067	1.3433	1.3767	1.4067
1955	1.12	1.12	1.12	1.12	1.12	1.29	1.3267	1.36	1.3933	1.4233
1956	1.1	1.1	1.1	1.1	1.1	1.27	1.3067	1.34	1.3733	1.4033

1957	1.06	1.06	1.06	1.06	1.06	1.3267	1.3633	1.4	1.43	1.46
1958	1.08	1.08	1.08	1.08	1.08	1.43	1.4633	1.4967	1.5233	1.55
1959	1.06	1.06	1.06	1.06	1.06	1.22	1.2567	1.29	1.3233	1.35
1960	1.04	1.04	1.04	1.04	1.04	1.2833	1.3167	1.3467	1.3767	1.4033
1961	1.02	1.02	1.02	1.02	1.02	1.2967	1.33	1.36	1.39	1.4167
1962	0.99	0.99	0.99	0.99	0.99	1.3467	1.3833	1.4167	1.4467	1.4733
1963	0.96	0.96	0.96	0.96	0.96	1.35	1.3833	1.4133	1.44	1.4667
1964	0.95	0.95	0.95	0.95	0.95	1.2667	1.3	1.33	1.36	1.3867
1965	0.92	0.92	0.92	0.92	0.92	1.1833	1.22	1.2533	1.2867	1.3167
1966	0.86	0.86	0.86	0.86	0.86	1.1433	1.1767	1.2067	1.2333	1.26
1967	0.84	0.84	0.84	0.84	0.84	1.1867	1.22	1.25	1.28	1.3067
1968	0.87	0.87	0.87	0.87	0.87	1.2367	1.27	1.3	1.33	1.3567
1969	0.81	0.81	0.81	0.81	0.81	1.08	1.11	1.14	1.1667	1.1933
1970	0.74	0.74	0.74	0.74	0.74	1.1167	1.15	1.1833	1.2133	1.24
1971	0.73	0.73	0.73	0.73	0.73	1.0733	1.11	1.1433	1.1733	1.2
1972	0.67	0.67	0.67	0.67	0.67	1.1133	1.1467	1.1767	1.2033	1.23
1973	0.64	0.64	0.64	0.64	0.64	1.1333	1.1667	1.2	1.23	1.2567
1974	0.69	0.69	0.69	0.69	0.69	1.1567	1.19	1.2233	1.2567	1.2833
1975	0.79	0.79	0.79	0.79	0.79	1.2	1.2367	1.27	1.3	1.33
1976	0.76	0.76	0.76	0.76	0.76	1.0833	1.1167	1.1467	1.1767	1.2033
1977	0.7	0.7	0.7	0.7	0.7	1.03	1.0667	1.1	1.1333	1.16
1978	0.74	0.74	0.74	0.74	0.74	1.12	1.1533	1.1867	1.2167	1.2433
1979	0.71	0.71	0.71	0.71	0.71	1.0733	1.1067	1.1367	1.1667	1.1933
1980	0.79	0.79	0.79	0.79	0.79	1.1733	1.2067	1.24	1.27	1.2967
1981	0.81	0.81	0.81	0.81	0.81	1.09	1.1233	1.1567	1.1867	1.2133
1982	0.81	0.81	0.81	0.81	0.81	1.13	1.1633	1.1967	1.2267	1.2567
1983	0.85	0.85	0.85	0.85	0.85	1.2133	1.2467	1.28	1.31	1.3367
1984	0.8	0.8	0.8	0.8	0.8	1.0867	1.1233	1.1567	1.1867	1.2167
1985	0.87	0.87	0.87	0.87	0.87	1.1733	1.2067	1.24	1.27	1.2967
1986	0.9	0.9	0.9	0.9	0.9	1.0733	1.1133	1.1467	1.18	1.2133
1987	0.89	0.89	0.89	0.89	0.89	1.0333	1.07	1.1067	1.1367	1.1667
1988	0.86	0.86	0.86	0.86	0.86	1.0467	1.0833	1.12	1.15	1.18
1989	0.82	0.82	0.82	0.82	0.82	1.0767	1.11	1.14	1.17	1.2
1990	0.83	0.83	0.83	0.83	0.83	1.2033	1.2433	1.28	1.3133	1.3467
1991	0.82	0.82	0.82	0.82	0.82	1.2067	1.2433	1.28	1.31	1.34
1992	0.86	0.86	0.86	0.86	0.86	1.2533	1.2867	1.3167	1.3467	1.3733
1993	0.85	0.85	0.85	0.85	0.85	1.1233	1.16	1.19	1.2233	1.25
1994	0.79	0.79	0.79	0.79	0.79	1.1467	1.1833	1.2167	1.2467	1.2767
1995	0.91	0.91	0.91	0.91	0.91	1.3067	1.3433	1.3767	1.4067	1.4367
1996	0.9	0.9	0.9	0.9	0.9	1.1633	1.1967	1.2267	1.2567	1.28
1997	0.89	0.89	0.89	0.89	0.89	1.22	1.2533	1.2833	1.3133	1.34
1998	0.9	0.9	0.9	0.9	0.9	1.2033	1.24	1.2767	1.3067	1.3367
Average						1.2181	1.2534	1.2866	1.3173	1.3456

5.4. Sensitivity Analyses with Gradients of Distance to Stream

In estimating the sensitivity of red spruce growth according to variations of Distance to Stream, the elevation was classified into three ranges – high (>1850 m), buffer (1650 to 1850 m) and low (1400 to 1650 m). Therefore, the sensitivity of red spruce growth for Distance to Stream was computed and averaged for three classes (**1**, **2** and **3**) at three elevation ranges separately. The indices of high elevation were computed by $ARIM_{high}$ at 1900m and low elevation $ARIM_{low}$ at 1600m. The index values of buffer range were obtained by averaging values at 1700 m estimated by $ARIM_{low}$ and 1700 and 1800 m estimated by $ARIM_{high}$ (Distance to Stream headings are written in italics and underlined in the following table). The indices of $ARIM_{low}$ were modified by being divided by 2 in order to reduce the effects of this variable on modeling. This is because, in the sensitivity analyses, the indices of $ARIM_{low}$ for Distance to Stream were relatively higher than others. All values in the table are unitless indices of ARIMs.

Year	Distance to Stream (ARIM Index of $ARIM_{low}$: Original Value)			Distance to Stream (ARIM Index of $ARIM_{low}$: Modified Value = Original Value / 2)		
	1	2	3	1	2	3
1940	3.45	2.32	1.19	1.725	1.16	0.595
1941	3.28	2.15	1.02	1.64	1.075	0.51
1942	3.3	2.17	1.03	1.65	1.085	0.515
1943	3.43	2.3	1.17	1.715	1.15	0.585
1944	3.34	2.21	1.08	1.67	1.105	0.54
1945	3.37	2.24	1.11	1.685	1.12	0.555
1946	3.4	2.27	1.14	1.7	1.135	0.57
1947	3.41	2.28	1.14	1.705	1.14	0.57
1948	3.3	2.17	1.03	1.65	1.085	0.515
1949	3.43	2.3	1.16	1.715	1.15	0.58
1950	3.43	2.3	1.17	1.715	1.15	0.585
1951	3.45	2.32	1.19	1.725	1.16	0.595
1952	3.39	2.26	1.13	1.695	1.13	0.565
1953	3.2	2.07	0.94	1.6	1.035	0.47
1954	3.27	2.14	1	1.635	1.07	0.5
1955	3.32	2.18	1.05	1.66	1.09	0.525
1956	3.31	2.17	1.04	1.655	1.085	0.52
1957	3.42	2.29	1.16	1.71	1.145	0.58
1958	3.57	2.44	1.31	1.785	1.22	0.655

1959	3.26	2.13	1	1.63	1.065	0.5
1960	3.39	2.26	1.13	1.695	1.13	0.565
1961	3.43	2.3	1.17	1.715	1.15	0.585
1962	3.51	2.38	1.25	1.755	1.19	0.625
1963	3.55	2.42	1.29	1.775	1.21	0.645
1964	3.43	2.3	1.16	1.715	1.15	0.58
1965	3.32	2.18	1.05	1.66	1.09	0.525
1966	3.32	2.19	1.05	1.66	1.095	0.525
1967	3.4	2.27	1.14	1.7	1.135	0.57
1968	3.44	2.31	1.18	1.72	1.155	0.59
1969	3.27	2.14	1	1.635	1.07	0.5
1970	3.36	2.23	1.1	1.68	1.115	0.55
1971	3.31	2.18	1.05	1.655	1.09	0.525
1972	3.43	2.3	1.17	1.715	1.15	0.585
1973	3.48	2.35	1.21	1.74	1.175	0.605
1974	3.47	2.33	1.2	1.735	1.165	0.6
1975	3.44	2.31	1.18	1.72	1.155	0.59
1976	3.3	2.16	1.03	1.65	1.08	0.515
1977	3.26	2.13	1	1.63	1.065	0.5
1978	3.37	2.24	1.11	1.685	1.12	0.555
1979	3.34	2.2	1.07	1.67	1.1	0.535
1980	3.4	2.27	1.14	1.7	1.135	0.57
1981	3.27	2.13	1	1.635	1.065	0.5
1982	3.33	2.2	1.07	1.665	1.1	0.535
1983	3.42	2.29	1.16	1.71	1.145	0.58
1984	3.27	2.14	1.01	1.635	1.07	0.505
1985	3.34	2.21	1.08	1.67	1.105	0.54
1986	3.15	2.02	0.89	1.575	1.01	0.445
1987	3.1	1.97	0.84	1.55	0.985	0.42
1988	3.15	2.02	0.89	1.575	1.01	0.445
1989	3.25	2.12	0.98	1.625	1.06	0.49
1990	3.41	2.28	1.14	1.705	1.14	0.57
1991	3.44	2.3	1.17	1.72	1.15	0.585
1992	3.48	2.34	1.21	1.74	1.17	0.605
1993	3.29	2.16	1.02	1.645	1.08	0.51
1994	3.38	2.25	1.11	1.69	1.125	0.555
1995	3.51	2.38	1.25	1.755	1.19	0.625
1996	3.32	2.19	1.06	1.66	1.095	0.53
1997	3.41	2.28	1.14	1.705	1.14	0.57
1998	3.36	2.23	1.09	1.68	1.115	0.545
Average	3.36322	2.231695	1.099153	1.68161	1.11585	0.549576

Year	<i>Distance to Stream (ARIM Index of ARIM_{low} at 1700m: Original Value)</i>			<i>Distance to Stream (ARIM Index of ARIM_{low} at 1700m: Modified Value = Original Value/2)</i>		
	1	2	3	1	2	3
1940	4.2	3.06	1.93	2.1	1.53	0.965
1941	3.93	2.8	1.66	1.965	1.4	0.83
1942	3.94	2.8	1.67	1.97	1.4	0.835
1943	4.22	3.09	1.96	2.11	1.545	0.98
1944	4.04	2.91	1.78	2.02	1.455	0.89
1945	4.11	2.97	1.84	2.055	1.485	0.92
1946	4.2	3.07	1.94	2.1	1.535	0.97
1947	4.16	3.03	1.9	2.08	1.515	0.95
1948	3.96	2.82	1.69	1.98	1.41	0.845
1949	4.24	3.1	1.97	2.12	1.55	0.985
1950	4.2	3.07	1.94	2.1	1.535	0.97
1951	4.27	3.14	2.01	2.135	1.57	1.005
1952	4.17	3.04	1.91	2.085	1.52	0.955
1953	3.82	2.68	1.55	1.91	1.34	0.775
1954	3.93	2.8	1.67	1.965	1.4	0.835
1955	4.01	2.87	1.74	2.005	1.435	0.87
1956	3.99	2.85	1.72	1.995	1.425	0.86
1957	4.23	3.1	1.97	2.115	1.55	0.985
1958	4.47	3.34	2.21	2.235	1.67	1.105
1959	3.91	2.77	1.64	1.955	1.385	0.82
1960	4.12	2.98	1.85	2.06	1.49	0.925
1961	4.19	3.05	1.92	2.095	1.525	0.96
1962	4.4	3.27	2.14	2.2	1.635	1.07
1963	4.44	3.31	2.18	2.22	1.655	1.09
1964	4.22	3.08	1.95	2.11	1.54	0.975
1965	4.04	2.91	1.77	2.02	1.455	0.885
1966	4	2.87	1.74	2	1.435	0.87
1967	4.17	3.04	1.91	2.085	1.52	0.955
1968	4.26	3.12	1.99	2.13	1.56	0.995
1969	3.89	2.76	1.63	1.945	1.38	0.815
1970	4.14	3.01	1.88	2.07	1.505	0.94
1971	4.04	2.91	1.78	2.02	1.455	0.89
1972	4.25	3.12	1.99	2.125	1.56	0.995
1973	4.39	3.25	2.12	2.195	1.625	1.06
1974	4.37	3.24	2.1	2.185	1.62	1.05
1975	4.31	3.18	2.05	2.155	1.59	1.025
1976	4	2.86	1.73	2	1.43	0.865
1977	3.97	2.84	1.7	1.985	1.42	0.85
1978	4.15	3.02	1.89	2.075	1.51	0.945
1979	4.07	2.94	1.8	2.035	1.47	0.9
1980	4.22	3.09	1.96	2.11	1.545	0.98
1981	3.93	2.8	1.67	1.965	1.4	0.835
1982	4.07	2.93	1.8	2.035	1.465	0.9
1983	4.24	3.11	1.98	2.12	1.555	0.99
1984	3.96	2.83	1.7	1.98	1.415	0.85
1985	4.08	2.95	1.82	2.04	1.475	0.91

1986	3.75	2.62	1.48	1.875	1.31	0.74
1987	3.64	2.51	1.38	1.82	1.255	0.69
1988	3.73	2.6	1.47	1.865	1.3	0.735
1989	3.89	2.76	1.62	1.945	1.38	0.81
1990	4.28	3.15	2.02	2.14	1.575	1.01
1991	4.3	3.17	2.04	2.15	1.585	1.02
1992	4.33	3.2	2.06	2.165	1.6	1.03
1993	3.98	2.85	1.71	1.99	1.425	0.855
1994	4.17	3.03	1.9	2.085	1.515	0.95
1995	4.42	3.29	2.16	2.21	1.645	1.08
1996	4	2.86	1.73	2	1.43	0.865
1997	4.18	3.05	1.91	2.09	1.525	0.955
1998	4.14	3.01	1.88	2.07	1.505	0.94

Year	<i><u>Distance to Stream (ARIM Index of ARIM_{high} at 1700m)</u></i>			<i><u>Distance to Stream (ARIM Index of ARIM_{high} at 1800m)</u></i>		
	1	2	3	1	2	3
1940	1.3	1.3	1.3	1.23	1.23	1.23
1941	1.28	1.28	1.28	1.2	1.2	1.2
1942	1.25	1.25	1.25	1.16	1.16	1.16
1943	1.24	1.24	1.24	1.14	1.14	1.14
1944	1.23	1.23	1.23	1.12	1.12	1.12
1945	1.2	1.2	1.2	1.1	1.1	1.1
1946	1.21	1.21	1.21	1.12	1.12	1.12
1947	1.22	1.22	1.22	1.11	1.11	1.11
1948	1.21	1.21	1.21	1.11	1.11	1.11
1949	1.24	1.24	1.24	1.15	1.15	1.15
1950	1.22	1.22	1.22	1.12	1.12	1.12
1951	1.22	1.22	1.22	1.12	1.12	1.12
1952	1.24	1.24	1.24	1.15	1.15	1.15
1953	1.23	1.23	1.23	1.13	1.13	1.13
1954	1.23	1.23	1.23	1.13	1.13	1.13
1955	1.22	1.22	1.22	1.12	1.12	1.12
1956	1.2	1.2	1.2	1.1	1.1	1.1
1957	1.17	1.17	1.17	1.06	1.06	1.06
1958	1.2	1.2	1.2	1.08	1.08	1.08
1959	1.17	1.17	1.17	1.06	1.06	1.06
1960	1.15	1.15	1.15	1.04	1.04	1.04
1961	1.14	1.14	1.14	1.02	1.02	1.02
1962	1.12	1.12	1.12	0.99	0.99	0.99
1963	1.1	1.1	1.1	0.96	0.96	0.96
1964	1.09	1.09	1.09	0.95	0.95	0.95
1965	1.07	1.07	1.07	0.92	0.92	0.92
1966	1.02	1.02	1.02	0.86	0.86	0.86
1967	1	1	1	0.84	0.84	0.84
1968	1.04	1.04	1.04	0.87	0.87	0.87
1969	0.98	0.98	0.98	0.81	0.81	0.81
1970	0.93	0.93	0.93	0.74	0.74	0.74

1971	0.92	0.92	0.92	0.73	0.73	0.73
1972	0.87	0.87	0.87	0.67	0.67	0.67
1973	0.84	0.84	0.84	0.64	0.64	0.64
1974	0.88	0.88	0.88	0.69	0.69	0.69
1975	0.97	0.97	0.97	0.79	0.79	0.79
1976	0.95	0.95	0.95	0.76	0.76	0.76
1977	0.9	0.9	0.9	0.7	0.7	0.7
1978	0.93	0.93	0.93	0.74	0.74	0.74
1979	0.9	0.9	0.9	0.71	0.71	0.71
1980	0.97	0.97	0.97	0.79	0.79	0.79
1981	0.99	0.99	0.99	0.81	0.81	0.81
1982	0.98	0.98	0.98	0.81	0.81	0.81
1983	1.01	1.01	1.01	0.85	0.85	0.85
1984	0.97	0.97	0.97	0.8	0.8	0.8
1985	1.03	1.03	1.03	0.87	0.87	0.87
1986	1.06	1.06	1.06	0.9	0.9	0.9
1987	1.05	1.05	1.05	0.89	0.89	0.89
1988	1.03	1.03	1.03	0.86	0.86	0.86
1989	0.98	0.98	0.98	0.82	0.82	0.82
1990	0.99	0.99	0.99	0.83	0.83	0.83
1991	0.98	0.98	0.98	0.82	0.82	0.82
1992	1.03	1.03	1.03	0.86	0.86	0.86
1993	1.01	1.01	1.01	0.85	0.85	0.85
1994	0.96	0.96	0.96	0.79	0.79	0.79
1995	1.06	1.06	1.06	0.91	0.91	0.91
1996	1.05	1.05	1.05	0.9	0.9	0.9
1997	1.05	1.05	1.05	0.89	0.89	0.89
1998	1.05	1.05	1.05	0.9	0.9	0.9

Year	Distance to Stream (ARIM Index of ARIM _{high})			<i>Distance to Stream (ARIM Index of ARIM_{high} of Buffer Zone at 1650 - 1850m)</i>		
	1	2	3	1	2	3
1940	1.23	1.23	1.23	1.54333	1.35333	1.165
1941	1.2	1.2	1.2	1.48167	1.29333	1.10333
1942	1.16	1.16	1.16	1.46	1.27	1.08167
1943	1.14	1.14	1.14	1.49667	1.30833	1.12
1944	1.12	1.12	1.12	1.45667	1.26833	1.08
1945	1.1	1.1	1.1	1.45167	1.26167	1.07333
1946	1.12	1.12	1.12	1.47667	1.28833	1.1
1947	1.11	1.11	1.11	1.47	1.28167	1.09333
1948	1.11	1.11	1.11	1.43333	1.24333	1.055
1949	1.15	1.15	1.15	1.50333	1.31333	1.125
1950	1.12	1.12	1.12	1.48	1.29167	1.10333
1951	1.12	1.12	1.12	1.49167	1.30333	1.115
1952	1.15	1.15	1.15	1.49167	1.30333	1.115

1953	1.13	1.13	1.13	1.42333	1.23333	1.045
1954	1.13	1.13	1.13	1.44167	1.25333	1.065
1955	1.12	1.12	1.12	1.44833	1.25833	1.07
1956	1.1	1.1	1.1	1.43167	1.24167	1.05333
1957	1.06	1.06	1.06	1.44833	1.26	1.07167
1958	1.08	1.08	1.08	1.505	1.31667	1.12833
1959	1.06	1.06	1.06	1.395	1.205	1.01667
1960	1.04	1.04	1.04	1.41667	1.22667	1.03833
1961	1.02	1.02	1.02	1.41833	1.22833	1.04
1962	0.99	0.99	0.99	1.43667	1.24833	1.06
1963	0.96	0.96	0.96	1.42667	1.23833	1.05
1964	0.95	0.95	0.95	1.38333	1.19333	1.005
1965	0.92	0.92	0.92	1.33667	1.14833	0.95833
1966	0.86	0.86	0.86	1.29333	1.105	0.91667
1967	0.84	0.84	0.84	1.30833	1.12	0.93167
1968	0.87	0.87	0.87	1.34667	1.15667	0.96833
1969	0.81	0.81	0.81	1.245	1.05667	0.86833
1970	0.74	0.74	0.74	1.24667	1.05833	0.87
1971	0.73	0.73	0.73	1.22333	1.035	0.84667
1972	0.67	0.67	0.67	1.22167	1.03333	0.845
1973	0.64	0.64	0.64	1.225	1.035	0.84667
1974	0.69	0.69	0.69	1.25167	1.06333	0.87333
1975	0.79	0.79	0.79	1.305	1.11667	0.92833
1976	0.76	0.76	0.76	1.23667	1.04667	0.85833
1977	0.7	0.7	0.7	1.195	1.00667	0.81667
1978	0.74	0.74	0.74	1.24833	1.06	0.87167
1979	0.71	0.71	0.71	1.215	1.02667	0.83667
1980	0.79	0.79	0.79	1.29	1.10167	0.91333
1981	0.81	0.81	0.81	1.255	1.06667	0.87833
1982	0.81	0.81	0.81	1.275	1.085	0.89667
1983	0.85	0.85	0.85	1.32667	1.13833	0.95
1984	0.8	0.8	0.8	1.25	1.06167	0.87333
1985	0.87	0.87	0.87	1.31333	1.125	0.93667
1986	0.9	0.9	0.9	1.27833	1.09	0.9
1987	0.89	0.89	0.89	1.25333	1.065	0.87667
1988	0.86	0.86	0.86	1.25167	1.06333	0.875
1989	0.82	0.82	0.82	1.24833	1.06	0.87
1990	0.83	0.83	0.83	1.32	1.13167	0.94333
1991	0.82	0.82	0.82	1.31667	1.12833	0.94
1992	0.86	0.86	0.86	1.35167	1.16333	0.97333
1993	0.85	0.85	0.85	1.28333	1.095	0.905
1994	0.79	0.79	0.79	1.27833	1.08833	0.9
1995	0.91	0.91	0.91	1.39333	1.205	1.01667
1996	0.9	0.9	0.9	1.31667	1.12667	0.93833
1997	0.89	0.89	0.89	1.34333	1.155	0.965
1998	0.9	0.9	0.9	1.34	1.15167	0.96333
Average	0.933729	0.933729	0.933729	1.35585	1.16701	0.97839

5.5. The summary of sensitivity analysis of red spruce growth for four geospatial variables

Elevation was classified into five ranges (a), Aspect four ranges (b), Slope five ranges (c) and Distance to Stream three ranges (d). The five ranges of Slope and three ranges of Distance to Stream were divided by the natural breaks (Jenks) system of the Reclassify function in Spatial Analyst, ArcGIS 9.2, and the break ranges are displayed in parentheses in tables (c) and (d). The natural breaks (Jenks) system classifies the data into groups based on similar values and maximizing the differences between classes by dividing classes by relatively big differences in the data values (ArcGIS 9.2 Desktop Help: Natural breaks (Jenks)). All index values of red spruce growth are the averaged values of the period of 1940 to 1998. For Distance to Stream (DS), the original index values were modified by being divided by 2 because the relatively big ARIM indices make RSHM unrealistically sensitive to the DS variable. Also, all ARIM indices were modified by being multiplied by 10000 for GIS modeling and shown in the columns of ‘Modified ARIM Index’ of tables (a), (b) and (c).

(a)

	ARIM index	Elevations *10000 (Modified ARIM index)
Elevations (m)		
1400-1450	1.05	10500
1450-1550	1.07508475	10750.847
1550-1650	1.09915254	10991.525
1650-1850	1.28661017	12866.102
>1850	0.93372881	9337.2881

(b)

Elevation	ARIM index			Aspect*10000 (Modified ARIM index)		
Aspect (°)	High	Low	Buffering Zone	High	Low	Buffering Zone
North (0 – 45, 315 – 360)	0.93372881	1.0991525	1.286610169	9337.288136	10991.5254	12866.10169
East (45 – 135)	0.93372881	1.5628814	1.442259887	9337.288136	15628.8136	14422.59887

South (135 – 225)	0.93372881	0.7884746	1.18740113	9337.288136	7884.74576	11874.0113
West (225 – 315)	0.93372881	1.4944068	1.420282486	9337.288136	14944.0678	14202.82486

(c)

Elevation	ARIM index			Slope*10000 (Modified ARIM index)		
	Slope (°)	High	Low	Buffering Zone	High	Low
1 (0-11.68268)	0.93372881	0.8855932	1.218079096	9337.288136	8855.9322	12180.79096
2 (11.68268-19.471133)	0.93372881	0.9959322	1.253446328	9337.288136	9959.32203	12534.46328
3 (19.471133-26.529418)	0.93372881	1.0991525	1.286610169	9337.288136	10991.5254	12866.10169
4 (26.529418-33.100926)	0.93372881	1.1945763	1.317288136	9337.288136	11945.7627	13172.88136
5 (33.100926-62.307625)	0.93372881	1.2832203	1.34559322	9337.288136	12832.2034	13455.9322

(d)

Elevation	ARIM index			Distance to Stream*10000 (Modified ARIM index)		
	Distance to Stream (m)	High	Low	Buffering Zone	High	Low
1 (0-149.277172)	0.9337	1.6816	1.3558	9337.288136	16816.1017	13558.47458
2 (149.277172-482.280094)	0.9337	1.1158	1.1670	9337.288136	11158.4746	11670.0565
3 (482.280094-979.870667)	0.9337	0.5496	0.9784	9337.288136	5495.76271	9783.898305

Appendix 6

Data of Model Evaluation

6.1. Random points, RSHM and Vegetation of Overstory and Understory

1000 random points were generated on RSHM and saved as a shapefile using Generate Random Point Tool of Hawth's Analysis Tools in ArcGIS 9.2 extension. The predicted suitability indices of RSHM and the original habitat information of the digital vegetation maps for GSMNP, including presence/absence and dominance of red spruce, were collected on the random points using the Intersect Point Tool of Hawth's Analysis Tools in ArcGIS extension. All vegetation codes were explained in Madden et al. (2004), and the vegetation codes related to red spruce appear in Table 4.2. Geographical locations of random points, longitude and latitude, were estimated from the Universal Transverse Mercator (UTM) coordinate system.

Random point	Longitude	Latitude	RSHM Suitability	Overstory Dominant Vegetation	Overstory Second Vegetation	Overstory Third Vegetation	Understory Dominant Vegetation
1	300586.330	3962069.284	0	HxL	Sb		RKl
2	301870.523	3961932.546	0	OmHL			T/Rp
3	299364.123	3961711.591	0	OmHr			Kl
4	307127.018	3961685.393	0	OmHA			HD
5	306091.723	3961571.646	0	OmHL			HD
6	299224.824	3961497.496	0	OzHf	PI		PI/Km
7	306607.364	3961359.913	0	OzH			Rh
8	308595.483	3961166.658	0	OmHL			Tu/RI
9	304252.942	3960684.778	0	CHxL	OmH		HD
10	300582.165	3960570.823	0	PI/OzH			PI/Km
11	295676.137	3960476.999	0	HxL	MAL		HD
12	302525.161	3960245.535	0	PI/OzH			Kl
13	299713.439	3960151.453	0	HxL	OmH		T/Ri
14	305428.723	3959986.748	0	NHx	OmH		Rm
15	297408.002	3959770.617	0	OmHA			HD
16	305362.925	3959744.484	0	NHx			Kl
17	305224.069	3959645.627	0	OzHf			RI
18	308063.359	3959394.067	0	OzHf			RKm
19	287926.736	3959400.628	0	OzH/PI			HD
20	300334.022	3959277.463	0	CHx	T		Tu/Rm

21	302937.872	3959167.578	0	OmH			HD
22	302518.223	3959112.056	0	CHx-T			HD
23	292505.359	3959052.874	0	OmH	MALc		Tu/Rh
24	305018.059	3959048.138	0	Hth			T/Rh
25	291568.899	3958880.132	0	OmHL			HD
26	306719.105	3958968.036	0	CHxL			HD
27	288465.007	3958679.239	0	CHx			Rh
28	296219.005	3958459.468	0	CHxL/T			T/Ri
29	307661.895	3958609.481	0	OmHr			Rh
30	294586.288	3958418.206	0	OzHf			Kh
31	296295.907	3959463.346	0	CHxL			HD
32	293061.648	3958380.101	0	OmHL			HD
33	287430.578	3958281.123	0	OmHr			Tu/Ri
34	297049.847	3958132.508	0	OmHA			T/Ri
35	292777.849	3958161.332	0	OmHr			Rh
36	292375.027	3958167.898	0	CHxL			Tu/Rm
37	301025.186	3958190.669	0	CHxR	T		T/Ri
38	296038.380	3958003.524	0	OmH	T		Rl/Sd
39	292281.582	3957998.701	0	CHx	OmH		Tu/Rm
40	300589.854	3957963.849	0	OmHL			Tu/Rl
41	294047.520	3957794.848	0	HxL			Tu/Rl
42	283208.650	3957671.306	0	CHxA			T/Rl
43	284746.999	3957561.746	0	HxL			HD
44	296520.132	3957622.701	0	OmHr			T/Ri
45	290805.385	3957502.151	0	CHxL			Tu/Rh
46	291392.780	3957336.091	0	CHxL			T/Ri
47	283916.416	3957093.482	0	HxL			Pl/Km
48	303252.037	3957370.936	0	MOr			HD
49	303943.594	3957053.018	0	MOr/Sb			RKl
50	306270.887	3957391.546	0	OmH	OzHf		Rh
51	289495.060	3957050.958	0	OzHf	OmH		Rh
52	304175.735	3957266.580	0	OcH	NHx		HD
53	305194.118	3956883.366	0	OzHf	PI		Rl
54	303497.614	3957114.690	0	MOr/Sb			Rl
55	308413.664	3956837.137	0	OmH/T			Rm/Pls-T
56	279166.496	3956778.787	0	OzH			Plx/Ki
57	285883.498	3956733.644	0	HxL			HD
58	288736.022	3956725.243	0	CHx-T			Rh
59	279459.955	3956692.695	0	OzHf			HD
60	283276.072	3956685.264	0	HxL			Pl/Km
61	299328.673	3956579.682	0	HxA/T			T/Ri
62	294123.814	3956568.760	0	OmH			Tu/Ri
63	289189.946	3956528.891	0	CHx-T			T/Ri
64	296380.322	3956511.809	11289	S	NHxB		HD
65	278547.435	3956463.316	0	MALc			HD
66	284805.830	3956442.874	0	OzH			Pls/Km
67	309108.635	3956350.504	0	OmHr			RKm
68	293591.651	3956330.577	0	CHx-T			Tu/Ri
69	288911.185	3956210.581	0	OmH			HD
70	308215.365	3956185.974	0	OzH			Hth
71	297368.463	3956051.774	13359	Sb	S		HD

72	281877.194	3955978.701	0	OzH			Tu/Ri
73	298352.850	3955996.394	13359	NHx	Hth	S	T/Ri
74	287477.722	3955976.634	0	OzHf			Rm
75	288285.239	3956008.515	0	OmHr			Kl
76	305220.105	3955846.490	0	OmHr			Rh
77	293310.001	3955827.382	0	NHxR			HD
78	276426.416	3955811.664	0	HxL			HD
79	286735.352	3955801.922	0	CHxO			HD
80	297718.625	3955683.504	13359	S	Hth		Su/Rh
81	277783.889	3955620.318	0	OzH			Pls/Kp
82	276461.101	3955567.633	0	HxL			HD
83	297150.761	3955537.268	13359	Sb	S		HD
84	309250.431	3955463.574	0	T/NHxA			T/Rh
85	294513.554	3955316.703	0	NHxR			T/Rh
86	288881.286	3955224.413	11289	NHx			Rl/Sd
87	291147.717	3955191.378	0	NHxA			HD
88	280251.362	3955089.056	0	OzH			HD
89	287248.010	3955084.324	0	OzH			HD
90	283991.801	3955064.373	0	HxL			HD
91	294110.568	3955044.904	13359	NHxA-T			T/Ri
92	280151.540	3954942.591	0	OzH			HD
93	300170.185	3954958.324	0	HxAz			Km
94	299720.139	3954909.583	0	HxA			Rl
95	285805.620	3954942.681	0	OzH/PI			Kl
96	304151.432	3954857.657	0	CHxL			HD
97	300792.214	3954782.983	0	HxA			Rl
98	309569.087	3954676.956	0	OmHp/R			Km
99	305006.113	3954610.776	0	Plp			Kh
100	285654.768	3954661.410	0	HxL	MALc		Tu/Rl
101	309360.327	3954437.471	0	MOz			RKm
102	308560.785	3954407.687	0	T/NHxA			T-S/Rm
103	294422.075	3954447.145	13359	NHx			HD
104	283192.117	3954475.169	0	CHxR			HD
105	292586.176	3954288.431	11289	S	Hth		S/Rh
106	290160.776	3954318.795	0	NHxR-T			T/Rh
107	303864.982	3954301.968	0	PI/OzH			PI/Kh
108	295860.977	3954300.164	9617	F	NHx		HD
109	281029.094	3954088.246	0	HxL			Tu/Rm
110	295985.727	3954066.658	13359	S/F			Rl
111	283568.154	3954058.971	0	CHxA			Tu/Ri
112	294444.927	3954039.996	13359	S/NHx			S/Rh
113	287444.502	3953947.396	0	OmH			HD
114	271913.250	3954056.898	0	PI-OzH			K/Rp
115	282993.201	3953782.777	0	HxL			HD
116	293131.367	3953759.861	11289	S	Hth	Sb	S/Rh
117	278802.567	3953746.724	0	OzH			HD
118	291349.567	3953889.719	0	NHxR-T			HD
119	280303.573	3953588.749	0	OzH			PIx/Kl
120	281284.343	3953539.606	0	PI			Rh
121	275295.985	3953460.179	0	OmHp/R			HD
122	303043.637	3953428.600	0	HxAz			Rh

123	308237.804	3953417.402	11289	S/NHxA			S/Sb
124	305901.125	3953354.797	0	NHx			HD
125	305051.037	3953305.031	0	HxA			Rh
126	310324.015	3953271.012	0	PI	OzH		PI/Kh
127	281047.201	3953351.780	0	OzH			HD
128	287254.551	3953318.456	0	OmH			Tu/RI
129	290851.857	3953178.165	0	HxA			T/Rh
130	279134.978	3953058.623	0	OmHr			HD
131	265007.639	3952942.461	0	OcH			HD
132	282673.838	3952989.699	0	OzH			HD
133	267060.319	3952791.406	0	OzH			Rp
134	264339.499	3952718.497	0	OzH/PI			HD
135	292820.603	3953011.865	9617	NHx			T/Rh
136	265257.462	3952618.787	0	CHx			T/PIs/Rp
137	277436.811	3952782.677	0	PI			PIs/KI
138	300356.843	3952760.962	11289	Hth			Kh
139	291429.281	3952777.682	0	CHx			RI
140	292027.922	3952378.526	0	NHx-T			Rp/Sd
141	266922.208	3952417.724	0	OzH			RKp
142	304548.281	3952610.345	0	OzHf			Rh
143	293385.220	3952649.491	0	NHx-T			Rh
144	304963.822	3952508.691	0	NHxBI/R			Rh
145	297209.230	3952428.512	11289	NHxB			Rm
146	308406.672	3952395.076	13359	NHxR			HD
147	266737.594	3952367.016	0	CHxA			T/PIs/Rp
148	305253.900	3952816.579	0	HxL			HD
149	309216.190	3952718.166	0	NHxR			HD
150	287417.908	3952406.012	0	CHx-T			T/Ri
151	271423.783	3953642.761	0	MAL			HD
152	272063.053	3953571.032	0	MAL			T/Rp
153	268970.176	3953436.275	0	SV			Kp
154	276220.811	3952311.399	0	HxL			Tu/RI
155	270456.969	3952270.312	0	MAL			HD
156	263843.397	3952269.431	0	CHxA			T/PIs/Rp
157	298939.165	3952262.452	13359	NHxB			HD
158	281193.211	3952239.407	0	OzH			Km
159	259957.828	3952233.243	0	PI	OzH		HD
160	308023.230	3952219.275	13359	NHxR			KI
161	286160.784	3952165.312	0	CHx-T			T/Rh
162	305296.721	3952154.887	0	CHx			HD
163	288882.979	3952146.597	0	CHx-T			T/Ri
164	301924.171	3952120.517	0	NHx/T			Rh
165	283827.557	3952073.584	0	HxL			RI
166	308715.652	3952065.894	0	OmHp/R			KI
167	284935.086	3952020.239	0	HxL			Rm
168	286834.014	3952010.659	0	CHx-T			T/Ri
169	274471.102	3951927.201	0	OzH			RKi
170	280906.938	3951913.238	0	OzH			KI
171	274132.469	3951935.057	0	OzH			HD
172	284974.968	3951835.365	0	HxL			HD
173	256225.284	3951851.541	0	PI			HD

174	288294.159	3951813.224	0	HxA-T			Tu/Ri
175	280966.919	3951803.167	0	OzH			Kl
176	294534.293	3951757.796	13359	S/NHx			HD
177	255699.781	3951739.623	0	CHxA	Pls		Pls/Plx/RKp
178	267899.605	3951596.212	0	OzH			PI/Kp
179	310527.444	3951550.736	0	OmHA			Pls/Kh
180	288138.942	3951549.099	0	NHx-T			Tu/Ri
181	294790.026	3951516.952	9617	Sb	S-F		Fuh
182	276598.451	3951524.697	0	CHx			T/Ri
183	302923.598	3951365.496	0	NHx/T			T/Rh
184	256792.632	3951407.865	0	CHxA	OmH		Pls/Plx/Rp
185	279968.055	3951359.572	0	OmHr			HD
186	275495.234	3951309.999	0	HxL			HD
187	288505.118	3951309.814	0	NHx			HD
188	271502.894	3951291.869	0	CHx			HD
189	289411.113	3951248.766	0	HxA-T			T/Ri
190	279820.665	3951212.056	0	OmHr			PI/Kh
191	275262.919	3951211.871	0	V			HD
192	270588.232	3951208.872	0	OmHr	OcH		HD
193	265572.151	3951103.967	0	OzH			HD
194	271015.920	3951200.553	0	MAL	T		HD
195	274389.284	3951118.616	0	CHx	OmH		Tu/Rl
196	278748.904	3951026.847	0	OmHr			Rm
197	279795.812	3950913.225	9617	NHxR			Huh
198	309366.030	3950871.955	0	OmHR			HD
199	294248.712	3950841.522	13359	Sb	F	NHx	HD
200	255399.165	3950689.765	0	OmH			PI/Kp
201	299143.360	3950680.036	13359	S/NHx			S/T/Rh
202	286877.513	3950648.805	0	OzHf			Rm
203	268559.638	3950640.007	0	PI-OzH			PI/Kp
204	292382.076	3950524.201	13359	S/NHx			S/Ri
205	262484.965	3950506.992	0	OzH/PI			HD
206	303008.362	3950497.704	13359	S/NHx			T/Rh
207	275512.245	3950499.019	0	HxL			HD
208	308077.931	3950494.513	0	MOa			PI/Km
209	277758.009	3950490.125	0	CHxR			T/Ri
210	259308.172	3950404.821	0	OmH	HxL		HD
211	263132.866	3950360.590	0	OmHR			HD
212	261887.867	3950293.423	0	OzH/PI			HD
213	302910.578	3950384.881	13359	S/NHx			S/T/Ri
214	267246.437	3950144.388	0	OzH			Pls/Rp
215	255605.245	3949985.600	0	OmH	PI	Pls	PI/Km
216	257280.274	3950083.233	0	OmHr/Pls			Pls/Rp
217	296985.962	3949993.732	13359	NHxB			Rh
218	272966.718	3950097.362	0	OzH			Rm
219	272897.202	3950002.777	0	OmH			Rm
220	305068.980	3950027.901	13359	NHxA			HD
221	295236.483	3950197.758	13359	S/NHx			S/Rh
222	304045.591	3950220.122	13359	NHx			Rl
223	284960.572	3950043.810	0	NHxB			Rl
224	240692.323	3949869.269	0	OzH			T/Rp

225	243787.968	3949370.775	0	PI/OzH			PI/PIs/Kp
226	240069.886	3949651.283	0	OzH	OzHf		HD
227	240315.992	3948028.153	0	OmH			HD
228	240418.233	3949174.777	0	OzHf			HD
229	239621.107	3947276.327	0	OmH			HD
230	240976.030	3947113.938	0	MALc			HD
231	242983.126	3946863.249	0	PIs			T/PIs/Rp
232	240256.543	3946865.656	0	OzHf			T/Rp
233	244369.950	3946585.119	0	OzH			HD
234	244498.740	3946517.201	0	OmHA			HD
235	239125.622	3946651.908	0	OmH			HD
236	235451.239	3946857.037	0	OzHf			PI/Km
237	238447.763	3946381.145	0	CHxA-T			Rm
238	243720.108	3946250.415	0	OmHA			PI/PIs/Kp
239	236324.813	3946234.187	0	OmH			PIx/Ki
240	296021.066	3949839.051	13359	S			HD
241	273874.443	3949870.262	0	OmH			HD
242	257686.268	3949849.923	0	PI	PIs		HD
243	283163.483	3949733.219	0	CHxA			Rm
244	302137.454	3949682.688	13359	NHx	S	F	HD
245	290723.208	3949683.324	0	NHx			T/Rh
246	310158.538	3949692.052	0	OmHL			HD
247	287455.328	3949664.818	11289	S/NHx			HD
248	291579.722	3949568.336	11289	S			S/Ri
249	311275.437	3949563.341	0	PIp			PIx/Km
250	289081.763	3949550.134	13359	NHxB			S/Ri
251	254489.448	3949452.055	0	OzH/PI	PIs		PI/Km
252	298875.956	3949333.496	0	CHx	NHx		HD
253	294850.929	3949315.649	13359	NHx			Rh
254	277746.526	3949292.146	13359	S/NHxB			HD
255	271880.639	3949305.697	0	CHx	OmH		HD
256	297884.544	3949279.765	11289	S/NHxB			S/Ri
257	306086.633	3949222.757	0	NHxA/T			Rh
258	307335.559	3949118.344	11289	MOr	NHx		HD
259	269956.759	3948984.431	0	OmH			Ri
260	288515.274	3948980.843	11289	S/NHxB			HD
261	259511.062	3948962.704	0	CHx-T			PIs/Rm
262	313484.592	3948867.049	0	PI			HD
263	281297.308	3948886.601	0	NHxB			T/Ri
264	311945.865	3948789.192	0	OmHp/R			HD
265	281939.771	3948800.912	0	NHxY			HD
266	297938.348	3948689.512	13359	NHx			Ri/Sd
267	293095.344	3948662.941	11289	NHxB	Hth		S/Rh
268	308960.947	3948627.998	0	OmHA			T/Rh
269	305185.014	3948606.320	0	NHxA			T/Rh
270	261951.389	3948636.341	0	OzH			HD
271	296746.607	3948543.551	13359	NHxA			S/Ri
272	269949.198	3948536.534	0	CHx			HD
273	262689.054	3948530.604	0	MALc	T		RKI
274	307911.312	3948523.552	0	T/CHxA			T/Rh
275	287944.106	3948509.661	13359	S	Sb		S/Ri

276	311861.746	3948432.339	0	OzH/PI			PIs-T/Rh
277	270375.033	3948381.191	0	OmH			HD
278	297789.353	3948334.617	13359	NHx			Rl
279	303798.295	3948237.409	11289	Hth			Kh
280	312366.747	3948215.861	0	PIs-T	CHxA		PIs-T/Rm
281	261321.273	3948303.532	0	OzH/PI			HD
282	255470.687	3948209.639	0	PI			PI/Kl
283	304557.461	3948189.431	9617	OcH			HD
284	264643.043	3948192.813	0	OzHf	OmH		HD
285	302910.616	3948124.135	13359	Hth	HxA	S/T	Rh
286	299462.413	3947999.840	0	NHxA			Rh
287	265435.651	3947916.771	0	PI-OzH			Rm
288	268756.479	3947989.962	0	OzH			RKm
289	270733.894	3947955.788	0	OcH			HD
290	273612.321	3947885.017	0	OzHf			PI/Kh
291	311566.148	3947814.017	0	PIs	OmHp/R		PIs-T/Rm
292	277903.537	3947806.185	13359	S/NHxB			S/Rm
293	259636.462	3947778.298	0	OzH/PI			RKl
294	303973.082	3947764.161	9617	OzH	K		Rm
295	261120.039	3947749.702	0	OzH	PI		RKm
296	256670.239	3947752.039	0	OmH			HD
297	307115.971	3947684.278	0	OzHf			HD
298	311554.751	3947606.001	0	PIs	OmHp/R		PI/Kh
299	250906.211	3947604.184	0	PIs/OzHf	PI		HD
300	274722.083	3947590.248	0	NHxR			HD
301	255795.179	3947521.924	0	OmH	PIs		Km
302	306142.207	3947489.466	0	NHx			T/Ri
303	284347.873	3947432.961	13359	S/T			T/Ri
304	311745.008	3947391.360	0	PIs	OmHp/R		PI/Kh
305	286979.332	3947361.604	11289	S/NHxB			S/Rl
306	254731.666	3947345.798	0	OmH			PIs/Rp
307	312965.114	3947162.049	0	CHxA/T			HD
308	292184.250	3947134.747	13359	NHxB	S		HD
309	259870.362	3947070.071	0	PI-OzH			HD
310	267121.956	3947158.780	0	OzHf			HD
311	280970.948	3947059.342	11289	S/NHxB			HD
312	266234.760	3946988.603	0	CHx			HD
313	257580.629	3946977.968	0	OmH			Rh
314	279220.024	3946952.933	11289	S/NHxB			Rh
315	283970.997	3946900.764	13359	S/T			S/Rh
316	271388.218	3946861.806	0	NHx-T			T/Ri/Sd
317	262993.257	3946816.434	0	OzHf			HD
318	256584.658	3946769.964	0	PI/OzH	PIs		PI/Km
319	284463.951	3946751.947	0	NHxB			T/Ri
320	267481.142	3946737.505	0	V			HD
321	298903.872	3946711.811	0	W			Rh
322	263067.534	3946697.464	0	CHxR	OmHR		T/Rh
323	288231.108	3946661.719	9617	NHx	S		Rh
324	252084.770	3946677.856	0	OzHf/PIs	PI		PIs/Km
325	263139.307	3946665.592	0	CHxR	OmHR		T/Rh
326	284055.590	3946654.175	13359	NHx			S/Rh

327	264491.220	3946644.174	0	V	R		HD
328	292485.175	3946635.494	11289	S	Hth		S/Rh
329	295440.292	3946633.250	0	Hth			S/T/Rh
330	311605.591	3946587.036	0	CHxL			PIs-T/RI
331	309150.972	3946563.219	0	CHxO			RI
332	303542.611	3946524.920	9617	MOr			HD
333	286943.983	3946484.145	0	NHx-T			S/Rp
334	286207.365	3946422.290	13359	Hth	NHx		HD
335	252312.111	3946446.537	0	OzHf/PIs	PI		PIs/Km
336	314426.811	3946378.438	0	OmHp/R			HD
337	282801.091	3946366.635	13359	NHx			HD
338	255805.529	3946356.780	0	PI/OzH			PI/KI
339	235922.306	3947850.496	0	OzHf	PI		HD
340	261369.106	3946317.508	0	OzH	PI		HD
341	272111.969	3946285.357	0	NHx-T			T/Ri
342	279731.350	3946231.678	13359	S/NHxB			S/Rh
343	307975.281	3946183.293	0	T/CHxA			PIs/KI
344	310419.198	3946146.514	0	OmHp/R			PI/Km
345	257600.010	3946114.842	0	OmH	PIs		PIs/RK _m
346	277055.527	3946098.473	0	NHxR			RD
347	303504.126	3946052.147	0	T/OmH			T/Rh
348	303191.220	3946059.257	0	OcH			HD
349	265358.208	3946026.918	0	OzH	K	R	RKh
350	271826.328	3946029.623	0	OcH			Kh
351	256009.711	3945829.230	0	CHxL			HD
352	306179.411	3945793.618	0	CHx-T	OmHr	MAL	Rm
353	267267.562	3945706.935	0	OzHf			Kh
354	246944.819	3945902.734	0	OzH			HD
355	241039.222	3945970.312	0	OzH/PI			HD
356	307936.023	3945539.622	0	Wt			HD
357	299671.272	3945505.000	0	OmHA			HD
358	297221.751	3945446.188	13359	NHx			HD
359	302334.429	3945423.566	0	OmHA	MOr/Sb	Sb	HD
360	262260.125	3945584.518	0	OmHA			RI
361	267127.658	3945550.807	0	K	R		Kh
362	298337.206	3945373.446	0	MOr			HD
363	307110.509	3945317.102	0	CHxA	CHx		HD
364	312191.804	3945176.213	0	T/CHxA			PIs-T/Rm
365	239149.241	3945881.595	0	CHxA-T	PIs		PI/Ki
366	239070.885	3945479.308	0	PIs			T/Ri
367	236736.368	3945466.849	0	OzHf	PIs		PIs/Kp
368	234932.052	3945725.557	0	CHxA-T			RI
369	235415.780	3945253.363	0	PI-OzH	PIs		PI/Ki
370	251364.099	3945461.313	0	PI/OzH	PIs		Tu/PIsu
371	283615.047	3945330.275	13359	S(F)	F		Fuh
372	260638.649	3945374.445	0	OzH/PI			RKI
373	269848.700	3945160.374	0	CHx			RI
374	270377.445	3945396.563	0	OzH/PI			PI/Km
375	285566.810	3945176.761	11289	NHxA			HD
376	246308.017	3945041.881	0	OzH			HD
377	256621.230	3945426.142	0	OzHf	OmHr		HD

378	260545.335	3945088.163	0	CHx-T			HD
379	254411.974	3945294.180	0	PI	OzH	PIs	PIx/Kp
380	262311.766	3945047.182	0	CHx			HD
381	271866.829	3945161.629	0	Hx	R		Rh
382	246264.241	3945400.995	0	OzHf			HD
383	282829.601	3945168.891	13359	S(F)	F		S/Rp
384	288392.257	3945044.977	0	R	Hx		Rh
385	314554.648	3945027.180	0	OmHp/R			HD
386	282593.007	3945016.738	13359	S/F			HD
387	281898.247	3945001.686	13359	NHx			HD
388	259883.533	3944965.884	0	OzHf	OmHA		HD
389	243325.110	3944956.141	0	OzHf			HD
390	233939.528	3944905.971	0	OzHf			PI/KI
391	259177.797	3944886.617	0	OzH/PI			HD
392	304074.631	3944849.133	0	OmHA	MOr/K		HD
393	309659.203	3944832.861	0	PIs			PIx/KI
394	257461.654	3944820.247	0	CHx			Tu/RI
395	262527.233	3944809.357	0	OzH			HD
396	307327.029	3944821.244	0	OmHA			HD
397	275518.045	3944798.768	0	NHxB	NHxR		HD
398	257666.056	3944774.824	0	CHx			HD
399	263990.723	3944769.780	0	CHx	NHx		HD
400	249735.117	3944754.859	0	OzH			HD
401	311749.088	3944730.026	0	OmHA			Km
402	299125.553	3944734.170	0	CHx	OmHr		HD
403	260938.108	3944718.954	0	OmHr	CHx		HD
404	282919.992	3944723.507	13359	S/NHxB			HD
405	235493.915	3944712.794	0	OzHf			KI
406	312535.619	3944632.674	0	OmHp/R			PIx/Kh
407	262346.487	3944624.839	0	OmHr			HD
408	273858.769	3944601.486	0	CHxA-T			HD
409	309918.916	3944506.134	0	AL			HD
410	268607.219	3945633.060	0	CHxA			Rh
411	303684.487	3944387.490	0	HxBI/R			Huh
412	297928.867	3944405.267	0	MOr/K			RI/Sd
413	239393.258	3944366.243	0	OzHf			T/Ri
414	287903.019	3944380.985	0	S/NHx	T		T/Ri
415	268928.583	3944351.937	0	Hth	NHx		RKI
416	245165.102	3944264.976	0	OmHA			HD
417	244369.527	3944279.001	0	PI			PIsu
418	313647.508	3944171.690	0	CHxR			HD
419	258445.448	3944176.288	0	OzHf/PIs			T/Ri
420	265846.656	3944169.555	0	HxBI/R			Rh
421	242872.540	3944098.905	0	OmHp/R			HD
422	276203.242	3944066.371	0	S-T/R	NHxB		RI
423	260439.229	3944031.013	0	OmHr	HxBI		HD
424	291524.389	3944027.083	13359	NHx			HD
425	298669.607	3943994.240	0	NHxR			HD
426	303890.822	3943920.693	9617	HxBI/R			Rh
427	282758.144	3943859.518	13359	NHxB/S			Su/RI
428	246979.250	3943854.243	0	HxL			HD

429	242894.652	3943843.099	0	PIs/OzH			PIsu/Kp
430	253512.571	3943837.496	0	OzHf	OmHr		HD
431	248029.039	3943818.203	0	OzH			HD
432	313470.963	3943810.938	0	MOr/Sb	OmHA	MOr/K	HD
433	259030.785	3943756.464	0	CHx			HD
434	291284.527	3943766.413	13359	NHxB			PI/Ki
435	300548.935	3943725.218	0	HxBI	CHxA/T		Rh
436	256943.054	3943717.821	0	PI			PI/Ki
437	281904.524	3943718.445	11289	S/NHxB			Rh
438	310015.751	3943708.311	0	T/CHxA			PI/Kh
439	301009.960	3943687.523	0	HxA/T			T/Ri
440	276287.451	3943680.083	0	NHxB			RI
441	262080.112	3943672.562	0	HxA	T		T/Rp
442	269181.500	3943644.742	0	HxA	R		T/Rh
443	302786.968	3943635.578	11289	HxBI/R	HxA		Rh
444	305270.771	3943610.227	0	MOz	PI		Km
445	266619.956	3943593.593	11289	S	T	R	HD
446	282549.047	3943585.778	11289	NHxR	T		HD
447	310114.562	3943544.719	0	OmHA			PIs-T/Rm
448	264243.335	3943486.383	9617	T	NHxA	K	RKh
449	275507.168	3943433.621	11289	S/NHxB			S/Ri
450	256864.008	3943435.599	0	CHxL	CHx		HD
451	270920.074	3943431.221	0	CHxA-T			HD
452	297369.544	3943421.979	0	CHxA/T			HD
453	260378.375	3943352.419	0	HxA	T		T/Ri
454	283516.069	3943362.514	9617	T/NHxB			HD
455	288683.512	3943338.428	0	NHx			HD
456	280971.771	3943322.822	13359	NHxR	T		HD
457	310528.140	3943286.663	0	OmHA	HxBI		PI/Km
458	255930.412	3943305.116	0	CHxR			HD
459	256909.460	3943278.846	0	OmHA	OzH	OzHf	HD
460	291434.775	3943187.324	0	MOr/Sb	NHx		HD
461	275503.524	3943085.836	13359	S/NHxB			S/Rp
462	239905.034	3943083.772	0	T			Ri/Sd
463	257200.902	3943015.396	0	PI-OzH	PIs		HD
464	275059.183	3943034.762	13359	S	NHx		T/Rm
465	254227.119	3943044.204	0	CHx			HD
466	259658.016	3942973.044	0	OmHA	OzH		HD
467	248219.656	3942927.708	0	PIs			T/PIs/Ri
468	295551.097	3942893.035	0	NHxR			T/Ri
469	250454.530	3942853.067	0	V			HD
470	272422.210	3942874.133	0	CHxR			HD
471	245379.527	3942834.164	0	P			G
472	272628.611	3942807.609	0	NHxAz	HxBI/R	HxA	RKm
473	310602.174	3942767.308	0	PIs	OzH		T/Rm
474	302401.059	3942711.415	13359	NHxY			HD
475	238916.342	3942729.898	0	CHxA-T			RI
476	244770.154	3942803.376	0	HxL			HD
477	248606.516	3942628.069	0	CHxA			T/Rp
478	273308.697	3942573.439	0	OcH	K		Rm
479	311227.660	3942529.723	0	HxL			PIx/Km

480	281452.610	3942490.839	0	MOr/R-K			HD
481	282601.727	3942460.863	0	T/HxA			Rm
482	281373.204	3942449.270	0	MOr/R-K			HD
483	308803.844	3942416.060	0	CHx			T/Rm
484	250693.562	3942463.396	0	OzHf	PI		HD
485	235176.629	3942462.568	0	CHxA-T			T/Pls/Ri
486	256852.914	3942387.136	0	CHx			HD
487	244724.229	3942385.364	0	P			G
488	294643.326	3942325.411	0	NHxR			HD
489	291421.503	3942300.948	0	NHxA			HD
490	241663.486	3942345.754	0	Wt			HD
491	298943.388	3942189.086	0	OmHA	CHx		HD
492	277389.297	3942217.423	13359	S/NHxB	S/R		Su/Ri
493	254603.611	3942160.221	0	CHx			HD
494	281634.629	3942139.573	0	CHxA-T	HI		HD
495	311147.474	3942118.723	0	MOr	Pls		Plx/Km
496	246231.023	3942048.778	0	HxL			G
497	279232.554	3941877.064	0	NHxR			T/Ri
498	252477.285	3941896.444	0	PI/OzH			Plx/Ki
499	262587.449	3941877.845	0	CHx	T		Rl
500	287710.968	3941823.956	0	NHxR			HD
501	231622.256	3941810.735	0	OzHfA			PI/Kl
502	262074.677	3941834.914	0	CHxR	T		T/Rp
503	235020.144	3941780.743	0	OzHfA			PI/Ki
504	276652.076	3941825.523	13359	S(F)			HD
505	254835.555	3941870.683	0	PI	OzH		HD
506	282387.117	3941745.411	0	CHx/T	OmHr		HD
507	254768.362	3941729.988	0	OmH			Rl
508	287010.691	3941700.646	0	OzH			Rl
509	289081.463	3941673.753	0	T	CHxA		T/Ri
510	281725.015	3941686.857	0	NHxR			HD
511	286166.563	3941682.278	0	OmHr			HD
512	299340.881	3941608.079	0	MOr/Sb			HD
513	281181.561	3941637.497	0	NHxB	HxA		Rh
514	263042.953	3941638.275	0	CHx	R		Rh
515	248697.405	3941471.483	0	OzH			Kl
516	263638.303	3941525.081	0	NHx-T			Rh
517	259078.672	3941578.319	0	T/HxA			Rh
518	281770.610	3941472.515	9617	NHxR			HD
519	291491.938	3941383.013	0	HxL	HxBI		T/Ri
520	288017.209	3941316.582	0	NHxY	MOr/Sb		HD
521	308531.727	3941287.357	0	OzH/PI			Plx/Kh
522	299545.498	3941283.527	13359	NHxR			HD
523	265548.646	3941274.569	0	OcH	K		Rh
524	297485.332	3941290.799	0	OmHA			HD
525	298834.855	3941283.414	0	HxAz	T		HD
526	299246.349	3941234.159	0	NHxR			HD
527	275276.561	3941155.413	13359	S/NHxB			HD
528	264094.959	3941054.465	9617	NHx			HD
529	233749.223	3941054.366	0	CHxA-T			Plx/Kp
530	233712.875	3941227.340	0	OzH-Pls			Pls/Ri

531	242162.971	3941040.088	0	OzH			PIx/Kp
532	280076.257	3941051.844	0	HxA/T	MOr		T/Rm
533	234562.092	3940988.190	0	PI			PI/Ki
534	250110.747	3940851.628	0	CHxL	T		HD
535	277161.131	3940971.943	11289	NHxB	S		HD
536	270980.554	3940926.562	0	NHxR			T/Rh
537	234683.723	3940723.449	0	OmHA			PI/Ki
538	251477.729	3940739.351	0	CHxA-T			RI
539	274469.967	3940886.446	13359	NHxR			HD
540	236784.476	3940634.764	0	PI/OzH			PI/Ki
541	239936.272	3940618.964	0	OmHp/R			Rm
542	231701.343	3940408.928	0	OzHf			PI/Km
543	246331.227	3940433.084	0	CHxR			PI/Ki
544	284613.184	3940869.565	0	OmHA			HD
545	253923.551	3940403.552	0	NHxR	NHx		RI
546	234349.778	3940177.989	0	OzH/PI			HD
547	271019.883	3940631.905	0	Hth			Huh
548	257686.868	3940393.499	11289	NHxA/T	R	R	T/Rh
549	233123.085	3940018.180	0	OzH/PI			RI
550	270559.095	3940579.523	13359	S/T	NHx		T/Rh
551	231287.490	3939864.029	0	OzHfA			HD
552	236530.636	3939881.533	0	OmHR			HD
553	233007.318	3939829.440	0	OzHf			PI/Km
554	236022.666	3939787.701	0	OzHfA			HD
555	229458.966	3939676.064	0	OzH/PI			RI
556	245504.838	3939951.331	0	CHxR			HD
557	256118.885	3940180.902	0	HxBI	P		Rp/Sd
558	274646.881	3940568.611	13359	S/NHxB			HD
559	248565.405	3939916.604	0	CHx			T/Ri
560	237323.884	3939618.550	0	PI-OzH			PI/Ki
561	281573.438	3940681.572	0	NHxR/T			T/Ri
562	250969.439	3939929.318	0	CHxR			HD
563	243077.760	3939717.789	0	PI			Plu
564	242792.369	3939666.332	0	T			T/Ri
565	228555.424	3939272.428	0	HI			Ou
566	235415.401	3939383.356	0	OmH			HD
567	232175.561	3939231.293	0	PI/OzH			PIs/Ri
568	274694.288	3940424.416	13359	S/NHxB			HD
569	253163.999	3939637.349	0	T/NHxA	T	HxA	HD
570	265484.049	3940060.329	0	NHx	R		HD
571	265309.266	3940046.480	0	NHx			Rm
572	255146.516	3939661.712	11289	Hth			Rm
573	247287.312	3939355.230	0	OzH			T/Rh
574	247548.039	3939309.527	0	OmHA			HD
575	256549.014	3939598.792	11289	Hth	R		Hth
576	245649.945	3939191.278	0	CHxR			HD
577	248150.864	3939259.647	0	NHxR			Ri/Sd
578	244937.354	3939066.653	0	OmHA			Rp/Sd
579	231728.800	3938351.552	0	PI/OzH			PI/Km
580	239662.395	3938645.291	0	OmHp/R			Ri/Sd
581	288416.677	3940715.698	0	MOr			RKh

582	234147.741	3938396.052	0	OzH/PI			PIs/Ri
583	230602.766	3938179.207	0	PI-OzH	PI		HD
584	258227.456	3939378.171	9617	NHxR	T		HD
585	232734.417	3938122.996	0	OzH-PIs			PIsu/KI
586	257756.727	3939073.596	0	MOr			HD
587	274642.355	3939932.017	13359	S	NHxB	R	S/Ri
588	245539.297	3938361.190	0	OzH			HD
589	236170.413	3937826.859	0	PI/OzH			PI/KI
590	250110.213	3938530.252	0	NHxR			Rm
591	240320.743	3937933.972	0	OzHf			HD
592	271608.479	3937918.615	13359	S/F	NHxE	NHxB	Sui
593	268007.166	3937302.823	0	NHx			HD
594	272959.650	3939306.961	11289	S/NHx	T		Rh
595	244749.977	3937903.989	0	OzH			HD
596	291688.522	3938006.132	0	CHxR			RI/Sd
597	282841.585	3938938.268	9617	MOr	NHx		HD
598	287458.870	3938440.034	0	OzH			Rh
599	258332.704	3937899.270	0	OmH	T		T/Ri
600	286100.126	3937550.496	0	OzH			HD
601	291381.720	3940067.419	0	CHxR			HD
602	255803.741	3938375.267	0	Hth			Hth
603	249204.593	3937828.069	0	OzH			Tu/Rm
604	262746.992	3938638.246	0	Sb	NHx		RKI
605	249980.044	3937898.664	0	OmHA			HD
606	284573.829	3939910.466	0	HxA/T			Tu/Rm
607	246504.823	3937808.700	0	NHxR			HD
608	266786.258	3937653.743	13359	MOr/R-K			HD
609	245895.299	3937746.799	0	OzH			HD
610	286694.273	3939737.445	0	OmHA			HD
611	255907.419	3937776.288	0	NHxA-T			T/Ri
612	279086.059	3939550.853	0	CHxR/T	CHxA/T		Tu/RI
613	268908.579	3938623.376	11289	S			Ful/Si
614	252066.111	3938293.505	0	NHxR	MOr		HD
615	275894.037	3939070.417	11289	S/R	NHxB		S/Rh
616	283580.758	3937862.656	0	NHxR/T	CHxR		T/Rm
617	285981.909	3939121.041	0	CHxR			HD
618	270343.397	3938164.835	13359	S	NHx	F	Sui
619	274307.127	3939401.332	13359	S/NHxB	S/R		S/Ri
620	282238.424	3938968.783	0	CHx			HD
621	281334.877	3940068.022	0	CHxR/T			RI
622	293056.551	3940352.783	11289	MOr/Sb	NHx		HD
623	292579.831	3940746.250	9617	NHxY			HD
624	291895.131	3939776.139	0	OmHR			HD
625	271021.858	3938807.408	13359	NHx			HD
626	261401.392	3937688.186	0	NHxR/T			T/Rp
627	256921.624	3938701.952	0	MOr			HD
628	279038.237	3938113.158	0	CHx/T	CHxR		RI
629	273613.499	3939252.904	13359	S/NHxB	S/R		Si/Rh
630	260721.954	3937807.098	0	MOr			HD
631	289204.945	3938360.965	0	OzH	PI		Km
632	257199.228	3937916.654	0	CHx	T	OmH	HD

633	289951.359	3938720.516	0	OmHR			HD
634	279491.633	3939771.264	0	T/HxA			T/Rl
635	270597.481	3939441.274	13359	NHx-T	K		Rh
636	260704.947	3937636.428	0	NHxR/T			HD
637	247877.810	3938082.217	0	NHxB			T/Rp
638	246796.053	3938036.343	0	CHx			T/Rp
639	291452.924	3937927.452	0	OmHL			HD
640	257232.133	3937888.961	0	CHx	T	OmH	Rl
641	291968.031	3939675.646	0	NHxB	T		Rh
642	278745.446	3939811.443	0	NHxR/T	NHxA		Rl
643	279872.039	3939725.403	0	T/HxA			T/Ri
644	277904.415	3939792.731	11289	S/R	S/NHxB		S/Ri
645	281312.620	3939473.321	0	OmHA			Kh
646	279780.710	3939974.807	0	NHxA/T			T/Ri
647	234142.031	3937571.235	0	OmHr			HD
648	277314.087	3939586.947	11289	S/T	S/NHxB	NHxA	S/Ri
649	232631.662	3937206.863	0	PI-OzH	Pls		PI/Km
650	267171.232	3937210.971	13359	NHx			HD
651	238759.599	3937107.468	0	CHxL			HD
652	237345.529	3937071.207	0	OzH-Pls			T/Rm
653	271697.213	3937151.504	13359	S	R	K	HD
654	242994.337	3937005.364	0	OmHr			HD
655	228744.145	3936917.269	0	Hx			Km
656	242728.239	3936925.922	0	PI			HD
657	264806.372	3937058.438	0	NHx	R		HD
658	243813.042	3936902.906	0	OmHr			HD
659	269886.296	3937086.194	9617	NHx			HD
660	266306.661	3937007.475	0	NHx			HD
661	230034.876	3936483.989	0	OmH	R		HD
662	232196.827	3936509.019	0	PI/OzH			PI/Km
663	251491.654	3936737.348	0	OmHA	OzH		Rl
664	241629.537	3936597.242	0	OmHr			HD
665	253601.306	3936685.172	11289	MOr	NHxA		HD
666	240978.968	3936473.215	0	OzH			Kl
667	245788.579	3936531.145	0	MOr			HD
668	231220.735	3936280.712	0	OzHfA			HD
669	268821.156	3936877.671	11289	OcH			HD
670	229184.784	3936211.335	0	PI-OzH			PI/Km
671	230091.985	3936198.108	0	OzHfA			HD
672	247271.581	3936431.609	0	OmHA			HD
673	234158.152	3936167.822	0	OzHfA			HD
674	245161.818	3936289.873	0	CHx			T/Ri
675	256396.821	3936449.875	0	Hx	T		HD
676	272716.142	3936821.026	11289	S/NHx	NHx		Si/Rm
677	234875.478	3935948.637	0	OzHf			HD
678	251902.268	3936307.267	0	HxA			HD
679	261577.746	3936534.591	0	OmHA	OzH		HD
680	235878.922	3935921.765	0	PI/OzH			Kl
681	275711.436	3936862.824	11289	NHxB/S	NHxR		Rh
682	250614.045	3936213.688	0	OmHA			HD
683	269179.253	3936670.049	0	OmH			HD

684	266683.983	3936600.604	13359	NHx			HD
685	229147.856	3935603.169	0	PI-OzH			PI/Ki
686	240677.091	3935895.536	0	OzH			HD
687	278043.305	3936890.551	0	NHxA/T	S		T/Ri
688	229420.501	3935542.154	0	CHxL			PI/Km
689	255154.792	3936221.193	0	OmHr			Rl
690	277941.708	3936282.341	0	MOr	R-K		HD
691	291396.948	3935197.698	0	PI			HD
692	285358.629	3935367.872	13359	MOr/Sb	NHx		HD
693	271575.311	3935818.338	0	NHx			RKl
694	286607.966	3935563.176	0	NHxR			HD
695	257307.661	3935478.116	0	OmHr	HxF		T/Ri
696	245783.564	3935596.770	0	CHxA			T/Rp
697	277492.964	3935803.225	0	MOr	R-K		HD
698	281852.907	3936163.586	0	NHxA/T			Rh
699	283640.050	3935411.766	0	T/CHxA	OmHA		T/Rp
700	272859.407	3936061.595	0	NHx/T			Rl
701	249760.790	3935807.888	0	OmHr			Rp/Sd
702	282889.391	3936241.918	0	OmHr	CHxL		Rp/Sd
703	261355.990	3936166.017	0	OmH			HD
704	281822.261	3936359.307	0	PIs			PIs/Ki
705	268647.519	3935567.172	0	CHxL			HD
706	238657.319	3935349.902	0	CHxL			HD
707	256657.097	3935389.360	0	CHxL	CHx		Rm
708	281165.840	3936921.165	0	T/OmHA	CHx		T/Ri
709	271110.749	3935721.028	0	NHx			HD
710	243562.869	3935461.834	0	NHxR			Ri/Sd
711	289942.931	3935202.561	0	OmHA			HD
712	290741.449	3935483.527	0	PI/OzH			HD
713	279442.921	3936731.992	0	T/CHx	CHxR		T/Rp
714	253868.385	3935952.926	0	MOr	OmHA		HD
715	254305.422	3935723.231	0	MOr	OmHA		HD
716	286511.163	3936675.514	0	OmHR			HD
717	287533.066	3935423.563	0	OzH/PI			HD
718	287148.952	3936925.776	0	NHxY			HD
719	240042.048	3935323.963	0	OmHA			HD
720	289510.333	3934912.765	0	T	CHxA		Rl/Sd
721	283998.776	3934955.989	0	MOr/Sb	OmHA		HD
722	251585.747	3935222.912	0	CHxR/T			HD
723	262468.444	3935129.417	0	OmHr	OmHA		HD
724	289269.597	3934769.493	0	OzH			HD
725	257272.488	3935097.069	0	OmHr/PIs	T/HxF		Rp
726	264958.473	3935016.210	0	NHx			HD
727	258482.177	3935086.264	0	CHxR			Rp/Sd
728	265085.306	3934730.949	0	NHx			HD
729	282034.360	3934273.475	0	OmHA			HD
730	236490.229	3935243.396	0	OzH/PI			Kl
731	281854.883	3934197.590	0	OmHA			PIsu
732	275734.907	3934234.259	0	MOr/G			T/Ri
733	255325.903	3934722.769	0	OmHr			HD
734	292019.802	3933881.858	0	OzH			Rm

735	275863.830	3933890.613	0	MOr/G			T/Ri
736	246461.420	3934742.665	0	OzH			RKl
737	232484.938	3935064.457	0	OmHr			HD
738	254168.858	3933714.531	0	CHxO	CHxR		HD
739	263554.076	3933737.378	0	OmH			HD
740	240618.779	3933836.701	0	OmHA			HD
741	246214.331	3933590.946	0	OmHr			HD
742	229163.888	3935010.514	0	OzH/PI			Kh
743	242768.889	3934047.005	0	OmHA			HD
744	232884.540	3934579.427	0	PI			HD
745	247516.433	3933448.090	0	OmHr			HD
746	259858.831	3933571.716	0	OmHA			PI/Kl
747	229877.470	3935135.735	0	OzHf			HD
748	249480.157	3934387.291	0	PI			Kl
749	277365.160	3933877.474	0	OmHA			HD
750	236868.075	3934924.301	0	PI/OzH			PI/Kl
751	277609.996	3933679.296	0	OmHA			HD
752	265424.101	3934354.464	0	NHx	R		HD
753	245816.886	3934101.397	0	NHxR			HD
754	278634.571	3933964.736	0	OmHA	OzH		HD
755	270984.151	3933865.332	0	CHxL			T/Ri
756	248164.127	3934586.488	0	OmHr			HD
757	239380.200	3934291.705	11289	NHxR			HD
758	261800.919	3934361.692	0	OmHA			HD
759	271983.194	3934010.477	0	NHx-T	S		T/Ri
760	248700.674	3934553.683	0	OzH			Km
761	268259.153	3933826.988	0	OmH			HD
762	240721.621	3933809.966	0	OmHA			HD
763	237854.160	3933646.755	0	OzHfA			HD
764	231267.227	3935303.019	0	PI/OzH			HD
765	246825.066	3934118.529	0	CHxR			Rh
766	229324.820	3935021.974	0	OzH/PI			HD
767	283864.868	3933798.742	0	MOr/Sb	OmHA		Rl
768	237726.418	3935005.746	0	OzHf			HD
769	247016.623	3934019.766	0	OzH			RKl
770	230468.689	3933335.508	0	PI/OzH			PI/Kl
771	230402.934	3932879.182	0	OzH/PI			HD
772	307934.292	3940565.459	0	OzH/PI			PIs/Kh
773	304274.354	3940700.232	9617	CHxR	T		T/Rh
774	306016.867	3940512.078	0	MOr/Sb			HD
775	304691.871	3940232.170	0	CHxR	T		T/Ri
776	308585.953	3940071.170	0	T/CHx			T/Rl
777	308006.319	3940041.767	0	HxL	CHxA	PIs	T/Rl
778	311141.621	3939701.144	0	T/CHx			RKm
779	297087.181	3940170.349	0	HxL			HD
780	307343.704	3938586.094	0	T/R	HxA	CHxA	T/Ri
781	306141.894	3938139.211	0	NHxR/T			T/Rm
782	298765.452	3939509.049	0	MOr/Sb			RKm
783	305234.637	3937690.021	0	T/NHxA	T/R		T/Rh
784	303264.408	3938234.789	11289	S/NHxB			Rh
785	304795.595	3937425.039	11289	R	T/R		T/Rh

786	302821.096	3937997.132	11289	NHxY	S		HD
787	303102.859	3937521.578	11289	NHx	S/Sb		HD
788	302577.596	3937175.178	13359	NHxY	S/T		HD
789	302896.243	3936598.381	11289	NHxR	NHx		HD
790	298733.046	3938518.220	0	CHxR	T		HD
791	303531.237	3935368.340	13359	MOr/Sb			HD
792	298212.967	3938568.152	0	CHxR	T		HD
793	299984.970	3936874.500	0	CHx	T		HD
794	299130.368	3937543.812	0	PI-OzH			KI
795	298914.029	3937432.197	0	OmHA			HD
796	300880.318	3934955.419	0	CHx	CHxR		Ri/Sd
797	300249.600	3935406.078	0	CHx	T		HD
798	273770.367	3933557.820	0	OmHr			HD
799	269880.670	3933489.373	0	OmH			HD
800	291215.594	3933676.220	0	G			HD
801	247226.254	3933169.711	0	CHxR			HD
802	249554.046	3933132.726	0	HxL			HD
803	240071.002	3932905.480	0	CHxR			HD
804	265257.389	3933236.233	0	OmH			HD
805	288954.375	3933594.212	0	PI			RKm
806	282059.299	3933490.215	0	OmHA/Pis	OzH/PI		T/Rp
807	285880.992	3932744.359	0	NHxY			HD
808	272841.432	3932925.529	0	OzHf			Kh
809	254442.491	3932751.205	0	OmHA	PI		Pis/Ri
810	290112.225	3932991.441	0	HxL			PI/KI
811	285048.347	3932773.766	0	CHxO			HD
812	287258.208	3933507.107	0	CHxR			HD
813	245427.034	3932864.447	0	CHxR			HD
814	254257.579	3932960.250	0	OmH			Pis/Ri
815	274492.304	3932831.733	0	OmHA			HD
816	258921.405	3932846.594	0	OmHA	OcH		HD
817	242850.249	3932772.005	0	CHxR			HD
818	254943.685	3932703.029	0	CHx			HD
819	279460.072	3932972.206	0	CHx	OmHr		HD
820	267265.495	3933270.036	0	OzHf			HD
821	282368.928	3933420.973	0	OzH	Pis	PI	Pisu/Ki
822	278150.830	3932732.003	0	OmHA			Rm
823	241174.332	3932659.433	0	OmHA			HD
824	242656.729	3932663.100	0	OzH			HD
825	239930.787	3932610.229	0	OzH			HD
826	270800.888	3932655.756	0	OmHL			T/Ri
827	275015.067	3932659.824	0	OmHA			HD
828	232774.108	3932580.082	0	OzH/PI			HD
829	249580.505	3932600.100	0	HxL			Rm
830	289986.064	3932657.224	0	CHxA	T		HD
831	285288.589	3932600.054	0	NHxY	NHxR		HD
832	240122.389	3932510.604	0	OmHR			HD
833	278839.207	3932603.521	0	OmH			T/Ri
834	263590.418	3932491.273	13359	MOr/R-K	NHx		HD
835	275051.758	3932471.994	0	OmHA			HD
836	255432.846	3932415.130	0	OmHA	PI	OzH	HD

837	249723.929	3932342.631	0	CHxA			Rm
838	239925.924	3932251.238	0	CHxA-T			HD
839	280276.969	3932278.062	0	OmHA			Rl
840	288244.176	3932318.542	0	CHxA/T			HD
841	247232.432	3932216.926	0	OmHA			HD
842	273729.018	3932208.675	0	OmHR	CHx		HD
843	270443.549	3932290.182	0	OmH			Rl
844	283142.084	3932356.807	0	OzH			Rm
845	277076.932	3932245.521	0	OmHA			HD
846	287495.505	3932257.377	0	OmHA			Rm
847	241861.989	3932185.264	0	OmHA			HD
848	271265.507	3932132.164	0	CHx			HD
849	280445.041	3932121.558	0	OmHA			Rm
850	290479.859	3931942.504	0	CHxL			HD
851	276085.065	3932007.936	0	OmHA			HD
852	268974.504	3931924.923	0	OzHf			HD
853	261412.637	3931869.578	0	OmHA			HD
854	274434.455	3931852.022	0	HxBI	HxL/T	OmH	HD
855	274324.746	3931828.718	0	HxBI	HxL/T	OmH	HD
856	246348.387	3931820.583	0	Plr	OzH		HD
857	252209.560	3931786.869	0	OmH			HD
858	254075.088	3931787.777	0	CHx	OmH		HD
859	250056.871	3931688.391	0	Plp/OzH			T/Ri
860	258304.279	3931662.723	0	MAL	OmH		HD
861	253547.651	3931617.188	0	CHxL			HD
862	239058.412	3931609.797	0	OzH			HD
863	286674.514	3931593.559	0	OmHL			HD
864	266655.119	3931588.554	0	OmH			Rh
865	263919.168	3931590.785	0	NHx			HD
866	281363.054	3931546.387	0	OmHR	OmHA		HD
867	250142.582	3931474.087	0	OzHf			HD
868	263031.042	3931266.675	0	OcH			HD
869	274903.363	3931261.959	0	CHx	OmH		HD
870	240609.864	3931195.429	0	OzHf			HD
871	235724.917	3931168.537	0	OzH	Plr		PI/Ki
872	283935.805	3931172.519	0	OmHA	OmHr		HD
873	246288.950	3931140.488	0	OmHA			HD
874	240212.126	3931059.546	0	OmHr			HD
875	266818.467	3931021.442	0	OmH	Hx		HD
876	281084.400	3931021.277	0	OmHA	OzHf		HD
877	234471.351	3930948.132	0	OmHr			HD
878	248143.192	3930920.346	0	OmHR			HD
879	244635.974	3930914.057	0	OcH			HD
880	251535.776	3930891.042	0	OmHA	Hx		HD
881	249855.040	3930763.955	0	PI			HD
882	249526.665	3930759.234	0	OmHR			Rm
883	254990.371	3930720.373	0	OzHf	Plr		HD
884	241775.222	3930715.159	0	OzH	Plr		HD
885	242814.904	3930684.367	0	Plr	OzH		HD
886	274507.103	3930647.264	0	CHx	OmHL		HD
887	246793.143	3930580.898	0	OmHL			HD

888	255334.073	3930541.240	0	Plp			PIs/Ki
889	247653.970	3930538.470	0	Plr			HD
890	248150.340	3930535.418	0	PIs			HD
891	255903.256	3930537.680	0	OmH	Hx		HD
892	263685.283	3930363.915	0	OcH			HD
893	265168.215	3930409.438	0	OmH	OcH		HD
894	270134.702	3930322.375	0	OzH/PI			HD
895	273863.833	3930295.277	0	HxL	OmH		HD
896	235682.814	3930293.472	0	OzHf			HD
897	271074.064	3930288.800	0	CHx	OmH		HD
898	248370.466	3930247.881	0	PIs	PI	OmHA	T/Ri
899	261999.933	3930236.335	11289	OmH			HD
900	248570.243	3930215.926	0	PI/OzH			HD
901	262179.158	3930174.908	0	CHx			HD
902	274910.205	3930159.408	0	OmH			HD
903	241179.272	3930123.204	0	CHxL			HD
904	235289.997	3930110.690	0	Plp			PIsu/Ki
905	233994.060	3930100.688	0	PIv/OzH			HD
906	278300.078	3930034.071	0	OmH	HxL		HD
907	283195.265	3929965.720	0	OmHA			Rm
908	256014.844	3929939.888	0	OzH	PI	PIs	PI/Kp
909	256068.041	3929881.259	0	OzH	PI	PIs	HD
910	254203.469	3929816.413	0	OzHf	Plr		HD
911	269090.223	3929673.612	0	OmH	HxL		HD
912	284401.748	3929792.610	0	OzH			HD
913	282716.710	3929506.502	0	OzHf			HD
914	243351.684	3929540.179	0	OzH	Plr		HD
915	246251.797	3929463.508	0	Plr	OzH		PIx/Kp
916	260970.219	3929290.939	0	OzHf			HD
917	257664.274	3929374.088	0	OcH	OmHA		HD
918	273161.481	3929537.925	0	OmH			HD
919	263042.703	3929205.534	0	OmHL			HD
920	242799.457	3929059.275	0	OmHL			HD
921	242469.177	3929061.975	0	CHxL			T/Rm
922	255881.037	3929023.794	0	OmHA	Hx		HD
923	258931.016	3928882.007	0	CHx			HD
924	257435.033	3928822.418	0	OzHf	PI		HD
925	261080.535	3928714.610	0	OzHf			HD
926	259814.328	3928648.731	0	OzHf	PI	PIp	HD
927	254149.964	3928586.795	0	OmHr			HD
928	267138.819	3928576.658	0	MAL			Tu/Rm
929	237178.147	3928392.819	0	PIv-OzH			HD
930	235339.155	3929069.089	0	OzH/PI			HD
931	277304.162	3929089.075	0	CHx	OmH		HD
932	278831.681	3928774.323	0	PI/OzH	PIs		PIs/Ki
933	256382.072	3928306.016	0	OmHA	OzHf	PI	HD
934	261520.728	3928221.666	0	OmH	HxL		T/Ri
935	257309.802	3928139.943	0	OmHA	HxL	PIs	HD
936	265781.181	3928117.325	0	OmH			T/Rl
937	258026.395	3928082.387	0	HxL	OmHr		HD
938	247595.796	3928072.097	0	CHxO			HD

939	246298.961	3927991.762	0	OzHf			HD
940	272010.904	3927956.272	0	OzH	PI		HD
941	272363.285	3927688.562	0	OmH			HD
942	269564.107	3927631.111	0	OmH			HD
943	254021.953	3927575.502	0	OmHA			HD
944	244418.145	3927554.906	0	OmHr			HD
945	266539.241	3927561.682	0	OmH	Hx		HD
946	273515.426	3927474.548	0	OmH	HxL		HD
947	249961.749	3927400.485	0	OmHL			HD
948	263576.074	3927331.942	0	OmH			Rp/Sd
949	259245.199	3927264.209	0	OmHA	HxL	PI	HD
950	241449.926	3927133.537	0	HxL			PIsu
951	278466.692	3928165.454	0	PI-OzH			HD
952	277485.002	3927858.051	0	CHx			HD
953	280416.245	3927417.522	0	PI-OzH	PIs		PIx/Kp
954	278315.210	3927234.830	0	OzHf			PIx/Ki
955	278696.643	3926676.150	0	PI/OzH			HD
956	272881.130	3927112.794	0	OzH	PIs		HD
957	255719.055	3927118.333	0	OzH	PI	PIs	PI/Kp
958	253035.341	3927097.803	0	OmHr			HD
959	266156.982	3927073.389	0	OmH	OzH		HD
960	255027.049	3926895.259	0	OzH	PI	PIs	HD
961	262370.408	3926850.850	0	OmH			HD
962	270418.401	3926745.976	0	MAL			PI/Kp
963	251727.303	3926650.207	0	OmHr			HD
964	260560.276	3926599.054	0	OmHA	PI		HD
965	255022.489	3926547.757	0	PI	OmH		PI/Ki
966	271735.959	3926528.986	0	PI/OzH	PIs		HD
967	266178.118	3926438.820	0	OmHL			HD
968	269739.385	3926406.693	0	PI	OzH	PIs	HD
969	251424.769	3926243.176	0	OmHA	PIr		HD
970	266084.227	3926352.677	0	OmH	OzH	PIs	HD
971	267761.177	3926339.767	0	OzH			HD
972	268900.331	3926353.369	0	OzHf	PI		HD
973	271115.778	3926320.176	0	PI/OzH	Hx		HD
974	266678.081	3926002.325	0	OmH			HD
975	272350.135	3926092.886	0	OmH			HD
976	271615.919	3925979.797	0	PI	Hx		HD
977	249577.167	3926050.500	0	PI	OzH		HD
978	249345.195	3926020.316	0	PI	OzH		HD
979	260420.977	3925893.586	0	OmHA	HxL		HD
980	258380.423	3925768.414	0	HxL	OmH		HD
981	261090.603	3925507.618	0	HxL			HD
982	250739.132	3925695.879	0	W			W
983	272713.157	3925745.020	0	W			W
984	270561.877	3925339.792	0	Dd			HD
985	271348.010	3924768.449	0	W			W
986	274176.283	3925107.775	0	PI-OzH			HD
987	273811.040	3924963.253	0	W			W
988	261699.081	3924441.029	0	W			W
989	261735.801	3924448.955	0	W			W

990	264474.857	3924329.674	0	W			W
991	263462.278	3924136.710	0	OmH			HD
992	257790.913	3925186.881	0	OmH	PI	PIs	HD
993	257591.090	3925061.587	0	W			W
994	259583.408	3924993.751	0	HxL	PI		HD
995	259799.571	3924874.185	0	W			W
996	268233.023	3924709.306	0	W			W
997	270904.532	3924712.080	0	Grv			HD
998	270649.814	3924548.907	0	PI	Hx		HD
999	259415.790	3923596.033	-32768	W			W
1000	259390.370	3923330.105	-32768	W			W

6.2. Index values for the red spruce vegetation and new index values for RSHM

The indices of RSHM were reclassified, and new indices, ranging from 10 to 40, were assigned for RSHM to make comparison convenient. An index value of 10 indicates absence of red spruce and higher index value more suitable habitat: 0 and negative values \rightarrow 10, 9617 \rightarrow 20, 11289 \rightarrow 30 and 13359 \rightarrow 40. The original habitat information of red spruce on the random points is reclassified, and new indices, ranging from 10 to 40, were assigned based on presence/absence and dominance of red spruce. An index value of 10 indicates absence of red spruce, 20 represents understory, 30 third- and second-level vegetation of the overstory, and 40 the dominant overstory vegetation (Table 4.2). In reclassification, if two different vegetation types overlapped at the same location, then the upper class was just reflected in the index system. For example, when dominant vegetation is overlapped with second- or third-level vegetation, an index value of 40 was assigned for this habitat. All values do not have units because they are index values. RSHM index values and Vegetation index values on the random points were used for the Pearson Chi-square goodness of fit test for model evaluation.

Random point	RSHM Suitability	Overstory Dominant Vegetation	Overstory Second Vegetation	Overstory Third Vegetation	Understory Dominant Vegetation	<i>RSHM Index</i>	<i>Vegetation Index</i>
1	10	10	10	10	10	10	10
2	10	10	10	10	10	10	10
3	10	10	10	10	10	10	10
4	10	10	10	10	10	10	10
5	10	10	10	10	10	10	10
6	10	10	10	10	10	10	10
7	10	10	10	10	10	10	10
8	10	10	10	10	10	10	10
9	10	10	10	10	10	10	10
10	10	10	10	10	10	10	10
11	10	10	10	10	10	10	10
12	10	10	10	10	10	10	10
13	10	10	10	10	10	10	10
14	10	10	10	10	10	10	10
15	10	10	10	10	10	10	10
16	10	10	10	10	10	10	10
17	10	10	10	10	10	10	10
18	10	10	10	10	10	10	10
19	10	10	10	10	10	10	10
20	10	10	10	10	10	10	10
21	10	10	10	10	10	10	10
22	10	10	10	10	10	10	10
23	10	10	10	10	10	10	10
24	10	10	10	10	10	10	10
25	10	10	10	10	10	10	10
26	10	10	10	10	10	10	10
27	10	10	10	10	10	10	10
28	10	10	10	10	10	10	10
29	10	10	10	10	10	10	10
30	10	10	10	10	10	10	10
31	10	10	10	10	10	10	10
32	10	10	10	10	10	10	10
33	10	10	10	10	10	10	10
34	10	10	10	10	10	10	10
35	10	10	10	10	10	10	10
36	10	10	10	10	10	10	10
37	10	10	10	10	10	10	10
38	10	10	10	10	10	10	10
39	10	10	10	10	10	10	10
40	10	10	10	10	10	10	10
41	10	10	10	10	10	10	10
42	10	10	10	10	10	10	10
43	10	10	10	10	10	10	10
44	10	10	10	10	10	10	10
45	10	10	10	10	10	10	10
46	10	10	10	10	10	10	10

47	10	10	10	10	10	10	10
48	10	10	10	10	10	10	10
49	10	10	10	10	10	10	10
50	10	10	10	10	10	10	10
51	10	10	10	10	10	10	10
52	10	10	10	10	10	10	10
53	10	10	10	10	10	10	10
54	10	10	10	10	10	10	10
55	10	10	10	10	10	10	10
56	10	10	10	10	10	10	10
57	10	10	10	10	10	10	10
58	10	10	10	10	10	10	10
59	10	10	10	10	10	10	10
60	10	10	10	10	10	10	10
61	10	10	10	10	10	10	10
62	10	10	10	10	10	10	10
63	10	10	10	10	10	10	10
64	30	40	10	10	10	30	40
65	10	10	10	10	10	10	10
66	10	10	10	10	10	10	10
67	10	10	10	10	10	10	10
68	10	10	10	10	10	10	10
69	10	10	10	10	10	10	10
70	10	10	10	10	10	10	10
71	40	10	30	10	10	40	30
72	10	10	10	10	10	10	10
73	40	10	10	30	10	40	30
74	10	10	10	10	10	10	10
75	10	10	10	10	10	10	10
76	10	10	10	10	10	10	10
77	10	10	10	10	10	10	10
78	10	10	10	10	10	10	10
79	10	10	10	10	10	10	10
80	40	40	10	10	20	40	40
81	10	10	10	10	10	10	10
82	10	10	10	10	10	10	10
83	40	10	30	10	10	40	30
84	10	10	10	10	10	10	10
85	10	10	10	10	10	10	10
86	30	10	10	10	10	30	10
87	10	10	10	10	10	10	10
88	10	10	10	10	10	10	10
89	10	10	10	10	10	10	10
90	10	10	10	10	10	10	10
91	40	10	10	10	10	40	10
92	10	10	10	10	10	10	10
93	10	10	10	10	10	10	10
94	10	10	10	10	10	10	10

95	10	10	10	10	10	10	10	10
96	10	10	10	10	10	10	10	10
97	10	10	10	10	10	10	10	10
98	10	10	10	10	10	10	10	10
99	10	10	10	10	10	10	10	10
100	10	10	10	10	10	10	10	10
101	10	10	10	10	10	10	10	10
102	10	10	10	10	10	20	10	20
103	40	10	10	10	10	10	40	10
104	10	10	10	10	10	10	10	10
105	30	40	10	10	10	20	30	40
106	10	10	10	10	10	10	10	10
107	10	10	10	10	10	10	10	10
108	20	10	10	10	10	10	20	10
109	10	10	10	10	10	10	10	10
110	40	40	10	10	10	10	40	40
111	10	10	10	10	10	10	10	10
112	40	40	10	10	10	20	40	40
113	10	10	10	10	10	10	10	10
114	10	10	10	10	10	10	10	10
115	10	10	10	10	10	10	10	10
116	30	40	10	10	10	20	30	40
117	10	10	10	10	10	10	10	10
118	10	10	10	10	10	10	10	10
119	10	10	10	10	10	10	10	10
120	10	10	10	10	10	10	10	10
121	10	10	10	10	10	10	10	10
122	10	10	10	10	10	10	10	10
123	30	40	10	10	10	20	30	40
124	10	10	10	10	10	10	10	10
125	10	10	10	10	10	10	10	10
126	10	10	10	10	10	10	10	10
127	10	10	10	10	10	10	10	10
128	10	10	10	10	10	10	10	10
129	10	10	10	10	10	10	10	10
130	10	10	10	10	10	10	10	10
131	10	10	10	10	10	10	10	10
132	10	10	10	10	10	10	10	10
133	10	10	10	10	10	10	10	10
134	10	10	10	10	10	10	10	10
135	20	10	10	10	10	10	20	10
136	10	10	10	10	10	10	10	10
137	10	10	10	10	10	10	10	10
138	30	10	10	10	10	10	30	10
139	10	10	10	10	10	10	10	10
140	10	10	10	10	10	10	10	10
141	10	10	10	10	10	10	10	10
142	10	10	10	10	10	10	10	10

143	10	10	10	10	10	10	10
144	10	10	10	10	10	10	10
145	30	10	10	10	10	10	10
146	40	10	10	10	10	10	10
147	10	10	10	10	10	10	10
148	10	10	10	10	10	10	10
149	10	10	10	10	10	10	10
150	10	10	10	10	10	10	10
151	10	10	10	10	10	10	10
152	10	10	10	10	10	10	10
153	10	10	10	10	10	10	10
154	10	10	10	10	10	10	10
155	10	10	10	10	10	10	10
156	10	10	10	10	10	10	10
157	40	10	10	10	10	10	10
158	10	10	10	10	10	10	10
159	10	10	10	10	10	10	10
160	40	10	10	10	10	10	10
161	10	10	10	10	10	10	10
162	10	10	10	10	10	10	10
163	10	10	10	10	10	10	10
164	10	10	10	10	10	10	10
165	10	10	10	10	10	10	10
166	10	10	10	10	10	10	10
167	10	10	10	10	10	10	10
168	10	10	10	10	10	10	10
169	10	10	10	10	10	10	10
170	10	10	10	10	10	10	10
171	10	10	10	10	10	10	10
172	10	10	10	10	10	10	10
173	10	10	10	10	10	10	10
174	10	10	10	10	10	10	10
175	10	10	10	10	10	10	10
176	40	40	10	10	10	40	40
177	10	10	10	10	10	10	10
178	10	10	10	10	10	10	10
179	10	10	10	10	10	10	10
180	10	10	10	10	10	10	10
181	20	10	30	10	10	20	30
182	10	10	10	10	10	10	10
183	10	10	10	10	10	10	10
184	10	10	10	10	10	10	10
185	10	10	10	10	10	10	10
186	10	10	10	10	10	10	10
187	10	10	10	10	10	10	10
188	10	10	10	10	10	10	10
189	10	10	10	10	10	10	10
190	10	10	10	10	10	10	10

191	10	10	10	10	10	10	10
192	10	10	10	10	10	10	10
193	10	10	10	10	10	10	10
194	10	10	10	10	10	10	10
195	10	10	10	10	10	10	10
196	10	10	10	10	10	10	10
197	20	10	10	10	10	10	10
198	10	10	10	10	10	10	10
199	40	10	10	10	10	10	10
200	10	10	10	10	10	10	10
201	40	40	10	10	10	20	40
202	10	10	10	10	10	10	10
203	10	10	10	10	10	10	10
204	40	40	10	10	10	20	40
205	10	10	10	10	10	10	10
206	40	40	10	10	10	10	40
207	10	10	10	10	10	10	10
208	10	10	10	10	10	10	10
209	10	10	10	10	10	10	10
210	10	10	10	10	10	10	10
211	10	10	10	10	10	10	10
212	10	10	10	10	10	10	10
213	40	40	10	10	10	20	40
214	10	10	10	10	10	10	10
215	10	10	10	10	10	10	10
216	10	10	10	10	10	10	10
217	40	10	10	10	10	10	40
218	10	10	10	10	10	10	10
219	10	10	10	10	10	10	10
220	40	10	10	10	10	10	40
221	40	40	10	10	10	20	40
222	40	10	10	10	10	10	40
223	10	10	10	10	10	10	10
224	10	10	10	10	10	10	10
225	10	10	10	10	10	10	10
226	10	10	10	10	10	10	10
227	10	10	10	10	10	10	10
228	10	10	10	10	10	10	10
229	10	10	10	10	10	10	10
230	10	10	10	10	10	10	10
231	10	10	10	10	10	10	10
232	10	10	10	10	10	10	10
233	10	10	10	10	10	10	10
234	10	10	10	10	10	10	10
235	10	10	10	10	10	10	10
236	10	10	10	10	10	10	10
237	10	10	10	10	10	10	10
238	10	10	10	10	10	10	10

239	10	10	10	10	10	10	10
240	40	40	10	10	10	40	40
241	10	10	10	10	10	10	10
242	10	10	10	10	10	10	10
243	10	10	10	10	10	10	10
244	40	10	30	10	10	40	30
245	10	10	10	10	10	10	10
246	10	10	10	10	10	10	10
247	30	40	10	10	10	30	40
248	30	40	10	10	20	30	40
249	10	10	10	10	10	10	10
250	40	10	10	10	10	40	10
251	10	10	10	10	10	10	10
252	10	10	10	10	10	10	10
253	40	10	10	10	10	40	10
254	40	40	10	10	10	40	40
255	10	10	10	10	10	10	10
256	30	40	10	10	20	30	40
257	10	10	10	10	10	10	10
258	30	10	10	10	10	30	10
259	10	10	10	10	10	10	10
260	30	40	10	10	10	30	40
261	10	10	10	10	10	10	10
262	10	10	10	10	10	10	10
263	10	10	10	10	10	10	10
264	10	10	10	10	10	10	10
265	10	10	10	10	10	10	10
266	40	10	10	10	10	40	10
267	30	10	10	10	20	30	20
268	10	10	10	10	10	10	10
269	10	10	10	10	10	10	10
270	10	10	10	10	10	10	10
271	40	10	10	10	20	40	20
272	10	10	10	10	10	10	10
273	10	10	10	10	10	10	10
274	10	10	10	10	10	10	10
275	40	40	10	10	20	40	40
276	10	10	10	10	10	10	10
277	10	10	10	10	10	10	10
278	40	10	10	10	10	40	10
279	30	10	10	10	10	30	10
280	10	10	10	10	10	10	10
281	10	10	10	10	10	10	10
282	10	10	10	10	10	10	10
283	20	10	10	10	10	20	10
284	10	10	10	10	10	10	10
285	40	10	10	30	10	40	30
286	10	10	10	10	10	10	10

287	10	10	10	10	10	10	10
288	10	10	10	10	10	10	10
289	10	10	10	10	10	10	10
290	10	10	10	10	10	10	10
291	10	10	10	10	10	10	10
292	40	40	10	10	20	40	40
293	10	10	10	10	10	10	10
294	20	10	10	10	10	20	10
295	10	10	10	10	10	10	10
296	10	10	10	10	10	10	10
297	10	10	10	10	10	10	10
298	10	10	10	10	10	10	10
299	10	10	10	10	10	10	10
300	10	10	10	10	10	10	10
301	10	10	10	10	10	10	10
302	10	10	10	10	10	10	10
303	40	40	10	10	10	40	40
304	10	10	10	10	10	10	10
305	30	40	10	10	20	30	40
306	10	10	10	10	10	10	10
307	10	10	10	10	10	10	10
308	40	10	30	10	10	40	30
309	10	10	10	10	10	10	10
310	10	10	10	10	10	10	10
311	30	40	10	10	10	30	40
312	10	10	10	10	10	10	10
313	10	10	10	10	10	10	10
314	30	40	10	10	10	30	40
315	40	40	10	10	20	40	40
316	10	10	10	10	10	10	10
317	10	10	10	10	10	10	10
318	10	10	10	10	10	10	10
319	10	10	10	10	10	10	10
320	10	10	10	10	10	10	10
321	10	10	10	10	10	10	10
322	10	10	10	10	10	10	10
323	20	10	30	10	10	20	30
324	10	10	10	10	10	10	10
325	10	10	10	10	10	10	10
326	40	10	10	10	20	40	20
327	10	10	10	10	10	10	10
328	30	40	10	10	20	30	40
329	10	10	10	10	20	10	20
330	10	10	10	10	10	10	10
331	10	10	10	10	10	10	10
332	20	10	10	10	10	20	10
333	10	10	10	10	20	10	20
334	40	10	10	10	10	40	10

335	10	10	10	10	10	10	10
336	10	10	10	10	10	10	10
337	40	10	10	10	10	10	10
338	10	10	10	10	10	10	10
339	10	10	10	10	10	10	10
340	10	10	10	10	10	10	10
341	10	10	10	10	10	10	10
342	40	40	10	10	10	20	40
343	10	10	10	10	10	10	10
344	10	10	10	10	10	10	10
345	10	10	10	10	10	10	10
346	10	10	10	10	10	10	10
347	10	10	10	10	10	10	10
348	10	10	10	10	10	10	10
349	10	10	10	10	10	10	10
350	10	10	10	10	10	10	10
351	10	10	10	10	10	10	10
352	10	10	10	10	10	10	10
353	10	10	10	10	10	10	10
354	10	10	10	10	10	10	10
355	10	10	10	10	10	10	10
356	10	10	10	10	10	10	10
357	10	10	10	10	10	10	10
358	40	10	10	10	10	10	40
359	10	10	10	10	10	10	10
360	10	10	10	10	10	10	10
361	10	10	10	10	10	10	10
362	10	10	10	10	10	10	10
363	10	10	10	10	10	10	10
364	10	10	10	10	10	10	10
365	10	10	10	10	10	10	10
366	10	10	10	10	10	10	10
367	10	10	10	10	10	10	10
368	10	10	10	10	10	10	10
369	10	10	10	10	10	10	10
370	10	10	10	10	10	10	10
371	40	40	10	10	10	10	40
372	10	10	10	10	10	10	10
373	10	10	10	10	10	10	10
374	10	10	10	10	10	10	10
375	30	10	10	10	10	10	30
376	10	10	10	10	10	10	10
377	10	10	10	10	10	10	10
378	10	10	10	10	10	10	10
379	10	10	10	10	10	10	10
380	10	10	10	10	10	10	10
381	10	10	10	10	10	10	10
382	10	10	10	10	10	10	10

383	40	40	10	10	20	40	40
384	10	10	10	10	10	10	10
385	10	10	10	10	10	10	10
386	40	40	10	10	10	40	40
387	40	10	10	10	10	40	10
388	10	10	10	10	10	10	10
389	10	10	10	10	10	10	10
390	10	10	10	10	10	10	10
391	10	10	10	10	10	10	10
392	10	10	10	10	10	10	10
393	10	10	10	10	10	10	10
394	10	10	10	10	10	10	10
395	10	10	10	10	10	10	10
396	10	10	10	10	10	10	10
397	10	10	10	10	10	10	10
398	10	10	10	10	10	10	10
399	10	10	10	10	10	10	10
400	10	10	10	10	10	10	10
401	10	10	10	10	10	10	10
402	10	10	10	10	10	10	10
403	10	10	10	10	10	10	10
404	40	40	10	10	10	40	40
405	10	10	10	10	10	10	10
406	10	10	10	10	10	10	10
407	10	10	10	10	10	10	10
408	10	10	10	10	10	10	10
409	10	10	10	10	10	10	10
410	10	10	10	10	10	10	10
411	10	10	10	10	10	10	10
412	10	10	10	10	10	10	10
413	10	10	10	10	10	10	10
414	10	40	10	10	10	10	40
415	10	10	10	10	10	10	10
416	10	10	10	10	10	10	10
417	10	10	10	10	10	10	10
418	10	10	10	10	10	10	10
419	10	10	10	10	10	10	10
420	10	10	10	10	10	10	10
421	10	10	10	10	10	10	10
422	10	40	10	10	10	10	40
423	10	10	10	10	10	10	10
424	40	10	10	10	10	40	10
425	10	10	10	10	10	10	10
426	20	10	10	10	10	20	10
427	40	40	10	10	20	40	40
428	10	10	10	10	10	10	10
429	10	10	10	10	10	10	10
430	10	10	10	10	10	10	10

431	10	10	10	10	10	10	10
432	10	10	10	10	10	10	10
433	10	10	10	10	10	10	10
434	40	10	10	10	10	10	10
435	10	10	10	10	10	10	10
436	10	10	10	10	10	10	10
437	30	40	10	10	10	10	40
438	10	10	10	10	10	10	10
439	10	10	10	10	10	10	10
440	10	10	10	10	10	10	10
441	10	10	10	10	10	10	10
442	10	10	10	10	10	10	10
443	30	10	10	10	10	10	10
444	10	10	10	10	10	10	10
445	30	40	10	10	10	10	40
446	30	10	10	10	10	10	10
447	10	10	10	10	10	10	10
448	20	10	10	10	10	10	10
449	30	40	10	10	10	20	40
450	10	10	10	10	10	10	10
451	10	10	10	10	10	10	10
452	10	10	10	10	10	10	10
453	10	10	10	10	10	10	10
454	20	10	10	10	10	10	10
455	10	10	10	10	10	10	10
456	40	10	10	10	10	10	10
457	10	10	10	10	10	10	10
458	10	10	10	10	10	10	10
459	10	10	10	10	10	10	10
460	10	10	10	10	10	10	10
461	40	40	10	10	10	20	40
462	10	10	10	10	10	10	10
463	10	10	10	10	10	10	10
464	40	40	10	10	10	10	40
465	10	10	10	10	10	10	10
466	10	10	10	10	10	10	10
467	10	10	10	10	10	10	10
468	10	10	10	10	10	10	10
469	10	10	10	10	10	10	10
470	10	10	10	10	10	10	10
471	10	10	10	10	10	10	10
472	10	10	10	10	10	10	10
473	10	10	10	10	10	10	10
474	40	10	10	10	10	10	10
475	10	10	10	10	10	10	10
476	10	10	10	10	10	10	10
477	10	10	10	10	10	10	10
478	10	10	10	10	10	10	10

479	10	10	10	10	10	10	10
480	10	10	10	10	10	10	10
481	10	10	10	10	10	10	10
482	10	10	10	10	10	10	10
483	10	10	10	10	10	10	10
484	10	10	10	10	10	10	10
485	10	10	10	10	10	10	10
486	10	10	10	10	10	10	10
487	10	10	10	10	10	10	10
488	10	10	10	10	10	10	10
489	10	10	10	10	10	10	10
490	10	10	10	10	10	10	10
491	10	10	10	10	10	10	10
492	40	40	30	10	20	40	40
493	10	10	10	10	10	10	10
494	10	10	10	10	10	10	10
495	10	10	10	10	10	10	10
496	10	10	10	10	10	10	10
497	10	10	10	10	10	10	10
498	10	10	10	10	10	10	10
499	10	10	10	10	10	10	10
500	10	10	10	10	10	10	10
501	10	10	10	10	10	10	10
502	10	10	10	10	10	10	10
503	10	10	10	10	10	10	10
504	40	40	10	10	10	40	40
505	10	10	10	10	10	10	10
506	10	10	10	10	10	10	10
507	10	10	10	10	10	10	10
508	10	10	10	10	10	10	10
509	10	10	10	10	10	10	10
510	10	10	10	10	10	10	10
511	10	10	10	10	10	10	10
512	10	10	10	10	10	10	10
513	10	10	10	10	10	10	10
514	10	10	10	10	10	10	10
515	10	10	10	10	10	10	10
516	10	10	10	10	10	10	10
517	10	10	10	10	10	10	10
518	20	10	10	10	10	20	10
519	10	10	10	10	10	10	10
520	10	10	10	10	10	10	10
521	10	10	10	10	10	10	10
522	40	10	10	10	10	40	10
523	10	10	10	10	10	10	10
524	10	10	10	10	10	10	10
525	10	10	10	10	10	10	10
526	10	10	10	10	10	10	10

527	40	40	10	10	10	40	40
528	20	10	10	10	10	20	10
529	10	10	10	10	10	10	10
530	10	10	10	10	10	10	10
531	10	10	10	10	10	10	10
532	10	10	10	10	10	10	10
533	10	10	10	10	10	10	10
534	10	10	10	10	10	10	10
535	30	10	30	10	10	30	30
536	10	10	10	10	10	10	10
537	10	10	10	10	10	10	10
538	10	10	10	10	10	10	10
539	40	10	10	10	10	40	10
540	10	10	10	10	10	10	10
541	10	10	10	10	10	10	10
542	10	10	10	10	10	10	10
543	10	10	10	10	10	10	10
544	10	10	10	10	10	10	10
545	10	10	10	10	10	10	10
546	10	10	10	10	10	10	10
547	10	10	10	10	10	10	10
548	30	10	10	10	10	30	10
549	10	10	10	10	10	10	10
550	40	40	10	10	10	40	40
551	10	10	10	10	10	10	10
552	10	10	10	10	10	10	10
553	10	10	10	10	10	10	10
554	10	10	10	10	10	10	10
555	10	10	10	10	10	10	10
556	10	10	10	10	10	10	10
557	10	10	10	10	10	10	10
558	40	40	10	10	10	40	40
559	10	10	10	10	10	10	10
560	10	10	10	10	10	10	10
561	10	10	10	10	10	10	10
562	10	10	10	10	10	10	10
563	10	10	10	10	10	10	10
564	10	10	10	10	10	10	10
565	10	10	10	10	10	10	10
566	10	10	10	10	10	10	10
567	10	10	10	10	10	10	10
568	40	40	10	10	10	40	40
569	10	10	10	10	10	10	10
570	10	10	10	10	10	10	10
571	10	10	10	10	10	10	10
572	30	10	10	10	10	30	10
573	10	10	10	10	10	10	10
574	10	10	10	10	10	10	10

575	30	10	10	10	10	30	10
576	10	10	10	10	10	10	10
577	10	10	10	10	10	10	10
578	10	10	10	10	10	10	10
579	10	10	10	10	10	10	10
580	10	10	10	10	10	10	10
581	10	10	10	10	10	10	10
582	10	10	10	10	10	10	10
583	10	10	10	10	10	10	10
584	20	10	10	10	10	20	10
585	10	10	10	10	10	10	10
586	10	10	10	10	10	10	10
587	40	40	10	10	20	40	40
588	10	10	10	10	10	10	10
589	10	10	10	10	10	10	10
590	10	10	10	10	10	10	10
591	10	10	10	10	10	10	10
592	40	40	10	10	20	40	40
593	10	10	10	10	10	10	10
594	30	40	10	10	10	30	40
595	10	10	10	10	10	10	10
596	10	10	10	10	10	10	10
597	20	10	10	10	10	20	10
598	10	10	10	10	10	10	10
599	10	10	10	10	10	10	10
600	10	10	10	10	10	10	10
601	10	10	10	10	10	10	10
602	10	10	10	10	10	10	10
603	10	10	10	10	10	10	10
604	10	10	10	10	10	10	10
605	10	10	10	10	10	10	10
606	10	10	10	10	10	10	10
607	10	10	10	10	10	10	10
608	40	10	10	10	10	40	10
609	10	10	10	10	10	10	10
610	10	10	10	10	10	10	10
611	10	10	10	10	10	10	10
612	10	10	10	10	10	10	10
613	30	40	10	10	20	30	40
614	10	10	10	10	10	10	10
615	30	40	10	10	20	30	40
616	10	10	10	10	10	10	10
617	10	10	10	10	10	10	10
618	40	40	10	10	20	40	40
619	40	40	30	10	20	40	40
620	10	10	10	10	10	10	10
621	10	10	10	10	10	10	10
622	30	10	10	10	10	30	10

623	20	10	10	10	10	20	10
624	10	10	10	10	10	10	10
625	40	10	10	10	10	40	10
626	10	10	10	10	10	10	10
627	10	10	10	10	10	10	10
628	10	10	10	10	10	10	10
629	40	40	30	10	20	40	40
630	10	10	10	10	10	10	10
631	10	10	10	10	10	10	10
632	10	10	10	10	10	10	10
633	10	10	10	10	10	10	10
634	10	10	10	10	10	10	10
635	40	10	10	10	10	40	10
636	10	10	10	10	10	10	10
637	10	10	10	10	10	10	10
638	10	10	10	10	10	10	10
639	10	10	10	10	10	10	10
640	10	10	10	10	10	10	10
641	10	10	10	10	10	10	10
642	10	10	10	10	10	10	10
643	10	10	10	10	10	10	10
644	30	40	30	10	20	30	40
645	10	10	10	10	10	10	10
646	10	10	10	10	10	10	10
647	10	10	10	10	10	10	10
648	30	40	30	10	20	30	40
649	10	10	10	10	10	10	10
650	40	10	10	10	10	40	10
651	10	10	10	10	10	10	10
652	10	10	10	10	10	10	10
653	40	40	10	10	10	40	40
654	10	10	10	10	10	10	10
655	10	10	10	10	10	10	10
656	10	10	10	10	10	10	10
657	10	10	10	10	10	10	10
658	10	10	10	10	10	10	10
659	20	10	10	10	10	20	10
660	10	10	10	10	10	10	10
661	10	10	10	10	10	10	10
662	10	10	10	10	10	10	10
663	10	10	10	10	10	10	10
664	10	10	10	10	10	10	10
665	30	10	10	10	10	30	10
666	10	10	10	10	10	10	10
667	10	10	10	10	10	10	10
668	10	10	10	10	10	10	10
669	30	10	10	10	10	30	10
670	10	10	10	10	10	10	10

671	10	10	10	10	10	10	10
672	10	10	10	10	10	10	10
673	10	10	10	10	10	10	10
674	10	10	10	10	10	10	10
675	10	10	10	10	10	10	10
676	30	40	10	10	20	30	40
677	10	10	10	10	10	10	10
678	10	10	10	10	10	10	10
679	10	10	10	10	10	10	10
680	10	10	10	10	10	10	10
681	30	40	10	10	10	30	40
682	10	10	10	10	10	10	10
683	10	10	10	10	10	10	10
684	40	10	10	10	10	40	10
685	10	10	10	10	10	10	10
686	10	10	10	10	10	10	10
687	10	10	30	10	10	10	30
688	10	10	10	10	10	10	10
689	10	10	10	10	10	10	10
690	10	10	10	10	10	10	10
691	10	10	10	10	10	10	10
692	40	10	10	10	10	40	10
693	10	10	10	10	10	10	10
694	10	10	10	10	10	10	10
695	10	10	10	10	10	10	10
696	10	10	10	10	10	10	10
697	10	10	10	10	10	10	10
698	10	10	10	10	10	10	10
699	10	10	10	10	10	10	10
700	10	10	10	10	10	10	10
701	10	10	10	10	10	10	10
702	10	10	10	10	10	10	10
703	10	10	10	10	10	10	10
704	10	10	10	10	10	10	10
705	10	10	10	10	10	10	10
706	10	10	10	10	10	10	10
707	10	10	10	10	10	10	10
708	10	10	10	10	10	10	10
709	10	10	10	10	10	10	10
710	10	10	10	10	10	10	10
711	10	10	10	10	10	10	10
712	10	10	10	10	10	10	10
713	10	10	10	10	10	10	10
714	10	10	10	10	10	10	10
715	10	10	10	10	10	10	10
716	10	10	10	10	10	10	10
717	10	10	10	10	10	10	10
718	10	10	10	10	10	10	10

719	10	10	10	10	10	10	10
720	10	10	10	10	10	10	10
721	10	10	10	10	10	10	10
722	10	10	10	10	10	10	10
723	10	10	10	10	10	10	10
724	10	10	10	10	10	10	10
725	10	10	10	10	10	10	10
726	10	10	10	10	10	10	10
727	10	10	10	10	10	10	10
728	10	10	10	10	10	10	10
729	10	10	10	10	10	10	10
730	10	10	10	10	10	10	10
731	10	10	10	10	10	10	10
732	10	10	10	10	10	10	10
733	10	10	10	10	10	10	10
734	10	10	10	10	10	10	10
735	10	10	10	10	10	10	10
736	10	10	10	10	10	10	10
737	10	10	10	10	10	10	10
738	10	10	10	10	10	10	10
739	10	10	10	10	10	10	10
740	10	10	10	10	10	10	10
741	10	10	10	10	10	10	10
742	10	10	10	10	10	10	10
743	10	10	10	10	10	10	10
744	10	10	10	10	10	10	10
745	10	10	10	10	10	10	10
746	10	10	10	10	10	10	10
747	10	10	10	10	10	10	10
748	10	10	10	10	10	10	10
749	10	10	10	10	10	10	10
750	10	10	10	10	10	10	10
751	10	10	10	10	10	10	10
752	10	10	10	10	10	10	10
753	10	10	10	10	10	10	10
754	10	10	10	10	10	10	10
755	10	10	10	10	10	10	10
756	10	10	10	10	10	10	10
757	30	10	10	10	10	30	10
758	10	10	10	10	10	10	10
759	10	10	30	10	10	10	30
760	10	10	10	10	10	10	10
761	10	10	10	10	10	10	10
762	10	10	10	10	10	10	10
763	10	10	10	10	10	10	10
764	10	10	10	10	10	10	10
765	10	10	10	10	10	10	10
766	10	10	10	10	10	10	10

767	10	10	10	10	10	10	10
768	10	10	10	10	10	10	10
769	10	10	10	10	10	10	10
770	10	10	10	10	10	10	10
771	10	10	10	10	10	10	10
772	10	10	10	10	10	10	10
773	20	10	10	10	10	10	10
774	10	10	10	10	10	10	10
775	10	10	10	10	10	10	10
776	10	10	10	10	10	10	10
777	10	10	10	10	10	10	10
778	10	10	10	10	10	10	10
779	10	10	10	10	10	10	10
780	10	10	10	10	10	10	10
781	10	10	10	10	10	10	10
782	10	10	10	10	10	10	10
783	10	10	10	10	10	10	10
784	30	40	10	10	10	30	40
785	30	10	10	10	10	30	10
786	30	10	30	10	10	30	30
787	30	10	30	10	10	30	30
788	40	10	30	10	10	40	30
789	30	10	10	10	10	30	10
790	10	10	10	10	10	10	10
791	40	10	10	10	10	40	10
792	10	10	10	10	10	10	10
793	10	10	10	10	10	10	10
794	10	10	10	10	10	10	10
795	10	10	10	10	10	10	10
796	10	10	10	10	10	10	10
797	10	10	10	10	10	10	10
798	10	10	10	10	10	10	10
799	10	10	10	10	10	10	10
800	10	10	10	10	10	10	10
801	10	10	10	10	10	10	10
802	10	10	10	10	10	10	10
803	10	10	10	10	10	10	10
804	10	10	10	10	10	10	10
805	10	10	10	10	10	10	10
806	10	10	10	10	10	10	10
807	10	10	10	10	10	10	10
808	10	10	10	10	10	10	10
809	10	10	10	10	10	10	10
810	10	10	10	10	10	10	10
811	10	10	10	10	10	10	10
812	10	10	10	10	10	10	10
813	10	10	10	10	10	10	10
814	10	10	10	10	10	10	10

815	10	10	10	10	10	10	10
816	10	10	10	10	10	10	10
817	10	10	10	10	10	10	10
818	10	10	10	10	10	10	10
819	10	10	10	10	10	10	10
820	10	10	10	10	10	10	10
821	10	10	10	10	10	10	10
822	10	10	10	10	10	10	10
823	10	10	10	10	10	10	10
824	10	10	10	10	10	10	10
825	10	10	10	10	10	10	10
826	10	10	10	10	10	10	10
827	10	10	10	10	10	10	10
828	10	10	10	10	10	10	10
829	10	10	10	10	10	10	10
830	10	10	10	10	10	10	10
831	10	10	10	10	10	10	10
832	10	10	10	10	10	10	10
833	10	10	10	10	10	10	10
834	40	10	10	10	10	10	10
835	10	10	10	10	10	10	10
836	10	10	10	10	10	10	10
837	10	10	10	10	10	10	10
838	10	10	10	10	10	10	10
839	10	10	10	10	10	10	10
840	10	10	10	10	10	10	10
841	10	10	10	10	10	10	10
842	10	10	10	10	10	10	10
843	10	10	10	10	10	10	10
844	10	10	10	10	10	10	10
845	10	10	10	10	10	10	10
846	10	10	10	10	10	10	10
847	10	10	10	10	10	10	10
848	10	10	10	10	10	10	10
849	10	10	10	10	10	10	10
850	10	10	10	10	10	10	10
851	10	10	10	10	10	10	10
852	10	10	10	10	10	10	10
853	10	10	10	10	10	10	10
854	10	10	10	10	10	10	10
855	10	10	10	10	10	10	10
856	10	10	10	10	10	10	10
857	10	10	10	10	10	10	10
858	10	10	10	10	10	10	10
859	10	10	10	10	10	10	10
860	10	10	10	10	10	10	10
861	10	10	10	10	10	10	10
862	10	10	10	10	10	10	10

863	10	10	10	10	10	10	10
864	10	10	10	10	10	10	10
865	10	10	10	10	10	10	10
866	10	10	10	10	10	10	10
867	10	10	10	10	10	10	10
868	10	10	10	10	10	10	10
869	10	10	10	10	10	10	10
870	10	10	10	10	10	10	10
871	10	10	10	10	10	10	10
872	10	10	10	10	10	10	10
873	10	10	10	10	10	10	10
874	10	10	10	10	10	10	10
875	10	10	10	10	10	10	10
876	10	10	10	10	10	10	10
877	10	10	10	10	10	10	10
878	10	10	10	10	10	10	10
879	10	10	10	10	10	10	10
880	10	10	10	10	10	10	10
881	10	10	10	10	10	10	10
882	10	10	10	10	10	10	10
883	10	10	10	10	10	10	10
884	10	10	10	10	10	10	10
885	10	10	10	10	10	10	10
886	10	10	10	10	10	10	10
887	10	10	10	10	10	10	10
888	10	10	10	10	10	10	10
889	10	10	10	10	10	10	10
890	10	10	10	10	10	10	10
891	10	10	10	10	10	10	10
892	10	10	10	10	10	10	10
893	10	10	10	10	10	10	10
894	10	10	10	10	10	10	10
895	10	10	10	10	10	10	10
896	10	10	10	10	10	10	10
897	10	10	10	10	10	10	10
898	10	10	10	10	10	10	10
899	30	10	10	10	10	30	10
900	10	10	10	10	10	10	10
901	10	10	10	10	10	10	10
902	10	10	10	10	10	10	10
903	10	10	10	10	10	10	10
904	10	10	10	10	10	10	10
905	10	10	10	10	10	10	10
906	10	10	10	10	10	10	10
907	10	10	10	10	10	10	10
908	10	10	10	10	10	10	10
909	10	10	10	10	10	10	10
910	10	10	10	10	10	10	10

911	10	10	10	10	10	10	10
912	10	10	10	10	10	10	10
913	10	10	10	10	10	10	10
914	10	10	10	10	10	10	10
915	10	10	10	10	10	10	10
916	10	10	10	10	10	10	10
917	10	10	10	10	10	10	10
918	10	10	10	10	10	10	10
919	10	10	10	10	10	10	10
920	10	10	10	10	10	10	10
921	10	10	10	10	10	10	10
922	10	10	10	10	10	10	10
923	10	10	10	10	10	10	10
924	10	10	10	10	10	10	10
925	10	10	10	10	10	10	10
926	10	10	10	10	10	10	10
927	10	10	10	10	10	10	10
928	10	10	10	10	10	10	10
929	10	10	10	10	10	10	10
930	10	10	10	10	10	10	10
931	10	10	10	10	10	10	10
932	10	10	10	10	10	10	10
933	10	10	10	10	10	10	10
934	10	10	10	10	10	10	10
935	10	10	10	10	10	10	10
936	10	10	10	10	10	10	10
937	10	10	10	10	10	10	10
938	10	10	10	10	10	10	10
939	10	10	10	10	10	10	10
940	10	10	10	10	10	10	10
941	10	10	10	10	10	10	10
942	10	10	10	10	10	10	10
943	10	10	10	10	10	10	10
944	10	10	10	10	10	10	10
945	10	10	10	10	10	10	10
946	10	10	10	10	10	10	10
947	10	10	10	10	10	10	10
948	10	10	10	10	10	10	10
949	10	10	10	10	10	10	10
950	10	10	10	10	10	10	10
951	10	10	10	10	10	10	10
952	10	10	10	10	10	10	10
953	10	10	10	10	10	10	10
954	10	10	10	10	10	10	10
955	10	10	10	10	10	10	10
956	10	10	10	10	10	10	10
957	10	10	10	10	10	10	10
958	10	10	10	10	10	10	10

959	10	10	10	10	10	10	10
960	10	10	10	10	10	10	10
961	10	10	10	10	10	10	10
962	10	10	10	10	10	10	10
963	10	10	10	10	10	10	10
964	10	10	10	10	10	10	10
965	10	10	10	10	10	10	10
966	10	10	10	10	10	10	10
967	10	10	10	10	10	10	10
968	10	10	10	10	10	10	10
969	10	10	10	10	10	10	10
970	10	10	10	10	10	10	10
971	10	10	10	10	10	10	10
972	10	10	10	10	10	10	10
973	10	10	10	10	10	10	10
974	10	10	10	10	10	10	10
975	10	10	10	10	10	10	10
976	10	10	10	10	10	10	10
977	10	10	10	10	10	10	10
978	10	10	10	10	10	10	10
979	10	10	10	10	10	10	10
980	10	10	10	10	10	10	10
981	10	10	10	10	10	10	10
982	10	10	10	10	10	10	10
983	10	10	10	10	10	10	10
984	10	10	10	10	10	10	10
985	10	10	10	10	10	10	10
986	10	10	10	10	10	10	10
987	10	10	10	10	10	10	10
988	10	10	10	10	10	10	10
989	10	10	10	10	10	10	10
990	10	10	10	10	10	10	10
991	10	10	10	10	10	10	10
992	10	10	10	10	10	10	10
993	10	10	10	10	10	10	10
994	10	10	10	10	10	10	10
995	10	10	10	10	10	10	10
996	10	10	10	10	10	10	10
997	10	10	10	10	10	10	10
998	10	10	10	10	10	10	10
999	10	10	10	10	10	10	10
1000	10	10	10	10	10	10	10

6.3. Rprogramming for Chi-Square goodness of fit test

```
RSE <- read.table("ChiSquare4.csv", head=T, sep=",") # R language to read data table  
#ChiSquare4 is the data file including RSHM Index (Expected values) and Vegetation  
#index (Original values) values  
chisq.test(RSE) # Chi-Square test for data called RSE.
```

Appendix 7

Data of Global Warming Effects on Red Spruce Distribution Ranges

7.1. *Red spruce growth with Global Warming and Air pollution changes in ARIMs*

Red spruce growths were simulated for the period of 1940 to 2099 in ARIM_{high} and ARIM_{low} separately (Table (a) in Section 3.1) and were averaged for two periods, 1980-1999 and 2080-2099 (Table (b) in Section 3.2). The averaged values of the period of 1980 to 1999 were subtracted from the ones for the period of 2080 to 2099 (Table (c) in Section 3.2) to compare the changes of red spruce growth. In Table (c), the positive values mean increase of red spruce growth and the negative ones decrease.

(a)

Year	Global Warming Effects on Red Spruce Growth (ARIM Index of ARIM _{high})			Global Warming Effects on Red Spruce Growth (ARIM Index of ARIM _{low})		
	Air Pollution Changes Rate			Air Pollution Changes Rate		
	10% increases	No increase	10% decreases	10% increases	No increase	10% decreases
1940	1.27	1.25	1.24	1.22	1.22	1.21
1941	1.24	1.22	1.21	1.07	1.06	1.06
1942	1.2	1.19	1.17	1.08	1.07	1.07
1943	1.19	1.17	1.15	1.21	1.21	1.2
1944	1.18	1.16	1.14	1.12	1.12	1.11
1945	1.15	1.13	1.11	1.15	1.15	1.14
1946	1.17	1.15	1.13	1.19	1.19	1.18
1947	1.16	1.14	1.12	1.19	1.18	1.18
1948	1.17	1.15	1.12	1.08	1.08	1.07
1949	1.2	1.18	1.16	1.21	1.21	1.2
1950	1.17	1.16	1.13	1.21	1.2	1.2
1951	1.18	1.16	1.14	1.23	1.23	1.22
1952	1.2	1.18	1.16	1.18	1.17	1.17
1953	1.19	1.17	1.15	1	0.99	0.99
1954	1.18	1.16	1.14	1.06	1.05	1.05
1955	1.18	1.16	1.14	1.1	1.1	1.09
1956	1.15	1.13	1.11	1.09	1.09	1.08
1957	1.12	1.1	1.08	1.21	1.2	1.2
1958	1.14	1.12	1.1	1.34	1.34	1.33
1959	1.12	1.1	1.07	1.05	1.04	1.04

1960	1.1	1.08	1.06	1.17	1.16	1.15
1961	1.09	1.07	1.04	1.2	1.2	1.19
1962	1.07	1.04	1.01	1.29	1.29	1.28
1963	1.04	1.02	0.99	1.32	1.32	1.31
1964	1.03	1	0.97	1.21	1.2	1.19
1965	1.01	0.98	0.95	1.1	1.1	1.09
1966	0.96	0.92	0.89	1.1	1.09	1.08
1967	0.93	0.9	0.86	1.18	1.18	1.17
1968	0.96	0.93	0.9	1.22	1.21	1.2
1969	0.91	0.87	0.83	1.05	1.04	1.03
1970	0.85	0.81	0.77	1.15	1.14	1.13
1971	0.84	0.81	0.76	1.1	1.09	1.08
1972	0.79	0.75	0.71	1.21	1.2	1.19
1973	0.76	0.72	0.67	1.27	1.26	1.25
1974	0.81	0.77	0.72	1.26	1.25	1.24
1975	0.89	0.86	0.82	1.23	1.22	1.21
1976	0.86	0.83	0.79	1.08	1.07	1.06
1977	0.82	0.78	0.73	1.06	1.05	1.04
1978	0.85	0.81	0.77	1.16	1.15	1.14
1979	0.83	0.79	0.74	1.12	1.11	1.1
1980	0.89	0.86	0.82	1.19	1.18	1.17
1981	0.91	0.88	0.84	1.05	1.05	1.04
1982	0.91	0.88	0.84	1.12	1.11	1.1
1983	0.94	0.91	0.87	1.21	1.2	1.19
1984	0.9	0.86	0.82	1.06	1.05	1.04
1985	0.96	0.93	0.89	1.13	1.12	1.11
1986	0.99	0.96	0.93	0.95	0.94	0.93
1987	0.98	0.95	0.92	0.9	0.89	0.88
1988	0.96	0.92	0.89	0.95	0.94	0.93
1989	0.91	0.88	0.84	1.04	1.03	1.02
1990	0.92	0.89	0.85	1.21	1.2	1.19
1991	0.92	0.88	0.85	1.23	1.22	1.21
1992	0.95	0.92	0.89	1.26	1.25	1.24
1993	0.94	0.91	0.88	1.08	1.07	1.06
1994	0.89	0.86	0.82	1.17	1.16	1.15
1995	0.99	0.96	0.93	1.29	1.29	1.28
1996	0.99	0.96	0.93	1.1	1.1	1.09
1997	0.98	0.95	0.92	1.19	1.18	1.17
1998	0.98	0.95	0.92	1.15	1.14	1.13
1999	1	0.97	0.94	1.14	1.13	1.12
2000	0.87	0.85	0.83	1.16	1.16	1.15
2001	0.89	0.87	0.85	1.02	1.02	1.01
2002	0.89	0.87	0.86	1.09	1.09	1.09
2003	0.92	0.91	0.89	1.18	1.17	1.17
2004	0.88	0.86	0.84	1.03	1.03	1.03
2005	0.94	0.92	0.91	1.09	1.08	1.08
2006	0.97	0.96	0.94	0.91	0.91	0.9
2007	0.96	0.95	0.93	0.87	0.87	0.86

2008	0.94	0.92	0.9	0.91	0.9	0.9
2009	0.9	0.88	0.86	1.01	1	1
2010	0.9	0.89	0.87	1.19	1.18	1.18
2011	0.9	0.88	0.86	1.2	1.2	1.2
2012	0.94	0.92	0.9	1.24	1.23	1.23
2013	0.92	0.91	0.89	1.05	1.05	1.04
2014	0.87	0.86	0.84	1.14	1.13	1.13
2015	0.97	0.96	0.95	1.27	1.26	1.26
2016	0.97	0.96	0.94	1.08	1.07	1.07
2017	0.96	0.95	0.93	1.17	1.16	1.16
2018	0.97	0.95	0.94	1.13	1.13	1.13
2019	0.98	0.97	0.95	1.12	1.12	1.11
2020	0.85	0.85	0.85	1.15	1.15	1.15
2021	0.87	0.87	0.87	1.01	1.01	1.01
2022	0.87	0.87	0.87	1.08	1.08	1.08
2023	0.91	0.91	0.91	1.16	1.16	1.16
2024	0.86	0.86	0.86	1.02	1.02	1.02
2025	0.92	0.92	0.92	1.07	1.07	1.07
2026	0.96	0.96	0.96	0.89	0.89	0.89
2027	0.95	0.95	0.95	0.85	0.85	0.85
2028	0.92	0.92	0.92	0.89	0.89	0.89
2029	0.88	0.88	0.88	0.99	0.99	0.99
2030	0.89	0.89	0.89	1.16	1.17	1.17
2031	0.88	0.88	0.88	1.18	1.18	1.18
2032	0.92	0.92	0.92	1.22	1.22	1.22
2033	0.91	0.91	0.91	1.04	1.04	1.04
2034	0.85	0.85	0.85	1.12	1.12	1.12
2035	0.96	0.96	0.96	1.25	1.25	1.25
2036	0.95	0.96	0.96	1.06	1.06	1.06
2037	0.95	0.95	0.95	1.15	1.15	1.15
2038	0.95	0.95	0.95	1.11	1.11	1.12
2039	0.96	0.96	0.97	1.1	1.1	1.1
2040	0.84	0.85	0.87	1.13	1.13	1.14
2041	0.85	0.87	0.89	0.99	0.99	1
2042	0.85	0.87	0.89	1.06	1.06	1.07
2043	0.89	0.9	0.92	1.14	1.15	1.15
2044	0.84	0.86	0.88	1	1	1.01
2045	0.9	0.92	0.94	1.05	1.05	1.06
2046	0.94	0.96	0.97	0.87	0.87	0.88
2047	0.93	0.95	0.96	0.83	0.84	0.84
2048	0.9	0.92	0.94	0.87	0.87	0.88
2049	0.86	0.87	0.89	0.97	0.98	0.98
2050	0.87	0.88	0.9	1.14	1.15	1.15
2051	0.86	0.88	0.9	1.16	1.17	1.17
2052	0.9	0.92	0.94	1.2	1.21	1.21
2053	0.89	0.91	0.92	1.02	1.02	1.02
2054	0.83	0.85	0.87	1.1	1.11	1.11
2055	0.94	0.96	0.98	1.23	1.23	1.24

2056	0.94	0.95	0.98	1.05	1.05	1.06
2057	0.93	0.95	0.97	1.13	1.14	1.14
2058	0.93	0.95	0.97	1.09	1.1	1.1
2059	0.94	0.96	0.98	1.07	1.08	1.08
2060	0.82	0.85	0.88	1.11	1.11	1.12
2061	0.83	0.87	0.9	0.97	0.98	0.99
2062	0.83	0.87	0.91	1.04	1.05	1.06
2063	0.87	0.9	0.94	1.12	1.13	1.14
2064	0.82	0.86	0.89	0.97	0.98	0.99
2065	0.88	0.92	0.95	1.03	1.04	1.05
2066	0.92	0.95	0.99	0.85	0.85	0.86
2067	0.91	0.94	0.98	0.81	0.82	0.83
2068	0.88	0.92	0.95	0.85	0.85	0.86
2069	0.84	0.87	0.91	0.95	0.96	0.97
2070	0.85	0.88	0.92	1.12	1.12	1.13
2071	0.84	0.88	0.91	1.14	1.15	1.16
2072	0.88	0.91	0.95	1.18	1.19	1.2
2073	0.87	0.9	0.94	0.99	1	1.01
2074	0.81	0.85	0.89	1.08	1.09	1.1
2075	0.92	0.96	0.99	1.21	1.22	1.23
2076	0.92	0.95	0.99	1.03	1.04	1.05
2077	0.91	0.94	0.98	1.12	1.12	1.13
2078	0.91	0.95	0.99	1.07	1.08	1.09
2079	0.93	0.96	1	1.05	1.05	1.06
2080	0.8	0.85	0.9	1.08	1.1	1.11
2081	0.81	0.87	0.92	0.94	0.96	0.97
2082	0.81	0.87	0.92	1.01	1.03	1.04
2083	0.85	0.9	0.95	1.1	1.11	1.13
2084	0.8	0.85	0.91	0.95	0.96	0.98
2085	0.87	0.92	0.97	1.01	1.02	1.03
2086	0.9	0.95	1	0.82	0.83	0.84
2087	0.89	0.94	0.99	0.78	0.8	0.81
2088	0.87	0.91	0.97	0.82	0.83	0.85
2089	0.82	0.87	0.93	0.93	0.94	0.96
2090	0.83	0.88	0.94	1.09	1.1	1.12
2091	0.82	0.87	0.93	1.11	1.13	1.14
2092	0.86	0.91	0.97	1.16	1.18	1.19
2093	0.85	0.9	0.96	0.97	0.98	1
2094	0.79	0.85	0.91	1.05	1.07	1.08
2095	0.9	0.95	1.01	1.18	1.2	1.21
2096	0.9	0.95	1.01	1.01	1.02	1.04
2097	0.89	0.94	1	1.09	1.11	1.12
2098	0.89	0.95	1	1.04	1.06	1.07
2099	0.91	0.96	1.01	1.02	1.03	1.04

7.2. *Comparisons of Averaged Red Spruce Growths between Two Periods (1980-1999 and 2080-2099)*

(b)

Elevation Range	Period	Air Pollution Change Rates		
		10% increase	0% increase	10% decrease
High Elevation	1980-1999	0.9455	0.914	0.8795
	2080-2099	0.853	0.9045	0.96
Low Elevation	1980-1999	1.121	1.1125	1.1025
	2080-2099	1.008	1.023	1.0365

(c)

Elevation Range	Air Pollution Change Rates		
	10% increase	0% increase	10% decrease
High Elevation	-0.0925	-0.0095	0.0805
Low Elevation	-0.113	-0.0895	-0.066
Buffer Zone (1650-1850)	-0.10275	-0.0495	0.00725

(d)

Elevation Range	Air Pollution Change Rates (Modified values)		
	10% increase	0% increase	10% decrease
High Elevation	-925	-95	805
Low Elevation	-1130	-895	-660
Buffer Zone (1650-1850)	-1027.5	-495	72.5

* Buffer Zone was calculated by averaging ARIM indices of ARIM_{high} (High Elevation) and ARIM_{low} (Low Elevation). These values were multiplied by 10,000 to apply them to map algebra modifications (Table (d)).